Chiral Nuclear Dynamics II

From Quarks to Nuclei to Compact Stars

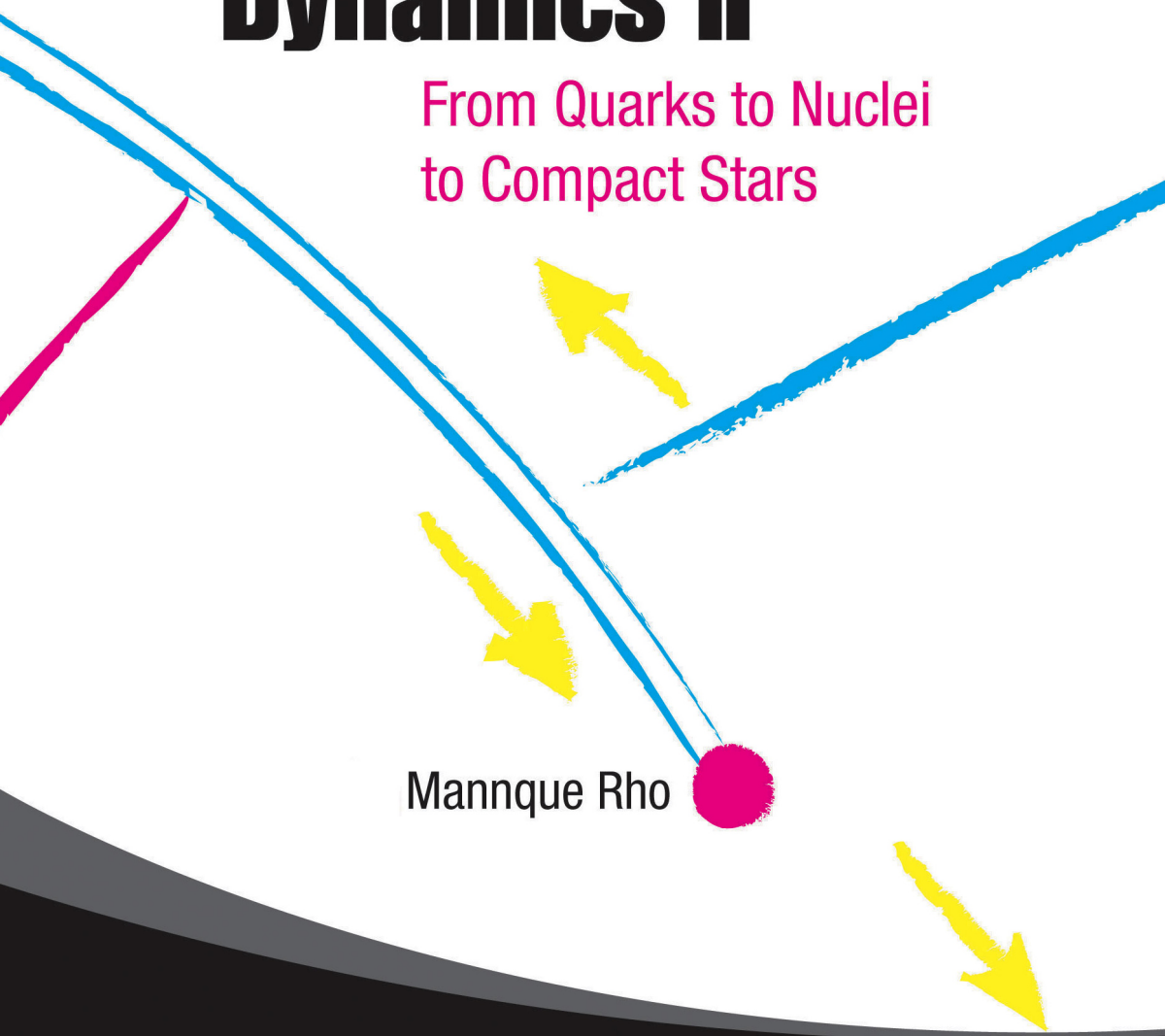

Mannque Rho

World Scientific

Chiral Nuclear Dynamics II

From Quarks to Nuclei to Compact Stars

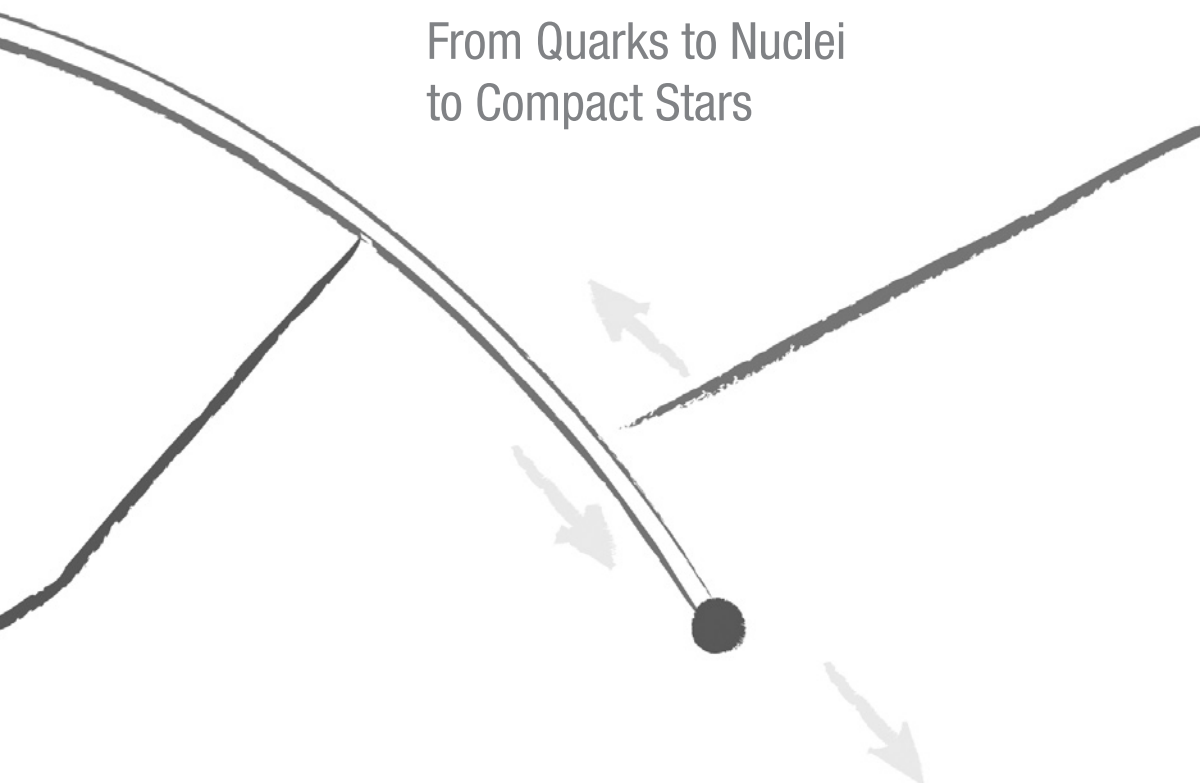

This page intentionally left blank

Chiral Nuclear Dynamics II

From Quarks to Nuclei to Compact Stars

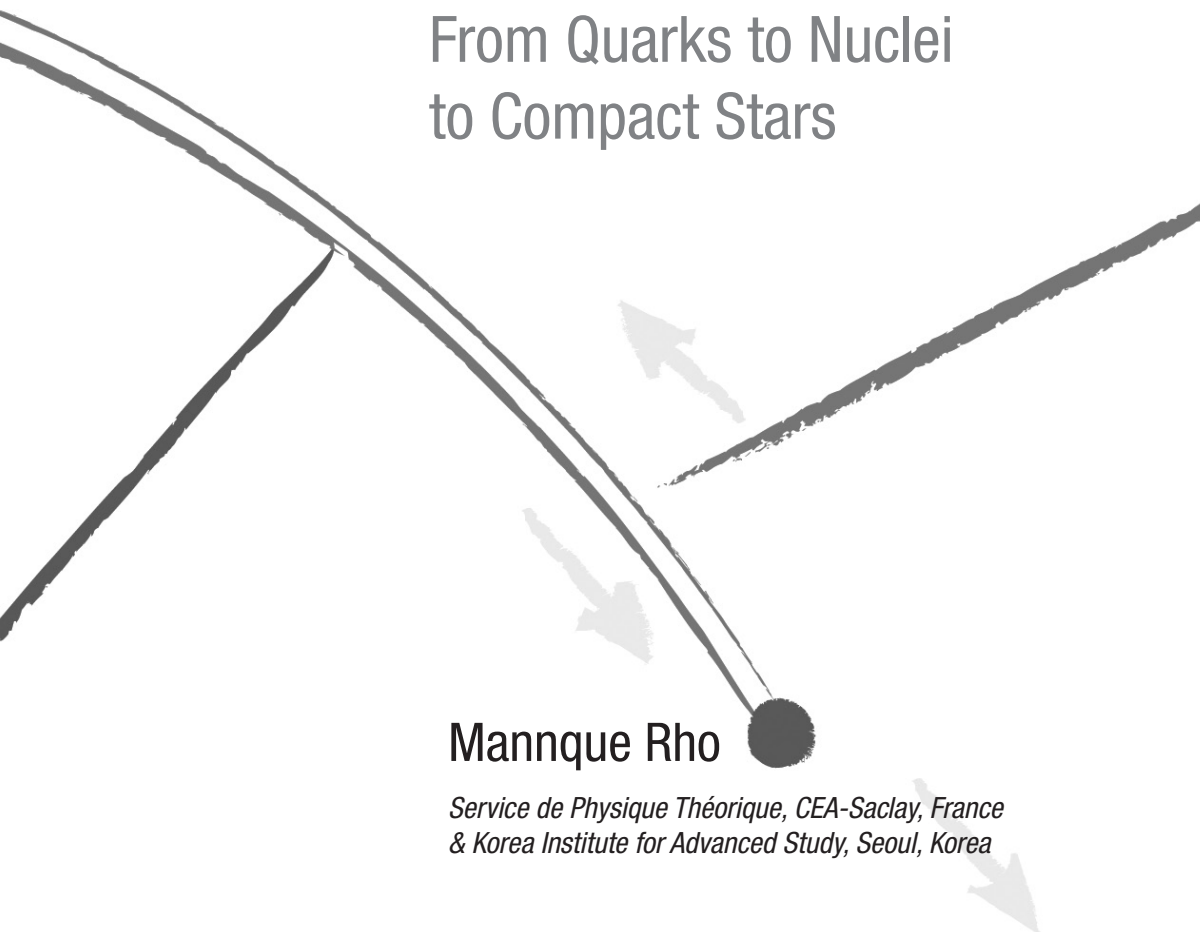

Mannque Rho

Service de Physique Théorique, CEA-Saclay, France
& Korea Institute for Advanced Study, Seoul, Korea

World Scientific

NEW JERSEY • LONDON • SINGAPORE • BEIJING • SHANGHAI • HONG KONG • TAIPEI • CHENNAI

Published by

World Scientific Publishing Co. Pte. Ltd.

5 Toh Tuck Link, Singapore 596224

USA office: 27 Warren Street, Suite 401-402, Hackensack, NJ 07601

UK office: 57 Shelton Street, Covent Garden, London WC2H 9HE

British Library Cataloguing-in-Publication Data
A catalogue record for this book is available from the British Library.

CHIRAL NUCLEAR DYNAMICS II (2nd Edition)
From Quarks to Nuclei to Compact Stars

ISBN-13 978-981-270-588-4
ISBN-10 981-270-588-0

Printed in Singapore.

To Oliver

This page intentionally left blank

Preface

This monograph is a sequel to the previous volume entitled *Chiral Nuclear Dynamics* (CND-I for short) that I co-authored with Maciek Nowak and Ismail Zahed and it develops further on the main theme of, and presents new perspectives on, the topics treated in that volume. The present volume is not intended to replace or improve on what was treated there. Apart from a mini-summary, I will skip essentially all the chapters dealing with basic concepts contained in CND-I up to Chapter 6 and pick up some of the issues that have either not been completely dealt with or touched on only briefly in the second half of CND-I, and expand them in the light of new developments that have generated renewed interest in the past decade.

What motivated me to write this volume was the need for a *single* unified framework that puts under a systematic control a large variety of phenomena taking place in hadronic matter under normal as well as extreme conditions of high temperature and high density. There is admittedly no such framework available at present that is truly realistic, but a first attempt is made in this monograph to see to what extent such a framework can be formulated. As such, though ambitious, the scope is rather limited. The subject matter treated in this volume belongs properly to the domain of nuclear physics, nowadays categorized more as hadronic physics than as nuclear physics. The core of the matter, which will be further elaborated upon in the Introduction, is intricately connected with the origin of hadron masses and is tied intimately with the fundamental structure of the complex vacuum associated with the strong interactions. But it also has striking ramifications on "standard" (or mundane) nuclear interactions. The recent intensive endeavor to unravel the phase structure of hadronic matter at very high temperature as in the environment of the Early Universe and at super-high density as in the core of compact stars highlights this matter in the guise of how chiral symmetry and confinement/deconfinement of quarks and gluons of QCD manifest themselves in Nature. Much of what might be happening in matter under the "extreme" conditions cannot be accessed directly and reliably by QCD *proper*, so one is forced to rely on models to access such environments. Various different models, mimicking the true theory of the strong interactions, QCD, have been studied extensively. However lacking experimental guidance and model-independent theoretical tools, they can address, at best, only

certain limited sectors of the strong interactions more or less disconnected from other sectors. This makes it difficult to assess the validity of the various scenarios proposed and to make falsifiable predictions in the conditions that are non-ordinary as one expects at high temperature/density.

Hadronic matter at high density illustrates what is meant above. The situation is similar for high temperature. The ultimate goal in studying matter much denser than nuclear matter would be to determine what the equation of state (EOS) is in the dense matter present in the deep interior of compact stars, either stabilized in binary pulsars or on the verge of collapse into black holes. One of the currently popular ideas is that certain compact stars may support quark matter in a variety of different forms. Now if the star had a core of quark matter, that would carry information on QCD at high density with its intriguing landscape of phases. Physicists would like to produce and study such a matter by laboratory experiments, by typically colliding nuclei on nuclei. Nucleons in nuclei are in interactions involving virtual as well as real mesons, so their interactions are effectively described in terms of hadrons, with their masses and coupling constants suitably determined in the condition in which the measurement is made and for which the theory is defined. The pertinent question is: How does the matter change over from nuclear matter – that we understand – to quark matter – that we do not – as the system is strongly compressed? There are currently two theoretical approaches to this issue. One is "bottom-up" which starts with what is known in the (zero-density) free space and then brings, perturbatively, the system to the state of extreme conditions. The other is "top-down" which starts at an asymptotic density for which QCD is well under control and goes down to a sub-asymptotic density relevant to compact stars. The accepted lore is that the first is well-defined at zero density and the second at asymptotic density. The question is: what happens in between? Here the situation is not at all clear.

In going from a dilute (zero-temperature) hadron state to a highly dense matter supposedly populated with quarks/gluons, one must encounter a variety of different "phases." At very low density, the matter is a Fermi gas. Next, one encounters Fermi liquid (nuclear matter), possibly condensed mesons, condensed Cooper pairs (color superconductivity) or quark matter and ultimately the color-flavor-locked state. At present each stage is handled separately. What happens in one has little connection to what happens in the other, for the simple reason that there is no systematic theoretical tool reliable enough to guide one to go from one to the other. Can one make a reasonable prediction of what might be happening in compact stars in this situation?

To address this question, let us see what is being done in the search for a "smoking gun" for chiral symmetry restoration at high temperature/density, which is one of the most puzzling and urgent issues in hadron physics. This has bearing on how hadronic masses are generated as I will elaborate in the Introduction, so it is a crucial issue for us. Current experimental and theoretical efforts work to

"restore" – partially or fully – chiral symmetry of the QCD vacuum by "melting" the quark condensate. This is done typically by studying spectral functions in the vector meson channels in heavy-ion collisions. Independent of whether or not such signals are visible in the spectral functions, one can ask whether the order parameter for chiral symmetry, namely, the quark condensate, can be isolated in a unique way from what takes place in the plethora of complex nuclear interactions involved in the experiments. Phrased differently, can one distinguish the would-be signal for full or partial restoration of chiral symmetry in dense medium from what might appear to be *mundane* phenomena in nuclei? I will argue that the answer to this is negative unless one is looking at processes in the close vicinity of the critical point where chiral symmetry is supposedly restored, an experimental condition that is difficult to access unencumbered by "trivial" complications. The matter must be much subtler than what we naively think. We are already familiar with one such situation in nuclear physics where the subtlety had challenged nuclear physicists for decades, namely, the meson exchange current. Yukawa's meson theory for nuclear forces dictated that there be meson exchange currents but it required the advent of chiral perturbation theory and the astute identification of the processes to look at, to unambiguously "see" how the mesons, and in particular, pions, intervene in nuclear processes.

We expect that the manifestation of chiral symmetry, and consequently the vacuum change of the strong interactions that govern the mass will be a lot subtler than the case of meson exchange currents. The currently available piece-meal treatments cannot provide a clear picture of what happens to the vacuum in nuclear interactions, be it under normal conditions or extreme conditions. In this volume, I will adopt a different strategy by starting with a (perhaps overly) simplified theory which is however not proven to be wrong but has the virtue of being adaptable to the whole range of conditions concerned. It has the definite advantage of being falsifiable at various stages as will be explicitly specified. I will accept the main premise of CND-I that the properties of many-nucleon systems, *i.e.*, nuclei, nuclear matter and hadronic matter at high density and/or high temperature can be deduced or guessed from the fundamental theory of the strong interactions and that this can be done by means of effective field theories consistent with Weinberg's "folk theorem," explained and followed closely in this volume. The best one can hope to do along this line is, then, to meet as many as possible the conditions required for the theorem. For this, I exploit the notion of hidden local symmetry developed by Harada and Yamawaki.

In the framework developed in this volume, limited to the minimum possible number of assumptions, we will see emerging an intricate connection between what *does* happen in standard nuclear processes under normal conditions that have been well studied and understood for decades and what *could* happen under extreme conditions that are as yet unexplored. For instance, what could be a signal for chiral phase transition at some high temperature and/or density with a vanish-

ing quark condensate that also indicates the vanishing hadron mass, is found to be intricately connected to such diverse objects or phenomena as tensor forces in normal nuclear interactions, meson exchange currents, Landau Fermi-liquid interactions, a Kohn-Sham-type density functional for nuclear matter, the anomalous gyromagnetic ratio, kaon condensation and the collapse of compact stars into black holes *etc.*

This monograph draws largely from work done and discussion with a large number of collaborators. It was most strongly influenced by Gerry Brown with whom I have worked on practically all aspects of the subjects treated and whose views pervade throughout the volume. The original inception of this monograph was already there when the volume CND-I was completed in mid-1990's but the major part of the material comes from the work done in Korea beginning from 1998 when I started to regularly visit Korea and work with Korean theorists, especially at Seoul National University, Korea Institute for Advanced Study, Hanyang University, and Pusan National University. Both Maciek Nowak and Ismail Zahed visited Korea with me on several occasions and contributed invaluably to the development of the field coined then as "astro-hadron physics" that combines hadron physics and astrophysics. I have had the great fortune of working with, and learning from, many Korean colleagues. Among them, I should mention Dong-Pil Min and his former students at Seoul National University who are now established theorists: Chang-Hwan Lee, Byung-Yoon Park, Tae-Sun Park, and Chaejun Song. Most of their contributions figure prominently in this volume. I should also mention Hyun Kyu Lee and Sang-Jin Sin of Hanyang University who helped me to better understand a variety of subtle issues on geometric phases, topology and renormalization group in hadron physics reflected throughout the volume. Also participating in the research with young Koreans in the years 1999–2003 were Kuniharu Kubodera of South Carolina, USA, Vicente Vento of Valencia, Spain and Bengt Friman of Darmstadt, Germany. The results of their research carried out in Korea make up important parts of this volume.

One of the most crucial developments that turned out to provide the validation of "Brown-Rho scaling" and form the foundation of the principal thesis developed here, is the remarkable but hitherto little appreciated work done by Masayasu Harada and Koichi Yamawaki of Nagoya University on hidden local symmetry in hadron dynamics. I am most grateful for extensive discussions and collaborations with them as well as with Chihiro Sasaki, whose thesis work offers the only consistent framework that I know of for confronting Nature with the notion of hidden local symmetry in matter under extreme conditions.

I would also like to acknowledge the kind help of Chang-Hwan Lee of Pusan National University on the astrophysics part of Chapters 10 and 11, which covers some of his works with Gerry Brown and the late Hans Bethe. For the more recent development on holographic dual QCD which opens up a new perspective in the field and of which I give a brief discussion, I would like to thank Deog Ki Hong

of Pusan National University, and Ho-Ung Yee and Piljin Yi of Korea Institute for Advanced Study.

Finally and above all, without the patient support and continuous encouragement of Helga, this volume would not have seen its day.

Mannque Rho

This page intentionally left blank

Contents

This page intentionally left blank

Chapter 1

Introduction

The core of this volume, the problem of "mass" of what we see around us, touches on one of the most profound issues in all areas of physics, be they condensed matter, nuclear or particle physics. This remains just as much of a mystery in nature as where the dark energy of the Universe comes from and what the dark matter of the Universe is. Though manifested differently in different areas of physics, it presents a basic puzzle. The origin of the mass of the particles familiar to nuclear physicists, namely, proton and neutron, belongs to this class of puzzles. Unlike the particles studied in high-energy machines, the proton is a mundane object, being a basic constituent of nuclei, that is accessible to laboratory scrutiny. Nonetheless its structure has remained up to date prominently mysterious. While the masses of all "visible" matters around us, molecules, atoms, nuclei *etc.* are more than 99% accountable in terms of the sum of the masses of the constituents, the nucleon being the basic constituent of them, the source of the nucleon (proton and neutron) mass itself is still more or less unknown. QCD tells us that a proton, say, is made primarily up of two up (u) quarks and one down (d) quark, with the strange (s) quark and heavier quarks entering into its structure only negligibly. Since the quarks involved have tiny masses, nearly zero on hadronic scale, $\sim 98\%$ of the proton mass must be coming from something other than the *basic* constituents of the proton. So the question is: Where do $\sim 98\%$ of the proton mass come from?

In CND-I, it was explained how the rearrangement of the complex vacuum can be responsible for the generation of the mass and for much of the properties of strong interaction dynamics as we observe them. The phenomenon was attributed to "spontaneous" break-down of chiral symmetry – which is an exact symmetry if one ignores the (tiny) quark masses. Although it is not yet proven, the dynamical breaking of chiral symmetry may also be intricately connected with the confinement of quarks and gluons. In this volume, we shall accept this possibility and ask, if the mass of hadrons is dynamically generated from the complex vacuum structure, can one unravel the mechanism of the mass generation by reversing the process, namely tweaking the vacuum so that the mass be made to dynamically "disappear"? One may think of this as going backwards in time in the evolution of the Universe from high temperature/density to what it is now.

In short, the main subjects of this volume consist of exploring how this can be done in the terrestrial and space laboratories and how to explain what have been so far observed in consistency in a language that models the fundamental theory of strong interactions.

In contrast to the time of the writing of CND-I when little empirical information was available, some, though incomplete, experimental data have accumulated which could now enable us to answer some part of the question posed above. Hadrons are being heated in heavy-ion collisions to high temperature, say, several hundreds of MeV, allowing us to have a glimpse of the Universe at the age of $\sim 10^{-6}$ second after the Big Bang. Hadronic matter is, and will be soon, compressed to a density several times the nuclear matter density, mimicking the conditions that are supposed to be present in the interior of compact stars. These processes bring hadronic matter to a temperature or density at which the spontaneously broken chiral symmetry is restored or/and the quarks and gluons get deconfined. Along the way the matter experiences a variety of conditions in which the mass and coupling constants get modified significantly, influencing crucially the properties of hadrons living in these environments. QCD should be undoubtedly the right theory to address all these issues but a direct use of QCD for *all* such issues is out of reach at this point. We are thus forced to resort to effective field theory (EFT for short) formalism.

We develop the appropriate languages to address this issue in this volume. We do this chiefly in two different ways. One way is to pick up what was touched on in CND-I, namely approaching effective field theory from the quark-gluon picture via what is called the Cheshire Cat Principle (Chapter 3). This is a "bottom-up" approach in the sense that we go up in energy scale to probe strong interactions at the relevant kinematic regime. The other is via holographic dual QCD based on AdS/CFT from string theory. This approach, touched on only briefly in Chapters 5 and 6, which is being actively developed at the time of writing of this volume may be classified as a "top-down" approach since it is based on a string-theory idea. The end product in both cases is effective chiral Lagrangian theory. In our case, the EFT tool to use is the hidden local symmetry (HLS) theory. We make a detailed exposition of the latter approach in Chapter 5. This may not be the only way to approach the issue, but we find this to be the easiest and most efficient way.

To make contact with the traditional nuclear physics, we treat few-nucleon nuclei in Chapter 4. Our theme is *continuity* in physics between the "old" way of doing things and the "new" way that is anchored on more modern view. In addition we aim to illustrate the power of the EFT approach in nuclear physics *proper* where the temperature is low and the density is not high. The focus will be on the predictive power of the EFT in nuclear physics. Here certain predictions – free of arbitrary parameters – are made by means of effective field theory combined with traditional many-body approaches based on accurate and sophisticated phenomenological techniques. The import of this exercise is that EFT can supplement and improve on – not replace – the standard nuclear physics approach (SNPA for short). What makes

EFT valuable in nuclear physics is that it can make predictions that go beyond what was feasible in standard nuclear physics approaches.

The skyrmion picture that figured centrally in CND-I reappears in a different guise in Chapters 6, in particular in making certain predictions of novel structure at high density. The skyrmion as a baryon re-emerges in the gravity dual description of QCD that comes from string theory. What makes this development noteworthy is that in a realistic holographic dual QCD (or AdS/QCD), low-energy strongly-coupled dynamics is captured by hidden local symmetry theory with an infinite tower of vector mesons coupled to the Goldstone pions ($\mathrm{HLS}_{K=\infty}$ for short) and the entire baryon degrees of freedom are encoded in the theory as solitons. The soliton in that theory is an instanton in 5D Yang-Mills theory or equivalently a skyrmion in 4D $\mathrm{HLS}_{K=\infty}$ theory. It turns out that the effect of infinite tower is totally encapsulated in a 5D instanton and gives rise to a baryon structure which is *drastically different* from that of the Skyrme model based on pion-only chiral Lagrangians. It leads to a natural justification of chiral perturbation theory that works well in the structure of low-lying baryons as well as of nuclei. Being at a seminal stage, however, not much is known of the property of holographic-QCD skyrmions in medium, so we can say nothing of what that new skyrmion picture implies for dense baryonic matter. What we will do is to consider the skyrmion description where hidden local symmetry will be truncated so that only the lowest members of the tower ρ, ω and ϕ figure as relevant vector degrees of freedom ($\mathrm{HLS}_{K=1}$ for short to be distinguished from $\mathrm{HLS}_{K=\infty}$). Such an object is not well understood even at the level of one baryon, so our treatment of many-baryon systems will be qualitative at best.

The hidden local symmetry $\mathrm{HLS}_{K=1}$ developed by Harada and Yamawaki is described in detail in Chapter 5. One can think of $\mathrm{HLS}_{K=1}$ as a truncated model of $\mathrm{HLS}_{K=\infty}$ in which all the members of the tower *except for the lowest* are integrated out. Quantum treatment of $\mathrm{HLS}_{K=1}$ theory at one-loop level predicts what constitutes the principal mechanism of how the mass can disappear in heat bath or in dense medium. This is signalled at the chiral restoration phase transition – driven by temperature and/or density – by what is called "vector manifestation" (VM for short). At the VM fixed point, the vector meson mass, generically denoted by m_V, vanishes (when the quark masses are ignored corresponding to the "chiral limit") proportionally to the quark condensate $\langle\bar{q}q\rangle$ which plays the role of a chiral order parameter. Although not established rigorously, the effect of the infinite tower remnant in $\mathrm{HLS}_{K=1}$ can be interpreted in terms of the parameter a of the $\mathrm{HLS}_{K=1}$ Lagrangian. The parameter a takes the value of 2 in free space but will approach 1 at the VM fixed point.

How the mass changes as the vacuum changes under extreme conditions of high temperature and high density is treated in Chapter 7. Here the VM fixed point of $\mathrm{HLS}_{K=1}$ controls what can happen in relativistic heavy ion collisions where temperature can be hundreds of MeV. As for dense matter, the $\mathrm{HLS}_{K=1}$ contains no explicit fermions, hence no baryons. They could in principle be generated as described in

Chapter 6 as skyrmions but in the absence of workable techniques, quasiquarks (or constituent quarks) are introduced in a hidden local symmetric way to $\mathrm{HLS}_{K=1}$ Lagrangian. It is found that the VM fixed point is also reached when chiral symmetry is restored by density. In all cases, the vanishing of the mass m_V and a approaching 1 play an important role in the change of hadron properties in medium. How this intricate chiral symmetry manifestation, which appears different from the standard scenario exemplified by sigma models, affects nuclear matter at the normal nuclear matter density at zero temperature is discussed in Chapter 8. Here the scaling relation proposed a decade and half ago – called "Brown-Rho scaling" – makes a contact with the prediction of $\mathrm{HLS}_{K=1}$ theory with the VM fixed point.

Strangeness at high density, in particular kaon condensation and possibly dense kaon bound nuclei, are treated from different vantage points in Chapter 9. A particular importance will be given to the approach that starts from the VM fixed point of hidden local symmetry theory, that makes a remarkably simple prediction that kaons will condense at a density ~ 3 times the nuclear matter density. This prediction will be the basis of the discussions on compact stars in Chapter 11. Other forms of dense matter that could figure at higher densities are discussed in Chapter 10. They are treated in the light of the "continuity" adopted in this volume. As such, it is not meant to be general. Nor can it directly confront the physics of compact stars as the intermediate steps are missing. In fact, there are generically two obstacles in confronting the physics of compact stars in terms of what's discussed in this chapter. On the one hand, there is a vast variety of theoretical models in the literature that differ in details but cannot be precise enough to make falsifiable predictions. $\mathrm{HLS}_{K=1}$, having been largely unexplored up to date in the density regime relevant for compact stars, is no exception in this regard. On the other hand, while there are a wealth of observations on properties of compact stars, they are not specific enough to confirm or falsify specific theoretical models. In other words, it is difficult to pin down what it is that a certain observation is telling us. Thus the discussion in Chapter 10, which addresses certain aspects of the most interesting density regime where perturbative QCD can make statements, cannot – and does not – directly address the properties of compact stars *per se*.

Some specific aspects of compact stars that bear on the equation of state of dense matter make up the content of Chapter 11. The focus will be on the neutron star mass which is the most important astrophysical observable that can be directly compared with theoretical results. In this chapter, an approach that departs drastically from conventional approaches found in the literature will be adopted. It will consist of assuming that the first phase transition that occurs beyond the nuclear matter density is kaon condensation and it determines the fate of compact stars, *i.e.* as to whether a star becomes a neutron star or collapses to a black hole. This would imply that other states at high densities discussed in Chapter 10 would be rendered irrelevant to compact stars.

Due to the limitation of the scope, we won't be able to adequately confront such related astrophysical issues as the formation and evolution processes of neutron stars, prospects for gravitational waves and gamma-ray bursts involving compact stars, neutron star cooling, and the neutrino signals in the process of neutron star formation. Even though these observations may not be able to provide directly details of the inside structure of neutron stars, they will certainly supply very useful information on masses and populations of compact objects.

The conclusion we can draw at at this point via-à-vis with compact stars is that a lot more work is needed and a great deal of discovery, both theoretical and experimental, are in store. The penultimate goal of probing dense hadronic matter via compact stars remains a challenge for the future.

In exposing the principal structure of this volume, we will take for granted some of the basic premises that are treated in CND-I. For completeness, we make a mini-summary of the basic elements that we will have in mind in this volume. They will be stated without explanation.

Confinement

We will take it for granted that at zero temperature and zero density, quarks and gluons are confined and that at some temperature $T_{c_1} > 0$ and some density $n_{c_1} > n_0$ where $n_0 \simeq 0.16$ fm^{-3} is the normal nuclear matter density, quarks and gluons are deconfined. How this happens which we take as unknown will not be addressed.

Chiral symmetry

We will be mainly dealing with the up (u) and down (d) quarks but will consider the strange (s) quark as well. We will be mostly considering the "chiral limit" where $m_u \approx m_d \approx m_s \approx 0$ although in nature, the u- and d-quark masses are a few MeV and the s-quark mass ~ 100 MeV. Unless otherwise stated, these will be referred to as "light quarks." The QCD Lagrangian is invariant under chiral transformations. This is the $SU(N_f)_L \times SU(N_f)_R$ chiral symmetry.[1] Thus both the left (L) and right (R) currents or alternatively the vector and axial vector currents are conserved. The conservation of the vector current is not affected if the quark masses are turned on provided the vector ($V = L + R$) symmetry is unbroken but the axial current will have a term proportional to the quark mass if the quark mass is not zero.

This symmetry of Lagrangian can, however, be broken by the vacuum. It turns out that the vector symmetry remains unbroken by the vacuum (Vafa-Witten theorem, see below) but the axial symmetry is broken, as we know from Goldstone theorem. It is now understood – and supported by nature – that the symmetry associated with the light quarks in the zero-mass limit is spontaneously broken below some temperature T_{c_2} and some density n_{c_2}. The present understanding is $T_{c_2} \simeq 170 - 190$ MeV and $n_{c_2} \simeq (3 - 10)n_0$. The latter is more or less unknown.

[1] There are in addition an unbroken $U(1)_V$ symmetry corresponding to baryon charge and anomalous $U(1)_A$ which will be mentioned below.

Whether the critical temperature and density (T_{c_2}, n_{c_2}) for chiral restoration are the same as or different from the deconfinement points (T_{c_1}, n_{c_1}) is not known. We will encounter the situation in which deconfinement may take place before chiral symmetry is restored, *i.e.* $T_{c_1} < T_{c_2}$. There are no known models that indicate the converse takes place. Unless otherwise stated, we shall take them coincident. Lattice results are not at odds with this choice. It will be taken for granted that the $SU(N_f) \times SU(N_f)$ chiral symmetry is spontaneously broken to the diagonal subgroup $SU(N_f)_{V=L+R}$. Thus we will have $(N_f^2 - 1)$ Goldstone (or with quark masses, pseudo-Goldstone) bosons, π and a massive η'.

Anomalies

Certain symmetries of QCD present in the "bare" Lagrangian are broken by quantum effects intimately tied to the complex vacuum structure. Such a phenomenon breaks the current conservation unlike the spontaneous breaking which leaves the relevant currents conserved. This is what is called "quantum anomaly" or "anomaly" in short. Among a variety of anomalies associated with QCD proper and effective theories thereof, what concerns us are the scale invariance and the axial $U(1)$ symmetry in the limit of zero mass.

- *Trace anomaly:*
  The QCD Lagrangian with no quark masses is scale invariant. So the energy-momentum tensor $\theta_{\mu\nu}$ is traceless at the classical level. However at the quantum level due to an anomaly, scale invariance is broken so the trace of the energy-momentum tensor has a non-zero value[2] $\theta^\mu_\mu = -\frac{\beta(g)}{2g}\mathrm{Tr}G^2_{\mu\nu}$. The non-vanishing trace of $\theta_{\mu\nu}$ means that there is a scale in the theory, so the scale invariance present in the Lagrangian is broken. If one defines a dilation current D_μ, the scale anomaly means that the dilatation current is not conserved. The divergence of the dilatation current is equal to the trace of $\theta_{\mu\nu}$.

  We will later observe, based on lattice data, that the vacuum expectation value of $G^2_{\mu\nu}$, *i.e.* r $\langle 0|G^2|0\rangle$, could be decomposed into two components "soft" and "hard," $\langle 0|G^2|0\rangle = \langle 0|G^2|0\rangle_{soft} + \langle 0|G^2|0\rangle_{hard}$. The "soft" component will be interpreted later as due to spontaneous breaking of scale invariance and the "hard" component to explicit breaking of scale invariance. It is understood, though not rigorously proven, that spontaneous breaking of the scale invariance is possible only if there is explicit breaking. This feature will play an important role in some parts of this volume.
- $U(1)_A$ *anomaly*
  While the $SU(N_f)$ axial currents are conserved, spontaneously broken in low temperature and low density regime, and assumed to be restored at T_{c_2}

[2]With non-zero quark mass there is an additional term on the RHS of the form $+\sum_f m_f(1+\gamma_f)\bar{q}_f q_f$ with γ_f the anomalous dimension for the quark field q_f.

and n_{c_2}, the $U(1)$ axial current is not conserved due to a triangle anomaly. The consequence is that the would-be Goldstone boson η' is not massless even in the chiral limit. The anomaly is believed to remain in the chirally restored phase. In this volume, this anomaly will not figure importantly.

Large N_c

QCD in the large N_c limit provides useful information on nonperturbative aspects of the strong interactions. In nature, N_c is 3 but in some sense which cannot be given a precise meaning, $N_c = 3$ can be considered much bigger than the number of flavors $N_f = 2, 3$. In terms of the power of N_c factors, the following counting can be done:

- *Gluons*
  The counting in the gluon sector is done in terms of the 't Hooft constant $\lambda = g^2 N_c$. This is taken to be $\mathcal{O}(1)$. [3] Thus $g^2 \sim \mathcal{O}(1/N_c^2)$. Planar diagrams dominate, with non-planar graphs being suppressed by $1/N_c$ or higher.
- *Mesons*
  The leading contribution to correlation functions is the sum of planar graphs which is $\mathcal{O}(N_c)$. Meson-meson couplings are down by powers of $1/N_c$. For instance, 3-meson interactions scale as $1/\sqrt{N_c}$, 4-meson interactions $1/N_c$ *etc.* The mass of the $\bar{q}q$-type mesons is $\mathcal{O}(N_c^0)$. They appear as sharp resonances. Exotics are suppressed by $\mathcal{O}(1/N_c)$ or higher.
- *Baryons*
  Baryon mass scales as $\mathcal{O}(N_c)$. This follows from the fact that N_c quarks are needed to make a "color" singlet. This plays an important role in what follows. Roughly

$$m_B \sim N_c \sim 1/g^2 \tag{1.1}$$

  where g is the color gauge coupling. The mass being inversely proportional to g^2 indicates that the baryon can be considered as a soliton in a weak coupling theory. Indeed the skyrmion description of baryons is intimately tied to this scaling as we will see later. Simple counting shows that $g_A \sim N_c$, $f_\pi \sim \sqrt{N_c}$ and $g_{\pi NN} \sim N_c^{3/2}$. There are a variety of relations between the skyrmion model and non-relativistic quark models in the large N_c limit which are listed in CND-I, which we will use without entering into details.

[3] In holographic QCD discussed in several chapters that follow, λ will be taken to be large in the sense that an expansion is made in $1/\lambda$.

Vafa-Witten theorem

Modulo some plausible assumptions, vector symmetries in vector-like theories like QCD are argued to be free from spontaneous symmetry breaking. The examples relevant to us are baryon number, isospin *etc.* One of the assumptions is that Lorentz invariance holds. Since the systems we will be considering in this volume will break explicitly Lorentz invariance (by temperature and/or density), this Vafa-Witten theorem does not directly apply, although it will be a useful guide in writing down the Lorentz-invariant part of effective theories.

Anomaly matching

In order for an effective theory to be consistent with a fundamental theory, the anomaly in EFT should be identical to the anomaly in the fundamental theory. This is 't Hooft anomaly matching condition. In QCD, this means that in the hadronic world where hadrons are composites of quarks and gluons, there must be a massless, colorless object which couples to the axial current and photon and reproduces exactly the triangle anomaly. The Goldstone pion is such an object. This condition will prove to be quite relevant in the chiral structure of the nucleon treated in Chapter 8.

Chapter 2

Multi-Facets Of QCD In Matter

In this chapter, we elaborate and extend some of the key points as required for exposing the general structure of this volume.

As one of the three ingredients of the Standard Model, quantum chromodynamics (QCD) is a complete theory by itself, renormalizable in the standard sense. It is thus believed that strongly interacting matter should be completely describable once QCD is solved exactly. Up to now, however, nobody has found how to obtain reliable solution of QCD in the nonperturbative regime we are concerned with. QCD has three distinctive characteristics: confinement, spontaneous breaking of chiral symmetry and asymptotic freedom. In certain kinematical regime where asymptotic freedom prevails, a systematic weak-coupling expansion can in principle be carried out to an arbitrary accuracy to reliably calculate physical observables. However, in the kinematical regime that we are interested in in this volume, that is, for many hadrons in strong interactions under extreme conditions such as at high temperature as in relativistic heavy ion collisions and at high density presumably found in the deep interior of the densest compact stars stable against collapse into black holes, QCD cannot yet be solved, so we have limited guidance, if any, from the fundamental theory. To address this issue, we need to understand how the quarks are confined and how chiral symmetry with massless quarks is spontaneously broken. These issues are inherently nonperturbative and nonlinear.

The fact that we have no trustful QCD solution in that regime does not of course mean that we do not know what's going on in nature. Indeed we know quite a lot from particle and nuclear physics of many decades, what is going on in conditions that are amenable to laboratory test. Nuclear physics is a highly mature and accurate science. What is needed is the proper tool to make a bridge from the conditions so far studied in the currently available laboratories to the extreme conditions that are needed to address the problems we are interested in. In looking for such a tool, we encounter multiple facets in the manifestations of QCD.

The Cheshire Cat phenomenon

The basic question to be addressed is how the fundamental degrees of freedom of QCD, namely, quarks and gluons, manifest themselves in the strong interactions involving many hadrons. This entails an inherently highly nonperturbative approach to QCD. Most likely connected to the origin of the mass mentioned in the Introduction is the role of constituents of the matter. Down to the scale of the nucleus, the constituents are "visible" in the sense that the constituents can be extracted from the system and scrutinized directly. Thus a nucleus can be shown explicitly to consist of nucleons. But here the explicitness of the constituents ends. Quarks and gluons that are believed to be the constituents of the nucleon are confined, so one cannot see them isolated. Whenever they appear, they are accompanied by others, in hadrons or in jets, in such a way that the measured quantities are always colorless. This is the problem of confinement. So the first issue is: How does confinement manifest itself in physical processes? The precise answer to this is as yet unknown. One line of thinking that we find helpful, if not rigorous, in making progress leads to the concept of what is called "Cheshire Cat principle (CCP)." A modern aspect of this issue – figured importantly in CND-I – will be treated in the next chapter.

The CCP relies on the complex vacuum structure of QCD, in particular, the spontaneous breaking by the vacuum of chiral symmetry (χSB for short) associated with the (near) masslessness of the up (u), down (d) and (sometimes) strange (s) quarks. As mentioned, it is not known whether χSB and confinement are intrinsically related. A recent development from holographic dual QCD that relates the strong-coupling regime of QCD to supergravity solution indicates that they could be either coincident or separate with the χSB scale higher than confinement scale. The simplest and most practical picture that incorporates quark-gluon confinement is that given by the MIT bag model. Here the quarks and gluons are confined within a bag of radius ~ 1 fm. Within the bag, the quarks and gluons are weakly interacting, reflecting asymptotic freedom, and cannot go out of the bag by confinement which is effected in the MIT bag mode with boundary conditions that prevent the color carriers from leaking out. This picture, however, does not take into account that there is chiral symmetry, which is exact if the quark masses are taken to be zero. The bag breaks chiral symmetry explicitly. Since the bag is representative of the "vacuum," there is nothing wrong with the bag "breaking" chiral symmetry. What is wrong is that while chiral symmetry can be broken by the vacuum, it should not in the equation of motion of the quarks. But the axial current of the MIT bag model is not conserved because of the MIT bag boundary condition. It implies that chiral symmetry is not correctly implemented. It is now fairly well understood that correctly implementing chiral symmetry leads to the structure of the outside of the bag which is quite different from that of the MIT bag. In fact spontaneous breaking of chiral symmetry necessitates that zero mass pseudoscalar modes, *i.e.* pions, be excited. Restoring the conservation of the axial current requires therefore modify-

ing the bag boundary conditions. In doing so, one is led to what is now known as "chiral bag model."

Putting boundary conditions to assure the continuity of the axial current introduces two subtle effects into the theory. One is a quantum anomaly effect due to an *induced* axial current due to the boundary condition for the pion field. It induces the baryon charge to leak out of the bag. Since this "anomaly" is an artifact of the boundary, the fractionized baryon charge that leaks out must be *absorbed* by the topological soliton configuration of the pions living outside, thereby assuring the conservation of the quantized baryon charge of the baryon. The other effect is that the boundary condition for the $U(1)_A$ boson, η', induces a quantum anomaly that makes the color leak out of the bag. There is no colored field outside of the bag to absorb this leaking color in contrast to the pion field which can absorb the baryon charge. To assure the conservation of the color, one must therefore impose a boundary condition – which breaks color gauge invariance – to absorb the leaking color. Thus one has a Lagrangian which breaks color gauge invariance at the classical level but when quantized, the color gets restored. This is contrary to the baryon charge conservation.

The net effect of what's given above can be captured in the "Cheshire Cat phenomenon" that states that the confinement radius encoded in the bag boundary condition is not a physical quantity. That is to say, physics should not depend on the bag or "confinement" size. This is the "Cheshire Cat Principle" (CCP for short). It is possible that there is an *exact* CCP in (1+1) dimensions with a minimum number of degrees of freedom. But it is difficult, if not impossible, to establish such an exact CCP in (3+1) dimensions where the relevant degrees of freedom are vastly greater. By incorporating a sufficiently large number of massive degrees of freedom in a manner discussed in what follows (*e.g.*, an infinite tower of hidden local gauge fields), QCD could be more accurately approximated in low-energy domains. Thus in the regime where asymptotic freedom does not prevail, one should be able to shrink the bag size to near zero. This is the limit where baryons appear as skyrmions. Depending upon the kinematic conditions, for instance, the nucleon can be described as a big MIT-type bag with three confined quarks coupled only to pionic fluctuations as in the "cloudy bag model" or three quarks bound in a potential generated by the pion hedgehog field as in the "chiral quark soliton model" or as a soliton with fluctuating meson fields with the confinement size shrunk to zero as in the skyrmion model. The "chiral bag" picture interpolates between the two extremes without substantially changing physics. We claim that these are all different facets of QCD, some of which have been treated in [Nowak, Rho and Zahed 1996].

Hidden local symmetry and holographic duality

Another important facet of QCD in the nonperturbative sector is the emergence of symmetries, local or global, that are not directly visible in the fundamental the-

ory, QCD. Particularly relevant for us is the emergence of hidden local symmetry, possibly with an infinite tower of (flavor) gauge degrees of freedom. Confinement makes "colors" invisible, that is, no colored hadrons are around in isolation. We see a variety of global symmetries, *e.g.*, chiral symmetry and flavor symmetry *etc.* but no manifest gauge symmetries. However it is known [Weinberg 1997b] that out of effective field theories with no evident gauge and/or global symmetries, one can *always* generate a theory with *any broken gauge symmetry* or conversely, starting from a gauge theory whose gauge symmetry is broken spontaneously, one can *always* have a local effective field theory that shows no vestige of the starting gauge invariance. This in fact sets the stage for generating hidden local symmetry theory.

The emergence of such gauge symmetry is a generic phenomenon that will figure importantly throughout the volume. One of the most celebrated and perhaps the most controversial cases is the spin-charge separation of the electron in high-T superconductivity. Suppose one starts with electrons only, with short-ranged interactions. Now there can be phases where the electron separates into a new fermion f and a boson b as

$$e(x) = b(x) f^\dagger(x). \tag{2.1}$$

Under the local transformations,

$$\begin{aligned} b(x) &\to e^{ih(x)} b(x), \\ f(x) &\to e^{ih(x)} f(x), \end{aligned} \tag{2.2}$$

the electron field remains unchanged. Clearly the new fields are "redundant." One can exploit this redundancy to make the symmetry a gauge symmetry by introducing gauge fields which are not *visible* in the original theory with the electrons. This symmetry is an emerging one.

For us, the relevant theory is the effective field theory of pions for low energy pion interactions. This effective field theory is governed by chiral symmetry and involves the Goldstone pion field $U = e^{i\pi/F_\pi} \in SU(N_f)_L \times SU(N_f)_R / SU(N_f)_{L+R}$. Now this field can be written in terms of "redundant" left and right fields $\xi_{L,R}$ as

$$U = \xi_L^\dagger \xi_R. \tag{2.3}$$

At very low energy, the dynamics is given by the Goldstone bosons,[1] *i.e.* pions, with a Lagrangian written with the least number of derivatives. Such a term is dictated by low-energy theorems, *i.e.* current algebras. Furthermore in the limit that the number of colors N_c becomes large, that's the Lagrangian to describe the baryons in terms of skyrmions. Thus low-energy dynamics within a given kinematic regime is entirely governed by the chiral field (2.3). Now just like the electron field (2.1), the

[1] In reality with non-zero quark masses, these should be called pseudo-Goldstones but we are not going to make the distinction. Unless stated otherwise, we will be considering the chiral limit but it should not be forgotten that quark masses do play important roles in certain quantities.

chiral field U remains unchanged by the local transformation $h(x) \in SU(N_f)_{L+R}$

$$\xi_{L,R} \to h(x)\xi_{L,R}. \tag{2.4}$$

The original chiral theory in terms of U field can be made a gauge theory by introducing "hidden" gauge fields $A^{\mu}_{L,R}$. This gives rise to hidden local symmetry theory of Harada and Yamawaki [Harada and Yamawaki 2003] which makes up one of the principal parts of what is discussed in this volume. Now as mentioned above, symmetry arguments alone can lead to an arbitrary theory when one goes up in scale. When constructed bottom-up as an emergence phenomenon, the theory needs to be "ultraviolet (UV)-completed" to the fundamental theory in order to make the theory truly predictive. In our case, it is QCD to which the effective theory should be "completed" and Harada-Yamawaki theory does this, effectively, by matching the current-current correlators in the effective theory to those in QCD.

To go even further, one can put this gauge theory on a lattice and "deconstruct" the fifth dimension, arriving at a Yang-Mills gauge theory in five dimensions. This corresponds to a local gauge theory with an infinite tower of vector fields coupled to pions. This is an emergent ("bottom-up") gauge symmetry involving an infinite tower of vector mesons. The gauge symmetry can also be obtained "top-down." In this connection, the modern development brings a surprise, *i.e. holographic duality*. A holographic dual QCD based on the notion of holographic duality of AdS/CFT shows that at low-energy, hadron interactions can be encapsulated in 5-D Yang-Mills Lagrangian, which when written in 4 dimensions, gives rise to a hidden local symmetry theory involving pions and an infinite tower of vector mesons in the bulk with a correct chiral symmetry structure. When all the members of the tower other than the lowest and the pion are integrated out, the resulting theory could be identified with the Harada-Yamawaki hidden local symmetry theory with the "bare" parameters of the HLS Lagrangian given by the bulk sector of string theory. The "UV completion" is here rendered automatically by the higher-dimension bulk theory. It is possible that the higher-dimension bulk theory in weak-coupling limit at which the solution is available does not fully correspond to QCD proper. Remarkably, baryons in this theory must come out as skyrmions since there are no explicit fermionic degrees of freedom. In fact, the 4-D skyrmion in an infinite tower of vector mesons is just the instanton in the Euclidean 4-D of the 5-D Yang-Mills Lagrangian. This then elevates the skyrmion to a higher level of sophistication.

Quark-hadron continuity

The above discussion hints at a web of continuity between QCD degrees of freedom and hadronic degrees of freedom in free space. Now going to medium, there are another web of dualities that emerge from the dynamics. Lattice gauge calculations are conclusively showing that as the temperature goes above a certain critical temper-

ature $T_c \sim 190$ MeV while keeping the chemical potential μ equal to zero, hadronic matter of realistic flavor content – that is, two light flavors (u and d) and one medium heavy flavor (s) – makes a smooth cross-over transition [Aoki *et al.* 2006; Wilczek 2006]. Experimental data indicate that the matter above T_c is in a strongly coupled state with a very low shear viscosity, perhaps a near perfect liquid, totally unlike the quark-gluon plasma that had been predicted – and widely advertized – previously. The structure of that state is not understood yet, but it appears to be a state which could be accessed more directly by holographic dual QCD than QCD proper. There appears to be a continuity from below T_c to above T_c without phase change or change that involves singularity.

The matter seems to be a lot subtler at high density. At asymptotic density where perturbative treatment is applicable, QCD makes an unambiguous prediction that the matter will undergo a "transition" to a color superconducting state that "locks" the color and flavor. This state is referred to as "color-flavor locked" (CFL) phase. As we shall discuss in a chapter below, there is a possibility that the CFL phase persists all the way down to the density regime at which normal matter joins quark matter. If this happens, then there is *no phase transition* between the normal hadronic matter and the color superconducting matter since both are in a phase with the chiral symmetry spontaneously broken, albeit with two different order parameters. There will then be one-to-one correspondence between the hadrons below the critical density n_c and the hadrons above. This phenomenon is referred to as "hadron-quark continuity" or equivalently "quark-hadron continuity."

There is an intriguing way of understanding this "quark-hadron continuity" in terms of the skyrmion description of baryons in both the hadron and CFL phases. As mentioned above, baryons in the hadronic phase are skyrmions that emerge from the meson theory with an infinite tower of vector mesons. It turns out that baryons in the color-flavor locked superconducting phase can also be viewed as skyrmions – called "superqualitons" – in a local symmetric form present in the CFL phase. It is then reasonable to interpret the quark-hadron continuity as a skyrmion-superqualiton continuity. When baryonic matter is compressed to high density, the matter can undergo a transition to superqualiton matter without change of symmetries, with chiral symmetry spontaneously broken in both sectors. What phenomena take place at the boundary is completely unknown at present. But one can imagine various theoretically interesting phenomena that can intervene at the boundary. As an example, one of the possibilities discussed in the volume is a skyrmion-half-skyrmion transition which resembles the deconfined quantum critical phenomenon discussed in condensed matter physics.

Weinberg "theorem" on effective field theory

In going from QCD to nuclei to nuclear matter to hot and/or dense matter, one encounters another sort of "continuity." Although there is a direct attempt to tackle

many-body problems in the strong interactions, say, by lattice simulations, at the present stage of development, multi-nucleon systems, not to mention nuclear matter and denser matter, are out of reach of the first principle technique. The only tool available for this is the effective field theory approach. In constructing EFT strategy, Weinberg's "folk theorem" plays a particularly important role. We quote the "theorem" directly from [Weinberg 1997a]:"When you use quantum field theory to study low-energy phenomena, then according to the folk theorem you're not really making any assumption that could be wrong, unless of course Lorentz invariance or quantum mechanics or cluster decomposition is wrong, provided you don't say specifically what the Lagrangian is. As long as you let it be the most general possible Lagrangian consistent with the symmetries of the theory, you're simply writing down the most general theory you could possibly write down. ... Effective field theory was first used in this way to calculate processes involving soft π mesons, that is, π mesons with energy less than about $2\pi F_\pi \approx 1200$ MeV. The use of effective quantum field theories has been extended more recently to nuclear physics where although nucleons are not soft they never get far from their mass shell, and for that reason can be also treated by similar methods as the soft pions. Nuclear physicists have adopted this point of view, and I gather that they are happy about using this new language because it allows one to show in a fairly convincing way that what they've been doing all along (using two-body potentials only, including one-pion exchange and a hard core) is the correct first step in a consistent approximation scheme.... "

We should stress that one of the main themes of this volume is indeed that what nuclear physicists have been doing, albeit in a language different from that of QCD proper, constitutes a correct first step or doorway to unraveling the physics under extreme conditions treated in this volume. To go beyond what the standard nuclear physics approach has achieved thus far is one of the ultimate goals of this volume for which we will use the "folk theorem" as a guiding principle. There is no rigorous proof for this theorem but as Weinberg states, it is difficult to imagine that it can go wrong. We must however state to begin with that we do not have at our disposal a theory which fully meets the conditions required to satisfy the theorem but each improvement we make in writing down the effective Lagrangian will constitute a step toward "verifying" this theorem.

This page intentionally left blank

Chapter 3

Cheshire Cat Phenomenon

As a first case of continuity in many-body hadronic physics, we consider the phenomenon known as *Cheshire Cat* and its associated *Cheshire-Cat Principle* (CCP). This matter is treated in detail in CND-I. What we will do in this volume is to rephrase the essential features of the phenomenon in terms of a local gauge symmetry and give a non-trivial case where the CCP can be interpreted to be in action, *i.e.* what is known as the "proton spin problem" viewed from the chiral bag point of view. How this view is related to other models purporting to solve the problem is not clear and will not be discussed.

3.1 Motivation

It has been a long-standing puzzle why the quark-gluon degrees of freedom of QCD do not show up explicitly somewhere in nuclear processes. Of course, the colored quarks and gluons are confined and hence cannot be taken out of the "jail" in which they are confined and be observed separately although we do not know exactly how that happens. It is still quite puzzling why their imprints do not show up in low-energy phenomena taking place in nuclear many-body systems. This is particularly disturbing since one would think that given the highly quantitative understanding that we have of nuclear processes, quark presence should somehow manifest itself – if not directly – in subtle discrepancies between what one measures and what one calculates in terms solely of hadronic variables. So far no such discrepancy has shown up.

It is instructive to compare the situation with another long-standing problem of nuclear physics which, however, is now well-understood, namely, meson-exchange currents. Nuclear force generated by the exchanges of mesons π, ρ, ω *etc.* implies that when a nucleus is probed by an external field, say, the electroweak fields, in addition to the usual single-particle currents, there are exchange currents of n-body form for $n \geq 2$ mediated by the exchange of those mesons that generate nuclear forces. Some of the exchange currents can be interpreted as reflecting that the external field responds to nucleons in occupied states, that is, through Pauli

exclusion principle. But the exclusion principle correction is not the only or even dominant story. In fact, as we will show in the next chapter, one can make a systematic chiral counting of effective theory of chiral symmetry and finds that many-body currents are a natural consequence of imposing the symmetry of QCD. This was discussed systematically in [Chemtob and Rho 1971] in terms of Feynman graphs for S-matrix and was put in a chiral perturbation theory framework two decades later [Rho 1991]. A prediction with an unprecedent high accuracy for the presence of such an exchange current was made for the process $n + p \to d + \gamma$ at thermal energy [Park, Min and Rho 1995; Park, Min and Rho 1996], obtaining a close agreement with the experimental data supporting the earlier calculation of Riska and Brown [Riska and Brown 1973]. This provided an unambiguous evidence that meson-exchange currents are *real* in Nature. We now realize that this is no big deal in the present understanding of nuclear dynamics. Here the mesons that mediate both the nuclear force and the exchange currents are particles that are observed on-shell, so there is nothing so unusual about it although it required a precise understanding of one-body processes and a systematic chiral counting before multi-body processes could be sorted out.

The situation with quarks and gluons is a totally different matter. The quarks and gluons can appear virtually but cannot be seen on-shell. Color gauge invariance forbids it. So there is the problem as to whether their presence can *in principle* be manifested in an unambiguous way in physical processes and can be sorted out from standard macroscopic processes.

We will see that the underlying principle that makes such a distinction impossible at low energy is the *Cheshire Cat Principle (CCP)*. We will develop that notion in this chapter and see that it leads to a variety of "dualities" in modeling of low-energy QCD. What is principally at work is the chiral symmetry in the broken phase. As for confinement, there are two classes of models: One with explicit confinement and the other without explicit confinement but making an implicit assumption of confinement in the sense that only color singlet states figure in the description.

3.2 Chiral Bag Picture

Given the absence of a "derivation" of an effective theory from QCD applicable in the regime that we are concerned with, the best we can do at present is to "construct" the simplest possible workable model that implements confinement[1] and chiral symmetry in the Nambu-Goldstone mode consistent with large N_c. Having no effective field theory (EFT) of confinement that can be used as a workable framework for our purpose, we shall implement it by the MIT bag description [Johnson 1975]. Many people have attempted to "derive" from first principles of QCD the bag structure as a confinement mechanism, but there is none yet which

[1] By confinement we will always mean the confinement of quarks and gluons.

is fully satisfactory and implementable in practical calculations. The simplest way to proceed is to impose a rigid confining bag boundary, but there is nothing other than convenience to use a rigid boundary condition. As we will describe precisely below, one can equally work with a "soft" or "fuzzy" or "cloudy" boundary – and there have been numerous discussions on the variation. Details differ but one can get a fairly accurate idea by taking the simplest, and this is what we will do here with a sharp boundary. We will later mention what happens when we relax the sharp boundary.

We separate the space into inside the bag V (taken to be spherical but could be of any shape), the outside $\bar{V}$ and the surface ∂V as depicted in Fig. 3.1. The total action for what may be called "Cheshire bag model" (CBM in short) is given by the action, say, for $SU(N_f)_L \times SU(N_f)_R$ (for $N_f = 3$) [2]

$$\begin{aligned} S &= S_V + S_{\bar{V}} + S_{\partial V}, \qquad (3.1)\\ S_V &= \int_V d^4x \left(\bar{\psi} i \not{D} \psi - \frac{1}{2g_c^2} \mathrm{tr}\ G_{\mu\nu} G^{\mu\nu} \right) + \cdots \\ S_{\bar{V}} &= \frac{f^2}{4} \int_{\bar{V}} d^4x \left(\mathrm{Tr}\ \partial_\mu U^\dagger \partial^\mu U + \frac{1}{4N_f} m_{\eta'}^2 (\ln U - \ln U^\dagger)^2 \right) + \cdots + S_{WZ}, \\ S_{\partial V} &= \frac{1}{2} \int_{\partial V} d\Sigma^\mu \left\{ (n_\mu \bar{\psi} U^{\gamma_5} \psi) + i \frac{g_c^2}{16\pi^2} K_{5\mu} (\mathrm{Tr}\ \ln U^\dagger - \mathrm{Tr}\ \ln U) \right\} . \end{aligned}$$

Here ψ is the quark field $\psi^T = (uds)$, G_μ the octet gluon field, $G_{\mu\nu}$ the gluon field tensor, g the "color" gauge coupling [3] and K_5^μ is the (properly regularized) "Chern-Simons current"

$$K_5^\mu = \epsilon^{\mu\nu\alpha\beta} (G_\nu^a G_{\alpha\beta}^a - \frac{2}{3} g_c f^{abc} G_\nu^a G_\alpha^b G_\beta^c), \qquad (3.2)$$

the chiral field U is

$$U = e^{i\eta'/f_0} e^{2i\pi/f} \qquad (3.3)$$

and U^{γ_5} is

$$U^{\gamma_5} = e^{i\eta'\gamma_5/f_0} e^{2i\pi\gamma_5/f}. \qquad (3.4)$$

We have written $d\Sigma^\mu$ for an area element with n^μ the normal vector, *i.e.* $n^2 = -1$ and picked outward-normal, and used loosely the decay constants f_0 and f which will be specified more precisely later. The action (3.1) contains full hadron dynamics for baryons at low-energy ($E \ll \Lambda_\chi$ where Λ_χ is the chiral symmetry scale) including anomaly structure, the derivation of which is too involved to go into in this volume and in fact is not needed. The details with precise definitions can be found in

[2] The color gauge coupling constant is denoted g_c, to be distinguished from the hidden gauge coupling constant g used in this volume. Also unless otherwise stated, we will be discussing the three-flavor case in what follows.

[3] Note that "tr" stands for color trace and "Tr" for flavor trace. We use the normalization for the group generators $\mathrm{Tr}(t^a t^b) = \frac{1}{2}\delta^{ab}$ and likewise for the color.

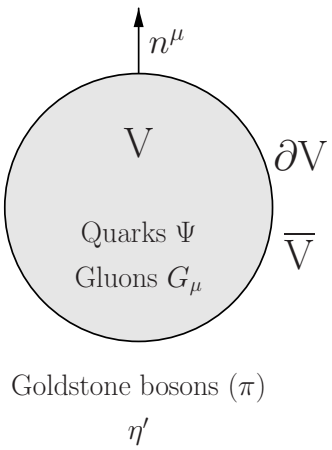

Fig. 3.1 A spherical chiral bag for "deriving" a four-dimensional Cheshire-Cat bag model. ψ represents the doublet quark field of u and d quarks for $SU(2)$ flavor or the triplet of u, d and s for $SU(3)$ flavor and π the triplet π^+, π^-, π^0 for $SU(2)$ and the octet pseudoscalars π, K, $\bar{K}$ and η for $SU(3)$. The axial singlet meson η' figures in the axial anomaly.

CND-I [Nowak, Rho and Zahed 1996]. The physical meaning of the action (3.1) – which looks complicated – will be explained better in a following subsection where we will consider the exact situation in (1+1) dimensions. One should of course keep in mind that physics in 4D is not necessarily encapsulated in 2D, so there are many caveats. Let us simply describe here what each term represents, with focus on the terms that we will consider later for an illustrative example, the so-called "proton spin."

(1) The action S_V is the QCD action in quark-gluon variables with the ellipses standing for the quark mass term, assumed to hold within the bag volume. The quarks ψ and gluons G_μ are confined in the volume V.
(2) The action in the complementary volume $\bar{V}$ consists of hadron fields, here, the octet pseudoscalars π, the first term being the current algebra term, the second term the η' mass term representing the broken $U(1)_A$ symmetry, *i.e.* $U(1)_A$ anomaly, S_{WZ} the five-dimensional Wess-Zumino term present for the number of flavors $N_f \geq 3$, and the ellipses stand for higher derivatives, pseudoscalar mass terms and terms involving vector and other massive fields.
(3) The surface action $S_{\partial V}$ is a bit subtler, so requires more detailed explanation. The first term is the usual MIT bag boundary term suitably made chirally symmetric with the π field. It confines, classically, outside of the bag not only the octet pion field but also the singlet field η' field associated with $U(1)_A$. The time variation of this field on the surface generates an anomaly which makes the color charge carried by the quarks and gluons leak outside. This leakage is

caused by a quantum anomaly effect. Now the raison d'être of the second term is to prevent this leakage since the leakage produces the violation of the color gauge invariance.

The full model (3.1) has not been sufficiently worked out, so one cannot say with certainty whether the theory describes nature correctly and whether it is predictive enough to be tested quantitatively experimentally. It has, however, the conceptual appeal in that it accommodates various aspects of desired baryonic properties. One such case, *i.e.* the proton spin problem, is discussed in detail below.

3.2.1 *Cheshire Cat as a gauge artifact*

The notion of Cheshire Cat phenomenon (CCPh) can be best illustrated in (1+1) dimensions. The implication of CCPh is that the "bag" implementing confinement in the sense of the bag model is an artifact that has no strict physical meaning. An elegant way to view this is to interpret the "bag" as a gauge artifact and treat it as a gauge degree of freedom. Thus a description in terms of a particular "bag radius" that was thought to represent the size of confinement region in the MIT bag model can be interpreted as a particular gauge fixing. In this view, confinement size has no physical meaning. In principle, when formulated completely, physics should be strictly equivalent for *all* gauge choices ("bag radii") one makes. This is a drastically different way – even in this 21st century – of looking at the classical confinement embodied by the MIT bag. We discuss this elegant and ingenious idea following Damgaard, Nielsen and Sollacher [Damgaard, Nielsen and Sollacher 1992a; Damgaard, Nielsen and Sollacher 1992b]. The idea can be best described in (1+1) dimensions since there the argument is exact, and in path-integral formulation. There is nothing to suggest that the same cannot hold in (3+1) dimensions.

Consider the case of massless fermions coupled to external vector $\mathcal{V}_\mu$ and axial-vector $\mathcal{A}_\mu$ fields, the generating functional [4] of which (in Minkowski space) is [5]

$$Z[\mathcal{V},\mathcal{A}] = \int [d\psi][d\bar{\psi}] e^{iS}, \tag{3.5}$$

$$S = \int d^2x \bar{\psi}\gamma^\mu \left(i\partial_\mu + \mathcal{V}_\mu + \mathcal{A}_\mu\gamma_5\right)\psi.$$

One can get from this functional the massless Thirring model if one adds a term $\sim \mathcal{V}^\mu\mathcal{V}_\mu$ and integrates over the vector field. One can get the massive Thirring model if one adds scalar and pseudoscalar sources in addition. In this sense, the model is quite general. Now do the field redefinition while *enlarging the space* by

[4] We remind the readers that all physical observables can in principle be computed once the generating functional is obtained. So the statements made below are fully quantum mechanical.

[5] Our convention is as follows. The metric is $g_{\mu\nu} = \mathrm{diag}(1,-1)$ with Lorentz indices $\mu,\nu = 0,1$ and the γ matrices are in Weyl representation, $\gamma_0 = \gamma^0 = \sigma_1$, $\gamma_1 = -\gamma^1 = -i\sigma_2$, $\gamma_5 = \gamma^5 = \sigma_3$ with the usual Pauli matrices σ_i.

introducing a fictitious field θ,

$$\psi(x) = e^{i\theta(x)\gamma_5}\chi(x)\ , \quad \bar{\psi}(x) = \bar{\chi}(x)e^{i\theta(x)\gamma_5}. \tag{3.6}$$

Since this is just a change of symbols, the generating functional is unmodified:

$$Z[\mathcal{V},\mathcal{A}] = \int [d\chi][d\bar{\chi}]\, J\, e^{iS'}, \tag{3.7}$$

$$S' = \int d^2x \bar{\chi}\gamma^\mu \left(i\partial_\mu + \mathcal{V}_\mu + \mathcal{A}_\mu\gamma_5 - \partial_\mu\theta(x)\gamma_5\right)\chi$$

where J is the Jacobian of the transformation which can be readily calculated:

$$J = \exp\left\{ i\int d^2x \left(\frac{1}{2\pi}\partial_\mu\theta\partial^\mu\theta + \frac{1}{\pi}\epsilon^{\mu\nu}\mathcal{V}_\mu\partial_\nu\theta - \frac{1}{\pi}\mathcal{A}_\mu\partial^\mu\theta \right) \right\}. \tag{3.8}$$

This nontrivial Jacobian arises due to the fact that the measure is not invariant under local chiral transformation (3.6). The important thing to note is that since *by definition* (3.5) and (3.7) are the same, the physics should not depend upon $\theta(x)$. The latter is redundant. Therefore – modulo an infinite constant which requires gauge fixing as described below, we may integrate over the field $\theta(x)$ in (3.7) without changing physics. Doing the integral in the path integral amounts to elevating the redundant $\theta(x)$ to a dynamical variable. Now if we rewrite (3.7) in terms of $\mathcal{L}'$ defined as

$$Z[\mathcal{V},\mathcal{A}] = \int [d\chi][d\bar{\chi}] e^{i\int d^2x\mathcal{L}'}, \tag{3.9}$$

$$\begin{aligned}\mathcal{L}' = {} & \bar{\chi}\gamma^\mu \left(i\partial_\mu + \mathcal{V}_\mu + \mathcal{A}_\mu\gamma_5 - \partial_\mu\theta\gamma_5\right)\chi \\ & + \frac{1}{2\pi}\partial_\mu\theta\partial^\mu\theta + \frac{1}{\pi}\epsilon^{\mu\nu}\mathcal{V}_\mu\partial_\nu - \frac{1}{\pi}\mathcal{A}_\mu\partial^\mu\theta,\end{aligned} \tag{3.10}$$

we uncover a (hidden) local gauge symmetry, namely, that (3.10) is invariant under the transformation

$$\chi(x) \to e^{i\alpha(x)\gamma_5}\chi(x)\,, \quad \bar{\chi}(x) \to \bar{\chi}(x)e^{i\alpha(x)\gamma_5}, \quad \theta(x) \to \theta(x) - \alpha(x) \tag{3.11}$$

provided of course the Jacobian is again taken into account. Thus by introducing a new dynamical field θ, we have gained a gauge symmetry at the expense of enlarging the space. This is a notion that is exploited later and throughout this volume in (emergent) hidden gauge symmetries that will play the pivotal role in describing hadron phenomena under extreme conditions.

Now in order to quantize the theory, we have to fix the gauge. To do this we pick a θ by a general gauge condition

$$\Phi(\theta) = 0. \tag{3.12}$$

Then following the standard text-book (Faddeev-Popov) method, we write

$$Z[\mathcal{V},\mathcal{A}] = \int [d\chi][d\bar{\chi}][d\theta]\delta(\Phi[\theta])|\det(\frac{\delta\Phi}{\delta\theta})|e^{i\int d^2x\mathcal{L}'}. \tag{3.13}$$

Note that if we choose $\Phi = \theta$, we recover the original generating functional (3.5) which describes everything in terms of fermions. We would like to choose the gauge condition relevant to the physics of the chiral bag we are dealing with. There the axial current plays an essential role. A suitable choice is

$$\Phi[\theta, \chi, \bar{\chi}] = \Delta \int_{x_0}^{x} d\eta^{\nu} \bar{\chi}(\eta)\gamma_{\nu}\gamma_5\chi(\eta) + (1-\Delta)\frac{1}{\pi}\theta(x) = 0 \tag{3.14}$$

which corresponds to partitioning the total axial current into the fraction Δ of the bosonic (pionic) piece and the fraction $(1-\Delta)$ of the fermionic (quark) piece [Damgaard, Nielsen and Sollacher 1992a]. This may be called a "Cheshire Cat gauge." We will not dwell on the proof which is rather technical but just mention that the functional integral does not depend upon the path of this line integral. The Faddeev-Popov determinant corresponding to (3.14) comes out to be [6]

$$\det\left(\frac{\delta\Phi}{\delta\alpha}\right) = \det\left(-\frac{1}{\pi}\right). \tag{3.17}$$

The Cheshire Cat structure is manifested in the choice of Δ. If one takes $\Delta = 0$, we have the pure fermion theory as one can see trivially. If one takes instead $\Delta = 1$, one obtains after some calculation (see paper [Damgaard, Nielsen and Sollacher 1994] for details)

$$Z[\mathcal{V}, \mathcal{A}] = \text{const.} \times \int [d\theta] e^{i\int d^2x \mathcal{L}^{\theta}} \tag{3.18}$$

with

$$\mathcal{L}^{\theta} = \frac{1}{2}\partial_{\mu}\theta\partial^{\mu}\theta - \frac{1}{\sqrt{\pi}}\epsilon^{\mu\nu}\mathcal{V}_{\mu}\partial_{\nu}\theta + \frac{1}{\sqrt{\pi}}\mathcal{A}_{\mu}\partial^{\mu}\theta. \tag{3.19}$$

This is just the bosonized form of the fermion theory coupled to the vector fields. The Cheshire Cat statement is that the theory is identical for *any* arbitrary value of Δ.

[6] To see this write the constraint

$$\begin{aligned}\delta(\Phi[\theta, \bar{\chi}, \chi]) &= \int [db] e^{i\int d^2x\, b\,\Phi} \\ &= \int [db] e^{i\int d^2x\ \mathcal{L}_{g.f.}}\end{aligned} \tag{3.15}$$

defining the gauge-fixing Lagrangian $\mathcal{L}_{g.f.}$. Now do the (infinitesimal) gauge transformation (3.11) on (3.15). We have

$$\delta_{\alpha}\mathcal{L}_{g.f.} = -\frac{1}{\pi}\{(1-\Delta)+\Delta\}\alpha \tag{3.16}$$

where the first term in curly bracket comes from the shift in θ and the second term from the Fujikawa measure. Now the right-hand side of this equation is just $b\delta_{\alpha}\Phi$, from which follows equation (3.17).

One can go further and take Δ to be a local function. In this case, one can continuously change representation from one region of space-time to another, choosing different gauge fixing conditions in different space-time regions. This leads to a smooth Cheshire bag. The standard chiral bag model [Brown and Rho 1988] corresponds to the gauge choice

$$\Delta(x) = \Theta(\mathbf{x} - \mathbf{z}) \tag{3.20}$$

with $\mathbf{z} = \hat{r}R$. The usual bag boundary conditions employed in phenomenological studies arise after certain suitable averaging over part of the space and, hence, are a specific realization of the Cheshire Cat scheme. Possible discontinuities or anomalies caused by sharp boundary conditions used in actual calculations should not be considered to be defects of the effective model. An interesting conclusion of this point of view is that one can in principle construct an *exact* Cheshire Cat model without knowing the exact bosonized version of the theory considered.

Since CCP in (3+1) dimensions is in practice not exact, using the strategy of hidden gauge symmetry (here $U(1)$ associated with $\theta(x)$) provides certain flexibility at the expense of non-uniqueness that goes with the specific gauge choice. Depending upon what processes one studies, a certain gauge choice might be more efficient than others. Thus for long-wavelength processes, a gauge closer to $\Delta = 1$ could be more efficient in capturing the strong interaction physics whereas processes sampling short distances would do better with gauge choices closer to $\Delta = 0$. [7]

3.2.2 *Baryon charge and the exact Cheshire Cat phenomenon*

As an illustration of how CCP works in the "chiral bag gauge" (3.20), consider how the baryon charge "leaks" out of the bag into the meson sector in two dimensions where the CCP can be formulated exactly. This gives us a general idea how the principle works. Later we will make a leap to reality in four dimensions and mention how much one can take over from the (1+1) case. We shall suggest that the result is generic and should not sensitively depend upon details of the models. Thus other models of similar structure containing the same symmetries – *e.g.*, chiral quark soliton model – could be equally used. We will leave the construction of CCP or approximate CCP to the aficionados of their own favorite models.

We write the action in (1+1) dimensions simplifying the Lagrangian (3.1) and keeping only the relevant terms for our purpose

$$S = S_V + S_{\tilde{V}} + S_{\partial V} \tag{3.21}$$

[7] We will note later that working with hidden gauge invariance where vector mesons figure as hidden gauge fields is more powerful than gauge-fixed theories in describing hot/dense matter in the vicinity of chiral restoration.

where

$$S_V = \int_V d^2x \bar{\psi} i\gamma^\mu \partial_\mu \psi + \cdots , \tag{3.22}$$

$$S_{\tilde{V}} = \int_{\tilde{V}} d^2x \frac{1}{2}(\partial_\mu \phi)^2 + \cdots \tag{3.23}$$

and $S_{\partial V}$ is the boundary term which plays a crucial role. Here the ellipses stand as in (3.1) for other terms such as interactions, fermion masses *etc.* consistent with the assumed symmetries. Unlike in the (3+1) dimensional case, one can write down the boundary term in a unique way subject to chiral symmetry, the discrete symmetries $\mathcal{P}$, $\mathcal{C}$ and $\mathcal{T}$ and the constraint that there be no decoupled boundary conditions, that is to say, that the boundary conditions involve only ψ and ϕ fields. It has the simple form

$$S_{\partial V} = \int_{\partial V} d\Sigma^\mu \left\{ \frac{1}{2} n_\mu \bar{\psi} e^{i\gamma_5 \phi/f} \psi \right\} \tag{3.24}$$

with the ϕ "decay constant" $f = 1/\sqrt{4\pi}$.[8]

At the classical level, the action (3.21) gives rise to the bag confinement, namely that, inside the bag, the fermion (which we shall call "quark" from now on although we are not in the real world) obeys (dropping the mass terms)

$$i\gamma^\mu \partial_\mu \psi = 0 \tag{3.25}$$

while the boson (which we will call "pion") satisfies

$$\partial^2 \phi = 0 \tag{3.26}$$

subject to the boundary conditions on ∂V

$$in^\mu \gamma_\mu \psi = -e^{i\gamma_5 \phi/f} \psi, \tag{3.27}$$

$$n^\mu \partial_\mu \phi = f^{-1} \bar{\psi} (\frac{1}{2} n^\mu \gamma_\mu \gamma_5) \psi. \tag{3.28}$$

Equation (3.27) is the familiar "MIT confinement condition" with chiral symmetry implemented, which is simply a statement of the classical conservation of the vector current $\partial_\mu j^\mu = 0$ or $\bar{\psi} \frac{1}{2} n^\mu \gamma_\mu \psi = 0$ at the surface, while Eq. (3.28) is just the statement of the conserved axial vector current $\partial_\mu j_5^\mu = 0$ (ignoring the possible explicit masses of the quark and the pion at the surface).

The crucial point of our discussion here is that these classical observations are invalidated by quantum mechanical effects. In particular, whereas the axial current continues to be conserved, the vector current fails to do so due to "quantum anomaly." In field theory without boundaries, there is no anomaly in the vector current. With the bag, however, *the vector anomaly occurs due to the "artificial" boundary we elected which acts as an induced local axial field.*

[8] We should stress that in contrast, we cannot establish the same unique relation in (3+1) dimensions: What is given in (3.1) is not unique.

There are several ways of seeing that something is amiss in the picture with the classical conservation law, with slightly different interpretations. The simplest is the "infinite hotel scenario" [Nadkarni, Nielsen and Zahed 1985; Nielsen and Wirzba 1987]. For definiteness, let us imagine that the quark is "confined" in the space $-\infty \leq r \leq R$ with a boundary at $r = R$. Now the vector current $j_\mu = \frac{1}{2}\bar{\psi}\gamma_\mu\psi$ is conserved inside the "bag"

$$\partial^\mu j_\mu = 0, \qquad r < R. \tag{3.29}$$

If one integrates this from $-\infty$ to R in r, one gets the time-rate change of the fermion (*i.e.* quark) charge

$$\dot{Q} \equiv \frac{d}{dt}Q = 2\int_{-\infty}^{R} dr\partial_0 j_0 = 2\int_{-\infty}^{R} dr\partial_1 j_1 = 2j_1(R) \tag{3.30}$$

which is just

$$\bar{\psi}n^\mu\gamma_\mu\psi, \qquad r = R. \tag{3.31}$$

This vanishes classically as we mentioned above. But quantum mechanically, this is not correct. The reason is that it is ill-defined locally in time. In other words, $\psi^\dagger(t)\psi(t+\epsilon)$ goes like ϵ^{-1} and so is singular as $\epsilon \to 0$. To circumvent this difficulty, we regulate the bilinear product by point-splitting in time

$$j_1(t) = \bar{\psi}(t)\frac{1}{2}\gamma_1\psi(t+\epsilon), \qquad \epsilon \to 0. \tag{3.32}$$

Now using the boundary condition

$$\begin{aligned} i\gamma_1\psi(t+\epsilon) &= e^{i\gamma_5\phi(t+\epsilon)/f}\psi(t+\epsilon) \\ &\approx e^{i\gamma_5\phi(t)/f}[1 + i\epsilon\gamma_5\dot{\phi}(t)/f]e^{\frac{1}{2f^2}[\phi(t),\phi(t+\epsilon)]}\psi(t+\epsilon), \quad r = R \end{aligned} \tag{3.33}$$

and the commutation relation

$$[\phi(t), \phi(t+\epsilon)] = i\ \mathrm{sign}\epsilon = \pm i, \tag{3.34}$$

we obtain

$$j_1(t) = -\frac{i}{4f}\epsilon\dot{\phi}(t)\psi^\dagger(t)\psi(t+\epsilon) = \frac{1}{4\pi f}\dot{\phi}(t) + O(\epsilon), \qquad r = R \tag{3.35}$$

where we have used $\psi^\dagger(t)\psi(t+\epsilon) = \frac{i}{\pi\epsilon} + [\text{regular}]$, the boundary condition (3.27) and $f^2 = (4\pi)^{-1}$. Thus quarks can flow out or in if the pion field varies in time. But they cannot simply disappear into nowhere if we impose that the fermion (quark) number be conserved. To see what happens, rewrite (3.35) using the surface tangent

$$t^\mu = \epsilon^{\mu\nu}n_\nu. \tag{3.36}$$

We have

$$t \cdot \partial\phi = \frac{1}{2f}\bar{\psi} n \cdot \gamma \psi = \frac{1}{2f}\bar{\psi} t \cdot \gamma\gamma_5 \psi, \qquad r = R \tag{3.37}$$

where we have used the relation $\bar{\psi}\gamma_\mu\gamma_5\psi = \epsilon_{\mu\nu}\bar{\psi}\gamma^\nu\psi$ valid in two dimensions. Equation (3.37) together with (3.28) is nothing but the bosonization relation

$$\partial_\mu\phi = f^{-1}\bar{\psi}(\frac{1}{2}\gamma_\mu\gamma_5)\psi \tag{3.38}$$

at the point $r = R$ and time t. As is well known, this is a particular feature of (1+1) dimensional fields that makes one-to-one correspondence between fermions and bosons.

Equation (3.30) with (3.35) is the vector anomaly. What it says is that the vector charge, which in this case is equivalent to the fermion (quark) number inside the bag, is not conserved. Physically, what happens is that the amount of fermion number ΔQ corresponding to $\Delta t\dot{\phi}/\pi f$ is pushed into the Dirac sea at the bag boundary, and so is lost from inside and gets accumulated at the pion side of the bag wall. Since the fermion charge is to be conserved, this accumulated baryon charge must be carried by something residing in the meson sector, namely the pion field outside. For this to be realized, the pion field must support a soliton. In the present model, we find that one unit of fermion charge $Q = 1$ is partitioned as

$$\begin{aligned} Q = 1 &= Q_V + Q_{\tilde{V}}, \\ Q_{\tilde{V}} &= \theta/\pi, \\ Q_V &= 1 - \theta/\pi \end{aligned} \tag{3.39}$$

with

$$\theta = \phi(R)/f. \tag{3.40}$$

We thus learn that the quark charge is partitioned into the bag and outside of the bag, without however any dependence of the total on the size or location of the bag boundary. This partition is exact. In the (1+1)-dimensional case, one can calculate other physical quantities such as the energy, response functions and, more generally, partition functions and show that the physics does not depend upon the presence of the bag. We could work with quarks alone, or pions alone or any mixture of the two. If one works with the quarks alone, we have to do a proper quantum treatment to obtain something which one can obtain in mean field with the pions alone. In some situations, the hybrid description is more economical than the pure ones. *The complete independence of the physics on the bag – size or location– is the "Cheshire Cat Principle" (CCP) with the corresponding mechanism referred to as "Cheshire Cat Mechanism" (CCM).*

We went into a great deal of detailed reasoning in arriving at the exact CCP in 2D. This will be the only luxury we can entertain and savor in this volume

where calculations can be done explicitly and simply. In what follows dealing with the real world, we are unable to make such a clear-cut reasoning and calculations. In 4D, things are vastly more complicated. There is no known bosonization technique for four dimensions. So whatever is bosonized in 4D must be approximate. Furthermore, it cannot be captured in a simple form, involving most likely an infinite number of boson fields as we observe in holographic QCD (see Chapter 5). Nonetheless an approximate CCP does hold and works even quantitatively in certain processes. All topological quantities like the baryon charge do obey exact CCP. The baryon charge is partitioned in a similar way in (3+1) as in (1+1) dimensions as first shown for the magic chiral angle $\theta = \pi/2$ [Rho, Goldhaber and Brown 1983] and then later generalized for any angle [Goldstone and Jaffe 1983].[9] Nontopological quantities such as masses, static properties and also some nonstatic properties satisfy it approximately but rather well. They are described in various reviews [Nowak, Rho and Zahed 1996; Rho 1994; Hosaka and Toki 1996] and won't be repeated here – except for the celebrated case of the flavor singlet axial charge of the proton described below. A lot more work is needed to construct a reliable and efficient chiral Lagrangian taking into account the vector-meson degrees of freedom – that emerge, e.g., from holographic dual QCD – and carry out calculations that account for a multitude of subtle effects encoded in the Lagrangian to either confirm or falsify the model.

3.3 Cheshire Cat Principle in Nature

3.3.1 *Flavor singlet axial charge* $a^0 \equiv g_A^0$

We illustrate how an *approximate* CCP works in one of the most subtle phenomena in nucleon structure, namely, the as-yet unsettled case of the proton spin which is connected to the flavor singlet axial charge of the nucleon. This problem has been studied extensively not only in the context of hadronic models but also from the point of view of QCD proper. For a review and references, see Bass [Bass 2005]. The objective of the present discussion is not so much to give *the solution* to the problem per se – which does not yet exist – but to illustrate the subtlety involved in the way the CC *can* manifest in a problem of this sort. In fact, it suggests that there can be many ways to explain the spin problem, some more in line with QCD than others. It is possible that some are correct and related to each other. Whether or not one or more explanations of a particular class are confirmed by experiments in disfavor of others is not clear.

Following the work of [Lee, Min, Park, Rho and Vento 1999], we derive the flavor singlet axial current (FSAC for short) from the Cheshire bag model (CBM) (3.1). We write the axial current A_μ ($\equiv J_{5\mu}$) in the CBM as a sum of two terms, one from the interior of the bag and the other from the outside populated by the meson field

[9] The baryon charge is conserved with $Q_{\bar{V}} = \frac{B}{\pi}(\theta - \sin\theta\cos\theta)$ for baryon number B.

η' (how to account for the Goldstone pion fields is known; they will be taken into account for the baryon charge leakage)

$$A^\mu = A^\mu_B \Theta_B + A^\mu_M \Theta_M. \tag{3.41}$$

For notational simplicity, we will omit the flavor (singlet) index in the current. We shall use the short-hand notations $\Theta_B = \theta(R-r)$ and $\Theta_M = \theta(r-R)$ – assuming a spherical bag configuration – with R the radius of the bag. We interpret the $U_A(1)$ anomaly as given in this model by[10]

$$\partial_\mu A^\mu = \frac{\alpha_s N_f}{2\pi} \sum_a \vec{E}^a \cdot \vec{B}^a \Theta_B + f m_\eta^2 \eta \Theta_M \tag{3.42}$$

where $\alpha_s = g_c^2/4\pi$, $\vec{E}$ and $\vec{B}$ are, respectively, color electric and magnetic fields and f is the η' decay constant. We are assuming here that in the nonperturbative sector outside of the bag, the only relevant $U_A(1)$ degree of freedom is the massive η' field. This allows us to write

$$A^\mu_M = A^\mu_\eta = f \partial^\mu \eta \tag{3.43}$$

with the divergence

$$\partial_\mu A^\mu_\eta = f m_\eta^2 \eta. \tag{3.44}$$

It turns out to be more convenient to write the current as

$$A^\mu = A^\mu_{B_Q} + A^\mu_{B_G} + A^\mu_\eta \tag{3.45}$$

such that

$$\partial_\mu (A^\mu_{B_Q} + A^\mu_\eta) = f m_\eta^2 \eta \Theta_M, \tag{3.46}$$

$$\partial_\mu A^\mu_{B_G} = \frac{\alpha_s N_f}{2\pi} \sum_a \vec{E}^a \cdot \vec{B}^a \Theta_B. \tag{3.47}$$

The subindices Q and G imply that these currents are written in terms of quark and gluon fields respectively. In writing (3.46), the up and down quark masses are ignored. Since we are dealing with an interacting theory, there is no unique way to separate the different contributions from the gluon, quark and η components. In particular, the separation we adopt, (3.46) and (3.47), is neither unique nor gauge invariant although the sum is without ambiguity. This separation, however, is found to lead to a natural partition of the contributions in the framework of the bag description for the confinement mechanism that is used here.

We now discuss individual contributions from each term, shown in Fig. 3.2.

[10] In what follows, we drop prime in η'.

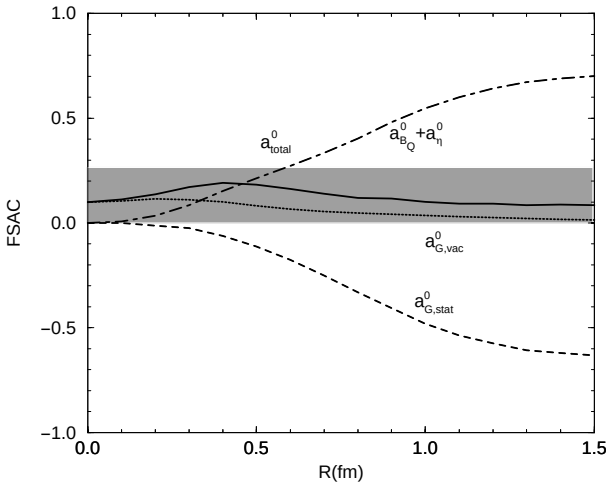

Fig. 3.2 Various contributions to the flavor singlet axial current of the proton as a function of bag radius R and comparison with the experiment: (a) quark plus η (or "matter") contribution ($a^0_{B_Q} + a^0_\eta$), (b) the contribution of the static gluons due to quark source ($a^0_{G,stat}$), (c) the gluon Casimir contribution ($a^0_{G,vac}$), and (d) their sum (a^0_{total}). The shaded area corresponds to the range admitted by experiments.

- **The quark current** $A^\mu_{B_Q}$

The quark current is given by

$$A^\mu_{B_Q} = \bar{\Psi}\gamma^\mu\gamma_5\Psi \tag{3.48}$$

where Ψ should be understood to be the *bagged* quark field. Therefore the quark current contribution to the FSAC (flavor singlet axial current) is given by

$$a^0_{B_Q} = \langle p| \int_B d^3r \bar{\Psi}\gamma_3\gamma_5\Psi|p\rangle. \tag{3.49}$$

The calculation of this type of matrix elements in the CBM is, as described above, nontrivial due to the baryon charge leakage between the interior and the exterior through the Dirac sea. But how to do this in an unambiguous way is known. The leakage produces an R dependence which would otherwise be absent. One finds that there is no contribution for zero radius, that is, in the pure skyrmion scenario for the proton. The contribution grows as a function of R towards the pure MIT result.

- **The meson current** A^μ_η

Due to the coupling of the quark and η fields at the surface, we can simply write

the η contribution in terms of the quark contribution,

$$a_\eta^0 = \frac{1+y_\eta}{2(1+y_\eta)+y_\eta^2}\langle p|\int_B d^3r\bar{\Psi}\gamma_3\gamma_5\Psi|p\rangle \tag{3.50}$$

where $y_\eta = m_\eta R$. Since the η field has no topological structure, its contribution also vanishes in the skyrmion ($R = 0$) limit. Due to the baryon charge leakage, however, this contribution increases slowly as the bag increases. This illustrates how the dynamics of the exterior can be tied to that of the interior by boundary conditions. We may summarize the analysis of these two contributions by stating that no trace of the CCP is apparent from the "matter" contribution $(a_{B_Q}^0 + a_\eta^0)$. As shown in Fig. 3.2, there is a sensitive dependence on R. Thus if an approximate CCP were to emerge, the only possibility would be that the gluons play the crucial role!

Let us now look at the gluon contribution. The gluon current is split into two pieces

$$A_{B_G}^\mu = A_{G,stat}^\mu + A_{G,vac}^\mu\,. \tag{3.51}$$

The first term arises from the quark and η sources, while the latter is associated with the properties of the vacuum of the model. One might worry that this contribution could not be split into these two terms without double counting. However this worry is unfounded. Technically, it is easy to check it by noticing that the former acts on the quark Fock space and the latter on the gluon vacuum. Thus, one can interpret the former as a one-gluon exchange correction to the quantity. One can also show this intuitively by making the analogy to the condensate expansion in QCD, where the perturbative terms and the vacuum condensates enter additively to the lowest order.

- **The gluon static current** $A_{G,stat}^\mu$

Let us first describe the static term.

We ignore the η coupling for the time being. Afterwards, the η contribution can be added. The boundary conditions for the gluon field would correspond to the original MIT ones. The quark current is the source term that remains in the equations of motion after performing a perturbative expansion in the QCD coupling constant, *i.e.* the quark color current

$$g_c\bar{\Psi}_0\gamma_\mu\lambda^a\Psi_0 \tag{3.52}$$

where the Ψ_0 fields represent the lowest cavity modes. In this lowest mode approximation, the color electric and magnetic fields are given by

$$\vec{E}^a = g_c\frac{\lambda^a}{4\pi}\frac{\hat{r}}{r^2}\rho(r) \tag{3.53}$$

$$\vec{B}^a = g_c \frac{\lambda^a}{4\pi}\left(\frac{\mu(r)}{r^3}(3\hat{r}\vec{\sigma}\cdot\hat{r}-\vec{\sigma}) + (\frac{\mu(R)}{R^3}+2M(r))\vec{\sigma}\right) \tag{3.54}$$

where ρ is related to the quark density ρ' as[11]

$$\rho(r,\Gamma) = \int_\Gamma^r ds\rho'(s)$$

and μ, M to the vector current density

$$\mu(r) = \int_0^r ds\mu'(s),$$
$$M(r) = \int_r^R ds\frac{\mu'(s)}{s^3}.$$

The lower limit Γ is taken to be zero in the MIT bag model – in which case the boundary condition is satisfied only *globally*, that is, after averaging – and $\Gamma = R$ in the so called *monopole solution* – in which case, the boundary condition is satisfied *locally*. We take the latter since consistency with the CCP condition rules out the MIT condition.

We now proceed to introduce the η field. We perform the same calculation with, however, the color boundary conditions of (3.1) taken into account. In the approximation of keeping the lowest non-trivial term, the boundary conditions take the form

$$\hat{r}\cdot\vec{E}^a_{stat} = \frac{N_f g_c^2}{8\pi^2 f}\hat{r}\cdot\vec{B}^a_g\eta(R) \tag{3.55}$$

$$\hat{r}\times\vec{B}^a_{stat} = -\frac{N_f g_c^2}{8\pi^2 f}\hat{r}\times\vec{E}^a_g\eta(R). \tag{3.56}$$

Here $\vec{E}^a_g$ and $\vec{B}^a_g$ are the lowest order fields given by (3.53) and (3.54) and $\eta(R)$ is the meson field at the boundary. The η field is given by

$$\eta(\vec{r}) = -\frac{g_{NN\eta}}{4\pi M}\vec{S}\cdot\hat{r}\frac{1+m_\eta r}{r^2}e^{-m_\eta r} \tag{3.57}$$

where the coupling constant is determined from the surface conditions.

Note that the magnetic field is not affected by the new boundary conditions, since $\vec{E}^a_g$ points into the radial direction. The effect on the electric field is just a change in the charge, *i.e.*

$$\rho_{stat}(r) = \rho(r,\Gamma) + \rho_\eta(R) \tag{3.58}$$

where

$$\rho_\eta(R) = \frac{N_f g_c^2}{64\pi^3 M}\frac{g_{NN\eta}}{f}(1+y_\eta)e^{-y_\eta}. \tag{3.59}$$

[11] Note that the quark density that figures here is associated with the color charge, *not* with the quark number (or rather the baryon charge) that leaks due to the hedgehog pion.

The contribution to the FSAC arising from these fields is determined from the expectation value of the anomaly

$$a^0_{G,stat} = \langle p| - \frac{N_f \alpha_s}{\pi} \int_B d^3 r x_3 \vec{E}^a_{stat} \cdot \vec{B}^a_{stat} |p\rangle. \tag{3.60}$$

One finds that including the η contribution in $\rho_{stat}(r)$ brings a non-negligible modification to the FSAC but does not modify the result qualitatively. The result as one can see in Fig. 3.2 shows that this contribution is zero at $R = 0$ but increases as R increases with, however, the sign opposite to that of the matter field, largely canceling the R dependence of the matter contribution. We should remark here that there is a drastic difference between the effect of the MIT-like electric field and that of the monopole-like electric field: The former is totally incompatible with the Cheshire Cat property, whereas the latter remains consistent independently of whether or not the η contribution is included in ρ_{stat}.

• **The gluon Casimir current** $A^\mu_{G,vac}$

Up to this point, the FSAC is zero for $R = 0$ and non-zero for $R \neq 0$. This is in principle a violation of the CCP although the magnitude of the violation is small. We now show that it is the vacuum contribution through Casimir effects that the CCP is restored. The calculation is subtle involving renormalization of the Casimir effects, the details of which are to be found in [Lee, Min, Park, Rho and Vento 1999]. Here we summarize the salient feature of the contribution.

The quantity to calculate is the gluon vacuum contribution to the flavor singlet axial current of the proton, which can be gotten by evaluating the expectation value

$$\langle 0_B| - \frac{N_f \alpha_s}{\pi} \int_V d^3 r x_3 (\vec{E}^a \cdot \vec{B}^a) |0_B\rangle \tag{3.61}$$

where $|0_B\rangle$ denotes the vacuum inside the bag. To calculate this, we invoke at this point *the CCP which states that at low energy, hadronic phenomena do not discriminate between QCD degrees of freedom (quarks and gluons) on the one hand and meson degrees of freedom (pions, etas,...) on the other, provided that all necessary quantum effects (e.g., quantum anomalies) are properly taken into account.* If we consider the limit where the η excitation is a long wavelength oscillation of zero frequency, the CCP asserts that it does not matter whether we choose to describe the η, in the interior of the infinitesimal bag, in terms of quarks and gluons or in terms of mesonic degrees of freedom. This statement, together with the color boundary conditions, leads to an extremely simple and useful *local* formula

$$\vec{E}^a \cdot \vec{B}^a \approx -\frac{N_f g_c^2}{8\pi^2} \frac{\eta}{f} \frac{1}{2} G^2, \tag{3.62}$$

where only the term up to the first order in η is retained in the right-hand side. Here we adapt this formula to the CBM. This means that the couplings are to be understood as the average bag couplings and the gluon fields are to be expressed in

the cavity vacuum through a mode expansion. That the surface boundary condition can be interpreted as a local operator is a rather strong CCP assumption which while justifiable for small bag radius, can only be validated *à posteriori* by the consistency of the result. This procedure is the substitute to the condensates in the conventional discussion.

Substituting Eq. (3.62) into Eq. (3.61) we obtain

$$\begin{aligned}\langle 0_B| - \frac{N_f\alpha_s}{\pi}\int_V d^3r x_3(\vec{E}^a\cdot\vec{B}^a)|0_B\rangle \\ \approx \left(-\frac{N_f\alpha_s}{\pi}\right)\left(-\frac{N_f g_c^2}{8\pi^2}\right)\frac{y(R)}{f_0}\langle p|S_3|p\rangle(N_c^2-1) \\ \sum_n\int_V d^3r(\vec{B}_n^*\cdot\vec{B}_n - \vec{E}_n^*\cdot\vec{E}_n)x_3\hat{x}_3,\end{aligned} \tag{3.63}$$

where we have used the fact that η has a structure of $(\vec{S}\cdot\hat{r})y(R)$. Since we are interested only in the first order perturbation, the field operator can be expanded by using MIT bag eigenmodes (the zeroth order solution). Thus, the summation runs over all the classical MIT bag eigenmodes. The factor (N_c^2-1) comes from the sum over the abelianized gluons.

The next steps are numerical calculations to evaluate the mode sum appearing in Eq. (3.63): (i) introduction of the heat kernel regularization factor to tame the divergences appearing in the sum and (ii) subtraction of the ultraviolet divergences. These procedures – which involve an intricate manipulation – are described in [Lee, Min, Park, Rho and Vento 1999]. Though its contribution ($a^0_{G,vac}$ in Fig. 3.2) is small compared with the others, it is indispensable for restoring, within the CBM scheme, the CCP at small R.

The lesson from this calculation is that as defined, neither the matter contribution nor the gluon contribution to a^0, both of which are non-gauge-invariant and CCP-violating, is physical. Only the total which is color gauge invariant and Cheshire-Cat gauge invariant is physical and CCP-preserving.

3.3.2 *"Charge-spin separation" for Cheshire Cat phenomena*

So what does the approximate CCP mean for hadron physics? Here we enter a philosophical question which will become totally irrelevant once QCD is solved in the nonperturbative. But such a solution will still take a long time to come. Even if QCD is fully solved, it would still be illuminating to have simpler and more intuitive pictures that describe what is happening. This is amply exemplified in nuclear physics.

One fascinating way to understand the CCP is to reason in analogy to what happens in condensed matter physics, in particular, high-T_c superconductivity. One idea that resembles what we are discussing, *i.e.* QCD with confinement, is the idea of spin-charge separation of an electron. According to this idea, an electron is not

a fundamental particle but a composite of spin and charge constituents which are independent dynamical degrees of freedom. The property of the electron manifests differently depending on the environment in which the electron is present. In matter-free space, its spin and charge, strongly correlated, is considered to be confined to each other. However, propagating in "dense" medium, its spin and charge are to separate and pick up their independent identities.

As noted Chapter 2, the redundancy in the electron field translates into an emergent local gauge invariance. Now in a space in which the electron propagates without interactions, the boson and fermion degrees of freedom are not independent degrees of freedom. They are "slaved" to each other, making up an "elementary" particle. However in a medium with strong correlations, they can separate and become independent degrees of freedom having their own separate identities. In this way, the spin and charge can separate. This means that the confinement and deconfinement can be realized in different environments. For instance, in condensed matter, the charge-spin separation is used for describing high temperature superconductivity in cuprates [Baskaran and Anderson 1988]. Another intriguing case discussed in Chapter 10 is the transition from a Néel magnetic state to a quantum paramagnetic state ("valence bond solid") – both of which are in "confinement" – via a quantum critical point at which the charge is fractionized with deconfined half-skyrmions as described in [Senthil *et al.* 2004].

It is appealing to speculate that what happens in the proton spin problem is similar to the charge-spin separation.

3.4 CCP and Multi-Facets of CBM

It should be clear from the definition of the CBM (Cheshire bag model) that the specific structure of the model will depend upon what degrees of freedom and physical ingredients are incorporated in the model and what physical processes are studied. Such quantities as topological baryon charge should surely be independent of the detailed dynamics. But such observables as the EM form factors must depend on what degrees of freedom are taken explicitly into account. In Chapters 5-7, we will show that the nature of vector dominance of nucleon form factors depends crucially on how many vector meson fields are taken into account. With the participation of an infinite tower of vector mesons as involved in holographic dual QCD (hQCD), the intrinsic (or "bag") size of the baryon, viewed as an instanton, is even zero, but if all other vector mesons than the lowest members are integrated out, then the intrinsic size of the proton is found to be ~ 0.4 fm, roughly half of its EM size. One may take this as a manifestation of CCP in terms of hidden local gauge fields. This is one further illustration that a variety of chiral symmetry models, different in appearance, but consistent with the CCP, could be applicable in different regimes of kinematics and environments. Here we briefly summarize what chiral models are available in the market and what they represent in terms of the CCP.

3.4.1 *Chiral quark-soliton model*

A model that uses solitonic structure for baryons which is a close variant of the chiral bag model is the "chiral quark-soliton model (CQSM)" of Diakonov and Petrov [Diakonov and Petrov 2000]. This model is based on two general properties shared by *all* chiral models, namely, the spontaneously broken chiral symmetry and large N_c approximations (with the quark confinement implicitly assumed). Instead of putting chiral symmetric boundary conditions delineating short-distance and long-distance physics, in CQSM, N_c quarks are bound by self-consistent (hedgehog) pion fields summarized by the effective "bare" Lagrangian [12] $\mathcal{L} = \bar{\Psi}(i\gamma \cdot \partial - \mathcal{M}U^{\gamma_5})\Psi$ where $\mathcal{M}$ is dynamically generated (or constituent-quark or quasiquark) mass matrix and $U^{\gamma_5} = e^{2i\pi\gamma_5/f_\pi}$ as given in (3.1) with f replaced by the pion decay constant f_π. Since the mass matrix is momentum and cut-off dependent, this is a nonlocal Lagrangian. When the mass matrix "dressed" by the pion field is suitably localized by derivative expansion, the Lagrangian should become highly non-linear. Higher derivative terms are to mock up dynamics of the bagged quarks in the chiral bag model or cloudy bag model (with or without more massive degrees of freedom). Given that the model is essentially based on the given symmetries and large N_c (with confinement assumed), there is no reason to expect basically different predictions from this model than from the generic CBM (3.1). Unsurprisingly one finds that the predictions made for baryon properties are quite similar to those of other models.

3.4.2 *Cloudy bag model*

In the spirit of CCP as a gauge artifact, one might choose to work with a "large" bag $R \sim 1$ fm in which case short-distance dynamics of the Cheshire bag model (CBM) (3.1) will be subsumed entirely in the bag, with long distance dynamics encoded in fluctuating pion fields. In this case, it would be a good approximation that all the baryon charge is lodged inside the bag. No or rather negligible solitonic structure will be attributed to the baryon: the pion field will have no hedgehog component. In this case, the axial current can be conserved globally and there is no *need* for the axial boundary condition in (3.1). The quarks will be confined by the vector current conservation as in the MIT bag model. However the pion couples to the quarks everywhere unlike the CBM of (3.1). So will other (heavier) mesons if they are needed (*e.g.*, for nuclei and nuclear matter). However by fiat, the bag size is big, say, of the order of hadron size, so the pion contributes only to long-distance dynamics with short-distance dynamics suppressed by the "form factor" given by the bag. What the CCP says is that what is given by this model with a big bag should be equivalent to CBM for *any* bag size, including zero size, with short-distance dynamics

[12] The generating functional with this Lagrangian would involve functional integrals over the pion field and the constituent quark fields $\bar{\Psi}$ and Ψ with a cutoff defined in the effective theory. This method resembles the "second decimation" in nuclear structure discussed in Chapter 8.

subsumed in the bag taken over progressively by a tower of vector meson fields as the bag size is shrunk as in hidden local symmetry theory developed below. This model, referred to as "cloudy bag model," that implements chiral symmetry without recourse to the topological structure of baryons has been extensively developed by Thomas and his collaborators [Thomas, Theberge and Miller 1981; Thomas 1982; Matevosyan, Miller and Thomas 2005] with a considerable phenomenological success.

3.4.3 *Skyrmion model*

In the limit that the bag size is shrunk to a point in accordance of CCP in the Cheshire bag model (3.1), one obtains the skyrmion model of the baryon. The skyrmion picture for baryons follows naturally in holographic dual QCD that comes from string theory as described in Chapter 5. This topic, extensively covered in CND-1 in the framework of the original Skyrme model, will be picked up again in Chapter 6 of this volume where it will be suggested that the skyrmion description with the Goldstone fields alone, *i.e.* the original Skyrme model, is in fact inaccurate and that vector meson fields *must* be incorporated for correctly describing baryons as solitons. That this must be so is not hard to see from the discussions given above. It will also be seen that many-nucleon systems under extreme conditions could be more profitably studied in terms of skyrmions in heat bath or at high density. We should mention that in the large N_c limit the skyrmion model is equivalent to the constituent quark model.

3.4.4 *Heavy baryon chiral perturbation approach*

Shrinking to a point as given by the instanton baryon described in Chapter 5 in the 't Hooft limit and coupling to fluctuating pions leads, in accordance with Weinberg "theorem," to chiral perturbation theory for pion-nucleon interactions and nuclear forces, *i.e.* effective field theory of nuclei and nuclear matter. The point-like nucleon structure allowing it to be described as a local field naturally arises in holographic dual QCD where it is found that the size of the baryon is mostly given by the exchange of an infinite tower of vector mesons (see Chapter 5). A systematic chiral expansion then represents *another facet of CBM* at very low energy and in many-body systems. This matter will be the topic of Chapter 4.

This page intentionally left blank

Chapter 4

Effective Field Theory For Nuclei

In this chapter, we treat the baryons as pointlike local fields coupled with pion fields in consistency with the assumed symmetries, especially chiral symmetry, and other basic properties of the fundamental theory QCD. Such a point-like local field for baryons could be justified in holographic dual QCD if the latter were proven to represent QCD proper. We will develop an argument that the baryon as an instanton configuration "squeezed" to a point by the infinite tower of vector mesons arises in a certain limiting process. In the preceding chapter, we classified this picture as one belonging to the case where the Cheshire Cat principle applies. We will focus on many-body systems where the role of effective field theory can be exposed in close contact with Nature. This will be the first illustration of how Weinberg theorem stated in Chapter 2 can be implemented in hadronic and nuclear processes.

4.1 Role of Effective Field Theory in Nuclear Physics

In nuclear physics, even though we are dealing with many-body systems, the "accepted" fundamental theory is QCD. Effective field theory (EFT for short) is supposed to be an approach which can ultimately reproduce the fundamental theory at low energy. Our task is to set up an approximate EFT scheme which comes as close as possible to the truth encoded in QCD. There is no clear-cut evidence that nuclear physics can be entirely understood in terms of explicit QCD variables (quarks and gluons) or put differently, QCD can be "tested" unambiguously in nuclear physics. By now, however, this question has become akin to asking whether condensed matter systems can be understood in terms of QED. In this volume, we adopt Weinberg's "folk theorem" [Weinberg 1997a] precisely stated in Chapter 2 and simply eschew the issue on the applicability or the test of QCD in nuclear physics.

So what is the task of an effective field theory in nuclear physics?

In the literature, two possible philosophical attitudes are taken in addressing this question. One is to set up a well-defined effective theory, albeit within a very

restricted domain of applicability, say, in energy/momentum, or in the number of nucleons involved in the system and investigate whether and how the intended theory does what it is supposed to do. Here one works with a well-defined set of rules for calculations and then *rigorously* follow the rules and confirm that the strategy works. We shall call this "rigorous EFT" (RigEFT for short). In this approach, given strong constraints imposed by the consistency with the strict power counting (or more generally chiral counting) and the rapid proliferation of input parameters at higher orders, one is severely limited to low orders of chiral perturbation expansion, which makes it unfeasible to address the complex dynamics of the wide-ranging real nuclear systems. In this class of approach is what we might call "toy EFT" where an EFT with the least complexity taken into account is solved fully, consistently with the set of rules adopted. The "pionless EFT" ($\not\pi$EFT) to be described below belongs to this subclass. The other philosophy – which in some sense is drastically different from the $\not\pi$EFT – is to take it for granted that EFT should work in nuclear physics and exploit the power of EFT to make calculations that cannot be accessed solely by the well-developed standard many-body technique. This is a more pragmatic approach aiming at describing *real* nuclear phenomena more widely and more painlessly than RigEFT. This approach is dubbed "more effective effective theory" (MEEFT) to suggest that it exploits both the power of EFT and the precision of the standard nuclear physics approach.

4.2 Standard Nuclear Physics Approach and EFT

4.2.1 *The power of SNPA*

The standard approach to physics of finite nuclei and normal nuclear matter has been to determine first highly sophisticated phenomenological two-nucleon potentials implemented with multi-nucleon (typically three-nucleon) potentials fit to a large body of experimental data and solve the many-body problem as accurately as possible. This approach, on a microscopic level, has reached an impressively precise description of nuclei up to mass number $A = 10$ [Pieper, Wiringa and Carlson 2004] with ground and excited state energies within $\sim$ 1-2% and on a more macroscopical level, to heavy nuclei. The solution requires massive numerical computations, which lead some to think that this approach is inferior to, or less elegant than, analytical approaches. But in the present era of computer revolution, that cannot be a valid complaint as it does not make the work any less fundamental than analytical calculations. This approach which we call in this volume "standard nuclear physics approach (SNPA)" exploits two-nucleon potentials that fit scattering data up to momenta $\sim$ 300 MeV with a χ^2/datum $\lesssim 1.4$. The success of this approach has been extensively reviewed in [Carlson and Schiavilla 1998; Pieper and Wiringa 2001] and we will not elaborate any further on it, although we will refer to it in this and later chapters. We consider it a grave shortsight and a

setback to ignore the accuracy achieved by the SNPA and discard it on the ground that it is not "derived" in an EFT formalism. Our point of view which we will develop here is that we should – and can naturally – incorporate it in the framework of an EFT in such as way as to allow us to systematically control possible corrections brought in by more fundamental and systematic formulations.

4.2.2 *The power of EFT*

In assessing both the power and the limitation of the SNPA, the physical observables to look at are not only the spectra of nuclear states but also response functions involving their wave functions and currents. For the latter, the standard procedure that has been mostly employed is to write down the currents in terms of the single-particle operators – called impulse approximation – which are typically the most important and then make, often less important, corrections due to the presence of multi-body operators constructed from the exchange of mesons, called "meson-exchange currents," in an effective phenomenological Lagrangian field theory. This approach was systematized a long time ago in [Chemtob and Rho 1971]. In many of the applications since then, this approach has given results that compare well with experiments. But within the framework of many-body theory based on phenomenological potentials, there is no unique or systematic way to assess what the size of the corrections that are calculated or guessed at is, so when the calculated value disagrees with experiments, there is no well-defined and systematic way to improve the calculation. Thus one can make post-dictions but rarely *predictions* or calculations that are free of free parameters. This is one place where EFT can come in and offer an invaluable help.

What is the true use of an EFT?

To show that QCD works is not the objective. Weinberg's theorem implies that *QCD should work in nuclei if one works hard enough*. This we are witnessing in the construction of two-body potentials in χPT.[1] Let us return to the points mentioned in Section 4.1. What have been done in the literature in the past in addressing the issue in question are the following:

- One direction belonging to the RigEFT class – followed by a large number of workers in the field – is to limit oneself to a well-defined, but drastically simplified, EFT Lagrangian and then study this as rigorously as possible within the framework of suitably well-defined rules. A case that has been particularly widely studied is the pionless ($\not\pi$) Lagrangian approach in which *all* but nu-

[1] To be more specific, we note from an updated review [Machleidt and Entem 2005] that the N^3LO chiral perturbation calculation of the two-body potential fits the 1999 data base *np* scattering below 290 MeV with a χ^2/datum=1.10 while the sophisticated phenomenological potential Av18 fits it with χ^2/datum=1.04. To see how high-order χPT terms work, one can compare the χ^2/datum=36.2 and 10.1, respectively, for NLO and N^{2}LO. At present, the N^{3}LO calculation is the best one can do, and it is unlikely that the SNPA potential will soon be superseded by high-order chiral perturbation.

cleon fields are integrated out. Given the limited range of nuclear interactions involved, it is necessarily limited in scope and so far achieved no more than *reproducing* what is, already, well and accurately described in SNPA. While this approach has the advantage to directly address problems that can lead to exact statements, such as the phenomenon of renormalization-group limit cycle, Efimov effect *etc.* (see, *e.g.*, [Hammer 2005]), it lacks genuine predictiveness.

An approach that belongs to the RigEFT class but tends to approach the MEEFT class takes the nucleon and the pion as the relevant degrees of freedom and calculate to as high an order as feasible and as consistently as possible within the tenet of chiral perturbation theory. This calculation is also severely limited for the simple reason that the number of unknown constants increases rapidly as the chiral order increases. We will have little to say on this approach. But when we say RigEFT without specification, we will mean both this and the pionless EFT.

- The other direction which will be adopted in this volume (see [Rho 2002; Rho 2006] for an earlier discussion along the same line) is to exploit the strategy of an EFT to calculate quantities that neither the SNPA nor QCD proper *separately* can do, that is, to make "predictions".[2] The strategy is to exploit both the full machinery of SNPA *and* the power of EFT in a scheme that is consistent with the symmetries of QCD to make *parameter-free* calculations that can be confronted with Nature. We will tacitly assume that systematic high-order chiral perturbation calculations of the potentials will eventually provide quantitative support to the potentials used in the SNPA. Up to the order calculated, this assumption is justified [Machleidt and Entem 2005].

4.3 Chiral Lagrangians

4.3.1 *Relevant scales and degrees of freedom*

When applied to nuclear systems, EFT involves a hierarchy of scales in the interactions. In nuclear physics, the nucleon is the core degree of freedom that figures as a *matter field* defining the system, with the pion being the lightest mesonic degree of freedom. What other degrees of freedom must enter in the dynamics depends upon what process one is studying. If the kinematics probed is of the scale $E \ll m_V$ where m_V is the mass of the light-quark vector mesons, the lightest of which are the ρ and the ω, then one may integrate out all heavy mesons – vectors as well as scalars – and work with the baryon and the pion only. This regime is accessible by a chiral perturbation theory (χPT) for physics of dilute nuclear systems, *e.g.*, few-nucleon systems. If one works to high enough order in chiral perturbation theory, one should be able to understand most, if not all, of nuclear physics taking

[2] By predictions, here as well as in what follows, we always mean parameter-free calculations with error estimates of what might be left out in the approximations, *e.g.*, the truncation, involved.

place within the given restricted kinematic domain, although in some cases, it is more convenient and simpler to introduce heavier degrees of freedom explicitly (as for instance the ρ, ω, a_1, σ *etc*). When one is studying systems involving a scale $E \ll m_\pi$, where m_π is the pion mass, then one might even integrate out the pion as well, as is done in $\not\pi$EFT. How this program works is described in numerous lecture notes, one recent reference of which is [Kaplan 2005].

It should be remarked that even when $\not\pi$ EFT is fully justified, that is, pions are *not* indispensable, as in certain cases, it proves to be much more powerful and predictive to keep pions as effective degrees of freedom. We will encounter such a situation when we discuss the so-called "chiral filter mechanism." One finds that having explicit pion degrees of freedom with their associated low-energy theorems can give a highly simplified and efficient description of processes which would require much harder work if the pion were integrated out.

More significantly, the explicit presence of pions is now known to be the dominant element in describing the structure of light nuclei. In particular, to quote Wiringa [Wiringa 2006], "the success of the simple model [of light nuclei] supports the idea that the one-pion exchange is the dominant force controlling the structure of light nuclei ..."[3]

As one probes denser systems such as nuclear matter and denser matter, due to Brown-Rho (BR) scaling (discussed in Chapters 5-9), the vector meson mass drops and near chiral restoration, becomes comparable to the pion mass. In this case, one cannot integrate out the vector mesons; the vector fields have to be endowed with local gauge invariance, so that systematic chiral perturbation can be done with the vector mesons included [Harada and Yamawaki 2003].

4.3.2 *Vector mesons and baryons*

In the next chapter, a hidden local symmetry (HLS) involving an infinite tower of gauge fields coupled to pions in a chirally symmetric way will be seen to emerge bottom-up from low-energy and also top-down from string theory via holographic duality. It will be shown there that the hidden local symmetry approach of Harada and Yamawaki [Harada and Yamawaki 2003] with the light-quark vector mesons arises as a truncated version of the holographic dual QCD (hQCD). Restricted to

[3]To continue the quote:"In Green's function Monte Carlo calculations of $A \leq 12$ nuclei with realistic interactions, the expectation value of the one-pion-exchange potential is typically 70-75% of the total potential energy. The importance of pion-exchange forces is even greater when one considers that much of the intermediate range attraction in the NN interaction can be attributed to uncorrelated two-pion exchange with the excitation of intermediate $\Delta(1220)$ resonances. In addition, two-pion exchange between three nucleons is the leading term in $3N$ interactions, which are required to get the empirical binding in light nuclei. In particular, the $3N$ forces provide the extra binding required to stabilize the Borromean nuclei ^{6,8}He and ^{9}Be." It would seem therefore that first integrating out the pion and then correcting with higher order (derivative) terms is like first throwing away the baby with the bath water and then trying to recover the baby piece by piece.

the lowest members of the vector mesons, *i.e.* the ρ and ω, it is the Wilsonian matching to QCD that makes the theory a bona-fide effective theory of QCD. In the simplest form of HLS theory with $N_f = 3$, there are the octet pseudo-Goldstone bosons and nonet of vector mesons coupled gauge invariantly. Baryon fields do not figure explicitly. But it is a complete theory at low energy, so baryons must appear as solitons. Although there have been efforts to construct skyrmions with a chiral Lagrangian with vector mesons incorporated (see [Weigel 1996] for references) – and it is now clear that vector mesons must be present in the skyrmion structure [Rho 2007a], very little is understood of such hidden local symmetry skyrmions. For the purpose of this section, instead of generating baryons as solitons, we will simply introduce baryon fields explicitly.

4.3.3 *Baryon fields*

As mentioned, baryon fields will be treated as matter fields. It is generally accepted that this is consistent with Weinberg's theorem as long as the momentum transfer involved is $\ll \Lambda$ where Λ is the cutoff. We consider baryons made up of u, d and s quarks, *i.e.* $SU(3)_f$.[4] We want the baryon field B to transform under (vector flavor) $SU(3)_V$ as

$$B \to VBV^\dagger \tag{4.1}$$

with $V \in SU(3)_{L+R=V}$. Now how does B transform under $SU(3)_L \times SU(3)_R$? Here there is no unique way as long as it is consistent with the symmetries of QCD. For our purpose, the most convenient choice is to have it transform as [Georgi 1984]

$$B \to hBh^\dagger \tag{4.2}$$

with h encoding the hidden local symmetry of the chiral field U

$$U = \xi_L^\dagger \xi_R. \tag{4.3}$$

with the transformations

$$\xi_L \to h\xi_L g_L^\dagger, \tag{4.4}$$
$$\xi_R \to h\xi_R g_R^\dagger. \tag{4.5}$$

Here h is a complicated local function of $g_L \in SU(3)_L$, $g_R \in SU(3)_R$ and U, the explicit form of which is not needed. When $g_L = g_R = V$, it is just a constant $h = V$.

[4] The s quark figures insignificantly in non-strange nuclear systems and nuclear matter. But we keep it for generality and for later purpose.

We define in unitary gauge $\xi_L^\dagger = \xi_R = e^{i\pi/F_\pi}$

$$\tilde{A}_\mu = \frac{i}{2}\left(\xi^\dagger\partial_\mu\xi - \xi\partial_\mu\xi^\dagger\right), \tag{4.6}$$

$$\tilde{V}_\mu = \frac{1}{2}\left(\xi^\dagger\partial_\mu\xi + \xi\partial_\mu\xi^\dagger\right), \tag{4.7}$$

$$D_\mu B = \partial_\mu + [\tilde{V}_\mu, B] \tag{4.8}$$

transforming under $SU(3)_V$ as [5]

$$\tilde{V}_\mu \to h(\partial_\mu + \tilde{V}_\mu)h^\dagger, \tag{4.9}$$

$$\tilde{A}_\mu \to h\tilde{A}_\mu h^\dagger, \tag{4.10}$$

$$D_\mu B \to hD_\mu B h^\dagger. \tag{4.11}$$

Now what we need to do is to write the Lagrangian $\mathcal{L}_{inv}$ invariant and the Lagrangian $\mathcal{L}_{non}$ non-invariant under the given transformation. Thus

$$\begin{aligned}\mathcal{L}_{inv} &= \mathrm{Tr}\bar{B}(i\gamma^\mu D_\mu - m_0)B - D\mathrm{Tr}\bar{B}\gamma^\mu\gamma_5\{\tilde{A}_\mu, B\} \\ &\quad -F\mathrm{Tr}\bar{B}\gamma^\mu\gamma_5[\tilde{A}_\mu, B] + \cdots, \end{aligned}\tag{4.12}$$

$$\begin{aligned}\mathcal{L}_{non} &= a_1\mathrm{Tr}\bar{B}(\xi^\dagger M\xi^\dagger + \mathrm{h.c})B + a_2\mathrm{Tr}\bar{B}B(\xi^\dagger M\xi^\dagger + \mathrm{h.c.}) \\ &\quad +a_3\mathrm{Tr}(MU + \mathrm{h.c.})\mathrm{Tr}\bar{B}B + \cdots. \end{aligned}\tag{4.13}$$

Here the ellipses stand for higher order terms, either in derivatives or in quark mass terms or in combination of both, M is the chiral-symmetry-breaking mass matrix, m_0 is the dynamically generated mass of the baryon which is of order ~ 1 GeV, *i.e.* the chiral scale and D, F, a_i are constants to be fixed.

In nuclear physics at low energy we are considering, the nucleon is non-relativistic, so it makes sense to go to the non-relativistic form of the Lagrangian. One may formulate it relativistically but contact with SNPA is made more directly in the non-relativistic approach. A nice way of going to the non-relativistic form is the heavy-baryon formalism employed in heavy-baryon chiral perturbation theory [Jenkins and Manohar 1991]. To do this, define

$$B_v(x) = e^{im_0 v\cdot\gamma v\cdot x}B(x) \tag{4.14}$$

where v_μ is the velocity four-vector for the baryon and introduce the spin operator S_v^μ that satisfies

$$v_\mu S_v^\mu = 0,\ S_v^2 B_v = -\frac{3}{4}B_\nu, \tag{4.15}$$

and

$$\{S_v^\mu, S_v^\mu\} = \frac{1}{2}(v^\mu v^\nu - \eta^{\mu\nu}), \tag{4.16}$$

[5] The "induced" vector and axial-vector fields are denoted $\tilde{V}_\mu$ and $\tilde{A}_\mu$, respectively, to be distinguished from the hidden local fields V_μ and A_μ that will figure in the coming chapters.

$$[S_v^\mu, S_v^\nu] = i\epsilon^{\mu\nu\alpha\beta} v_\alpha S_{v\beta}. \tag{4.17}$$

In terms of these definitions, we can rewrite $\mathcal{L}_{inv}$ as

$$\begin{aligned}\mathcal{L}_{inv} = \; & \mathrm{Tr}\bar{B}_v v_\mu D^\mu B_v + 2D\mathrm{Tr}\bar{B}_v S_v^\mu \{\tilde{A}_\mu, B_v\} \\ & + 2F\mathrm{Tr}\bar{B}_v S_v^\mu [\tilde{A}_\mu, B_v] + \cdots \end{aligned} \tag{4.18}$$

In this form, the mass term m_0 disappears, so the chiral counting comes out, as we wanted, without having to worry about the cancelation between the mass term and the time derivative on the baryon field. Similar forms can be written down for the chiral symmetry non-invariant terms.

The Lagrangians written above in bilinears in the baryon field are applicable in the one-nucleon sector. With these Lagrangians in various approximations, one can systematically treat one baryon problem including interactions with pions and external fields. We won't dwell on this problem in this volume. If one is interested in this topic, there are some good reviews in the literature which show that chiral perturbation theory does work well and could even be improved as one goes to higher orders and as more precise experimental data become available. In what follows and in other sections of this volume, we will take this "success" for granted.

Here we are interested in few- and many-nucleon systems. When there are more than one nucleon in the system, one has multi-nucleon terms involving $2n$ fermion fields for $n > 2$. Thus we have

$$\mathcal{L}_{2n-fermi} = \sum_a (\bar{B}\Gamma_{a\mu} B)(\bar{B}\Gamma_a'^\mu B) + \cdots \tag{4.19}$$

where the ellipses now stand for higher number of Fermi fields and Γ and Γ' are various Lorentz structures involving derivatives *etc.* subject to the necessary symmetry constraints of QCD.

4.4 Pionless EFT ($\not\pi$EFT)

As mentioned, if one is interested in nuclear processes where the energy scale is much less than the pion mass, one may integrate out the pion as well. The resulting Lagrangian containing only the massive nucleons has no chiral symmetry since there are no pions anymore. But chiral symmetry is not violated. It is just that chiral symmetry is an irrelevant symmetry here. It is easy to write down the effective Lagrangian

$$\mathcal{L}_{\not\pi} = N^\dagger (i\partial_t + \nabla^2/2m) N + C(N^\dagger N)^2 + C'((NN)^\dagger (N\nabla^2 N) + \cdots \tag{4.20}$$

where N stands for the nucleon doublet replacing the baryon field B. The ellipses stand for terms with spin and flavor matrices and other derivative terms of the same order with and without spin and isospin factors *etc.* The Lagrangian should be Galilean invariant.

Given the extreme simplicity of the pionless Lagrangian, the power counting rule is equally simple, allowing one to do a systematic and consistent calculation, in principle, to high orders. It is just a power series in p/Λ where p is the probe momentum and Λ is the cutoff scale defining the momentum space considered. In practice it makes no sense to go to very high orders since unknown parameters increase rapidly. Further complications can arise if one is interested in many-nucleon systems where the Fermi momentum which is of order of a few times the pion mass enters, but this theory makes no sense there anyway.

Now what can we learn with this? It can work for two-body and perhaps three-body systems for which the SNPA has scored a great success already, but the procedure gets rapidly unmanageable when it goes to the really interesting problem like the solar *hep* and the related *hen* process that involve four-body interactions. (We will return to this problem below.) It has no pions, and hence quantities which are rendered easy to understand when pions are present (*e.g.*, various low-energy theorems) are made difficult, if not impossible, to treat. Being a toy model, on the other hand, it allows, thanks to the simplicity of the Lagrangian, a systematic and rigorous description – unfeasible in other approaches – of certain, though restricted, low-energy processes. But it should be mentioned that the physical processes that can be treated are mostly, if not all, those which have been well reproduced in SNPA with well-defined corrections (*e.g.*, those processes which are subsumed in effective range theory).

As an illustration, consider $n + p \to d + \gamma$ at low energy. This process to which we will return for MEEFT has been treated by the model with some success [Kaplan 2005]. The *np* capture at thermal energy is accurately measured and so can offer an excellent process to check the theory with. Now this process is dominated by an isovector $M1$ operator, so in (4.20), we need the interaction C term for the ${}^3S_1$ channel, a C' term for both ${}^3S_1$ and ${}^1S_0$ channels and the couplings to the magnetic photon [Kaplan 2005]

$$\mathcal{L}_B^{1b} = eN^\dagger(\kappa_S + \kappa_V\tau_3)\frac{\sigma\cdot\mathbf{B}}{2m}N \tag{4.21}$$

and

$$\mathcal{L}_B^{2b} = eL_1(N^T P_i N)^\dagger(N^T\overline{P}_3 N)B_i \tag{4.22}$$

where $\kappa_{S/V} = \frac{1}{2}(\kappa_p \pm \kappa_n)$ with $\kappa_p = 2.79$ and $\kappa_n = -1.91$. Here P_i and $\overline{P}_3$ are, respectively, the ${}^3S_1$ and ${}^1S_0$ projection operators.[6] The constant C in (4.20) is obtained by fitting the deuteron binding energy and the C' from the effective range in NN scattering. But there is one unknown constant L_1 which cannot be *à priori* fixed: There is no other experiment than the *np* capture that involves this term. Hence no true prediction can be made. It is not, however, totally devoid of value

[6]The projection operators are given explicitly by $P_i = \frac{1}{\sqrt{8}}\sigma_2\sigma_i\tau_2$ and $\overline{P}_i = \frac{1}{\sqrt{8}}\sigma_2\tau_2\tau_i$ with $\mathrm{Tr}(P_i^\dagger P_j) = \frac{1}{2}\delta_{ij}$ and similarly for $\overline{P}_i$.

since once L_1 is fixed from the np capture experiment, one can then turn the process around and calculate the inverse process $\gamma + d \to n + p$ as a function of the photon energy. It works fairly well up to, say, $E_\gamma \sim 10$ MeV. This is relevant for big-bang nucleosynthesis. One should, however, recognize that there is no real gain in theoretical understanding in this approach because the SNPA can do just as well with well-defined two-body corrections.

4.5 More Effective EFT

4.5.1 *Weinberg's counting rule*

We now turn to a more predictive EFT scheme. To exploit the accuracy and power of SNPA, we adopt the Weinberg counting rule.[7] In fact, the Weinberg counting[Weinberg 1990; Weinberg 1991] is the only way known that the SNPA can be *naturally* "married" with an EFT. Since the aim here is to exploit the powers of both SNPA and EFT, we refer to it as "more effective EFT (MEEFT)."

The Weinberg counting consists essentially of two steps. In the first step, one defines the nuclear potential as the sum of 2-particle irreducible diagrams – irreducible in the sense that they contain no purely nucleonic intermediate states – and truncates the sum at some order n in the standard chiral perturbation power counting. The potential is dominated by two-body irreducible terms, with n-body terms for $n > 2$ suppressed by the power counting. In the second step, the potential so constructed is used to solve the Lippman-Schwinger or Schrödinger equation. This corresponds to incorporating "reducible" graphs that account for infrared enhancement (or singularities) associated with bound states. Now the potential will then include one or more pion exchanges and local multi-fermion interactions that represent massive degrees of freedom (such as the vector mesons ρ, ω *etc.*) that are "integrated out." The approach then can automatically be applied equally to two-nucleon processes as well as to many-nucleon processes with the outputs in the form of physical observables, namely, scattering cross sections, energy spectra, response functions to external fields *etc.* Wave functions make an indispensable part of the scheme, so the theory enables one to calculate things not only in few-body systems but also across the periodic table. Contact with "rigorous" EFT – in the sense of power counting assured in pionless EFT – can be made only for few-body systems. However systematic higher order chiral corrections to the estimates made in SNPA can be made with certain error estimates for processes that involve heavy nuclei, *e.g.*, lead nuclei, a feat that has not been feasible up to date in the $\not\pi$EFT approach

The Weinberg counting rule explains naturally that n-body forces for $n > 2$ are

[7] Historically, the first effort to incorporate Weinberg counting in nuclear physics was made in a 1981 Erice lecture [Rho 1982] based on Weinberg's 1979 paper on $\pi\pi$ scattering [Weinberg 1979]. The 1981 Erice lecture contains the core idea behind the application of chiral perturbation theory to nuclear problems. Unfortunately the discussion was incomplete because the role of nucleons in the counting was inadvertently left out.

suppressed relative to 2-body forces, and n-body currents are normally subdominant to one-body current, known in nuclear physics as impulse approximation. These are familiar things in SNPA, but in MEEFT, they go beyond SNPA in that one can in practice make a systematic account for corrections to the SNPA results that are guided by an effective field theory strategy. What this means is that in calculating response functions to external fields, one can use the accurate state-of-the art wave functions that have been constructed since a long time in SNPA to make predictions that are otherwise not feasible in the RigEFT approach. We will illustrate this point below.

There is of course a price to pay for this "predictive power." One of them is possible ambiguity in the regularization procedure which separates high-energy and low-energy physics. Where to do the separation is completely arbitrary and the observables calculated should not depend on the separation point. This is the statement of the renormalization group invariance. However to the extent that one calculates in certain approximations, one cannot make the independence perfect. How best to do this, one must admit, is sometimes more an art than science.

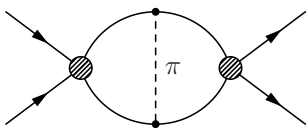

Fig. 4.1 A two-loop diagram that requires higher-order counter term in the leading order graph in ≠EFT.

For example, one of the problems arises when the two-loop graph with a pion exchange between two nucleons of Fig. 4.1 treated as a Feynman diagram is calculated in dimensional regularization. The problem lies in treating this graph strictly in the sense of perturbation theory. If one writes the dimension as $d = 4-2\epsilon$ letting $\epsilon \to 0$ at the end, then one finds that this graph diverges as

$$\sim \frac{1}{\epsilon} m_\pi^2. \tag{4.23}$$

This represents the logarithmic dependence on scale $\sim \ln \mu$. This scale dependence needs to be canceled by a counter term that goes like $\sim m_\pi^2$. In the power counting of the theory, this comes at higher order than that assigned to the pion exchange in Weinberg counting, since m_π^2 counts as $\mathcal{O}(Q^2)$. This means that when one solves Schrödinger equation with the pion exchange included in the potential consisting of irreducible terms, one has an inconsistency in chiral counting, since the pion exchange needs to be regulated by a counter term higher order in the Weinberg counting.

Now how did this "basic" problem not hamper development in SNPA? The answer is that what happens in nuclei is not wholly accessed by perturbative renormalization that is obstructed by the above problem. The fact that one is solving Schrödinger equation illustrates that nuclear problems are inherently nonperturbative and the above inconsistency arises because one is doing a strict perturbation calculation. This difficulty is essentially sidestepped by MEEFT that we will discuss in the following section.

There is also an indication that this regularization difficulty can even be *formally* remedied [Pavon Valderrama and Ruis Arriola 2005; Pavon Valderrama and Ruis Arriola 2006; Nogga, Timmermans and van Kolck 2005; Epelbaum and Meissner 2006]. The most serious is the singularity of tensor interactions in partial waves where the interaction is attractive. For large cutoff Λ, say, greater than vector meson mass, spurious bound states can be generated. Of course the cutoff has a physical meaning in effective theories as elaborated below and picking a cutoff bigger than what is appropriate is meaningless, so this problem is in a sense academic. However even for low enough cutoff, there may be unacceptably large cut-off dependence. The situation gets more serious in certain channels where counter terms are infrared-enhanced. However it turns out that one can add a counter term in each partial wave where this sensitivity is present and avoid this difficulty, at least to the leading order [Nogga, Timmermans and van Kolck 2005]. This issue is further discussed in [Epelbaum and Meissner 2006]. It is not clear that this problem continues to arise at higher orders and more work is needed in this area. At present, the MEEFT predictions described below are free from this difficulty.

4.5.2 *Strategy of MEEFT*

What is crucial for a viable MEEFT is to have very accurate wave functions. Let us suppose that we do have wave functions that give a good description of spectra and response functions for a range of mass numbers. *The basic requirement is that the wave functions so obtained possess the correct long-distance properties governed by chiral symmetry.* We shall assume that the wave functions we use meet this requirement. It would be highly surprising if fitting a large number of low-energy data, both scattering and current matrix elements, were achieved without a good account of the long-distance physics associated with chiral symmetry. We can therefore assume that the currents we construct in Weinberg's scheme incorporating one or more pion exchanges given by leading order chiral expansion should be consistent with the (SNPA) wave functions up to that order, with possible uncertainty in the current residing in higher orders. Shorter-distance properties of the range $\lesssim (2m_\pi)^{-1}$ in the phenomenological potentials used to generate the wave functions are not unique, but they should not affect long wavelength probes we are interested in. If we can assure cutoff independence in the relevant range of cutoff values consistent with the physics we are interested in, that should be good enough for

the predictive power. The support for this comes from the RGE argument to be discussed in a section below. Now the strategy in computing response functions is to calculate the irreducible contributions to the current vertex functions to the order that is correctly implemented in the wave functions from the point of view of chiral counting. In doing this, we can roughly separate into two classes of processes: those processes that are "chiral-filter protected" and those that are not. The former processes are accurately calculable given accurate wave functions with small error bars since the effects are primarily controlled by soft-pion theorems. The latter is less well controlled by low-energy theorems and hence brings in certain uncertainties. We will show, however, that with an astute implementation of SNPA, one can calculate certain processes belonging to the second class with fair accuracy. We will treat both classes below.

4.5.3 *The chiral filter*

We will be dealing with a slowly varying weak external field that acts only once at most. Thus in the chiral counting, the external field that does not bring in small parameter such as the external momentum or the pion mass lowers by one order two-body corrections relative to the single-particle process to the counting that goes into the potential. This is essentially because of the minimal coupling of the external field which replaces one derivative in the two-body terms by the external field that contribute to the potential. This means that if we know the potential to n-th chiral order, then there can be a two-body current which, *when not suppressed by symmetry*, is determined to the same order, further corrections being suppressed by two chiral orders. This makes the calculation of the correction terms extremely accurate. This in a nut-shell summarizes what "chiral filter" is. It will be defined more precisely below in confronting Nature. We should point out that this does not take place if the external field brings in small parameters such as external momentum or the pion mass into the current operators. It is known that this chiral filter is operative with the isovector $M1$ and the axial-charge operators in nuclei[Kubodera, Delorme and Rho 1978], but not with the isoscalar $M1$ and the Gamow-Teller operators as we will see later.

The idea of chiral filter was a guiding principle when EFT formalism was not available for nuclear physics. In chiral perturbation theory, chiral filter is automatic as pointed out in [Rho 1991], so there appears to be nothing special in it when one does a systematic chiral expansion to high enough order, but the intuitive power associated with pion dynamics is completely lost when the pion is integrated out as in the pionless EFT. An illustrative example is the thermal np capture (described below) which can be predicted without any parameters in MEEFT, but as mentioned above, can at best be postdicted with one unknown parameter in the pionless theory. Another striking case which will be discussed in Chapter 8 after introducing the notion of Brown-Rho scaling is the "Warburton ratio" in forbidden

β transitions in heavy nuclei. According to Weinberg's theorem, this process will *ultimately* be accessed by a "rigorous EFT (RigEFT)" but it will be a long time before succeeding to reach that stage. The power of MEEFT is that the notion of chiral filter allows to make a prediction quickly and painlessly without going through a horrendous labor as will be needed for a RigEFT. Moreover, even if one were able to describe certain simple processes with small uncertainty with a systematic chiral counting with or without pion, the insight and simplicity brought in by chiral filter would be lost.

4.5.4 *Working of MEEFT*

In order to illustrate how the chiral filter mechanism works out in nature, let us study the response functions in the mass number A system and where we have at our disposal accurate wave functions for $A-1$, A and $A+1$ systems. We shall do so with few-nucleon systems. For heavy nuclei and nuclear matter, we cannot proceed in the same approach and obtain a comparable accuracy. For that purpose, we need to develop the notion of "double decimation" as is done in Chapter 8.

We want to treat specifically $A = 2, 3, 4$ systems on the same footing. The processes we are interested in are

$$\begin{aligned} n + p &\to d + \gamma, \\ p + p &\to d + e^+ + \nu_e, \\ \nu_e + d &\to e^- + p + p, \\ p + {}^3\mathrm{He} &\to {}^4\mathrm{He} + e^+ + \nu_e \end{aligned} \tag{4.24}$$

and

$$\begin{aligned} e + d &\to e + d, \\ \mu({}^3\mathrm{H}) &\pm \mu({}^3\mathrm{He}). \end{aligned} \tag{4.25}$$

The processes (4.24) are of interest not only for nuclear physics but also for astrophysical studies. The first three processes were postdicted in the pionless theory with undetermined (free) parameters [Chen, Rupak and Savage 1999b; Kong and Ravndal 2001] while the last (*hep*) remains out of reach even for postdiction. The third process is one of the class of reactions for SNO processes studied in EFT [Ando, Song, Park, Fearing and Kubodera 2003], involving both the charge current (CC) processes

$$\begin{aligned} \nu_e + d &\to e^- + p + p, \\ \bar{\nu}_e + d &\to e^+ + n + n \end{aligned} \tag{4.26}$$

and the neutral current (NC) processes

$$\nu_l + d \to \nu_l + p + n,$$
$$\bar{\nu}_l + d \to \bar{\nu}_l + p + n. \tag{4.27}$$

Here the subscript l stands for e, μ, τ. These neutrino processes are very closely related to the pp process as they are governed by the same operators, albeit at different kinematics.

The processes listed in (4.25) are electromagnetic. The first, electron-deuteron scattering, can be treated in various forms of EFT with some accuracy for momentum transfers $Q^2 < 1$ GeV^2 whereas the remaining observables have been calculated parameter-free *only* in MEEFT.

All the observables of (4.24) and (4.25) have been treated in SNPA, but various calculations gave different results ranging in some cases over several orders of magnitude. The problem there was that there was no systematic way of estimating errors involved and making corrections. We will see how the chiral filter works in enabling one to make an accurate calculation for the isovector transition in the np capture and how it provides a way to approach the processes that are *not* protected by the chiral filter. All of the processes in question will be calculated $free$ of arbitrary parameters.

4.5.4.1 *What does the chiral filter say?*

Historically, it was the special role played by the "soft" pion that led to an early and simple understanding [Riska and Brown 1973] of the thermal np capture process in (4.24). The development up to date in EFT has shown that the chiral filter mechanism is automatically included in a systematic chiral expansion in MEEFT [Rho 1991], so, as mentioned, there is nothing special in it from the point of view of chiral dynamics. Even so, there is a power in it, *viz*, in pin-pointing where and in which way pions can play a prominent role in certain processes, without requiring to go to higher orders in chiral expansion ridden with unknown parameters. This was first noticed in the application of current algebras, *i.e.* soft-pion theorems, to the nuclear processes of the type given in (4.24) [Kubodera, Delorme and Rho 1978] and subsequently justified in χPT [Rho 1991]. The argument went as follows.

In MEEFT, effective currents are characterized by the number of nucleons involved in the transition. The leading one in the chiral counting is the single-particle operator – called one body or "impulse", then the next subleading one is two-particle (two-body) followed by three-particle *etc.* The Weinberg counting says that in the processes we are concerned with in the long wave-length regime, we can limit ourselves to up to two-body. We will verify that three-body and higher-body corrections can be ignored within the accuracy we are aiming at.[8] Now among two-body currents, the leading correction is given by the one-pion exchange as depicted

[8]Contrast this to the $\not\pi$EFT where n-body currents for all $n > 1$ appear at the leading order.

in Fig. 4.2. This is the longest-range correction. Shorter-ranged corrections involve

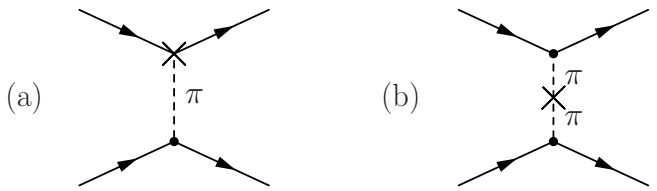

Fig. 4.2 Two-body currents with one soft-pion exchange which dominate whenever unsuppressed by kinematics or symmetry. The cross stands for the current. Both (a) and (b) contribute to the vector current but only (a) contributes to the axial current.

pion loop diagrams and corresponding counter terms to regulate the divergences as well as to account for chiral counting. If the one-pion exchange contribution can contribute unsuppressed by kinematics or symmetries, then we can estimate the leading corrections totally free of parameters. Since the πNN vertex is known, what matters then will be the vertex $\mathcal{J}_\mu \pi NN$ where $\mathcal{J}_\mu = J^a_\mu$ (vector current) or $J^a_{5\mu}$ (axial-vector current) with the index a standing for the isospin (flavor). Now the longest wavelength process that enters here is the graph with the pion being "soft." When the pion is soft, there is a low-energy theorem that gives for the vector current J^a_μ

$$\sim \mathcal{O}(\frac{\breve{q}}{m_N}) \qquad \text{for} \quad \mu = 0, \tag{4.28}$$

$$\sim \frac{g_A}{F_\pi}\epsilon^{3ab}\frac{\tau^a}{2}\sigma \quad \text{for} \quad \mu = 1,2,3 \tag{4.29}$$

and for the axial vector current $J^a_{5\mu}$

$$\sim \frac{1}{F_\pi}\epsilon^{abc}V^c_0 \quad \text{for} \quad \mu = 0, \tag{4.30}$$

$$\sim \mathcal{O}(\frac{\breve{q}}{m_N}) \qquad \text{for} \quad \mu = 1,2,3. \tag{4.31}$$

where $\breve{q}$ stands for typical momentum scale involved in the process. Here $m_N \sim 1$ GeV is the lowest baryon (*i.e.* nucleon) mass. The characteristic momentum scale involved, *i.e.* the momentum carried by the nucleon responding to the external field, is assumed to be much smaller than the baryon mass scale. What these results imply is quite simple. They say that the two-body corrections are dominated by the soft-pion exchanges in the space component of the vector current, *e.g.*, the isovector $M1$ transition and in the time component of the axial vector current, *e.g.*, the first forbidden beta transitions $J^\pm \to J^\mp$ with $\Delta T = 1$. As a corollary, we learn that the two-body currents for the time component of the vector current, *e.g.*, the

Table 4.1 Various contributions to the vector current relative to the one-body charge $V^0 \sim \mathcal{O}(1)$. The last row gives the ratio of 2-body over 1-body matrix elements.

	V^i	V^0
one-body current	$\mathcal{O}(Q^1)$	$\mathcal{O}(Q^0)$
two-body (leading)current	$\mathcal{O}(Q^2)$	$\mathcal{O}(Q^3)$
two-body (one loop)current	$\mathcal{O}(Q^4)$	$\mathcal{O}(Q^4)$
M_{2B}/M_{1B}	$\mathcal{O}(Q^1)$	$\mathcal{O}(Q^3)$

charge operator and the space component of the axial current, *e.g.*, the Gamow-Teller transition, have no reason to be suppressed. In contrast, the leading order one-body current has the opposite behavior, namely, the space component of the one-body vector current and the time component of the one-body axial current are suppressed relative to the other components. Table 4.1 illustrates the chiral orders involved for the vector current in this way of counting. A similar scaling applies to the axial current.

4.5.4.2 *Sketch of the calculational procedure*

While the calculation involves a conceptually simple procedure, the details are rather complicated. We shall therefore skip the details and, instead, present a brief sketch of the calculational procedure with a focus on the essential concepts.

In the Weinberg counting scheme, the relevant quantity is the index ν in the chiral counting of the electroweak currents. In the present case, it is sufficient to focus on "irreducible graphs" in Weinberg's classification. Irreducible graphs are organized according to the chiral index ν given by

$$\nu = 2(A - C) + 2L + \sum_i \nu_i \,, \tag{4.32}$$

where A is the number of nucleons involved in the process, C the number of disconnected parts, and L the number of loops; ν_i is the chiral index $\nu_i \equiv d_i + e + \frac{n_i}{2} - 2$ of the i-th vertex where d_i is the number of derivatives, e the number of the external field ($= 1$) and n_i the number of internal nucleon lines, all entering the i-th vertex. One can show that a diagram characterized by Eq. (4.32) involves an n_B-body transition operator, where $n_B \equiv A - C + 1$. The physical amplitude is expanded with respect to ν. The leading-order one-body GT operator belongs to ν=0. Compared with this operator, a Feynman diagram with a chiral index ν is suppressed by a factor of $(\breve{q}/\Lambda_\chi)^\nu$, where $\breve{q}$ is a typical three-momentum scale or the pion mass, and $\Lambda_\chi \sim 1$ GeV is the chiral scale. We denote this in short as Q^ν. In our case it is important to take into account also the kinematic suppression of the time component

of the nucleon four-momentum. We note

$$v \cdot p_l \sim v \cdot p_l' \sim v \cdot k_l \sim \frac{\breve{q}^2}{m_N}, \tag{4.33}$$

where p_l^μ ($p_l'^\mu$) denotes the initial (final) momentum of the l-th nucleon, and $k_l^\mu \equiv (p_l' - p_l)^\mu$. Therefore, each appearance of $v \cdot p_l$, $v \cdot p_l'$ or $v \cdot k_l$ carries two powers of $\breve{q}$ instead of one, which implies that ν increases by two units rather than one. Thus, if we denote by $q^\mu = (q_0, \mathbf{q})$ the momentum transferred to the leptonic pair in, *e.g.*, the *pp* and *hep* processes in Eqs. (4.24), then $q_0 \sim |\mathbf{q}| \sim \breve{q}^2/\Lambda_\chi \sim \mathcal{O}(Q^2)$ rather than $\mathcal{O}(Q)$ as naive counting would suggest. These features turn out to simplify the calculation considerably.

In what follows, unless stated otherwise, we will always write correction terms relative to the leading-order terms. Since the leading-order terms in the currents are of $\mathcal{O}(Q^0)$, a chiral order corresponding to the index ν will be referred to as $\mathcal{O}(Q^\nu)$. (In the literature, one finds the notation N^{n}LO with n a non-negative integer. This means n-th order term relative to the leading order without regards to the power ν. We shall also use this notation whenever there is no ambiguity.) In the discussions that follow, we shall limit ourselves to $\mathcal{O}(Q^3)$ although one can go to $\mathcal{O}(Q^4)$ for certain operators as was done in the published calculation [Park *et al.* 2003].

We now briefly sketch the structure of one-body (1B) and two-body (2B) current operators that are consistent with the chiral counting. Actual calculations involve much more involved discussions which we will simply avoid here.

The current in momentum space is written as

$$\mathcal{J}^\mu(\mathbf{q}) = J^\mu(\mathbf{q}) + J_5^\mu(\mathbf{q}) = \int d\vec{x}\, \mathrm{e}^{-i\mathbf{q}\cdot\vec{x}} \mathcal{J}^\mu(\vec{x}). \tag{4.34}$$

We shall use the notations $J^\mu = (V^0, \mathbf{V})$, $\quad J_5^\mu = (A^0, \mathbf{A})$.

Table 4.2 Contributions from each type of current at $\mathbf{q} = 0$. The entry of "–" indicates the absence of contribution. "1B-RC" stands for relativistic corrections to the one-body operators, and "2B-1L" for one-loop 2-body contributions including counter term contributions.

J^μ	$\nu = 0$	$\nu = 1$	$\nu = 2$	$\nu = 3$	$\nu = 4$
$\mathbf{A}$	1B	–	1B-RC	2B	1B-RC, 2B-1L and 3B
A^0	–	1B	2B	1B-RC	1B-RC, 2B-1L
$\mathbf{V}$	–	1B	2B	1B-RC	1B-RC, 2B-1L
V^0	1B	–	–	2B	1B-RC, 2B-1L and 3B

The chiral counting of the electroweak currents is summarized in Table 4.2, where the non-vanishing contributions at $\mathbf{q} = 0$ are indicated. This table shows how the counting goes for each component of the currents:

- $\nu = 0$: One-body $\mathbf{A}$ and V^0: $\mathbf{A}$ gives the Gamow-Teller (GT) operator, while V^0 is responsible for the charge operator.

- $\nu = 1$: One-body A^0 and $\mathbf{V}$: A^0 gives the axial-charge operator while $\mathbf{V}$ gives the $M1$ operator.
- $\nu = 2$: Two-body tree current with $\nu_i = 0$ vertices, namely, the soft-pion-exchange current. This is the leading correction protected by chiral filter to the one-body $M1$ and axial-charge operators carrying an odd orbital angular momentum.
- $\nu = 3$: Two-body tree currents with $\sum_i \nu_i = 1$. These are leading corrections to the GT and V^0 operators carrying an even orbital angular momentum. These are chiral-filter *unprotected* and hence involve constants that are not given by chiral symmetry considerations (*i.e.* soft-pion theorems) alone.
- $\nu = 4$: All the components of the electroweak current receive contributions of this order. They consist of two-body one-loop corrections as well as leading-order (tree) three-body corrections. Among the three-body currents, however, there are no six-fermion contact terms proportional to $(\bar{N}N)^3$, because there is no derivative at the vertex and hence no external field.

In this subsection we will deal with the isovector currents, returning to the isoscalar currents below.

One can easily see that the counting rule for $\mathbf{V}$ is the same as for A^0, and the counting rules for V^0 and $\mathbf{A}$ are the same. The behavior of $\mathbf{V}$ and A^0 summarized in Table 4.2 represents the chiral filter mechanism: $\mathbf{V}$ and A^0 are chiral-filter-protected. By contrast, V^0 and $\mathbf{A}$ are chiral-filter-unprotected.

We now show the explicit expressions for the relevant currents. This is to give an idea what sorts of operators are involved in view of the general discussion given above. Up to $\mathcal{O}(Q^3)$, the 1B currents in coordinate representation are well-known in the literature,

$$
\begin{aligned}
\tilde{V}^0(l) &= \tau_l^- \mathrm{e}^{-i\mathbf{q}\cdot\mathbf{r}_l}\left[1 + i\mathbf{q}\cdot\sigma_l \times \mathbf{p}_l \frac{2\mu_V - 1}{4m_N^2}\right], \\
\tilde{\mathbf{V}}(l) &= \tau_l^- \mathrm{e}^{-i\mathbf{q}\cdot\mathbf{r}_l}\left[\frac{\overline{\mathbf{p}}_l}{m_N}\left(1 - \frac{\overline{\mathbf{p}}_l^2}{2m_N^2}\right) + i\frac{\mu_V}{2m_N}\mathbf{q}\times\sigma_l + i\sigma_l \times \overline{\mathbf{p}}_l\, q_0 \frac{2\mu_V - 1}{4m_N^2}\right], \\
\tilde{A}^0(l) &= -g_A \tau_l^- \mathrm{e}^{-i\mathbf{q}\cdot\mathbf{r}_l}\left[\frac{\sigma_l\cdot\overline{\mathbf{p}}_l}{m_N}\left(1 - \frac{\overline{\mathbf{p}}_l^2}{2m_N^2}\right)\right], \\
\tilde{\mathbf{A}}(l) &= -g_A \tau_l^- \mathrm{e}^{-i\mathbf{q}\cdot\mathbf{r}_l}\left[\sigma_l + \frac{2(\overline{\mathbf{p}}_l\,\sigma_l\cdot\overline{\mathbf{p}}_l - \sigma_l\,\overline{\mathbf{p}}_l^2) + i\mathbf{q}\times\overline{\mathbf{p}}_l}{4m_N^2}\right],
\end{aligned}
\tag{4.35}
$$

where $\mu_V \simeq 4.70$ is the isovector anomalous magnetic moment of the nucleon and $\tau_l^- \equiv \frac{1}{2}(\tau_l^x - i\tau_l^y)$. The tildes in Eq. (4.35) imply that the currents are given in the coordinate space representation, and $\mathbf{p}_l = -i\nabla_l$ and $\overline{\mathbf{p}}_l = -\frac{i}{2}\left(\overrightarrow{\nabla}_l - \overleftarrow{\nabla}_l\right)$ act on the wave functions.

We next consider the two-body (2B) currents. Because of the chiral filter protection, the two-body operators $\mathbf{V}_{\rm 2B}$ and $A^0_{\rm 2B}$ are determined unambiguously. These have no unknown parameters. The processes dominated by these operators can be

calculated nearly parameter-free. The $V^0_{\rm 2B}$ operator does not appear up to the order under consideration, so we will forget it. The two-body currents that concern us are given in the center-of-mass (c.m.) frame in coordinate space with a cut-off Λ by

$$\begin{aligned}
\mathbf{V}_{12}(\mathbf{r}) &= -\frac{g_A^2 m_\pi^2}{12 f_\pi^2}\tau_\times^- \,\mathbf{r}\,\left[\sigma_1\cdot\sigma_2\, y^\pi_{0\Lambda}(r) + S_{12}\, y^\pi_{2\Lambda}(r)\right] \\
&\quad -i\frac{g_A^2}{8 f_\pi^2}\mathbf{q}\times\left[\mathcal{O}_\times y^\pi_{0\Lambda}(r) + \left(\mathcal{T}_\times - \frac{2}{3}\mathcal{O}_\times\right) y^\pi_{1\Lambda}(r)\right], \\
A^0_{12}(\mathbf{r}) &= -\frac{g_A}{4 f_\pi^2}\tau_\times^-\left[\frac{\sigma_+\cdot\hat{\mathbf{r}}}{r} + \frac{i}{2}\mathbf{q}\cdot\hat{\mathbf{r}}\,\sigma_-\cdot\hat{\mathbf{r}}\right] y^\pi_{1\Lambda}(r), \\
\mathbf{A}_{12}(\mathbf{r}) &= -\frac{g_A m_\pi^2}{2 m_N f_\pi^2}\Bigg[\left[\frac{\hat{c}_3}{3}(\mathcal{O}_+ + \mathcal{O}_-) + \frac{2}{3}\left(\hat{c}_4 + \frac{1}{4}\right)\mathcal{O}_\times\right] y^\pi_{0\Lambda}(r) \\
&\quad + \left[\hat{c}_3(\mathcal{T}_+ + \mathcal{T}_-) - \left(\hat{c}_4 + \frac{1}{4}\right)\mathcal{T}_\times\right] y^\pi_{2\Lambda}(r)\Bigg] \\
&\quad + \frac{g_A}{2 m_N f_\pi^2}\Big[\frac{1}{2}\tau_\times^-(\overline{\mathbf{p}}_1\,\sigma_2\cdot\hat{\mathbf{r}} + \overline{\mathbf{p}}_2\,\sigma_1\cdot\hat{\mathbf{r}})\frac{y^\pi_{1\Lambda}(r)}{r} \\
&\quad + \delta_\Lambda(r)\,\hat{d}^R\mathcal{O}_\times\Big],
\end{aligned} \tag{4.36}$$

where $\mathbf{r} = \mathbf{r}_1 - \mathbf{r}_2$, $S_{12} = 3\sigma_1\cdot\hat{\mathbf{r}}\,\sigma_2\cdot\hat{\mathbf{r}} - \sigma_1\cdot\sigma_2$, and

$$\mathcal{O}^k_\odot \equiv \tau^-_\odot\sigma^k_\odot, \quad \mathcal{O}_\odot \equiv \tau^-_\odot\sigma_\odot, \quad \mathcal{T}_\odot \equiv \hat{\mathbf{r}}\,\hat{\mathbf{r}}\cdot\mathcal{O}_\odot - \frac{1}{3}\mathcal{O}_\odot, \tag{4.37}$$

with

$$\odot = \pm,\times, \quad \tau^-_\odot \equiv (\tau_1\odot\tau_2)^- \equiv (\tau_1\odot\tau_2)^x - i(\tau_1\odot\tau_2)^y, \quad \sigma_\odot \equiv (\sigma_1\odot\sigma_2). \tag{4.38}$$

The cut-off dependent quantities are specified below. Note that in (4.36), it is only in $\mathbf{A}_{12}(\mathbf{r})$ that undetermined parameters appear. We will show how they can be fixed unambiguously from the accurate experiment on the triton beta decay, the crucial feature that renders the approach truly predictive.

Note that up to the order considered, the vector current is completely free of parameters to be fixed.

4.5.4.3 *How the cutoff Λ enters*

The two-body currents derived in momentum space given above are valid only up to a certain cutoff Λ. This implies that, when we go to coordinate space, the currents must be regulated. With the cutoff having a physical meaning in our scheme, there are no divergences and no perturbative counter term problem encountered in the $\not\pi$EFT. In performing Fourier transformation to derive the r-space representation of a transition operator, we can use a variety of different regulators, and physics should not be sensitive to the specific form of the regulator. A simple and convenient

regularization is of the Gaussian form

$$S_\Lambda(\mathbf{k}^2) = \exp\left(-\frac{\mathbf{k}^2}{2\Lambda^2}\right). \tag{4.39}$$

In terms of this function, the regularized delta and Yukawa functions take the form

$$\begin{aligned}
\delta^{(3)}_\Lambda(r) &\equiv \int \frac{d^3\mathbf{k}}{(2\pi)^3}\, S^2_\Lambda(\mathbf{k}^2)\, \mathrm{e}^{i\mathbf{k}\cdot\mathbf{r}}\,, \\
y^\pi_{0\Lambda}(r) &\equiv \int \frac{d^3\mathbf{k}}{(2\pi)^3}\, S^2_\Lambda(\mathbf{k}^2)\, \mathrm{e}^{i\mathbf{k}\cdot\mathbf{r}} \frac{1}{\mathbf{k}^2 + m^2_\pi}, \\
y^\pi_{1\Lambda}(r) &\equiv -r\frac{\partial}{\partial r} y^\pi_{0\Lambda}(r), \\
y^\pi_{2\Lambda}(r) &\equiv \frac{1}{m^2_\pi} r \frac{\partial}{\partial r} \frac{1}{r} \frac{\partial}{\partial r} y^\pi_{0\Lambda}(r)\,.
\end{aligned} \tag{4.40}$$

As noted above, the chiral-filter-protected operators $\mathbf{V}_{12}(\mathbf{r})$ and $A^0_{12}(\mathbf{r})$ are given by the soft-pion exchange and hence will contain the Yukawa functions. Given the wave functions, the matrix elements of these operators are unambiguously given with insignificant dependence on the cutoff due to the shorter-ranged function $y^\pi_{1\Lambda}(r)$. On the other hand, the chiral-filter-unprotected operator $\mathbf{A}_{12}(\mathbf{r})$ contains, in addition to the long-ranged Yukawa term $y^\pi_{0\Lambda}(r)$ and the short-ranged $y^\pi_{2\Lambda}(r)$ with the fixed $\hat{c}$ coefficients, (smeared) delta function terms containing the only parameter of the theory $\hat{d}^R$ as one can see from (4.36).

4.5.4.4 *Physical meaning of* Λ

Unlike in a renormalizable field theory where the cutoff is to be sent to ∞, the cutoff parameter Λ in EFT defines the physics of the system we are interested in. This is not a defect of the theory. In fact there is no strictly renormalizable field theory known in the real world; the cutoff always is finite in theories of the real world. In our case, a reasonable range of Λ may be inferred as follows. According to the general *tenet* of chiral perturbation theory (χPT), Λ larger than $\Lambda_\chi \simeq 4\pi f_\pi \simeq m_N$ has no physical meaning. In this sense, worrying about what happens when the cutoff is taken to ∞ – sometimes found in the literature of nuclear EFT – is unwarranted. Meanwhile, since the pion is an explicit degree of freedom in our scheme, Λ should be much larger than the pion mass to ascertain that genuine low-energy contributions are properly included. These considerations lead us to adopt as a natural range Λ = 500-800 MeV, in the range where the lowest-lying vector mesons intervene.

There is a subtlety in handling the delta-function appearing in the two-body currents (4.36) that we need to discuss before proceeding further. This is important particularly for our later treatment of the axial current. We will see later that a similar argument can be made for the chiral-filer unprotected vector current. For definiteness, let us take Λ = 500, 600 and 800 MeV. Now the procedure is that for each of these values of Λ one adjusts $\hat{d}^R$ – the only parameter in the theory – to

reproduce the experimental value of the triton beta decay rate Γ^t_β. To determine $\hat{d}^R$ from Γ^t_β, one calculates Γ^t_β from the matrix elements of the current operators evaluated for accurate A=3 nuclear wave functions. What is important here is to maintain consistency between the treatments of the A=2, 3 and 4 systems, including the same regularization applied to all processes. In the numerical work of [Park *et al.* 2003], the Argonne v_{18} (Av18) potential [Wiringa, Stoks and Schiavilla 1995] for all these nuclei plus the Urbana-IX (Av18/UIX) three-nucleon potential for the $A \geq 3$ systems were used. As long as the potential is "realistic" in the sense that it has the correct long-range part and fits scattering data accurately, it should not matter what potential one uses. This is guaranteed by the RGE argument on V_{low-k} reviewed in [Brown and Rho 2004a; Brown, Holt, Lee and Rho 2006]. If it were to have an appreciable dependence, it would mean simply that the scheme could not be trusted.

The values of $\hat{d}^R$ determined in this manner are:

$$\begin{aligned} \hat{d}^R &= 1.00 \pm 0.07 \qquad \text{for } \Lambda = 500 \text{ MeV}, \\ \hat{d}^R &= 1.78 \pm 0.08 \qquad \text{for } \Lambda = 600 \text{ MeV}, \\ \hat{d}^R &= 3.90 \pm 0.10 \qquad \text{for } \Lambda = 800 \text{ MeV}, \end{aligned} \tag{4.41}$$

where the errors correspond to the experimental uncertainty in Γ^t_β. Note that they vary widely as a function of the cut-off. These values determined in the three-body system will be used below in both two-body and four-body systems.

4.5.5 *Predictions of MEEFT*

4.5.5.1 *Thermal np capture*

We first look at the case where a clean prediction can be made free of short-distance ambiguity, *i.e.* the total cross section at thermal energy for the well-known process

$$n + p \to d + \gamma. \tag{4.42}$$

Here the isovector $M1$ operator dominates. There are corrections from the isoscalar currents (isoscalar $M1$ and $E2$, see Eq. (4.48)) but they are suppressed by three orders of magnitude, so to the accuracy involved, we can ignore them for the total cross section. The calculation presented here represents a χPT improvement on the earlier Riska-Brown work [Riska and Brown 1973] which exploited the Chemtob-Rho procedure [Chemtob and Rho 1971]. In the next subsection, we will discuss the polarization observables for which the isoscalar currents figure prominently.

As was first predicted in [Kubodera, Delorme and Rho 1978], the isovector $M1$ operator has the chiral filter protection, so the principal correction to the leading one-body $M1$ operator of $\mathcal{O}(Q)$ – relative to the one-body term as prescribed above – comes from a one soft-pion exchange graph at $\mathcal{O}(Q^2)$. One can verify that the next chiral correction comes at $\mathcal{O}(Q^4)$. (There are corrections of $\mathcal{O}(Q^3)$ but they are

in principle known since they are relativistic corrections to the one-body current.) With the $\mathcal{O}(Q^4)$ one-loop corrections to the vertices, the chiral filter argument predicts simply that the one-pion exchange with the parameters completely fixed by chiral symmetry should dominate the two-body current. There is also a small $\mathcal{O}(Q^4)$ correction coming from one-loop graph involving two-pion exchanges. The result of the calculation which involves only the cutoff to be taken care of, here represented by the cut-off radius in coordinate space (referred in nuclear physics to as "hard-core radius"), is given in Fig. 4.3 from [Park, Min and Rho 1995].[9] The various contributions given therein correspond to the following. The "tree"

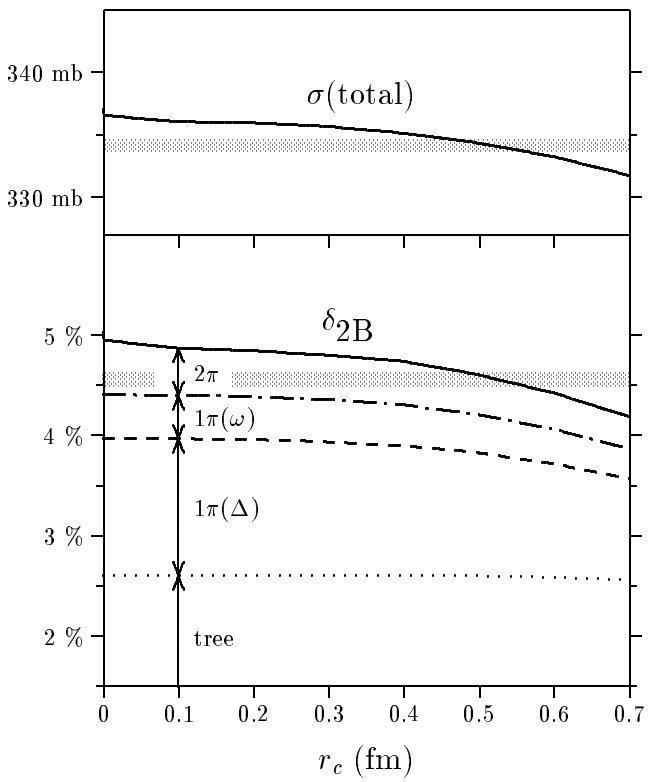

Fig. 4.3 Total capture cross section $\sigma_{\rm cap}$ (top) and the corrections relative to the single-particle $M1$ matrix elements denoted δ's (bottom) vs. the cut-off r_c. The solid line represents the total contributions and the experimental values are given by the shaded band indicating the error bar. The dotted line gives $\delta_{\rm tree}$, the dashed line $\delta_{\rm tree} + \delta_{1\pi}^{\Delta}$, the dot-dashed line $\delta_{\rm tree} + \delta_{1\pi} = \delta_{\rm tree} + \delta_{1\pi}^{\Delta} + \delta_{1\pi}^{\omega}$ and the solid line the total ratio, $\delta_{\rm 2B}$.

[9]The use of the hard-core cutoff $r_c \neq 0$ suppressed a contact $\mathcal{O}(Q^4)$ term which should be there. Since it is a term with its range shorter than that given by the hard core radius, it was assumed to be subsumed in the error bar assigned to it based on the variation over the range of radii considered. This problem is treated with more rigor in [Song, Lazauskas, Park and Min 2007] in calculating the magnetic moments of the trinucleons. We will come back to this problem.

corresponds to the soft one-pion exchange term (of $\mathcal{O}(Q)$) with the constants at the vertices given by renormalized quantities that can be picked from experiments. The terms with $1\pi(\omega, \delta)$ represent one pion exchange with the vertices resonance-saturated with the ω and Δ. The "2π" represents 2π exchange one-loop corrections of $\mathcal{O}(Q^4)$.

Note the remarkably weak dependence on the cut-off radius r_c, ranging from 0 to 0.7 fm which we can take as an *à posteriori* check of the consistency of the procedure. Taking into account the variation over this range as a measure of the error involved in the calculation, the prediction is

$$\sigma_{th} = 334 \pm 2 \ \text{mb} \tag{4.43}$$

to be compared with the experimental value

$$\sigma_{ex} = 334.2 \pm 0.5 \ \text{mb}. \tag{4.44}$$

By fully taking into account the $\mathcal{O}(Q^4)$ terms and with a more careful treatment of the cutoff as is done below (for the trinucleon magnetic moments), one could bring the accuracy of the theory within the experimental uncertainty.

4.5.5.2 *Polarization observables in np capture*

We now turn to the case where while the chiral filter protection is not available, one can still make a rather accurate prediction. Together with the *hep* process discussed below, this represents a highly non-trivial case where the MEEFT works surprisingly well. It concerns the isoscalar matrix elements in the *np* capture process (4.42) which contribute insignificantly to the total capture rate and hence are ignored in giving the theoretical value but could be measured. The process involved is the polarized process

$$\vec{n} + \vec{p} \to d + \gamma. \tag{4.45}$$

We discuss, based on the work of [Park, Kubodera, Min and Rho 2002], how a parameter-free prediction on spin-dependent observables of this process at threshold can be made.

To bring out the main points of the calculation, we need to specify in more detail than what we did above for the total capture rate, what sorts of matrix elements are involved.

The process (4.45) receives, apart from contributions from the isovector $M1$ matrix element (M1V) between the initial ${}^1S_0$ ($T = 1$) and the final deuteron ($T = 0$) state, the isoscalar $M1$ matrix element (M1S) and the isoscalar $E2$ (E2S) matrix element between the initial ${}^3S_1$ ($T = 0$) and the final deuteron ${}^3S_1 - {}^3D_1$ states. While the spin-averaged cross section $\sigma_{unpol}(np \to d\gamma)$ is totally dominated by M1V, since the initial ${}^1S_0$ state has $J = 0$, the M1V cannot yield spin-dependent

effects, whereas M1S and E2S can. This means that the spin-dependent observables in (4.45) are extremely sensitive to small isoscalar matrix elements.

We recall that the isoscalar matrix elements, M1S and E2S, are examples of the "chiral-filter unprotected" observable. Furthermore it is well known that the one-body contribution of M1S is highly suppressed due to the orthogonality between the initial ${}^3S_1$ and the final deuteron state, in addition to the small isoscalar magnetic moment of the nucleon. The soft-pion exchange is also suppressed, there being no isoscalar $\mathcal{B}^\mu \pi NN$ vertex in the leading order chiral Lagrangian, where $\mathcal{B}^\mu$ is the external isoscalar field that couples to the baryonic current. Due to this double suppression, the size of M1S becomes even comparable to that of E2S, which is a higher-order multipole and hence, in normal circumstances, can be ignored. This situation suggests that we must go up to an unusually high chiral order before getting sensible estimates of the isoscalar matrix elements that govern the spin observables in (4.45). However, remarkably, MEEFT allows us to make a systematic and reasonably reliable estimation of M1S and E2S with no free parameters.

We write the transition amplitude as

$$\langle \psi_d, \gamma(\hat{k},\lambda)|\mathcal{T}|\psi_{np}\rangle = \chi_d^\dagger \, \mathcal{M}(\hat{k},\lambda)\, \chi_{np} \tag{4.46}$$

with

$$\begin{aligned}\mathcal{M}(\hat{k},\lambda) = \; & \sqrt{4\pi}\frac{\sqrt{v_n}}{2\sqrt{\omega}A_s}\Big[i(\hat{k}\times\hat{\epsilon}_\lambda^*)\cdot(\sigma_1-\sigma_2)\,\mathrm{M1V} \\ & -i(\hat{k}\times\hat{\epsilon}_\lambda^*)\cdot(\sigma_1+\sigma_2)\,\frac{\mathrm{M1S}}{\sqrt{2}} \\ & +(\sigma_1\cdot\hat{k}\sigma_2\cdot\hat{\epsilon}_\lambda^* + \sigma_2\cdot\hat{k}\sigma_1\cdot\hat{\epsilon}_\lambda^*)\frac{\mathrm{E2S}}{\sqrt{2}}\Big]\end{aligned} \tag{4.47}$$

where v_n is the velocity of the projectile neutron, A_s is the deuteron normalization factor $A_s \simeq 0.8850$ fm$^{-1/2}$, and χ_d (χ_{np}) denotes the spin wave function of the final deuteron (initial np) state. The emitted photon is characterized by the unit momentum vector $\hat{k}$, the energy ω and the helicity λ, and its polarization vector is denoted by $\hat{\epsilon}_\lambda \equiv \hat{\epsilon}_\lambda(\hat{k})$. The amplitudes M1V, M1S and E2S represent the isovector $M1$, isoscalar $M1$ and isoscalar $E2$ contributions, respectively.[10] These quantities are defined in such a manner that they all have the dimension of length, and the cross section for the unpolarized np system takes the form

$$\sigma_{unpol} = |\mathrm{M1V}|^2 + |\mathrm{M1S}|^2 + |\mathrm{E2S}|^2 \,. \tag{4.48}$$

As shown above, the isovector $M1$ amplitude was calculated [Park, Min and Rho 1995] very accurately up to $\mathcal{O}(Q^3)$. The result expressed in terms of M1V is: $\mathrm{M1V} = 5.78 \pm 0.03$ fm, which should be compared to the empirical value $\sqrt{\sigma_{unpol}^{exp}} = 5.781 \pm 0.004$ fm. So we need to focus on the isoscalar matrix elements. The isoscalar

[10] These amplitudes are real at threshold.

matrix elements are given by

$$\begin{aligned} \text{M1S} &\equiv -\frac{\sqrt{2}\omega^{\frac{3}{2}}}{\sqrt{v_n}}\langle\psi_d^{J_z=1}|\mu^z|\psi_t^{J_z=1}\rangle, \\ \text{E2S} &\equiv \frac{\omega^{\frac{5}{2}}}{\sqrt{8}\sqrt{v_n}}\langle\psi_d^{J_z=1}|Q^{33}|\psi_t^{J_z=1}\rangle \end{aligned} \tag{4.49}$$

with

$$\begin{aligned} \vec{\mu} &= \frac{1}{2}\int d^3\vec{x}\,\vec{x}\times\mathbf{J}_{\rm EM}(\vec{x}), \\ Q^{ij} &= \int d^3\vec{x}\,(3x^ix^j-\delta^{ij}\vec{x}^2)J^0_{\rm EM}(\vec{x}), \end{aligned} \tag{4.50}$$

where $J^\mu_{\rm EM}(\vec{x})$ is the EM current. Now the measurable quantities are the photon circular polarization P_γ and the anisotropy η_γ defined in terms of the angular distribution of photons with helicity $\lambda=\pm1$ denoted $I_\lambda(\theta)$ where θ is the angle between $\hat{k}$ (direction of photon emission) and a quantization axis of nucleon polarization. For polarized neutrons with polarization $\vec{P}_n$ incident on unpolarized protons, P_γ is defined by

$$P_\gamma \equiv \frac{I_{+1}(0^\circ)-I_{-1}(0^\circ)}{I_{+1}(0^\circ)+I_{-1}(0^\circ)}\,. \tag{4.51}$$

With both protons and neutrons polarized (along a common quantization axis) with polarizations $\vec{P}_n$ and $\vec{P}_p$, respectively, the anisotropy η_γ is defined by

$$\eta_\gamma \equiv \frac{I(90^\circ)-I(0^\circ)}{I(90^\circ)+I(0^\circ)}\,, \tag{4.52}$$

where $I(\theta)=I_{+1}(\theta)+I_{-1}(\theta)$ is the angular distribution of total photon intensity (regardless of their helicities). These quantities are given in terms of $\vec{P}_{p,n}$ and the ratios of matrix elements

$$\mathcal{R}_{\rm M1}\equiv\frac{\rm M1S}{\rm M1V}\,,\quad \mathcal{R}_{\rm E2}\equiv\frac{\rm E2S}{\rm M1V}\,. \tag{4.53}$$

See [Park, Kubodera, Min and Rho 2002] for explicit formulas.

The matrix elements M1S and E2S have been computed to $\mathcal{O}(Q^4)$ in the chiral counting defined above that involves up to one-loop graphs. It turns out, to the order considered, that E2S is given entirely by the one-body matrix elements, with the two-body correction estimated to be $\text{E2S}_{\rm 2B}=(0.00\pm0.01)\times10^{-3}$ fm for the whole range of $r_c=(0.01\sim0.8)$ fm. Combining the one-body and two-body contributions, it is found to be

$$\text{E2S}=(1.40\pm0.01)\times10^{-3}\text{ fm}. \tag{4.54}$$

Thus the most interesting quantity is the two-body contribution to M1S denoted $\text{M1S}_{\rm 2B}$. One naively would think that there would be too many parameters to the

chiral order involved to make a parameter-free prediction. It turns out, however, that this is not the case. There is one unknown parameter that appears at $\mathcal{O}(Q^3)$ in the form of a contact counter term denoted g_4' in [Park, Kubodera, Min and Rho 2002] that, however, can be determined entirely by the (isoscalar) deuteron magnetic moment. This means that apart from the cut-off Λ or r_c in the coordinate space, there is no unknown parameter in the theory. $\mathrm{M1S}_{\mathrm{2B}}$ is of the form

$$\mathrm{M1S}_{\mathrm{2B}} = a(r_c) + g_4' b(r_c) \tag{4.55}$$

where both $a(r_c)$ and $b(r_c)$ diverge for $r_c \to 0$, but otherwise are completely determined for any $r_c \neq 0$. The second term comes from the contact (counter) term which is of delta function in coordinate space. The premise of the consistency of EFT dictates that the sum of the total MS1=$\mathrm{MS1}_{\mathrm{1B}}$+$\mathrm{MS1}_{\mathrm{2B}}$ be insensitive to the cut-off r_c within the physically reasonable range defined above. This is indeed what comes out. For the wide-ranging values of $r_c = 0.01, 0.2, 0.4, 0.6, 0.8$ fm, fitting to the deuteron magnetic moment requires the corresponding g_4' to be $g_4' = 5.06, 2.24, 0.73, 0.31$. Again, although the g_4' varies strongly in the range considered, the total M1S varies negligibly: M1S$\times 10^3$ fm^{-1} = $-$(2.849, 2.850, 2.852, 2.856, 2.861). This allows to predict the M1S to a high accuracy:

$$\mathrm{M1S} = (-2.85 \pm 0.01) \times 10^{-3} \text{ fm}\,, \tag{4.56}$$

where the error bar stands for the r_c-dependence.

This accurate prediction has, however, remained untested experimentally. We should underline at this point that exactly the same situation will arise in the solar *pp* and *hep* calculation that will be given below.

It is interesting to compare the surprisingly precise prediction (4.56) with what one obtains in $\not\pi$EFT[Chen, Rupak and Savage 1999b]. Because of the dominance of the single-particle matrix element with the next-order corrections suppressed, one obtains roughly the same E2S in $\not\pi$EFT as in MEEFT. The situation is quite different, however, for M1S. Here due to the "accidental" suppression of the leading order (one-body) isoscalar $M1$ operator, the next-order term, though down formally by $\mathcal{O}(Q^3)$, is substantially bigger than naively expected. Thus in the $\not\pi$EFT calculation, the leading order correction cannot be completely pinned down by the deuteron magnetic moment alone as in the case of MEEFT. There is an undetermined constant which cannot be taken into account, making the calculation of the M1S uncertain by $\sim 60\%$ or more. Thus both M1V and M1S are not truly predictable in the $\not\pi$EFT approach.

4.5.5.3 *Deuteron form factors*

An objection may be raised at this point against the above claim of success on the basis of (in)consistency in the chiral counting. The highly "sophisticated" wave function that is used in the calculation can in principle account for *all* orders of chiral expansion in the relevant kinematic regime, whereas the currents are calculated to

a finite order N^{n}LO for $n < \infty$. This means that there is in a strict sense an inconsistency in chiral counting at order $n+1$. Given that *all* calculations based on systematic expansion involve truncation at a certain level of accuracy, none of *any* "precise" theoretical results can rigorously claim to be *entirely* consistent. So the relevant question is: Is the possible inconsistency serious?

There is no fully satisfactory answer to this question in the case at hand. Here we would like to show that at least within the few-body systems we are discussing here, there is no indication for serious inconsistency. To illustrate this point, we take the well-tested case of the electron-deuteron elastic scattering

$$e + d \to e + d \tag{4.57}$$

at low momentum transfers $Q = \sqrt{-q^2} \lesssim 0.8$ GeV. This process has been analyzed both in RigEFT and in MEEFT with the currents computed to $\mathcal{O}(Q^3)$. At the end of this subsection, we will comment on how one can understand the well-known "Q_d problem" in terms of the chiral filter mechanism.

The process (4.57) involves precisely the same EM current that figured in the polarization observables in the *np* capture (4.45) discussed above. It is isoscalar and hence in the terminology introduced above, multi-body corrections are chiral-filter unprotected. This means that relative to the leading one-body (isoscalar) current – which is "accidentally" suppressed by the isoscalar magnetic moment of the nucleon, the corrections are suppressed at least by $\mathcal{O}(Q^2)$. At that order, short-distance dynamics uncontrollable by chiral symmetry plays an extremely important role as we saw above and will encounter again below. As remarked, one expects that it is in processes that are not protected by chiral filter that the possible inconsistency in chiral counting of MEEFT, if any, should show up.

Our chief point can be made based on the work by Phillips [Phillips 2007]. In this work, it was found that the ratios of the form factors provided more useful information on the working of EFT than the form factors by themselves. Our discussion will focus on both the comparison between the RigEFT and MEEFT in their *confronting* experimental data.

To define notations, we write the differential cross section for electron-deuteron scattering in the lab frame as

$$\frac{d\sigma}{d\Omega} = \frac{d\sigma}{d\Omega}_0 \left[A(Q^2) + B(Q^2) \tan^2\left(\frac{\theta_e}{2}\right) \right]. \tag{4.58}$$

Here θ_e is the electron scattering angle, and $\frac{d\sigma}{d\Omega}_0$ is the cross section for electron scattering from a point particle of charge $|e|$ and mass M_d, *i.e.* the deuteron mass, in one-photon exchange approximation. The Coulomb (C), electric quadrupole (Q)

and magnetic (M) form factors figure in A and B as

$$A = G_C^2 + \frac{2}{3}\eta G_M^2 + \frac{8}{9}\eta^2 M_d^4 G_Q^2, \tag{4.59}$$

$$B = \frac{4}{3}\eta(1+\eta)G_M^2 \tag{4.60}$$

with $\eta = Q^2/(4M_d^2)$. These form factors are normalized so that at zero momentum transfer,

$$G_C(0) = 1, \tag{4.61}$$

$$G_Q(0) = Q_d, \tag{4.62}$$

$$G_M(0) = \mu_d \frac{M_d}{m_N}, \tag{4.63}$$

where Q_d is the quadrupole moment and μ_d the magnetic moment of the deuteron. The ratios in question

$$\frac{G_C}{G_E^{(s)}} \quad \text{and} \quad \frac{G_Q}{G_E^{(s)}} \quad \text{and} \quad \frac{G_M}{G_M^{(s)}}, \tag{4.64}$$

with $G_E^{(s)}$ and $G_M^{(s)}$ the isoscalar single-nucleon electric and magnetic form factors, respectively, are argued to be better behaved than the chiral expansion for G_C, G_Q and G_M themselves.

We will focus on the calculations performed to $\mathcal{O}(Q^3)$ for the potential and for the current in one-photon-exchange approximation.[11] At higher orders, the g_4'-type corrections enter crucially in G_M which we will not consider.

As given, we mean by RigEFT the calculation of the form factors with the wave functions obtained with a potential computed up to $\mathcal{O}(Q^3)$ and the currents computed to the same order. This represents a fully consistent EFT. By MEEFT, we mean calculating the matrix elements with the current computed to order $\mathcal{O}(Q^3)$ and the wave functions obtained with SNPA potentials, *i.e.* the "high-quality realistic potentials." The SNPA potentials used by Phillips are the Nijm93 [Stoks, Klomp, Terheggen and de Swart 1994] and CD-Bonn [Machleidt 2001] potentials. These potentials have the common feature of having correct long-range part (*i.e.* one pion exchange) with differing short-range part but fit to NN scattering to momenta ~ 2 fm^{-1}. This feature is shared by other high-quality potentials such as the Argonne v_{18} potential [Wiringa, Stoks and Schiavilla 1995] used in the solar neutrino processes described below. We take the Nijm93 and CD-Bonn potentials as representative "accurate" potentials.

In Fig. 4.4 is reproduced the charge form factor up to momentum transfer of $Q \sim 0.8$ fm^{-1}. In Fig. 4.5 is given the ratio G_C/G_Q.

[11] One can count this as we have done above for the currents as relative to the leading order charge operator which is of $\mathcal{O}(Q^0)$.

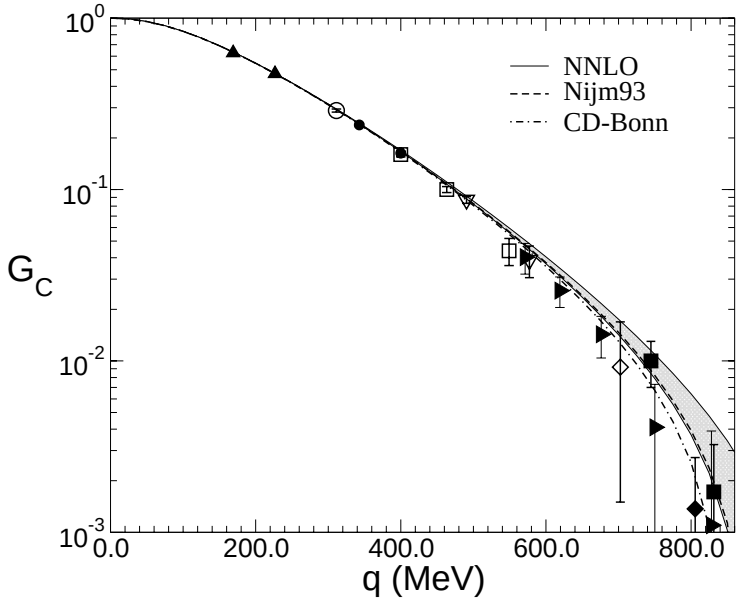

Fig. 4.4 Results for the charge form factor G_C as a function of $|\mathbf{q}| \equiv \sqrt{Q^2}$ from [Phillips 2007] (copyright 2006 by IOP Publishing Ltd). Here "NNLO" represents RigEFT computed to $\mathcal{O}(Q^3)$ in the convention used here. The shaded area indicates the range of uncertainty in the theoretical values. "Nijm93" and "CD-Bonn" represent MEEFT with the given potentials, the difference between the two indicating, roughly, the uncertainty involved in MEEFT. For the experimental data and more details of the calculations, see [Pillips 2007].

It is clear in comparing various calculations described in detail in [Phillips 2007] and the experimental data that due to large error bars of the experimental form factors, it is not possible to discriminate the optimal RigEFT results and the MEEFT results. Nor is it possible to gauge whether there is any serious inconsistency in the EFT counting rule which is inevitable in MEEFT. Indeed the uncertainty in MEEFT which may be manifested in the difference between two "reliable" potentials employed in [Phillips 2007], here represented by the Nijm93 and CD-Bonn potentials, is shown to be considerably less than the uncertainty manifested in different treatments of higher-order terms in the RigEFT approach. In fact, within the present precision of the experimental data, it seems reasonable to conclude that the MEEFT is superior in predictiveness to RigEFT. As mentioned, this is a case of chiral-filter unprotected processes, which can be subject to errors caused by the counting inconsistency.

One lesson we can draw from the consideration of the deuteron EM form factors is that it illustrates the subtle nature of the chiral filter mechanism, manifested as the "two sides of the same coin." Consider for this the $E2$ response of deuterium as we discussed above for both the polarized np capture process and the deuteron

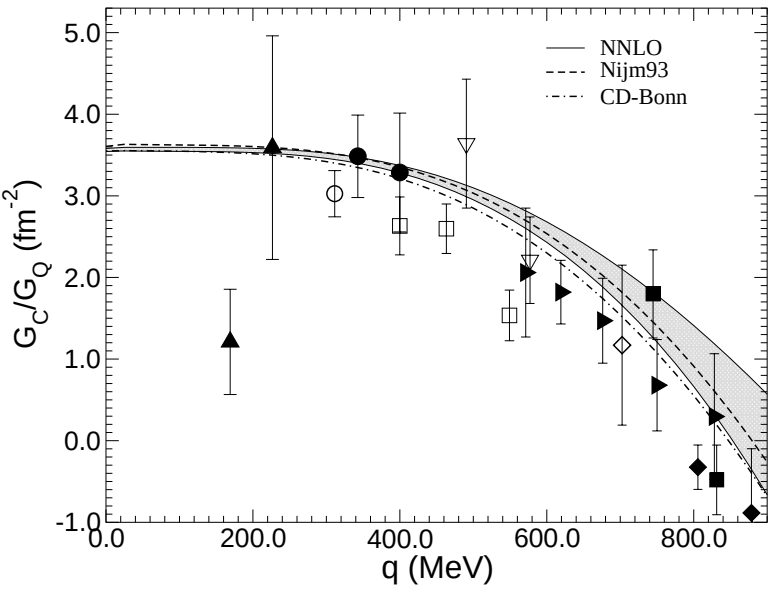

Fig. 4.5 Results for the ratio G_C/G_Q. See Fig. 4.4 for notations and reference.

EM form factors. As noted above, the $E2$ matrix element (denoted E2S) for the np capture is calculable in both ⧸EFT and MEEFT up to the chiral order that involves no free parameters (*i.e.* $\mathcal{O}(Q^3)$ in MEEFT). This is easy to see with the pions included. One notes that the $1/m_N$ corrections which come at $\mathcal{O}(Q^3)$ are essentially governed by chiral symmetry (*i.e.* pions) and Poincaré invariance and hence more or less model-independent [Phillips 2007]. Furthermore the next-order terms, *i.e.* of $\mathcal{O}(Q^4)$, are also calculable parameter-free as shown by Park *et al.* However the resulting prediction for the deuteron quadrupole moment Q_d undershoots the experiment by 2-3%. This is a "huge" discrepancy considering the accuracy achieved in the $M1$ matrix elements. As suggested by Phillips [Phillips 2007], the possible solution to this "Q_d problem" is in zero-range $\mathcal{O}(Q^5)$ terms – with, however, undetermined coefficients – that represent short-distance physics in a way analogous to the g_4' term in the isoscalar $M1$ transitions discussed above and the $\hat{d}^R$ term in the isovector Gamow-Teller transitions discussed below. What is common in all the cases considered here is that the single-particle matrix elements are unnaturally suppressed, making correction terms particularly important, sometimes even dominant. Now, when chiral-filter protected, the leading corrections dictated by chiral symmetry dominate and hence account for most, if not all, of the required matrix elements. However when chiral-filter unprotected as in the Q_d case in question, even though one may be able to calculate, free of parameters, one or two next-order corrections which are intrinsically suppressed to start with, they do not saturate the

corrections. One has to go to an arbitrarily high order generated by short-distance interactions before the corrections can, if at all, be put under control.

4.5.5.4 *Predicting the solar neutrino processes*

Now we are ready to make a precise statement on the key prediction of the MEEFT approach. They are the solar *pp* and *hep* processes. We note here that the calculation of the *hep* process has not yet been achieved by the RigEFT method.

To treat the axial-current entering in these processes, we need to fix the unknown constants in the axial two-body operator (4.36), *i.e.* $\mathbf{A}_{12}(\mathbf{r})$. Now in $\mathbf{A}_{12}(\mathbf{r})$, $\hat{c}_{3,4}$ are fixed from $\pi - N$ scattering, so that leaves only one parameter to be fixed, *i.e.* $\hat{d}^R$, multiplying the delta function term. Actually there are two unknown terms $\hat{d}_{1,2}$ in $\mathbf{A}_{12}(\mathbf{r})$ originating from a term of the form in the current

$$-\frac{g_A}{m_N f_\pi^2}\left[2\hat{d}_1(\tau_1^- \sigma_1 + \tau_2^- \sigma_2) + \hat{d}_2 \tau_\times^a \sigma_\times\right] \tag{4.65}$$

but it turns out from Fermi statistics that only one combination

$$\hat{d}^R \equiv \hat{d}_1 + 2\hat{d}_2 + \frac{1}{3}\hat{c}_3 + \frac{2}{3}\hat{c}_4 + \frac{1}{6} \tag{4.66}$$

figures in all the relevant processes that we are concerned with. This parameter $\hat{d}^R$ is analogous to g_A' that figures in the isoscalar *np* capture treated above. The argument why this is the only relevant combination is given in the paper [Park *et al.* 2003] which should be consulted for details. It follows from symmetry considerations.

Once $\hat{d}^R$ is fixed by fitting a well-measured quantity in a specific system, *i.e.* the triton beta decay in the present case, then it is fixed *once and for all independently of the mass number* involved. The corresponding matrix element is determined for *any* system given the wave functions. The reason for the universality of $\hat{d}^R$ (and also g_A') is that the corresponding operator is shorter-ranged and hence should be independent of the density of the system as long as the probe momentum, *e.g.*, the Fermi momentum, is much less than the cutoff scale. If there were uncertainty due to regularization which would be the case if there were a strong mismatch in the chiral counting between the wave functions which are obtained by empirical fits and the current operators which are computed to a certain order in the chiral counting, then physical quantities would exhibit dependence on the cutoff, that is, on the regulator. Thus an *à posteriori* justification of the procedure would be the cutoff independence. This is not a rigorous justification, but it is the best one can do in any effective theories which limited to a finite order, are, by definition, an approximation.

We illustrate how this strategy works for the second (and third) and fifth processes of (4.24) relevant to solar neutrino problems.

• **The pp process:**

We will here focus on the pp process. The same argument applies to the neutrino processes (4.26) and (4.27). We decompose the matrix element of the GT operator into one-body and two-body parts

$$\mathcal{M} = \mathcal{M}_{1\mathrm{B}} + \mathcal{M}_{2\mathrm{B}} \ . \tag{4.67}$$

Since the one-body term is independent of the cutoff and very well known in SNPA, we discuss only the two-body term.

The properly regularized two-body GT matrix elements for the pp process read

$$\begin{aligned}
\mathcal{M}_{2\mathrm{B}} = \frac{2}{m_N f_\pi^2}\int_0^\infty dr\ \Big\{\ & \frac{m_\pi^2}{3}\left(\hat{c}_3 + 2\hat{c}_4 + \frac{1}{2}\right) y^\pi_{0\Lambda}(r)\, u_d(r)\, u_{pp}(r) \\
& -\sqrt{2}\frac{m_\pi^2}{3}\left(\hat{c}_3 - \hat{c}_4 - \frac{1}{4}\right) y^\pi_{2\Lambda}(r)\, w_d(r)\, u_{pp}(r) \\
& +\frac{y^\pi_{1\Lambda}(r)}{12r}\Bigg[\Big[u_d(r) - \sqrt{2}w_d(r)\Big]\, u'_{pp}(r) \\
& -\Big[u'_d(r) - \sqrt{2}w'_d(r)\Big]\, u_{pp}(r) + \frac{3\sqrt{2}}{r} w_d(r) u_{pp}(r)\Bigg] \\
& - \hat{d}^R \delta^{(3)}_\Lambda(r)\, u_d(r) u_{pp}(r)\ \Big\},
\end{aligned} \tag{4.68}$$

where $u_d(r)$ and $w_d(r)$ are the S- and D-wave components of the deuteron wave function, and $u_{pp}(r)$ is the ${}^1\mathrm{S}_0$ pp scattering wave (at zero relative energy). The results are given for the three representative values of Λ in Table 4.3; for convenience, the values of $\hat{d}^R$ given in Eq. (4.41) are also listed. The table indicates that, although the value of $\hat{d}^R$ is highly sensitive to Λ, $\mathcal{M}_{2\mathrm{B}}$ is surprisingly stable against the variation of Λ within the stated range. In view of this high stability, we believe that we are on the conservative side in adopting the estimate $\mathcal{M}_{2\mathrm{B}} = (0.039 \sim 0.044)$ fm. Since the leading single-particle term is independent of Λ, the total amplitude $\mathcal{M} = \mathcal{M}_{1\mathrm{B}} + \mathcal{M}_{2\mathrm{B}}$ is Λ-independent to the same degree as $\mathcal{M}_{2\mathrm{B}}$. The Λ-independence of the physical quantity $\mathcal{M}$ is a crucial feature of the result in our present study. The relative strength of the two-body contribution as compared with the one-body contribution is

$$\delta_{2\mathrm{B}} \equiv \frac{\mathcal{M}_{2\mathrm{B}}}{\mathcal{M}_{1\mathrm{B}}} = (0.86 \pm 0.05)\ \%. \tag{4.69}$$

Despite that this process is not protected by the chiral filter, we have achieved an accuracy unprecedented in nuclear physics. This aspect will be exploited for the case of the *hep* process below.

We now give, for completeness, the threshold S factor, $S_{pp}(0)$, needed for solar neutrino processes. Adopting the accurately determined value $G_V = (1.14939 \pm$

$0.00065) \times 10^{-5}$ GeV^{-2}, we obtain

$$S_{pp}(0) = 3.94 \times \left(\frac{1+\delta_{2B}}{1.01}\right)^2 \left(\frac{g_A}{1.2670}\right)^2 \left(\frac{\Lambda_{pp}^2}{6.91}\right)^2$$
$$= 3.94 \times (1 \pm 0.0015 \pm 0.0010 \pm \epsilon) \tag{4.70}$$

in units of 10^{-25} MeV-b. Here the first error is due to uncertainties in the input parameters in the one-body part, while the second error represents the uncertainties in the two-body part; $\epsilon(\approx 0.001)$ denotes possible uncertainties due to higher chiral order contributions. To make a formally rigorous assessment of ϵ, we must evaluate loop corrections and higher-order counter terms. Although an $\mathcal{O}(Q^4)$ calculation would not involve any new unknown parameters, it is a non-trivial task. Furthermore loop corrections necessitate a more elaborate regularization scheme since the naive cutoff regularization used here violates chiral symmetry at loop orders. (This difficulty, however, is not insurmountable.) All these caveats notwithstanding, a careful analysis indicates that the error quoted above is most likely conservative.

It is somewhat surprising that the short-range physics is so well controlled in MEEFT at the order considered. In the conventional treatment of MEC, one derives the coordinate space representation of a MEC operator by applying ordinary Fourier transformation (with no restriction on the range of the momentum variable) to the amplitude obtained in momentum space; this corresponds to setting $\Lambda = \infty$ in Eq. (4.39). Short-range correlation has to be implemented in an ad hoc manner to account for the short-distance ignorance. In MEEFT, the inclusion of the $\hat{d}^R$ term, with its strength renormalized as described here, properly takes into account the short-range physics inherited from the integrated-out degrees of freedom above the cutoff, thereby drastically reducing the undesirable (or unphysical) sensitivity to short-distance physics. It is undoubtedly correct to say that this procedure is not rigorously justified on the basis of strict chiral counting but it should be stressed that what we might call "ansatz" as it stands is a giant leap from the SNPA prescription for "short-range correlation."

- **The *hep* process:**

This process is a lot more complicated than the *pp* process involving up to four nucleons, both in bound and scattering states. n-body currents for $n = 3, 4$

Table 4.3 The strength $\hat{d}^R$ of the contact term and the two-body GT matrix element, $\mathcal{M}_{2B}$, for the *pp* process calculated for representative values of Λ.

Λ (MeV)	$\hat{d}^R$	$\mathcal{M}_{2B}$ (fm)
500	1.00 ± 0.07	$0.076 - 0.035\ \hat{d}^R \simeq 0.041 \pm 0.002$
600	1.78 ± 0.08	$0.097 - 0.031\ \hat{d}^R \simeq 0.042 \pm 0.002$
800	3.90 ± 0.10	$0.129 - 0.022\ \hat{d}^R \simeq 0.042 \pm 0.002$

could be calculated but are ignored in the discussion given here, since they are of higher chiral order than what is considered. To make contact with the literature and also to avoid crowding with unilluminating formulas, we use the notation of the classic SNPA paper on the subject (MSVKRB in short) [Marcucci *et al.* 2001], focusing on the essential part of our MEEFT strategy. The GT-amplitudes will be given in terms of the reduced matrix elements, $\overline{L}_1(q;A)$ and $\overline{E}_1(q;A)$.[12] Since these matrix elements are related to each other as $\overline{E}_1(q;A) \simeq \sqrt{2}\,\overline{L}_1(q;A)$, with the exact equality holding at q=0, we consider here only one of them, $\overline{L}_1(q;A)$. For the three exemplary values of Λ, Table 4.4 gives the corresponding values of $\overline{L}_1(q;A)$ at $q \equiv |\mathbf{q}|$=19.2 MeV and zero c.m. energy; for convenience, the values of $\hat{d}^R$ in Eq. (4.41) are also listed. We see from the table that the variation of the two-body GT amplitude (row labeled "2B-total") is only ∼10% for the range of Λ under study. It should be pointed out that the Λ-dependence in the total GT amplitude is made more pronounced by the drastic but "accidental" cancelation between the one-body and two-body terms, but this amplified Λ-dependence still lies within acceptable levels.

Table 4.4 Values of $\hat{d}^R$ and $\overline{L}_1(q;A)$ (in fm$^{3/2}$) for the *hep* process calculated as functions of the cutoff Λ. Three- and four-boy exchange currents are assumed to be ignorable. The individual contributions from the one-body (1B) and two-body (2B) operators are also listed.

Λ (MeV)	500	600	800
$\hat{d}^R$	1.00 ± 0.07	1.78 ± 0.08	3.90 ± 0.10
$\overline{L}_1(q;A)$	−0.032	−0.029	−0.022
1B	−0.081	−0.081	−0.081
2B (without $\hat{d}^R$)	0.093	0.122	0.166
2B ($\propto \hat{d}^R$)	−0.044	−0.070	−0.107
2B-total	0.049	0.052	0.059

Summarizing the results obtained, we arrive at a prediction for the *hep* S-factor useful for solar neutrino processes:

$$S_{hep}(0) = (8.6 \pm 1.3) \times 10^{-20}\ \text{keV-b}\,, \tag{4.71}$$

where the "error" spans the range of the Λ-dependence for Λ=500–800 MeV.

- **Confronting nature**

There is no laboratory information on the *hep* process and the only information we have at present is the analysis of the Super-Kamiokande data [Fukuda *et al.* 2001] which gives an upper limit of the solar *hep* neutrino flux, $\Phi(hep)^{\rm SK} < 40 \times 10^3$ cm^{-2}s^{-1}. The standard solar model [Bahcall, Pinsonneault and Basu 2001] using

[12] The detailed expressions are not important for this discussion. What matters is the behavior of these matrix elements as the cutoff is varied.

the *hep* S-factor of MSVKRB [Marcucci *et al.* 2001] predicts $\Phi(hep)^{\rm SSM} = 9.4\times10^3$ cm^{-2}s^{-1}. The use of the central value of our estimate, Eq. (4.71), of the *hep* S-factor would slightly lower $\Phi(hep)^{\rm SSM}$ but with the upper limit compatible with $\Phi(hep)^{\rm SSM}$ in [Bahcall, Pinsonneault and Basu 2001]. A significantly improved estimate of $S_{hep}(0)$ in Eq. (4.71) is expected to be useful for further discussion of the solar *hep* problem.

One can reduce the uncertainty in Eq. (4.71). To do so, one would need to reduce the Λ-dependence in the two-body GT term. By the EFT strategy, the cutoff dependence should diminish as higher order terms are included. In fact, the somewhat rapid variation seen in $\hat{d}^R$ and in the $^3S_1$ contribution to $S_{hep}(0)$ as Λ approaches 800 MeV may be an indication that there is need for higher chiral order terms or alternatively the explicit presence of the vector-mesons (ρ and ω) with mass $m_V \lesssim \Lambda$. We expect that the higher order correction would make the result for $\Lambda = 800$ MeV come closer to those for $\Lambda = 500, 600$ MeV. This possibility is taken into account in the error estimate given in Eq. (4.71).

4.5.5.5 *Magnetic moments of the trinucleons*

Given highly precise wave functions of the tri-nucleon systems ^{3}H and ^{3}He, we can predict their magnetic moments with the EM currents calculated to $\mathcal{O}(Q^3)$. To this order, the magnetic moment operator consists of the known one-body operators including relativistic corrections (see Eq. (4.35)) and two-body operators as given in (4.36). Three-body currents contribute at the next order and so are ignored. Up to this order, there are only two undetermined terms of zero-range that come as counter terms, representing very short-range interactions lodged in higher order terms that are ignored. One is the isoscalar term, denoted g_4', already encountered in the polarization observables in np capture (4.45) and another an isovector contact term, to be denoted as g_{4V}, that contributes to the isovector $M1$ matrix element of the np capture process.[13] The former is fixed by the deuteron magnetic moment and the latter by the np capture rate which as we saw, is dominated by the isovector $M1$ operator. In coordinate space with a suitable smoothing of the delta function with a cutoff Λ as defined before, the two-body "counter-term" magnetic moment operator is of the form

$$\boldsymbol{\mu}_{12}^{CT} = \frac{1}{2m_N}[g_4'(\boldsymbol{\sigma}_1+\boldsymbol{\sigma}_2) + g_{4V}(\tau_1\times\tau)_2^z(\boldsymbol{\sigma}_1\times\boldsymbol{\sigma}_2)]\delta_\Lambda^{(3)}(\boldsymbol{r})j_0(qR). \quad (4.72)$$

We should note that these two terms subsume a large number of terms which in general would be difficult to pin down empirically or theoretically. Remarkably though, a symmetry consideration similar to that which led to one constant $\hat{d}^R$ in the axial current case intervenes here and gives only one term each in the isoscalar

[13] This term was dropped in [Park, Min and Rho 1995; Park, Min and Rho 1996] as it was cut off by the hard core and subsumed in the error bar. Here it comes in because the cutoff is set at the scale of vector mesons with the "hard core" smoothed accordingly.

and isovector channels. Similarly as in the case of $\hat{d}^R$, because of their short-range nature, they are "universal" in the sense that they are independent of the mass number A.

An impressively accurate calculation was performed by Song *et al* [Song, Lazauskas, Park and Min 2007] using the Av18/UIX potential (*i.e.* the Argonne v_{18} 2-body plus Urbana IX 3-body potential) referred to in Section 4.5.4.4. They obtained (in units of nuclear magneton)[14]

$$\begin{aligned} \mu^{th}(^3\mathrm{H}) &= 3.035 \pm 0.013, \\ \mu^{th}(^3\mathrm{He}) &= -2.198 \pm 0.013 \end{aligned} \tag{4.73}$$

where the error bars represent theoretical uncertainties associated with possible higher order terms reflected in the cutoff dependence *etc.* These values should be compared with the experimental values $\mu^{exp}(^3\mathrm{H}) = 2.979$ and $\mu^{exp}(^3\mathrm{He}) = -2.128$.

The standard nuclear physics approach (SNPA) with the same accurate potentials which takes into account certain 2- and 3-body exchange currents along the line of [Chemtob and Rho 1971] developed in the pre-χPT era has achieved a comparable agreement with the experimental values (see, *e.g.*, [Marcucci, Riska and Schiavilla 1998]). Here the methodology is quite similar. However one should note that as stressed before, the power of the MEEFT approach is that it provides an estimate of what errors could be involved in the approximations made and indicates what to calculate to improve the calculation, whereas the SNPA approach does not offer that guidance. A disadvantage of the SNPA would be that if the calculation disagreed with experiments, one would be at a loss as to how to improve it. This does not mean that the SNPA should be abandoned as some advocates of RigEFT claimed. On the contrary, it reinforces the notion that the SNPA should constitute a part – an indispensable one at that – of the MEEFT scheme.

4.5.5.6 *Further implications of the $\hat{d}^R$ term*

The short-range two-body axial current proportional to $\hat{d}^R$ in (4.36) can intervene in an important way in different processes. It is a four-Fermi axial current, so it couples to an axial field, internal or external. For instance, it can couple to the pion via PCAC and can give rise to the three-body force that governs short-distance interaction as given by Fig. 4.6. As noted by [Gårdestig and Phillips 2006], this will enable one to pin down the three-body force with a fairly good accuracy. An example that involves external fields that we discuss here is the process of the type

$$\gamma NN \leftrightarrow \pi NN \tag{4.74}$$

[14]The authors used different "high-quality" potentials with and without 3-body potentials and confirmed that the results are highly insensitive to the possible model dependence in the potential, essentially consistent with the argument made above on the validity of counting in using the potential.

where the pion involved is soft. This process – which is a two-body analog to the Kroll-Ruderman term in photo-pion production on a nucleon – can be used to extract – highly reliably – the neutron-neutron scattering length which is difficult to pin down with small error bars, and here the $\hat{d}^R$ term plays the same role as in the solar neutrino processes discussed above to assure a model independent MEEFT. It offers an extremely interesting case that illustrates the power of MEEFT.

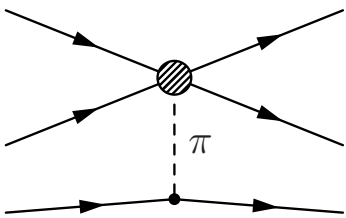

Fig. 4.6 The dominant short-ranged 3-body force mediated by the $\hat{d}^R$ term (indicated by the blob) exchanging a pion with the third nucleon. Here the solid lines stand for nucleon lines, and the broken line for the pion.

It has been shown in [Gårdestig and Phillips 2006] that the uncertainty in the neutron-neutron scattering length can be reduced to $\lesssim 0.05$ fm. Let us discuss how this comes about.

Data from radiative pion capture experiments

$$\pi^- + d \to n + n + \gamma \tag{4.75}$$

dominate the accepted value

$$a_{nn} = -18.59 \pm 0.40 \ \text{ fm}. \tag{4.76}$$

Now it turns out that ± 0.3 fm out of ± 0.4 fm in the error bar arises from the short-distance uncertainty and hence in order to reduce the error substantially below the ± 0.3 fm, it is necessary to control the short-distance component of the force. It is here that the $\hat{d}^R$ term accurately determined above can come in. The basic idea goes as follows. For soft pion, the process (4.75) goes through the same current as the solar *pp* process (apart from the Coulomb interaction) via PCAC. The relevant Lagrangian is of the form

$$\delta\mathcal{L} = -\frac{2\hat{d}_1 g_A}{m_N f_\pi^2} N^\dagger S \cdot u N N^\dagger N \tag{4.77}$$

where $u_\mu = f_\pi^{-1}(-\tau_a \partial_\mu \pi_a - \epsilon_{3ab}\mathcal{V}_\mu \pi_a \pi_b + f_\pi \mathcal{A}_\mu + \mathcal{O}(\pi^3))$ with $\mathcal{V}_\mu$ ($\mathcal{A}_\mu$) being external vector (axial-vector) field. The coefficient $\hat{d}_1$ here is, apart from a constant,

essentially the soft-pion limit of the coefficient $\hat{d}^R$, so the idea is to determine the coefficient $\hat{d}_1$ for a given short-distance scale parameter which, in the case of the *pp* process, was the cutoff Λ. Then using the same prescription for short-distance treatment, one computes the capture process (4.75) using the $\hat{d}_1$ in a suitable range of the short-distance cutoff parameter. The crucial idea is that an approximate renormalization group invariance (in the Wilsonian sense) is achieved if, within the reasonable range of cutoff parameters, the physical observable is insensitive to the change of the cutoffs. The procedure taken in [Gårdestig and Phillips 2006] to implement this strategy was as follows. For both the deuteron and scattering wave functions, they are calculated from $r = \infty$ to a matching radius R – which plays the role of delineating short from long distance – using the one-pion exchange potential, and for $r < R$, a spherical well potential is assumed, the wave function of which is matched to the $r > R$ wave function. This procedure is applied to both the *pp* process and the pion capture (4.75), with the Coulomb effect suitably taken into account into the former. The coefficient $\hat{d}_1$ is an important part of the $\hat{d}^R$ that governs the *pp* process as given by the result (4.70). The result comes out to be

$$\begin{aligned} \hat{d}_1 = \; & -1.27 \text{ for } R = 1.4 \text{ fm}, \; 0.48 \text{ for } R = 2.2 \text{ fm}, \\ & 4.29 \text{ for } R = 3.0 \text{ fm}. \end{aligned} \tag{4.78}$$

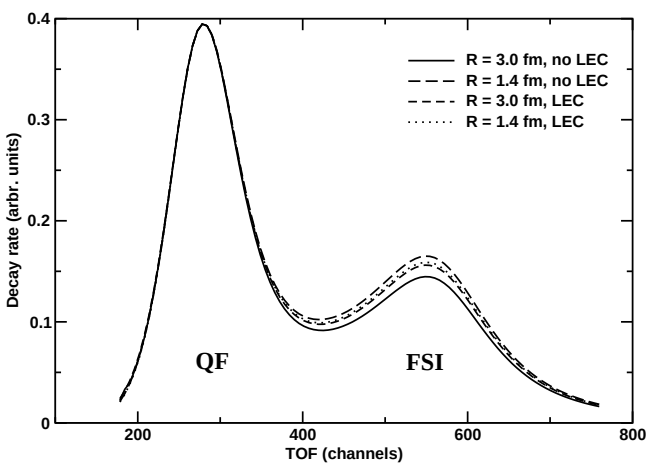

Fig. 4.7 The $\pi^- d \to nn\gamma$ neutron time-of-flight distribution calculated by [Gårdestig and Phillips 2006] (copyright 2006 by the APS), for two widely-separated R values, without and with the $\hat{d}_1$ contribution. The supplement of the γn lab. angle is $\theta_3 = 0.075$ rad and $a_{nn} = -18.5$ fm. The labels QF (quasi-free) and FSI indicate where the corresponding kinematics are dominant. "LEC" and "no LEC" correspond, respectively, to with and without the $\hat{d}_1$ term taken into account.

As in the solar neutrino case, the $\hat{d}_1$ varies widely for a range of the matching radius, but the result for the radiative capture process (4.75) comes out to be highly

insensitive to R. In Fig. 4.7 is shown the capture rate for R ranging widely from 1.4 fm to 3.0 fm. This illustrates how well the short-distance physics is captured by the simple procedure as in the *pp* case: while the results differ widely for the two different values of R without the $\hat{d}_1$ term (the curves with "no LEC"), they are markedly close when the $\hat{d}_1$ term is taken into account (the curves with "LEC") in the "FSI" region where the effect is more significant. A careful analysis of [Gårdestig and Phillips 2006] suggests that this procedure will be able to reduce the short-distance uncertainty in the determination of the *nn* scattering length by a factor of 3 relative to the value available up to date, to, say, $\lesssim 0.05$ fm.

4.6 EFT "Completion" of SNPA

One can now clarify how EFT comes in to *complete* the SNPA. This can be illustrated by the results of the *hep* process. In SNPA approaches, two-body corrections have been made in a procedure suggested a long time ago in [Chemtob and Rho 1971]. As discussed in [Park *et al.* 2003], there are two serious problems with this procedure. The first is that without the guidance of the EFT counting rule, terms of various chiral order are mixed in at the level of computing leading-order exchange current terms. This raises the question of consistency. Since the corrections are chiral-filter unprotected, this inconsistency in chiral counting could generate big errors. The second is more serious, having to do with the shorter-range interaction of the $\hat{d}^R$ type. In the procedure of the SNPA, short-range interactions with the range shorter than the hard-core radius r_c are killed by short-range correlations. This simply means that, roughly speaking, terms of the $\hat{d}^R$ type are missing. Without the MEEFT strategy, what comes in as corrections can be largely arbitrary. One can see from Table 4.4 that without the balance from the $\hat{d}^R$ term, the corrections are strongly dependent on the cut-off r_c and hence totally arbitrary, with the result differing by several factors for different cut-offs. This arbitrariness is neatly circumvented by the MEEFT procedure at the level where the calculation can be done without unknown parameters.

4.7 EFT for Heavy Nuclei and Nuclear Matter

So far we have discussed how to exploit EFT in few-nucleon systems. Can one extend the same strategy to heavier nuclei on the one hand and to nuclear matter on the other? Ultimately we would like to go to densities higher than that of nuclear matter so as to enter the regime where phase transitions to other forms of states (such as kaon condensation, quark matter *etc.*) are presumed to take place.

In RigEFT, one might try to do high-order χPT starting with a chiral Lagrangian appropriate for n-body systems but defined at zero density (*i.e.* "free space") by including diagrams involving n nucleons. A possible way to arrive at nuclear matter

in this way was suggested sometime ago by Lynn [Lynn 1993] which was to first construct a non-topological soliton, namely, "chiral liquid," and then to quantize the system to describe fluctuations around the soliton solution. (This is similar in spirit to what is called "double-decimation approach" mentioned below and described in more detail in Chapter 8.) This Lynn program has not yet been successfully worked out, so one cannot say how well it fares and how far it can go. Now in a much more practical way, one might extend the MEEFT method we described above for few-nucleon systems to many-nucleon systems with the "realistic" two-body potentials used efficiently in the few-body problems, supplemented with three-body and perhaps more-body potentials. The standard nuclear physics approach belongs to this class of approaches, but so far without the proper incorporation of chiral symmetry. The question then is: How should one go about formulating an MEEFT that is applicable to heavy nuclei and nuclear matter?

This question is addressed in [Brown and Rho 2004a; Brown, Holt, Lee and Rho 2006] after introducing the notion of hidden local symmetry in which vector mesons enter importantly as relevant degrees of freedom. Here we mention merely that when one approaches the nuclear matter saturation density with the intention of going beyond the nuclear matter density, it is much more astute to approach the problem via multiple decimations in the renormalization group sense rather than going in one step as one does in the standard χPT approach.

Just to illustrate the basic idea, consider the density regime near the nuclear saturation density, $n \sim 0.16$ fm^{-3}. (Things can become considerably subtler at higher densities and this problem will be treated in the subsequent chapters.) Now what characterizes nuclear matter is the presence of the Fermi surface. It is understood that many-body interactions in the presence of Fermi surfaces generically lead – with certain exceptions that we are not concerned with here – to an RG fixed point, known as "Fermi liquid fixed point"[Shankar 1994] (more on this in Chapter 8). This suggests that starting from a chiral Lagrangian defined at zero density, it makes a better sense to do the first decimation from the chiral scale $\Lambda_\chi \sim 4\pi f_\pi \sim 1$ GeV to the scale at which the effective interactions between nucleons in medium are defined, say, $\Lambda_{eff} \sim 2-3m_\pi$ and then make the second decimation to the Fermi liquid fixed point by going from Λ_{eff} to the Fermi surface. In both of these decimations, Brown-Rho scaling treated in Chapters 6-8 is found to play an essential role. It will turn out that this procedure is consistent with the vector manifestation phenomenon of hidden local symmetry theory described in [Harada and Yamawaki 2003; Brown and Rho 2004a; Brown, Holt, Lee and Rho 2006] and explained in detail in Chapters 5, 7 and 8. The bridge to dense matter where chiral phase transition can take place is then made through a mapping to hidden local symmetry with the vector manifestation.

This page intentionally left blank

Chapter 5

Hidden Local Symmetry For Hadrons

In the preceding chapter, we treated nucleons as pointlike local fields figuring as *matter fields* coupled to the lowest bosonic excitations, *i.e.*, Goldstone (or more precisely pseudo-Goldstone) fields[1] with all other massive excitations implicitly integrated out.[2] In this chapter, we address the question of what the effective field theory of QCD could be for processes at kinematics that are applicable to phase changes taking place at high temperature and high density. What we would like to write down is a theory that is applicable up to, say, the vector meson mass $\lesssim 800$ MeV. This leads to the concept of hidden local symmetry (HLS). As mentioned, hidden local symmetry *naturally* emerges from holographic QCD which exploits a possible holographic duality between 4D QCD and 5D gravity along the AdS/CFT conjecture [Sakai and Sugimoto 2005]. If this top-down approach to strong interactions is correct, then we may take it that the low-energy physics is *entirely* given by hidden local symmetry theory with its full anomaly structure.[3] In the next chapter, baryonic excitations "invisible" (or more precisely, not explicitly present) in the HLS Lagrangian will emerge from the mesonic theory as skyrmions in 4D or instantons in 5D. We will give a first theoretical "justification" for treating baryons as point-like objects in certain limits, pointing to a possible set-up for chiral perturbation theory χPT, developed in the preceding chapter. We will develop in this chapter HLS theory, viewed both ways, namely, bottom-up as an emergence and

[1] We remind the readers that unless otherwise stated, we will not make the distinction between Goldstone bosons (with zero quark mass) and pseudo-Goldstone bosons (with non-zero quark mass).

[2] Given a complete theory, *e.g.*, QED, one can integrate out *explicitly* the degrees of freedom, *e.g.*, electrons, that are not needed in the kinematic regime considered. In our case, we do not have such a luxury and we rarely do the explicit integrating-out. Implicit integrating-out means that the effect of those degrees of freedom that are integrated out is inherited in the parameters of the resulting effective theory, most – if not all – of which are not fixed by the original theory. The subtlety involved in writing down effective theories that capture the original fundamental theory, such as anomalies *etc.*, was discussed in CND-I.

[3] Scalar degrees of freedom which play an important role in hot/dense matter are not present in this approach. They are presumably closely connected with the quark condensate and need to be taken into account. How to do this in hidden gauge symmetry and holographic dual QCD approach is not known yet. They will however be invoked somewhat *ad hoc* in Chapter 7 in treating processes that take place at high temperature.

top-down as a reduction. How this approach affects baryons and hot/dense matter will be discussed in the following chapters.

5.1 Emergence of Local Flavor Symmetry

One does not find in field theory text books flavor symmetry appearing as local gauge symmetry. We will discuss here how local flavor symmetry naturally *emerges* and how it can be exploited to a great advantage in hadron physics.

Effective theory in strong interaction physics is well defined at very low energy with pions, but as one increases the energy, one encounters heavier-mass hadrons. The pseudoscalar mesons like kaons (K) can be incorporated into the pseudo-Goldstone family by increasing the flavor group from SU(2) – where pions live – to SU(3) but the vector mesons like the ρ meson with spin 1 do not have an immediate habitat. How does one treat the spin-1 vector mesons, that are heavier, observed in nature? If one is restricting observation to a very low energy for which one can restrict oneself to tree order, there are several equivalent ways of introducing vector mesons as summarized in [Harada and Yamawaki 2003]. In nuclear physics, one samples whole range of energy scales, so one would naturally like to incorporate the scales corresponding to that of the vector mesons ρ, ω *etc*, and perhaps towers of them as one sees in nature, as a way of incorporating short-wavelength effects. How does one do that? As one probes shorter distances, one needs to include in the Lagrangian, going beyond the well-established quadratic current algebra term, higher dimension or derivative terms involving not only pions but also vector mesons, for instance, terms of the form

$$\sim \frac{1}{16\pi^2}\mathrm{Tr}A^4, \quad \sim \frac{1}{16\pi^2}\mathrm{Tr}(\partial A)^2, \cdots \tag{5.1}$$

where A_μ is a vector-meson field. Such terms are naturally generated when one calculates higher orders by doing loop calculations from leading-order terms, and consistent perturbative schemes require that equivalent terms be added to renormalize the loop terms. Without systematic ways of accounting for higher order terms, it will require an arduous book-keeping to correctly put all terms of the same order. This is where symmetry considerations help. Indeed, local gauge symmetry can do this in a highly efficient way. For instance, all higher order terms like the ones in (5.1) can be completely and neatly collected in an expansion in terms of "covariant derivatives" $(D_\mu^n\Sigma)^m$ (with n and m even integers) if one elevates the vector field to a local gauge field by introducing a gauge degree of freedom Σ

$$\sim \frac{1}{16\pi^2}\mathrm{Tr}|D_\mu\Sigma|^4, \quad \sim \frac{1}{16\pi^2}\mathrm{Tr}|D^2\Sigma|^2, \cdots \tag{5.2}$$

In unitary gauge $\Sigma = 1$, this gives rise to (5.1).

To illustrate how this can be done, we follow the discussion of [Arkani-Hamed *et al.* 2003] and consider the simple "moose" graph Fig. 5.1 with two sites occupied

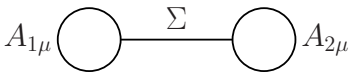

Fig. 5.1 The moose diagram with two sites and one link.

by the gauge fields $A_{1\mu}$ and $A_{2\mu}$ and one non-linear sigma model link field $\Sigma = e^{i\pi/f}$. This represents the gauge symmetry $SU(n)_1 \times SU(n)_2$ with the link field transforming as

$$\Sigma \to g_2^{-1}\Sigma g_1 \tag{5.3}$$

with $g_i \in SU(n)_i$. The Lagrangian invariant under this gauge symmetry has the form

$$\mathcal{L} = -\frac{1}{2g_1^2}\mathrm{Tr}F_{1\mu\nu}^2 - \frac{1}{2g_2^2}\mathrm{Tr}F_{2\mu\nu}^2 + f^2\mathrm{Tr}|D_\mu\Sigma|^2 + \cdots \tag{5.4}$$

with the covariant derivative defined by[4]

$$D_\mu\Sigma = \partial_\mu - iA_{1\mu}\Sigma + i\Sigma A_{2\mu}. \tag{5.5}$$

Now what is the physics of this gauge invariant theory? To answer this question, we fix the gauge to the unitary gauge

$$\Sigma = 1. \tag{5.6}$$

Then the Lagrangian (5.4) becomes

$$\mathcal{L} = -\frac{1}{2g_1^2}\mathrm{Tr}F_{1\mu\nu}^2 - \frac{1}{2g_2^2}\mathrm{Tr}F_{2\mu\nu}^2 + f^2\mathrm{Tr}(A_{1\mu} - A_{2\mu})^2 + \cdots . \tag{5.7}$$

Now let $g_1 = 0$. Then the massless A_1 decouples and we wind up with

$$\mathcal{L} = -\frac{1}{2g_2^2}\mathrm{Tr}F_{2\mu\nu}^2 + f^2\mathrm{Tr}A_{2\mu}^2 + \cdots \tag{5.8}$$

which is a Lagrangian describing a massive vector excitation with the mass

$$m_{A_2} = fg_2. \tag{5.9}$$

Thus physics-wise, the gauge invariant theory with Goldstone bosons is equivalent to the massive gauge non-invariant theory without Goldstone bosons. We could have worked equally well with (5.4) or (5.8). It is clear that the local gauge invariance is really a fictitious symmetry. However it is not a vacuous stuff. It allows to do the systematic accounting as described above. More importantly for systems that interest us where the vacuum is changed by temperature and density, it allows us to make predictions that are difficult, if not impossible, to do with a theory

[4]Recall the notation $A_\mu = A_\mu^a T^a$ where T^a is the generator of the gauge group normalized $\mathrm{Tr}T^aT^b = \frac{1}{2}\delta^{ab}$.

without local gauge invariance. We will see that this is the case with the hidden local symmetry theory developed for the strong interactions by Bando *et al.* [Bando *et al.* 1988] at tree order and extended by Harada and Yamawaki [Harada and Yamawaki 2003] to loop orders.

5.2 Tower of Hidden Gauge Fields

The way hidden gauge symmetry appears is quite generic, emerging in all areas of physics. One of the most tantalizing cases is the one in condensed matter physics mentioned above, namely, the charge-spin separation mediated by an emerging gauge field. Another example which is quite analogous to this is the emergence of general coordinate invariance in the AdS/CFT duality [Horowitz and Polchinski 2006]. Here we describe how an infinite tower of local gauge fields naturally emerge in the strong interactions. The hidden local symmetry that we will extensively exploit in this volume will be the simplest version of the hidden gauge structure.

5.2.1 *Simplest open moose diagram*

The example given above, (5.4), involved only one set of Goldstone bosons which are ultimately eaten up to give the vector mesons the mass, that is, have them become the longitudinal components of the massive vector mesons. When we want to study what happens at low energy in the strong interactions, the most important ingredients are the pions $\pi^{\pm}$, π^0 in the $SU(2)$ flavor sector if one is not interested in strangeness or the octet of pseudoscalar mesons in the $SU(3)$ flavor sector if strange flavor is involved. These are real particles. We need to have this set of pseudoscalar mesons left over in the spectrum. The simplest way to implement this is to consider a situation with three sites as in Fig. 5.2 corresponding to $K = 1$, with the local gauge field ρ_μ in the middle and the left and right sites becoming boundary conditions possessing global chiral symmetries L and R. For generality, we consider the global symmetries to be $SU(N)_L$ and $SU(N)_R$. Now, we let the vector field be connected to the boundaries by the link fields written as Σ_L and Σ_R. In this volume we shall be mostly using the notation of [Harada and Yamawaki 2003] where the link fields are written with ξ. The relations are $\Sigma_L = \xi_L^\dagger$ and $\Sigma_R = \xi_R$. What we are doing is a description of the model in a theory space – not a physical space – corresponding to the symmetry $G_{global} \times H_{local}$ where $G = SU(N)_L \times SU(N)_R$ and H is the diagonal subgroup $SU(N)$, to which G is broken down. The "local symmetry" H_{local} is completely broken so there are two sets of Goldstone bosons: the ξ fields can be written as[5]

$$\xi_{\rm L,R} = e^{i\sigma/F_\sigma} e^{\mp i\pi/F_\pi} \ , \quad [\, \pi = \pi^a T_a \, , \, \sigma = \sigma^a T_a] \ , \tag{5.10}$$

[5] Unless otherwise stated, $F_{\pi,\sigma}$ are parameters to be distinguished from physical constants such as the pion decay constant which will be written as f_π.

where π denote the Nambu-Goldstone (NG) bosons associated with the spontaneous breaking of G chiral symmetry, and σ denote the NG bosons[6] associated with the spontaneous breaking of the local H_{local} symmetry. Define the covariant derivative involving the vector (gauge) field which we shall write generically as $V_\mu \equiv V_\mu^a T^a$

$$D_\mu \xi_{\rm L,R} = \partial_\mu \xi_{\rm L,R} - i V_\mu \xi_{\rm L,R} \tag{5.11}$$

and 1-forms (known as Maurer-Cartan 1-forms)

$$\alpha_{\perp\mu} = \left(\partial_\mu \xi_{\rm R} \cdot \xi_{\rm R}^\dagger - \partial_\mu \xi_{\rm L} \cdot \xi_{\rm L}^\dagger\right)/(2i) \ , \tag{5.12}$$

$$\alpha_{\parallel\mu} = \left(\partial_\mu \xi_{\rm R} \cdot \xi_{\rm R}^\dagger + \partial_\mu \xi_{\rm L} \cdot \xi_{\rm L}^\dagger\right)/(2i) \ , \tag{5.13}$$

which transform as

$$\alpha_{\perp\mu} \to h(x) \cdot \alpha_{\perp\mu} \cdot h^\dagger(x) \ , \tag{5.14}$$

$$\alpha_{\parallel\mu} \to h(x) \cdot \alpha_{\parallel\mu} \cdot h^\dagger(x) - i\partial_\mu h(x) \cdot h^\dagger(x) \ . \tag{5.15}$$

The vector field transforms as

$$V_\mu \to h(x) \cdot V_\mu \cdot h^\dagger(x) - i\partial_\mu h(x) \cdot h^\dagger(x) \ . \tag{5.16}$$

Define the "covariantized 1-forms"

$$\widehat{\alpha}_{\perp\mu} = \frac{1}{2i}\left(D_\mu \xi_{\rm R} \cdot \xi_{\rm R}^\dagger - D_\mu \xi_{\rm L} \cdot \xi_{\rm L}^\dagger\right) \ , \tag{5.17}$$

$$\widehat{\alpha}_{\parallel\mu} = \frac{1}{2i}\left(D_\mu \xi_{\rm R} \cdot \xi_{\rm R}^\dagger + D_\mu \xi_{\rm L} \cdot \xi_{\rm L}^\dagger\right) \ . \tag{5.18}$$

The relations of these covariantized 1-forms to $\alpha_{\perp\mu}$ and $\alpha_{\parallel\mu}$ in Eqs. (5.12) and (5.13) are given by

$$\begin{aligned} \widehat{\alpha}_{\perp\mu} &= \alpha_{\perp\mu} \ , \\ \widehat{\alpha}_{\parallel\mu} &= \alpha_{\parallel\mu} - V_\mu \ . \end{aligned} \tag{5.19}$$

The covariantized 1-forms $\widehat{\alpha}_{\perp\mu}$ and $\widehat{\alpha}_{\parallel\mu}$ in Eqs. (5.17) and (5.18) now transform homogeneously:

$$\alpha_{\perp,\parallel}^\mu \to h(x) \cdot \alpha_{\perp,\parallel}^\mu \cdot h^\dagger(x) \ . \tag{5.20}$$

Thus we have the following two invariants:

$$\mathcal{L}_{\rm A} \equiv F_\pi^2 \, {\rm Tr}\left[\widehat{\alpha}_{\perp\mu}\widehat{\alpha}_\perp^\mu\right] \ , \tag{5.21}$$

$$a\mathcal{L}_{\rm V} \equiv F_\sigma^2 \, {\rm Tr}\left[\widehat{\alpha}_{\parallel\mu}\widehat{\alpha}_\parallel^\mu\right] = F_\sigma^2 \, {\rm Tr}\left[\left(V_\mu - \alpha_{\parallel\mu}\right)^2\right] \ . \tag{5.22}$$

[6]The σ is not to be confused with the scalar in linear sigma model or the scalar excitation coupled to 2π channel.

The most general Lagrangian made out of $\xi_{\rm L,R}$ and $D_\mu \xi_{\rm L,R}$ with the lowest derivatives – which defines the Bando *et al* Lagrangian [Bando *et al.* 1988] – is thus given by

$$\mathcal{L} = \mathcal{L}_{\rm A} + a\mathcal{L}_{\rm V} \tag{5.23}$$

with

$$a = \frac{F_\sigma^2}{F_\pi^2}. \tag{5.24}$$

These are the leading-order terms, and higher derivative terms can then be constructed using the covariant derivatives. Mass terms would also figure at higher order. For the moment, we will ignore the mass terms, postponing their consideration to later.

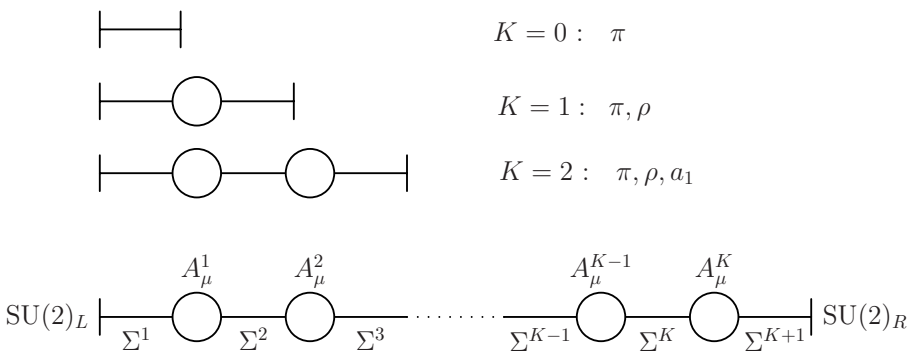

Fig. 5.2 The moose diagram corresponding to the Lagrangian Eq. 5.27 for $N_f = 2$. $K = 0$ represents nonlinear sigma model for pions; $K = 1$ represents a hidden local symmetry Lagrangian describing π and ρ; and $K = 2$ represents a description of π, ρ, and a_1. The gauge coupling g_i is restored in the figure to indicate that it is connected to the i-th site. The link variables Σ are related to $\xi_L^\dagger = \Sigma_L$ and $\xi_R = \Sigma_R$ of Harada and Yamawaki.

5.2.2 *General open moose*

To generalize the structure of the Lagrangian, let us slightly rewrite (5.23) in terms of $\Sigma_L = \xi_L^\dagger$ and $\Sigma_R = \xi_R$

$$\mathcal{L} = \frac{F_\pi^2}{4}\mathrm{Tr}\{|D_\mu \Sigma_L|^2 + |D_\mu \Sigma_R|^2 + \kappa |D_\mu U|^2\} \; - \frac{1}{2}\,\mathrm{Tr}\,[\rho_{\mu\nu}\rho^{\mu\nu}] \tag{5.25}$$

with

$$U = \Sigma_L \Sigma_R \; . \tag{5.26}$$

Here we have added the kinetic energy term for the gauge field. In the usual approach to hidden local symmetry, one imagines this kinetic energy term arising as a quantum-loop effect. Later we will see that such a term arises naturally as an effective theory of QCD.

As written in the form of (5.25), the mixing of the L and R symmetries is encoded in a non-zero coefficient κ which can be given in terms of a of (5.23), *i.e.*, $\kappa = a^{-1} - 1$. When $a = 1$, the mixing disappears and it corresponds to $\kappa = 0$ in (5.25). In this case, we are left with a linear combination of the L and R terms without coupling between them. One can visualize this Lagrangian in the theory space as Fig. 5.2 and refer to this linear form as an "open moose" diagram local in theory space. We will come back to this issue of chiral symmetry since $a = 1$ or $\kappa = 0$ can play an important role in hadron physics. For the moment, it is interesting to extend the open moose diagram to an infinite linear chain (letting $K \to \infty$ in Fig. 5.2)

$$\mathcal{L} = \sum_{j=1}^{K+1} \frac{f_j^2}{4} \mathrm{Tr}|D_\mu \Sigma^j|^2 \ - \sum_{j=1}^{K} \frac{1}{2g_j^2} \mathrm{Tr}\left[F_{\mu\nu}^j F^{j\mu\nu}\right] \ . \tag{5.27}$$

Here we have replaced the "pion decay constant" F_π by a generalized constant f^j corresponding to the j-th link field and $g\rho_{\mu\nu}$ by $F_{\mu\nu}^j$ to accommodate $K \geq 1$ gauge fields. The covariant derivatives are of the form now

$$D_\mu \Sigma^1 = \partial_\mu \Sigma^1 + i\Sigma^1 A_\mu^1, \tag{5.28}$$

$$D_\mu \Sigma^k = \partial_\mu \Sigma^k - i A_\mu^{k-1} \Sigma^k + i\Sigma^k A_\mu^1, \tag{5.29}$$

$$D_\mu \Sigma^{K+1} = \partial_\mu \Sigma^{K+1} - i A_\mu^K \Sigma^{K+1} \ . \tag{5.30}$$

where $1 < k < K$.

The model (5.27) which was first considered by Son and Stephanov as a model for low-energy QCD [Son and Stephanov 2004] describes $K + 1$ nonlinear sigma model fields $\Sigma^k \in SU(N_f)$ mediated by K hidden gauge fields A_μ^k. This has a linear "moose" structure in the sense of that of $\kappa = 0$ for the $K = 1$ case displayed above: The mixing terms are not present. This situation – *i.e.*, the absence of mixing terms – is referred to as "locality in theory space." This is just one way of constructing a model that resembles the nearest-neighbor interaction in condensed matter systems. We will see later what is so special about this "locality."

The pion field π is given by

$$\Sigma^1 \Sigma^2 \cdots \Sigma^K \equiv U = e^{2i\pi/f}. \tag{5.31}$$

5.2.3 *Spectrum of the open moose*

The tree order spectrum of (5.27) for $K < \infty$ turns out to consist of towers of vector mesons[Son and Stephanov 2004]. For $K = 0$, it is the usual chiral model with the pion fields only. For $K = 1$, it is hidden local theory with $a = 1$. For $K = 2$, it is

a theory-space-local hidden local theory with ρ and a_1 and so on. For $K = \infty$ it represents an infinite tower. One can see this in the mass spectrum of the vector mesons. There are K gauge degrees of freedom, so to exhibit physical degrees of freedom in the vacuum, one can choose the unitary gauge

$$\Sigma^k = 1 \quad \text{for all k.} \tag{5.32}$$

To get the mass spectrum at tree order, one expands the Lagrangian (5.27) to quadratic order in gauge fields,

$$\begin{aligned} \delta\mathcal{L} &= \sum_{k=1}^{K+1} f_k^2 \mathrm{Tr}[(A_\mu)^{k-1} - (A_\mu)^k]^2 \\ &\equiv \sum_{(k,j)=1}^{K} (M^2)_{kj} \mathrm{Tr} A_\mu^k A_\mu^j, \end{aligned} \tag{5.33}$$

Diagonalizing the mass matrix M, one finds the mass eigenvalues m_n with $n = 1, 2, \cdots, K$. The $n = 1$ state corresponds to the lowest ρ meson and the $n = 2$ to the lowest a_1 meson *etc.* Odd n states correspond to vector mesons, and even n to axial vector mesons. Vectors and axial vectors alternate to infinity. This infinite tower structure of vector mesons will emerge naturally from holographic dual QCD described below.

5.2.4 *Dimensional deconstruction*

The model (5.27) represented by $K < \infty$ corresponds to a finite lattice Lagrangian where the lattice sites – except for the boundaries – are occupied by gauge fields. One can think of this equivalently as a five-dimensional theory with the fifth dimension latticized. When K goes to ∞, one can replace the theory by a continuum theory. The link field can be interpreted as the Wilson line

$$U(x) = P e^{i \int_0^\epsilon dx_5 A_5(x, x_5)}. \tag{5.34}$$

On the lattice,

$$\Sigma^j \approx 1 + i\epsilon A_5(x_5) + \cdots \tag{5.35}$$

where the lattice size is denoted ϵ (we reserve a – the usual notation for the lattice size – for the ratio F_σ^2/F_π^2.). Then our moose action with the Lagrangian (5.27) in the limit $K \to \infty$ can be rewritten as a 5-D Yang-Mills action in a "warped" background,

$$S = -\int d^4x dz \frac{1}{2g(z)^2} \sqrt{g} \mathrm{Tr}(F_{AB} F^{AB}) \tag{5.36}$$

where $A = 0, 1, 2, 3, 4$. The determinant of the metric – which is curved – enters in the expression. The role of the fifth dimension is to represent the energy scale

in 4-D field theory, extending from the infrared to the ultraviolet, conventionally referred to as "infrared (IV) brane" and "ultraviolet (UV) brane," respectively. The space is compactified by putting boundary conditions at the two branes.

In working with the action (5.36), the metric (gravity) is taken to be non-dynamical (except when temperature is involved in which case black hole arises). Physics depends on what the background metric is. Its specific structure depends on the details of both the deviation from conformal invariance at the UV brane and chiral symmetry breaking at the IR brane. At present, there are two approaches to exploiting the action (5.36). One is to infer the bulk action from what one assumes for the 4D "surface" action corresponding to QCD. This is admittedly phenomenological and is referred to as "bottom-up" approach that we will refer to as "AdS/QCD." The other is to introduce in the gravity background transverse to the 4-D space time flavor "probe branes" and obtain the warped metric from string action in weak coupling limit corresponding, via AdS/CFT duality, to large N_c and large 't Hooft constant ($\lambda \equiv g^2_{YM} N_c$) limit in the gauge theory sector. This approach is a "top-down" approach that we will refer to as "holographic dual QCD" or hQCD in short.[7] We briefly summarize the two approaches.

5.3 AdS/QCD and hQCD

5.3.1 *Objectives*

The recent development in applying the concept and the methodology of AdS/CFT duality to low-energy hadron dynamics, referred to as AdS/QCD or holographic QCD, brings out two related issues from opposite directions, one top-down from string theory and the other bottom-up from low-energy chiral effective field theory of mesons and baryons.

From the string theory point of view, what one is interested in is to assess to what extent the gravity theory in the bulk sector in a controlled weak coupling limit can address, via duality, the strongly coupled dynamics of QCD, and if so, how well and how far. In this respect, the aim there is to "post-dict" what is established in low-energy hadron dynamics and try to reproduce what has been well understood in low-energy effective theories. The principal goal here is to establish the raison-d'être of string theory in the strong interaction sector. On the other hand, from the low-energy effective theory perspective on which we will elaborate in some detail below, the aim is, if it is firmly established that AdS/QCD or hQCD has definite connection to real QCD, whether it can make clear-cut and falsifiable predictions on processes that are difficult to access by QCD proper.

A notable example of this sort is the prediction by AdS approaches of low shear

[7] In the literature, some authors use AdS/QCD and hQCD interchangeably making no distinction between the bottom-up and top-down. In what follows, we will adhere to the distinction whenever possible.

viscosity in matter at high temperature above the chiral restoration point [Kovtun, Son and Starinets 2005], which is presumed to be observed at RHIC. Given the complete inability of the QCD proper to handle this regime, this development gives a hope that the AdS/QCD (or hQCD) approach could provide a powerful tool going beyond perturbative QCD and elucidate strongly-coupled matter under extreme conditions that are otherwise inaccessible. At present, however, in the paucity of better understanding, it is not clear whether the current "explanation" of the properties of quark-gluon plasma at RHIC reflects directly certain specific properties of nonperturbative QCD or whether they are simply in a same universality class unspecific to dynamics. In fact, recent works suggest that the prediction could be common to all AdS-based models regardless of details.

Another example of this sort is the exploitation of the conformal structure of AdS/CFT to deduce the analytic form of the frame-independent light-front wave-functions of hadrons which could allow the computation of various observables that are found to be difficult to obtain in QCD proper [Brodsky and de Teramond 2006].

Here we would like to zero in on a more specific set of problems that are typically of strong-coupling QCD and are very difficult to access by established QCD techniques, namely chiral dynamics of hadrons, in particular, baryons at low energy but high density. Pions are relatively well-understood from the chiral Lagrangian approach to QCD, but baryons remain more difficult to pin down. This may account for the reason why in the chiral lagrangian approach, baryons are either put in by hand as point-like objects or built up as solitons (*i.e.*, skyrmions) from mesons. The former suffers from the lack of theoretical justification as a local field when the energy scale reaches the inverse of its Compton wavelength as evidenced in the growing number of unknown parameters, while the latter in its simplest approximation does not fare well in phenomenology. Attempts to marry the two pictures are often difficult, given the relatively large size of the skyrmion.

As mentioned, there are essentially two approaches to this issue, one which is a phenomenological bottom-up approach that inputs as much as known of the gauge sector into the bulk sector to make contact with string theory in a manageable limit, and the other is top-down from string theory in certain limits to predict the gauge theory sector in the strong coupling limit.

5.3.2 *Bottom-up approach*

Here the basic idea is that given the gravity/gauge duality which implies that QCD in 4-D has a holographic dual in 5-D, the field content of the 5-D theory is chosen such that the dynamics of spontaneously broken chiral symmetry is holographically reproduced [Erlich, Katz, Son and Stephanov 2005; Da Rold and Pomarol 2005; Hirn and Sanz 2005]. The metric is taken in a "conformally flat" form with a "warp factor" $w(z)$

$$ds^2 = w(z)^2(\eta_{\mu\nu}dx^\mu dx^\nu - dz^2) \tag{5.37}$$

where $\mu = (0, ..., 3)$ and $x^5 = z$. The AdS metric corresponds to $w(z) = l/z$ with l being the AdS curvature radius. The theory is defined on the line element $l_1 < z < l_0$ with boundary conditions put at $l_{0,1}$. The UV boundary $z = l_0$ at which conformal invariance is assumed to be operative acts as a regulator to cancel ultraviolet divergences. The boundary condition on the gauge fields L_μ and R_μ at $z = l_0$ required by the holographic principle is given by the value of the sources of the vector and axial-vector currents in 4-D theory.[8] The IR boundary $z = l_1$ plays the role of a mass gap $\Delta \sim 1/l_1$ and it is at this point that conformal as well as chiral symmetry is broken. The chiral symmetry breaking to the diagonal subgroup is assured by the boundary condition $L_\mu(x^\mu, z = l_1) = R_\mu(x^\mu, z = l_1)$.

With the metric (5.37), the correlators $G_{V,A}(-Q^2)$ reproduce in the large Euclidean limit the logarithmic term of the QCD correlator given by

$$G_{V,A}(-Q^2) = -\frac{N_c}{12\pi^2}\left\{c + \log\left(\frac{Q^2}{\mu^2}\right) + \mathcal{O}(\alpha_s)\right\} + \frac{1}{12\pi}\alpha_s\langle G^2\rangle Q^{-4} + \binom{-1}{11/7}\frac{28}{9}\pi\alpha_s\langle\bar{q}q\rangle^2 Q^{-6} + \mathcal{O}(Q^{-8}), \quad (5.38)$$

where c is a subtraction constant. However with the metric of the form (5.37), the Q^{-2d} terms with $d = 2, 3, ...$ that break conformal symmetry are missing from the bulk sector. In order to recover these terms, there are two ways to proceed. One is to deform the warp factor in the metric $w(z)$ so as to reproduce these terms [Hirn, Rius and Sanz 2006] without introducing any other fields. This procedure seems somewhat arbitrary as it is not clear what it means physically. An alternative method is to introduce a scalar field whose vacuum expectation value (VEV) is responsible for the breaking of chiral symmetry [Erlich, Katz, Son and Stephanov 2005; Da Rold and Pomarol 2005], *e.g.*, the quark condensate, scale invariance *etc.* In this approach, the action takes the form

$$S = -\int d^5x\sqrt{g}\mathrm{Tr}\left\{\frac{1}{2g_5^2}(F_L^2 + F_R^2) + |D\Phi|^2 - M_\Phi^2|\Phi|^2\right\} \quad (5.39)$$

where $D_A\Phi = \partial_A\Phi + iL_A\Phi - i\Phi R_A$ and $L_A = L_A^a T^a$. In this case the gluon condensate is still missing. However chiral symmetry breaking is reflected in the difference $(G_V - G_A)$ for which the gluon condensate cancels out. The log term gives a relation between the 5-D gauge coupling g_5 and N_c

$$N_c = \frac{12\pi^2 l}{g_5^2}. \quad (5.40)$$

Similarly to the metric at the UV brane [Hirn, Rius and Sanz 2006], the background metric associated with the IR brane in addition to a mass gap is also

[8] This is presumably connected with the "ultraviolet completion."

intricate. With the simple conformal metric, the spectrum of mesons with high spin or high radial excitation is known not to come out correctly as we will comment below. On the other hand, one can manufacture a particular geometry constrained at the infrared regime that can make the spectrum come out right [Karch, Katz, Son and Stephanov 2006] but the origin of such a geometry is not known from string theory. Thus both the UV and IR behavior of the background metric is quite specific to QCD.

It is, however, amazing how well this theory with simple warp factor reproduces the properties of the pion and the vector mesons we are familiar with.

- **Goldstone bosons**
  A massless 4-D spin zero mode arises with the boundary conditions at the UV and IR branes with the conformal invariance broken only at the IR brane. This can be identified with the pionic excitation. It is related to the fifth component of the 5-D gauge field via the Wilson line

$$U(x) = \mathcal{P}\{e^{i\int_{l_1}^{l_0} dz R_5(x,z)}\} \times \mathcal{P}\{e^{i\int_{l_1}^{l_0} dz L_5(x,z)}\} \tag{5.41}$$

  with $R_5 = A_{R5}$ and $L_5 = A_{L5}$. The pion decay constant is given by

$$f_\pi^{-2} = g_5^2 \int_{l_1}^{l_0} \frac{dz}{w(z)}. \tag{5.42}$$

  With the scalar degrees of freedom implemented to account for the Q^{-6} term in the correlators, the Gell-Mann-Oakes-Renner formula can be reproduced [Erlich, Katz, Son and Stephanov 2005]. The Gasser-Leutwyler p^4 terms L_i for $i = 1, 2, 3, 9, 10$ in chiral perturbation theory (χPT) can also be extracted in the model in a reasonable agreement with experiments [Hirn and Sanz 2005; Hirn, Rius and Sanz 2006].
- **Vector mesons**
  To describe vector excitations, one does what is known as "Kaluza-Klein decomposition" which consists of separation of (x_μ, z) coordinates. For instance, for the vector field $V_\mu(x,z) \equiv \frac{1}{2}(L_\mu(x,z) + R_\mu(x,z))$, one factorizes

$$V_\mu(x,z) = \sum_{n=1}^{\infty} V_\mu^{(n)}(x)\phi_n^V(z) \tag{5.43}$$

  and likewise for $A_\mu(x,z) \equiv \frac{1}{2}(L_\mu(x,z) - R_\mu(x,z))$. The wave functions $\phi(z)$ – a profile in the fifth direction – are determined by the equation of motion that captures the spread in the fifth dimension with boundary conditions at the UV and IR branes and likewise for A. This yields the infinite tower of alternating vector and axial-vector mesons we encountered in dimensionally deconstructed QCD. The spectrum given by the conformal metric, going like $M_{V_n,A_n} \sim n$, does not agree with the Regge behavior, but with a suitable change in the

background geometry, one can make the spectrum come out as $M_{V_n,A_n} \sim \sqrt{n}$ as needed.

Other phenomenology from this bottom-up formulation resembles that of the top-down approach given below.

5.3.3 *Top-down approach*

Instead of guessing the metric as above, here one tries to derive from string theory the appropriate metric in a particular approximation. One starts from string theory, choose the backgrounds so that such essential features as confinement, chiral symmetry breaking *etc.* present in QCD be reproduced. The idea is to bring flavors in AdS background as gauge fields living on the world volume of flavor branes. This approach would ultimately give the background geometry needed for a realistic dual picture to QCD, predicting the UV and IR behaviors rather than put in by hand as in the bottom-up approach described above. To describe the top-down approach in a self-contained way, we would need to go into full string theory machineries. At present, one is limited to the leading order in the 't Hooft constant $\lambda = g_{YM}^2 N_c$ and the number of colors N_c and the limit that the number of flavors is much less than the number of colors, $N_f \ll N_c$, corresponding to the probe approximation or "quenched approximation." It is only in these limits that one has a controllable tool in the bulk (gravity) sector. All these technicalities are way beyond the scope of this volume, so we will limit ourselves to summarizing the most essential outcome of the approach which is expected to survive at least qualitatively future modifications.

For conformally invariant gauge theories, the dual string theory is defined with a metric of the product $AdS_5 \times W$ living in 10-D. The coordinates on the AdS space are the usual 4-D Minkowski coordinates x^μ with $x^\mu = (0, 1, 2, 3)$ and the fifth coordinate z that runs from $z = 0$ at the horizon of the Poincaré patch to $z = \infty$ at its boundary. The W lives in the remaining 5D. As before, the z is related to the energy scale probed in the quantum field theory. In this model, $z = 0$ is *chosen* to correspond to the IR at which conformal invariance is broken and $z = \pm\infty$ to the UV. QCD is not a conformally invariant theory. At high energy/momentum, the conformal symmetry is broken by trace anomaly giving rise to the dimensional transmutation, and at low energy, it is completely broken with mass gap. The hope here is that the strategy of conformal invariant theory can be suitably modified on the metric so that the conformally invariant metric $AdS_5 \times W$ can still be used.

Now flavor-free objects such as glueballs, pomerons *etc.* live in the 6D transverse to the space-time, coupling to the flavors living in the flat space-time at subleading order in N_c. For high-energy scattering of hadrons in which Pomerons dominate, one would have to consider the excitations in the transverse dimensions. This is being studied for both $t < 0$ and $t > 0$ at large $|t|$ where t is the momentum transfer [Brower, Polchinski, Strassler and Tan 2007]. For our purpose, however, we can think of the transverse space going into the warp factor which is a function

of the coordinates on W multiplying the AdS metric. The metric would generically take the form

$$ds^2 = e^{A(y)}\eta_{\mu\nu}dx^\mu dx^\nu + G_{\perp mn}dy^m dy^n. \tag{5.44}$$

The holographic dual model that implements confinement-deconfinement and spontaneous breaking of chiral $U(N_f)_L \times U(N_f)_R$ constructed by Sakai and Sugimoto [Sakai and Sugimoto 2005; Sakai and Sugimoto 2006] (SS model for short) seems to be quite realistic, so we shall focus on that model. In a nut-shell, the idea is to construct a supergravity dual to the YM theory in the background given by a stack of N_c D4 branes describing colored gluons and then insert N_f $D8/\overline{D8}$ probe branes extended along x^μ with $\mu = 0, 1, 2, 3$ to represent N_f flavors of L/R quarks in the background of the D4 branes. One makes the approximation that $N_c \gg N_f$ (probe approximation) and then ignores the back-reaction of the probes on the D4 background. In the W coordinates, S^1 wrapped by D4 branes breaks supersymmetry – by boundary conditions – and there is an $SO(5)$ symmetry which acts as a rotation on S^4. The SUSY breaking makes the fermions in the adjoint rep massive and scalars also in the adjoint rep pick up large mass by radiative corrections, so both decouple from the zero mass gauge fields – which are the gluons. QCD does not have excitations charged in $SO(5)$, so one makes the assumption that the charged objects decouple leaving behind only those states invariant under $SO(5)$ symmetry which are identified as the physical degrees of freedom.

There are then colored objects as the fluctuation modes of open strings with at least one end located on N_c D4 branes, *i.e.*, gluons from D4-D4 strings and flavor quarks from D4-D8 (or antiquarks from D4-$\bar{D}8$) strings. In the supergravity approximation in the bulk sector which corresponds to taking the 't Hooft limit $\lambda = g^2_{YM}N_c \to \infty$ in the gauge field sector, confinement is interpreted as the loss of color information behind the horizon caused by the large spatial curvature in the fifth direction. What is left then as physical degrees of freedom are the fluctuation modes, namely, the color-singlet mesons in the supergravity background. The SS model astutely implements local $U(N_f)_L \times U(N_f)_R$ symmetry broken down to local $U(N_f)_V$ symmetry, correctly representing (global) chiral symmetry of QCD in 4D. The upshot of the derivation is that we have in the large λ and N_c limit a 5D Yang-Mills action with $U(N_f)$ flavor symmetry in a curved space plus a Chern-Simons term that encodes anomalies. The resulting 5D Yang-Mills action is of the form of (5.36) which is given in the notation of [Sakai and Sugimoto 2005] by[9]

[9]We avoid delving into the lengthy and involved derivation of this formula which requires the background of string theory which is beyond the scope of this volume. See [Hong, Rho, Yee and Yi 2007b] for the details and relevant references. We will be content with carefully specifying the assumptions that go into the arguments developed therein.

$$S_{YM} = \kappa \int d^4x dz \Bigg(-\frac{1}{2} K^{-1/3}(z) \mathrm{Tr}[F_{\mu\nu} F^{\mu\nu}] + K(z) M_{\mathrm{KK}}^2 \mathrm{Tr}[F_{\mu z} F^{\mu z}] + \mathcal{O}(F^3) \Bigg), \tag{5.45}$$

where $K(z)$ is the induced measure of 5-dimensional space-time given by

$$K(z) = 1 + z^2 \tag{5.46}$$

and the constant κ is related to N_c and the 't Hooft constant $\lambda \equiv N_c g_{YM}^2$ by

$$\kappa = \frac{\lambda N_c}{108\pi^3}\,. \tag{5.47}$$

The mass M_{KK} in Eq. (5.45) that sets the compactification scale that sends off all higher modes of string theory roughly corresponds to the chiral scale we are concerned with. The five dimensional (5D) gauge field A_M ($M = 0, 1, 2, 3, z$) transforms as

$$A_M(x^\mu, z) \to g(x^\mu, z) \cdot A_M(x^\mu, z) \cdot g^\dagger(x^\mu, z) - i\partial_M g(x^\mu, z) \cdot g^\dagger(x^\mu, z)\,, \tag{5.48}$$

We will return below to a (brief) discussion of the action (5.45) via-à-vis with hidden local symmetry with an infinite tower of vector mesons in 4D (denoted $\mathrm{HLS}_{K=\infty}$) and its relevance to $\mathrm{HLS}_{K=1}$ that we will be focusing on for applying to systems of our interest.

5.3.4 *Vector dominance*

To confront nature, we need to go to 4D. In going to 4-D from 5-D, there is one gauge degree of freedom at one's disposal. There are two convenient choices:

(1) One possible choice is

$$A_z(x^\mu, z) = 0. \tag{5.49}$$

This can be obtained by the gauge transformation

$$A_M(x^\mu, z) \to A_M^g = g(x^\mu, z)(A_M(x^\mu, z) + i\partial_M) g^\dagger(x^\mu, z) \tag{5.50}$$

with $M = (\mu, z)$ and

$$g(x^\mu, z) = P \exp\{-i \int_0^z dz' A_z(x^\mu, z')\}. \tag{5.51}$$

In this gauge, chiral symmetry is manifest with the pion field appearing in the boundary conditions at $z = \pm\infty$. As will be made clear in the next chapter, this theory is a generalized form of Harada-Yamawaki HLS theory involving an

infinite tower of vector mesons with coefficients of the Lagrangian fixed by the bulk sector. The intrinsic parity-odd sector of the theory is given by the 5-D Chern-Simons term which when reduced to 4-D gives rise to the well-known Wess-Zumino term, again involving the infinite tower. When the 4-D gauge fields are set equal to zero – which is not the same as integrating out the vector fields, the remaining Lagrangian is precisely the Lagrangian that corresponds to the skyrmion Lagrangian with the Skyrme quartic term. One may think of this as a *derivation* of the Skyrme Lagrangian in a certain limit, but the coefficient of the Skyrme term should not be identified with an effect of the lowest member of the vector tower.

(2) The other choice, modulo a constant factor, is

$$A_z(x^\mu, z) \simeq \pi. \tag{5.52}$$

In this gauge, vector dominance is manifest. In the intrinsic parity-odd sector, there are no terms involving more than one pion field and no contact terms with electroweak fields, so they are all totally vector-dominated. This means that the familiar 5-D Wess-Zumino term is absent and hence topology must be carried by the vector fields. It is interesting that even certain strong interactions, *e.g.*, $\pi\pi$ scattering, are vector-dominated.

5.3.5 *Instanton baryons*

In the holographic dual QCD formulated in terms of Goldstone bosons and vector fields, baryons *must* appear as instantons in five dimensions and skyrmions in four dimension. Indeed in the top-down approach, the baryon can be identified as D4 brane wrapped on S^4 which can be in turn identified as an instanton on D8 brane [Sakai and Sugimoto 2005; Sakai and Sugimoto 2006]. It is important to note that in the $A_z(x^\mu, z) \simeq \pi$ gauge, the skyrmion structure must involve hidden gauge fields in a crucial way including the topology. The skyrmion structure will be discussed in the next chapter where we will show how important the infinite tower is in the structure of the nucleon, in particular in the full vector-dominance structure of the electroweak form factors. It will be seen that the skyrmion structure is drastically modified from the standard picture based on the Skyrme model with a strong implication on many-body nuclear systems viewed as skyrmions with large winding numbers. Seen from the 5D perspective, the baryon will be a point-like instanton, allowing it to be treated as a local baryon field and providing a support to low-energy baryon chiral perturbation theory.

5.4 HLS$_{K=1}$ from Holographic Dual QCD

While chiral symmetry in hQCD is a local symmetry in 5 dimensions, it becomes a global symmetry when reduced to 4 dimensions. However it is possible to rewrite

the Lagrangian in terms of an infinite number of hidden local gauge fields, leading to $\mathrm{HLS}_{K=\infty}$ which we implicitly took for granted above. This turns out to allow us to obtain $\mathrm{HLS}_{K=1}$ by integrating out all but the lowest member of the tower in hQCD. This is an important element for later discussions on hidden local symmetry in hot/dense medium since we do not yet know how to apply $\mathrm{HLS}_{K=\infty}$ to matter under extreme conditions. In this section, we show how $\mathrm{HLS}_{K=1}$ can be obtained from hQCD of Sakai and Sugimoto as formulated in [Harada, Matsuzaki and Yamawaki 2006].

5.4.1 *Going from 5D to 4D*

We start from the 5D action (5.45) of SS [Sakai and Sugimoto 2005]. We take the $A_z(x^\mu, z) \equiv 0$ gauge (with $\mu = 0, 1, 2, 3$) which makes chiral symmetry manifest. This gauge choice still leaves a residual gauge symmetry, $h(x^\mu) = g(x^\mu, z = 0)$, which is precisely the hidden local symmetry (HLS) that we are familiar with:

$$A_\mu(x^\mu, z) \to h(x^\mu)\, \{A_\mu(x^\mu, z) + i\partial_\mu\}\, h^\dagger(x^\mu)\,. \tag{5.53}$$

In this gauge the Goldstone boson fields appear in the boundary conditions for the gauge field A_μ as

$$A_\mu(x^\mu, z = \pm\infty) = \alpha_\mu^{R,L}(x^\mu)\,, \tag{5.54}$$

where

$$\alpha_\mu^{R,L}(x^\mu) = i\xi_{R,L}(x^\mu)\partial_\mu\xi_{R,L}^\dagger(x^\mu) \tag{5.55}$$

which transform under the HLS in the same way as in Eq. (5.53). The L and R chiral fields appear at the boundary,

$$\xi_{R,L}(x^\mu) = e^{\frac{i\sigma(x^\mu)}{F_\sigma}} \cdot e^{\pm\frac{i\pi(x^\mu)}{F_\pi}}\,. \tag{5.56}$$

We would like to reduce to 4D and have the 4D vector fields transform hidden local invariantly. This can be done by mode-expanding

$$\begin{aligned} A_\mu(x^\mu, z) = {} & \alpha_\mu^R(x^\mu)\phi^r(z) + \alpha_\mu^L(x^\mu)\phi^l(z) \\ & + \sum_{k\geq 1} V_\mu^{(k)}(x^\mu)\phi_k(z)\,, \end{aligned} \tag{5.57}$$

where the functions ϕ^r, ϕ^l and ϕ_k ($k = 1, 2, \ldots$) form a complete set in the z-coordinate space and will be obtained by the equation of motion along the z direction. The $V_\mu^{(k)}$ fields are the hidden local fields we are interested in in 4D. When the expansion (5.57) is plugged into the 5D YM action (5.45) and integrated over the fifth direction, we get an infinite-tower HLS action.

We recall that the manifest gauge invariance is required to formulate a systematic χPT with the vector mesons put on the same footing as the Goldstone bosons.

Now, for focusing on processes that take place at very low energy $E \ll M_{KK}$, we may choose to integrate out *all* except for the lowest members $K = 1$ (or $K = 2$ if needed) and write the resultant action in terms of the latter, denoted ρ_μ for convenience, appropriate for chiral perturbation expansion. To do this we define 1-forms as before

$$\widehat{\alpha}_{\mu||}(x^\mu) = \frac{\alpha^R_\mu(x^\mu) + \alpha^L_\mu(x^\mu)}{2} - g\rho_\mu(x^\mu)\,, \tag{5.58}$$

$$\widehat{\alpha}_{\mu\perp}(x^\mu) = \frac{\alpha^R_\mu(x^\mu) - \alpha^L_\mu(x^\mu)}{2}\,. \tag{5.59}$$

Using these 1-forms, we can formally write down the familiar gauge-invariant chiral Lagrangian

$$\mathcal{L} = \tilde{F}_\pi^2 \mathrm{Tr}[\widehat{\alpha}_{\mu\perp}\widehat{\alpha}^\mu_\perp] + \tilde{F}_\sigma^2 \mathrm{Tr}[\widehat{\alpha}_{\mu||}\widehat{\alpha}^\mu_{||}] - \frac{1}{2}\mathrm{Tr}[\rho_{\mu\nu}\rho^{\mu\nu}] + \mathcal{L}_{(4)}\,, \tag{5.60}$$

where $\mathcal{L}_{(4)}$ is constructed by the $\mathcal{O}(p^4)$ terms. The contact with hQCD with its infinite tower is made in the constants $\tilde{F}_{\pi,\sigma}$ and the coefficients that appear in $\mathcal{L}_{(4)}$.

Integrating out the higher modes is worked out in [Harada, Matsuzaki and Yamawaki 2006]. The resulting Lagrangian is put in the form of (5.60) with the 5D gauge field $A_\mu(x_\mu, z)$ written in terms of "renormalized" coefficients as

$$\begin{aligned} A_\mu(x^\mu, z) = {} & \alpha^R_\mu(x^\mu)\varphi^r(z) + \alpha^L_\mu(x^\mu)\varphi^l(z) \\ & + g\rho_\mu(x^\mu)\varphi(z)\,. \end{aligned} \tag{5.61}$$

The upshot is that the ρ field embedded into the 5D gauge field with the effect of the higher members of the tower can be shoved into the wavefunctions in the fifth dimension, φ^r, φ^l and φ. Harada *et al.* were able to express the constants of the Lagrangian (5.60) in terms of the parameters figuring in hQCD Lagrangian, namely, N_c, λ and M_{KK} and the integrals of the 5D wavefunctions in the fifth direction.

5.4.2 *Doing quantum corrections*

The Lagrangian (5.60) is obtained in the weak coupling approximation in the gravity sector, applicable in the large N_c and λ limit in the field theory sector. One would like to compute $1/N_c$ and $1/\lambda$ corrections – quantum corrections – so as to confront Nature. That would require higher order calculations in the string theory sector but it is not known how this can be done. One possible way to circumvent this

difficulty was proposed in [Harada, Matsuzaki and Yamawaki 2006]. The idea is as follows. One takes the Lagrangian (5.60) as a *bare* Lagrangian determined at a matching scale Λ_M with the parameters fixed by matching to hQCD. Given this *bare* Lagrangian, quantum loop corrections can be done in the field theory sector in the same way as we describe below with $\mathrm{HLS}_{K=1}$ with a matching to QCD via correlators. This procedure seems to work fairly well. For instance, it can reproduce the KSRF relations and give vector dominance in the pion form factor with the ground-state ρ only.

There is however a big difference in its predictive nature. In $\mathrm{HLS}_{K=1}$ with vector manifestation, *i.e.* HLS/VM, the parameters in the effective theory inherit "intrinsic background dependence (IBD)" – with the background being temperature, density *etc* – from various condensates in the QCD correlators. The parameters therefore "slide" as temperature and/or density varies, an ingredient necessary to obtain in particular the striking properties associated with the vector manifestation fixed point. Thus IBD plays a crucial role in hot/dense medium. In order for hQCD to implement this property, one would have to do higher order loop calculations in the gravity sector. Given that hQCD has its own built-in "ultraviolet completion," such a calculation should in principle be doable. However such loop calculations in hQCD have not been worked out and furthermore, it is not clear whether the built-in ultraviolet completion gives correct high energy properties that are consistent with QCD proper. In other words, it is not clear whether one can approach the weak-coupling QCD regime for which higher lying KK modes in hQCD become relevant. There will be further comments on this matter in what follows.

5.5 Hidden Local Symmetry and the "Vector Manifestation"

5.5.1 $HLS_{K=1}$: Hidden local symmetry à la Bando *et al.*

We shall now focus on 4-D hidden local symmetry. As explained above, the $\mathrm{HLS}_{K=1}$ can be considered as a truncated theory of $\mathrm{HLS}_{K=\infty}$ with the effects of those vector mesons that are integrated out lodged in the role of quarks and gluons of QCD to which HLS will be matched by Wilsonian matching.

The basic chiral field is the unitary matrix field U

$$U = exp(2i\pi/F_\pi) \tag{5.62}$$

with $U \in SU(N_f)$. As we saw above, we can introduce a string of "redundant" fields by writing

$$U = \xi_L^\dagger \xi^1 \times \cdots \xi^{K-1} \xi_R. \tag{5.63}$$

This has K redundant degrees of freedom which can be elevated to K gauge degrees of freedom by introducing K local vector fields. Bando *et al* construct the $K = 1$

HLS theory setting

$$\xi^1 = \xi^2 = \cdots = \xi^{K-1} = 1. \tag{5.64}$$

This theory is $\mathrm{HLS}_{K=1}$ referred to above.

5.5.2 *$HLS_{K=1}$ with loop corrections*

So far we have been discussing the structure of the theory at tree order which is essentially what phenomenological Lagrangian approaches can do. Here we are interested in the quantum structure of this theory, that is, going to loop orders. It turns out that the quantum structure of the theory brings out several remarkable features that are not evident from the tree-order and that pertain to properties of hadrons in medium. This aspect is sometimes not appreciated in the literature. That is because at the tree level used in phenomenological calculations, various different approaches are all equivalent as long as symmetries are properly accounted for [Harada and Yamawaki 2003]. For instance, such approaches as (1) massive Yang-Mills (e.g, external gauging), (2) tensor fields and (3) HLS all give the same results at the tree level or semiclassical level as one applies to matter in medium. It is at the quantum level that the HLS approach gives results that are different from other approaches, in introducing vector mesons in the description when one is considering matter under extreme conditions.

To begin, we shall consider the three-flavor case in the chiral limit, so we are setting the current quark masses of up, down and strange flavors equal to zero.

As emphasized before, making the theory with vector mesons local gauge invariant enables one to go beyond the mass scale of the vector mesons taken into account and to identify where the theory breaks down. As noted, the scale is set by the dimensionful scale $\sim 4\pi m_V/g \sim 4\pi f_\pi$ where f_π is the pion decay constant ~ 93 MeV. This is the scale at which new physics must intervene, with the effective field theory given by HLS being no longer applicable. One should then find a different theory which has correct ultraviolet behavior to replace the effective theory. In strong interaction physics, it is obviously QCD. The strategy we shall use here is the one adopted by Harada and Yamawaki, *viz*, that at a suitable delineating scale $\Lambda_M \sim 4\pi f_\pi \sim 1$ GeV, the effective theory HLS should be matched to QCD. This may be considered as a sort of "ultraviolet completion."

The Lagrangian (5.23) is the leading order in derivative expansion $\sim \mathcal{O}(p^2)$ resulting from integrating out the degrees of freedom lying above the matching scale. For specific calculations, we need to go to the next order, *i.e.* $\mathcal{O}(p^4)$, in the expansion. To construct the corresponding Lagrangian, we need to include field strengths of the external left and right fields denoted respectively by $\mathcal{L}_\mu$ and $\mathcal{R}_\mu$,

$$\begin{aligned}
\mathcal{L}_{\mu\nu} &= \partial_\mu \mathcal{L}_\nu - \partial_\nu \mathcal{L}_\mu - i\,[\mathcal{L}_\mu\,,\,\mathcal{L}_\nu]\ , \\
\mathcal{R}_{\mu\nu} &= \partial_\mu \mathcal{R}_\nu - \partial_\nu \mathcal{R}_\mu - i\,[\mathcal{R}_\mu\,,\,\mathcal{R}_\nu]\ .
\end{aligned} \tag{5.65}$$

We convert these into the fields which transform as adjoint representations under the HLS:

$$\widehat{\mathcal{L}}_{\mu\nu} \equiv \xi_{\rm L}\mathcal{L}_{\mu\nu}\xi_{\rm L}^\dagger \ , \quad \widehat{\mathcal{R}}_{\mu\nu} \equiv \xi_{\rm R}\mathcal{R}_{\mu\nu}\xi_{\rm R}^\dagger \ , \tag{5.66}$$

which transform homogeneously

$$\begin{aligned} \widehat{\mathcal{L}}_{\mu\nu} &\to h(x)\cdot\widehat{\mathcal{L}}_{\mu\nu}\cdot h^\dagger(x) \ , \\ \widehat{\mathcal{R}}_{\mu\nu} &\to h(x)\cdot\widehat{\mathcal{R}}_{\mu\nu}\cdot h^\dagger(x) \ . \end{aligned} \tag{5.67}$$

Moreover, it is convenient to introduce the following combinations:

$$\begin{aligned} \widehat{\mathcal{V}}_{\mu\nu} &\equiv \frac{1}{2}\left[\widehat{\mathcal{R}}_{\mu\nu} + \widehat{\mathcal{L}}_{\mu\nu}\right] \ , \\ \widehat{\mathcal{A}}_{\mu\nu} &\equiv \frac{1}{2}\left[\widehat{\mathcal{R}}_{\mu\nu} - \widehat{\mathcal{L}}_{\mu\nu}\right] \ . \end{aligned} \tag{5.68}$$

For general N_f, there are 35 $\mathcal{O}(p^4)$ terms, a complete list of which can be found in [Tanabashi 1993]. We will not list them here. We shall simply write down those terms that will be used in the next subsection,

$$\mathcal{L}_{(4)z} = z_1\,{\rm Tr}\left[\hat{\mathcal{V}}_{\mu\nu}\hat{\mathcal{V}}^{\mu\nu}\right] + z_2\,{\rm Tr}\left[\hat{\mathcal{A}}_{\mu\nu}\hat{\mathcal{A}}^{\mu\nu}\right] + z_3\,{\rm Tr}\left[\hat{\mathcal{V}}_{\mu\nu}V^{\mu\nu}\right] + \cdots \tag{5.69}$$

where the ellipses stand for additional terms we shall not deal with here and z's are constants to be fixed empirically or theoretically.

5.5.2.1 *Wilsonian matching*

The effective field theory with (5.23) and (5.69) should apply at a scale below Λ_M. Since HLS$_{K=1}$ does not contain the a_1 meson, we choose the Λ_M below the a_1 mass, say, around 1 GeV. This is strictly a matter of choice. The physics of a_1 should be lodged then in (5.69). How it makes its input in a specific process is what we wish to discuss here. In principle it should not matter much where one takes it as long as it's near $\sim 4\pi f_\pi$, below the a_1 mass 1260 MeV. The canonical value that will be chosen is 1.1 GeV, following Harada and Yamawaki who have used this value in their extensive analyses. Baryons do not figure explicitly in this theory, since in the large N_c limit, they are much heavier. If needed, they can be generated as skyrmions as required in holographic dual QCD mentioned above (see Chapter 6 for more details). Above Λ_M, the relevant degrees of freedom are the elements of QCD, namely, quarks and gluons and below Λ_M, they are the pions and the vector mesons ρ_μ. *The crucial assumption that remains yet unjustified is that there is a region of energy scale Δ in which one can match the physics in terms of the QCD variables to that in terms of the effective variables.* This means that within the range Δ around Λ_M one can write the *bare* EFT Lagrangian in terms of quantities determined by QCD.

So the question is: What is this effective Lagrangian?

To give a precise definition, let us consider the generating functional both in QCD and in EFT,

$$Z_{QCD}[J] = \int [Dq][D\bar{q}][DG] e^{iS_{QCD}(q,\bar{q},G:J)}, \tag{5.70}$$

$$Z_{EFT}[J] = \int [DU] e^{iS_{EFT}(U,\mathcal{P}:J)} \tag{5.71}$$

where G stands for the gluon field, U for the set of effective fields that figure in the effective theory and $\mathcal{P}$ for set of parameters that represent the effective theory. Here J is the external source. Now the generating functionals at the scale $E = \Lambda_M$ are equal to each other by construction, and the parameters of the EFT are then given by

$$Z_{EFT}[J]|_{E=\Lambda_M} = e^{iS_{EFT}(U,\mathcal{P},J)|_{\Lambda_M}} = Z_{QCD}[J]|_{E=\Lambda_M}. \tag{5.72}$$

What this means is that the physics at $E = \Lambda_M$ is exactly given by the tree diagrams with the effective Lagrangian $\mathcal{L}_{EFT}$ with the parameters of the Lagrangian fixed by the QCD quantities defined at that scale. Thus to determine the parameters, one can simply compare physical quantities given by the tree graphs of $\mathcal{L}_{EFT}$ with the QCD quantities given at the same scale. This can be done by looking at the current correlators as described below.

Before we determine the parameters of $\mathcal{L}_{EFT}$ at the given scale, let us clarify the meaning and role of the effective Lagrangian so obtained. As mentioned, the physics at $E = \Lambda_M$ is given by the tree diagrams with this Lagrangian. This Lagrangian should, however, describe best the physics of energy $E \ll \Lambda_M$. To calculate physical amplitudes at $E = E_0 \ll \Lambda_M$, we need to "decimate" down to E_0. This decimation is precisely doing quantum corrections. The efficient way of doing this is via renormalization group equations.

To summarize: the Lagrangian obtained thereby through the matching is nothing but the *bare* Lagrangian that constitutes the classical action that enters in the Feynman path integral for the generating functional.

Let us give a very simplified description of how the matching can be done. It is convenient to exploit the axial-vector and vector correlators defined as

$$\begin{aligned}
\int d^4x e^{ipx} \left\langle 0 \left| T\, J^a_{5\mu}(x) J^b_{5\nu}(0) \right| 0 \right\rangle &= \delta^{ab} \left(p_\mu p_\nu - g_{\mu\nu} p^2 \right) G_A(p^2) \ , \\
\int d^4x e^{ipx} \left\langle 0 \left| T\, J^a_{\mu}(x) J^b_{\nu}(0) \right| 0 \right\rangle &= \delta^{ab} \left(p_\mu p_\nu - g_{\mu\nu} p^2 \right) G_V(p^2) \ .
\end{aligned} \tag{5.73}$$

In the HLS theory we are interested in, these two-point functions are well described by the tree contributions including $\mathcal{O}(p^4)$ terms when the momentum is around the matching scale, $Q^2 \sim \Lambda_M^2$. By combining $\mathcal{O}(p^4)$ terms in Eq. (5.69) with the leading terms in Eq. (5.23), the correlators in the HLS are given by [Harada and Yamawaki

2003] (with $Q^2 = -p^2$)

$$G_A^{(\mathrm{HLS})}(Q^2) = \frac{F_\pi^2(\Lambda)}{Q^2} - 2z_2(\Lambda) \ , \tag{5.74}$$

$$G_V^{(\mathrm{HLS})}(Q^2) = \frac{F_\sigma^2(\Lambda)}{M_\rho^2(\Lambda) + Q^2}\left[1 - 2g^2(\Lambda)z_3(\Lambda)\right] - 2z_1(\Lambda) \ , \tag{5.75}$$

where we defined

$$M_\rho^2(\Lambda) \equiv g^2(\Lambda)F_\sigma^2(\Lambda) \ . \tag{5.76}$$

The same correlators are evaluated by the OPE up to $\mathcal{O}(1/Q^6)$ [Shifman, Vainshtein and Zakharov 1979a; Shifman, Vainshtein and Zakharov 1979b]:

$$G_A^{(\mathrm{QCD})}(Q^2) = \frac{1}{8\pi^2}\left(\frac{N_c}{3}\right)\left[-\left(1 + \frac{3(N_c^2-1)}{8N_c}\frac{\alpha_s}{\pi}\right)\ln\frac{Q^2}{\mu^2}\right. \tag{5.77}$$
$$\left. + \frac{\pi^2}{N_c}\frac{\left\langle\frac{\alpha_s}{\pi}G_{\mu\nu}G^{\mu\nu}\right\rangle}{Q^4} + \frac{\pi^3}{N_c}\frac{96(N_c^2-1)}{N_c^2}\left(\frac{1}{2} + \frac{1}{3N_c}\right)\frac{\alpha_s\left\langle\bar{q}q\right\rangle^2}{Q^6}\right] ,$$

$$G_V^{(\mathrm{QCD})}(Q^2) = \frac{1}{8\pi^2}\left(\frac{N_c}{3}\right)\left[-\left(1 + \frac{3(N_c^2-1)}{8N_c}\frac{\alpha_s}{\pi}\right)\ln\frac{Q^2}{\mu^2}\right. \tag{5.78}$$
$$\left. + \frac{\pi^2}{N_c}\frac{\left\langle\frac{\alpha_s}{\pi}G_{\mu\nu}G^{\mu\nu}\right\rangle}{Q^4} - \frac{\pi^3}{N_c}\frac{96(N_c^2-1)}{N_c^2}\left(\frac{1}{2} - \frac{1}{3N_c}\right)\frac{\alpha_s\left\langle\bar{q}q\right\rangle^2}{Q^6}\right] ,$$

where μ is the renormalization scale of QCD and the N_c-dependence is written down explicitly.

In writing down the QCD correlators in the form given above, an assumption is made

$$\langle\bar{q}q\bar{q}q\rangle \propto \langle\bar{q}q\rangle^2. \tag{5.79}$$

That such a relation holds with a certain constant is clear, since when chiral symmetry is restored with the vanishing order parameter $\langle\bar{q}q\rangle = 0$, the vector correlator $G_V^{(\mathrm{QCD})}(Q^2)$ must be equal to the axial-vector correlator $G_A^{(\mathrm{QCD})}(Q^2)$. There cannot be an additional term on the RHS of (5.79) that does not vanish as $\langle\bar{q}q\rangle \to 0$. This must also be true when the system studied is not Lorentz invariant as in the case of medium with temperature and/or density treated below.

We require that the current correlators in the HLS in Eqs. (5.74) and (5.75) be matched at the matching scale Λ_M to those in QCD in Eqs. (5.77) and (5.78). There is a subtlety – and perhaps an ambiguity – in doing this because we are matching two quantities that are supposed to be valid in two different regimes. In HLS, the derivative expansion with Q taken as a "small" parameter, hence in positive power of Q, is used; this means that the current correlators are valid in the low-energy region. On the other hand, the OPE is an asymptotic expansion in negative power of Q, and hence is valid in the high energy region. Thus the validity of the matching

requires the existence of high-low energy duality in some region in the scale where the two expansions overlap. As stipulated above, we are assuming that this can be done. Whether this works or not cannot be mathematically proven and so has been justified only *à posteriori* by showing that the scheme works [Harada and Yamawaki 2003].

Since we are calculating the current correlators in the HLS including the first non-leading order $[\mathcal{O}(p^4)]$, we expect that we can match the correlators with those in the OPE up to the first derivative. Note that both $G_A^{(\mathrm{QCD})}$ and $G_V^{(\mathrm{QCD})}$ explicitly depend on μ. Such dependence is assigned to the parameters $z_2(\Lambda)$ and $z_1(\Lambda)$. However, the difference between two correlators has no explicit dependence on μ. Thus our first Wilsonian matching condition is given by

$$\begin{aligned}
&\frac{F_\pi^2(\Lambda_M)}{\Lambda_M^2} - \frac{F_\sigma^2(\Lambda_M)}{\Lambda_M^2 + M_\rho^2(\Lambda_M)}\left[1 - 2g^2(\Lambda_M) z_3(\Lambda_M)\right] - 2\left[z_2(\Lambda_M) - z_1(\Lambda_M)\right] \\
&\quad = \frac{4\pi(N_c^2-1)}{N_c^2}\frac{\alpha_s \langle\bar{q}q\rangle^2}{\Lambda_M^6} \ . \qquad (5.80)
\end{aligned}$$

We also require that the first derivative of $G_A^{(\mathrm{HLS})}$ in Eq. (5.74) match that of $G_A^{(\mathrm{QCD})}$ in Eq. (5.77), and similarly for G_V's in Eqs. (5.75) and (5.78). This requirement gives the following two Wilsonian matching conditions

$$\begin{aligned}
\frac{F_\pi^2(\Lambda_M)}{\Lambda_M^2} &= -Q^2 \frac{d}{dQ^2} G_A^{(\mathrm{QCD})}(Q^2)\Big|_{Q^2=\Lambda_M^2} \\
&= \frac{1}{8\pi^2}\left(\frac{N_c}{3}\right)(1+\delta_A) \ , \\
\delta_A &\equiv \frac{3(N_c^2-1)}{8N_c}\frac{\alpha_s}{\pi} + \frac{2\pi^2}{N_c}\frac{\left\langle \frac{\alpha_s}{\pi} G_{\mu\nu}G^{\mu\nu}\right\rangle}{\Lambda_M^4} \\
&\quad + \frac{288\pi(N_c^2-1)}{N_c^3}\left(\frac{1}{2} + \frac{1}{3N_c}\right)\frac{\alpha_s\langle\bar{q}q\rangle^2}{\Lambda_M^6} \ , \qquad (5.81)
\end{aligned}$$

$$\begin{aligned}
&\frac{F_\sigma^2(\Lambda_M)}{\Lambda_M^2}\frac{\Lambda_M^4\left[1 - 2g^2(\Lambda_M) z_3(\Lambda_M)\right]}{\left[\Lambda_M^2 + M_\rho^2(\Lambda_M)\right]^2} = -Q^2\frac{d}{dQ^2} G_V^{(\mathrm{QCD})}(Q^2)\Big|_{Q^2=\Lambda_M^2} \\
&\quad = \frac{1}{8\pi^2}\left(\frac{N_c}{3}\right)(1+\delta_V) \ , \\
&\delta_V \equiv \frac{3(N_c^2-1)}{8N_c}\frac{\alpha_s}{\pi} + \frac{2\pi^2}{N_c}\frac{\left\langle \frac{\alpha_s}{\pi} G_{\mu\nu}G^{\mu\nu}\right\rangle}{\Lambda_M^4} \\
&\quad - \frac{288\pi(N_c^2-1)}{N_c^3}\left(\frac{1}{2} - \frac{1}{3N_c}\right)\frac{\alpha_s\langle\bar{q}q\rangle^2}{\Lambda_M^6} \ . \qquad (5.82)
\end{aligned}$$

Corrections from ρ and/or π loops to the LHS of Eqs. (5.81) and (5.82) are of higher order in the present counting scheme, and hence are left out.

The above three equations (5.80), (5.81) and (5.82) are the Wilsonian matching conditions. These determine the *bare* parameters of the HLS without much ambiguity. Especially, the second condition (5.81) determines the ratio $F_\pi(\Lambda_M)/\Lambda_M$ directly from QCD. It should be noticed that the above Wilsonian matching conditions determine the absolute value and the explicit dependence of bare parameters of HLS on the parameters of underlying QCD such as N_c (not just scaling properties in the large N_c limit) and $\Lambda_{\rm QCD}$ *as well as, most importantly for nuclear physics, on the dependence of the quark and gluon condensates on external conditions such as density and temperature.* The latter dependence reflects QCD vacuum structure in a heat bath (the Early Universe) or in a compressed environment (neutron stars) and cannot be obtained by perturbation from zero density/temperature vacuum or without matching to QCD. We shall refer to this dependence as "intrinsic background (temperature/density) dependence."[10]

5.5.2.2 *Vector manifestation (VM)*

The hidden local symmetry *and* the matching to QCD determine the bare parameters $F_\pi(\Lambda_M)$, $g(\Lambda_M)$ and $a(\Lambda_M)$ in terms of the quark condensate $\langle\bar{q}q\rangle$, the gluon condensate $\langle G_{\mu\nu}G^{\mu\nu}\rangle$ and the QCD gauge coupling constant α_s at the scale Λ_M. The matching procedure makes a unique prediction on what happens to the HLS parameters at the point where chiral symmetry is restored.[11] This is the feature which distinguishes HLS theory from "standard" sigma-model approaches.

To see what happens in this theory under extreme conditions, first we define what we mean by chiral restoration. This is done in terms of the QCD order parameter, the quark condensate $\langle\bar{q}q\rangle$. The chiral symmetry spontaneously broken (Goldstone) phase is characterized by $\langle\bar{q}q\rangle \neq 0$ and the chiral symmetry restored (Wigner) phase by $\langle\bar{q}q\rangle = 0$. Now setting $\langle\bar{q}q\rangle \to 0$ in the matching conditions (5.80), (5.81) and (5.82), one finds that

$$g(\Lambda_M) \to 0 \ , \tag{5.83}$$

$$a(\Lambda_M) = \frac{F_\sigma^2(\Lambda_M)}{F_\pi^2(\Lambda_M)} \to 1 \ , \tag{5.84}$$

$$z_1(\Lambda_M) - z_2(\Lambda_M) \to 0 \ , \tag{5.85}$$

$$F_\pi^2(\Lambda_M) \to (F_\pi^{\rm crit})^2 \equiv \frac{N_c}{3}\left(\frac{\Lambda_M}{4\pi}\right)^2 \cdot 2(1+\delta_A^{\rm crit}) \neq 0 \tag{5.86}$$

with

$$\delta_A^{\rm crit} \equiv \delta_A|_{\langle\bar{q}q\rangle=0} = \frac{3(N_c^2-1)}{8N_c}\,\frac{\alpha_s}{\pi} + \frac{2\pi^2}{N_c}\frac{\left\langle\frac{\alpha_s}{\pi}G_{\mu\nu}G^{\mu\nu}\right\rangle}{\Lambda_M^4} > 0 \quad (\ll 1) \ . \tag{5.87}$$

[10]The point which will recur throughout the volume is that this intrinsic dependence which plays a crucial role for the vector manifestation described below is missing in all other works that do not use the gauge invariant procedure adopted here.

[11]Whether or not chiral symmetry is restored makes strict sense only in the chiral limit where the quark masses are taken to be zero. This is how we will understand the terminology.

One of the important consequences of the above properties is that the *parametric mass* $M_\rho^2(\Lambda)$ defined in (5.76) – the mass that figures in the HLS Lagrangian – goes to zero

$$M_\rho^2(\Lambda) \to 0 \ \text{ as } \langle\bar{q}q\rangle \to 0. \tag{5.88}$$

It turns out (more on this later) that RG flow equations show that $g = 0$ and $a = 1$ are the fixed points. This means that once g and a are at the fixed point, they remain there no matter what the scale is. Therefore at the point where $\langle\bar{q}q\rangle = 0$, we have $g = 0$ and $a = 1$ independently of the scale (*i.e.* scale invariant). But since the QCD dictates that the condensate be zero at the chiral restoration, g and a will flow to the fixed point as one dials the external conditions such as temperature and/or density. But this is not the case with the F_π. Note that $F_\pi(\Lambda_M)$ remains non-zero when the condensate vanishes. But we know that the on-mass-shell pion decay constant must vanish at chiral restoration since it is the order parameter in hadronic variable. Therefore the pion decay constant must flow as the scale is changed. Now remaining on the point at which $g = 0$ and $a = 1$, only the pion loops will contribute to the RGE for F_π as the vector mesons decouple. As with all the loops involving scalars, the pion loop will be divergent: in the Wilsonian RGE, it will correspond to a $D = 2$ singularity in dimensional regularization and a quadratic divergence in the cut-off regularization. The one-loop RGE is of the form (see below)

$$\mu\frac{d}{d\mu}F_\pi^2(\mu) = \frac{N_f}{(4\pi)^2}\mu^2 \ . \tag{5.89}$$

The solution is

$$F_\pi^2(0) = F_\pi^2(\Lambda_M) - \frac{N_f}{2(4\pi)^2}\Lambda_M^2 \tag{5.90}$$

where $F_\pi^2(\Lambda_M)$ is given by Eq. (5.86) which is a known quantity for given α_s, $\langle G_{\mu\nu}G^{\mu\nu}\rangle$ and Λ_M. Interpreting that $F_\pi(0)$ is related to $\langle\bar{q}q\rangle$ as order parameter, we set $F_\pi^2(0) = 0$ at $\langle\bar{q}q\rangle = 0$. Equation (5.90) gives the condition for the only unknown, *i.e.* N_f, in the equation at $\langle\bar{q}q\rangle = 0$, that is, the critical number of flavor at which chiral symmetry is restored. The precise value of the critical N_f^c depends on rather poorly known gluon condensate, so it is not possible to pin down the number but the analysis [Harada and Yamawaki 2003] indicates $N_f^c \sim 5$. There are results from lattice QCD which give generally larger but conflicting values for N_f^c. The lattice measurement by Iwasaki *et al* [Iwasaki *et al* 2004] gives $6 < N_f^c < 7$ whereas Appelquist *et al* [Appelquist, Fleming and Neil 2007] find $8 < N_f^c < 12$. For our purpose, what is important is that at the chiral restoration, one is at the fixed point $g = 0$ and $a = 1$ with $F_\pi(0) \equiv f_\pi = 0$. The corresponding fixed point with $F_\pi(0) = 0$ is the "vector manifestation (VM) fixed point" reached when chiral symmetry is restored (in the chiral limit).

5.5.2.3 *"Dropping mass" and local gauge symmetry*

The hidden gauge coupling g going to zero as one reaches chiral restoration means that the "parametric mass" of the vector meson goes to zero and so does the width of the vector meson (since the width goes as $\sim g^n$ with $n \geq 2$ as explained later). Thus the notion that the vector meson mass is "small" – used in setting up a chiral perturbation strategy with the vector mesons and the pions – becomes more appropriate. This is where the local gauge symmetry we advocate plays an important role. To see this, consider doing loop calculations with the vector meson appearing in the internal line of the loop. The propagator in an arbitrary gauge is

$$\frac{1}{p^2 - M_\rho^2}\left[g_{\mu\nu} - (1-\alpha)\frac{p_\mu p_\nu}{p^2 - \alpha m_\rho^2}\right] , \tag{5.91}$$

where α is the gauge fixing parameter. This propagator is well defined in the limit of $M_\rho \to 0$ except for the gauge $\alpha = \infty$ which is the unitary gauge. If one were to use the unitary gauge, then the propagator would be ill-defined, and it would be cumbersome to calculate loop corrections as one approaches chiral restoration where $M_\rho \to 0$. Gauge invariance assures that no terms of $1/M_\rho^2$ appear in the loop calculation. This is relevant when we consider high temperature and/or high density matter at which the theory predicts the "dropping" of the mass. Gauge non-invariant Lagrangians cannot handle this feature in a simple and transparent way, and hence can lead to misleading results on the properties of hadrons in hot and/dense matter.

5.5.2.4 *Scaling near the VM fixed point*

It is important to understand how various quantities in HLS theory scale in the order parameter of chiral symmetry, *i.e.* the quark condensate, as the latter goes to zero. This will have an important ramification in studying hadrons in matter. Matter makes the system break Lorentz invariance, so the discussion is a bit trickier but for the moment we work with Lorentz invariant systems, coming back to Lorentz-symmetry breaking later. Let us consider driving the system toward chiral restoration by dialing the number of flavors N_f to the critical value. Here Lorentz invariance is preserved. We shall do this taking both the number of colors N_c and N_f to be large.

First let us see how the bare parameters $g(\Lambda; N_f)$ and $a(\Lambda; N_f)$ approach the VM fixed point in Eqs. (5.83) and (5.84). Taking the limits $g^2(\Lambda) \ll 1$, $M_\rho^2(\Lambda)/\Lambda^2 = g^2(\Lambda)a(\Lambda)F_\pi^2(\Lambda)/\Lambda^2 \ll 1$ and $F_\sigma^2(\Lambda)/F_\pi^2(\Lambda) - 1 = a(\Lambda) - 1 \ll 1$ in the Wilsonian matching condition (5.80), we obtain

$$g^2(\Lambda)\left(\frac{F_\pi^2(\Lambda)}{\Lambda^2}\right)^2 - (a(\Lambda)-1)\frac{F_\pi^2(\Lambda)}{\Lambda^2} + 2g^2(\Lambda)z_3(\Lambda)\frac{F_\pi^2(\Lambda)}{\Lambda^2} - 2\left[z_2(\Lambda) - z_1(\Lambda)\right]$$
$$= \frac{4(N_c^2-1)\pi}{N_c^2}\frac{\alpha_s\langle\bar{q}q\rangle^2}{\Lambda^6} . \tag{5.92}$$

In the large N_c limit, $F_\pi^2 \sim \mathcal{O}(N_c)$, $\alpha_s \sim \mathcal{O}(1/N_c)$ and $\langle\bar{q}q\rangle \sim \mathcal{O}(N_c)$, we expect the first term to dominate, so as $N_f \to N_f^c$,

$$g^2(\Lambda) \sim \frac{\alpha_s}{N_c^2}\,\langle\bar{q}q\rangle^2 \ . \tag{5.93}$$

Now the mass formula

$$M_\rho^2(\Lambda) = a(\Lambda) g^2(\Lambda) F_\pi^2(\Lambda) \tag{5.94}$$

becomes, on-shell,

$$m_\rho^2 = a(m_\rho) g^2(m_\rho) F_\pi^2(m_\rho). \tag{5.95}$$

Since $M_\rho^2(\Lambda)|_{\langle\bar{q}q\rangle=0} = 0$ for any Λ, so $m_\rho = M_\rho^2(\rho)$ will go to zero in the same limit. Furthermore

$$\frac{m_\rho^2}{F_\pi^2(m_\rho)} = a(m_\rho) g^2(m_\rho) \to \langle\bar{q}q\rangle^2. \tag{5.96}$$

Thus the vector meson mass goes to zero faster than the pion decay constant as chiral restoration is approached.

An important point to stress here (that will be used later) is that the vector meson mass goes linear in the quark condensate near the VM fixed point.

5.6 Phenomenology with HLS$_{K=1}$

Although our main theme here is that HLS/VM is potentially most powerful in medium, we discuss how it fares at low energy outside of the medium. In fact, it comes out to work just as well as the nonlinear sigma model without vector mesons does in confronting Nature in hadronic interactions at low energy. This gives a compelling support to its validity as a reliable effective field theory of QCD. In this section, we discuss a few such issues.

5.6.1 *Doing chiral perturbation theory*

Chiral perturbation theory (χPT) based on nonlinear sigma model is reformulated here in terms of HLS/VM.

5.6.1.1 *Chiral counting for the vector mesons in χPT*

In the HLS theory, thanks to the gauge invariance, it is possible to perform the derivative expansion systematically even when vector mesons are present. In χPT with HLS, the vector meson mass is considered as *small* compared with the chiral symmetry breaking scale Λ_χ, by assigning $\mathcal{O}(p)$ to the HLS gauge coupling

[Georgi 1989a; Georgi 1989b; Tanabashi 1993]:

$$g \sim \mathcal{O}(p)\,. \tag{5.97}$$

In fact, in HLS theory, the vector meson mass drops to the level of the pion mass when the strongly interacting system is put in heat bath or compressed to high density, so the loops computed with the vector mesons in the loop interior can become important. This means that chiral perturbation calculation should be treated with the vector mesons put on the same footing as the pions. It is here that hidden local symmetry has its power. Other methods such as antisymmetric tensor field method, matter field method *etc.* are not readily amenable to this task.

The argument applies both to with and without a_1, so we discuss the former case. This will be needed for a later subsection. We can adopt the same order assignment for both ρ and a_1 mesons in the HLS$_{K=2}$, *i.e.* $m_\rho \sim m_{a_1} \sim \mathcal{O}(p)$. This counting is contrasted to the tensor field counting, $m_\rho^2 \sim \mathcal{O}(1)$. This is the most important part in the counting rules in the HLS. Now the ρ field (and a_1 field) is counted as $\mathcal{O}(1)$. So the kinetic term of the HLS gauge boson is counted as $\mathcal{O}(p^2)$ which is of the same order as the kinetic term of the pseudoscalar meson.

At the next order, $\mathcal{O}(p^4)$ for general N_f, there are many terms, say, 35 counter terms for the ρ field [Tanabashi 1996]. We will need only three of them given in Eq. (5.69). The calculational strategy is to do the chiral expansion with the above counting rule and then take the N_f value, 2 or 3, called for the calculation. This method turns out to be surprisingly successful in medium-free space where the vector meson is massive.[12] It should be more suitable in medium where the vector meson mass is predicted to diminish.

Using the above counting rule, we can systematically incorporate the quantum corrections to several physical quantities.

Let us be more precise as to what we mean by "smallness" of the expansion parameter $m_{\rho,a_1}/\Lambda_\chi$. Similarly to the smallness of m_ρ/Λ_χ discussed in [Harada and Yamawaki 2003], the smallness of the expansion parameters $m_{a_1}/\Lambda_\chi \ll 1$ can be justified for large number of colors N_c of QCD as follows: In the large N_c limit, the (parametric) pion decay constant F_π scales as $\sqrt{N_c}$ which implies that Λ_χ scales as $\Lambda_\chi \sim 4\pi F_\pi \sim \sqrt{N_c}$. On the other hand, the masses of vector and axial-vector mesons, m_{ρ,A_1}, do not scale with N_c. So the ratios $m_{\rho,A_1}^2/F_\pi^2$ scale as $1/N_c$, and become small in the large N_c QCD:

$$\frac{m_{\rho,A_1}^2}{\Lambda_\chi^2} = \frac{m_{\rho,A_1}^2}{(4\pi F_\pi)^2} \;\sim\; \frac{1}{N_c} \;\ll\; 1. \tag{5.98}$$

[12] Although we develop our arguments in the chiral limit, symmetry breaking can be systematically taken into account. The resulting phenomenology comes out to be remarkably successful. See [Benayoun *et al.* 2007] for a recent account.

Thus we can perform the derivative expansion in the large N_c limit, and extrapolate the results to the real-life QCD with $N_c = 3$.

5.6.1.2 *Loop calculations*

Since we will need the a_1 degree of freedom for a later discussion, we work with the HLS$_{K=2}$ defined below by the HLS$_{K=2}$ Lagrangian (5.172) which encompasses HLS$_{K=1}$. Quantum corrections to the five leading-order parameters of the HLS$_{K=2}$ Lagrangian from the π, ρ and a_1 mesons have been performed by Harada and Sasaki [Harada and Sasaki 2005] and by Hidaka *et al* [Hidaka, Morimatsu and Ohtani 2006]. The calculation is rather lengthy and the formulas are involved. We make the briefest possible sketch of the results here which we will need later and return to them for more details.

The calculation was done by using the background field method in 't Hooft-Feynman gauge. In this calculation, as stressed above, it is important to include the quadratic divergences to obtain the RGEs in the Wilsonian sense as described in [Harada and Yamawaki 2003]. One uses the dimensional regularization and identifies the quadratic divergences with the presence of poles of ultraviolet origin at $n = 2$. This can be done by the following replacement in the Feynman integrals:

$$\int \frac{d^n k}{i(2\pi)^n} \frac{1}{-k^2} \to \frac{\Lambda^2}{(4\pi)^2}\,,$$

$$\int \frac{d^n k}{i(2\pi)^n} \frac{k_\mu k_\nu}{\left[-k^2\right]^2} \to -\frac{\Lambda^2}{2(4\pi)^2} g_{\mu\nu}\,. \tag{5.99}$$

On the other hand, the logarithmic divergence is identified with the pole at $n = 4$:

$$\frac{1}{\bar{\epsilon}} + 1 \to \ln \Lambda^2\,, \tag{5.100}$$

where

$$\frac{1}{\bar{\epsilon}} \equiv \frac{2}{4-n} - \gamma_E + \ln(4\pi)\,, \tag{5.101}$$

with γ_E being the Euler constant.

The quantities we are interested in are the two-point functions of $\bar{V}^\mu$-$\bar{V}^\nu$, $\bar{A}^\mu$-$\bar{A}^\nu$, $\bar{\mathcal{A}}^\mu_\perp$-$\bar{A}^\nu$ and $\bar{\mathcal{A}}^\mu_M$-$\bar{\mathcal{A}}^\nu_\perp$, which we express as $\Pi^{\mu\nu}_{\bar{V}\bar{V}}$, $\Pi^{\mu\nu}_{\bar{A}\bar{A}}$, $\Pi^{\mu\nu}_{\bar{\mathcal{A}}_\perp\bar{A}}$, $\Pi^{\mu\nu}_{\bar{\mathcal{A}}_M\bar{\mathcal{A}}_\perp}$, respectively. We divide each of these two-point functions into two parts as

$$\Pi^{\mu\nu}(p) = \Pi^S(p^2) g^{\mu\nu} + \Pi^{LT}(p^2)(p^2 g^{\mu\nu} - p^\mu p^\nu)\,. \tag{5.102}$$

At the bare level, the relevant parts are expressed as

$$\begin{aligned}
\Pi^{(\mathrm{bare})S}_{\bar{V}\bar{V}} &= a_{\mathrm{bare}}F^2\,,\\
\Pi^{(\mathrm{bare})LT}_{\bar{V}\bar{V}} &= -\frac{1}{g^2_{\mathrm{bare}}} + 2z^{LR}_{\mathrm{bare}}\,,\\
\Pi^{(\mathrm{bare})S}_{\bar{A}\bar{A}} &= (b_{\mathrm{bare}} + c_{\mathrm{bare}})F^2\,,\\
\Pi^{(\mathrm{bare})LT}_{\bar{A}\bar{A}} &= -\frac{1}{g^2_{\mathrm{bare}}} - 2z^{LR}_{\mathrm{bare}}\,,\\
\Pi^{(\mathrm{bare})S}_{\bar{\mathcal{A}}_\perp\bar{A}} &= -b_{\mathrm{bare}}F^2\,,\\
\Pi^{(\mathrm{bare})S}_{\bar{\mathcal{A}}_M\bar{\mathcal{A}}_\perp} &= d_{\mathrm{bare}}F^2\,,
\end{aligned} \tag{5.103}$$

where z^{LR}_{bare} is the coefficient of $\mathcal{O}(p^4)$ terms proportional to $\mathrm{Tr}\left[L_{\mu\nu}\xi_M R^{\mu\nu}\xi^\dagger_M\right]$. The constant F is defined below in (5.168). From Eq. (5.103), the divergences proportional to $g^{\mu\nu}$ in the two-point functions are renormalized by $a_{\mathrm{bare}}, b_{\mathrm{bare}}, c_{\mathrm{bare}}$ and d_{bare} and those proportional to $(p^2g^{\mu\nu} - p^\mu p^\nu)$ are renormalized by g_{bare} and z^{LR}_{bare}. Thus the renormalization conditions are

$$\begin{aligned}
a_{\mathrm{bare}}F^2 + \Pi^S_{\bar{V}\bar{V}}\big|_{\mathrm{div}} &= (\mathrm{finite})\,,\\
-b_{\mathrm{bare}}F^2 + \Pi^S_{\bar{\mathcal{A}}_\perp\bar{A}}\big|_{\mathrm{div}} &= (\mathrm{finite})\,,\\
c_{\mathrm{bare}}F^2 + \Pi^S_{\bar{A}\bar{A}}\big|_{\mathrm{div}} + \Pi^S_{\bar{\mathcal{A}}_\perp\bar{A}}\big|_{\mathrm{div}} &= (\mathrm{finite})\,,\\
d_{\mathrm{bare}}F^2 + \Pi^S_{\bar{\mathcal{A}}_M\bar{\mathcal{A}}_\perp}\big|_{\mathrm{div}} &= (\mathrm{finite})\,,\\
-\frac{1}{g^2_{\mathrm{bare}}} + \frac{1}{2}\left[\Pi^{LT}_{\bar{V}\bar{V}}\big|_{\mathrm{div}} + \Pi^{LT}_{\bar{A}\bar{A}}\big|_{\mathrm{div}}\right] &= (\mathrm{finite})\,.
\end{aligned} \tag{5.104}$$

From the above renormalization conditions follow the renormalization group equations (RGEs) for the parameters a, b, c, d and the $\mathrm{HLS}_{K=2}$ gauge coupling g.

5.6.1.3 *Comparison with experiments*

A detailed analysis with $\mathrm{HLS}_{K=1}$is available and reviewed in [Harada and Yamawaki 2003; Benayoun *et al.* 2007]. We need not repeat what is given there. It suffices to mention that in all quantities so far studied, the χPT with $\mathrm{HLS}_{K=1}$works just as well as the classic pion-only χPT does.

5.6.2 *Weinberg sum rules*

We shall now look at some of the sum rules that are closely associated with chiral symmetry. In particular we examine how one can interpret Weinberg sum rules [Weinberg 1967], KSRF relation *etc.*

First define the spectral functions of the vector (V) and axial-vector (A) currents:

$$\frac{1}{2\pi}\int d^4x e^{ipx}\langle 0|J^a_\mu(x)J^b_\nu(0)|0\rangle = \delta^{ab}(p_\mu p_\nu - g_{\mu\nu}p^2)\rho_V(p^2)\ , \tag{5.105}$$

$$\frac{1}{2\pi}\int d^4x e^{ipx}\langle 0|J^a_{5\mu}(x)J^b_{5\nu}(0)|0\rangle = \delta^{ab}(p_\mu p_\nu - g_{\mu\nu}p^2)\rho_A(p^2) + \delta^{ab}p_\mu p_\nu \rho^0_A(p^2)\ , \tag{5.106}$$

where $\rho^0_A(p^2)$ is the spin 0 component of the spectral function and $\rho_{V,A}(p^2)$ the spin 1 component. In terms of these spectral functions, the Weinberg sum rules read

$$\int_0^\infty ds s^{-1}\left[\rho_V(s) - \rho_A(s)\right] = F_\pi^2\ , \tag{5.107}$$

$$\int_0^\infty ds\ \left[\rho_V(s) - \rho_A(s)\right] = 0\ . \tag{5.108}$$

The resonance saturation assumption that ρ_V is dominated by the ρ meson [13] and ρ_A by the a_1 meson lead to

$$\frac{g_\rho^2}{m_\rho^2} = F_\pi^2 + \frac{g_{a_1}^2}{m_{a_1}^2}, \tag{5.109}$$

$$g_\rho^2 = g_{a_1}^2\ . \tag{5.110}$$

Now with $g_\rho = agF_\pi^2$, these give

$$\frac{m_\rho^2}{m_{a_1}^2} = 1 - 1/a \tag{5.111}$$

which for $a = 2$ leads to the Weinberg mass formula

$$m_{a_1} = \sqrt{2}m_\rho. \tag{5.112}$$

One notes that when $a = 1$ – which we will argue holds in nature violating vector dominance, the ratio $\frac{m_\rho^2}{m_{a_1}^2}$ goes to zero or $m_{a_1} \to \infty$ for finite m_ρ meaning that the ρ mass goes to zero while the a_1 stays massive. This is a signal that at $a = 1$, the vector dominance hypothesis makes no sense. In fact, it breaks down in $\mathrm{HLS}_{K<\infty}$ as we will see later.

In Harada-Yamawaki theory $\mathrm{HLS}_{K=1}$, a_1 has been integrated out and hence the resonance saturation approximation does not make sense. It will be necessary to look at the sum rules as they are in terms of the spectral functions given by the theory. In terms of the correlators defined in (5.73), the first Weinberg sum rule (5.107) reads

$$\left[-Q^2G_V(Q^2) + Q^2G_A(Q^2)\right]|_{Q^2=0} = F_\pi^2\ . \tag{5.113}$$

[13] That is, $\rho_V(s) \simeq g_\rho^2\delta(s - m_\rho^2)$.

This is trivially satisfied by the HLS correlators (5.75) and (5.74) at the tree level. It turns out to be satisfied also at one loop level [Harada and Yamawaki 2003]. It is easy to understand how this can happen at one loop order in the theory. Although the a_1 is not present, it is the $\pi\rho$ complex in the bubble that mocks up the a_1.

The key point here is that Weinberg sum rules are not violated in HLS/VM. This point is important later when we consider what happens at chiral restoration where the ρ and a_1 become degenerate as implied by the Weinberg sum rule in the limit that $F_\pi \to 0$. In other words, even if there is no explicit a_1, HLS/VM is consistent with the symmetry constraints implicit in the Weinberg sum rule.

The interplay between a_1 and the Weinberg sum rules in $\mathrm{HLS}_{K=2}$ theory will be discussed below.

5.6.3 *Pion mass difference*

Calculating the π^+ - π^0 mass difference $\Delta m_\pi^2 \equiv m_{\pi^+}^2 - m_{\pi^0}^2$ in HLS has an interesting feature that will be exploited below and in Chapters 9 and 10, namely that the fixed point value $a = 1$ is applicable even for the situation that departs from the VM fixed point with $g \neq 0$ and $f_\pi \neq 0$. The calculation in HLS is straightforward and is unambiguous once the matching point Λ_M is fixed [Harada, Tanabashi and Yamawaki 2003].

The mass difference is given by the one photon exchange pion self-energy graph. For this, the photon field A_μ is introduced in the external field as $\mathcal{L}_\mu = \mathcal{R}_\mu = e\,Q\,A_\mu$, where e is the electromagnetic coupling and Q the electromagnetic charge matrix of the diagonal form: $\mathrm{diag}(Q) = (2/3, -1/3, -1/3)$. In order to include the photon loop, we need to add the kinetic term of the photon field to the $\mathcal{O}(p^2)$ HLS Lagrangian. Since HLS is cut off at Λ_M, the degrees of freedom lying above Λ_M, namely quarks and gluons, that are integrated out, give rise to a "counter term" which has the form

$$\sim \alpha_{\mathrm{em}}\,\kappa\,\mathrm{Tr}\left[QUQU^\dagger\right], \tag{5.114}$$

where κ is a constant to be determined, $U = \xi_L^\dagger \xi_R = e^{2i\pi/F_\pi(\Lambda_M)}$ and $\alpha_{\mathrm{em}} = e^2/4\pi$ is the fine structure constant. This contribution to the mass splitting is the "bare" mass term, and is given by

$$\Delta m_\pi^2\big|_{\mathrm{bare}} = \alpha_{\mathrm{em}}\,\Omega(\Lambda_M)/F_\pi^2(\Lambda_M) \equiv \alpha_{\mathrm{em}}\,\omega(\Lambda_M)\ . \tag{5.115}$$

It is easy to see that this term can be fixed by the Wilsonian matching. To do so, the usual current algebra formula for Δm_π^2 is written in terms of the full current correlators (5.73):

$$\Delta m_\pi^2 = (3\alpha_{\mathrm{em}}/4\pi)\int_0^\infty dQ^2\,Q^2\Delta\Pi(Q^2)/F_\pi^2(0), \tag{5.116}$$

where $\Delta\Pi(Q^2) \equiv G_A(Q^2) - G_V(Q^2)$ and $F_\pi(0) \equiv f_\pi (\neq F_\pi(\Lambda_M))$ the physical decay

constant of π. Now the matching amounts to identifying the high energy part of the integral for $Q^2 > \Lambda_M^2$ as the bare term Eq. (5.115):

$$\omega(\Lambda_M) = \frac{3}{4\pi}\int_{\Lambda_M^2}^{\infty} dQ^2 Q^2 \frac{\Delta\Pi^{(\mathrm{QCD})}(Q^2)}{F_\pi^2(0)} = \frac{8}{3}\frac{\alpha_s \langle\bar{q}q\rangle^2}{F_\pi^2(0)\Lambda_M^2} \ , \tag{5.117}$$

where $\Delta\Pi^{(\mathrm{QCD})}(Q^2)$ is given by the operator product expansion (OPE) in QCD [Shifman, Vainshtein and Zakharov 1979a; Shifman, Vainshtein and Zakharov 1979b],

$$\Delta\Pi^{(\mathrm{QCD})}(Q^2) = [4\pi(N_c^2-1)/N_c^2][(\alpha_s \langle\bar{q}q\rangle^2)/Q^6]. \tag{5.118}$$

Taking $N_f = 3$, $(\Lambda_M\,,\,\Lambda_{\mathrm{QCD}}) = (1.1\,,\,0.4)\,\mathrm{GeV}$ and $\langle\bar{q}q\rangle_{1\mathrm{GeV}} = -\,(225 \pm 25\,\mathrm{MeV})^3$, one gets from Eq. (5.115) and Eq. (5.117)

$$\Delta m_\pi^2\big|_{\mathrm{bare}} = \alpha_{\mathrm{em}}\omega(\Lambda_M) \approx 211\,\mathrm{MeV}^2. \tag{5.119}$$

Next we need to compute the divergent part of one-loop contribution to the π_a-π_b two point function from the photon loop in the HLS. Taking into account the quadratic divergences coming from scalar loops, one finds that the RGE for ω is

$$\mu\frac{d\omega}{d\mu} = -\frac{1}{2\pi}\left[(1-a)\mu^2 + 3a\,M_\rho^2\right] \ . \tag{5.120}$$

This has to be solved together with the RGE's for a, F_π and M_ρ.

At this point, we can make an enormous simplification by assuming that $a = 1$ holds everywhere. In fact, this is found to be a good approximation for all the analyses made in [Harada and Yamawaki 2003]. We will have further occasions to find that a is close to 1 in nature.

With $a = 1$, the quadratic divergence disappears and (5.120) reduces to

$$\mu\frac{d\omega}{d\mu} = -\frac{3}{2\pi}M_\rho^2 \ . \tag{5.121}$$

Numerically solving Eq. (5.121) together with RGE for M_ρ as in [Harada and Yamawaki 2003] leads to

$$\Delta m_\pi^2 = \alpha_{\mathrm{em}}\omega(0) \simeq 1223\,\mathrm{MeV}^2 \ , \tag{5.122}$$

for a typical case $(\Lambda\,,\,\Lambda_{\mathrm{QCD}}) = (1.1\,,\,0.4)\,\mathrm{GeV}$. There are typically about 10% error in this estimate that comes from the uncertainty in the various parameters. This result should be compared with the experiment $\Delta m_\pi^2|_{\mathrm{exp.}} = 1261\,\mathrm{MeV}^2$. Large N_c considerations imply $a \simeq 1.3$, not exactly equal to 1. However the result obtained with this value of a for the mass difference differs only un-appreciably from the $a = 1$ prediction.

That $a \simeq 1$ has several implications in gauge theory. As mentioned before, it gives rise to "theory space locality" and the little Higgs phenomenon in the Standard Model. It is also connected with the dimensional deconstruction for QCD

and as mentioned above, may be relevant for possible connections to holographic dual QCD. In matter at high density, the approach $a \to 1$ will be associated – in Chapter 10 – with the emergence of global symmetry called "vector symmetry."

5.6.4 *Perturbing from the VM point*

We have learned that χPT with HLS based on the bare Lagrangian determined at the matching scale works fairly well in free space. For certain processes where chiral symmetry plays a singular role, it can be easier to start from the VM point and treat the departure from the VM by perturbation. As we shall describe later, this is potentially a powerful approach when we are looking at processes that take place in medium or in finite temperature. One particularly important example is kaon condensation in dense neutron star matter treated in Chapter 9.

As an illustration of how starting from VM fixed point seems to work even far away from the fixed point, we consider the mass splitting between the parity doublet of heavy-light quark hadrons. The argument applies to both baryons and mesons that contain both heavy quarks and light quarks. This problem was previously worked out starting from a chiral Lagrangian constructed in the free-space vacuum that incorporates heavy-quark symmetry in heavy-light systems [Nowak, Rho and Zahed 1993; Nowak, Rho and Zahed 2004]. This approach treated in CND-I may be called "bottom-up." Here we shall look at open heavy-quark systems from the starting point of the vector manifestation, *i.e.* top-down. This top-down approach is found to give more or less the same result as the bottom-up approach.

Denote the heavy quark by Q and the light quark by q. Then the configuration we are interested in is of the form $\bar{q}Q$. The ground state of such mesons which we will denote as $\mathcal{M}$ has the quantum numbers $J^P = 0^-$. In the limit that the mass of Q is taken infinite and that of q zero, the $J^P = 1^-$ state is degenerate with the ground state. What we are interested in is the splitting between the ground state multiplet $(0^-, 1^-)$ and the first excited states $(0^+, 1^+)$.

5.6.4.1 *Heavy quark symmetry*

To be as self-contained as possible, we briefly summarize the notion of heavy quark symmetry.

Like the approximate light quark flavor symmetry, *i.e.* chiral symmetry in the light quark sector of QCD where the current quark masses are not strictly equal to zero, the approximate heavy quark symmetry for $\Lambda_{\rm QCD}/m_Q \ll 1$ is a powerful tool for doing computations. In the limit that $m_Q \to \infty$, dynamics of the heavy quark Q becomes independent of its mass and spin [Isgur and Wise 1989]. The four velocity of the heavy quark v_μ is fixed. The size of the meson is of order $1/\Lambda_{\rm QCD}$, so the typical momentum scale of the light degrees of freedom is of order $\Lambda_{\rm QCD}$. We decompose as we did in Chapter 4 for (heavy) baryons the four momentum of

the heavy quark into

$$p_\mu = m_Q v_\mu + k_\mu \,, \tag{5.123}$$

where k_μ is the residual momentum which is of order $\Lambda_{\rm QCD}$. The heavy-quark propagator

$$\frac{-(p_\mu \gamma^\mu + m_Q)}{p^2 - m_Q^2 + i\epsilon} \tag{5.124}$$

simplifies to

$$\frac{-1}{v \cdot k + i\epsilon} \,. \tag{5.125}$$

Note that the propagator is independent of the heavy quark mass m_Q and γ matrices. The same independence holds for the vertices involving heavy quarks. Since the heavy quark is sitting with an infinite mass, the spin of the heavy quark does not flip by the interaction with the light degrees of freedom – which is of order $\Lambda_{\rm QCD}$. Thus the heavy-quark spin is conserved. This means that if there are N_f heavy quarks with the same four velocity, the effective heavy quark theory has an $SU(2N_f)$ spin-flavor symmetry [Isgur and Wise 1989].

Consider now the heavy-light meson multiplet. For the hadrons containing a single heavy quark Q, there is an $SU(2)$ spin symmetry between Q with up-spin, $Q(\uparrow)$ and Q with down-spin, $Q(\downarrow)$. Thus the hadrons with the spin combined $\uparrow$ and $\downarrow$ with the spin of the light degrees of freedom $s_{\rm light}$ are the spin partners to each other. Thus for each $s_{\rm light}$, there is a degenerate doublet with the total spin s_+ and s_-:

$$s_\pm = s_{\rm light} \pm \frac{1}{2} \,. \tag{5.126}$$

Hadrons in the ground state with one light antiquark have $s_{\rm light} = 1/2$ and negative parity. The meson with $J^P = 0^-$ is the spin partner of the one with $J^P = 1^-$. We shall call these chiral doublet.

5.6.4.2 *Constructing effective Lagrangians*

We wish to construct an effective Lagrangian containing the approximate chiral $SU(3)_{\rm L} \times SU(3)_{\rm R}$ symmetry in the light-quark sector and the heavy quark symmetry in the heavy-quark sector. We first describe how to construct the Lagrangian defined at the VM fixed point. Then, we account for the effect of spontaneous chiral symmetry breaking by adding a *bare* parameter for the mass splitting in the heavy sector and taking into account the deviation of the HLS parameters from the VM fixed point.

5.6.4.3 *The fixed point Lagrangian*

• **Light-meson sector**

At the VM fixed point characterized by $(g, a) = (0, 1)$, the relevant 1-forms are

$$\alpha_{\parallel\mu} = \frac{1}{2i}\left(\partial_\mu \xi_{\rm R}\cdot\xi_{\rm R}^\dagger + \partial_\mu \xi_{\rm L}\cdot\xi_{\rm L}^\dagger\right) ,$$
$$\alpha_{\perp\mu} = \frac{1}{2i}\left(\partial_\mu \xi_{\rm R}\cdot\xi_{\rm R}^\dagger - \partial_\mu \xi_{\rm L}\cdot\xi_{\rm L}^\dagger\right) . \tag{5.127}$$

Note that these 1-forms do not contain the HLS gauge field since the gauge coupling g vanishes at the VM fixed point. It is convenient to define the (L,R) 1-forms:

$$\alpha_{R\mu} = \alpha_{\parallel\mu} + \alpha_{\perp\mu} = \frac{1}{i}\partial_\mu \xi_{\rm R}\cdot\xi_{\rm R}^\dagger ,$$
$$\alpha_{L\mu} = \alpha_{\parallel\mu} - \alpha_{\perp\mu} = \frac{1}{i}\partial_\mu \xi_{\rm L}\cdot\xi_{\rm L}^\dagger , \tag{5.128}$$

which can be viewed as belonging to the chiral representation $(1, 8)$ and $(8, 1)$, respectively. They transform under chiral $SU(3)_{\rm L} \times SU(3)_{\rm R}$ as

$$\alpha_{R\mu} \to g_{\rm R}\alpha_{R\mu}g_{\rm R}^\dagger ,$$
$$\alpha_{L\mu} \to g_{\rm L}\alpha_{L\mu}g_{\rm L}^\dagger . \tag{5.129}$$

In terms of these 1-forms, the HLS Lagrangian at the VM fixed point can be written as

$$\mathcal{L}^*_{\rm light} = \frac{1}{2}F_\pi^2\,{\rm tr}\left[\alpha_{R\mu}\alpha_R^\mu\right] + \frac{1}{2}F_\pi^2\,{\rm tr}\left[\alpha_{L\mu}\alpha_L^\mu\right] , \tag{5.130}$$

where the $*$ affixed to the Lagrangian denotes that it is a fixed-point Lagrangian, and F_π denotes the bare pion decay constant. Note that the physical pion decay constant f_π vanishes at the VM fixed point by the quadratic divergence, although the bare one is non-zero.

• **Heavy-meson sector**

Next we construct the Lagrangian of the heavy meson sector defined at the chiral restoration point identified as the VM fixed point. Introduce two heavy-meson fields $\mathcal{H}_R$ and $\mathcal{H}_L$ transforming under chiral ${\rm SU(3)_R} \times {\rm SU(3)_L}$ as

$$\mathcal{H}_R \to \mathcal{H}_R\, g_{\rm R}^\dagger , \quad \mathcal{H}_L \to \mathcal{H}_L\, g_{\rm L}^\dagger . \tag{5.131}$$

In terms of these fields together with the light-meson 1-forms $\alpha^\mu_{L,R}$, the fixed point Lagrangian of the heavy mesons takes the form

$$\begin{aligned}\mathcal{L}^*_{\rm heavy} = &-{\rm Tr}\left[\mathcal{H}_R i v_\mu \partial^\mu \bar{\mathcal{H}}_R\right] - {\rm Tr}\left[\mathcal{H}_L i v_\mu \partial^\mu \bar{\mathcal{H}}_L\right] \\ &+ m_0\,{\rm Tr}\left[\mathcal{H}_R\bar{\mathcal{H}}_R + \mathcal{H}_L\bar{\mathcal{H}}_L\right] \\ &+ 2k\,{\rm Tr}\left[\mathcal{H}_R\alpha_{R\mu}\gamma^\mu\frac{1+\gamma_5}{2}\bar{\mathcal{H}}_R + \mathcal{H}_L\alpha_{L\mu}\gamma^\mu\frac{1-\gamma_5}{2}\bar{\mathcal{H}}_L\right] ,\end{aligned} \tag{5.132}$$

where v_μ is the velocity of the heavy meson, m_0 represents the mass generated by the interaction between the heavy quark and the "pion cloud" surrounding the heavy quark which cannot distinguish the doublet, and k is a real constant to be determined.

5.6.4.4 *Effects of spontaneous chiral symmetry breaking*

We consider what happens in the broken phase where chiral symmetry is spontaneously broken. In the conventional scenario of chiral-symmetry manifestation à la linear sigma model, the effect of spontaneous chiral symmetry breaking is expressed by the vacuum expectation value of the scalar fields. In the VM, on the other hand, it is signaled by the HLS Lagrangian departing from the VM fixed point: There the gauge coupling constant $g \neq 0$ and we acquire the kinetic term of the HLS gauge bosons $\mathcal{L}_{\rho\text{kin}} = -\frac{1}{2}\text{Tr}\,[\rho_{\mu\nu}\rho^{\mu\nu}]$. The derivatives in the HLS 1-forms become the covariant derivatives, so $\alpha_{L\mu}$ and $\alpha_{R\mu}$ are covariantized to

$$\begin{aligned} \partial_\mu &\to D_\mu = \partial_\mu - ig\rho_\mu, \\ \alpha_{R\mu} &\to \hat{\alpha}_{R\mu} = \alpha_{R\mu} - g\rho_\mu, \\ \alpha_{L\mu} &\to \hat{\alpha}_{L\mu} = \alpha_{L\mu} - g\rho_\mu. \end{aligned} \tag{5.133}$$

These 1-forms transform as $\hat{\alpha}_{R(L)\mu} \to h\,\hat{\alpha}_{R(L)\mu}h^\dagger$ with $h \in [SU(3)_{\text{V}}]_{\text{local}}$.

Although $a = 1$ at the VM fixed point, generally $a \neq 1$ in the broken phase. We therefore expect to have a term of the form $\frac{1}{2}(a-1)F_\pi^2\text{Tr}[\hat{\alpha}_{L\mu}\hat{\alpha}_R^\mu]$. Thus the Lagrangian for the light mesons takes the following form:

$$\begin{aligned} \mathcal{L}_{\text{light}} = &\frac{a+1}{4}F_\pi^2\text{Tr}[\hat{\alpha}_{R\mu}\hat{\alpha}_R^\mu + \hat{\alpha}_{L\mu}\hat{\alpha}_L^\mu] \\ &+ \frac{a-1}{2}F_\pi^2\text{Tr}[\hat{\alpha}_{R\mu}\hat{\alpha}_L^\mu] + \mathcal{L}_{\rho\text{kin}}. \end{aligned} \tag{5.134}$$

By using $\hat{\alpha}_{\parallel\mu}$ and $\hat{\alpha}_{\perp\mu}$ given in Eqs. (5.17) and (5.18), this Lagrangian can be rewritten as

$$\mathcal{L}_{\text{light}} = F_\pi^2\text{Tr}[\hat{\alpha}_{\perp\mu}\hat{\alpha}_\perp^\mu] + F_\sigma^2\text{Tr}[\hat{\alpha}_{\parallel\mu}\hat{\alpha}_\parallel^\mu] + \mathcal{L}_{\rho\text{kin}}, \tag{5.135}$$

which is nothing but the $\text{HLS}_{K=1}$ Lagrangian [Harada and Yamawaki 2003].

We next consider the spontaneous breaking of chiral symmetry in the heavy-meson sector. One of the most important effects of the symmetry breaking is to generate the mass splitting between the odd parity multiplet and the even parity multiplet [Nowak, Rho and Zahed 1993]. This effect can be represented by the Lagrangian of the form:

$$\mathcal{L}_{\chi\text{SB}} = \frac{1}{2}\Delta M\,\text{Tr}\left[\mathcal{H}_L\bar{\mathcal{H}}_R + \mathcal{H}_R\bar{\mathcal{H}}_L\right]\ . \tag{5.136}$$

Here ΔM is the *bare* parameter corresponding to the mass splitting between the two multiplets. An important point of this approach is that the bare ΔM can be

determined by matching the EFT with QCD as we will show below in section 5.6.4.8: The matching will show that ΔM is directly proportional to the quark condensate:

$$\Delta M \sim \langle \bar{q}q \rangle. \tag{5.137}$$

5.6.4.5 *Lagrangian in parity eigenfields*

In order to compute the mass splitting between $\mathcal{M}$ and $\tilde{\mathcal{M}}$, it is convenient to go to the corresponding fields in parity eigenstate, H (odd-parity) and G (even-parity) as defined, *e.g.*, in [Nowak, Rho and Zahed 2004];

$$\begin{aligned} \mathcal{H}_R &= \frac{1}{\sqrt{2}} \left[G - iH\gamma_5 \right] \ , \\ \mathcal{H}_L &= \frac{1}{\sqrt{2}} \left[G + iH\gamma_5 \right] \ . \end{aligned} \tag{5.138}$$

Here, the pseudoscalar meson P and the vector meson P^*_μ are included in the H field as

$$H = \frac{1 + v_\mu \gamma^\mu}{2} \left[i\gamma_5 P + \gamma^\mu P^*_\mu \right] \ , \tag{5.139}$$

and the scalar meson Q^* and the axial-vector meson Q_μ are in G as

$$G = \frac{1 + v_\mu \gamma^\mu}{2} \left[Q^* - i\gamma^\mu \gamma_5 Q_\mu \right] \ . \tag{5.140}$$

In terms of the H and G fields, the heavy-meson Lagrangian *departing from* the VM fixed point is of the form

$$\mathcal{L}_{\text{heavy}} = \mathcal{L}_{\text{kin}} + \mathcal{L}_{\text{int}} \ , \tag{5.141}$$

with

$$\mathcal{L}_{\text{kin}} = \text{Tr} \left[H \ (iv_\mu D^\mu - M_H) \, \bar{H} \right] - \text{Tr} \left[G \ (iv_\mu D^\mu - M_G) \, \bar{G} \right] \ , \tag{5.142}$$

$$\begin{aligned} \mathcal{L}_{\text{int}} = k \Bigg[& \text{Tr}[H\gamma_\mu\gamma_5\hat{\alpha}^\mu_\perp \bar{H}] - \text{Tr}[Hv_\mu\hat{\alpha}^\mu_\parallel \bar{H}] \\ & + \text{Tr}[G\gamma_\mu\gamma_5\hat{\alpha}^\mu_\perp \bar{G}] + \text{Tr}[Gv_\mu\hat{\alpha}^\mu_\parallel \bar{G}] \\ & - i\text{Tr}[G\hat{\alpha}_{\perp\mu}\gamma^\mu\gamma_5\bar{H}] + i\text{Tr}[H\hat{\alpha}_{\perp\mu}\gamma^\mu\gamma_5\bar{G}] \\ & - i\text{Tr}[G\hat{\alpha}_{\parallel\mu}\gamma^\mu\bar{H}] + i\text{Tr}[H\hat{\alpha}_{\parallel\mu}\gamma^\mu\bar{G}] \Bigg], \end{aligned} \tag{5.143}$$

where the covariant derivatives acting on $\bar{H}$ and $\bar{G}$ are defined as

$$D_\mu \bar{H} = (\partial_\mu - ig\rho_\mu)\,\bar{H}\ , \quad D_\mu \bar{G} = (\partial_\mu - ig\rho_\mu)\,\bar{G}\ . \tag{5.144}$$

We have defined M_H and M_G as the masses of the parity-odd multiplet H and the parity-even multiplet G, respectively. They are related to m_0 and ΔM as

$$M_H = -m_0 - \frac{1}{2}\Delta M\ ,$$

$$M_G = -m_0 + \frac{1}{2}\Delta M\ . \tag{5.145}$$

The mass splitting between G and H is therefore given by

$$M_G - M_H = \Delta M\ . \tag{5.146}$$

5.6.4.6 *Calculation at the matching point*

In the spirit of HLS theory, the bare parameter $\Delta M_{\rm bare}$ which carries information on QCD should be determined by matching the EFT correlators to QCD ones. Here we are concerned with the pseudoscalar correlator G_P and the scalar correlator G_S. In the EFT sector, the correlators at the matching scale are of the form [14]

$$G_P(Q^2) = \frac{F_D^2 M_D^4}{M_D^2 + Q^2},$$

$$G_S(Q^2) = \frac{F_{\tilde{D}}^2 M_{\tilde{D}}^4}{M_{\tilde{D}}^2 + Q^2}, \tag{5.147}$$

where F_D ($F_{\tilde{D}}$) denotes the D-meson ($\tilde{D}$-meson) decay constant and the space-like momentum $Q^2 = (M_D + \Lambda_M)^2$ with Λ_M being the matching scale. We note that the heavy quark limit $M_D \to \infty$ should be taken with Λ_M kept fixed since Λ_M must be smaller than the chiral symmetry breaking scale characterized by $\Lambda_\chi \sim 4\pi f_\pi$. Then, Q^2 should be regarded as $Q^2 \simeq M_D^2$ in the present framework based on the chiral and heavy quark symmetries. If we ignore the difference between F_D and $F_{\tilde{D}}$ which can be justified by the QCD sum rule analysis, then we get

$$\begin{aligned}\Delta_{SP}(Q^2) &\equiv G_S(Q^2) - G_P(Q^2) \\ &\simeq \frac{3F_D^2 M_D^3}{M_D^2 + Q^2}\Delta M_D.\end{aligned} \tag{5.148}$$

[14] Here and in what follows, the heavy meson is denoted D with the open charm heavy meson in mind. However the arguments (except for the numerical values) are generic for all heavy mesons $\mathcal{M}$.

In the QCD sector, the correlators G_S and G_P are given by the operator product expansion (OPE) as [Narison 1988]

$$\begin{aligned} G_S(Q^2) &= G(Q^2)\big|_{\rm pert} \\ &\quad + \frac{m_H^2}{m_H^2+Q^2}\left[- m_H\langle\bar{q}q\rangle + \frac{\alpha_s}{12\pi}\langle G^{\mu\nu}G_{\mu\nu}\rangle\right], \\ G_P(Q^2) &= G(Q^2)\big|_{\rm pert} \\ &\quad + \frac{m_H^2}{m_H^2+Q^2}\left[m_H\langle\bar{q}q\rangle + \frac{\alpha_s}{12\pi}\langle G^{\mu\nu}G_{\mu\nu}\rangle\right], \end{aligned} \tag{5.149}$$

where m_H is the heavy-quark mass. To the accuracy we are aiming at, the OPE can be truncated at $\mathcal{O}(1/Q^2)$. The explicit expression for the perturbative contribution $G(Q^2)\big|_{\rm pert}$ is available in the literature but we do not need it since it drops out in the difference. From these correlators, the Δ_{SP} becomes

$$\Delta_{SP}(Q^2) = -\frac{2m_H^3}{m_H^2+Q^2}\langle\bar{q}q\rangle. \tag{5.150}$$

Equating Eq. (5.148) to Eq. (5.150) and neglecting the difference $(m_H - M_D)$, we obtain the following matching condition:

$$3F_D^2\,\Delta M \simeq -2\langle\bar{q}q\rangle. \tag{5.151}$$

Thus at the matching scale, the splitting is

$$\Delta M_{\rm bare} \simeq -\frac{2}{3}\frac{\langle\bar{q}q\rangle}{F_D^2}. \tag{5.152}$$

As announced, the *bare* splitting is indeed proportional to the light-quark condensate. The quantum corrections do not change the dependence on the quark condensate as we verify below.

5.6.4.7 *Quantum correction*

Given the bare Lagrangian whose parameters are fixed at the matching scale Λ_M, the next step is to decimate the theory à la Wilson to the scale at which ΔM is measured. This amounts to calculating quantum corrections to the mass difference ΔM in the framework of the present EFT.

This calculation turns out to be surprisingly simple for $a \approx 1$. If one sets $a = 1$ which is the approximation we are adopting here, α_L does not mix with α_R in the light sector, and then α_L couples to only $\mathcal{H}_L$ and α_R to only $\mathcal{H}_R$. As a result $\mathcal{H}_{L(R)}$ cannot connect to $\mathcal{H}_{R(L)}$ by the exchange of α_L or α_R. Only the ρ-loop links between the fields with different chiralities as shown in Fig. 5.3. This approximation has been verified to be reliable since corrections to the result with $a = 1$ come only at higher loop orders [see the next paragraph]. The diagram shown in Fig. 5.3

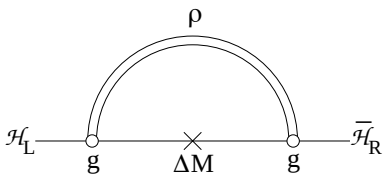

Fig. 5.3 Diagram contributing to the mass difference.

contributes to the two-point function

$$\Pi_{LR}\Big|_{\rm div} = -\frac{1}{2}\Delta M\, \mathcal{C}_2(N_f)\, \frac{g^2}{2\pi^2}\Big(1-2k-k^2\Big)\ln\Lambda, \tag{5.153}$$

where $\mathcal{C}_2(N_f)$ is the second Casimir defined by $\sum_a (T_a)_{ij}(T_a)_{jl} = \mathcal{C}_2(N_f)\delta_{il}$ with i, j and l denoting the flavor indices of the light quarks. This divergence is renormalized by the bare contribution of the form $\Pi_{LR,\rm bare} = \frac{1}{2}\Delta M_{\rm bare}$. Thus the renormalization-group equation (RGE) takes the form

$$\mu\frac{d\,\Delta M}{d\mu} = \mathcal{C}_2(N_f)\, \frac{g^2}{2\pi^2}\Big(1-2k-k^2\Big)\Delta M. \tag{5.154}$$

To the order we are interested in at this point, we may ignore the scale dependence in g and k. Then the solution is simple:

$$\Delta M = \Delta M_{\rm bare} \times C_{\rm quantum}\ , \tag{5.155}$$

where we define $C_{\rm quantum}$ by

$$C_{\rm quantum} = \exp\Big[-\mathcal{C}_2(N_f)\, \frac{g^2}{2\pi^2}\Big(1-2k-k^2\Big)\ln\frac{\Lambda}{\mu}\Big]\ . \tag{5.156}$$

This shows manifestly that the mass splitting is dictated by the bare' splitting $\Delta M_{\rm bare}$ proportional to $\langle\bar{q}q\rangle$ corrected by the quantum effect $C_{\rm quantum}$.

Next we lift the condition $a = 1$ made in the above analysis. For this purpose, we compute the quantum effects to the masses of 0^- (P) and 0^+ (Q^*) D-mesons by calculating the one-loop corrections to the two-point functions of P and Q^* denoted by Π_{PP} and $\Pi_{Q^*Q^*}$. It is found that, amazingly, the resultant form of the quantum correction exactly agrees with the previous one which was obtained by taking $a = 1$. To arrive at this result, it is essential that P (or P^*_μ) be the chiral partner of Q^* (or Q_μ) as follows: The loop diagrams have power and logarithmic divergences. However, all the divergences of the diagrams with pion loop are exactly canceled among themselves since the internal (or external) particles are chiral partners. In a similar way, the exact cancelation takes place in the diagrams with σ loop. Finally, the logarithmic divergence from the ρ loop does contribute to the mass difference. This shows that the effect of spontaneous chiral symmetry breaking introduced as the deviation of a from 1 does not get transferred to the heavy sector. Thus, even

in the case of $a \neq 1$, the bare mass splitting is enhanced by only the vector meson loop, with the pions not figuring in the quantum corrections at least at one-loop order. Solving the corresponding RGE which is identical to Eq. (5.154), we obtain the same mass splitting as the one given in Eq. (5.155).

The message here is that $a \approx 1$ is a good approximation in this chiral doubler problem as in other cases that we have considered elsewhere.

5.6.4.8 *Mass splitting*

We can now make a numerical prediction for the mass splitting of the chiral doublers in the open charm system. (Here D denotes the open charm meson *proper*.) Since we are considering the chiral limit, strictly speaking, a precise comparison with the experiments (*i.e.* BaBar and CLEO II), where the light quark is an s quark whose mass cannot be ignored in practice, is not feasible. But it gives the basic idea which is qualitatively correct.

Determining the bare mass splitting from the matching condition (5.152) requires the quark condensate at that scale and the D-meson decay constant F_D. For the quark condensate, we shall use the so-called "standard value" $\langle\bar{q}q\rangle = -(225 \pm 25\,\mathrm{MeV})^3$ at 1 GeV. Extrapolated to the scale $\Lambda_M = 1.1$ GeV we shall adopt here, this gives

$$\langle\bar{q}q\rangle_{\Lambda_M} = -(228 \pm 25\,\mathrm{MeV})^3. \tag{5.157}$$

Unfortunately this value is not firmly established, there being no consensus on it. The values found in the literature vary widely, even by a factor of ~ 2. As for the D-meson decay constant, we take as a typical value $F_D = 0.205 \pm 0.020\,\mathrm{GeV}$ obtained from the QCD sum rule analysis [Narison 2005]. Plugging the above input values into Eq. (5.152), we obtain

$$\Delta M_{\mathrm{bare}} \simeq 0.19\,\mathrm{GeV}\ . \tag{5.158}$$

By taking $\mu = m_\rho = 771\,\mathrm{MeV}$, $\Lambda = \Lambda_M = 1.1\,\mathrm{GeV}$, $g = g(m_\rho) = 6.27$ determined via the Wilsonian matching for $(\Lambda_M, \Lambda_{\mathrm{QCD}}) = (1.1, 0.4)\,\mathrm{GeV}$ in [Harada and Yamawaki 2003] and $k \simeq 0.59$ extracted from the $D^* \to D\pi$ decay in Eq. (5.156), we find for $N_f = 3$

$$C_{\mathrm{quantum}} = 1.6\ . \tag{5.159}$$

This is a sizable quantum correction involving only the vector meson. If one takes into account the uncertainties involved in the condensate and the decay constant, the quantum-corrected splitting ΔM comes out to be

$$\Delta M \approx 0.31 \pm 0.12\,\mathrm{GeV}\ . \tag{5.160}$$

Despite the uncertainty involved, (5.160) is a pleasing result. It shows that the splitting is indeed of the size of the constituent quark mass of a chiral quark

$\Sigma \sim m_p/3 \sim 310$ MeV and is directly proportional to the quark condensate.[15] This prediction is surprisingly close to the result of the bottom-up approach of [Nowak, Rho and Zahed 2004] where ΔM comes out to be ~ 340 MeV and to the experimental value ~ 350 MeV of BaBar and CLEO II.

5.7 HLS with ρ and a_1: $\mathrm{HLS}_{K=2}$

5.7.1 *$\mathrm{HLS}_{K=2}$ Lagrangian*

We turn to hidden local symmetry Lagrangian that includes both the ρ and a_1 multiplets which generalizes the $K = 1$ Lagrangian (5.25) along the "moose" strategy outlined above. Most of the explicit applications given in this volume are done with the ρ alone with the a_1 integrated out, that is, $\mathrm{HLS}_{K=1}$, but we will need the properties of the axial a_1 meson for discussing some of physical observables. We call this $K = 2$ HLS written as $\mathrm{HLS}_{K=2}$. The construction follows Harada and Sasaki [Harada and Sasaki 2005] and Hidaka, Morimatsu and Ohtani [Hidaka, Morimatsu and Ohtani 2006].

The $\mathrm{HLS}_{K=2}$ Lagrangian is based on the $G_{\mathrm{global}} \times G_{\mathrm{local}}$ symmetry, where $G_{\mathrm{global}} = [SU(N_f)_L \times SU(N_f)_R]_{\mathrm{global}}$ is the chiral symmetry and $G_{\mathrm{local}} = [SU(N_f)_L \times SU(N_f)_R]_{\mathrm{local}}$ is the $K = 2$ hidden local symmetry. The symmetry $G_{\mathrm{global}} \times G_{\mathrm{local}}$ is spontaneously broken down to flavor diagonal $SU(N_f)_V$. The basic quantities are the $\mathrm{HLS}_{K=2}$ gauge bosons L_μ and R_μ and three matrix valued variables ξ_L, ξ_R and ξ_M which are introduced as

$$U = \xi_L^\dagger \xi_M \xi_R \,, \tag{5.161}$$

where $N_f \times N_f$ special-unitary matrix U is a basic ingredient of chiral perturbation theory. The transformation property of U under the chiral symmetry is of course the same as in $\mathrm{HLS}_{K=1}$:

$$U \to g_L U g_R^\dagger \,, \tag{5.162}$$

with $g_{L,R} \in [SU(N_f)_{L,R}]_{\mathrm{global}}$. The variables ξ's transform as

$$\begin{aligned} \xi_{L,R} &\to h_{L,R} \cdot \xi_{L,R} \cdot g_{L,R}^\dagger \,, \\ \xi_M &\to h_L \cdot \xi_M \cdot h_R^\dagger \,, \end{aligned} \tag{5.163}$$

with $h_{L,R} \in [SU(N_f)_{L,R}]_{\mathrm{local}}$. The $\mathrm{HLS}_{K=2}$ gauge fields L_μ and R_μ transform as

$$\begin{aligned} L_\mu &\to h_L (i\partial_\mu + L_\mu) h_L^\dagger \,, \\ R_\mu &\to h_R (i\partial_\mu + R_\mu) h_R^\dagger \,. \end{aligned} \tag{5.164}$$

[15] In anticipation of what is to come in Chapter 7, we note that $\Delta M \to 0$ as $\langle \bar{q}q \rangle \to 0$ giving a direct signal for chiral restoration. This is a superior tool for probing chiral symmetry in hot/dense medium than dileptons in heavy ion collisions.

The covariant derivatives of $\xi_{L,R,M}$ are defined by

$$\begin{aligned} D_\mu \xi_L &= \partial_\mu \xi_L - i L_\mu \xi_L + i \xi_L \mathcal{L}_\mu \,, \\ D_\mu \xi_R &= \partial_\mu \xi_R - i R_\mu \xi_R + i \xi_R \mathcal{R}_\mu \,, \\ D_\mu \xi_M &= \partial_\mu \xi_M - i L_\mu \xi_M + i \xi_M R_\mu \,, \end{aligned} \tag{5.165}$$

where $\mathcal{L}_\mu$ and $\mathcal{R}_\mu$ are the external gauge fields introduced by gauging $G_{\rm global}$ symmetry.

We complement the Maurer-Cartan 1-form written for $\mathrm{HLS}_{K=1}$ with an extra one,

$$\begin{aligned} \hat{\alpha}^\mu_{L,R} &= D^\mu \xi_{L,R} \cdot \xi^\dagger_{L,R}/i \,, \\ \hat{\alpha}^\mu_M &= D^\mu \xi_M \cdot \xi^\dagger_M/(2i) \,, \end{aligned} \tag{5.166}$$

which transform as

$$\begin{aligned} \hat{\alpha}^\mu_{L,R} &\to h_{L,R} \hat{\alpha}^\mu_{L,R} h^\dagger_{L,R} \,, \\ \hat{\alpha}^\mu_M &\to h_L \hat{\alpha}^\mu_M h^\dagger_R \,. \end{aligned} \tag{5.167}$$

It is convenient to construct four independent terms, with the lowest derivatives, invariant under $G_{\rm global} \times G_{\rm local}$:

$$\begin{aligned} \mathcal{L}_V &= F^2 \mathrm{tr}\big[\hat{\alpha}_{\parallel\mu} \hat{\alpha}^\mu_\parallel\big] \,, \\ \mathcal{L}_A &= F^2 \mathrm{tr}\big[\hat{\alpha}_{\perp\mu} \hat{\alpha}^\mu_\perp\big] \,, \\ \mathcal{L}_M &= F^2 \mathrm{tr}\big[\hat{\alpha}_{M\mu} \hat{\alpha}^\mu_M\big] \,, \\ \mathcal{L}_\pi &= F^2 \mathrm{tr}\big[(\hat{\alpha}_{\perp\mu} + \hat{\alpha}_{M\mu})(\hat{\alpha}^\mu_\perp + \hat{\alpha}^\mu_M)\big] \,, \end{aligned} \tag{5.168}$$

where F is the parameter carrying the mass dimension 1 and $\hat{\alpha}_{\parallel,\perp}$ are defined as

$$\hat{\alpha}^\mu_{\parallel,\perp} = \big(\xi_M \hat{\alpha}^\mu_R \xi^\dagger_M \pm \hat{\alpha}^\mu_L\big)/2 \,. \tag{5.169}$$

With the gauge field strength tensors

$$\begin{aligned} L_{\mu\nu} &= \partial_\mu L_\nu - \partial_\nu L_\mu - i\big[L_\mu, L_\nu\big] \,, \\ R_{\mu\nu} &= \partial_\mu R_\nu - \partial_\nu R_\mu - i\big[R_\mu, R_\nu\big] \,, \end{aligned} \tag{5.170}$$

the kinetic term of the gauge bosons can be written as

$$\mathcal{L}_{\rm kin}(L_\mu, R_\mu) = -\frac{1}{2g^2} \mathrm{Tr}\big[L_{\mu\nu} L^{\mu\nu} + R_{\mu\nu} R^{\mu\nu}\big] \,, \tag{5.171}$$

with g being the gauge coupling constant of the $\mathrm{HLS}_{K=2}$. There is only one gauge coupling g due to the parity invariance.

By combining the four terms in Eq. (5.168) together with the kinetic term of the gauge fields in Eq. (5.171), the $\mathrm{HLS}_{K=2}$ Lagrangian is given by

$$\mathcal{L} = a\mathcal{L}_V + b\mathcal{L}_A + c\mathcal{L}_M + d\mathcal{L}_\pi + \mathcal{L}_{\rm kin}(L_\mu, R_\mu) \,, \tag{5.172}$$

where a, b, c and d are dimensionless parameters to be determined by the underlying QCD.

5.7.2 *Fixed points*

With the presence of the axial vectors, the fixed point structure becomes richer. In fact, three fixed points are uncovered [Harada and Sasaki 2005; Hidaka, Morimatsu and Ohtani 2006]. To be complete, one should also consider scalar degrees of freedom since they figure in certain multiplet structure and more significantly in observables we discuss in Chapter 7, but scalars have not yet been implemented in a systematic way in hidden local symmetry approach.

Although Weinberg sum rules come out of the RG calculations [Hidaka, Morimatsu and Ohtani 2006], it turns out to be simpler if one imposes them to start with as was done in [Harada and Sasaki 2005].

We start by recalling the definitions of the correlators given in Eq. (5.73)

$$\begin{aligned}
&\int d^4x e^{ipx} \left\langle 0 \left| T\, J^a_{5\mu}(x) J^b_{5\nu}(0) \right| 0 \right\rangle = \delta^{ab} \left(p_\mu p_\nu - g_{\mu\nu} p^2 \right) G_A(p^2) \ , \\
&\int d^4x e^{ipx} \left\langle 0 \left| T\, J^a_{\mu}(x) J^b_{\nu}(0) \right| 0 \right\rangle = \delta^{ab} \left(p_\mu p_\nu - g_{\mu\nu} p^2 \right) G_V(p^2) \ , . \qquad (5.173)
\end{aligned}$$

At the leading (or tree) order of the $\mathrm{HLS}_{K=2}$, the current correlators $G_{A,V}$ with $Q^2 = -p^2$ are

$$\begin{aligned}
G_A(Q^2) &= \frac{F_\pi^2}{Q^2} + \frac{F_{a_1}^2}{M_{a_1}^2 + Q^2} \, , \\
G_V(Q^2) &= \frac{F_\rho^2}{M_\rho^2 + Q^2} \, , \qquad (5.174)
\end{aligned}$$

where the a_1 and ρ decay constants are defined in terms of the Lagrangian (5.172) by

$$\begin{aligned}
F_{a_1}^2 &= \left(\frac{g_{a_1}}{M_{a_1}} \right)^2 = \frac{b^2}{b+c} F^2 \, , \\
F_\rho^2 &= \left(\frac{g_\rho}{M_\rho} \right)^2 = a F^2 \, . \qquad (5.175)
\end{aligned}$$

The corresponding correlators in QCD variables were given above (Section 5.5.2.1) in OPE up to $\mathcal{O}(1/Q^6)$ based on the work of [Shifman, Vainshtein and Zakharov 1979a; Shifman, Vainshtein and Zakharov 1979b]. What we need is the difference,

$$G_A^{(\mathrm{QCD})}(Q^2) - G_V^{(\mathrm{QCD})}(Q^2) = \frac{32\pi}{9} \frac{\alpha_s \langle \bar{q} q \rangle^2}{Q^6} \ . \qquad (5.176)$$

Since the above forms of the correlators in the OPE are valid in the high energy region, we consider the difference of the correlators in the $\mathrm{HLS}_{K=2}$ in the energy

region higher than the a_1 meson mass, *i.e.* $Q^2 \gg M_A^2$. In the high energy region, two correlators in $\mathrm{HLS}_{K=2}$ given in Eq. (5.174) can be expanded as

$$\begin{aligned} G_A(Q^2) &= \frac{F_\pi^2 + F_{a_1}^2}{Q^2} - \frac{F_{a_1}^2 M_{a_1}^2}{Q^4} + \frac{F_{a_1}^2 M_{a_1}^4}{Q^6}\,, \\ G_A(Q^2) &= \frac{F_\rho^2}{Q^2} - \frac{F_\rho^2 M_\rho^2}{Q^4} + \frac{F_\rho^2 M_\rho^4}{Q^6} \end{aligned} \tag{5.177}$$

which yields

$$\begin{aligned} G_A(Q^2) - G_V(Q^2) = {} & \frac{F_\pi^2 + F_{a_1}^2 - F_\rho^2}{Q^2} \\ & + \frac{F_{a_1}^2 M_{a_1}^2 - F_\rho^2 M_\rho^2}{Q^4} + \frac{F_{a_1}^2 M_{a_1}^4 - F_\rho^2 M_\rho^4}{Q^6}\,. \end{aligned} \tag{5.178}$$

Now we require that the high energy behavior of the difference between two correlators in the $\mathrm{HLS}_{K=2}$ match with that in the OPE: $G_A(Q^2) - G_V(Q^2)$ in the $\mathrm{HLS}_{K=2}$ scales as $1/Q^6$. This requirement implies

$$\begin{aligned} F_\pi^2 + F_{a_1}^2 &= F_\rho^2\,, \\ F_{a_1}^2 M_{a_1}^2 &= F_\rho^2 M_\rho^2\,, \end{aligned} \tag{5.179}$$

These relations are the pole saturated forms of the Weinberg first and second sum rules [Weinberg 1967]. In terms of the parameters of the $\mathrm{HLS}_{K=2}$ Lagrangian (5.172), these relations can be satisfied if we take

$$a = b\,, \quad d = 0\,. \tag{5.180}$$

The relations (5.180) apply at the matching scale. In what is by now a routine procedure, we determine how they flow as the scale is varied. For this, one would have to compute the RGE's for a, b and d. Although the RGE's at one-loop order are very complicated (see Appendix B in [Harada and Sasaki 2005]), the flow equations for $(a-b)$ and d satisfying (5.180) turns out to be extremely simple. For $a = b$ and $d = 0$, the flow equations come out as

$$\mu \frac{d(aF^2)}{d\mu} = \frac{N_f}{(4\pi)^2}\left[\mu^2 + 3ag^2F^2\right], \tag{5.181}$$

$$\mu \frac{d(bF^2)}{d\mu} = \frac{N_f}{(4\pi)^2}\left[\mu^2 + 3ag^2F^2\right], \tag{5.182}$$

$$\mu \frac{d(dF^2)}{d\mu} = 0\,, \tag{5.183}$$

so

$$\mu\frac{d(a-b)}{d\mu} = 0\,, \tag{5.184}$$

$$\mu\frac{d(d)}{d\mu} = 0\,. \tag{5.185}$$

What this means is that the Weinberg sum rules expressed in terms of the leading order parameters are not renormalized by one loop quantum corrections in $\mathrm{HLS}_{K=2}$ theory. This also means that the $\mathrm{HLS}_{K=2}$ theory that satisfies the Weinberg sum rules has "theory space locality" at one-loop quantum level.

In going further to study the fixed point structure of $\mathrm{HLS}_{K=2}$, we shall impose the Weinberg sum rules and it is this imposition that makes the discussion remarkably simple. Hidaka *et al* [Hidaka, Morimatsu and Ohtani 2006] do not impose the Weinberg sum rules in their analysis. Instead they *obtain* that the Weinberg sum rules are satisfied for the flow that lead to the fixed points.

We can exploit the non-renormalization theorem (5.184) and (5.183) to uncover the fixed points in $\mathrm{HLS}_{K=2}$ theory. First we find from (5.176) and the Weinberg sum rules that

$$F_\rho^2 M_\rho^2 \left(M_{A_1}^2 - M_\rho^2\right) = \frac{32\pi\alpha_s}{9}\langle\bar{q}q\rangle^2\,. \tag{5.186}$$

Expressed in terms of the $\mathrm{HLS}_{K=2}$ Lagrangian, and showing only those quantities that change with scale, (5.186) implies the relation

$$a^2\cdot c\cdot g^4 \propto \langle\bar{q}q\rangle^2\,. \tag{5.187}$$

This means that as the quark condensate – the order parameter of chiral symmetry – goes to zero, the product $a\cdot c\cdot g$ goes to zero. So at least one among a, c and g must go to zero. In order to determine which one is responsible for $a\cdot c\cdot g\to 0$, let us look at the RG equations given the Weinberg sum rule conditions $a-b=0$ and $d=0$,

$$\mu\frac{d(a)}{d\mu} = \frac{N_f}{(4\pi)^2}\left[\mu^2/F^2 + 3ag^2\right], \tag{5.188}$$

$$\mu\frac{d(c)}{d\mu} = \frac{N_f}{(4\pi)^2}\left[2\mu^2/F^2 + 6cg^2\right], \tag{5.189}$$

$$\mu\frac{dg^2}{d\mu} = -\frac{N_f}{(4\pi)^2}\frac{43}{3}g^4\,. \tag{5.190}$$

One can see from these equations that neither $a=0$ nor $c=0$ can be a fixed point whereas $g=0$ can be. Thus we see immediately that under the constraint that the Weinberg sum rules be held at the matching point,

$$g\to g^\star = 0 \tag{5.191}$$

as the quark condensate is dialled to zero. Since the parametric masses of the ρ and a_1 are all proportional to g, we find that both of them go to zero simultaneously at the fixed point.

5.7.3 *Phase structures for different fixed points*

While we have uncovered the fixed point $g^\star = 0$, what about the flow behavior of the other parameters $a(= b)$ and c ? To answer this question we look at the RGE's (5.188)-(5.190). For this, it is convenient to three define dimensionless quantities

$$\begin{aligned} X(\mu) &= \frac{N_f}{2(4\pi)^2}\frac{\mu^2}{a(\mu)F^2}\,, \\ Y(\mu) &= \frac{N_f}{2(4\pi)^2}\frac{\mu^2}{c(\mu)F^2}\,, \\ G(\mu) &= \frac{N_f}{2(4\pi)^2}g^2(\mu)\,. \end{aligned} \tag{5.192}$$

In terms of these, the RGE's (5.188)-(5.190) read

$$\begin{aligned} \mu\frac{dX}{d\mu} &= 2X(1-X-3G)\,, \\ \mu\frac{dY}{d\mu} &= 2Y(1-2Y-6G)\,, \\ \mu\frac{dG}{d\mu} &= -\frac{86}{3}G^2\,. \end{aligned} \tag{5.193}$$

These RGE's have, apart from one trivial fixed point $(X^*, Y^*, G^*) = (0, 0, 0)$, three non-trivial fixed points

$$\begin{aligned} &\text{A}: \quad (X^*, Y^*, G^*) = (0, 1/2, 0)\,, \\ &\text{B}: \quad (X^*, Y^*, G^*) = (1, 0, 0)\,, \\ &\text{C}: \quad (X^*, Y^*, G^*) = (1, 1/2, 0)\,. \end{aligned} \tag{5.194}$$

What these fixed points correspond to can be seen clearly by looking at the ratio of the parametric masses

$$\frac{M_\rho^2(\mu)}{M_{a_1}^2(\mu)} = \frac{Y(\mu)}{X(\mu)+Y(\mu)}\quad . \tag{5.195}$$

The fixed points (5.194) describe the flow

$$\text{VM}\ :\ M_\rho^2/M_{a_1}^2\ \to\ 0\,, \tag{5.196}$$

$$\text{GL}\ :\ M_\rho^2/M_{a_1}^2\ \to\ 1\,, \tag{5.197}$$

$$\text{HB}\ :\ M_\rho^2/M_{a_1}^2\ \to\ 1/3 \tag{5.198}$$

while

$$M_\rho \;\to\; 0\,, \quad M_{a_1} \;\to\; 0\,. \tag{5.199}$$

Here, (5.196) represents the generalized VM scenario where the ρ mass goes to zero faster than the a_1 mass, (5.197) the standard sigma model scenario which is called "Ginzburg-Landau" where the ρ joins the a_1 as a chiral partner, and (5.198) a hybrid of VM and LG.

5.7.4 *Multiplet structure and vector dominance*

The three different fixed points imply different multiplet structures and different responses to the electromagnetic field. This difference will be important for looking for the signal of chiral restoration in relativistic heavy ion collisions. Consider flavor $SU(2)$ for which the states that we need to focus on are the ρ, a_1, π and s (often labeled as σ in nuclear physics literature and as ϕ in Chapter 8). Define the mixing angle ψ in terms of κ as

$$\cos\psi = \sqrt{1-\kappa}\,, \qquad \sin\psi = \sqrt{\kappa}\,. \tag{5.200}$$

with

$$\kappa = \frac{Y}{X+Y} \tag{5.201}$$

with X and Y defined in (5.192). Then we can write

$$\begin{aligned}
|s\rangle &= |(N_f, N_f^*) \oplus (N_f^*, N_f)\rangle\,, \\
|\pi\rangle &= |(N_f, N_f^*) \oplus (N_f^*, N_f)\rangle \sin\psi \\
&\quad + |(1, N_f^2-1) \oplus (N_f^2-1, 1)\rangle \cos\psi\,, \\
|\rho\rangle &= |(1, N_f^2-1) \oplus (N_f^2-1, 1)\rangle\,, \\
|a_1\rangle &= |(N_f, N_f^*) \oplus (N_f^*, N_f)\rangle \cos\psi \\
&\quad - |(1, N_f^2-1) \oplus (N_f^2-1, 1)\rangle \sin\psi\,,
\end{aligned} \tag{5.202}$$

where $N_f = 2$. Note that here the vectors ρ and a_1 correspond to the longitudinal components. At the fixed points, we find the multiplet structure

$$\begin{aligned}
&\text{VM} \;:\; \sin\psi \;\to\; 0\,, \\
&\text{GL} \;:\; \cos\psi \;\to\; 0\,, \\
&\text{HB} \;:\; \sin\psi \;\to\; \sqrt{\frac{1}{3}}\,, \quad \cos\psi \;\to\; \sqrt{\frac{2}{3}}\,.
\end{aligned} \tag{5.203}$$

This is just a symmetry structure. Whether or not they become degenerate is a dynamical issue which the symmetry alone cannot decide. However, in certain application of the VM idea discussed in Chapter 7 (*e.g.*, the STAR ρ^0/π^- ratio), there is requirement that all of these modes become massless at the critical point

(in the chiral limit). This feature has yet to be established by experiments or theory (on lattice). The proper approach would be to find the way to incorporate scalar degrees of freedom that is compatible with this multiplet structure.

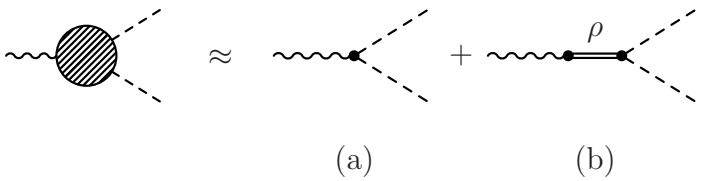

Fig. 5.4 Leading contributions to the electromagnetic form factor of the pion. (a) direct $\gamma\pi\pi$ and (b) $\gamma\pi\pi$ mediated by ρ-meson exchange.

Thus the VM mode describes the longitudinal ρ joining the π with the s joining the a_1, the GL mode describes the ρ joining the a_1 with the s joining the π, *i.e.* the sigma model structure, and the HB describing a mixture of the two.

5.7.5 *Vector dominance and the fixed points*

Next we consider how the notion of vector dominance gets affected by the different fixed point structure. The pion couples to the EM field directly (a) and via the ρ meson (b) as in Fig. 5.4. The direct photon-π-π coupling $g_{\gamma\pi\pi}$ is given by

$$g_{\gamma\pi\pi} = 1 - \frac{1}{2}\frac{F_\sigma^2}{F_\pi^2}(1-\kappa^2)\,. \tag{5.204}$$

For $a = b$ and $d = 0$, this becomes

$$g_{\gamma\pi\pi} = (1-\kappa)/2\,. \tag{5.205}$$

Thus as the chiral symmetry restoration point is approached, we have

$$\begin{aligned} &\text{VM} \;:\; g_{\gamma\pi\pi} \;\to\; \frac{1}{2}\,,\\ &\text{GL} \;:\; g_{\gamma\pi\pi} \;\to\; 0\,,\\ &\text{HB} \;:\; g_{\gamma\pi\pi} \;\to\; \frac{1}{3}\,. \end{aligned} \tag{5.206}$$

It is interesting that vector dominance which seems to be broken away from the vacuum for GL gets restored at the fixed point. For the two cases of VM and HB, vector dominance is violated at their respective fixed point.

5.7.6 *Infinite tower and the VD*

In Subsection 5.3.4 above, we mentioned that hadronic processes are vector dominated in the holographic description. How this affects the nucleon EM structure will be discussed in the next chapter where the problem arises in connection with the solitonic (*i.e.* instantonic) structure of baryons. Here we briefly discuss how the vector dominance discussed above in terms of the lowest member of the tower gets modified by the presence of the infinite tower for the pion form factor. It will be seen that the "violation" of vector dominance near the VM viewed in terms of the lowest member(s) picks up a different meaning.

In the Sakai-Sugimoto model of $\text{HLS}_{K=\infty}$ [Sakai and Sugimoto 2005], the electromagnetic (EM) form factor of the pion is given by

$$F_1^\pi(Q^2) = \sum_{k=0}^{\infty} \frac{g_{v^{(k)}} g_{v^{(k)}\pi\pi}}{Q^2 + m^2_{v^{(k)}}} \tag{5.207}$$

with the normalization

$$F_1^\pi(0) = \sum_{k=0}^{\infty} \frac{g_{v^{(k)}} g_{v^{(k)}\pi\pi}}{m^2_{v^k}} = 1 \tag{5.208}$$

where $v^{(k)}$ stands for the k-th vector meson in the ρ channel with the index $k = 0, 1, 2, ..., \infty$ labeling the vector mesons in the tower. Now to what extent the vector meson with index k contributes to the form facto is described by the sum rule (5.208). The numerical result comes out to be

$$F_1^\pi(0) = 1 = 1.310 - 0.346 + 0.0505 - 0.0128 + ... = 1.002. \tag{5.209}$$

More than $\sim 99\%$ of the sum rule is saturated by the first four vector mesons in the ρ channel. We will see in the next chapter that the same saturation holds in the nucleon EM form factors. It is interesting that in this infinite tower picture, the lowest vector meson overshoots the sum rule by $\sim 30\%$. Naively the VD violation attributed to $a < 2$ in HLS/VM theory discussed above can be attributed to the participation of the remaining members of the tower.

Chapter 6

Skyrmions

6.1 Preliminary Remarks

As we will see in Chapters 7-10, the state of hadronic matter at densities greater than that of nuclear matter is very poorly understood. Unlike in hot medium, QCD proper is more or less powerless except at very low density and very high asymptotic density. The only known theoretical approach of QCD in the nonperturbative regime, *i.e.* lattice simulation, cannot yet access the density regime involved because of the notorious sign problem. At very low density, there is a wealth of data from experiments with finite nuclei and at asymptotically high density, perturbative QCD should apply. But the phenomenological extrapolation to densities greater than that of nuclear matter using effective models as described in Chapter 4 and theoretical extrapolation from an infinite density at which perturbative QCD is applicable to densities in the vicinity of that of nuclear matter – treated in Chapter 10 – are highly unreliable. At present, the only theoretically justifiable tool that can in principle capture QCD – but is largely undeveloped – is, as we will describe below, the skyrmion approach to baryons of the baryon number B for $1 \leq B \leq \infty$. The modern development of skyrmion structure that emerges from holographic QCD lends further support to this assertion.

At low densities treated in the preceding chapters, effective field theories, with the nucleon treated as a local field, adequately model QCD in the sense of Weinberg's folk theorem. However it is not clear how to extend the strategy applicable there directly to nuclear matter, hot and/or dense matter. A possible strategy for accessing such systems will be discussed in Chapter 8, which will involve multiple (or at least two) decimations in the renormalization group sense. In this chapter, we will address the problem from the point of view of many-nucleon systems treated as skyrmions with large baryon (winding) number, $B(W) \to \infty$. We shall work mainly with the classic Skyrme model with pions only, mentioning only briefly the potential role of the lightest vector mesons ρ and ω, in dealing with dense matter and chiral restoration phase transition.[1] We shall, however, treat in some detail the

[1]The skyrmion description for baryons (of the winding number B) with the Skyrme Lagrangian [Skyrme 1962] consisting of the quadratic current algebra term and the quartic Skyrme

nucleon structure that follows from hidden local symmetry Lagrangian with an infinite tower of vector mesons following Sakai-Sugimoto model [Sakai and Sugimoto 2005; Sakai and Sugimoto 2006] of holographic dual QCD (hQCD for short). We will find a drastically different structure from what one finds in the Skyrme model, which suggests that hadronic matter built with the Skyrme model – without vector mesons – may not be realistic.

6.2 Skyrmions in QCD

6.2.1 *A little history in nuclear physics*

The Skyrme model invented by Skyrme in late 1950's and early 1960's [Skyrme 1962] had remained as a mere curiosity, totally unrecognized by both particle and nuclear physicists, until 1983 when it was resurrected as a bona-fide model for baryons consistent with QCD in the large N_c limit [Witten 1983; Adkins, Nappi and Witten 1983]. The main reason for this neglect was that there were quark models, all trying to mock up what might be in the nonperturbative sector of QCD, such as constituent quark model, MIT bag model *etc.* which appeared as promising microscopic pictures of the baryons.

It was argued by the aficionados of the MIT bag model – mostly particle theorists – until late in 1970's that the point-like nucleon fields exchanging mesons as in the old Yukawa picture used by nuclear physicists should be abandoned and replaced by the picture of the bags of confined quarks overlapping with each other and interacting within the bag by exchanging weakly interacting gluons. Since the confinement size described by the *bag size* of a radius $R \sim 1$ fm to be compared with the average inter-particle distance $d_{NN} \sim 2$ fm between pairs of nucleons in heavy nuclei implied that nucleons are close-packed in nuclei, the Yukawa picture was thought to be absurd. But the standard nuclear physics worked very well up to that point. So the big question was: How can the picture depicted variably as "grapefruits in a salad bowl" or even worse as a "pea-soup" be reconciled with the highly successful shell-model picture with the nucleons treated as point particles exhibiting distinctive single particle nature in the standard nuclear structure approach?

As a way out of this conflict, nuclear theorists proposed in 1979 the "little bag" with a radius of $\sim 1/3$ fm [Brown and Rho 1979]. In hindsight, the original argument given in [Brown and Rho 1979] turned out to be incorrect. The correct modern version of the "little bag" was given in Chapter 3, where we saw that the basic idea of the little bag essentially survived as an approximation of a more general picture of the Cheshire bag model (CBM). Here we will briefly sketch the original

term with pion fields only will always be referred to as "Skyrme model." When unspecified as such, we will mean in a generic sense a skyrmion model that takes into account, as needed, other relevant (massive) mesonic degrees of freedom, *e.g.*, vector-meson fields.

reasoning which led to the model and ultimately to the adoption of the skyrmion as the correct ingredient of the nucleon in nuclear physics.

The MIT bag model, while implementing confinement by fiat, did not have one of the basic ingredients of QCD for nuclear physics, namely, the spontaneously broken chiral symmetry. There was no pion, *i.e.* the Goldstone excitation degenerate (in the chiral limit) with the vacuum; the pion was also a bag in the model. This defect was remedied (as detailed in Chapter 3) by requiring that the pion field be coupled at the boundary to the quark lodged inside the bag [Chodos and Thorn 1975; Brown and Rho 1979]. (There is an alternative picture which allows the pion field to penetrate the bag and couple to the quarks inside the bag. This is the "cloudy bag model" described in the previous chapter [Thomas, Theberge and Miller 1981; Thomas 1982]. To account for the bulk of physics, the bag size had to be "big" in this model.) Now the argument of [Brown and Rho 1979] was that the pion cloud covering the bag outside would put a pressure on, and squash, the bag when the bags are inside nuclear medium so the bag becomes effectively small, say $\sim 1/3$ of the size it has in free space, allowing two little bags exchanging the pions to give the desired Yukawa force. We now know how this "shrinking" of the bag can be made consistently with topological properties of the baryon charge. The existence of a little bag as an optimal model was, however, indicated empirically in the presence of a $\sim 0.2 - 0.3$ fm core in large angle high-energy proton-proton scattering at the time [Orear 1978] and, more recently, in inelastic structure function of the proton [Petronzio 2003]. This is also the size one observes in the proton form factor measured in the electron scattering at large momentum transfer [Bijker and Iachello 2004]. Later we will see how this structure can be interpreted in terms of the vector manifestation of hidden local symmetry and the violation of the vector dominance (VD) and equivalently in terms of an infinite tower of vector mesons encapsulated in the instanton baryon in 5D.

6.2.2 *Little bag and skyrmion*

We saw in Chapter 3 that the bag picture can be made chirally symmetric by populating pions outside the bag with suitable boundary conditions on the bag surface. When quantized, the baryon charge is shared between inside and outside of the bag, the inside by the (complementary) fractionalized quark baryon charge and the outside the fractionalized topological charge. The partition is such that the total charge remains integral as required by the integer quantization of the baryon charge. The Cheshire Cat principle [Nowak, Rho and Zahed 1996; Rho 1994] then says that physics should be independent of the size of the bag in which the quark degrees of freedom reside. In Chapter 3, this was stated as a gauge invariance. What is relevant for the present chapter is that in the limit that the bag radius shrinks to zero, one is left with a description of the baryon in terms of the skyrmion picture of the baryon, the baryon charge becoming entirely topological.

In reality, this Cheshire Cat mechanism is only approximate except in topological quantities. Thus neither the bag picture nor the skyrmion picture can be pushed to its extreme. This means that in describing the nucleon, one would have to make a compromise. The best comprise is made when the baryon charge is shared equally between the bag with quarks and the outside in the pion cloud. This is obtained at the "magic angle" $\theta = \pi/2$ in the skyrmion profile function. Roughly speaking this is the angle which would give the bag size corresponding to the "core size" $\sim 1/3$ fm observed in the proton structure [Orear 1978; Petronzio 2003].

6.3 Skyrmions and Vector Mesons

6.3.1 *Multiple scales*

As stressed in Chapters 4 and 8, because of the multiple scales involved in the physics of many-body hadronic systems, a variety of strategies appropriate for different scales using effective field theories need be combined. In fact the simplest effective strategy described in [Brown and Rho 2004a] is the "double-decimation" approach that involves a RG decimation down to the scale of chiral symmetry breaking (denoted Λ_χ) and another from the chiral symmetry scale to a Fermi-liquid scale (denoted Λ_{FS}). There are, in the literature, various different models that have been extensively studied, such as, to cite a few, Nambu-Jona-Lasinio (NJL) model and the models mentioned in Chapter 3, *i.e.* chiral bag model, cloudy bag model, chiral quark-soliton model *etc.* The skyrmion picture has the advantage to provide a unified approach to many-body physics starting from a large N_c effective Lagrangian for nucleons and treating on the same footing elementary baryons, as well as nuclei, nuclear matter and dense matter.

Much work has been done in confronting the standard Skyrme model with nature [Nowak, Rho and Zahed 1996; Zahed and Brown 1986]. It is, however, clear that even in the large N_c limit, the Skyrme Lagrangian is far from realistic. We will see below some of the basic difficulties of the Skyrme model. As mentioned, we learn from the holographic dual model that the baryons must arise as skyrmions in a theory that has an infinite tower of vector mesons whereas the Skyrme model represents a model when all the vectors are arbitrarily set equal to zero. Here we first consider a much simpler model, namely, the soliton implied by the hidden local symmetry (HLS) theory of Bando *et al.* [Bando *et al.* 1988; Harada and Yamawaki 2003] which takes into account only the ρ and ω mesons.

6.3.2 *HLS Lagrangian "light" ($HLS_{K=1}$)*

The Lagrangian we will use is an $SU(3)$ Lagrangian, reduced according to the need for our purpose. For what follows in this chapter, the action we will need can be

written in three parts as [Scoccola, Min, Nadeau and Rho 1989][2]

$$\Gamma = \Gamma_0 + \Gamma_{\rm mass} + \Gamma_{\rm an} \tag{6.1}$$

where Γ_0 is the HLS action given in Chapter 5[3]

$$\Gamma_0 = \int d^4x \left(\mathcal{L}_A + a\mathcal{L}_V - \frac{1}{2g^2} \,\mathrm{Tr}\,[V_{\mu\nu} V^{\mu\nu}] \right) + \Gamma_0', \tag{6.2}$$

where

$$\mathcal{L}_{\rm A} \equiv F_\pi^2 \,\mathrm{tr}\,[\widehat{\alpha}_{\perp\mu} \widehat{\alpha}_\perp^\mu] \ , \tag{6.3}$$

$$a\mathcal{L}_{\rm V} \equiv F_\sigma^2 \,\mathrm{tr}\left[\widehat{\alpha}_{\parallel\mu} \widehat{\alpha}_\parallel^\mu\right] = F_\sigma^2 \,\mathrm{tr}\left[\left(V_\mu - \alpha_{\parallel\mu}\right)^2\right] \tag{6.4}$$

with

$$\hat{\alpha_{\perp\mu}} = \left(\partial_\mu \xi_{\rm R} \cdot \xi_{\rm R}^\dagger - \partial_\mu \xi_{\rm L} \cdot \xi_{\rm L}^\dagger\right)/(2i) \ , \tag{6.5}$$

$$\hat{\alpha_{\parallel\mu}} = \left(\partial_\mu \xi_{\rm R} \cdot \xi_{\rm R}^\dagger + \partial_\mu \xi_{\rm L} \cdot \xi_{\rm L}^\dagger\right)/(2i) \ - V_\mu, \tag{6.6}$$

and

$$\xi_{\rm L,R} = e^{i\sigma/F_\sigma} e^{\mp i\pi/F_\pi} \ , \quad [\,\pi = \pi^a T_a \,,\, \sigma = \sigma^a T_a] \ . \tag{6.7}$$

Here Γ_0' is an $\mathcal{O}(p^4)$ gauged Skyrme term [4] which in unitary gauge is of the form

$$\Gamma_0' = \eta^2 \int d^4x \mathrm{Tr}[U^\dagger D_\mu U, U^\dagger D_\nu U]^2, \tag{6.8}$$

where η is some unknown constant, $\Gamma_{\rm mass}$ is a chiral symmetry breaking mass term which we will take – dropping the pion mass when compared with the kaon mass – as

$$\Gamma_{\rm mass} = \frac{F_\pi^2}{6} m_K^2 \int d^4x [\mathrm{Tr}(\xi_L^\dagger \xi_R + \xi_R^\dagger \xi_L - 2) - \sqrt{3}\mathrm{Tr}(\lambda^8(\xi_L^\dagger \xi_R + \xi_R^\dagger \xi_L))] \tag{6.9}$$

and $\Gamma_{\rm an}$ is the anomalous action which takes the form

$$\Gamma_{\rm an} = \Gamma_{WZ}^0 + \frac{N_c}{16\pi^2} \int_{M^4} \sum_{i=1}^{4} c_i \mathcal{L}_i \tag{6.10}$$

where Γ_{WZ}^0 is the "irreducible" Wess-Zumino action containing only the pseudoscalar fields (that contains topology) and the second term is a homogeneous term

[2] Here and in what follows in this chapter, we will not distinguish the parametric decay constant F_π and the physical decay constant f_π which are the same in the order we are considering and hence will be used interchangeably.

[3] We shall reserve the notation ρ for the non-strange vector mesons and use V for the $SU(3)$ vector field.

[4] It is perhaps worth repeating that this term appears naturally in dimensional deconstruction of QCD [Hill and Zachos 2005; Brihaye, Hill and Zachos 2004] and holographic dual QCD [Sakai and Sugimoto 2005; Sakai and Sugimoto 2006] discussed in the preceding chapter.

that is required to satisfy the anomalous Ward identity but is not topological: it is of the form

$$\mathcal{L}_1 = i\mathrm{Tr}(\hat{a}_L^3\hat{a}_R - \hat{a}_R^3\hat{a}_L), \tag{6.11}$$

$$\mathcal{L}_2 = i\mathrm{Tr}(\hat{a}_L\hat{a}_R\hat{a}_L\hat{a}_R), \tag{6.12}$$

$$\mathcal{L}_3 = i\mathrm{Tr}F_V(\hat{a}_L\hat{a}_R - \hat{a}_R\hat{a}_L), \tag{6.13}$$

$$\mathcal{L}_4 = i\mathrm{Tr}(\hat{F}_L + \hat{F}_R)(\hat{a}_L^3\hat{a}_R - \hat{a}_R^3\hat{a}_L) \tag{6.14}$$

with, written in the form notation,

$$\hat{a}_{L(R)} = \frac{1}{i}D_\mu\xi_{L(R)}\xi_{L(R)}^\dagger dx^\mu. \tag{6.15}$$

$$F_V = dV - iV^2 \ , \quad \hat{F}_{L,R} = \xi_{L,R}\mathcal{F}_{L,R}\xi_{L,R}^\dagger \ . \tag{6.16}$$

Here $\mathcal{F}$ is the external gauge field which we shall not specify. If needed, they can appear by suitably gauging the subgroup of the global symmetry. In this chapter, we will not need the external fields, so $\mathcal{L}_4$ will not figure. The hidden gauge field denoted V_μ has the components

$$V_\mu = \frac{g}{\sqrt{2}}\begin{pmatrix} \omega_\mu + \rho_\mu & \sqrt{2}K_\mu^* \\ \sqrt{2}K_\mu^{*\dagger} & \phi_\mu \end{pmatrix} \ . \tag{6.17}$$

The coefficients c_i are determined by the processes involving ω, π^0, γ and γ^*. When best-fit to data at tree order, they come out to be [Harada and Yamawaki 2003]

$$c_3 \approx 1, \quad c_1 - c_2 \approx 1. \tag{6.18}$$

This combination of c_i's implies that there is no direct ω-3π coupling. The absence of the direct coupling is the characteristic feature of the holographic dual model of QCD of Sakai and Sugimoto [Sakai and Sugimoto 2005]. As will be elaborated further in what follows, these values of the coefficients could have an important role in dense baryonic matter, because it suppresses the $B_\mu\omega^\mu$ coupling where B_μ is the baryon current (defined below) and hence some of the repulsion due to the ω meson in dense medium. In considering the $S > 0$ skyrmions below, however, we will use the combination $c_1 - c_2 = 2$ and $c_3 = 0$ as used for the hyperons in [Scoccola, Min, Nadeau and Rho 1989]. The only reason for taking this combination is that it makes the numerical calculation much simpler than that of (6.18). No results are available at the time of this writing with the coefficients (6.18), so one cannot say whether there will be qualitative differences between the two.

6.3.3 SU(2) *skyrmion*

To have contact with the standard discussion of ungauged skyrmions of the Skyrme model (as discussed in the monograph CND-I [Nowak, Rho and Zahed 1996]), we first consider the two-flavor skyrmions most relevant to nuclear physics. We will

return later to the structure of three-flavor skyrmions for baryons with strange quarks.

Our task here is to construct a skyrmion soliton using a Lagrangian that comes as close as possible to HLS. In so doing, we will make a drastic simplification without, however, losing essential features of the model. Since we are in the two-flavor space, the pseudoscalar K and the strange vector K^* do not come in. Among the vector mesons, only the ρ and ω are taken into account.

6.3.3.1 *Stabilizing the soliton*

In the Skyrme model, the quartic Skyrme term is essential for the topological stability of the soliton, *i.e.* it evades the Derrick-Hobart collapse. The microscopic origin of this term has been a mystery. While it makes the soliton escape from the Derrick-Hobart collapse, it seems to capture a lot more than the relevant chiral scale ~ 1 GeV. If one were to follow chiral perturbation theory (χPT) philosophy and take the most general Lagrangian to the chiral order corresponding to the Skyrme term, *i.e.* $\mathcal{O}(p^4)$,[5] the resulting chiral Lagrangian which has several $\mathcal{O}(p^4)$ terms reduces approximately to the Skyrme-type term for $N_f = 2$ in the large N_c limit [Bijnens, Colangelo and Gasser 1994]. It should be noted, however, that one cannot attach a great importance to this observation. In fact, if one naively assumes (which HLS theory says is unjustified) that the ρ meson is heavy and can be integrated out, then the kinetic energy term of the vector meson does indeed give the Skyrme term $\frac{1}{32e^2}\mathrm{Tr}[U^\dagger\partial_\mu U, U^\dagger\partial_\nu U]^2$ where e can be identified with the gauge coupling g. However, in HLS/VM, this "derivation" cannot be valid since the coupling should scale as $g \sim \mathcal{O}(p)$ as required by the counting that the ρ meson is as "light" as the pion. In the HLS chiral counting, the kinetic energy term of the ρ must go as $\mathcal{O}(p^2)$ like the pion kinetic energy term and hence cannot be responsible for the stabilization of the soliton.[6]

That the Skyrme term must arise from some other excitations than the ρ meson is indicated in the recent development of holographic dual QCD (hQCD). In fact, when all the fields of the tower of vector mesons that result from the compactification of the 5D YM theory are set equal to zero, what remains is just the Skyrme model with the quadratic current algebra term and the quartic Skyrme term with the fixed coefficients and nothing else. Now since the lowest member of the tower ρ considered in HLS theory cannot give rise to the Skyrme term in the sense of HLS/VM, it must be the higher-lying vector mesons in the infinite tower that are responsible for the

[5] This is essentially the same counting as in Chapter 4. We do make the distinction however since the counting made in Chapter 4 is more appropriate for nuclear few-body systems than what is used in the context of this chapter.

[6] As noted below, even in the presence of the Skyrme quartic term, the soliton shrinks to a point in the presence of the infinite tower of the vector mesons. The stabilization is gotten by a Coulomb-type term coming from the (5D) Chern-Simons term.

Skyrme term that provides the stabilization.[7] We will see this in the structure of the gauged skyrmion discussed below.

Now what about the ω meson? Assume for the moment that there is a direct coupling between ω and 3 pions. This would give rise to the $B_\mu\omega^\mu$ coupling. If one does not make the assumption that the ω mass is infinite, then it turns out that the resulting soliton sits on a saddle point and hence unstable as discussed in [Igarashi *et al.* 1985]. If there is a direct coupling $B_\mu\omega^\mu$ and if the ω can be integrated out, then the six derivative term considered by Adkins and Nappi a long time ago results and gives stabilization [Adkins and Nappi 1984]. However, as mentioned above, both the phenomenology [Harada and Yamawaki 2003] and hQCD indicate that there is no direct $\omega\pi^3$ coupling. The absence of this direct coupling will be welcome for the physics of hadronic matter at high density.

The conclusion then is that the *gauged* Skyrme term that comes out of the five-dimensional gauge theory – dimensionally reduced to 4-D – could be responsible for the stabilization of the skyrmion. Neither the lowest lying ρ meson nor the ω meson does the job. This observation has an important consequence on the equation of state of hadronic matter at high density as will be discussed later.

6.3.3.2 *Gauged skyrmion with the ρ meson*

Since there is no ω coupling to three pions and hence to the baryon current B_μ for the coefficient (6.18) in the induced WZ term, the ω field decouples in the $SU(2)$ skyrmion structure. Thus we wind up with what is an essentially gauged Skyrme Lagrangian, with the nonabelian gauge field ρ_μ. The Lagrangian is roughly equivalent to Harada-Yamawaki HLS Lagrangian gauge fixed to unitary gauge [8]. The soliton that results from such a Lagrangian is the Skyrme-Wu-Yang hedgehog solution with the energy given by

$$4\pi E(g, F_\pi, \kappa) = \frac{1}{2g^2}\int d^3x \mathrm{Tr} F_{ij}^2 + \frac{F_\pi^2}{4}\int d^3x \{\mathrm{Tr}(D_j U^\dagger D_j U) + \kappa^2 \mathrm{Tr}[D_i U^\dagger, D_j U]^2\} \quad (6.19)$$

where $D_\mu U = \partial_\mu U - ig[\rho_\mu, U]$ and $\kappa^2 = \eta^2/F_\pi^2$ (we follow the notation of Brihaye *et al.* [Brihaye, Hill and Zachos 2004] [9]) For simplicity we will continue ignoring the chiral symmetry breaking mass term. The qualitative features are not affected by this term, although doing phenomenology would require its presence. This sys-

[7] In [Hill 2002], it is argued that the gauged Skyrme Lagrangian is gotten from the 5D Yang-Mills Lagrangian of hQCD when dimensionally reduced to 4D with only the lowest vector meson multiplet ρ taken into account and that the resulting skyrmion is stabilized by the gauged Skyrme term which could be identified as representing short-distance effects inherited from the high-lying vector mesons not figuring explicitly in the Lagrangian.

[8] As will see below, the gauge fixing hides an interesting phenomenon which has to do with half-skyrmions and a topological phase associated with it. This seems to indicate that the gauge-fixed skyrmion cannot be a good description as density increases since with a gauge-fixed Lagrangian, one cannot describe the dropping mass of the ρ and ω mesons.

[9] In the standard notation of the Skyrme model, $\kappa^2 = (8e^2F_\pi^2)^{-1}$.

tem which we shall call "gauged skyrmion" in contrast to the ordinary ungauged skyrmion was studied first by Igarashi *et al.* [Igarashi *et al.* 1985] a long time ago. The spherical Skyrme-Wu-Yang ansatz for a unit winding number is

$$\rho_i = \frac{1-\mathcal{K}(r)}{gr}\epsilon_{ijk}\frac{\tau^j}{2}\hat{x}^k \equiv \frac{G(r)}{gr}\epsilon_{ijk}\frac{\tau^j}{2}\hat{x}^k,$$
$$U = e^{if(r)\hat{\mathbf{x}}\cdot\tau} = \cos f(r) + if(r)\hat{\mathbf{x}}\cdot\tau. \tag{6.20}$$

To bring out the distinctive feature of the gauged skyrmion, we first recall a few well-known features of the soliton of the ungauged Skyrme Lagrangian which is obtained by setting $\mathcal{K}(r) = 1$ or equivalently by dropping the ρ term in the gauged skyrmion Lagrangian. The energy of the system is

$$E = \frac{F_\pi^2}{2}\int_0^\infty dr\{(rf' - \kappa\frac{\sin^2 f}{r})^2 + 2\sin^2 f(1-\kappa f')^2 + 6\kappa f'\sin^2 f\}. \tag{6.21}$$

Now the first two terms are positive definite, and the last term is a total derivative which is related to the baryon number, so the energy of the soliton has the bound known as the Bogomol'ny topological lower bound

$$E_{B=1} > E_{\text{topological}} \tag{6.22}$$

where

$$E_{\text{topological}} = \frac{3\pi}{2}\kappa F_\pi^2. \tag{6.23}$$

The soliton can never saturate the bound unlike in the BPS monopole case, because there are no self-dual chiral fields. Specifically the first two terms in (6.21) cannot vanish simultaneously. As it stands, the bound goes to zero if one sets $\kappa \to 0$ and goes to infinity as $\kappa \to \infty$. This observation has an interesting ramification on the interpretation of the Skyrme term on which we will have more to say later (in connection with what is called Brown-Rho scaling).

Suppose the ρ is very massive. In this case, one can integrate it out to obtain $\eta^2 = \kappa^2 F_\pi^2 = \frac{1}{8g^2}$. Since in HLS theory with the vector manifestation (see Chapter 5) the gauge coupling g is driven to zero as temperature and/or density of the medium is increased, that would correspond to increasing κ. This implies that the skyrmion mass keeps increasing as one approaches the vector manifestation point at which g goes to zero proportionally to the quark condensate. This is clearly unreasonable as it contradicts the basic premise of HLS with the VM fixed point.

The situation changes drastically when the hidden gauge particles figure in the soliton structure. To see this, substitute (6.20) into (6.19) and re-scale r and κ by $1/(gF_\pi)$ and get

$$E = \frac{F_\pi}{g}\int_0^\infty dr\{4\mathcal{K}'^2 + \frac{2(\mathcal{K}^2-1)^2}{r^2} + \frac{r^2 f'^2}{2}$$
$$+\mathcal{K}^2\sin^2 f + \kappa^2\mathcal{K}^4\frac{\sin^4 f}{2r^2} + \kappa^2\mathcal{K}^2 f'^2\sin^2 f\}\ . \tag{6.24}$$

The baryon number is given by the soliton field U, so the condition that the baryon number be quantized requires that

$$f(0) = n\pi,\ f(\infty) = 0 \tag{6.25}$$

with an integer n for the winding number. As for the gauge field, one notes that the second term under the integral $\frac{2(\mathcal{K}^2-1)^2}{r^2}$ diverges at $r = 0$, so to have the energy finite $\mathcal{K}$ should equal 1 at the origin and vanish at infinity,

$$\mathcal{K}(0) = 1,\ \mathcal{K}(\infty) = 0. \tag{6.26}$$

The topological lower bound of this system has been studied by various authors for the theory corresponding to (6.24). It is given by [Brihaye, Hill and Zachos 2004]

$$E_{\text{topological}} = \frac{2\pi F_\pi}{\sqrt{g^2 + (\frac{4}{3\kappa F_\pi})^2}}\,. \tag{6.27}$$

In this formula, g can be taken as small as one wishes without getting into difficulty. Furthermore as the gauged Skyrme term becomes large, the bound becomes independent of κ, and instead becomes proportional to F_π/g, with the scale being set by the gauge coupling.

Solutions to the equations of motion that follow from (6.24) are available in numerical forms [Brihaye, Hill and Zachos 2004]. The differences from the ungauged skyrmion structure can be qualitatively summarized as follows:

(1) The scales of the two functions $f(r)$ and $\mathcal{K}(r)$ tend to resolve as in the Born-Oppenheimer problems and as in the monopole in the large Higgs mass limit.
(2) For large κ, f stays nearly constant up to $r = R$ at which f' changes from zero abruptly to $\pi R/r^2$, while $\mathcal{K}$ goes rapidly to zero at $r = R$. R depends weakly on κ.
(3) Asymptotically f goes as $\sim 1/r$, whereas it goes as $\sim 1/r^2$ in the case of the ungauged skyrmion.
(4) In the vicinity of R, the skyrmion structure is dominated by the scale $r \sim \sqrt{\kappa}$, whereas in the ungauged case, it is $r \sim \kappa$.
(5) For large κ, the energy is more or less independent of κ in contrast to the ungauged case where $E \sim \kappa$.

6.3.3.3 *Defects of the Skyrme soliton*

We learned above that the gauged skyrmion is basically different from the ungauged one, the Skyrme model. Here we argue that the Skyrme model, in fact, does not adequately describe the physics of baryons, be that for single baryon or for many-baryons systems, suggesting that the presence of vector mesons is mandatory to improve the model.

We recall from the preceding chapter that the Skyrme model results if *all* gauge fields in the infinite tower of the holographic QCD model are equal to zero, as shown by Sakai and Sugimoto [Sakai and Sugimoto 2006]. Including, in the Skyrme model, the pion mass term, and re-scaling the coordinates so that the energy and length units are given in terms of $F_\pi/2e$ and $1/eF_\pi$ respectively, we get the Lagrangian

$$L = \int d^3x \left\{ -\frac{1}{2}\mathrm{Tr}(R_\mu R^\mu) + \frac{1}{16}\mathrm{Tr}([R_\mu . R_\nu]^2) + \bar{m}^2\mathrm{Tr}(U-1) \right\} \tag{6.28}$$

and the energy of the classical static skyrmion

$$E_0 = \frac{F_\pi}{2e}\int d^3x \left\{ -\frac{1}{2}\mathrm{Tr}(R_i R_i) + \frac{1}{16}\mathrm{Tr}([R_i, R_i]^2) + \bar{m}^2\mathrm{Tr}(U-1) \right\}, \tag{6.29}$$

with $R_\mu \equiv (\partial_\mu U)U^\dagger$ and $\bar{m} = m_\pi/(F_\pi e)$. Assuming that the $B = 1$ skyrmion is spherically symmetric, we take the hedgehog form

$$U_0(\mathbf{x}) = \exp(if(r)\hat{\mathbf{x}}\cdot\tau)\,. \tag{6.30}$$

In order to get solutions that are eigenstates of spin and isospin, the standard approach is to quantize the rotational zero modes of the skyrmion as a rigid body, which yields multiplets of equal spin and isospin. To do this, write in spherical polar coordinates (r, θ, ϕ) the hedgehog configuration rigidly rotating around the ϕ-axis [Battye, Krusch and Sutcliffe 2006]

$$U = \cos f + i \sin f(\tau_3 \cos\theta + \sin\theta(\tau_1 \cos(\phi+\omega t) + \tau_2 \sin(\phi+\omega t)). \tag{6.31}$$

Substituting this into (6.28), we have

$$L = \frac{1}{2}\mathcal{I}\Omega^2 - E_0 \tag{6.32}$$

where $\Omega = \omega e F_\pi/2$,

$$E_0 = \frac{2\pi F_\pi}{e}\int_0^\infty dr \left\{ r^2 f'^2 + 2\sin^2 f(1+f'^2) + \frac{\sin^4 f}{r^2} + 2\bar{m}^2 r^2(1-\cos f) \right\}, \tag{6.33}$$

and $\mathcal{I}$ is the moment of inertia

$$\mathcal{I} = \frac{8\pi}{3e^2 F_\pi}\int_0^\infty \{\sin^2 f(r^2(1+f'^2)\} dr. \tag{6.34}$$

Quantizing (6.32), one gets the familiar expression for the rotational band

$$E = E_0 + \frac{J(J+1)}{2\mathcal{I}} \tag{6.35}$$

where $J = \Omega\mathcal{I}$ is the spin which is a conserved quantity. The spin takes the values from $1/2$ to $N_c/2$, so in the case of $N_c = 3$, this formula describes the nucleon with $J = 1/2$ and the Δ with $J = 3/2$.

To evaluate the energy (6.35), one needs the profile function $f(r)$ which can be gotten by solving the classical equation of motion. There is no analytical solution

to that; it was solved numerically first in [Jackson and Rho 1983; Adkins, Nappi and Witten 1983]. There is however a very simple form deduced by Atiyah and Manton from instanton solution [Atiyah and Manton 1989] which has a parameter, λ, that can be determined by variational principle

$$f(r) = \zeta_\lambda(r) = \pi\left[1 - \frac{r}{\sqrt{r^2+\lambda^2}}\right]. \tag{6.36}$$

Then (6.33) and (6.34) take the form

$$E_0 = \frac{2\pi F_\pi}{e}\int_0^\infty dr\left\{\lambda(r^2{\zeta_1'}^2 + 2\sin^2\zeta_1) + \frac{1}{\lambda}\sin^2\zeta_1(2{\zeta_1'}^2 + \sin^2\zeta_1)\right.$$
$$\left.+2\lambda^3\bar{m}^2r^2(1-\cos\zeta_1)\right\}, \tag{6.37}$$

and

$$\mathcal{I} = \frac{8\pi}{3e^2F_\pi}\int_0^\infty \lambda\{\sin^2\zeta_1(r^2(\lambda^2+{\zeta_1'}^2) + \sin^2\zeta_1)\}dr. \tag{6.38}$$

This allows us to express E_0 and $\mathcal{I}$ in terms of integrals that can be computed numerically. The energy takes the form

$$E_0(\lambda) = a\lambda + b/\lambda + c\lambda^3 \tag{6.39}$$

where a, b and c are numbers given by the integrals. Now minimizing with respect to λ, we have

$$\lambda^2 = \frac{-a + \sqrt{a^2+8cb}}{4c}. \tag{6.40}$$

Assuming the $\bar{m}$ is small and hence c is small, then we have

$$\lambda^2 = b/a + \mathcal{O}(c^2). \tag{6.41}$$

This number has been computed [Atiyah and Manton 1989]

$$\lambda^2 = 2.11. \tag{6.42}$$

This solution turns out to give the energy to the accuracy of 99.1% of the exact numerical solution of the differential equation. This is remarkable and indicates an intimate relation between instantons and skyrmions as evidenced in holographic dual QCD approach. (For a recent development, see [Eto, Nitta, Ohashi and Tong 2005].)

There are three parameters, F_π, e and m_π, but there are two relations, E_0 and $\mathcal{I}$. Fixing one parameter, then the other two can be determined from the two equations. There are roughly three ways to choose the parameters to do physics.

(1) One is to take m_π as given by experiment, $m_\pi \simeq 138$ MeV and fix the two remaining parameters by fitting to the masses of the nucleon and the Δ [Adkins, Nappi and Witten 1983]. Then other properties of the nucleon and the Δ such

as the magnetic moments, axial coupling constants and other static properties can be computed. The results are recorded extensively in the literature, so need not be repeated here. What matters for our purpose is that the resulting parameter F_π comes out to be about a half of the experimental value $f_\pi = 93$ MeV. There is nothing to compare with e; it is not directly related to the ρ-meson vector coupling as pointed out elsewhere (see [Igarashi *et al.* 1985]). Now the fact that the Lagrangian parameter F_π is so different from the physical pion decay constant f_π is quite disturbing as we will see later. This is because the Lagrangian one starts with is supposed to be valid in the large N_c limit, and in that limit, F_π, for instance, is a bit larger than the physical value [Harada and Yamawaki 2003], not smaller as is found here. Furthermore, it turns out that "with the experimental value of the pion mass the standard values of F_π and e are in the region for which there is no spinning skyrmion solution for the Δ" [Battye, Krusch and Sutcliffe 2006]. This means that the standard Skyrme parameters are most likely the artifacts of the rigid-body approximation.

(2) Another approach which has just been studied at the time of this writing is not to approximate the spinning skyrmions as rigid bodies but allow them to deform and break spherical symmetry [Battye, Krusch and Sutcliffe 2006]. This requires extensive numerical calculations. The outcome of the calculation is that there is a set of consistent solutions for the spinning skyrmions only for the pion mass in the range 280 MeV $\lesssim m_\pi \lesssim$ 350 MeV. Even for this, F_π that is needed is less than half of the experimental value of ~ 93 MeV, again far from what it should be in the large N_c limit.

(3) The third approach is to take into account the Casimir effect which is $\mathcal{O}(N_c^0)$ term in the N_c counting, subleading with respect to the classical soliton energy E_0 which is $\mathcal{O}(N_c)$ but leading order with respect to the rotational energy that separates the Δ from the nucleon. As mentioned in [Nowak, Rho and Zahed 1996], this seems to be the best way to compute the baryon properties with skyrmions, but it is difficult to compute the Casimir energies and so far, even after more than two decades since the the skyrmion picture was resurrected, there is no single reliable calculation of this contribution that can be used for a global analysis. There are several reasons, however, why the Casimir effect should be taken seriously: It cannot be simply lumped into parameters of the Lagrangian. First of all, in the baryon mass, while the $N - \Delta$ splitting is of order of 10% of the classical soliton mass, one expects the Casimir energy to be of order of $\sim$ 50% of E_0. It also turns out that in the chiral bag model [Rho, Goldhaber and Brown 1983; Nowak, Rho and Zahed 1996; Rho 1994] the Casimir effect plays a crucial role in describing not only the mass of the baryon but also the "proton spin" structure discussed in Chapter 3. Without the Casimir effect, there is no way to explain the bag-radius independence of both the mass and the flavor singlet axial charge and the smallness of the flavor-singlet axial charge in the chiral bag model. As described, once the large

Casimir energy of the order of ~ -500 MeV is taken into account, there is no difficulty in understanding the mass of the nucleon, the $N - \Delta$ splitting, the g_A for the neutron decay. The lack of calculations that account for this contribution, unfortunately, does not allow at this moment to know whether this approach actually solves the problem.

What the results as they stand are telling us is that the Skyrme model defined with the quadratic current algebra term and the quartic Skyrme term cannot be taken as a quantitative model to describe nature with. As we shall see later in this chapter, there is strong evidence for the importance of vector-meson degrees of freedom in the nucleon structure, *e.g.*, nucleon form factors.

6.3.4 *Nuclei as skyrmions*

Nuclei with baryon number $B > 1$ should also be described as skyrmions with winding number B. In fact, we will discuss later the case where $B = \infty$ for nuclear matter. What comes out at the classical skyrmion level depends extremely sensitively on what one takes for the pion mass. So far, skyrmions for $B > 1$ have not been appropriately quantized. However, one would like to see what they look like at the classical level and see whether there is any resemblance to real nuclei.

To see the role of the pion mass in the Skyrme model, let us take the usual form of the Skyrme model with the pion mass varied arbitrarily [Battye and Sutcliffe 2006; Houghton and Magee 2007]. In the chiral limit where the pion mass is zero, one finds that "minimum-energy multi-skyrmions come out shell-like, with the baryon density localized on the edges of a polyhedron that is approximately spherical and generically of the fullerene-type." This is not at all like what nuclei should look like. However, when pion mass is introduced there are qualitative changes. It is found that the fullerene structures collapse to a stable flat structure, displaying clustering into lower baryon numbers, typically of three and four. Such clustering, particularly of the alpha structure, is prominent in nuclear structure and one might be tempted to believe that after quantization, skyrmions come closer to nature.

As noted above for a single skyrmion, one typically needs a larger pion mass than what it should be and the qualitatively significant role played by the mass for multi-skyrmions looks suspicious. In view of the role played by vector mesons discussed below, we believe this signals – once more – a general defect in skyrmions constructed with pion field alone.

6.3.5 SU(3) *Skyrmions:* $S > 0$ *baryons*

Skyrmions that carry strangeness are interesting not only for their intrinsic role in the structure of strange baryons but also for the possible existence of exotic baryons, exotic in the sense that they cannot be described in terms of N_c valance quarks as the naive quark model seems to dictate. The example is the Θ^+ pentaquark that

presumably consists, at the most naive level, of four u and d quarks and one anti-s-quark, *i.e.* $qqqq\bar{s}$. There have been a flurry of experimental works in search of strangeness $S > 0$ baryons since the first announcement of the observation of the Θ^+ in 2003, and at the moment, the jury is not out. It is not our purpose here to either confirm or refute theoretically whether such a baryon is predicted by theory. Our theory is not developed quantitatively enough to do so. What interests us is to describe the important role the vector mesons are theoretically predicted to play in the structure of $S > 0$ baryons, with a focus on the $S = 1$ baryon with the quantum number of Θ^+. To do so we use the action (6.1) which was successfully applied to the hyperons, *i.e.* $S = -1, -2, -3$ baryons by Scoccola *et al.* [Scoccola, Min, Nadeau and Rho 1989].

6.3.5.1 *Kaon-soliton bound skyrmions*

In the approach introduced for hyperons by Callan and Klebanov (CK) [Callan and Klebanov 1985] which is more realistic in handling the strangeness degree of freedom than the approach based on three-flavor collective rotation (see [Nowak, Rho and Zahed 1996]), particularly in the K^+ sector as we will see shortly, the strangeness is carried by the pseudo-Goldstone field K, and baryons with strangeness are constructed by binding the kaon to the $SU(2)$ soliton. Now the $SU(2)$ soliton is the same as what was described above, which means that the classical configurations $f(r)$ or the hedgehog U_0 and $A(r)$ are given *ab initio*. The back-reaction from the fluctuating field on the $SU(2)$ skyrmion is ignored. The kaon appears as a fluctuating field, and the CK approach was to introduce the kaon field fluctuating around the pionic hedgehog configuration U_0 as

$$\xi_0 U_K \xi_0 \tag{6.43}$$

where

$$\xi_0 = \sqrt{U_0} \tag{6.44}$$

and

$$\ln U_K = \frac{i\sqrt{2}}{F_\pi} \begin{pmatrix} 0 & K \\ K^\dagger & 0 \end{pmatrix}. \tag{6.45}$$

This suggests taking the ξ field as [Scoccola, Min, Nadeau and Rho 1989] [10]

$$\xi_L^\dagger = \xi_0 \sqrt{U_K}, \qquad \xi_R = \sqrt{U_K} \xi_0. \tag{6.46}$$

Substituting the CK ansatz into the simplified HLS Lagrangian (6.1)), keeping terms quadratic in the kaon field and reinstating the pseudo-Goldstone mass terms, we

[10] Note that this is just an ansatz and is of course not unique. There may be other forms that could lead to better results, but there has been no systematic study on this matter.

get the Lagrangian density[11]

$$\mathcal{L} = \mathcal{L}_{\mathrm{SU(2)}} + \mathcal{L}_{\mathrm{KK*}} + \mathcal{L}_{\mathrm{K*kin}} + \mathcal{L}_{an} \tag{6.47}$$

where $\mathcal{L}_{\mathrm{SU(2)}}$ is the $SU(2)$ Lagrangian, $\mathcal{L}_{\mathrm{KK*}}$ is the non-anomalous part of the kaon Lagrangian including kaon interaction with the vector mesons

$$\begin{aligned}\mathcal{L}_{\mathrm{KK*}} = &(D_\mu K)^\dagger D^\mu K - K^\dagger \left(m_K^2 - a_\mu^{(0)} a^{\mu(0)}\right) K \\ &-\frac{a}{2}\mathrm{Tr}\left[(v_\mu^{(0)} + iq_\mu^{(0)})(K(D_\mu K)^\dagger - D_\mu K K^\dagger)\right] \\ &+aF_\pi^2 g^2 \left(\frac{1}{gF_\pi} a_\mu^{(0)} K + K_\mu^*\right)^\dagger \left(\frac{1}{gF_\pi} a^{\mu(0)} K + K^{*\mu}\right),\end{aligned} \tag{6.48}$$

$\mathcal{L}_{\mathrm{K*kin}}$ is the kinetic energy term for the strange vector meson $K^\star$

$$\mathcal{L}_{\mathrm{K*kin}} = -\frac{1}{2}(K_{\mu\nu}^{*\dagger} K^{*\mu\nu} + 2iK_\mu^{*\dagger} q^{\mu\nu(0)} K_\nu^*) \tag{6.49}$$

and $\mathcal{L}_{an}$ is what one obtains when the ansatz is substituted into the anomalous Lagrangian (6.10)

$$\begin{aligned}\mathcal{L}_{an} = +\left(\frac{iN_c}{4F_\pi^2}\right) \Big\{ &(\tfrac{2}{2} - \tfrac{3}{4}c_{12}) B^{\mu(0)} \left((D_\mu K)^\dagger K - K^\dagger D_\mu K\right) + c_{12} K^\dagger (i\frac{3g}{4}\omega_0 B^0) K \\ &-c_{12}\frac{gF_\pi}{3\pi^2}\epsilon^{\mu\nu\lambda\rho}\left(K_\mu^* a_\nu^{(0)} a_\lambda^{(0)} D_\rho K - (D_\mu K)^\dagger a_\nu^{(0)} a_\lambda^{(0)} K_\rho^*\right) \\ &-c_{12}\frac{1}{3\pi^2}\epsilon^{\mu\nu\lambda\rho}(D_\mu K)^\dagger \left\{a_\nu^{(0)}, (v_\lambda^{(0)} + iq_\lambda^{(0)})\right\}_+ D_\rho K \Big\} \\ &+c_3\mathcal{L}_3\end{aligned} \tag{6.50}$$

with $c_{12} = c_1 - c_2$ and where

$$K_{\mu\nu}^* = \mathcal{D}_\mu K_\nu^* - \mathcal{D}_\nu K_\mu^*, \tag{6.51}$$

$$q_{\mu\nu}^{(0)} = \partial_\mu q_\nu^{(0)} - \partial_\nu q_\mu^{(0)} - i[q_\mu^{(0)}, q_\nu^{(0)}]. \tag{6.52}$$

Here $v_\mu/a_\mu = \frac{1}{2}\left(\xi_L \partial_\mu \xi_L^\dagger \pm \xi_R \partial_\mu \xi_R^\dagger\right)$ and $q_\mu = \vec{\tau}\cdot\vec{\rho}_\mu + \omega_\mu$. The superscript (0) denotes the classical configuration. In this expression, we differentiate two kinds of covariant derivatives:

$$D_\mu = (\partial_\mu + v_\mu^{(0)}), \tag{6.53}$$

$$\mathcal{D}_\mu = (\partial_\mu - iq_\mu^{(0)}). \tag{6.54}$$

Recent developments in $\mathrm{HLS}_{K=1}$ and $\mathrm{HLS}_{K=\infty}$ indicate that the complete vector dominance in the anomalous Lagrangian implies the coefficients in (6.50) to be

$$c_1 - c_2 \approx c_3 \approx 1. \tag{6.55}$$

[11] For simplicity, we are dropping pion mass terms compared with the kaon mass.

These will be referred to as "vector-dominance anomaly coefficients." The hyperon spectrum studied in [Scoccola, Min, Nadeau and Rho 1989] and $S = +1$ baryon studied in [Park, Min and Rho 2004] were, instead, calculated with the anomaly coefficients

$$c_1 - c_2 = 2, \quad c_3 = 0. \tag{6.56}$$

We shall discuss the result of calculations with these coefficients.[12] For the hyperon spectrum with $S < 0$, this should not be serious since it is insensitive to the coefficients. However, it is highly probable that the $S > 0$ spectra be considerably modified from those given by (6.56). Therefore our discussion may only be qualitative, not quantitative. It serves to highlight the possible role that the vector mesons can play in the structure of the positive strangeness baryons. Just as in the nucleon structure, the effect could be qualitatively important.

The key point of the approach presented here is that the presence of K^* modifies especially the terms of first order in time derivative, which distinguishes $S = \pm 1$ fluctuations. It should be recalled that in the model with pseudoscalars only as in [Callan and Klebanov 1985], such a term arises uniquely from the "irreducible" Wess-Zumino term. We shall refer to the terms that distinguish $S = \pm 1$ fluctuations *other* than the irreducible WZ term as "WZ-like terms." We have many such WZ-like terms. They originate not only from the homogeneous Wess-Zumino term but also from the covariant derivatives with the static ω configuration as a gauge potential. The most striking result is that in addition to the irreducible WZ term, $+(iN_c/4f_\pi^2)B^{\mu(0)}((D_\mu^{(0)}K)^\dagger K - K^\dagger D_\mu^{(0)}K) \times \frac{2}{2}$, of the Callan-Klebanov Lagrangian, there are additional terms from the homogeneous part of the anomalous Lagrangian (6.50). However, this does not necessarily mean that the $S = +1$ fluctuation will now feel an attractive interaction with the skyrmion. One can easily check that when the vector mesons are integrated out, the additional terms are exactly canceled by (i) the term with the non-vanishing time component of $q_{\mu=0}^{(0)}$(=the classical ω configuration) in the third line of Eq. (6.47), with the $\omega_{(0)}$ replaced by its infinite mass limit $\omega_{(0)}^\infty$, and (ii) the eighth line in Eq. (6.47), with K_μ^*'s replaced by their infinite mass limit which can be read off from the fourth line as

$$K_\mu^{*\infty} = \frac{-1}{gf_\pi} a_\mu^{(0)} K. \tag{6.57}$$

This shows the consistency of the present formulation, even though the coefficients are not the best fit to nature.

Now the crucial point of this approach: With finite vector meson masses as required in $\mathrm{HLS}_{K=1}$ theory, the cancelation becomes imperfect. The deviation of $\omega_{(0)}$ from its infinite mass limit $\omega_{(0)}^\infty$ is such that $\langle \omega_{(0)}/\omega_{(0)}^\infty \rangle < 1$ independently of fluctuations in the strangeness direction. Thus the incomplete cancelation effectively reduces the net strength of the Wess-Zumino attraction in the $S = -1$

[12] Unfortunately no calculations were available at the time of writing of this volume for the "vector dominance coefficients" $c_1 - c_2 = c_3 = 1$.

channel, which was the motivation of introducing the vectors in [Scoccola, Min, Nadeau and Rho 1989] to solve the over-binding problem for the hyperons in the Callan-Klebanov model. What was not noticed in [Scoccola, Min, Nadeau and Rho 1989] was however, that the K^*_μ solution depends strongly on its strangeness. In the case of the $S = -1$ fluctuation, the closer it is to $K^{*\infty}_\mu$, the more exact the cancelation among the WZ-like terms becomes. Thus the net strength of the Wess-Zumino attraction becomes stronger approaching the irreducible strength. As for the $S = +1$ fluctuation, however, the opposite phenomenon takes place; the more K^*_μ deviates from its infinite mass limit, the less cancelation among the WZ-like terms occurs. The sum of the irreducible Wess-Zumino term and the WZ-like terms can then give an *attraction*, although the fourth term in the Lagrangian prevents K^*_μ from deviating too much from $K^{*\infty}_\mu$.

It is straightforward, though tedious, to solve the equations of motion for K and K^* moving in the background potentials provided by the static soliton configuration sitting at the origin. This was done in [Park, Min and Rho 2004].

Through the background potentials, K and K^* are strongly coupled. Since the soliton solution is invariant only under the simultaneous rotations in the spatial and isospin spaces, the eigenstates are classified by their "grand spin" quantum number λ associated with the operator $\mathbf{\Lambda} = \mathbf{L} + \mathbf{S} + \mathbf{I}$, where $\mathbf{L}$, $\mathbf{S}$ and $\mathbf{I}$ are the angular momentum, spin and isospin operators.

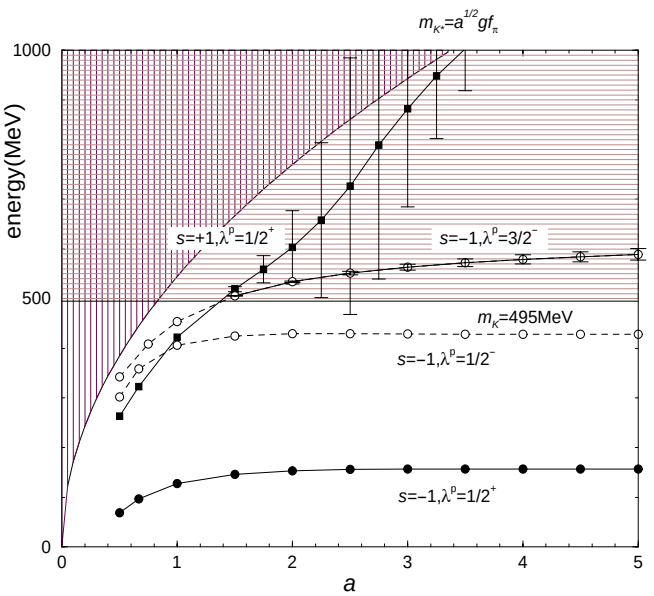

Fig. 6.1 The eigenenegies of $S = \pm 1$, $\lambda^P = \frac{1}{2}^{\pm}, \frac{3}{2}^{-}$ states obtained for various a values. The width of the resonance in the K^+-skyrmion channel is given by the error bar.

To have an idea, let us first take the *bare* Lagrangian obtained by Harada and Yamawaki [Harada and Yamawaki 2003] by matching the EFT correlators to the QCD ones at $\Lambda = 1.1$ GeV. This corresponds to taking large N_c limit. The resulting parameters obtained in [Harada and Yamawaki 2003] are: $F_\pi \approx 145$ MeV, $g \approx 3.69$ and $a \approx 4/3$. These parameters differ from the physical values by the loop corrections which are down by $1/N_c$. We expect the soliton mass to be too big compared with the physical mass of the nucleon without $\mathcal{O}(N_c^0)$ (*e.g.*, Casimir) corrections (which of course should be calculated), but what is relevant for us is the effective mass of K^+ in the background of the skyrmion. The calculation shows that the K^+ is bound classically as shown in Fig. 6.1. The binding energy turns out to be not appreciably big, around 3 MeV, but the sign of the mass shift is robust.

Since nature seems to indicate that a is close to 1,[13] it would be interesting to be able to "dial" a toward 1 and see how the system evolves. This operation is rather intricate and non-trivial, however, because of various "consistency conditions" associated with the VM as can be seen in [Harada and Yamawaki 2003]. For instance, much of the low-energy hadron dynamics can be understood with a set to its fixed-point value 1 while the other parameters of the Lagrangian, such as g and the parametric F_π, depart from their fixed point values. This comes about because there are subtle connections between various parameters controlled by the fact that the theory flows to the VM fixed point. Since what one is interested in is the qualitative question as to how the K^+-soliton system behaves in the presence of the vector mesons, particularly an infinite tower of them, we shall simply fix all the model parameters to the empirical values except for a which we vary: $N_c = 3$, $f_\pi = 93$ MeV, $m_\pi = 140$ MeV, $m_K = 495$ MeV and $g = 5.85$. Now in interpreting the results, one should keep in mind at least two constraints that one has at one's disposal. One is that the (leading N_c) *bare* Lagrangian of Harada and Yamawaki mentioned above does give a bound K^+-soliton system. The other is that at $a = 1$, chiral symmetry is realized with $F_\pi = F_\sigma$ where $\langle 0|A^\mu|\pi\rangle = ip^\mu F_\pi$ and $\langle 0|V^\mu|\sigma\rangle = ip^\mu F_\sigma$. We will return to this matter in Chapter 10 where it will be interpreted as an emergence of Georgi's vector symmetry.

We then come to the question as to what the physical meaning of a going near 1 is. In $\mathrm{HLS}_{K=1}$ theory, it means the vector dominance is violated and there is a contact coupling for the photon to, say, the pion. This is at odds in free space with what is known experimentally. However, in heat bath, as mentioned, the constant a is driven to 1 at the VM fixed point. As mentioned, in $\mathrm{HLS}_{K=1}$ theory, the vector dominance is violated in the nucleon EM form factor even in free space. We will see later that with an infinite tower, the size of the nucleon becomes tiny, much smaller than the Compton wavelength, and the form factor is given by the vector dominance with an infinite tower. This means that the pion form factor in heat bath and the nucleon form factor in free space must be getting contributions from the higher-lying members of the tower. This also means that the fact that baryonic

[13] As in the chiral doubler structure, the π^+-π^0 mass difference, the nucleon form factor *etc.*

environment entails a going to 1 implies that baryonic structure in terms of the skyrmion picture requires higher-lying vector mesons, possibly the infinite tower.

The solutions for the K^+-soliton system we have so obtained are summarized in Fig. 6.1. Plotted there are the eigenenergies vs. a of the bound states or the resonance states found in $S = \pm 1$, $\lambda^P = \frac{1}{2}^{\pm}, \frac{3}{2}^-$ channels. The widths of the resonance states in the kaon-soliton channel are indicated by error bars, which, however, may not be interpreted in the present form as the physical width of the Θ^+. To be realistic, the system should be (collective) quantized for such an interpretation. It is remarkable in Fig. 6.1 that the $S = -1$ states depend little on a for the relevant range $a \geq 1$ (or as long as the corresponding mass parameter m_{K^*} is larger than m_K). This means that the structure of the $S < 0$ states, well described with [Scoccola, Min, Nadeau and Rho 1989] or without [Callan and Klebanov 1985] vector mesons, will not be affected by the change in a. There are two bound states stable against the change of a which correspond, when quantized, to the normal $S = -1, -2$ hyperons with positive parity or $\Lambda(1405)$ with negative parity and one bound state or narrow-width resonance corresponding to $\Lambda(1520)$ with negative parity. On the other hand, the $S = +1$ state is *extremely* sensitive to the value of a. What this shows clearly is that a full account of the infinite tower of the vector mesons or in $\mathrm{HLS}_{K=1}$ a proper treatment of the a parameter would be – once again – needed to be able to make a reliable prediction on $S > 0$ exotic baryons.

6.3.5.2 *Deeply bound K^- in nuclei*

An interesting application of the kaon-soliton bound state approach is to study strongly interacting systems at high density. For instance, one can explore strongly bound K^-N^n systems with $n = 2, 3, \cdots, \infty$. There the principal mechanism will be the Wess-Zumino and Wess-Zumino like terms. This matter will be discussed in Chapter 9 both for deeply bound nuclei such as strange nuggets called "$KaoN$" and kaon condensation in compact star matter. The idea will be to embed one or more K^-'s in the dense skyrmion background that is described in the next section. In all cases, hidden gauge symmetry with the VM (vector manifestation) fixed point will figure importantly.

6.4 Dense Skyrmion Matter and Chiral Transition

We now extend the Skyrme model to dense matter, going beyond normal nuclear matter to the density at which chiral symmetry is restored. This is a topic that will eventually be relevant to the structure of compact stars described in Chapter 11. To do this we shall take the Skyrme model implemented with the dilaton field χ to take into account the trace anomaly of QCD [Brown and Rho 1991]. A detailed treatment is given in [Lee, Park, Rho and Vento 2003] which we will follow closely here. In accounting for the trace anomaly of QCD in the skyrmion description,

it is a reasonable approximation to assume that the gluon degree of freedom that enters into hadron dynamics – hence in terms of hadronic variables – comprises of two components, "soft glue" and "hard glue" (sometimes called "epoxy"). This separation plays a crucial role in understanding heavy-ion dynamics as discussed in Chapter 7.[14] As discussed there, the trace anomaly is given by both the soft glue and the hard glue,

$$\theta^\mu_\mu = \sum_q m_q \bar{q}q - \frac{\beta(g)}{g}\left[(\mathrm{Tr}G_{\mu\nu}G^{\mu\nu})_{\mathrm{soft}} + (\mathrm{Tr}G_{\mu\nu}G^{\mu\nu})_{\mathrm{hard}}\right] \tag{6.58}$$

where $\beta(g)$ is the beta function of QCD. Now as the system reaches the critical point at which chiral restoration takes place, as for instance at the critical temperature T_c, the soft glue "melts," whereas the hard glue is, in the first approximation, unaffected in the vicinity of the critical point, disappearing only at high temperature or high density. The soft glue is therefore the component which is supposed to be tied directly to chiral symmetry, that is, the quark condensate, so melting soft glue will be the same as melting the quark condensate. The condensation of the soft glue is then to represent a *spontaneous* breaking of scale invariance, whereas the condensation of the hard glue is to represent the *explicit* breaking of scale invariance. In this discussion, we never deal with the hard (epoxy) component. As long as the explicit breaking of the scale invariance is present, there remains dimensional transmutation in QCD.

Now the rationale for the role of the dilaton field that interpolates the soft glue is that the mean field of the scalar field which should depend on the background of the medium, namely, density and/or temperature, plays the role of the "intrinsic background dependence (IBD)" of hidden local symmetry theory of Harada and Yamawaki [Harada and Yamawaki 2003] which is required by the Wilsonian matching to QCD *in medium*. This aspect played a crucial role in the original formulation of Brown-Rho scaling but remained largely unrecognized in the community. It should be admitted that there is no rigorous derivation starting from QCD of the above statement.

Although quantitative aspect of the dynamics would require the full panoply of vector mesons considered above, the essential idea is captured in the simple model Lagrangian of the following form that includes the pion mass term [Ellis and Lanik 1985; Brown and Rho 1991]

$$\begin{aligned}\mathcal{L} = &\frac{f_\pi^2}{4}\left(\frac{\chi}{f_\chi}\right)^2 \mathrm{Tr}(\partial_\mu U^\dagger \partial^\mu U) + \frac{1}{32e^2}\mathrm{Tr}([U^\dagger\partial_\mu U, U^\dagger \partial_\nu U])^2 + \frac{f_\pi^2 m_\pi^2}{4}\left(\frac{\chi}{f_\chi}\right)^3 \\ &\times \mathrm{Tr}(U + U^\dagger - 2) + \frac{1}{2}\partial_\mu\chi\partial^\mu\chi - V(\chi)\,.\end{aligned} \tag{6.59}$$

[14] This separation will be explained more precisely in Chapter 7 using a lattice result measured in temperature. It will also figure particularly importantly in Brown-Rho scaling described in Chapter 8.

Table 6.1 Parameter sets for the dilaton χ.

	m_χ	f_χ	G_0
set A	550 MeV	240 MeV	0.004 GeV^4
set B	720 MeV	240 MeV	0.007 GeV^4
set C	1000 MeV	240 MeV	0.012 GeV^4

We have denoted the vacuum expectation value of the dilaton field χ as f_χ, a constant which describes the spontaneous breaking of scale invariance *in the presence of* an explicit breaking. The spontaneous breaking of the scale symmetry can be reproduced by the potential $V(\chi)$ for the scalar field – the last term of Eq. (6.59) – which is adjusted in the Lagrangian (6.59) so that $V' = dV/d\chi = 0$ and $d^2V/d\chi^2 = m_\chi^2$ at $\chi = f_\chi$. The explicit breaking of scale symmetry associated with the hard glue, not directly linked to explicit chiral symmetry breaking, is not written down in (6.59).[15]

The vacuum state of the Lagrangian at zero baryon number density is defined by $U = 1$ and $\chi = f_\chi$. We will take the latter to be positive, and therefore the field values around the vacuum will be positive. The fluctuations of the pion and the scalar (dilaton) fields about this vacuum, defined through

$$U = \exp(i\vec{\tau}\cdot\vec{\phi}/f_\pi), \quad \text{and} \quad \chi = f_\chi + \tilde{\chi}, \tag{6.60}$$

give physical meaning to the model parameters: f_π as the pion decay constant, m_π as the pion mass, f_χ as the scalar decay constant, and m_χ as the scalar mass. For the pions, we shall use their empirical values (in free space) as $f_\pi = 93$ MeV and $m_\pi = 140$ MeV. We fix the Skyrme parameter e to 4.75 from the axial-vector coupling constant g_A as in [Jackson and Rho 1983; Nowak, Rho and Zahed 1996]. However, there is little information from experiments on the scalar field χ. We shall therefore take three exemplary cases given in Table 6.1 to see qualitative aspects of the problem. The sets A and B are reasonable values that bracket what nature represents, but the set C is most likely to be unrealistically high for the scalar we are dealing with. We take it as an illustrative case.

There are two points to be stressed here. The first is the quantities given above are the free-pace values, not fit values as found in the literature (*e.g.*, [Adkins, Nappi and Witten 1983]). The second point useful for later is that they are not to be scaling *in medium* as the intrinsic-background-dependent parameters of HLS/VM do. The scaling is to be encoded in the mean field of the χ field as originally proposed in [Brown and Rho 1991].

[15] We are tacitly assuming that the mixing of the "soft" and "hard" glues can be ignored, which means ignoring the possible mixing of quarkonium configurations with the gluonium.

6.4.1 *Single skyrmion*

In order to define our notations, let us first describe the single skyrmion[16] with the Lagrangian (6.59). $B = 1$ skyrmion was discussed above, so this part is somewhat redundant, but the context in which it figures here in the presence of the scalar χ field will be different.

The soliton solution with the baryon number $B = 1$ can be found by generalizing the spherical hedgehog ansatz of the original Skyrme model as

$$U_0(\vec{r}) = \exp(i\vec{\tau}\cdot\hat{r}F(r)), \text{ and } \chi_0(\vec{r}) = f_\chi C(r), \tag{6.61}$$

with two radial functions $F(r)$ and $C(r)$. The mass of the single soliton is given by

$$M_{B=1} = 4\pi\int_0^\infty r^2 dr \ \left[\frac{f_\pi^2}{2}C^2\left(F'^2 + 2\frac{\sin^2 F}{x^2}\right) + \frac{1}{2e^2}\frac{\sin^2 F}{x^2}\left(\frac{\sin^2 F}{x^2} + 2F'^2\right)\right.$$
$$\left. + f_\pi^2 m_\pi^2 C^3(1-\cos F) + \frac{{f_\chi}^2}{2}\left(C'^2 + \frac{m_\chi^2}{2}\{(C^4\ln C - \tfrac{1}{4}) + \tfrac{1}{4}\}\right)\right]. \tag{6.62}$$

where the prime stands for derivative with respect to r, and an explicit form of the dilaton potential is used. Variations of $M_{B=1}$ with respect to $F(r)$ and $C(r)$ lead to the equations of motion

$$\left(f_\pi^2 r^2 C^2 + \frac{2\sin^2 F}{e^2}\right)F''(r) + 2f_\pi^2(\ rC^2 + r^2 CC'\ )F'(r) - \frac{2\sin F\cdot\cos F}{e^2}F'^2(r)$$
$$-2f_\pi^2 C^2\sin F\cdot\cos F - \frac{2\sin^3 F\cdot\cos F}{e^2 r^2} - f_\pi^2 m_\pi^2 C^3 r^2\sin F = 0, \tag{6.63}$$

for $F(r)$ and

$$f_\chi^2 C''(r) + \frac{2f_\chi^2}{r}C'(r) - f_\pi^2 C(r)\left(F'^2(r) + \frac{2\sin^2 F}{r^2}\right) - 3f_\pi^2 m_\pi^2(1-\cos F)C^2(r)$$
$$+ f_\chi^2 m_\chi^2 C^3(r)\ln C(r) = 0, \tag{6.64}$$

for $C(r)$.

At infinity, the fields $U_0(\vec{r})$ and $\chi_0(\vec{r})$ should reach their vacuum values. The asymptotic behavior of the equations of motion reveals that the radial functions reach the corresponding vacuum values as

$$F(x) \sim \frac{e^{-m_\pi r}}{r}, \quad \text{and} \quad C(x) \sim 1 - \frac{e^{-m_\chi r}}{r}. \tag{6.65}$$

In order for the solution to carry a baryon number, U_0 has the value -1 at the origin, while there is no such topological constraint for $C(x = 0)$. All that is required is that it be a positive number below 1. The equations of motion tell us that for small x,

[16] Skyrmion in this subsection represents the soliton of the Skyrme Lagrangian.

$$F(x) \sim \pi - \alpha x + \gamma x^3 + O(x^5),$$
$$C(x) \sim C_0 + \beta x^2 + O(x^4). \tag{6.66}$$

The coupled equations of motion for $F(x)$ and $C(x)$ together with the boundary conditions (6.65) and (6.66) can be solved in various different ways. Shown in Fig. 6.2 are the profile functions $F(x)$ and $C(x)$ as a function of $x(= ef_\pi r)$. $F(r)$. Note that the resulting root mean-square-radius of the baryon charge

$$\langle r^2 \rangle^{1/2} = \left(\int d^3 r r^2 B^0(\vec{r}) \right)^{1/2} \tag{6.67}$$

shows little dependence on m_χ. On the other hand, the changes in $C(r)$ and the soliton mass are appreciable. As is obvious, the larger the scalar mass is, the smaller its coupling to the pionic field and the less its effect on the single skyrmion. In the limit of $m_\chi \to \infty$, the scalar field is completely decoupled from the pions and the model returns back to the original Skyrme model, where $C(r) = 1$, $M_{sol} = 1479$ MeV [17] and $\langle r^2 \rangle^{1/2} = 0.43$ fm. As for the soliton mass, note that M_{sol} scales approximately as (f_π/e) and the f_π^2 in the current algebra term of the Lagrangian is multiplied by $C^2(r)$. Thus, $C(r) \leq 1$ reduces the *effective* f_π inside the single skyrmion, so that the soliton mass decreases accordingly. For example, for the parameter set $m_\chi \approx 550$ MeV, $f_\chi \approx 240$ MeV and $G_0 \approx 0.004$ GeV (a typical set of values), the soliton mass gets 7% reduction and we expect that the effective f_π is reduced by the same amount in average in the region where the single skyrmion is located.

6.4.2 *Skyrmion crystal*

We now apply (6.59) to a skyrmion description of infinite matter, that is, a system of baryon number $B = \infty$. The discussion will be somewhat detailed, for we believe that with a better understanding of the role the infinite tower of vector mesons and hidden local symmetry (with a possible intervention of the dilaton field) play in baryon structure, a reliable and workable scheme could be developed along the line presented here for treating dense medium that defies direct approach from QCD proper.

For gaining a qualitative idea as to what happens to nuclear matter when squeezed to a high density, following [Lee, Park, Rho and Vento 2003], we take the crystal configuration made up of skyrmions, where each face-centered cubic (FCC) lattice site is occupied by a single skyrmion center with $U_0 = -1$ and each nearest neighboring pair is relatively rotated in isospin space by π with respect to

[17] With the parameters used in our discussion, the soliton mass is quite large compared with the physical nucleon mass. However, as discussed in [Nowak, Rho and Zahed 1996; Rho 1994] – and mentioned above, this should not upset the readers since there is ~ -0.5 GeV Casimir energy that has to be taken into account.

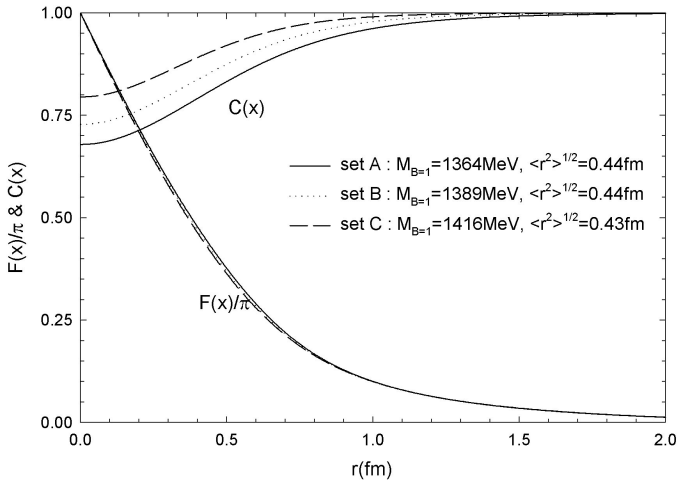

Fig. 6.2 Profile functions $F(x)$ and $C(x)$ as a function of x.

the line joining them.[18] At low density, the system maintains the original configuration, *i.e.* it appears as an FCC crystal with the dense centers of single skyrmions on each lattice sites. At high density, however, the system undergoes a phase transition to a body-centered cubic (BCC) crystal made up of half-skyrmions which possess a different topology from that of skyrmions [Goldhaber and Manton 1987; Kugler and Shtrikman 1989; Castillejo, Jones, Jackson and Verbaarschot 1989]. (This is described in detail, *e.g.*, in [Lee, Park, Min, Rho and Vento 2003]). Here, only half of the baryon number carried by the single skyrmion is concentrated at the original FCC sites, while the other half is concentrated at the center of the links connecting these points. This feature is illustrated in Fig. 6.3. We clarify the role of half-skyrmions in detail below and will be taken up in a different context in Chapter 10.

Let us denote the field configuration for the skyrmion field by $U_0(\vec{x}) = \sigma + i\vec{\tau}\cdot\vec{\pi}$ (with $\sigma^2 + \pi^2 = 1$) and $\chi_0(\vec{x})$ for the scalar field. The FCC configuration we are considering has the symmetries listed in Table 6.2. There, $2L$ is the size of the single FCC unit cell that contains 4 skyrmions. Thus the baryon number density is $\rho = 1/2L^3$. Normal nuclear matter density occurs at $\rho_0 = 0.17/\text{fm}^3$which corresponds to $L \sim 1.43$ fm. Note that the chiral σ field [19] (with $\sigma \propto \bar{q}q$) has exactly the same symmetries as those of the χ.

[18]The nuclear matter that we know of is of course not in a crystalline form but rather in a liquid form. It may be that small perturbation "will" melt the crystalline structure. However, as we will argue, the description of chiral phase transition based on the *change of topology* exploited here could be robust.

[19]This σ figuring in linear sigma model should not be confused with the longitudinal component of the ρ meson in HLS theory.

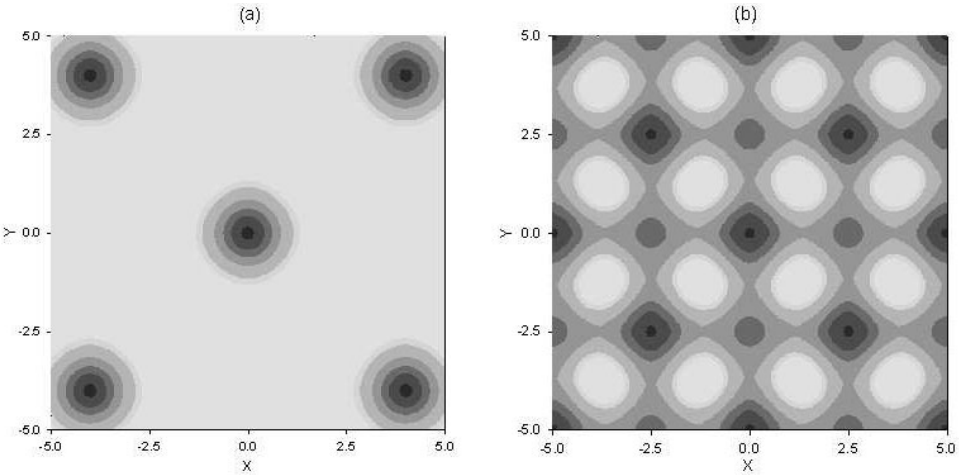

Fig. 6.3 The baryon number density of (a) the FCC Skyrme crystal at a density $n < n_c$ and (b) the half-skyrmion simple cubic crystal (CC) or BCC at a density $n \geq n_c$ where n_c is some critical density at which the two phases delineate.

Table 6.2 Symmetries of the FCC skyrmion crystal

symmetry	space	U_0	χ
reflection	$\vec{x} \to (-x, y, z)$	$U_0 \to (\sigma, -\pi_1, \pi_2, \pi_3)$	$\chi_0 \to \chi_0$
3-fold axis rotation	$\vec{x} \to (y, z, x)$	$U_0 \to (\sigma, \pi_2, \pi_3, \pi_1)$	$\chi_0 \to \chi_0$
4-fold axis rotation	$\vec{x} \to (x, z, -y)$	$U_0 \to (\sigma, \pi_1, \pi_3, -\pi_2)$	$\chi_0 \to \chi_0$
translation	$\vec{x} \to (x + L, y + L, z)$	$U_0 \to (\sigma, -\pi_1, -\pi_2, \pi_3)$	$\chi_0 \to \chi_0$

The field configurations obeying the above symmetries can be easily found by expanding the fields in terms of Fourier series as [Kugler and Shtrikman 1989]

$$\bar{\sigma}(\vec{x}) = \sum_{a,b,c} \beta_{abc} \cos(a\pi x/L) \cos(b\pi y/L) \cos(c\pi z/L), \tag{6.68}$$

and

$$\bar{\pi}_1(\vec{x}) = \sum_{h,k,l} \alpha_{hkl} \sin(h\pi x/L) \cos(k\pi y/L) \cos(l\pi z/L), \tag{6.69}$$

$$\bar{\pi}_2(\vec{x}) = \sum_{h,k,l} \alpha_{hkl} \cos(l\pi x/L) \sin(h\pi y/L) \cos(k\pi z/L), \tag{6.70}$$

$$\bar{\pi}_3(\vec{x}) = \sum_{h,k,l} \alpha_{hkl} \cos(k\pi x/L) \cos(l\pi y/L) \sin(h\pi z/L), \tag{6.71}$$

and finally

$$\chi_0(\vec{x}) = \sum_{a,b,c} \gamma_{abc} \cos(a\pi x/L) \cos(b\pi y/L) \cos(c\pi z/L). \tag{6.72}$$

The symmetries of Table 6.2 restrict the modes appearing in Eqs. (6.68) to (6.72) as follows;

(M1) if h is even, then k, l are restricted to odd numbers and a, b, c are to even numbers,
(M2) if h is odd, then k, l are restricted to even numbers and a, b, c are to odd numbers.

Furthermore, $\alpha_{hkl} = \alpha_{hlk}$ and $\beta_{abc} = \beta_{bca} = \beta_{cab} = \beta_{acb} = \beta_{cba} = \beta_{bac}$.

We can locate, without loss of generality, the centers of the skyrmions at the corners of the cube and at the centers of the faces by letting $\sigma = -1$ and $\pi_i (i = 1, 2, 3) = 0$ at those points. For the skyrmion field to have a definite integer baryon number per site, we should have $\sigma = +1$ and $\pi_i (i = 1, 2, 3) = 0$ at points such as $(L, 0, 0)$. This produces the constraint,

$$\sum_{a,b,c=\text{even}} \bar{\beta}_{abc} = 0 \ . \tag{6.73}$$

As for γ_{abc} associated with the scalar field, there is no such constraint, but the coefficients should be arranged to satisfy $\chi_0 \geq 0$, a consequence of our choice of vacuum.

If we had only the modes (M2) in the expansion, the configuration would then have an additional symmetry, namely, under the translation $\vec{x} \to (x + L, y, z)$ the field undergoes an $O(4)$ rotation by π in the σ, π_1 plane. Furthermore, in order to satisfy the constraint $\chi \geq 0$, χ must vanish identically. This configuration corresponds to the *half-skyrmion* CC mentioned above. Because of this additional symmetry, physical quantities such as the local baryon number density and the local energy density become completely identical around the points with $\sigma = -1$ and the points with $\sigma = +1$. Thus, one half of the baryon number carried by a single skyrmion is concentrated at the sites where the centers of the single skyrmion are expected to be in the FCC crystal. The other half of the baryon number is now concentrated on the links connecting those points, where the σ takes the value $+1$ and, in the original FCC configuration, the local baryon number density is rather low. As a consequence, the expectation value $\langle\sigma\rangle$ goes to zero, signaling the restoration of the spontaneously broken chiral symmetry. Both modes, (M1) and (M2), are included in the actual numerical procedure described next. The half-skyrmion crystal

configuration arises at high density where the expansion coefficients associated with the modes (M1) become small.

It should be stressed in anticipation of what we will describe below that the skyrmion-half-skyrmion transition could very well be free from possible lattice artifacts. This is because they are topological objects and topological objects, as long as they escape from the Derrick-Hobart collapse, are stable.

In order to obtain the coefficients, it suffices to minimize the energy per baryon E/B given by

$$\begin{aligned} E/B &= -\frac{1}{4}\int_{Box} d^3r \mathcal{L}_{\rm M}(U_0,\chi_0) \\ &= \frac{1}{4}\int_{Box} d^3x \left\{ \frac{f_\pi^2}{4}\left(\frac{\chi_0}{f_\chi}\right)^2 {\rm Tr}(\partial_i U_0^\dagger \partial_i U_0) + \frac{1}{32e^2}{\rm Tr}\left[U_0^\dagger\partial_i U_0, U_0^\dagger \partial_j U_0\right]^2 \right. \\ &\quad \left. + \frac{f_\pi^2 m_\pi^2}{4}\left(\frac{\chi_0}{f_\chi}\right)^3 {\rm Tr}(2 - U_0^\dagger - U_0) + \frac{1}{2}\partial_i\chi_0\partial_i\chi_0 + V(\chi_0)\right\} \end{aligned} \tag{6.74}$$

by taking the coefficients of the expansion as variational parameters. In Eq. (6.74), the subscript 'box' denotes that the integration is over a single FCC box and the factor 1/4 in front appears because the box contains baryon number four.

We can gain a simple idea of what's going on by taking χ_0 to be a constant:

$$\chi_0/f_\chi = X. \tag{6.75}$$

Then Eq. (6.74) can be approximately written as

$$E/B(X,L) = X^2(E_2/B) + (E_4/B) + X^3(E_m/B) + (2L^3)V(X) \tag{6.76}$$

where E_2, E_4 and E_m are, respectively, the contributions from the current algebra term, the Skyrme term and the pion mass term of the Lagrangian and $(2L^3)$ is the volume occupied by a single skyrmion. It can be understood as an effective potential for the chiral field *in medium*, modified by the coupling of the scalar to the background matter. With the parameter values used in [Lee, Park, Min, Rho and Vento 2003], say, for the Skyrme model without the scalar fields, the effective potentials $E/B(X)$ behave as shown in Fig. 6.4. At low density (larger L), the minimum of the effective potential is located slightly away from $X = 1$. As the density increases, the effective potential $V(\chi)$ develops another minimum at $X = 0$ which was an unstable extremum of the potential in free space. At $L \sim 1$ fm, the newly developed minimum can compete with the one near $X \sim 1$. At higher density, the minimum gets shifted to $X = 0$ where the system gets stabilized.

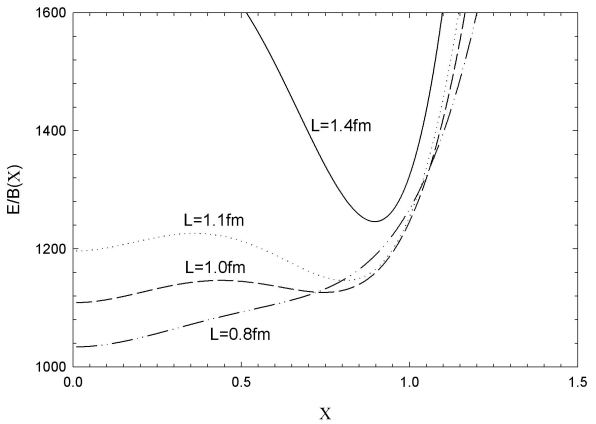

Fig. 6.4 Energy per single skyrmion as a function of the scalar field X for a given L. The results are obtained with the (E_2/B), (E_4/B), and (E_m/B) of [Lee *et al* 2003] and with the parameter sets B of Table 6.1.

In Fig. 6.5 is plotted $E/B(X_{min}, L)$ as a function of L. The figure in a small box is the corresponding value of X_{min} as function of L. There we see an explicit manifestation of a first-order phase transition. Although the discussion is perhaps a bit too naive, it essentially encodes the same physics as in the more rigorous treatment of χ_0 given below.

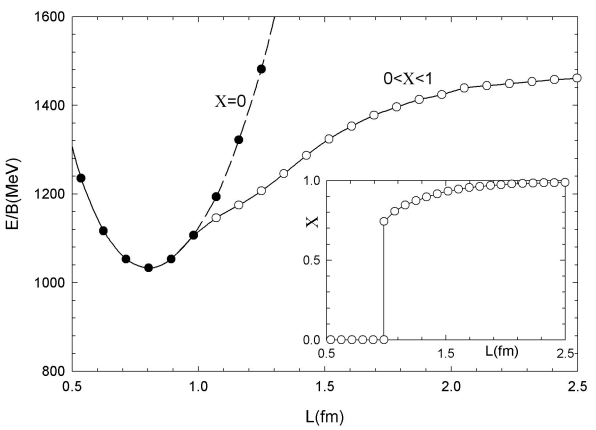

Fig. 6.5 Energy per single skyrmion as a function of L. The results are obtained by minimizing $E/B(X, L)$ with respect to X for a given L.

Given in Fig. 6.6 is the energy per baryon, E/B, as a function of the FCC box size parameter L. Each point corresponds to the lowest energy crystal configuration for the given value of L. The solid circles, solid squares and solid triangles are obtained with the parameter sets A, B, and C of Table 6.1, respectively. Furthermore, the black solid lines correspond to the single skyrmion FCC phase, while the gray lines to the half-skyrmion BCC phase. As we squeeze the system from $L = 6$ fm on, the skyrmion system undergoes at $L = L_{pt}$ a phase transition from the FCC single skyrmion configuration to the simple cubic crystal (CC) (or BCC) half-skyrmion configuration. The transition appears to be first order. In this toy model, $\chi_0(\vec{r})$ vanishes in the half-skyrmion phase.[20] The energy of the system comes only from the Skyrme term and the scalar field potential. The former roughly scales as $\sim 1/L$ and the latter exactly as L^3 (the volume of the box); explicitly,

$$E/B \sim a/L + 2V(\chi_0 = 0)L^3, \tag{6.77}$$

with a a constant.

Unsurprisingly, the implementation of the scalar field in the Skyrme model Lagrangian produces quite dramatic effects on the properties of the skyrmion matter. For example, the energy per baryon drops down to ~ 700 MeV. This can be understood since the potential energy between the skyrmions amounts to nearly 50% of the skyrmion mass and comes from the medium-range attraction generated by the scalar field.

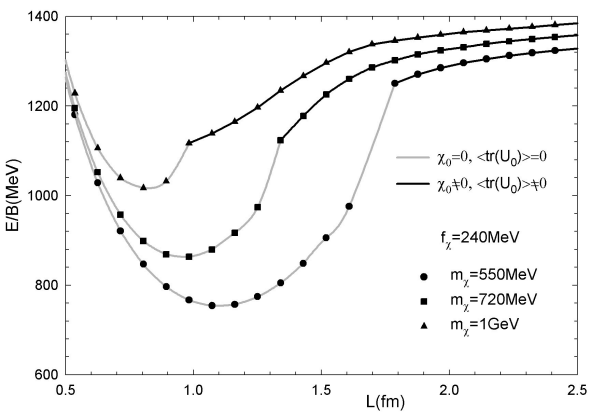

Fig. 6.6 Energy per single skyrmion as a function of the size parameter L. The solid circles, solid squares, solid triangles are the results obtained with the parameter sets A, B, and C, respectively.

[20] Below, we will see that more realistically, there is a region in the half-skyrmion phase in which $\chi_0(\vec{r})$ remains non-vanishing though chiral symmetry is restored.

In Fig. 6.7, $\langle\sigma\rangle$ and $\langle\chi_0/f_\chi\rangle$ – the averaged values of $\sigma(\vec{r})$ and $\chi_0(\vec{r})$ over space – are shown as a function of L. Here we denote by $\langle Q\rangle$ the average value of a quantity $Q(\vec{r})$ over the FCC box,

$$\langle Q\rangle = \frac{1}{8L^3}\int_{Box} d^3rQ(\vec{r}). \tag{6.78}$$

We observe that both quantities go to zero at the *same* phase transition point $L = L_{pt}$. However, for larger values of m_χ, the transition properties of the two quantities are different. Note that while $\sigma(\vec{r}) \neq 0$ locally and $\langle\sigma\rangle = 0$ is obtained by the averaging process, $\langle\chi_0/f_\chi\rangle = 0$ results because $\chi_0(\vec{r}) = 0$ throughout the whole space. We will take $\langle\chi_0\rangle$ as the *effective* value of f_χ, *i.e.* f_χ^*. We identify this as the vanishing of the "soft" part of the gluon condensate locked to the quark condensate that reflects chiral symmetry.

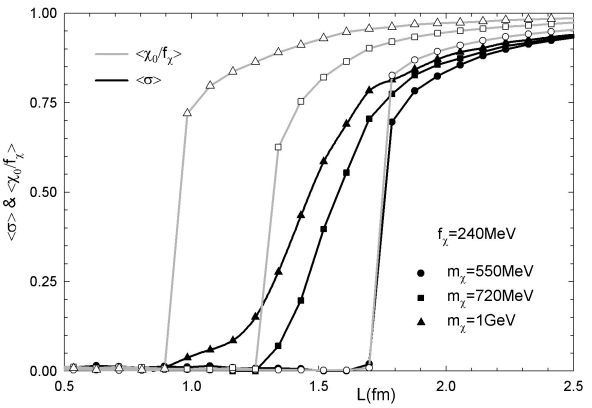

Fig. 6.7 $\langle\sigma\rangle$ and $\frac{\chi_0}{f_\chi}$ as a function of the size parameter L.

6.4.3 *Fluctuations on top of the skyrmion background and Brown-Rho scaling*

Given the structure of the medium defined in terms of skyrmions, we can now provide a natural description of mesonic fluctuations on top of this background. For this, the quantities of interest are scalar and pseudoscalar excitations. For this purpose, we take the ansatz

$$U(x) = \sqrt{U_\pi(x)}U_0(\vec{x})\sqrt{U_\pi(x)}, \qquad \chi(x) = \chi_0(\vec{x}) + \tilde{\chi}(x), \tag{6.79}$$

where $U_\pi = \exp(i\vec{\tau}\cdot\vec{\phi}/f_\pi)$. Expanding the Lagrangian (6.59) up to the second order in the fluctuating fields, we obtain [21]

$$\mathcal{L}(U,\chi) = \mathcal{L}_{\rm M}(U_0,\chi_0) + \mathcal{L}_{{\rm M},\chi} + \mathcal{L}_{{\rm M},\phi} + \mathcal{L}_{{\rm M},\phi\chi}, \tag{6.80}$$

where the subscript 'M' denotes the matter field, $\mathcal{L}_{\rm M}$ the Lagrangian density for the static configuration for the background matter and the various terms are given by

$$\mathcal{L}_{{\rm M},\phi} = \frac{1}{2}G_{ab}\dot{\phi}_a\dot{\phi}_b - \frac{1}{2}H^{ij}_{ab}(\vec{x})\partial_i\phi_a\partial_j\phi_b - \frac{1}{2}\left(\frac{\chi_0}{f_\chi}\right)^3 m_\pi^2\sigma(\vec{x})\phi_a^2 + \frac{1}{2f_\pi^2}\epsilon_{abc}\partial_\mu\phi_a\phi_b V_c^\mu(\vec{x}) \tag{6.81}$$

$$\mathcal{L}_{{\rm M},\chi} = \frac{1}{2}\partial_\mu\chi\partial^\mu\chi - \frac{1}{2}\left[m_\chi^2\left(\frac{\chi_0}{f_\chi}\right)^2\left(1+3\ln(\chi_0/f_\chi)\right) + \frac{2}{f_\chi^2}\frac{f_\pi^2}{4}{\rm Tr}(\partial_i U_0^\dagger\partial_i U_0) + \frac{6\chi_0}{f_\chi^3}f_\pi^2 m_\pi^2(1-\sigma(\vec{x}))\right]\chi^2 \tag{6.82}$$

$$\mathcal{L}_{{\rm M},\chi\phi} = \left(\frac{2\chi_0}{f_\chi^2}\frac{f_\pi}{4}{\rm Tr}(i(L_i-R_i)\tau^a)\right)\chi\partial^i\phi_a + \left(\frac{3\chi_0^2}{f_\chi^3}\frac{f_\pi m_\pi^2}{2}{\rm Tr}(i\tau_a U_0)\right)\chi\phi^a. \tag{6.83}$$

Here,

$$G_{ab}(\vec{x}) = \left(\frac{\chi_0}{f_\chi}\right)^2(\delta_{ab}+g_{ab}(\vec{x})) + \frac{1}{32e^2f_\pi^2}{\rm Tr}([R_i,\tilde{\tau}^a][R_i,\tilde{\tau}^b]), \tag{6.84}$$

$$H^{ab}_{ij}(\vec{x}) = G^{ab}\delta_{ij} + \frac{1}{32e^2f_\pi^2}{\rm Tr}\Big([R_i,R_j][\tilde{\tau}^a,\tilde{\tau}^b] - [R_i,\tilde{\tau}^b][R_j,\tilde{\tau}^a]\Big), \tag{6.85}$$

$$V_i^a(\vec{x}) = \left(\frac{\chi_0}{f_\chi}\right)^2\frac{i}{4}f_\pi^2{\rm Tr}[(L_i+R_i)\tau^a] + \frac{i}{16e^2}{\rm Tr}\Big([L_j,\tau^a][L_i,L_j] + [R_j,\tau^a][R_i,R_j]\Big), \tag{6.86}$$

where

$$g_{ab}(\vec{x}) = \tfrac{1}{4}{\rm Tr}(\tau_a U_0\tau_b U_0^\dagger - \tau_a\tau_b) = -(\pi^2\delta_{ab} - \pi_a\pi_b) \tag{6.87}$$

which comes from the current algebra term in the Lagrangian. Here L_i and R_i are defined by $L_i = (\partial_i U_0^\dagger)U_0$ and $R_i = (\partial_i U_0)U_0^\dagger$, respectively, in terms of the background matter fields.

One can see from these equations how the medium, represented by the background skyrmion field, influences the elementary excitations. In order to get an idea of the expected results, we show the tree level approximation where we have substituted the background field by its space average over the cell. In this way, we

[21] We shall drop the tilde on the fluctuating χ field since it is obvious.

obtain closed form expressions for the *in-medium parameters* showing their relation to their vacuum values.

Due to the symmetry of the background field, $\langle \mathrm{Tr}(i\tau_a U_0)\rangle$ vanishes in the averaging procedure and therefore there are no terms with $\chi\phi_a$ in $\mathcal{L}_{M,\chi\phi}$ to this order. The relevant terms arise from $\mathcal{L}_{M,\phi}$ and $\mathcal{L}_{M,\chi}$ and can be written as

$$\mathcal{L}_{M,\phi} = \frac{Z_\pi^2}{2}\dot{\phi}_a\dot{\phi}_a - \frac{m_\pi^{*2}Z_\pi^2}{2}\phi_a^2\cdots, \tag{6.88}$$

$$\mathcal{L}_{M,\chi} = \frac{1}{2}\dot{\chi}\dot{\chi} - \frac{m_\chi^{*2}}{2}\chi^2\cdots. \tag{6.89}$$

where the pion wave function renormalization constant Z_π, the in-medium pion mass m_π^* and scalar mass m_χ^* are defined as

$$Z_\pi^2 = \left\langle \left(\frac{\chi_0(\vec{x})}{f_\chi}\right)^2 (1 - \tfrac{2}{3}\pi^2(\vec{x}))\right\rangle \equiv \left(\frac{f_\pi^*}{f_\pi}\right)^2, \tag{6.90}$$

$$m_\pi^{*2}Z_\pi^2 = \left\langle \left(\frac{\chi_0(\vec{x})}{f_\chi}\right)^3 \sigma(\vec{x})\ m_\pi^2\right\rangle, \tag{6.91}$$

$$m_\chi^{*2} = \left\langle m_\chi^2\left(\frac{\chi_0(\vec{x})}{f_\chi}\right)^2\left(1 + 3\ln(\chi_0(\vec{x})/f_\chi)\right) + \frac{2}{f_\chi^2}\frac{f_\pi^2}{4}\mathrm{Tr}(\partial_i U_0^\dagger \partial_i U_0) + \frac{6\chi_0}{f_\chi^3}f_\pi^2 m_\pi^2(1-\sigma))\right\rangle. \tag{6.92}$$

The wave function renormalization constant Z_π gives the ratio of the in-medium pion decay constant f_π^* to the free one, and the above expression arises from the current algebra term with f_π in the Lagrangian. The other two equations reflect how the medium affects the effective masses of the mesons.

We show in Fig. 6.8 the ratios of the in-medium parameters relative to their free-space values. Only the results obtained with the parameter set B are presented. The other parameter sets yield similar results except that L_{pt} takes different values. It is important to note that at $L = L_{pt}$, *all* the ratios approach zero except for m_χ^*/m_χ.

Let us analyze these ratios in the light of the above equations and related work. As stated before, χ_0 and $\langle\sigma\rangle$ vanish in the dense matter phase. This is the reason for the vanishing of two of the above ratios. The non-vanishing of m_χ^*/m_χ is due to the existence of a pure background term which appears in the contribution to the in-medium scalar mass. This term substitutes in the dense matter phase the trace anomaly relation $\frac{1}{2}f_\chi m_\chi = \left(\frac{9}{8}\langle 0|\frac{\alpha_s}{\pi}G^2|0\rangle\right)^{1/2}$ by

$$\frac{1}{2}m_\chi^* f_\chi = \sqrt{\left\langle \frac{f_\pi^2}{8}\mathrm{Tr}(\partial_i U_0^\dagger \partial_i U_0)\right\rangle}, \tag{6.93}$$

which remains finite. It should be noted that this is an addition to the hard glue caused by the back-reaction of the skyrmion background to the density-modified

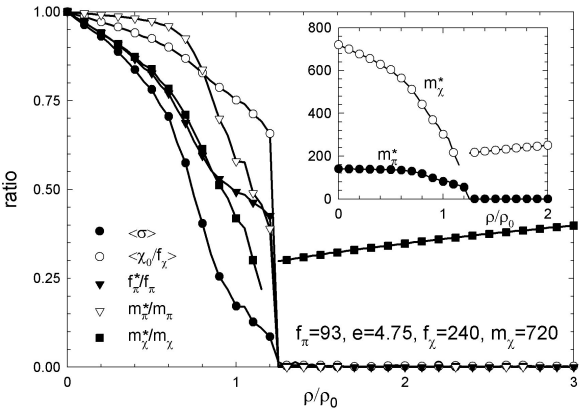

Fig. 6.8 The ratios of the in-medium parameters to the free space parameters. The graph in a small box shows the masses of the pion and the scalar.

vacuum that remains "unmelted" above the critical density. This seems to be an effect missing in the temperature case. The extra terms in Eq. (6.92), which are not proportional to m_χ^2, come from the properly scaled current algebra and the pion mass terms. In the (matter-free) vacuum, these terms describe the couplings of χ to the π's. In dense medium, χ couples to the static background matter fields which contribute to the χ mass.

The vanishing of the pion mass, which is, in the pure Skyrme model calculation, due to the vanishing of the $\langle\sigma\rangle$, shows the chiral behavior of χ_0, since the transition density for both phenomena is the same.

Table 6.3 The slope of the ratios near the origin

	f_π^*/f_π	m_π^*/m_π	f_χ^*/f_χ	m_χ^*/m_χ
set A	−0.21	−0.01	−0.14	−0.25
set B	−0.25	−0.03	−0.14	−0.28
set C	−0.12	−0.005	−0.07	−0.14

The phenomenon discussed above corresponds to "Brown-Rho" scaling discovered in 1991 [Brown and Rho 1991]. In the description of [Brown and Rho 1991], the density dependence comes solely from the change in the mean field χ^* with the corresponding change to the skyrmion structure ignored. Our present result corrects and gives a precise meaning to the scaling relation of [Brown and Rho 1991] which represents the "intrinsic density dependence" imposed on Harada-Yamawaki hidden local symmetry theory by the Wilsonian matching constraint [Harada and Yamawaki 2003]. Similarly, Eq. (6.90) compares to the corresponding f_π^*/f_π of [Brown and Rho 1991]. Again an additional factor, $(1 - \frac{2}{3}\vec{\pi}^2(\vec{x}))$, associated with the background property appears as a correction.

At low matter density, the ratio f_π^*/f_π can be fit to a linear function

$$\frac{f_\pi^*}{f_\pi} \sim 1 - 0.24(\rho/\rho_0) + \cdots . \tag{6.94}$$

At $\rho = \rho_0$, this yields $f_\pi^*/f_\pi = 0.76$ which is to be compared with $f_\pi^*/f_\pi \approx 0.78$ of [Brown and Rho 1991]. The ratio m_χ^*/m_χ scales similarly to f_π^*/f_π up to $\rho \sim \rho_0$. In Table 6.3, we list the slopes of the ratios. The inset figure in Fig. 6.8 shows the behavior of the masses m_π^* and m_χ^*. They become *nearly* degenerate close to the "critical" density.

6.4.4 *Pseudogap phase*

The skyrmion-half-skyrmion transition discussed above has an interesting interpretation in terms of what is called "pseudogap" phenomenon. This was first noticed in [Lee, Park, Rho and Vento 2004].

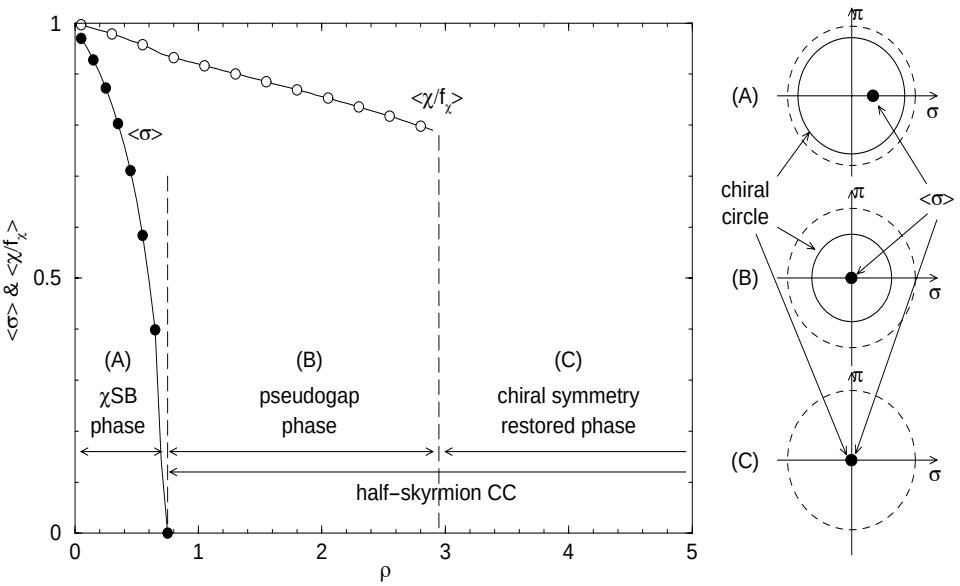

Fig. 6.9 Average values of $\sigma = \frac{1}{2}\mathrm{Tr}(U)$ and χ/f_χ of the lowest energy crystal configuration at a given baryon number density. Note that here ρ – not to be confused with the ρ meson figuring elsewhere – stands for density n.

In Fig. 6.9 we show the average values of $\sigma = \frac{1}{2}\mathrm{Tr}U$ and χ/f_χ over space, which provide direct information on the structure of the crystal and can be used as order parameters of the phase transition. What these data show is that there is a "phase transition" before the chiral restoration transition, at the density at

which the expectation value of σ vanishes. Recalling that the expectation value of σ is proportional to the quark condensate, this may indicate a change in the chiral symmetry structure due to destructive interference of the phase of the quark condensate with a non-vanishing modulus. In the case of the massive pions, such a phase transition is not abrupt but continuous, and this is the reason why one has failed to notice it in previous works with the pion mass. We identify this phase transition with $\langle\sigma\rangle = 0$ while $\langle\chi\rangle \neq 0$ as of a *pseudogap type*. The density at which the pseudogap phase transition appears is denoted as n_p. Since the vanishing of σ is possible because each skyrmion maps the chiral circle onto space in order to carry nontrivial baryon number, it is not clear whether the pseudogap phase is not an artifact of the skyrmion matter. A similar pseudogap structure was proposed in hot QCD [Zarembo 2002]. It is interesting to note an analogy to what is known in condensed matter physics as "deconfined quantum critical phenomenon" wherein the appearance of half-skyrmions signals a phase transition and that leads to a strongly non-Fermi liquid state. When the ground-state vector meson ρ is incorporated à la $\mathrm{HLS}_{K=1}$ in the construction of dense skyrmion matter, the pseudogap phase corresponds to $a = 1$ or $F_\sigma = F_\pi$, approaching Georgi's "vector limit" [Georgi 1989a; Georgi 1989b] when the gauge coupling g approaches zero. It can be identified with what is called "hadronic freedom" regime in Chapter 7. This matter will be discussed in Chapter 10.

The two step phase transition is schematically illustrated in Fig. 6.9.

To summarize:

(A) At low density ($n < n_p$ where n_p is the pseudogap threshold density), matter slightly reduces the vacuum value of the dilaton field from that of the baryon free vacuum. This implies a shrinking of the radius of the chiral circle by the same ratio. Since the skyrmion takes all the values on the chiral circle, the expectation value of σ is not located on the circle but inside the circle. Skyrmion matter at this density is in the chiral symmetry broken phase.

(B) At some intermediate densities ($n_p < n < n_c$ where n_c is the chiral restoration density), the expectation value of σ vanishes while that of the dilaton field is still nonzero. The skyrmion crystal is in a CC (or BCC) configuration made of half skyrmions localized at the points where $\sigma = \pm 1$. Since the average value of the dilaton field does not vanish, the radius of the chiral circle is still finite. Here, $\langle\sigma\rangle = 0$ implies that chiral symmetry is restored in the sense of Georgi's vector limit.

(C) At higher density ($n > n_c$), the phase characterized by $\langle\chi/f_\chi\rangle = 0$ becomes energetically favorable. Then, the chiral circle, describing the fluctuating pion dynamics, shrinks to a point.

In the case of massive pions, the chiral circle is tilted by the explicit symmetry breaking term. Thus the exact half-skyrmion CC, that requires a symmetry between points with values $\sigma = +1$ and $\sigma = -1$ cannot be constructed and consequently the

phase characterized by $\langle\sigma\rangle = 0$ cannot exist at any density. However, $\langle\sigma\rangle$ is always inside the chiral circle and its value drops much faster than that of $\langle\chi/f_\chi\rangle$. Thus, if the pion mass is small enough, a pseudogap phase can appear in the model.

6.4.4.1 *Skyrmion mass at high density*

The result that $\langle\chi/f_\chi\rangle$ does not vanish at the transition to the half-skyrmion phase suggests that the skyrmion mass does not vanish at that point. Roughly this can be understood since the skyrmion mass goes like

$$M \propto f_\pi \langle\chi/f_\chi\rangle. \tag{6.95}$$

This is reminiscent of the parity-doublet model discussed in the next chapter. It shares the feature that near the transition point, the skyrmion mass deviates from the naive BR scaling.

6.5 Holographic Skyrmion

In Subsection 6.3.3.2, we learned that in the presence of the ρ field, the skyrmion structure of the baryon changes drastically, including the stabilization mechanism. In this section, we discuss a novel skyrmion structure for baryons that arises when the infinite tower of vector mesons that emerges in holographic dual QCD are taken into account. Most surprisingly, we find the justification for treating the nucleon as a point-like local field, long exploited in nuclear physics, and offer a bona-fide – and the first – derivation of the total vector dominance for the nucleon EM form factor. This remarkable structure arises naturally from the 5D instanton configuration stabilized with a tiny size in the 't Hooft limit.

6.5.1 *Baryon as an instanton*

Consider the 5D YM action that is obtained in the large 't Hooft and N_c limit discussed in Chapter 5. We rewrite Eq. (5.45) – with somewhat more details than in Chapter 5 – as [Hong, Rho, Yee and Yi 2007b]

$$S_{YM} = -\int dx^4 dw\, \frac{1}{4e^2(w)}\, \mathrm{Tr} F_{MN} F^{MN} \tag{6.96}$$

with $(M, N) = 0, 1, 2, 3, 4$, where $e(w)$ is the position-dependent "electric coupling" reflecting the supergravity background and encoding "spread" in energy scale:

$$\frac{1}{e^2(w)} = \frac{(g_{YM}^2 N_c) N_c}{108\pi^3} M_{KK} \frac{U(w)}{U_{KK}}. \tag{6.97}$$

Here M_{KK} is the Kaluza-Klein mass that corresponds to the UV cutoff of the low-energy effective theory, w is the fifth coordinate written in a conformally flat form, $U(w)^3 = U_{KK}^3(1 + M_{KK}^2 w^2)$ and U_{KK} is the location of the horizon in the gravity

solution in the bulk sector. As given, the fifth coordinate w turns out to be finite $-w_{max} \leq w \leq w_{max}$ with $\omega_{max} \simeq 3.64/M_{KK}$.

When reduced to 4D, (6.96) encapsulates an infinite tower of vector and axial-vector mesons. In the broken phase, the gauge field A_μ, in the $A_5 \equiv A_z = 0$ gauge, has a mode expansion

$$A_\mu(x,w) = i\alpha_\mu(x)\psi_0(w) + i\beta_\mu(x) + \sum_n a_\mu^{(n)}(x)\psi_{(n)}(w) \ , \tag{6.98}$$

where $\hat{\Psi}_0(z) \equiv \psi_0(w(z)) = \frac{1}{\pi}\arctan\left(\frac{z}{U_{KK}}\right)$ which is odd under $w \to -w$, and in the unitary gauge in 4D,

$$\begin{aligned} \alpha_\mu &= \{\xi^{-1}, \partial_\mu \xi\} = \frac{2i}{f_\pi}\partial_\mu \pi + \cdots \ , \\ \beta_\mu &= \frac{1}{2}[\xi^{-1}, \partial_\mu \xi] = \frac{1}{2f_\pi^2}[\pi, \partial_\mu \pi] + \cdots \end{aligned} \tag{6.99}$$

with $\xi = e^{i\pi/f_\pi}$. The "wave functions" ψ_0 and ψ_n satisfy the equations of motion encoding spread in the z direction. The resulting theory is a 4-D action involving a massless scalar multiplet, *i.e.* pions and an infinite tower of hidden local symmetric vector mesons with alternating parity quite analogous to the bottom-up theory.

We would like to obtain baryons as solitons from (6.96). Unlike the conventional chiral Lagrangian approaches wherein baryons are realized as skyrmions, made of the pion field U only, as we couple higher massive vector mesons to the Skyrme action, the size-stabilizing mechanism for topological solitons is significantly affected by the massive vector mesons. If we approach this problem from the above five-dimensional viewpoint, it is advantageous to consider the problem as a five-dimensional one. It has been known for some time [Atiyah and Manton 1989] that what replaces the skyrmion in five dimensions is the instanton soliton since the two share the same topological winding number. However, what has not been clear is whether and how much of the instanton is born out of the skyrmion. We will show that the instanton interpretation of the baryon will give a very different route to the low energy effective dynamics of the baryons.

It is known in the string theory community that a $D4$ brane wrapping the compact S^4 corresponds to a baryon vertex on the $5D$ spacetime, which follows from an argument originally given by Witten [Witten 1998]. Here the Chern-Simons action plays an important role.[22] This object is an instanton in the action (6.96).

[22]Since the argument is technical – and we won't be going into details in this volume, although there are many interesting features that are of relevance to some of the issues discussed here, we put a min-resumé on the Chern-Simons term here for completeness. On the D4-brane, we have a Chern-Simons coupling of the form,

$$\mu_4 \int C_3 \wedge 2\pi\alpha' d\tilde{A} = 2\pi\alpha'\mu_4 \int dC_3 \wedge \tilde{A} \tag{6.100}$$

for D4 gauge field $\tilde{A}$. Wrapping D4 on S^4 which has a quantized dC_3 flux in this background, one finds that this flux induces N_c unit of electric charge. The Gauss constraint for $\tilde{A}$ demands that

Since an instanton has

$$\int \mathrm{Tr} F_{MN} F^{MN} = 2 \int \mathrm{Tr} F \wedge F = 16\pi^2 \tag{6.103}$$

a point-like instanton that is localized at $w = 0$ would have the energy

$$m_B^{(0)} \equiv \frac{4\pi^2}{e^2(0)} = \frac{(g_{YM}^2 N_c) N_c}{27\pi} M_{KK} \ . \tag{6.104}$$

This mass also equals that of an S^4 wrapped D4 located at $w = 0$, in accordance with the string theory picture of the instanton. If the instanton gets bigger, on the other hand, the configuration costs more and more energy, since $1/e^2(w)$ is an increasing function of $|w|$, thus the leading behavior of the instanton is to collapse to a point-like instanton. Thus, in the large λ limit, the baryon is a point-like object – the size of which going like $\sim 1/\sqrt{\lambda}$ – that can be treated as a local field. This is the description that has been used successfully in nuclear physics since Yukawa's meson theory. The departure from the point-like configuration will come from $1/\lambda$ and $1/N_c$ corrections, which would make the instanton configuration bigger somewhat like in chiral perturbation theory where the point-like heavy baryon gets "blown-up" by the meson cloud which emerges as higher chiral order corrections. It is interesting that the standard nuclear physics approach to the nucleons in terms of meson-exchange potentials and exchange currents naturally arises in this holographic dual theory.

Once we have the baryon as a quantized soliton, then from the invariance under local coordinate as well as local gauge symmetries on the D8 branes reduced along internal S^4, the leading 5D kinetic term for the baryon must simply be the standard Dirac kinetic term in the curved space. It is of the form [Hong, Rho, Yee and Yi 2007b]

the net charge should be zero, and thus the D4 can exist only if N_c fundamental strings end on it. In turn, the other end of fundamental strings must go somewhere, and the only place it can go is D8 branes. Thus a D4 wrapping S^4 looks like an object with N_c $U(1)$ charge with respect to the overall $U(1)$ of D8. This overall $U(1)$ charge is precisely the baryon number, so we identify the baryon as wrapped D4 with N_c fundamental strings sticking onto it.

Of course, things are more complicated than this since $D4$ can dissolve into D8 branes and become an instanton soliton on the latter. From D8's viewpoint, a D4 wrapped on S^4 once is interchangeable with the unit instanton

$$\frac{1}{8\pi^2} \int_{R^3 \times I} \mathrm{Tr} F \wedge F = 1 \tag{6.101}$$

as far as the conserved charge goes, which follows from a Chern-Simons term on D8,

$$\mu_8 \int_{R^{3+1} \times I \times S^4} C_5 \wedge 2\pi^2 (\alpha')^2 \mathrm{Tr} F \wedge F = \mu_4 \int_{R^{0+1} \times S^4} C_5 \wedge \frac{1}{8\pi^2} \int_{R^3 \times I} \mathrm{Tr} F \wedge F \tag{6.102}$$

which shows that a unit instanton couples to C_5 minimally, and carries exactly one unit of $D4$ charge. When the size of the instanton becomes infinitesimal, it can be freed from D8's, and this is precisely D4. From the viewpoint of D4, this corresponds to going from the Higgs phase into the Coulomb phase.

$$-i\int d^4xdw\left[\bar{\mathcal{B}}\gamma^m D_m\mathcal{B}+m_b(w)\bar{\mathcal{B}}\mathcal{B}+ig_5(w)\frac{\rho^2_{baryon}}{e^2(w)}\bar{\mathcal{B}}\gamma^{mn}F_{mn}\mathcal{B}\right]$$
$$-\int d^4xdw\frac{1}{4e^2(w)}\ \mathrm{Tr}\,F_{mn}F^{mn}+\text{C.S. term}\,, \tag{6.105}$$

where $\gamma^{mn}=[\gamma^m,\gamma^n]/2$, $\mathcal{B}$ is five-D baryon field, ρ_{baryon} is the stabilized size of the 5D instanton representing baryon, and $g_5(w)$ is a function whose value at $w=0$ is to be determined from the (collective) quantization of the soliton

$$g_5(0)=\frac{2\pi^2}{3}. \tag{6.106}$$

To go to four dimensions where we live, we do the Kaluza-Klein dimensional reduction. To do this, we mode expand $\mathcal{B}_{L,R}(x^\mu,w)=B_{L,R}(x^\mu)f_{L,R}(w)$ where $\gamma^5 B_{L,R}=\pm B_{L,R}$ are 4D chiral components, with the profile functions $f_{L,R}(w)$ satisfying the equation of motion in the fifth direction

$$\begin{aligned}\partial_w f_L(w)+m_b(w)f_L(w)&=m_B f_R(w)\ ,\\ -\partial_w f_R(w)+m_b(w)f_R(w)&=m_B f_L(w)\ ,\end{aligned} \tag{6.107}$$

in the range $w\in[-w_{max},w_{max}]$. The 4D Dirac field for the baryon is then reconstructed as

$$B=\begin{pmatrix}B_L\\ B_R\end{pmatrix} \tag{6.108}$$

and the eigenvalue m_B is the mass of the baryon mode $B(x)$.

Explicitly written, the baryonic action of (6.105) in 4D takes the form

$$\mathcal{L}_4=-i\bar{B}\gamma^\mu\partial_\mu B-im_B\bar{B}B+\mathcal{L}_{\text{vector}}+\mathcal{L}_{\text{axial}}\,, \tag{6.109}$$

with the four-dimensional nucleon mass m_B. This nucleon mass will generally differ from the five-dimensional mass, due to spread of the wavefunction $f_{L,R}$ along the fifth direction. However, this difference arises only as a subleading correction in the large N_c and large λ. Writing out the interaction terms explicitly, we have

$$\mathcal{L}_{\text{vector}}=-i\bar{B}\gamma^\mu\beta_\mu B-\sum_{k\geq 0}g_V^{(k)}\bar{B}\gamma^\mu a_\mu^{(2k+1)}B\,, \tag{6.110}$$

and the nucleon couplings to axial mesons, including pions, as

$$\mathcal{L}_{\text{axial}}=-\frac{ig_A}{2}\bar{B}\gamma^\mu\gamma^5\alpha_\mu B-\sum_{k\geq 1}g_A^{(k)}\bar{B}\gamma^\mu\gamma^5 a_\mu^{(2k)}B\,, \tag{6.111}$$

where various coupling constants $g_{V,A}^{(k)}$ as well as the pion-nucleon axial coupling g_A are calculated by suitable wave-function overlap integrals. In the above expression, the meson fields are written in the nucleon isospin representation.

6.5.2 *Chiral dynamics*

Making suitable assumptions consistent with large λ and N_c limit, we can compute from the Lagrangian (6.105) a variety of low-energy constants that are associated with chiral dynamics of the nucleon [Hong, Rho, Yee and Yi 2007b]. For instance, in terms of the wave functions $f_{L,R}(w)$ of (6.107) for the nucleon and $\psi_n(w)$ of (6.98), the nucleon axial coupling constant is given by

$$g_A \approx 2 \int_{-w_{max}}^{w_{max}} dw \; |f_L(w)|^2 \, \psi_0(w) \; . \tag{6.112}$$

With an appropriate account of the hedgehog structure of the instanton (or skyrmion) that provides the leading $1/N_c$ correction to the $\mathcal{O}(N_c)$ term plus a subleading term in λ – which roughly corresponds to the "quenched approximation" in lattice calculations, we get

$$g_A \approx 1.3 \tag{6.113}$$

to be compared with the experimental value of $g_A^{exp} = 1.27$. To the same approximation, we get the anomalous magnetic moments

$$\mu_p^{anomalous} \approx 1.8\mu_N, \quad \mu_n^{anomalous} \approx -1.8\mu_N \tag{6.114}$$

to be compared with the experiments $\mu_p^{exp} - 1 = 1.8\mu_N$ and $\mu_n^{exp} = -1.9\mu_N$ respectively.

Remarkably, the model provides the *first* ever theoretical prediction for the ratio

$$R = \frac{g_{\omega NN}}{3g_{\rho NN}} \approx 1.2 \tag{6.115}$$

deviating from the nonrelativistic quark model value $R = 1$. There is no direct experimental determination of this ratio which plays an important role in the nucleon-nucleon potential that figures in nuclear physics, the ω coupling playing a prominent role in the short-range interactions in nuclei. The phenomenological fits give the ratio in the range of $1.1 \leq R \leq 1.5$.

To repeat what was said above, an important aspect of the development here is that the point-like instanton picture for the baryon provides a theoretical justification for the long-standing practice in nuclear physics of using a local field for the nucleon as well as the current development of baryon chiral perturbation theory discussed in Chapter 4. It also leads to a theoretical "derivation" of vector dominance in nucleon electroweak form factors. In the past, vector dominance by the lightest vector mesons, so powerful in the pionic form factor, failed badly in the nucleon form factor. When the infinite tower of vector mesons are included, we find that both the EM and axial form factors of the nucleon are completely vector-dominated.

6.5.3 *Deriving vector dominance*

6.5.3.1 *"Old" vector dominance*

We saw in Chapter 5 how the infinite tower enters the structure of the EM form factor of the pion. The lowest four ρ mesons saturated the charge sum rule, $F^\pi(0) = 1$. It has been shown that the pion form factor for space-like momentum comes out to be very well in agreement with experiments with the four lowest vector mesons. Strangely though, it has been known since a long time that the lowest ρ is enough to dominate the form factor in full agreement with experiment. This may be an accident just as much as $a = 2$ in $\mathrm{HLS}_{K=1}$ which gives vector dominance was an accident.

When it comes to the nucleon form factor, the "old" vector dominance with the lowest members of the tower – ρ, ω and ϕ – does not work. In terms of $\mathrm{HLS}_{K=1}$, $a \approx 1$ with a maximal VD violation turns out to work much better. We briefly review this in order to better appreciate what the infinite tower does.

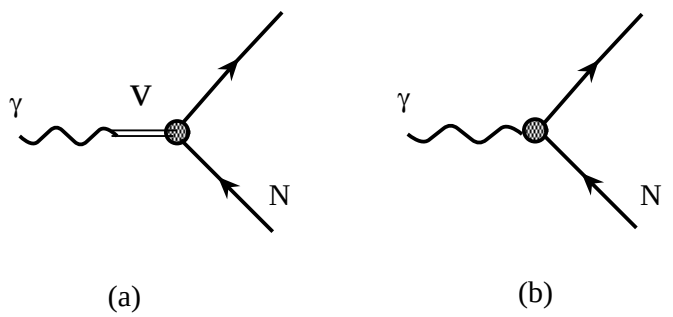

Fig. 6.10 (a) Photon coupling to the nucleon via vector meson V and (b) direct photon coupling to the nucleon. The blob represents the intrinsic form factor accounting for short-distance effects (referred to as "intrinsic core" in some circles) unaccounted for in the effective theory, *e.g.*, asymptotically free QCD property.

It has been known since a long time that the nucleon form factors at low momentum transfers cannot be fitted by a monopole form factor of the type $\sim 1/(1+cQ^2)$ with c a constant and $Q^2 = -q^2$. In fact, one obtains a much better fit by a dipole form factor of the form $\sim 1/(1+dQ^2)^2$ with $d \approx 1/(0.71\ \mathrm{GeV})^2$. This meant that the single-vector-meson mediated mechanism along the line of reasoning used for the pion form factors could not explain the process. This led to a two-component description Fig. 6.10 which can be put in the form [Bijker and Iachello 2004]

$$F_1(Q^2) = \frac{1}{2}\left[A(Q^2) + B(Q^2)\frac{m_\rho^2}{Q^2+m_\rho^2}\right] \tag{6.116}$$

with the normalization

$$A(0) + B(0) = 1. \tag{6.117}$$

In (6.116), the momentum dependence in A and B represents a form-factor effect corresponding to an "intrinsic" structure of the nucleon which is expected from both the confinement and the asymptotic behavior of perturbative QCD [Lepage and Brodsky 1980]. The first term corresponds to a direct coupling to the intrinsic component of the nucleon ("nucleon core" in short), Fig. 6.10b, and the second term via one or more vector mesons in the ρ channel, Fig. 6.10a. Let us for simplicity consider only one vector meson exchange. The same reasoning applies to the case where more than one vector mesons are considered. Making the reasonable assumption that the photon and the ρ meson couple to the nucleon core with a same form factor, one can rewrite (6.116) as

$$F_1(Q^2) = \frac{1}{2} h(Q^2) \left[(1 - \beta_\rho) + \beta_\rho \frac{m_\rho^2}{Q^2 + m_\rho^2} \right] \tag{6.118}$$

with the core form factor normalized as $h(0) = 1$. Perturbative QCD indicates that asymptotically $h(Q^2) \approx (1 + \gamma Q^2)^{-2}$. The coefficient γ is not given by the model but can be fixed by experimental data. One can make a very good fit to the data with (6.118) with the coefficients $\gamma \approx 0.52$ GeV^{-2} and $\beta_\rho \approx 0.51$ [Bijker and Iachello 2004].

Given that the two-component picture (6.118) works so well, one would like to understand what physics the first term represents. The conventional interpretation has been that it, with a size of ~ 0.4 fm, encodes the "short-distance" physics of the microscopic degrees of freedom of QCD that are extraneous to long-wavelength excitations – π, ρ *etc.* – in the baryon. One interpretation along that line of the core component was given in terms of a chiral bag in which quarks and gluons are confined with the broken chiral symmetry of QCD suitably implemented outside of the bag [Brown, Rho and Weise 1986]. The baryon charge was assumed to be divided roughly half and half between the quark-gluon sector and the hadron sector. This hybrid model met with a fair success in reproducing the data available up to late 1980's. Interestingly, it has been claimed that there is an (albeit indirect) evidence for a core of ~ 0.2 fm from the Nachtmann moment of the unpolarized proton structure function measured at JLab [Petronzio 2003]. Another interpretation for the core, which is equivalent to the chiral bag by the Cheshire Cat principle, is the skyrmion. Such a model in which the photon couples directly to a skyrmion of size ~ 0.4 fm and via the exchange of the lowest member of the vector-meson tower has been constructed [Holzwarth 1996]. With one parameter that represents the amount of direct coupling, the model is found to agree quite well with the dipole form factors up to $Q^2 \sim 1$ GeV^2 and can explain satisfactorily the deviation from the dipole form for $Q^2 \gtrsim 1$ GeV^2. What this implies is that the nucleon form factors at low momentum transfers, say, $Q^2 \lesssim 1$ GeV^2, can be well understood

given the three basic ingredients: (a) an extended object, (b) partial coupling to vector mesons and (c) relativistic recoil corrections.

6.5.3.2 *"New" vector dominance*

In a stark contrast to the old picture of vector dominance in the nucleon structure where the vector dominance by the ρ and ω is violated by the presence of a direct coupling of the photon to what is considered to be a "core" attributed to a quark-gluon structure, the nucleon form factor in hQCD is found to be given entirely by the same four vector mesons that enter in the pion form factor. To appreciate what this means, we recall from the work of Holzwarth [Holzwarth 1996] that in the skyrmion model with the pion field only – and no fluctuating vector mesons, the form factor is described dominantly by the skyrmion with pion fluctuations entering at higher chiral order. Thus the size of the nucleon – which is the slope of the form factor vs. the momentum transfer squared $(-6(d/dQ^2)F(Q^2)|_{Q^2=0})$ – is primarily given by the size of the skyrmion. One would naively think that in this holographic dual model, the instanton would replace the skyrmion of the Skyrme model in giving the form factors. It turns out that this is not the case.

To see this, consider how the mixing of the EM and hidden gauge vector fields enters the coupling of baryons with the electromagnetic vector field $\mathcal{V}$. Seemingly this case is very different from that of pions. For one thing, we have a minimal interaction term between baryons and the 5D gauge field, A, and this is inherited by $\mathcal{V}$ without modification since $\mathcal{V}$ is simply the non-normalizable part of A. Thus it may seem that we have a point-like interaction between baryons and $\mathcal{V}$. However, baryons also couple minimally to the 4D massive vectors, $a^{(2k+1)}$, which mix with $\mathcal{V}$ in the propagator. They show up in the baryon effective Lagrangian as

$$\int dw\ \bar{\mathcal{B}}\gamma^m A_m \mathcal{B} = \bar{B}\gamma^\mu \mathcal{V}_\mu B + \sum_k g^{(k)}_{V,min} \bar{B}\gamma^\mu a^{(2k+1)}_\mu B + \cdots \tag{6.119}$$

where the ellipses denote axial couplings to axial vectors as well as coupling to pions via α_μ and β_μ. Then, an additional contribution from the magnetic term shifts $g_{V,min}$ to $g_V = g_{V,min} + g_{V,mag}$ and we have

$$\bar{B}\gamma^\mu \mathcal{V}_\mu B + \sum_k g^{(k)}_V \bar{B}\gamma^\mu a^{(2k+1)}_\mu B + \cdots . \tag{6.120}$$

This interaction term, together with the mixing between the photons and massive vector meson, will generate electromagnetic form factors of the baryon.

Alternatively, we may use the canonically normalized vectors $v^{(k)}$ instead, where we have the vector-current couplings of type

$$\bar{B}\gamma^\mu \mathcal{V}_\mu B + \sum_k g^{(k)}_V \bar{B}\gamma^\mu (v^{(k)}_\mu - \zeta_k \mathcal{V}_\mu) B + \cdots \tag{6.121}$$

where

$$\zeta_k = \int dw \frac{1}{e(w)^2}\, \psi_{(2k+1)}(w)\ . \tag{6.122}$$

This is just a field re-parametrization, changing no physics. Now using normalization of the background wave functions in the w direction, one can show that

$$\sum_k g^{(k)}_{V,min}\zeta_k = 1 \tag{6.123}$$

and similarly,

$$\sum_k g^{(k)}_{V,mag}\zeta_k \ = 0 \tag{6.124}$$

and together they imply the crucial sum rule,

$$\sum_k g^{(k)}_V \zeta_k = 1. \tag{6.125}$$

Therefore, in this shifted basis, we have

$$\bar{B}\gamma^\mu \mathcal{V}_\mu B + \sum_k g^{(k)}_V \bar{B}\gamma^\mu (v^{(k)}_\mu - \zeta_k \mathcal{V}_\mu)B + \cdots = \sum_k g^{(k)}_V \bar{B}\gamma^\mu v^{(k)}_\mu B + \cdots . \tag{6.126}$$

As with the pion, we can see that the cubic electromagnetic interaction is again mediated entirely by intermediate massive vector mesons. Thus the isovector nucleon form factor is given by

$$F_V(Q^2) = 1 - \sum_k \frac{g^{(k)}_V \zeta_k Q^2}{Q^2 + m^2_{2k+1}} = \sum_k \frac{g^{(k)}_V \zeta_k m^2_{2k+1}}{Q^2 + m^2_{2k+1}} = \sum_k \frac{g_{v^{(k)}} g^{(k)}_V}{Q^2 + m^2_{2k+1}} \tag{6.127}$$

up to the electromagnetic charge operator. We used the sum rule $\sum_k g^{(k)}_V \xi_k = 1$ and defined $g_{v^{(k)}} = \zeta_k m^2_{2k+1}$.

It is found numerically that the isovector charge sum rule (6.125) is almost completely saturated by the four lowest vector mesons in the ρ channel just as in the pion form factor,

$$F_V(0) = 1 \simeq 1.393 - 0.338 - 0.183 + 0.178 \simeq 1.05. \tag{6.128}$$

It has not yet been fully verified, but the plausible conjecture is that the near complete saturation of the sum rule both in the pion and isovector nucleon form factors by the same isovector vector mesons is indicative of a hidden symmetry in the curvature of the 5D space-time at the hadronic scale.

6.5.3.3 *Generalized universality*

The saturation of the charge and magnetic sum rules suggest a new form of universality that generalizes the "old" universality $g_{\rho\pi\pi} = g_{\rho NN}$. This is based on the observation [23] that to a very good accuracy, we can set

$$(-)^k \zeta_k = 1/h \tag{6.129}$$

where h is a constant independent – within less than 1% – of the species k. Assuming that the pion charge sum rule is completely saturated by the four vector mesons, we arrive at the conclusion that [24]

$$\sum_{k=0}^{3} (-)^k g_{v^{(k)}\pi\pi} = h. \tag{6.131}$$

Since the same relation holds with a nucleon replacing the π in (6.131), h could be identified with the $\mathrm{HLS}_{K=\infty}$ gauge coupling constant and that

$$\sum_{k=0}^{3} (-)^k g_{v^{(k)}\pi\pi} \simeq \sum_{k=0}^{3} (-)^k g_{v^{(k)}NN}. \tag{6.132}$$

We could consider this as a "generalized universality" relation, although we have no rigorous argument for such a relation.

If the sum rules are saturated by the first four vector mesons, then an interesting question is how the relation $\sum_{k=4}^{\infty} \zeta_k g_{v^{(k)}\pi\pi} = \sum_{k=4}^{\infty} \zeta_k g_{v^{(k)}NN} = 0$ is satisfied and what it means vis-a-vis with the short-range structure of the nucleon.

6.5.3.4 *Nucleon EM form factors*

Let us see how the predicted vector-dominated nucleon form factors compare with nature [Hong, Rho, Yee and Yi 2007c].

The nucleon form factors are defined from the matrix elements of the external currents,

$$\langle p' |\, J^\mu(x)\, | p \rangle = e^{iqx}\, \bar{u}(p')\, \mathcal{O}^\mu(p, p')\, u(p)\,, \tag{6.133}$$

where $q = p' - p$ and $u(p)$ is the nucleon spinor of momentum p. By the Lorentz invariance and the current conservation, we expand the operator $\mathcal{O}^\mu$, assuming the

[23] It is not known whether (6.129) is an identity or a coincidence. It is an interesting possibility that this is a signal for the hidden symmetry mentioned above.

[24] This is reminiscent of the nonet relation in three flavor HLS_1

$$g_\rho/m_\rho^2 = 3g_\omega/m_\omega^2 = -(3/\sqrt{2})g_\phi/m_\phi^2 = 1/g \tag{6.130}$$

where g is the hidden gauge coupling constant.

CP invariance, as

$$\mathcal{O}^\mu(p,p') = \gamma^\mu \left[\frac{1}{2}F_1^s(Q^2) + F_1^a(Q^2)t^a\right] + i\frac{\sigma^{\mu\nu}}{2m_B}q_\nu \left[\frac{1}{2}F_2^s(Q^2) + F_2^a(Q^2)t^a\right], \tag{6.134}$$

where $m_B \simeq 940$ MeV is the nucleon mass and $t^a = \tau^a/2$. F_1^s and F_2^s are, respectively, the Dirac and Pauli form factors for isoscalar current, and similarly F_1^a, F_2^a for isovector currents.

Since they are matrix elements, the form factors contain all one-particle irreducible diagrams for two nucleons and one external current which are very difficult to calculate in QCD proper. However, the anti-de Sitter/conformal field theory (AdS/CFT) correspondence, found in certain type of string theory, enables us to compute such nonperturbative quantities like hadron form factors with some sensible approximations. According to the AdS/CFT correspondence, the low energy effective action of the gravity dual of QCD corresponds to the generating functional for the correlators of an operator $\mathcal{O}$ in QCD in the large N_c limit:

$$e^{iS_{5D}^{\rm eff}[\phi(\epsilon,x)]} = \left\langle \exp\left[-i\int_x \phi_0\,\mathcal{O}\right]\right\rangle_{\rm QCD}, \tag{6.135}$$

where $\phi(z,x)$ is a bulk field, acting as a source for $\mathcal{O}$ when evaluated at the UV boundary $z=\epsilon$. Furthermore, the normalizable mode of the bulk field is identified as the physical state in QCD, created by the operator $\mathcal{O}$.

Let us rewrite the relevant part of Eq. (6.105) – which is the gravity dual of low energy QCD with two massless flavors of Sakai and Sugimoto (SS) [Sakai and Sugimoto 2005] applied to instanton baryons in [Hong, Rho, Yee and Yi 2007a; Hong, Rho, Yee and Yi 2007b] – as

$$\begin{aligned} S_{5D}^{\rm eff} = &\int_{x,w} \left[-i\bar{\mathcal{B}}\gamma^m D_m\mathcal{B} - im_b(w)\bar{\mathcal{B}}\mathcal{B} + \kappa(w)\bar{\mathcal{B}}\gamma^{mn}F_{mn}\mathcal{B} + \cdots\right] \\ &+S_{\rm meson}, \end{aligned} \tag{6.136}$$

where $S_{\rm meson}$ is the effective action for the mesons. We have defined the coefficient $\kappa(w) = g_5(w)\rho^2_{baryon}/e^2(w)$ which can be estimated:

$$\kappa(w) \simeq \frac{0.18N_c}{M_{KK}}, \tag{6.137}$$

where $M_{KK} \simeq m_B$. The ellipses in the effective action (6.136) denote higher derivative operators, whose coefficients are difficult to estimate but are suppressed at low energy, $E < M_{KK}$.

Though the exact correspondence between the gravity dual and QCD is not established yet, we can compute the electromagnetic form factors for the nucleons in the SS model by assuming the correspondence. We first need to identify the dual bulk field of the external EM current, which is nothing but the bulk photon field.

Since the electric charge operator is the sum of isospin and the baryon operator,

$$Q = I_3 + \frac{1}{2}B, \tag{6.138}$$

we have to identify A_μ^3 and A_μ^B, the third component of the isospin gauge field and the $U(1)_B$ gauge field, respectively, as the photon field. Then all baryon bilinear operators in the effective action that couple to either $U(1)_B$ gauge fields or $SU(2)_I$ gauge fields will contribute to the EM form factors.

We now write the (nonnormalizable) photon field as

$$A_\mu(x,w) = \int_q A_\mu(q) A(q,w)\, e^{iqx}\ , \tag{6.139}$$

with boundary conditions that $A(w,q) = 1$ and $\partial_w A(q,w) = 0$ at the UV boundary, $w = \pm w_{\rm max}$ and the (normalizable) bulk baryon field as

$$\mathcal{B}(w,x) = \int_p \left[f_L(w) u_L(p) + f_R(w) u_R(p)\right] e^{ipx}\,. \tag{6.140}$$

Then, using the correspondence (6.135), one can read off the form factors from the effective action (6.105). We find for nucleons the Dirac form factor $F_1(q^2) = F_{1\rm min} + F_{1\rm mag}\, I_3$ with

$$F_{1\rm min}(q^2) = \int_{-w_{max}}^{w_{max}} dw\ |f_L(w)|^2\ A(q,w)\ , \tag{6.141}$$

$$F_{1\rm mag}(q^2) = 2\int_{-w_{max}}^{w_{max}} dw \kappa(w)\, |f_L(w)|^2\, \partial_w A(q,w) \tag{6.142}$$

where $F_{1\rm min}$ and $F_{1\rm mag}$ are, respectively, from the minimal and magnetic couplings. Similarly the Pauli form factor is given as $F_2(q^2) = F_2^3(q^2)\tau^3/2$ with

$$F_2^3(q^2)\,\tau^3 = 4 m_B\,\tau^3 \int_{-w_{max}}^{w_{max}} dw\, \kappa(w) f_L^*(w) f_R(w)\, A(q,w) \tag{6.143}$$

which comes solely from the magnetic coupling. We note that the form factors (6.141), (6.142) and (6.143) have corrections coming from higher order operators in the effective action (6.105), which are suppressed by powers of E/M_{KK} at low energy. However, it should be restressed that this result contains full quantum effects in the large N_c limit, because it is computed from the one-particle irreducible functional, summed over all loops, prescribed by AdS/CFT correspondence.

As shown above, we can replace the form factors by an infinite sum of vector-meson exchanges [Hong, Rho, Yee and Yi 2007b], if we expand the nonnormalizable photon field in terms of the normalizable vector meson ψ_{2k+1} of mass m_{2k+1} as

$$A(q,w) = \sum_k \frac{g_{v^{(k)}} \psi_{(2k+1)}(w)}{Q^2 + m_{2k+1}^2}\ , \tag{6.144}$$

where the decay constant of the k-th vector mesons is given as $g_{v^{(k)}} = m_{2k+1}^2 \zeta_k$ with

$$\zeta_k = \frac{\lambda N_c}{108\pi^3} M_{KK} \int_{-w_{max}}^{w_{max}} dw \frac{U(w)}{U_{KK}} \psi_{(2k+1)}(w) \,, \tag{6.145}$$

where U_{KK} is a parameter of the SS model and

$$dw = \frac{3}{2} \frac{U_{KK}^{1/2}}{M_{KK}} \frac{dU}{\sqrt{U^3 - U_{KK}^3}} \,. \tag{6.146}$$

The resulting EM form factors then take the form

$$F_1(Q^2) = F_{1,\min} + F_{1,\mathrm{mag}} \frac{\tau^3}{2} = \sum_{k=1}^{\infty} \left(g_{V,min}^{(k)} + g_{V,mag}^{(k)} \frac{\tau^3}{2} \right) \frac{\zeta_k m_{2k+1}^2}{Q^2 + m_{2k+1}^2} \tag{6.147}$$

$$F_2(Q^2) = F_2^3(Q^2) \frac{\tau^3}{2} = \frac{\tau^3}{2} \sum_{k=1}^{\infty} \frac{g_2^{(k)} \zeta_k m_{2k+1}^2}{Q^2 + m_{2k+1}^2} \,, \tag{6.148}$$

where

$$g_{V,min}^{(k)} = \int_{-w_{max}}^{w_{max}} dw \; |f_L(w)|^2 \, \psi_{(2k+1)}(w) \,, \tag{6.149}$$

$$g_{V,mag}^{(k)} = 2 \int_{-w_{max}}^{w_{max}} dw \, \kappa(w) \, |f_L(w)|^2 \, \partial_w \psi_{(2k+1)}(w) \,,$$

$$g_2^{(k)} = 0.18 N_c \times \frac{4 m_B}{M_{KK}} \times \int_{-w_{max}}^{w_{max}} dw f_L^*(w) f_R(w) \psi_{(2k+1)}(w) \,. \tag{6.150}$$

In the approximations adopted in the large N_c and λ limit, the parameters of the theory are completely fixed in the meson sector. We take from the analysis of Sakai and Sugimoto in the meson sector, for $N_c = 3$ and $f_\pi \approx 93$ MeV,

$$\lambda \approx 17, \quad M_{KK} \approx 0.94 \text{ GeV}. \tag{6.151}$$

There is a wealth of data, recently from the JLab, on the electromagnetic structure of the nucleon that give strong constraints on the models of the nucleon structure. In order to do a high-quality fit to the data ranging to the momentum transfer $Q^2 \sim 10$ GeV^2, a number of ingredients consistent with long and short-distance properties of QCD have to be properly implemented. Phenomenological models introduce *ad hoc* a number of parameters to fit the data over the range of kinematics available. Here we eschew the usual fitting. Instead, we shall simply take what is given by the model with the parameters completely fixed and see how far one can go in comparing with nature. Now since we are limited by the scale set by the KK mass $M_{KK} \sim 1$ GeV, we will limit to the space-like momentum transfer $Q^2 \lesssim 1$ GeV^2. This also means that we are going to miss certain asymptotic properties of the form factors. For instance, we will not be able to satisfy the asymptotic

behavior demanded by QCD proper, namely,

$$F_1(Q^2) \sim 1/Q^4,\ F_2(Q^2) \sim Q^6 \tag{6.152}$$

where F_1 and F_2 are, respectively, the Dirac and Pauli form factors defined above.

As noted, the charge and magnetic moment sum rules are saturated within a few % by the lowest four vector mesons. We will therefore truncate the infinite sum by the lowest four vector mesons and compute them numerically as done in [Hong, Rho, Yee and Yi 2007c]. For illustration, we will look at the proton form factors.

Using the wavefunctions calculated in [Hong, Rho, Yee and Yi 2007b] and the parameter values (6.151), we can write for the proton

$$\begin{aligned} F_1^p(Q^2) &\simeq \frac{0.958\ M_{KK}^2}{Q^2+0.67\ M_{KK}^2} - \frac{1.230\ M_{KK}^2}{Q^2+2.87\ M_{KK}^2} - \frac{0.628\ M_{KK}^2}{Q^2+6.59\ M_{KK}^2} + \frac{1.585\ M_{KK}^2}{Q^2+11.8\ M_{KK}^2} \\ F_2^p(Q^2) &\simeq \frac{1.855\ M_{KK}^2}{Q^2+0.67\ M_{KK}^2} - \frac{4.587\ M_{KK}^2}{Q^2+2.87\ M_{KK}^2} + \frac{4.547\ M_{KK}^2}{Q^2+6.59\ M_{KK}^2} - \frac{2.390\ M_{KK}^2}{Q^2+11.8\ M_{KK}^2}. \end{aligned} \tag{6.153}$$

In terms of these, the Sachs form factors – conventionally used in the field – for the proton are given by

$$G_M^p(Q^2) = F_1^p(Q^2) + F_2^p(Q^2)\,, \tag{6.154}$$

$$G_E^p(Q^2) = F_1^p(Q^2) - \frac{Q^2}{4m_B^2} F_2^p(Q^2) \tag{6.155}$$

where $m_B = m_N \approx M_{KK}$.

Equations (6.153) allows us to make very simple estimates.

(M1) **Proton charge and magnetic radii**:

$$r_{pe}{}^2 \equiv -6\ \frac{\mathrm{d}}{\mathrm{d}q^2}\left[\ln G_E(q^2)\right]\Big|_{q^2=0} \simeq (0.796\ \mathrm{fm})^2\,, \tag{6.156}$$

$$r_{pm}{}^2 \equiv -6\ \frac{\mathrm{d}}{\mathrm{d}q^2}\left[\ln G_M^p(q^2)\right]\Big|_{q^2=0} \simeq (0.744\ \mathrm{fm})^2\,. \tag{6.157}$$

These are to be compared with the experimental values

$$\tilde{r}_{pe}^{exp} = 0.895 \pm 0.018\ \mathrm{fm},\quad \tilde{r}_{pm}^{exp} = 0.855 \pm 0.035\ \mathrm{fm}. \tag{6.158}$$

Some comments are in order here.

We first note that both of the predicted radii are ~ 0.1 fm smaller than the experimental values. This deviation is in some sense expected since our estimate is reliable only when the number of colors and also the 't Hooft coupling λ are very large. In the SS model of QCD, the "core" radius of the nucleons

scales as $1/\sqrt{\lambda}$ and therefore the resulting core size $\Delta r \sim 0.1$ fm must be due to the subleading corrections, which are extremely difficult to estimate. What is noteworthy is that the core size which comes out to be ~ 0.4 fm when only the ground-state vector mesons are taken into account [Bijker and Iachello 2004], shrinks to ~ 0.1 fm in the presence of the tower of vector mesons, here encapsulated in the three higher-lying members. The full account of the tower may shrink the "core" size further with the higher tower playing the role of a major part of the intrinsic core or quark-bag degrees of freedom.

It appears that the underestimate of the root-mean-square radii, while static quantities, *e.g.*, magnetic moments, g_A *etc.* come out close to experimental values [Hong, Rho, Yee and Yi 2007a], is a generic feature of quenched approximations as noticed in quenched lattice calculations of vector and axial nucleon form factors [Sasaki and Yamazaki 2007].

(M2) **The ratio** $\mu_p G_E^p(Q^2)/G_M^p(Q^2)$:
We expect the ratios of form factors to be less sensitive than the form factors themselves to $1/N_c$ and $1/\lambda$ corrections and also to additional form factors representing asymptotic scaling which manifest themselves in the "core size." We therefore look at the ratio

$$R_1(Q^2) = \mu_p G_E^p(Q^2)/G_M^p(Q^2). \tag{6.159}$$

The result is plotted in Fig. 6.11 [Hong, Rho, Yee and Yi 2007c]. Given that the calculation is valid in the large N_c and λ limits and also in the chiral

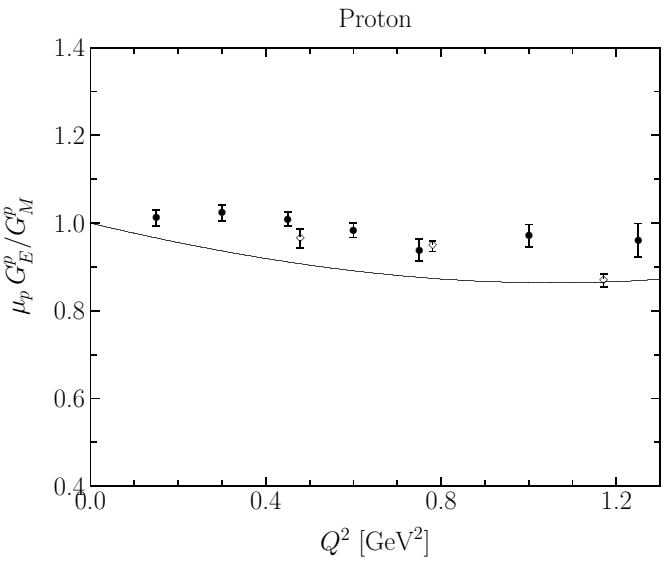

Fig. 6.11 The open circles are the polarization measurements at JLab and the filled circles are the data taken from Walker *et al.* The solid line is the prediction in the SS model.

limit, and above all that there are no free parameters, the agreement with experiments within, say, $\lesssim 10\%$ is quite surprising. However, the fact that the corrections cancel out largely in the ratio suggests that the R_1 belongs to the class of observables for which quenched approximations are applicable.

Other observables come out in agreement with nature within $\sim 10\%$ with the discrepancy readily understandable in terms of $1/N_c$ and $1/\lambda$ corrections [Hong, Rho, Yee and Yi 2007c].

6.6 Neutron Stars As Giant Skyrmions

If the skyrmion construction can access density high enough to describe the central density of neutron stars – not known phenomenologically since its determination can be done only indirectly, it could be used to make predictions for the properties of neutron stars. Such a skyrmion approach could provide certain insight into what the phenomenological Lagrangian approaches mostly employed in the field cannot offer. The advantages of the skyrmion description are:

- As shown above, the skyrmion structure can provide a natural "background" for excitations of the degrees of freedom – baryonic as well as mesonic, *e.g.*, pions, vector mesons *etc.* The intrinsic background dependence which plays an important role in triggering phase transitions in dense/hot matter is forced on them by the Wilsonian matching to QCD in HLS-type theory and tracks the vacuum changes caused by baryonic medium.
- One can systematically treat instabilities as density increases in mesonic channels, such as pseudo-Goldstone boson condensation.
- Change-over from the Nambu-Goldstone phase to the Wigner-Weyl phase, *i.e.* chiral restoration, can be treated in a way that is consistent for handling other instabilities that precede the chiral transition.

As of now, such an approach with the above advantages fully exploited for compact stars has not been developed. The main reason for this is that the theory is so constrained by the consistency conditions of chiral symmetry, large N_c and current quark masses *etc.* that it is difficult to carry out the full calculation that meets *all* the known requirements. We have discussed above the powerful aspect of the approach which on the one hand, provides a valuable insight into the structure of nuclear matter but on the other hand, makes a quantitative calculation difficult even for nuclear matter.

Broadly, two approaches to describing compact stars in terms of skyrmions have been discussed in the literature: (a) calculate the equation of state (EOS) of compact-star matter at high density using the skyrmion model and then insert the resulting EOS into the Tolman-Oppenheimer-Volkov (TOV) equation – as described in the next chapter, with the gravity entering in solving the TOV equation;

(b) couple the $B = \infty$ skyrmion to gravity and solve the resulting Einstein-Skyrme equation.

Neither avenue has been explored fully in the field. We will make only brief remarks on both.

6.6.1 *Skyrmion EOS*

The main property of the EOS that controls the structure of compact stars is how stiff or soft the EOS can be at a density relevant for the observed compact stars. To construct such an EOS, according to the thesis of this volume, one should take an HLS theory with a full account of relevant degrees of freedom, particularly those of vector mesons, to construct the skyrmion EOS. Such a construction is lacking. We saw above how the dense skyrmion matter in the Skyrme model can be constructed, but it has not been applied to compact stars. Therefore, it is not known what a realistic skyrmion EOS predicts for compact stars. What is available in the literature [Jaikumar and Ouyed 2006] is an EOS of an infinite matter consisting of $B = 1$ skyrmions interacting via coupling with the pions, the vector mesons ρ, ω and the dilaton χ associated with the trace anomaly of QCD. The mesonic degrees of freedom that figure in this approach are essentially the same as the ones used in the skyrmion lattice description of [Lee, Park, Rho and Vento 2003; Lee, Park, Min, Rho and Vento 2003]. However, there is a major difference in how the skyrmion structure is treated.

Although the reliability of the model is highly doubtful, one can learn from the results how to go about improving the approach. The EOS comes out to be quite stiff, even stiffer than the standard nuclear physics approach that is based on many-body interactions with phenomenological potentials (*e.g.*, the review by Heiselberg and Pandharipande [Heiselberg and Pandharipande 2000]). The stiffness allows the neutron star mass to be as heavy as $M \sim 3M\odot$. This result has been taken as a support for the recently reported neutron star mass of $M \gtrsim 2M_\odot$ [Nice *et al.* 2005] (on which we will comment in the next chapter). This conclusion cannot be taken too seriously, however. It is easy to see what could go wrong with this approach from what we have discussed so far. First of all, none of the advantages of the skyrmion description listed above is exploited in this treatment. Furthermore, this model is essentially the same as the (naive) Walecka linear mean field model with the nucleon treated as an elementary field with a partial and inadequate account of the intrinsic background (density) dependence crucial for a correct account of BR scaling. The repulsion, attributed mainly to the ω meson as in the Walecka model, is unrealistic as evidenced from the fact that in the *naive* Walecka linear mean-field model, chiral restoration transition cannot occur even at infinite density. The reason for this serious defect – which will be explained in the next chapter – is that the VM implied by HLS theory that requires the vector coupling g to drop at increasing density is missing in the model.

6.6.2 *Einstein-skyrmion star*

Instead of the $B = \infty$ skyrmion stabilized in the absence of gravity, or the matter composed of an infinite number of $B = 1$ skyrmions to be inserted into the TOV equation, one could consider a gravitating soliton from the action

$$S = \int_M d^4x\sqrt{-g}\left(\mathcal{L}_{sk} - \frac{R}{16\pi G}\right) \tag{6.160}$$

where $\mathcal{L}_{sk}$ is the Lagrangian for the skyrmion, R is the Ricci scalar and G is the Newton's constant. The idea is then to find a stable soliton configuration of this action and identify it as a compact star.

Such a model has been studied taking the Skyrme Lagrangian – with the pion field only – for $\mathcal{L}_{sk}$. What comes out of such a model, however, is found to be totally unsatisfactory, since the resulting properties of the soliton star are unnaturally sensitive to the soliton structure. For instance, different ansätze give drastically different results. If one takes the familiar hedgehog ansatz, usually picked for the $B = 1$ soliton, there are no stable solitons for $B \gg 1$. This result is not surprising since it is known that the hedgehog ansatz is unsuitable even for finite nuclei. Now if one takes the rational map ansatz which is found to give a more sensible description of nuclei at the classical level, then for baryon number corresponding to a typical neutron star, say, $B \sim 10^{58}$, the star radius comes out to be $\sim 10^{10}$ km [Piette and Probert 2007], while the typical neutron star radius is ~ 10 km. This looks totally absurd, and one may think that the notion of soliton star makes no sense. However, the authors of [Piette and Probert 2007] found that with only a mild modification of the rational map ansatz, it is possible to reduce the radius to a more sensible value, ~ 20 km.

It is clear that the whole issue on skyrmion stars is wide open. It was shown above that in the presence of vector mesons, in particular with the infinite tower, the mechanism for the soliton stabilization is drastically different from that of the Skyrme model. The Skyrme term plays no role for stabilization in the presence of even the lowest member of the tower of vector mesons. With the infinite tower encapsulated in the instanton configuration, it is the 5D Coulomb term that provides the necessary repulsion to prevent the collapse of the soliton. This suggests that the issue of stability and the mass/radius relation of the skyrmion stars could be totally different in holographic dual QCD.

Chapter 7

Hidden Local Symmetry In Hot/Dense Medium

This chapter is devoted to the application of the formalism developed in Chapter 5 to strongly interacting systems in heat bath and in dense medium. One of the outcomes most relevant to this volume will be a field-theoretic justification of Brown-Rho scaling described in detail in Chapter 8. We will first show how the structure of the theory is modified in hot/dense medium and then give applications to selected processes in heavy-ion physics, relegating (dense) compact star structure to Chapter 11. We will restrict the treatment mostly to $\mathrm{HLS}_{K=1}$ (with π, ρ and ω), and make extensions to generalized HLS, mostly $\mathrm{HLS}_{K=2}$ (with π, ρ, ω and a_1)[1], whenever we need other degrees of freedom. We shall have little to say on holographic dual QCD in hot/dense medium since this subject is at its infancy and nothing precise can be said at present. Unless otherwise specified, HLS will stand in this chapter for $\mathrm{HLS}_{K=1}$. Some of the quantities given in Chapter 5 will be redefined for convenience.

7.1 HLS in Heat Bath

We first treat hot medium and then turn to dense matter. The formalism is very similar for both cases.

7.1.1 *Vector manifestation at T_c*

Our first task is to show that in HLS theory, when a hadronic system is heated to temperature near the critical temperature where chiral symmetry is restored with $\langle\bar{q}q\rangle \to 0$, it is driven to the vector manifestation (VM) fixed point. The quantities we will study are the (flavor) gauge coupling constant g, the ratio of decay constants $a \equiv \frac{F_\sigma^2}{F_\pi^2}$ and the (physical) pion decay constant f_π (to be differentiated from the parametric constant F_π). In a matter at non-zero temperature or density, the reference frame is defined, so Lorentz invariance is broken, and each of these

[1] Although not treated explicitly, in the applications to hot/dense matter, a scalar denoted s or ϕ in this volume (σ in the literature) will be taken into consideration. This is somewhat *ad hoc* but could be justified in a more refined treatment of HLS.

quantities will consist of time component and space component which are different in general. To take into account this aspect of Lorentz non-invariance, one would have to carefully define relevant correlators in terms of different components. It turns, however, that near the chiral transition, the space and time components of the three quantities involved become equal to each other, that is, Lorentz invariance is *restored* at the critical point. We will show how this happens. This allows us to discuss the fixed-point structure driven by temperature in a Lorentz-invariant framework. Below, we shall first describe the Lorentz-invariant formulation and then justify the results in the non-Lorentz-invariant context.

7.1.2 *Lorentz-invariant formulas*

We start with Lorentz invariant *bare* HLS Lagrangian (5.23) or equivalently (5.25) in Chapter 5 with the parameters of the Lagrangian *intrinsically* dependent on temperature. The temperature dependence arises when the HLS correlators are matched to those of QCD at a certain matching scale since the QCD correlators involve gluon and quark condensates defined at a given temperature. Lorentz non-invariance introduces additional terms as described in the next subsection, but we simply pretend for the moment that they are not there except for the temperature dependence intrinsically embedded in the parameters of the Lagrangian from matching to QCD. We can then rewrite the correlators Eqs. (5.74) and (5.75) incorporating temperature dependence as

$$\begin{aligned} G_A^{(\mathrm{HLS})}(Q^2;T) &= \frac{F_\pi^2(\Lambda;T)}{Q^2} - 2z_2(\Lambda;T), \\ G_V^{(\mathrm{HLS})}(Q^2;T) &= \frac{F_\sigma^2(\Lambda;T)[1-2g^2(\Lambda;T)z_3(\Lambda;T)]}{{M_\rho}^2(\Lambda;T)+Q^2} - 2z_1(\Lambda;T) \end{aligned} \tag{7.1}$$

where Λ is the matching point, denoted Λ_M in the case in consideration, ${M_\rho}^2(\Lambda;T) = g^2(\Lambda;T)F_\sigma^2(\Lambda;T)$, and z_i's are $\mathcal{O}(p^4)$ counter terms as defined in Chapter 5. Matching the difference between the vector and axial-vector HLS correlators to that of QCD at the matching point $Q^2 = \Lambda_M^2$, we have

$$G_A^{(\mathrm{HLS})}(\Lambda_M;T) - G_V^{(\mathrm{HLS})}(\Lambda_M;T) \propto \frac{\langle\bar{q}q\rangle_T^2}{(\Lambda_M)^6}\,. \tag{7.2}$$

The simple result that the difference of the correlators is proportional to the square of the quark condensate holds at one loop order. Whether a relation of this type with the difference simply proportional to the quark condensate holds at higher loop orders is not yet settled, but the resulting vector manifestation fixed point can, however, be easily shown to be valid to *all* orders. In any case, the whole argument of HLS theory as developed in this volume crucially depends on this point. Another point which disturbs experts on QCD sum rules in matter is the approximation of the condensate of quartic quark fields, $\langle\bar{q}q\bar{q}q\rangle$, by the square of the

condensate of the bilinear quark fields, $\langle\bar{q}q\rangle^2$. The basic assumption, as mentioned in Chapter 5, that enters in the discussion is actually that

$$\langle\bar{q}q\bar{q}q\rangle \approx h\langle\bar{q}q\rangle^2 \tag{7.3}$$

where h is a non-negative constant, possibly dependent on temperature and/or density. As long as h is not much different from 1, there is no obstacle to the argument for the VM.

7.1.2.1 *Approaching the VM fixed point*

We wish now to see what happens as $T \to T_c$. The right-hand side of (7.2) vanishes since the condensate vanishes at chiral restoration. Now in order to see what happens to the left-hand side at T_c, we first have to know how F_π behaves near the critical temperature. As in free space, we match F_π's at the matching scale Λ_M and at T_c and get from Eq. (5.81) (for $N_c = 3$)

$$\frac{F_\pi^2(\Lambda_M;T_c)}{{\Lambda_M}^2} = \frac{1}{8\pi^2}\Big[1+\frac{\alpha_s}{\pi}+\frac{2\pi^2}{3}\frac{\langle\frac{\alpha_s}{\pi}G_{\mu\nu}G^{\mu\nu}\rangle_{T_c}}{{\Lambda_M}^4}\Big]\,. \tag{7.4}$$

We see that this cannot be zero. It is now easy to deduce from (7.2) that

$$g(\Lambda_M;T) \overset{T\to T_c}{\to} 0, \tag{7.5}$$

$$a(\Lambda_M;T) = F_\sigma^2(\Lambda;T)/F_\pi^2(\Lambda;T) \overset{T\to T_c}{\to} 1, \tag{7.6}$$

$$z_1(\Lambda_M;T) - z_2(\Lambda_M;T) \overset{T\to T_c}{\to} 0. \tag{7.7}$$

Now using the RGEs

$$\mu\frac{dg^2}{d\mu} \propto g^2,\ \mu\frac{da}{d\mu} \propto (a-1), \tag{7.8}$$

we conclude that $g = 0$ and $a = 1$ are the fixed point. Thus as $T \to T_c$, the system is driven to the vector manifestation fixed point $(g, a) = (0, 1)$ with $M_\rho^2 = ag^2F_\pi^2 = 0$.

7.1.2.2 *Pion decay constant*

Next we examine what happens to the (physical) pion decay constant at T_c. As noted above, the parametric $F_\pi(T_c)$ cannot be zero at any scale. This implies that if the physical pion decay constant (denoted f_π) is to go to zero at the critical temperature as befits the chiral symmetry order parameter, it must be the thermal loop corrections that cancel $F_\pi(T_c)$. The intrinsic temperature dependence alone sliding along, as the scale is varied, cannot do it.

As stressed in Chapter 5, in calculating the loop contributions for the pion decay constant, it is mandatory that the quadratic divergence that comes from the pion loop be taken into account [Harada and Yamawaki 2003]. In cutoff regularization

with the cutoff at Λ, the divergence goes like Λ^2. This must not be swept under the rug as is done when one naively uses dimensional regularization. Such quadratic divergence is also encountered in Nambu-Jona-Lasinio model for describing spontaneous symmetry breaking. In dimensional regularization, this corresponds to a divergence at $D = 4 - 2 = 2$ which needs to be subtracted. It featured crucially in Chapter 5 for chiral restoration at a critical number of flavors $N_f^c \sim 5$. The same reasoning can be applied in heat bath.

For the pion decay constant in heat bath, we need to compute the same loop graphs that enter in RGE for the free space value with, however, thermal propagators. There are no temperature-dependent counter terms. The calculation can be done in Matsubara (imaginary-time) formalism. Noting that near T_c, M_ρ can be taken to be much less than the temperature, one obtains a simple formula [Harada and Sasaki 2002],

$$f_\pi(T) \approx F_\pi^2(0;T) - \frac{N_f}{24}T^2 \quad \text{as} \quad T \to T_c \tag{7.9}$$

with

$$F_\pi^2(0;T) = F_\pi^2(\Lambda_M;T) - \frac{N_f^2}{2(4\pi)^2}(\Lambda_M)^2 \tag{7.10}$$

and from Eq. (5.81) for $N_c = 3$

$$F_\pi^2(\Lambda_M;T) = \frac{(\Lambda_M)^2}{8\pi^2}\left[1 + \frac{\alpha_s}{\pi} + \frac{2\pi^2}{3}\frac{\langle\frac{\alpha_s}{\pi}G^2\rangle_T}{(\Lambda_M)^4} + \frac{1408\pi}{9}\frac{\alpha_s\langle\bar{q}q\rangle_T^2}{(\Lambda_M)^6}\right]. \tag{7.11}$$

Now assuming that the left-hand side of (7.9) as the order parameter of chiral symmetry vanishes at $T = T_c$, we find

$$T_c^2 \approx \frac{24}{N_f}F_\pi^2(0;T_c). \tag{7.12}$$

This equation determines the critical temperature. With reasonable parameters for $N_f = 3$, this gives

$$T_c \approx 0.2 \text{ GeV}, \tag{7.13}$$

which is consistent with the phenomenological value $T_c \sim 175$ MeV and the lattice value 192 MeV.

7.1.2.3 *"Dropping mass"*

The next quantity we would like to look at is the ρ-meson (pole) mass as the temperature approaches T_c. Here we need to distinguish the *parametric mass* and the *pole mass*. The parametric mass $M_\rho = \sqrt{a}gF_\pi$ must go to zero linearly in g,

$$M_\rho \sim g \to 0. \tag{7.14}$$

This is because F_π does not go to zero at T_c. The parameter a varies little, say, from 2 to 1. Now what about the thermal loop contributions? In the limit that the parametric mass goes to zero as (7.14), the loop corrections go like $\sim T^2$, so the result for T near T_c is

$$\begin{aligned} m_\rho^2(T) &\approx M_\rho^2 + g^2 \frac{N_f}{2\pi^2} \frac{15 - a^2}{12} \frac{\pi^2}{6} T^2 \\ &\approx M_\rho^2 + \frac{7N_f}{72} g^2 T^2. \end{aligned} \tag{7.15}$$

We see therefore that both the parametric mass and the pole mass of the ρ-meson vanish proportionally to g. This is an important observation which plays a crucial role in discussing Brown-Rho scaling in Chapter 8.

7.1.2.4 *Width*

What happens to the ρ-meson width as the mass goes to zero? The answer to this question plays a key role in distinguishing the HLS theory with the vector manifestation (HLS/VM for short) from other models incorporating chiral symmetry: *very close to the critical temperature, the width must vanish faster than the mass, and hence the vector meson becomes even sharper closer to T_c than to $T = 0$.* The ρ-to-2π decay carries g^2 as long as there is phase space, so the natural width should go to zero as g^2. Furthermore the penetrability brings the m_ρ^3 factor, so the width must go like

$$\Gamma^\star/\Gamma \sim (\frac{m_\rho^\star}{m_\rho})^3 (\frac{g^\star}{g})^2 \sim (g^\star/g)^5 \ . \tag{7.16}$$

There is also what is called collisional width which cannot be computed in leading order in HLS theory without incorporating fermions. However in a HLS theory with fermions suitably incorporated, one expects the collisional width to also go as g^5. Thus, one arrives at the conclusion that the ρ-meson with its mass dropping to zero will be narrow-widthed near the chiral restoration regime. *This is a clear-cut prediction of the theory that is easily falsifiable by lattice or experiments.* This contrasts with the case at low temperature or low density where while the mass drops slightly, the width blows up instead due to many-body interactions [2] which are strong because of the strong coupling constant, *i.e.*, $g_{\pi NN} \gg 1$. We should stress that this would make it difficult to isolate and identify unambiguously the precursor for the dropping mass phenomenon at low temperature or density. It is only in the close vicinity of T_c that the dropping mass effect will be visible unambiguously. This observation applies also to dense matter.

[2] This blowing-up width has nothing obvious to do with change of chiral properties in medium. The phenomenological description of such behavior cannot be naively extended to temperature and/density where phase change can take place.

7.1.2.5 *Corrections from Lorentz non-invariance*

So far, we have simply ignored that Lorentz symmetry is broken in heat bath and dense medium. Here we discuss how the Lorentz symmetry breaking is manifested in what we have looked at above. To do this, it suffices to recognize that in medium, there is an additional four vector u^μ that represents breaking of Lorentz invariance due to the presence of the rest frame

$$u^\mu = (1, \vec{0}). \tag{7.17}$$

The presence of this vector gives rise to the tensor $u^\mu u^\nu$ in addition to $g^{\mu\nu}$. With these two tensors, the most general in-medium HLS Lagrangian can be systematically constructed [Harada, Kim and Rho 2002]

$$\begin{aligned}\tilde{\mathcal{L}} = &\left[(F^t_{\pi,\mathrm{bare}})^2 u_\mu u_\nu + F^t_{\pi,\mathrm{bare}} F^s_{\pi,\mathrm{bare}} (g_{\mu\nu} - u_\mu u_\nu)\right] \mathrm{Tr}\left[\hat{\alpha}^\mu_\perp \hat{\alpha}^\nu_\perp\right] \\ &+ \left[(F^t_{\sigma,\mathrm{bare}})^2 u_\mu u_\nu + F^t_{\sigma,\mathrm{bare}} F^s_{\sigma,\mathrm{bare}} (g_{\mu\nu} - u_\mu u_\nu)\right] \mathrm{Tr}\left[\hat{\alpha}^\mu_\parallel \hat{\alpha}^\nu_\parallel\right] \\ &+ \left[-\frac{1}{g^2_{L,\mathrm{bare}}} u_\mu u_\alpha g_{\nu\beta} - \frac{1}{2g^2_{T,\mathrm{bare}}} (g_{\mu\alpha} g_{\nu\beta} - 2u_\mu u_\alpha g_{\nu\beta})\right] \mathrm{Tr}\left[V^{\mu\nu} V^{\alpha\beta}\right] + \cdots .\end{aligned} \tag{7.18}$$

The subscript "bare" is added to show that it is a Lagrangian defined at the matching point. We have written here only the leading order terms, with the ellipses standing for higher derivative terms, chiral symmetry breaking (quark mass) terms *etc.* Below, to avoid overcrowding the subscripts we shall drop "bare" whenever there is no confusion. In (7.18), F^s_π (F^t_π) denotes the *parametric* spatial (temporal) pion decay constant and similarly $F^{s,t}_\sigma$ for the σ, and $V_{\mu\nu}$ is the field strength of V_μ. g_L and g_T correspond in medium, respectively, to the longitudinal and transverse components of the HLS gauge coupling g. We define the parametric π and σ velocities as

$$V^2_\pi = F^s_\pi / F^t_\pi, \qquad V^2_\sigma = F^s_\sigma / F^t_\sigma. \tag{7.19}$$

As explained in Chapter 5, the "bare" Lagrangian with which quantum corrections are to be computed is determined by matching HLS correlators to QCD ones. The difference in the present case is that the correlators are defined in medium, hence dependent on the background, *i.e.* temperature and density. The axial-vector and vector current correlators at the matching scale Λ_M, in other words, at the "bare level," are constructed in terms of "bare" parameters and consist of the longitudinal and transverse components:

$$G^{\mu\nu}_{A,V} = P^{\mu\nu}_L G^L_{A,V} + P^{\mu\nu}_T G^T_{A,V}, \tag{7.20}$$

where $P^{\mu\nu}_{L,T}$ are the longitudinal and transverse projection operators. The axial-vector current correlator in HLS at the matching scale Λ_M is given by the tree

graph given in terms of "bare" parameters [Harada, Kim and Rho 2002; Harada, Kim, Rho and Sasaki 2003]:

$$G^L_{A(\mathrm{HLS})}(p_0,\bar{p}) = \frac{p^2 F^t_\pi F^s_\pi}{-[p_0^2 - V_\pi^2 \bar{p}^2]} - 2p^2 z_2^L,$$
$$G^T_{A(\mathrm{HLS})}(p_0,\bar{p}) = -F^t_\pi F^s_\pi - 2\left(p_0^2 z_2^L - \bar{p}^2 z_2^T\right) \ , \tag{7.21}$$

where V_π is the bare pion velocity defined in (7.19), $V_\pi^2 = \frac{F^s_\pi}{F^t_\pi}$. The vector current correlators are written in a similar way:

$$G^L_{V(\mathrm{HLS})}(p_0,\bar{p}) = \frac{p^2\, F^t_\sigma F^s_\sigma \left(1 - 2g_L^2 z_3^L\right)}{-\left[p_0^2 - V_\sigma^2 \bar{p}^2 - M_\rho^2\right]} - 2p^2 z_1^L + \mathcal{O}(p^4) \ ,$$
$$G^T_{V(\mathrm{HLS})}(p_0,\bar{p}) = \frac{F^t_\sigma F^s_\sigma}{-\left[p_0^2 - V_T^2 \bar{p}^2 - M_\rho^2\right]}$$
$$\times \left[p_0^2\left(1 - 2g_L^2 z^L_{3,\mathrm{bare}}\right) - V_T^2 \bar{p}^2\left(1 - 2g_T^2 z_3^T\right)\right]$$
$$- 2\left(p_0^2 z_1^L - \bar{p}^2 z_1^T\right) + \mathcal{O}(p^4) \ . \tag{7.22}$$

In the above expressions, the bare vector meson mass in the rest frame, M_ρ, is of the form

$$M_\rho^2 \equiv g_L^2 F^t_\sigma F^s_\sigma \ , \tag{7.23}$$

the bare parameters for a^t and a^s are

$$a^t = \left(\frac{F^t_\sigma}{F^t_\pi}\right)^2, \quad a^s = \left(\frac{F^s_\sigma}{F^s_\pi}\right)^2, \tag{7.24}$$

and the bare σ and transverse ρ velocities,

$$V_\sigma^2 = \frac{F^s_\sigma}{F^t_\sigma}, \quad V_T^2 = \frac{g_L^2}{g_T^2}. \tag{7.25}$$

We should note here that, due to the Lorentz symmetry violation, two variables ξ_{L} and ξ_{R} included in the 1-forms $\hat{\alpha}^\mu_\perp$ and $\hat{\alpha}^\mu_\parallel$ in Eq. (7.18) are parameterized as

$$\xi_{\mathrm{L,R}} = e^{i\sigma/F^t_\sigma} e^{\mp i\pi/F^t_\pi} \ , \tag{7.26}$$

where $F^t_{\pi,\mathrm{bare}}$ and $F^t_{\sigma,\mathrm{bare}}$ are the bare parameters associated with the temporal decay constants of the pion and the σ. Note that it is the temporal components of the decay constants that figure in the chiral field (7.26) in heat bath.

To see that one gets the same fixed point as in the Lorentz-invariant case, one proceeds in two steps. First one shows that at the matching scale and as $T \to T_c$,

$$\begin{aligned} a^t &\to a^s \to 1, \\ g_L &\to g_T \to 0. \end{aligned} \tag{7.27}$$

Next one shows that at $T = T_c$, both a's and g's are renormalization-group invariant, so that the same conditions hold as one decimates down from the matching scale to the relevant scale.

The first step is easy to see. At the chiral restoration point, we expect that $G^L_{A(\mathrm{HLS})} = G^L_{V(\mathrm{HLS})}$ and $G^T_{A(\mathrm{HLS})} = G^T_{V(\mathrm{HLS})}$. These equalities must hold for any values of p_0 and $\bar{p}$ around the matching scale. Then (7.27) follows.

For the second step, first note that in medium, the vector meson field is normalized as

$$V_\mu = g_L \rho_\mu. \tag{7.28}$$

It is g_L that is involved. Now RGE for g implies that $g_L = 0$ is a fixed point. What is needed to be shown next is that given the $g_L = 0$ fixed point condition, $a^t = a^s = 1$ is also a fixed point. The argument for this demonstration is a bit involved requiring calculation of two-point functions at one loop order, so we won't go into it. See [Sasaki 2005] for details. The upshot of the calculation is that the $g_L = 0$ and $a^t = a^s = 1$ found at the matching scale and $T = T_c$ remain unrenormalized, that is, do not flow, as the scale is varied. Thus, the fixed point structure in Lorentz non-invariant case is identical to the fixed point structure in the Lorentz-invariant case.

It should be noted that as one approaches T_c, as $g_L \to 0$, the transverse vector meson at the critical point decouples, at any energy scale, from the vector current correlator. The VM condition for a^t and a^s leads to the equality between the π and σ velocities:

$$\begin{aligned} \left(V_\pi / V_\sigma\right)^4 &= \left(F^s_\pi F^t_\sigma / F^s_\sigma F^t_\pi\right)^2 \\ &= a^t / a^s \overset{T \to T_c}{\to} 1. \end{aligned} \tag{7.29}$$

This is easily understood from the point of view of the VM since the longitudinal vector meson becomes the chiral partner of the pion. We note that this condition $V_\sigma = V_\pi$ holds independently of the value of the bare pion velocity which is to be determined through the Wilsonian matching.

7.2 HLS in Dense Matter

In heat bath, we needed no fermionic degrees of freedom. Fermions do not figure in heat bath at zero chemical potential. In dense matter, however, we need them because density is supplied by fermions. Now in HLS theory with bosonic fields

only – which is a complete effective field theory by itself modeling QCD as seen in holographic dual QCD , baryons emerge as skyrmions. For dilute systems, this can be done by constructing skyrmions with the HLS Lagrangian as discussed in Chapter 5. As argued there, it should be possible to describe dense matter in the skyrmion framework and address chiral symmetry properties including Brown-Rho scaling. In doing so, however, the notion of the vector manifestation (VM) could not be exploited in a transparent way: A dilaton degree of freedom had to be introduced to simulate the VM effect in dense skyrmion matter [Park, Rho and Vento 2008]. In this section, our objective is to see that the VM fixed point is indeed reached also by density. Now the natural way of introducing fermions via topological excitations, *i.e.* skyrmions, faces a difficulty in that the fermionic degrees of freedom brought in by a skyrmion construction are baryons with integral topological charges which are not relevant degrees of freedom near the chiral restoration point. As in the high temperature case, near chiral restoration, the relevant degrees of freedom are more likely to be the quasiquarks or constituent quarks. Unfortunately we do not know how to generate quasiquarks as skyrmions. The idea that a quasiquark could be obtained as a colored soliton, named qualiton, was proposed by Kaplan in 1991 [Kaplan 1991], but it turns out that the qualiton is not a stable object [Frishman, Hanany and Karliner 1996], so generating quasiquarks from skyrmions appears to be problematic. The instability of such an object was also noticed in solitons built in NJL model [Alkofer, Song and Zahed 1991]. [3] Furthermore the half-skyrmion phase above the flash point described in Chapters 6 and 10 could play an important role.

In the absence of a more rigorous way of introducing quasiquarks (or any equivalent fermion degrees of freedom), we will simply incorporate them as 1/3-baryon-charge objects coupled (flavor) gauge invariantly to HLS fields.

7.2.1 *Dense HLS Lagrangian*

To introduce fermion degrees of freedom, we simply assume that near the chiral transition density approached from below, baryons turn into quasiquarks (or constituent quarks) which then figure in providing density.[4] Denoting the quasiquark field by ψ, we write the fermion part of the Lagrangian in leading order as

$$\begin{aligned}\delta\mathcal{L}_F &= \bar{\psi}(x)(iD_\mu\gamma^\mu - \mu\gamma^0 - m_q)\psi(x) \\ &\quad + \bar{\psi}(x)\left(\kappa\gamma^\mu\hat{\alpha}_{\parallel\mu}(x) + \lambda\gamma_5\gamma^\mu\hat{\alpha}_{\perp\mu}(x)\right)\psi(x) \end{aligned} \tag{7.30}$$

[3] We will see in Chapter 10 that the qualiton could be an *appropriate* degree of freedom at asymptotic density where color-flavor locking sets in. There the qualiton will emerge in a quark-hadron transmutation as a stable colorless excitation with an integer baryon charge.

[4] We should point out a caveat here to presage some of the serious consistency problems we will face later. For instance, in the chiral limit, the quasiquarks can become massless at the VM fixed point (discussed below). At that point, there are also massless pions. This means that there are too many massless degrees of freedom and hence the 't Hooft anomaly cancelation condition will not be satisfied. Now whether this is a serious defect or not is not clear. It deserves further considerations.

where m_q is the dynamical quark (quasiquark or constituent quark) mass, $D_\mu\psi = (\partial_\mu - ig\rho_\mu)\psi$ and κ and λ are constants to be specified later. $\hat{\alpha}_{\parallel\mu}$ and $\hat{\alpha}_{\perp\mu}$ are the covariantized Maurer-Cartan 1-forms defined in Chapter 5. The part of the Lagrangian that contains only HLS fields is simply that given by the usual HLS (5.23) and (7.30).

Consider matching at the scale Λ_M. In the background of non-zero density, the matching scale will depend upon density or chemical potential μ. We use the same notation as in the vacuum with the μ dependence understood. At the scale Λ_M, the correlators are given by tree contributions and hence by the usual HLS Lagrangian only. Since there is no flow, (7.30) which can figure only at loop order does not enter. Thanks to Lorentz symmetry, it suffices to replace the temperature T by the chemical potential μ in Eq. (7.1):

$$G_A^{(\mathrm{HLS})}(Q^2) = \frac{F_\pi^2(\Lambda_M;\mu)}{Q^2} - 2z_2(\Lambda_M;\mu)\,,$$

$$G_V^{(\mathrm{HLS})}(Q^2) = \frac{F_\sigma^2(\Lambda_M;\mu)\left[1 - 2g^2(\Lambda_M;\mu)z_3(\Lambda_M;\mu)\right]}{M_\rho^2(\Lambda_M;\mu) + Q^2} - 2z_1(\Lambda_M;\mu)\,. \qquad (7.31)$$

As was done above in heat bath, one matches these correlators to those of QCD given at fixed chemical potential μ and obtain the *bare* parameters of the HLS Lagrangian defined at scale Λ_M. Since the condensates of the QCD correlators are density dependent, the *bare* parameters of the Lagrangian must clearly be density dependent. This is completely analogous to the temperature case. This density dependence in the HLS sector that we referred to above as "intrinsic density dependence" can be understood in the following way. First of all, the matching scale Λ_M will have an intrinsic density dependence. Secondly, the degrees of freedom Φ_H lodged above the scale Λ_M which in full theory are in interactions with the nucleons in the Fermi sea will, when integrated out for EFT, leave their imprint of interactions – which is evidently density-dependent – in the coefficients of the Lagrangian.[5]

In the QCD correlators, going to the chiral-symmetry-restored phase with $\langle\bar{q}q\rangle_{\mu_c} = 0$ implies that at $\mathcal{M} = \Lambda_M$, [6]

$$G_V^{(QCD)}(Q^2;\mu_c) = G_A^{(QCD)}(Q^2;\mu_c) \qquad (7.32)$$

[5]Much like intrinsic temperature dependence, this "intrinsic density dependence" is generally absent in low loop-order calculations that employ effective Lagrangians whose parameters are fixed by comparing with experiments in the matter-free space. Much as in the temperature case, such theories lack the essential elements that drive the system to the VM fixed point at high density.

[6]In this part of the chapter, we reserve μ for chemical potential and denote renormalization scale by $\mathcal{M}$.

which implies by matching that

$$G_V^{(HLS)}(Q^2;\mu_c) = G_A^{(HLS)}(Q^2;\mu_c). \tag{7.33}$$

From (7.31) follows, in a complete parallel to the temperature case, that

$$\begin{aligned} &g(\Lambda_M;\mu) \underset{\mu\to\mu_c}{\longrightarrow} 0\ , \qquad a(\Lambda_M;\mu) \underset{\mu\to\mu_c}{\longrightarrow} 1\ , \\ &z_1(\Lambda_M;\mu) - z_2(\Lambda_M;\mu) \underset{\mu\to\mu_c}{\longrightarrow} 0\ . \end{aligned} \tag{7.34}$$

Note that this result imposes no condition for $F_\pi(\Lambda_M;\mu_c)$. This is again identical to what happens in temperature.

Given (7.34) at $\mu = \mu_c$, how the parameters vary as they flow to on-shell is governed by the RGEs. With the contribution from the fermion loops given by (7.30) added, the RGEs now read

$$\begin{aligned} \mathcal{M}\frac{dF_\pi^2}{d\mathcal{M}} &= C[3a^2g^2F_\pi^2 + 2(2-a)\mathcal{M}^2] - \frac{m_q^2}{2\pi^2}\lambda^2 N_c\,, \\ \mathcal{M}\frac{da}{d\mathcal{M}} &= -C(a-1)[3a(1+a)g^2 - (3a-1)\frac{\mathcal{M}^2}{F_\pi^2}] + a\frac{\lambda^2}{2\pi^2}\frac{m_q^2}{F_\pi^2}N_c\,, \\ \mathcal{M}\frac{dg^2}{d\mathcal{M}} &= -C\frac{87-a^2}{6}g^4 + \frac{N_c}{6\pi^2}g^4(1-\kappa)^2\,, \\ \mathcal{M}\frac{dm_q}{d\mathcal{M}} &= -\frac{m_q}{8\pi^2}[(C_\pi - C_\sigma)\mathcal{M}^2 - m_q^2(C_\pi - C_\sigma) + M_\rho^2 C_\sigma - 4C_\rho] \end{aligned} \tag{7.35}$$

where $C = N_f/\left[2(4\pi)^2\right]$ and

$$\begin{aligned} C_\pi &\equiv (\frac{\lambda}{F_\pi})^2\frac{N_f^2-1}{2N_f}\,, \\ C_\sigma &\equiv (\frac{\kappa}{F_\sigma})^2\frac{N_f^2-1}{2N_f}\,, \\ C_\rho &\equiv g^2(1-\kappa)^2\frac{N_f^2-1}{2N_f}. \end{aligned}$$

Quadratic divergences are present also in the fermion loop contributions as in the pion loops contributing to F_π. Note that since $m_q = 0$ is a fixed point, the fixed-point structure of the other parameters is not modified. Specifically, when $m_q = 0$, $(g,a) = (0,1)$ is a fixed point. Furthermore $X \equiv \frac{N_f}{2(4\pi)^2}\frac{\Lambda_M^2}{F_\pi^2(\Lambda_M)} = 1$ remains a fixed point. Therefore $(X^\star, a^\star, G^\star, m_q^\star) = (1,1,0,0)$ is the VM fixed point (where $G \equiv \frac{N_f}{2(4\pi)^2}g^2(\Lambda_M)$).

7.2.2 *Hadrons near $\mu = \mu_c$*

Let us see what the above result implies for hadrons near μ_c. To do this we define the in-medium on-shell quantities

$$\begin{aligned} &F_\pi = F_\pi(\mathcal{M}=0;\mu)\ , \\ &g = g\big(\mathcal{M}=M_\rho(\mu);\mu\big)\ , \quad a = a\big(\mathcal{M}=M_\rho(\mu);\mu\big)\ , \end{aligned} \tag{7.36}$$

where M_ρ is determined from the on-shell condition:

$$\begin{aligned} M_\rho^2 &= M_\rho^2(\mu) \\ &= a\big(\mathcal{M}=M_\rho(\mu);\mu\big) g^2\big(\mathcal{M}=M_\rho(\mu);\mu\big) F_\pi^2\big(\mathcal{M}=M_\rho(\mu);\mu\big). \end{aligned} \tag{7.37}$$

Then, the parameter M_ρ is renormalized in such a way that it becomes the pole mass at $\mu = 0$.

We first look at the "on-shell" pion decay constant f_π. At $\mu = \mu_c$, it is given by

$$f_\pi(\mu_c) \equiv f_\pi(\mathcal{M}=0;\mu_c) = F_\pi(0;\mu_c) + \Delta(\mu_c) \tag{7.38}$$

where Δ is dense hadronic contribution arising from fermion loops involving (7.30). It has been shown (see [Harada, Kim and Rho 2002]) that up to $\mathcal{O}(p^6)$ in the power counting, $\Delta(\mu_c) = 0$ at the fixed point $(g, a, m_q) = (0, 1, 0)$. Thus [7]

$$f_\pi(\mu_c) = F_\pi(0;\mu_c) = 0. \tag{7.39}$$

This may be taken as the signal for chiral symmetry restoration. Since

$$F_\pi^2(0;\mu_c) = F_\pi^2(\Lambda_M;\mu_c) - \frac{N_f}{2(4\pi)^2}\Lambda_M^2, \tag{7.40}$$

and at the matching scale Λ_M, $F_\pi^2(\Lambda_M;\mu_c)$ is given by a QCD correlator at $\mu = \mu_c$ – presumably measured on lattice, (7.39) – if taken at its face value – would allow μ_c to be computed from

$$F_\pi^2(\Lambda_M;\mu_c) = \frac{N_f}{2(4\pi)^2}\Lambda_M^2\ . \tag{7.41}$$

This is analogous to the formula (5.90) that holds for obtaining the critical number of flavors in free space. In order for this equation to have a solution at the critical density, it is found to be necessary that [Harada, Kim and Rho 2002]

$$F_\pi(\Lambda_M;\mu_c)/F_\pi(\Lambda_M;0) \approx \sqrt{3/5} \approx 0.77. \tag{7.42}$$

We do not have at present a reliable estimate of the density dependence of the QCD correlator to verify this condition, but the decrease of F_π of this order in medium looks quite reasonable as one can see as follows. For instance, one can deduce what

[7] Contrast $F_\pi(0;\mu_c) = 0$ to $F_\pi(0;T_c) \neq 0$. This difference may be an artifact of the ambiguity mentioned above in the role of quasiquarks in HLS theory.

the ratio is at nuclear matter density from deeply bound pionic states [Kienle and Yamazaki 2004]

$$f_\pi^*(n_0)/f_\pi \approx 0.81. \tag{7.43}$$

Since $F_\pi(\Lambda_M; n_0) \approx f_\pi^*(n_0)$, we see from Eqs. (7.42) and (7.43) that the scaling is nearly constant from the nuclear matter density to the chiral transition density. This observation will be used in calculating kaon condensation in compact star matter in Chapter 9.

Next we compute the ρ pole mass near μ_c. The calculation is straightforward, so we just quote the result. With the inclusion of the fermionic dense loop terms, the pole mass, for $M_\rho, m_q \ll k_F$ (where k_F is the Fermi momentum), is of the form

$$m_\rho^2(\mu) = M_\rho^2(\mu) + g^2\, G(\mu)\ , \tag{7.44}$$

$$G(\mu) = \frac{\mu^2}{2\pi^2}[\frac{1}{3}(1-\kappa)^2 + N_c(N_f c_{V1} + c_{V2})]\ . \tag{7.45}$$

At $\mu = \mu_c$, we have $g = 0$ and $a = 1$ so that $M_\rho(\mu) = 0$ and since $G(\mu_c)$ is non-singular, $m_\rho = 0$. Thus, the fate of the ρ meson at the critical density is as follows: *As μ_c is approached, the ρ becomes sharper and lighter with the mass vanishing at the critical point in the chiral limit.* The vector meson meets the same fate as at the critical temperature described in Sec. 7.1.

So far we have focused on the critical density at which the Wilsonian matching clearly determines $g = 0$ and $a = 1$ without knowing much about the details of the current correlators. Here we consider how the parameters flow as function of chemical potential μ. In low density region, we expect that the "intrinsic" density dependence of the bare parameters is small. If we ignore the intrinsic density effect, we may then resort to a theorem by Morley and Kislinger (MK) [Morley and Kislinger 1979] which states that given an RGE in terms of $\mathcal{M}$, one can simply trade in μ for $\mathcal{M}$ for dimensionless quantities and for dimensionful quantities with suitable calculable additional terms. The results are

$$\begin{aligned}
\mu\frac{dF_\pi^2}{d\mu} &= -2F_\pi^2 + C[3a^2g^2F_\pi^2 + 2(2-a)\mu^2] - \frac{m_q^2}{2\pi^2}\lambda^2 N_c \\
\mu\frac{da}{d\mu} &= -C(a-1)[3a(1+a)g^2 - (3a-1)\frac{\mu^2}{F_\pi^2}] + a\frac{\lambda^2}{2\pi^2}\frac{m_q^2}{F_\pi^2}N_c \\
\mu\frac{dg^2}{d\mu} &= -C\frac{87-a^2}{6}g^4 + \frac{N_c}{6\pi^2}g^4(1-\kappa)^2 \\
\mu\frac{dm_q}{d\mu} &= -m_q - \frac{m_q}{8\pi^2}[(C_\pi - C_\sigma)\mu^2 - m_q^2(C_\pi - C_\sigma) + M_\rho^2 C_\sigma - 4C_\rho]\ ,
\end{aligned} \tag{7.46}$$

where F_π, a, g, *etc.* are understood as $F_\pi(\mathcal{M} = \mu; \mu)$, $a(\mathcal{M} = \mu; \mu)$, $g(\mathcal{M} = \mu; \mu)$, and so on.

It should be stressed that the MK theorem supposedly applies in the given form to "fundamental theories" such as QED but not without modifications to effective

theories such as the one we are considering. The principal reason is that there is a change of relevant degrees of freedom from above Λ_M where QCD variables are relevant to below Λ_M where hadronic variables figure. Consequently, we do not expect Eq. (7.46) to apply in the vicinity of μ_c. Specifically, near the critical point, the *intrinsic density dependence* of the bare theory will become indispensable and the naive application of Eq. (7.46) should break down. One can see this clearly in the following example: The condition $g(\mathcal{M} = \mu_c; \mu_c) = 0$ that follows from the QCD-HLS matching condition, would imply, when (7.46) is naively applied, that $g(\mu) = 0$ for *all* μ. This is obviously incorrect. Therefore, near the critical density, the *intrinsic density dependence* must be included in the RGE: Noting that the RGE for the gauge coupling g in Eq. (7.46) is for $g(\mathcal{M} = \mu; \mu)$, we may write the RGE for g corrected by the *intrinsic density dependence* as

$$\mu\frac{d}{d\mu}g(\mu;\mu) \quad = \mathcal{M}\frac{\partial}{\partial\mathcal{M}}g(\mathcal{M};\mu)\bigg|_{\mathcal{M}=\mu} + \mu\frac{\partial}{\partial\mu}g(\mathcal{M};\mu)\bigg|_{\mathcal{M}=\mu}, \tag{7.47}$$

where the first term on the right-hand-side reproduces Eq. (7.46) and the second term appears due to the *intrinsic density dependence*. Note that $g = 0$ is a fixed point when the second term is neglected (this follows from (7.46)), so it is not obvious how it will remain a fixed point with the second term included. The μ dependence away from the critical density remains unknown. This is one important reason, among others, why dense matter is poorly understood even in HLS/VM theory. In view of the total lack of guide from lattice measurements, this makes the interpretation of some heavy-ion processes, *i.e.* dilepton production, which are affected by density and compact star properties difficult to assess as we will see below and in Chapters 8 and 10.

One can bypass some of the difficulties mentioned above in the vicinity of the critical point, however. The Wilsonian matching of the correlators at $\Lambda_M = \Lambda_\chi$ (where Λ_χ is the chiral symmetry scale ~ 1 GeV) allows one to see how the ρ mass scales very near the critical density as near the critical temperature. For this purpose, it suffices to look at the intrinsic density dependence of M_ρ. We find that close to μ_c

$$M_\rho^2(\Lambda;\mu) \sim \frac{\langle\bar{q}q(\mu)\rangle^2}{F_\pi^2(\Lambda;\mu)\Lambda^2} \tag{7.48}$$

which implies that

$$\frac{m_\rho^\star}{m_\rho} \sim \frac{\langle\bar{q}q\rangle^\star}{\langle\bar{q}q\rangle}. \tag{7.49}$$

Here the star denotes density dependence. Note that Eq. (7.49) is consistent with the "Nambu scaling" [Brown and Rho 2004b].

7.3 Hadronic Freedom

There is an important new concept we can develop as temperature or density goes near the critical point at which the gauge coupling g goes to zero as the vector manifestation predicts. In this section, we address the question as to what happens when a hot matter cools down from the critical temperature or a compressed matter is decompressed from the critical density. The latter is not very well understood, but there are indications from both lattice and experiments what might be happening in a hot matter. We shall discuss this matter in detail and make a brief comment on the problem of density later. What emerges is an interesting notion of "hadronic freedom."

In relativistic heavy ion processes at RHIC (and at ALICE/LHC in the future), one expects that hot (and dense) matter is produced at a temperature $T > T_c$ and then cools below T_c before the matter is detected in the laboratories. Now at T_c, the gauge coupling is zero and the vector mesons decouple, but what happens as the system cools will dictate much of what is observed in the detector. According to the recent lattice calculation [Cheng *et al.* 2006], the critical temperature is located at $T_c = 192$ MeV. In conjunction with results from RHIC experiments, we can locate the temperature at which hadrons in hot medium go nearly one shell, called "flash temperature," $T_{flash} \sim 120$ MeV. Thus, we envision that there is a region between T_{flash} and T_c where the vector manifestation would imply that the interactions will be weak. We call this region "hadronic freedom region."[8]

7.3.1 *Melting of "soft" glue and chiral restoration*

We can identify the region of hadronic freedom from lattice measurements of gluon condensate. We show in Fig. 7.1 the behavior of the gluon condensate $\langle G^2_{\mu\nu}\rangle$ in the presence of light dynamical quarks in heat bath as a function of temperature measured on lattice by Miller [Miller 2000; Miller 2007]. The result shows that the gluon condensate in the presence of dynamical quarks stays constant up to some temperature which we will call T_1 and then drops rapidly down to some $\langle G^2\rangle \neq 0$ as temperature reaches near the chiral restoration temperature T_c and then stays nonzero beyond above T_c. That roughly half of the gluon condensate remains condensed above T_c was first noticed on lattice in 1989 [Lee 1989]. This suggests that the gluon condensate be divided *roughly* into two components

$$\langle G^2\rangle_T = \langle G^2\rangle_T^{soft} + \langle G^2\rangle_T^{hard} \tag{7.50}$$

[8]The "hadronic freedom" that results from the gauge coupling going to zero at the ultraviolet should be distinguished from "asymptotic freedom" of QCD. The renormalization group equation for the hidden gauge coupling has an ultraviolet fixed point that resembles that of QCD. But the theory we are dealing with is an effective field theory defined up to the cutoff at the matching scale, whereas QCD – which is asymptotically free – is a renormalizable theory where the cutoff is to be sent off to infinity. What is meant here by "freedom" is that within the scale applicable to the effective theory, there is an ultraviolet fixed point at which the gauge interaction vanishes.

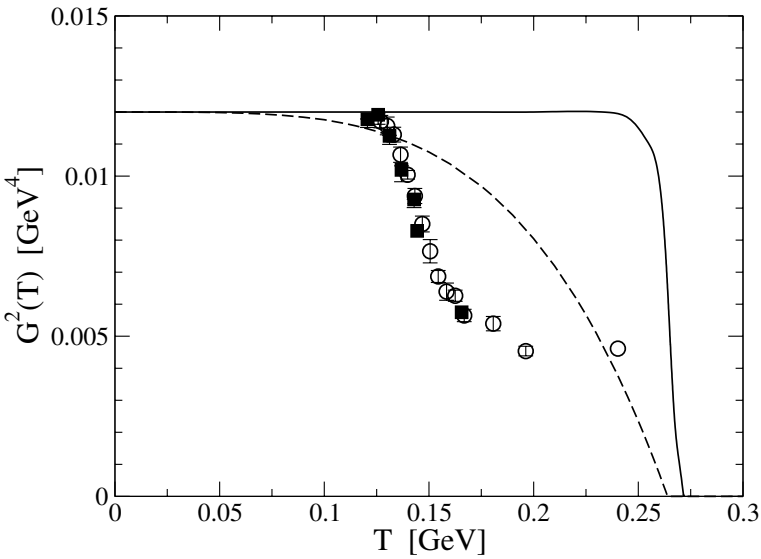

Fig. 7.1 $G^2(T)$ vs. T from [Miller 2000]. The lines show the gluon condensates for SU(3) (solid) and the ideal gluon gas (broken) in comparison with that of the light dynamical quarks denoted by the open circles and the heavier ones with filled squares. The error bars are included when significant. The physical units are for $G^2(T)$ [GeV^4] and T [GeV].

where the subscript "soft" and "hard" denote the scale of the condensate. This separation was found in Chapter 6 to be quite useful for constructing dense skyrmion matter. Here we can explicitly associate the hard component that remains condensed as one goes up across the critical temperature T_c, with an *explicit* breaking of scale invariance caused by the trace anomaly of QCD and the soft component to a *spontaneous* breaking of scale invariance. The dimensional transmutation of QCD implies that scale invariance remains broken until when the QCD gauge coupling constant goes to zero. What lattice result indicates is that at some temperature near T_c, the melting of the soft glue is locked to the unbreaking of spontaneous broken scale invariance.

To see more precisely what the above statement means, we look at the trace anomaly in heat bath in the chiral limit

$$\langle\theta^\mu_\mu\rangle \propto -g\left[\langle G^2\rangle_T^{soft} + \langle G^2\rangle_T^{hard}\right]. \tag{7.51}$$

As stated, it is believed that the scale symmetry is broken both explicitly by the trace anomaly *and* spontaneously by the vacuum. The hard and soft components pertain, respectively, to the former and to the latter. Normally with an internal continuous symmetry, the equation of motion is invariant under the

symmetry transformation and hence the corresponding symmetry current J_μ is conserved, *i.e.* $\partial_\mu J^\mu = 0$, regardless of whether the symmetry is spontaneously broken or unbroken. Spontaneous breaking of conformal symmetry, however, manifests itself quite differently because the symmetry can be spontaneously broken *only if* it is broken explicitly [Freund and Nambu 1968; Zumino 1970]. What this means is that the effective potential contains both a component which spontaneously breaks *both* chiral invariance and scale invariance and a component which is chiral invariant but scale non-invariant. The first term of (7.51) corresponds to the former and the second to the latter. One may want to associate the first component with the divergence of a dilatation current D_μ but note that unlike internal symmetries, its divergence cannot be zero because it is a part of the trace of energy-momentum tensor which gets contribution from the spontaneous breaking. It is this intricate locking between the explicit breaking and the spontaneous breaking that leads to this unusual relation.

What we are arguing is that it is the first component of the trace anomaly (7.51) which melts at T_c in Miller's lattice calculation and hence tracks the properties of chiral symmetry. This is in fact the reasoning for dense medium used in [Brown and Rho 1991] to derive BR scaling in terms of an interpolating dilaton field χ. This point – much misinterpreted in the literature, *e.g.*, [Birse 1994]), – will be made clearer in Chapter 8.

Our important point in relation to heavy-ion observables is that the temperature at which the soft glue starts melting be identified as the flash temperature, mentioned above, defined as follows. The flash point is defined [Shuryak and Brown 2003] as the temperature at which going down from the critical temperature, the ρ meson gets 90% on its mass shell and at which the ρ meson starts decaying into two pions. It was determined from the STAR data that this corresponds to a temperature ~ 120 MeV. One can see that this is roughly where the soft glue starts melting in Miller's lattice data, *i.e.* $T_1 \approx T_{flash}$. We therefore associate this point with the point at which chiral symmetry "starts" being restored as temperature increased.

We are now equipped with the terminologies to define precisely what we mean by *hadronic freedom*. We see in the lattice result that the soft glue melts very quickly after the flash point. We associate this with the rapid drop of the hidden gauge coupling constant from T_{flash} to T_c. Since interactions in HLS theory are governed by the gauge coupling constant, this implies that interactions diminish quickly within the temperature range. For simplicity, we will simply assume that they are negligible.

7.4 Applications

The HLS formalism developed above in medium gives extremely simple and unambiguous predictions in hot and dense medium which differ in a distinctive way from the standard sigma model scenario. They should be readily verifiable or fal-

sifiable. At the time of writing of this volume, none has been checked in either directions. Here, we discuss a few examples in temperature and in density to give one an idea where things stand. We cannot yet make a detailed comparison with available heavy-ion data.

7.4.1 *Pion velocity near critical temperature T_c*

There are several quantities measured in laboratory experiments and lattice simulations that can be eventually checked against. Here we treat the pion velocity. Since Lorentz invariance is broken in a heat bath, the relevant Lagrangian is (7.18) which we reproduce here for convenience:

$$\begin{aligned}\tilde{\mathcal{L}} = &\left[(F^t_{\pi,\mathrm{bare}})^2 u_\mu u_\nu + F^t_{\pi,\mathrm{bare}} F^s_{\pi,\mathrm{bare}} \left(g_{\mu\nu} - u_\mu u_\nu\right)\right] \mathrm{tr}\left[\hat{\alpha}^\mu_\perp \hat{\alpha}^\nu_\perp\right] \\ &+ \left[(F^t_{\sigma,\mathrm{bare}})^2 u_\mu u_\nu + F^t_{\sigma,\mathrm{bare}} F^s_{\sigma,\mathrm{bare}} \left(g_{\mu\nu} - u_\mu u_\nu\right)\right] \mathrm{tr}\left[\hat{\alpha}^\mu_\parallel \hat{\alpha}^\nu_\parallel\right] \\ &+ \left[-\frac{1}{g^2_{L,\mathrm{bare}}} u_\mu u_\alpha g_{\nu\beta} - \frac{1}{2g^2_{T,\mathrm{bare}}} \left(g_{\mu\alpha} g_{\nu\beta} - 2u_\mu u_\alpha g_{\nu\beta}\right)\right] \mathrm{tr}\left[V^{\mu\nu} V^{\alpha\beta}\right] + \cdots \,,\end{aligned} \tag{7.52}$$

with the parameters to be determined at the matching point by matching the HLS correlators to the QCD ones. We recall here that, due to the Lorentz symmetry violation, two variables ξ_L and ξ_R included in the 1-forms $\hat{\alpha}^\mu_\perp$ and $\hat{\alpha}^\mu_\parallel$ in Eq. (7.52) are parameterized as

$$\xi_{\mathrm{L,R}} = e^{i\sigma/F^t_\sigma} e^{\mp i\pi/F^t_\pi} \,. \tag{7.53}$$

We also need the terms of $\mathcal{O}(p^4)$ for the present analysis:

$$\bar{\mathcal{L}}_{z_2} = \left[2z^L_{2,\mathrm{bare}} u_\mu u_\nu g_{\nu\beta} + z^T_{2,\mathrm{bare}} \left(g_{\mu\alpha} g_{\nu\beta} - 2u_\mu u_\alpha g_{\nu\beta}\right)\right] \mathrm{tr}\left[\hat{\mathcal{A}}^{\mu\nu} \hat{\mathcal{A}}^{\alpha\beta}\right] \,, \tag{7.54}$$

where the parameters $z^L_{2,\mathrm{bare}}$ and $z^T_{2,\mathrm{bare}}$ are the in-medium counterparts of the vacuum parameter $z_{2,\mathrm{bare}}$ and likewise for $\hat{\mathcal{A}}^{\mu\nu}$ defined in Chapter 5.

As stated before, the approach to the chiral restoration point should be characterized by the equality between the axial-vector and vector current correlators in QCD, $G_A - G_V \to 0$ for $T \to T_c$. The EFT should satisfy this also for any values of p_0 and $\bar{p}$ near matching point provided the following conditions are met: $(g_{L,\mathrm{bare}}, g_{T,\mathrm{bare}}, a^t_{\mathrm{bare}}, a^s_{\mathrm{bare}}) \to (0,0,1,1)$ for $T \to T_c$. As in dense medium, this implies that at the tree or bare level, the longitudinal mode of the vector meson

becomes the real NG boson and couples to the vector current correlator, while the transverse mode decouples. A non-renormalization theorem by Sasaki [Sasaki 2004] shows that $(g_L, a^t, a^s) = (0, 1, 1)$ is a fixed point of the RGEs satisfied at any energy scale. Thus, the VM condition is given by

$$(g_L, a^t, a^s) \to (0, 1, 1) \quad \text{for} \quad T \to T_c. \tag{7.55}$$

The VM condition for a^t and a^s leads to the equality between the π and σ (*i.e.* longitudinal vector meson) velocities:

$$\left(V_\pi/V_\sigma\right)^4 \equiv \left(F_\pi^s F_\sigma^t / F_\sigma^s F_\pi^t\right)^2 = a^t/a^s \overset{T\to T_c}{\to} 1. \tag{7.56}$$

This is easy to understand in the VM scenario since the longitudinal vector meson becomes the chiral partner of the pion. This equality holds at T_c whatever the value of the bare pion velocity obtained at the matching point.

7.4.1.1 *Standard sigma model scenario*

Before we get into the discussion on HLS predictions, it is instructive to see what we can expect in chiral models without the light vector-meson degrees of freedom. Here, the basic assumption is that near chiral restoration, there is no instability in the channel of the degrees of freedom that have been integrated out. In this pion-only case, the appropriate effective Lagrangian for the axial correlators is the in-medium chiral Lagrangian dominated by the current algebra terms, [9]

$$\mathcal{L}_{eff} = \frac{f_\pi^{t\,2}}{4}\left(\mathrm{Tr}\nabla_0 U \nabla_0 U^\dagger - v_\pi^2 \mathrm{Tr}\partial_i U \partial_i U^\dagger\right) - \frac{1}{2}\kappa \mathrm{ReTr} M^\dagger U + \cdots \tag{7.57}$$

where v_π is the pion velocity, M is the mass matrix introduced as an external field, U is the standard chiral field, κ is a dimension-3 object related to the light-quark condensate that we do not need to specify, and the covariant derivative $\nabla_0 U$ is given by $\nabla_0 U = \partial_0 U - \frac{i}{2}\mu_A(\tau_3 U + U\tau_3)$ with μ_A the axial isospin chemical potential. As usual, the ellipses stand for higher order terms in spatial derivatives and covariant derivatives.

The quantities that we need to study are the vector isospin susceptibility (VSUS) χ_V and the axial-vector isospin susceptibility (ASUS) χ_A defined in terms of the vector charge density $J_a^0(x)$ and the axial-vector charge density $J_{5a}^0(x)$ by the Euclidean correlators:

$$\delta_{ab}\chi_V = \int_0^{1/T} d\tau \int d^3\vec{x} \langle J_a^0(\tau, \vec{x}) J_b^0(0, \vec{0})\rangle_\beta, \tag{7.58}$$

$$\delta_{ab}\chi_A = \int_0^{1/T} d\tau \int d^3\vec{x} \langle J_{5a}^0(\tau, \vec{x}) J_{5b}^0(0, \vec{0})\rangle_\beta \tag{7.59}$$

[9] Here we need not make distinction between f_π (physical pion decay constant) and F_π (parametric pion decay constant).

where $\langle\ \rangle_\beta$ denotes thermal average and

$$J_a^0 \equiv \bar{\psi}\gamma^0\frac{\tau^a}{2}\psi, \quad J_{5a}^0 \equiv \bar{\psi}\gamma^0\gamma^5\frac{\tau^a}{2}\psi \tag{7.60}$$

with the quark field ψ and the τ^a Pauli matrix the generator of the flavor $SU(2)$. Given the effective action described by (7.57) *with possible non-local terms ignored*, then the axial susceptibility (ASUS) takes the simple form

$$\chi_A = -\frac{\partial^2}{\partial\mu_A^2}\mathcal{L}_{eff}|_{\mu_A=0} = {f_\pi^t}^2. \tag{7.61}$$

The principal point to note here is that *as long as the effective action is given by local terms (subsumed in the ellipses) involving the U field, this is the whole story*: There is no other contribution to the ASUS than the temporal component of the pion decay constant.

Next one assumes that at the chiral phase transition point $T = T_c$, the restoration of chiral symmetry dictates the equality

$$\chi_A = \chi_V. \tag{7.62}$$

While there is no lattice information on χ_A, χ_V has been measured as a function of temperature [Gottlieb *et al.* 1987; Brown and Rho 1996]. In particular, it is established that

$$\chi_V|_{T=T_c} \neq 0, \tag{7.63}$$

which leads to the conclusion that

$$f_\pi^t|_{T=T_c} \neq 0. \tag{7.64}$$

On the other hand, it is expected – and confirmed by lattice simulations – that the space component of the pion decay constant f_π^s should vanish at $T = T_c$. One therefore arrives at

$$v_\pi^2 \sim f_\pi^s/f_\pi^t \to 0, \quad T \to T_c. \tag{7.65}$$

This is the main conclusion of the standard chiral theory [Son and Stephanov 2002].

What this means physically is as follows. The pole mass of the pion m_π^p in a heat bath is related to the screening mass m_π^s via ${m_\pi^p}^2 = v_\pi^2({m_\pi^s}^2 + \vec{k}^2)$. Thus, the vanishing of the pole mass would imply in this scenario the vanishing of the pion velocity. In some sense, this result would indicate a maximal violation of Lorentz invariance.

To check whether this prediction is free of caveat, let us see what one obtains for the VSUS when one applies the same reasoning to the vector correlators. The effective Lagrangian for calculating the vector correlators is of the same form as the ASUS, Eq. (7.57), except that the covariant derivative is now defined with the vector isospin chemical potential μ_V as $\nabla_0 U = \partial_0 U - \frac{1}{2}\mu_V(\tau_3 U - U\tau_3)$. Now if one

assumes as was done above for χ_A that possible *non-local terms* can be dropped, then the SUS is given by

$$\chi_V = -\frac{\partial^2}{\partial \mu_V^2}\mathcal{L}_{eff}|_{\mu_V=0} \tag{7.66}$$

which can be easily evaluated from the Lagrangian. One finds that

$$\chi_V = 0 \tag{7.67}$$

for all temperature. While it is expected to be zero at $T = 0$, the vanishing χ_V for $T \neq 0$ is at variance with the lattice data at $T = T_c$. This gives a warning to the pitfall of the simple result obtained for the ASUS.

The sigma model prediction (7.65) can be simply understood from the fact that in the absence of other degrees of freedom, χ_A is directly related to the f_π^t and χ_A is equal to χ_V at the chiral restoration point. Since χ_V is seen to be nonzero, f_π^t does not vanish at T_c, whereas the space component f_π^s does. Now one can ask why χ_A should be given entirely by f_π^T at T_c. There is no reason why there should not be some additional contributions to χ_A than f_π^t. Indeed, this is the defect of the pion-only sigma model scenario. We will see below that when the ρ meson goes massless at T_c, the longitudinal component of the ρ meson contributes to χ_A on the same footing as the π, and hence the observation that the non-vanishing of χ_V implies non-vanishing of f_π^t is invalidated. We will see below that this is because the contribution of massless vector mesons cannot be approximated in a localized form.

7.4.1.2 *HLS/VM scenario*

In the presence of the ρ meson in HLS, it comes out that $(f_\pi^t, f_\pi^s) \to (0, 0)$ and $\chi_A \to \chi_V \neq 0$ as $T \to T_c$. For this we should start with (7.18) and work with broken Lorentz invariance. This means that we have to consider the condensates like $\bar{q}\gamma_\mu D_\nu q$ in the current correlators. It turns out, however, as we will detail later, that in HLS/VM theory, such invariance breaking appears as a small correction compared with the main term of $1+\frac{\alpha_s}{\pi}$ in the Lorentz invariant matching condition

$$\frac{F_\pi^2(\Lambda)}{\Lambda^2} = \frac{1}{8\pi^2}\left(\frac{N_c}{3}\right)\left[1 + \frac{3(N_c^2-1)}{8N_c}\frac{\alpha_s}{\pi} + \frac{2\pi^2}{N_c}\frac{\left\langle \frac{\alpha_s}{\pi} G_{\mu\nu}G^{\mu\nu}\right\rangle}{\Lambda^4} + \frac{288\pi(N_c^2-1)}{N_c^3}\left(\frac{1}{2}+\frac{1}{3N_c}\right)\frac{\alpha_s\left\langle\bar{q}q\right\rangle^2}{\Lambda^6}\right]. \tag{7.68}$$

This implies that the difference between $F^t_{\pi,\mathrm{bare}}$ and $F^s_{\pi,\mathrm{bare}}$ is small compared with their own values, or equivalently, the bare π velocity defined by $V^2_{\pi,\mathrm{bare}} \equiv F^s_{\pi,\mathrm{bare}}/F^t_{\pi,\mathrm{bare}}$ is close to one. We will give an estimate of the correction to this bare pion velocity later.

Now, given the result that $V_{\pi,\mathrm{bare}} = 1$, we need to compute the quantum corrections so as to compare with nature. Here, Sasaki's non-renormalization theorem [Sasaki 2004] comes to help. The argument for the theorem goes as follows. At $T \ll T_c$, the pion velocity – denoted v_π for physical quantity – receives hadronic thermal correction from the pion field, of the form

$$v_\pi^2(T) \simeq V_\pi^2 - N_f \frac{2\pi^2}{15} \frac{T^4}{(F_\pi^t)^2 M_\rho^2} \quad \text{for} \quad T < T_c. \tag{7.69}$$

Here, the longitudinal component of the ρ field (called σ in this volume) is suppressed by the Boltzmann factor $\exp[-M_\rho/T]$, and hence only the pion loop contributes to the pion velocity. Now approach T_c. Then the vector meson mass drops toward zero due to the VM and the Boltzmann factor $\exp[-M_\rho/T]$ is no longer a suppression factor. Thus, at tree order, the contribution from the longitudinal vector meson (σ) exactly cancels the pion contribution. Similarly, the quantum correction generated from the pion loop is exactly canceled by that from the σ loop. Accordingly, we conclude

$$v_\pi(T) = V_{\pi,\mathrm{bare}}(T) \qquad \text{for} \quad T \to T_c. \tag{7.70}$$

In sum, the pion velocity in the limit $T \to T_c$ is protected by the VM against both quantum and hadronic loop corrections at one loop order [Sasaki 2004]. This implies that $(g_L, a^t, a^s, V_\pi) = (0, 1, 1, \text{any})$ forms a fixed line for four RGEs of g_L, a^t, a^s and V_π. When a point on this fixed line is selected through the matching procedure (this is explained in detail in [Harada, Kim, Rho and Sasaki 2004]), that is to say when the value of $V_{\pi,\mathrm{bare}}$ is fixed, the present result implies that the point does not move in a subspace of the parameters. Approaching the chiral symmetry restoration point, the physical pion velocity itself will flow to the fixed point.

Let us now discuss corrections due to the breaking of Lorentz invariance to the bare pion velocity. To define the language for this issue, we need the definitions of the vector and axial-vector correlators in heat bath

$$G_A^{\mu\nu}(p_0 = i\omega_n, \vec{p}; T)\delta_{ab} = \int_0^{1/T} d\tau \int d^3\vec{x} e^{-i(\vec{p}\cdot\vec{x} + \omega_n \tau)} \left\langle J_{5a}^\mu(\tau, \vec{x}) J_{5b}^\nu(0, \vec{0}) \right\rangle_\beta , \tag{7.71}$$

$$G_V^{\mu\nu}(p_0 = i\omega_n, \vec{p}; T)\delta_{ab} = \int_0^{1/T} d\tau \int d^3\vec{x} e^{-i(\vec{p}\cdot\vec{x} + \omega_n \tau)} \left\langle J_a^\mu(\tau, \vec{x}) J_b^\nu(0, \vec{0}) \right\rangle_\beta \tag{7.72}$$

where $\omega_n = 2n\pi T$ is the Matsubara frequency, $(a, b) = 1, \ldots, N_f^2 - 1$ denotes the flavor index and $\langle\ \rangle_\beta$ the thermal average. The correlators for Minkowski momentum are obtained by the analytic continuation of p_0.

For calculating the pion velocity, we only need to focus on the axial-vector correlator. We decompose it into

$$G_A^{\mu\nu}(q_0, \vec{q}) = q^2 P_L^{\mu\nu} G_A^L(q_0, \bar{q}) + q^2 P_T^{\mu\nu} G_A^T(q_0, \bar{q}) \ , \tag{7.73}$$

where $\bar{q} = |\vec{q}|$ and the polarization tensors are given by

$$\begin{aligned} P_T^{\mu\nu} &\equiv g_i^\mu \left(\delta_{ij} - \frac{q_i q_j}{\bar{q}^2}\right) g_j^\nu \\ &= (g^{\mu\alpha} - u^\mu u^\alpha)\left(-g_{\alpha\beta} - \frac{q^\alpha q^\beta}{\bar{q}^2}\right)(g^{\beta\nu} - u^\beta u^\nu) \ , \\ P_L^{\mu\nu} &\equiv -\left(g^{\mu\nu} - \frac{q^\mu q^\nu}{q^2}\right) - P_T^{\mu\nu}. \end{aligned} \tag{7.74}$$

As we now know, the bare Lagrangian is determined at the matching scale Λ_M through the matching and is expressed in terms of the bare parameters as the sum of Eqs. (7.52) and (7.54). From this bare Lagrangian, the current correlator at the matching scale is constructed as follows:

$$\begin{aligned} G^L_{A(\mathrm{HLS})}(q_0, \bar{q}) &= \frac{F^t_{\pi,\mathrm{bare}} F^s_{\pi,\mathrm{bare}}}{-[q_0^2 - V^2_{\pi,\mathrm{bare}}\bar{q}^2]} - 2z^L_{2,\mathrm{bare}} \ , \\ G^T_{A(\mathrm{HLS})}(q_0, \bar{q}) &= -\frac{F^t_{\pi,\mathrm{bare}} F^s_{\pi,\mathrm{bare}}}{q^2} - 2\frac{q_0^2 z^L_{2,\mathrm{bare}} - \bar{q}^2 z^T_{2,\mathrm{bare}}}{q^2} \ , \end{aligned} \tag{7.75}$$

where $V^2_{\pi,\mathrm{bare}} = F^s_{\pi,\mathrm{bare}}/F^t_{\pi,\mathrm{bare}}$ is the bare pion velocity defined above. For matching with the QCD correlators, it is convenient to expand $G_A^{(\mathrm{HLS})L}$ in Eq. (7.75) in terms of $\bar{q}^2/(-q^2)$:

$$G_A^{(\mathrm{HLS})L(0)}(-q^2) = \frac{F^t_{\pi,\mathrm{bare}} F^s_{\pi,\mathrm{bare}}}{-q^2} - 2z^L_{2,\mathrm{bare}} \ , \tag{7.76}$$

$$G_A^{(\mathrm{HLS})L(1)}(-q^2) = \frac{F^t_{\pi,\mathrm{bare}} F^s_{\pi,\mathrm{bare}}(1 - V^2_{\pi,\mathrm{bare}})}{(-q^2)^2}. \tag{7.77}$$

Calculating the QCD correlators in heat bath at the scale Λ_M is more involved because of the loss of Lorentz invariance. Here the analysis relies heavily on what has been done in the calculation of QCD sum rules in medium which we avoid going into as the discussion is quite complicated and unilluminating. The object that enters is the thermal expectation value of tensors of dimension d and twist $\tau = d - s$ (where $s = 2k$ is the spin), *i.e.* $A^{2k+\tau,\tau}_{\mu_1\cdots\mu_{2k}}$ and $C^{2k+\tau,\tau}_{\mu_1\cdots\mu_{2k}}$ *etc.* Of particular importance for the deviation from Lorentz invariance is with $d = 6$ and $\tau = 2$, *e.g.*,

$$A^{6,2}_{\mu_1\mu_2\mu_3\mu_4} = i\left\langle \mathcal{S}T\left(\bar{q}\gamma_{\mu_1} D_{\mu_2} D_{\mu_3} D_{\mu_4} q\right)\right\rangle_\rho \ , \tag{7.78}$$

where $\mathcal{S}T$ stands for making the operators symmetric and traceless with respect to the Lorentz indices.

Now the higher the twist, the more power-suppressed the tensors are. So the approximation is to take the lowest twist terms, *i.e.* $\tau = 2$. Then only $A^{6,2}_{\mu_1\mu_2\mu_3\mu_4}$ need to be considered. Unfortunately, there is no direct QCD information on this quantity, so it has to be evaluated with a model. This makes the result highly model dependent. The usual approximation is to use dilute gas picture with light mesons

taken into account. At low temperature, the pion gas picture is reasonable in which case one finds that

$$A^{6,2(\pi)}_{\alpha\beta\lambda\sigma} = \Big[p_\alpha p_\beta p_\lambda p_\sigma - \frac{p^2}{8}\big(p_\alpha p_\beta g_{\lambda\sigma} + p_\alpha p_\lambda g_{\beta\sigma} + p_\alpha p_\sigma g_{\lambda\beta} + p_\beta p_\lambda g_{\alpha\sigma} + p_\beta p_\sigma g_{\alpha\lambda} + p_\lambda p_\sigma g_{\alpha\beta}\big) + \frac{p^4}{48}\big(g_{\alpha\beta}g_{\lambda\sigma} + g_{\alpha\lambda}g_{\beta\sigma} + g_{\alpha\sigma}g_{\beta\lambda}\big)\Big] A^\pi_4 \ , \tag{7.79}$$

where A^π_4 carries the temperature dependence. With $m^2_\pi = 0$ in the chiral limit, the terms with p^2 and p^4 in Eq. (7.79) drop out. Now we make an assumption that goes with the VM scenario, that is, as $T \to T_c$ from below, since the σ (the longitudinal component of the ρ) joins the pion, the ρ also contributes as

$$A^\rho_4|_{T_c} \simeq A^\pi_4|_{T_c}. \tag{7.80}$$

In terms of this, the deviation from the velocity of light at the bare level is

$$\delta_{bare} = 1 - V^2_{\pi,bare} \propto \frac{T^6}{\Lambda^6_M} A^{\rho+\pi}_4. \tag{7.81}$$

As is made clear in the discussion, a precise calculation of δ cannot be made at the present stage of development. A rough calculation taking reasonable ranges of QCD parameters, $\Lambda_M = 0.8 - 1.1\,\mathrm{GeV}$, $\Lambda_{QCD} = 0.30 - 0.45\,\mathrm{GeV}$ and the range of critical temperature $T_c = 0.15 - 0.20\,\mathrm{GeV}$, we get

$$\delta_{\mathrm{bare}}(T_c) = 0.0061 - 0.29\,, \tag{7.82}$$

where the Λ_M dependence of $A^\pi_{2,4}$ is ignored as it is expected to be suppressed by more than $1/\Lambda^6_M$. Thus, we find the *bare* pion velocity to be close to the speed of light:

$$0.71 \lessapprox V_{\pi,\mathrm{bare}}(T_c) \lessapprox 0.99\,. \tag{7.83}$$

Now, invoking Sasaki's non-renormalization theorem [Sasaki 2004] which is applicable here as well, *i.e.* $v_\pi(T_c) = V_{\pi,\mathrm{bare}}(T_c)$, we arrive at the physical pion velocity at chiral restoration:

$$0.71 \lessapprox v_\pi(T_c) \lessapprox 0.99 \tag{7.84}$$

which differs definitely from the pion-only sigma model prediction $v_\pi(T_c) \simeq 0$.

7.4.1.3 *Measuring the pion velocity near T_c*

The drastic difference in predictions for v_π near T_c between the sigma model scenario, $v_\pi \sim 0$ and the HLS/VM scenario, $v_\pi \sim 1$ should be testable by experiments or lattice calculations. In fact this issue has been addressed in connection with a HBT puzzle found in the STAR data at RHIC [Cramer, Miller, Wu and Yoon 2005] which measured the momentum correlations between two pions emitted from 200 GeV Au+Au collisions. The pions were supposed to be emitted from a hot matter

in the chirally restored state and hence carry information about the pion dispersion relation in that state. The dispersion relation presumably gives information on the pion pole mass which could be related in the pion rest frame to the pion velocity v_π times the pion screening mass m_π^{screen}. Knowing what the pion screening mass is at T_c, one may be able to extract the pion velocity. The analysis in [Cramer, Miller, Wu and Yoon 2005] is inconclusive as to whether v_π is near zero as predicted in the standard sigma model scenario or near 1 as predicted by the HLS/VM scenario. More work is needed to rule out one of the two alternatives.

7.4.2 *Vector and axial vector susceptibilities near critical temperature T_c*

To see better what makes the HLS/VM scenario so different from the sigma model scenario, let us look in more detail at both the axial-vector susceptibility (ASUS) and the vector susceptibility (VSUS) in Minkowski space. In terms of the axial

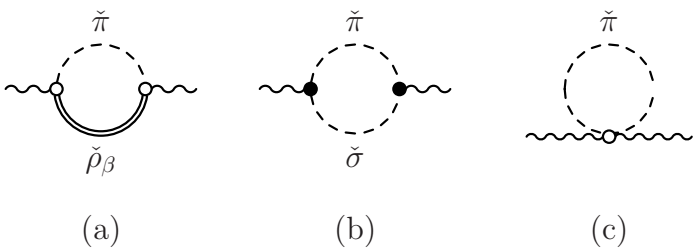

Fig. 7.2 Feynman diagrams contributing to the $\overline{\mathcal{A}}_\mu$-$\overline{\mathcal{A}}_\nu$ two-point function. Here $\check{\pi}$ represents the quantum pion field and likewise for the others.

correlator (7.71) and the vector correlator (7.72), the ASUS and VSUS for non-singlet currents in the static, *i.e.* low-momentum, limit are given as

$$\begin{aligned}\chi_A(T) &= 2N_f \lim_{\vec{p}\to 0}\lim_{p_0\to 0}\left[G_A^{00}(p_0,\vec{p};T)\right] \ , \\ \chi_V(T) &= 2N_f \lim_{\vec{p}\to 0}\lim_{p_0\to 0}\left[G_V^{00}(p_0,\vec{p};T)\right] \ ,\end{aligned} \tag{7.85}$$

where we have included the normalization factor of $2N_f$. Computing the correlators involves two-point functions up to one-loop order. The one-loop graphs for the axial vector-axial vector two-point functions are given in Fig. 7.2, and those for the vector-vector two-point functions in Fig. 7.3. The calculations go through the same steps as in the cases discussed above, though it is rather involved to compute the graphs.

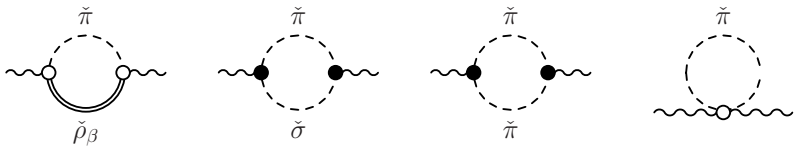

Fig. 7.3 Feynman diagrams contributing to the $\overline{\mathcal{V}}_\mu$-$\overline{\mathcal{V}}_\nu$ two-point function. Same symbols as Fig. 7.2.

The results can be summarized in the form

$$\chi_A(T) = 2N_f F_\pi^2(T;0) + A(M_\rho(T), a(T) : T),$$
$$\chi_V(T) = B(M_\rho(T), a(T) : T) \tag{7.86}$$

where A and B are complicated functions involving the two-point functions of the diagrams in Figs. 7.2 and 7.3 and $F_\pi^2 = F_\pi^s F_\pi^t$. The complicated functions A and B simplify enormously when both $M_\rho \to 0$ and $a \to 1$ as one approaches the vector manifestation fixed point $(M_\rho, a) = (0, 1)$,

$$A \to \frac{N_f^2}{12} T^2,$$
$$B \to \frac{N_f^2}{6} T^2. \tag{7.87}$$

So at $T = T_c$,

$$\chi_A(T_c) = 2N_f f_\pi^2(T_c) + \frac{N_f^2}{6} T_C^2, \tag{7.88}$$

$$\chi_V(T_c) = \frac{N_f^2}{6} T_c^2. \tag{7.89}$$

In writing (7.88), we have used the relations Eqs. (7.9) to (7.11) to bring in the physical pion decay constant at T_c which is zero, so one sees from (7.89) that

$$\chi_A(T_c) = \chi_V(T_c) = \frac{N_f^2}{6} T_c^2. \tag{7.90}$$

There are two notable points in these results. The first is that unlike in the standard sigma model where χ_A is proportional to f_π^t, χ_A has two terms, one the pion decay constant $f_\pi = \sqrt{f_\pi^s f_\pi^t}$ which goes to zero and the other additional loop correction from the σ – the longitudinal component of the ρ meson – which does not vanish. Thus, χ_A has a non-zero value which has nothing to do with f_π^t. This means that the ρ going massless has a crucial contribution to the ASUS, particularly at

T_c. This is the major difference from the standard sigma model scenario where the possibility of the massless ρ contributing is ignored.

The next point is that χ_V is measured in lattice [Gottlieb *et al.* 1987]. The prediction (7.90) is consistent with the available value of [Gottlieb *et al.* 1987]. Unfortunately, however, the susceptibility must be quite sensitive to the quark mass and the result of [Gottlieb *et al.* 1987] is obtained in quenched and heavy-quark approximation. Thus, it may not make sense to compare the prediction made in the chiral limit and the lattice data. Also on the theoretical side, as pointed out above, there is a serious caveat and that has to do with the possible degrees of freedom associated with quasiquarks. In fact, the HLS/VM theory assumes that the relevant degrees of freedom are the pion and the ρ (and ω). Suppose that there are constituent quarks or quasiquarks with mass above some temperature, say, the flash temperature introduced above in the vicinity of T_c. Their mass must be small so as to contribute to the susceptibility. Their contribution at one loop order is found to be $\chi_V^{quasiquark}|_{T_C} \simeq \frac{N_f N_c}{3} T_c^2$. This is substantial and cannot be ignored if the quasiquarks do enter in the picture. Lattice calculation in the chiral limit or HLS/VM calculation with massive quarks will be needed for the test of the prediction.

7.4.3 *Spectral function of the ρ meson*

One would like to be able to "see" experimentally, directly or indirectly, how hadrons behave in hot and/or dense medium. The ultimate goal here would be to expose the effect of chiral symmetry in the guise of critical opalescence in an environment provided by terrestrial laboratories. Since both hot matter and dense matter are produced by strong interactions, the most prominent tool being relativistic heavy ion collision,[10] one needs probes that do not suffer interactions in transporting information. The natural probe for this is thought to be the photon. Perhaps neutrinos could be used for that purpose but, for the moment, this is not yet feasible. Thus, dileptons have been exploited as possible "snapshots" of the properties of hadrons propagating in hot and/or dense medium, supposedly unencumbered by final-state interactions. Measurements have been made at SPS/CERN, RHIC and JLab to extract the ρ spectral function that is supposed to carry the needed information. We will give arguments, though without going into details, that this intuitive idea at its naive level is most likely incorrect. Even so, the spectral function is a theoretically well-defined quantity and can be calculated in HLS/VM.

We consider the spectral function for $T \neq 0$ and $n = 0$. The density effect has not been systematically worked out in a consistent approach, so we can say practically nothing as to what density does to the spectral function.. The first careful study of the spectral function in the ρ meson channel in HLS was carried out by Harada and Sasaki [Harada and Sasaki 2006]. We will restrict our discussions to this approach,

[10] Producing dense medium with strangeness flavor will be discussed in Chapter 9.

although there have been numerous papers giving thermal spectral functions in various phenomenological models including both temperature and density.

7.4.3.1 *$\rho\pi\pi$ and $\gamma\pi\pi$ couplings in hot medium and violation of vector dominance*

In order to address the problem of the spectral function, it is useful to look at the EM form factor of the pion in medium. Here we consider the medium at a finite temperature T. The crucial ingredient for this analysis is the *intrinsic* temperature dependence explained in detail in Section 7.1.2. Here we review the quantities relevant to the problem to recall the essential points.

The "bare" parameters of the effective Lagrangian, *i.e.* HLS, are determined by integrating out high frequency modes above the matching scale. When those degrees of freedom are integrated out in hot (and/or dense) medium, the bare parameters must necessarily be dependent on temperature (and/or density). This is intuitively obvious since those degrees of freedom, *i.e.* hadrons, have an internal structure composed of quarks and gluons [Harada and Yamawaki 2001; Harada, Kim and Rho 2002]. It will turn out that these *intrinsic temperature/density effects* play more important roles in higher temperature/density region than thermal/dense loop effects, especially near the phase transition point.

Within the matching scheme, the intrinsic dependence is determined once one has information on the quark and gluon condensates as a function of temperature (and/or density) and the running QCD coupling constant. The condensates could ultimately be calculated on lattice. However, they are not yet available in specific forms. What one can do at present is to infer from presently available lattice and experimental data, though they are far from complete.

First, we recall that near T_c where the VM is applicable, we can write the difference between the vector and axial-vector correlators in the form

$$G_A^{(\mathrm{HLS})}(Q^2) - G_V^{(\mathrm{HLS})}(Q^2) \simeq g^2(\Lambda;T)\left(\frac{F_\pi^2(\Lambda;T)}{\Lambda^2}\right)^2 - (a(\Lambda)-1)\,\frac{F_\pi^2(\Lambda;T)}{\Lambda^2}$$
$$+2g^2(\Lambda;T)\,z_3(\Lambda;T)\,\frac{F_\pi^2(\Lambda;T)}{\Lambda^2} - 2\left(z_2(\Lambda;T) - z_1(\Lambda;T)\right)\ . \tag{7.91}$$

Near T_c, this implies [Harada and Sasaki 2002; Harada and Sasaki 2004],

$$\begin{aligned} &g^2(\Lambda;T) \propto \langle\bar{q}q\rangle_T^2 \\ &a(\Lambda;T) - 1 \propto \langle\bar{q}q\rangle_T^2 \quad \text{for } T \simeq T_c\,. \end{aligned} \tag{7.92}$$

This shows that the bare parameters evolve in temperature as the quark condensate does, thus manifesting the property of chiral symmetry of the "vacuum." However, this reasoning applies only very near the VM point.

To interpolate the intrinsic dependence between $T = 0$ and near $T = T_c$, we rely on the lattice data on gluon condensate of Miller [Miller 2007]. In [Brown, Lee and Rho 2005; Brown, Holt, Lee and Rho 2006], these lattice data were interpreted as

indicating that up to what we call flash temperature T_{flash}, the soft glue remains unmelted and hence the intrinsic temperature dependence can be ignored. The temperature effect then will be entirely accounted for by hadronic thermal corrections. Only above the T_{flash} does the soft glue start to melt with the VM behavior, *i.e.* BR scaling, becoming applicable. The above features can be summarized as

$$\begin{aligned} &\text{For } T < T_{flash} \quad \begin{cases} g(\Lambda;T) = (\text{constant}) \\ a(\Lambda;T) - 1 = (\text{constant}) \end{cases} \\ &\text{For } T > T_{flash} \quad \begin{cases} g(\Lambda;T) \propto \langle \bar{q}q \rangle_T \\ a(\Lambda;T) - 1 \propto \langle \bar{q}q \rangle_T^2 \ . \end{cases} \end{aligned} \tag{7.93}$$

We follow Harada and Sasaki [Harada and Sasaki 2006], assuming that the quark condensate scales as $(T_c - T)^{1/2}$ as one finds in the mean field approximation, to write the temperature dependence of the bare g and a as

$$\begin{aligned} g(\Lambda;T) &= \theta(T_{flash} - T) g(\Lambda;T=0) \\ &\quad + \theta(T - T_{flash}) g(\Lambda;T=0) \left(1 - \frac{T^2 - T_{flash}^2}{T_c^2 - T_{fash}^2}\right)^{1/2} , \\ a(\Lambda;T) &= \theta(T_{flash} - T) a(\Lambda;T=0) + \theta(T - T_{flash}) \\ &\quad \times \left[1 + \{a(\Lambda;T=0) - 1\} \left(1 - \frac{T^2 - T_{flash}^2}{T_c^2 - T_{flash}^2}\right)\right] , \end{aligned} \tag{7.94}$$

where θ is the step function. We will ignore possible temperature dependence of the matching scale Λ in hot matter. Since the Wilsonian matching conditions do not indicate substantial temperature dependence on the ratio $F_\pi(\Lambda;T)/\Lambda$ as well as on the parameter $z_3(\Lambda;T)$, we may assume that the bare z_3 and bare F_π do not have any significant T dependence:

$$\begin{aligned} z_3(\Lambda;T) &\simeq z_3(\Lambda;0) , \\ F_\pi(\Lambda;T) &\simeq F_\pi(\Lambda;0) . \end{aligned} \tag{7.95}$$

In order to compute physical quantities, we need to bring the scale in the parameters from the matching scale $\mu = \Lambda$ at which they are determined to the physical scale where the measurement is made. This quantum renormalization effect is given by the renormalization group equations computed at one-loop order in [Harada and Yamawaki 2003]. This (quantum) effect provides the temperature dependent pa-

rameters at the physical scale

$$\begin{aligned}
\bar{g} &= g(\mu = m_\rho; T)\,, \\
\bar{a} &= a(\mu = m_\rho; T)\,, \\
\bar{z}_3 &= z_3(\mu = m_\rho; T)\,, \\
\bar{F}_\pi &= F_\pi(\mu = 0; T)\,, \\
\bar{F}_\sigma &= \sqrt{\bar{a}} F_\pi(\mu = m_\rho; T)\,, \\
\bar{M}_\rho &= \bar{g}\bar{F}_\sigma\,.
\end{aligned} \tag{7.96}$$

Here the bar indicates renormalized quantity. Next one computes thermal loop effects with these parameters. The loop terms give corrections to the vector mass in the form

$$\begin{aligned}
m_\rho^2(T) = \bar{M}_\rho^2 + N_f \bar{g}^2 \Big[&-\frac{\bar{a}^2}{12} G_2(\bar{M}_\rho; T) \\
&+ \frac{5}{4} J_1^2(\bar{M}_\rho; T) + \frac{33}{16} \bar{M}_\rho^2 F_3^2(\bar{M}_\rho; \bar{M}_\rho; T) \Big]\,,
\end{aligned} \tag{7.97}$$

where m_ρ is defined at the rest frame of the ρ meson, $p_\mu = (m_\rho, \vec{0})$ [11] and to the pion decay constants as

$$\begin{aligned}
(f_\pi^t(T))^2 &= \bar{F}_\pi^2 - N_f \left[I_2(T) - \frac{\bar{a}}{\bar{M}_\rho^2} (I_4(T) - J_1^4(\bar{M}_\rho; T)) \right]\,, \\
f_\pi^t(T) f_\pi^s(T) &= \bar{F}_\pi^2 - N_f \left[I_2(T) + a \left\{ \frac{1}{3\bar{M}_\rho^2} (I_4(T) - J_1^4(\bar{M}_\rho; T)) - J_1^2(\bar{M}_\rho; T) \right\} \right]\,.
\end{aligned} \tag{7.98}$$

The functions J, G, F and I are listed in the Appendix of [Harada and Sasaki 2006].

For a numerical analysis, as in [Harada and Sasaki 2006], one takes $T_c = 170\,\mathrm{MeV}$ and $T_f = 0.7\,T_c$ as proposed in [Brown, Lee and Rho 2005; Brown, Lee and Rho 2006]. The bare parameters of the HLS Lagrangian at $T = 0$ via the Wilsonian matching for $\Lambda_{\mathrm{QCD}} = 0.4\,\mathrm{GeV}$ and $\Lambda = 1.1\,\mathrm{GeV}$ ($N_c = 3$ and $N_f = 3$) as prescribed in [Harada and Yamawaki 2003] are summarized in Table 7.1.

We are now ready to show the results.

It turns out that to one-loop order, there are no hadronic thermal loop contributions to the $\rho\pi\pi$ and $\gamma\pi\pi$ couplings appearing in the imaginary part of the photon propagator, so

[11] In medium the full vector meson propagator consists of the longitudinal and transverse parts, D_L and D_T. These two components of the vector meson mass defined as the pole positions of D_L and D_T are identical at rest frame.

Table 7.1 Input parameters. The values listed in the second line are fixed by performing the Wilsonian matching at $T = 0$ with $\langle\bar{q}q\rangle_{1\text{GeV}} = -(0.25)^3$ GeV^3 and $\langle\frac{\alpha_s}{\pi}G_{\mu\nu}G^{\mu\nu}\rangle = 0.012$ GeV^4.

f_π [GeV]	m_ρ [GeV]	Λ_{QCD} [GeV]	Λ [GeV]
0.09246	0.7758	0.4	1.1
$F_\pi(\Lambda)$ [GeV]	$a(\Lambda)$	$g(\Lambda)$	$z_3(\Lambda)\times 10^3$
0.149	1.31	3.63	-2.55
m_π [GeV]	T_c [GeV]	T_f	—
0.13957	0.17	$0.7\,T_c$	—

$$\bar{g}_{\rho\pi\pi}(T) = \bar{g}\,\frac{\bar{a}(0)}{2}\,, \tag{7.99}$$

$$\bar{g}_{\gamma\pi\pi}(T) = 1 - \frac{\bar{a}(0)}{2}\,. \tag{7.100}$$

where $\bar{a}(0)$ is defined as

$$\bar{a}(0) = \frac{\bar{F}_\sigma^2}{\bar{F}_\pi^2}\,. \tag{7.101}$$

Thus, these two coupling constants essentially run in temperature by the intrinsic effect.

In Fig. 7.4 is given the schematic temperature dependence of $\bar{g}_{\rho\pi\pi}(T)$ and $\bar{g}_{\gamma\pi\pi}(T)$. It is easy to understand the rapid drop of the parametric $\rho\pi\pi$ coupling $\bar{g}_{\rho\pi\pi}$ above the flash temperature in Fig. 7.4(a). It is caused by the dropping of the gauge coupling proportionally to the drop of the quark condensate – which is the intrinsic effect. Fig. 7.4(b) shows the violation of VD as the temperature increases. In the temperature region below the flash temperature $\bar{g}_{\gamma\pi\pi}$ is almost zero with $a \approx 2$. But above the flash temperature, the parameter $\bar{a}(0)$ starts to decrease from 2 to 1 due to the intrinsic effect as given in Eq. (7.94). This causes an increase of $\bar{g}_{\gamma\pi\pi}$ toward 1/2, thereby leading to the strong violation of the VD. We would like to see what the above two effects do to the pionic form factor and the ρ spectral function.

7.4.3.2 *EM form factor of the pion and the ρ spectral function*

The first we would like to know is what happens to the EM coupling to hadrons when the temperature effects are taken into account. The most well-studied quantity is the EM form factor of the pion where the vector dominance works remarkably well in matter-free space.[12] The leading corrections are depicted in Fig. 7.5. The figure (a) represents the direct photon coupling to the pion and the figure (b) via the vector meson ρ. In terms of HLS parameters, the first comes multiplied by the factor $(a-2)/2$ and the second by the factor $a/2$. Thus, in free space with

[12] Perhaps accidentally as remarked in the preceding chapter.

$a = 2$, the direct coupling vanishes, leaving the second term that is mediated by the ρ exchange. This is the well-known vector dominance (VD). On the other hand, when the VM fixed point is arrived at, $a \to 1$, and then the VD is violated with the direct coupling coming with the same weight as the vector-mediated term. We showed above that as the temperature exceeds the flash temperature, a quickly approaches 1 with an obvious consequence on the pionic form factor.

Let us first see how well HLS theory can reproduce in free space the pionic form factor and to what extent the VD is exact. The parameters of the bare Lagrangian were determined by the Wilsonian matching with, as the inputs, the ρ mass $m_\rho = 775.8$ MeV and the pion decay constant $f_\pi = 92.46$ MeV. The resulting bare parameters are [Harada and Yamawaki 2003]

$$\begin{aligned} a(0) &= 1.94\,, \\ g(m_\rho) &= 6.02\,, \\ z_3(m_\rho) &= -3.87 \times 10^{-3}\,, \end{aligned} \tag{7.102}$$

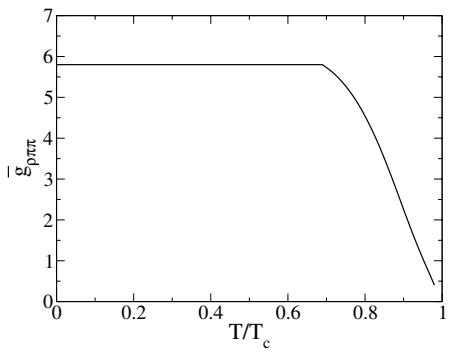

(a)

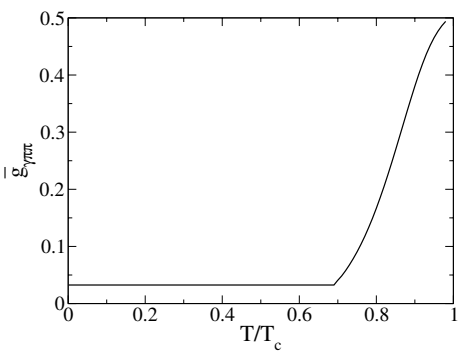

(b)

Fig. 7.4 Temperature dependence of (a) the parametric $\rho\pi\pi$ coupling $\bar{g}_{\rho\pi\pi}$ and (b) the parametric direct-$\gamma\pi\pi$ coupling $\bar{g}_{\gamma\pi\pi}$.

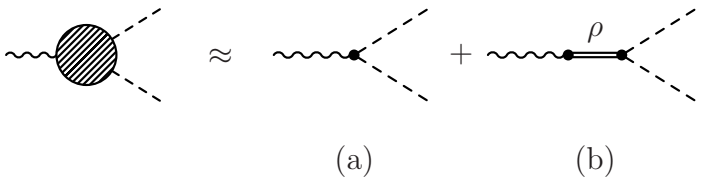

Fig. 7.5 Leading contributions to the electromagnetic form factor of the pion. (a) direct $\gamma\pi\pi$ and (b) $\gamma\pi\pi$ mediated by ρ-meson exchange.

for the QCD scale $\Lambda_{\rm QCD} = 0.4\,\text{GeV}$ and the matching scale $\Lambda_M = 1.1\,\text{GeV}$. Note that the value for $a(0)$ close to 2 indicates that in this theory the form factor is very close to a perfect VD. The prediction – in the sense that there is no free parameter – for the time-like regime is given in Fig. 7.6.[13]

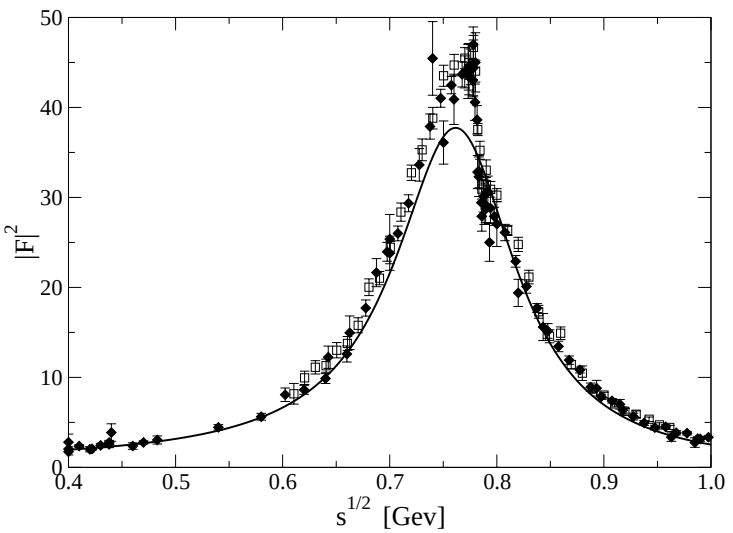

Fig. 7.6 Time-like electromagnetic form factor of the pion as a function of the invariant mass $\sqrt{s}$ at zero temperature. The solid curve is the parameter-free prediction of the theory. From [Harada and Sasaki 2006] (copyright 2006 by the APS).

Let us next see what one can say about the pionic form factor in hot medium. This problem is closely connected with the spectral function of the ρ meson in

[13]The extra peak at the ω invariant mass observed in the experiments is missing because here the $\rho - \omega$ mixing is not taken into account. This can be readily improved.

medium which is a controversial subject of study in unraveling how chiral symmetry manifests itself at high temperature and/or density. Here we will be concerned with what the EFT theory within the well-defined framework of the $\mathrm{HLS}_{K=1}$ predicts for the spectral function. Confronting dilepton data in relativistic heavy ion collisions requires a lot more work which will involve taking into account not only straightforward (and mundane) many-body effects but also the experimental conditions. We shall eschew doing this for the reason given below.

The relevant quantity for both the pion form factor and the spectral function is the imaginary part of the photon propagator at temperature T, $\Pi(s;T)$, where s is the invariant mass of the dilepton to which the ρ decays, $s = M^2$. The pionic form factor $\mathcal{F}(s;T)$ is related to $\mathrm{Im}\Pi(s;T)$ by

$$\mathrm{Im}\Pi(s;T) = \frac{1}{6\pi\sqrt{s}}\left(\frac{s-4m_\pi^2}{4}\right)^{3/2}|\mathcal{F}(s;T)|^2\,, \tag{7.103}$$

with the pion mass m_π. The differential dilepton production rate integrated over the photon three-momentum is related to the same by

$$\frac{dN}{ds}(s;T) = \int \frac{d^3\vec{q}}{2q_0}\frac{dN}{d^4q}(q_0,\vec{q};T)\,, \tag{7.104}$$

with $q_0 = \sqrt{\vec{q}^2+M^2}$, where

$$\frac{dN}{d^4q}(q_0,\vec{q};T) = \frac{\alpha^2}{\pi^3 M^2}\frac{1}{e^{q_0/T}-1}\mathrm{Im}\Pi(q_0,\vec{q};T)\,, \tag{7.105}$$

with $\alpha = e^2/4\pi$ the electromagnetic coupling constant and $q_\mu = (q_0,\vec{q})$ the four momentum of the virtual photon. In terms of the temperature-dependent renormalized parameters given above, the pion form factor is of the form

$$\begin{aligned}\mathcal{F}(s;T) &= \bar{g}_{\gamma\pi\pi}(T)\\ &\quad + \frac{g_\rho(s;T)\cdot\bar{g}_{\rho\pi\pi}(T)}{m_\rho^2(T)-s-\theta(s-4m_\pi^2)im_\rho(T)\Gamma_\rho(s;T)}\end{aligned} \tag{7.106}$$

where $\Gamma_\rho(s;T)$ is the in-medium ρ width and $g_\rho(s;T)$ is the in-medium $\rho-\gamma$ mixing constant. In this expression, the pion mass is assumed to be temperature-independent. This is reasonable since being a pseudo-Goldstone boson, it should be insensitive to strong interactions.

Both $\Gamma_\rho(s;T)$ and $g_\rho(s;T)$ are readily calculated within the formalism. The behavior of these quantities is easy to guess from the temperature dependence of the parameters established above. The width gets a small contribution from the hadronic thermal corrections, so that it increases slightly up to the flash temperature and then drops to zero proportionally to g^2 beyond the flash temperature.[14] In a similar way, the $\rho-\gamma$ coupling g_ρ decreases only slightly because of the hadronic

[14] Or even as fast as $\sim g^5$. More on this below.

thermal correction which is negative up to flash point and then drops to zero beyond the flash point linearly in g. In Fig. 7.7 are shown the pion form factor and the dilepton rate vs. the invariant mass $\sqrt{s}$ as a function of temperature. For illustration we have picked three temperatures, one before, one at and one after the flash temperature T_{flash}.

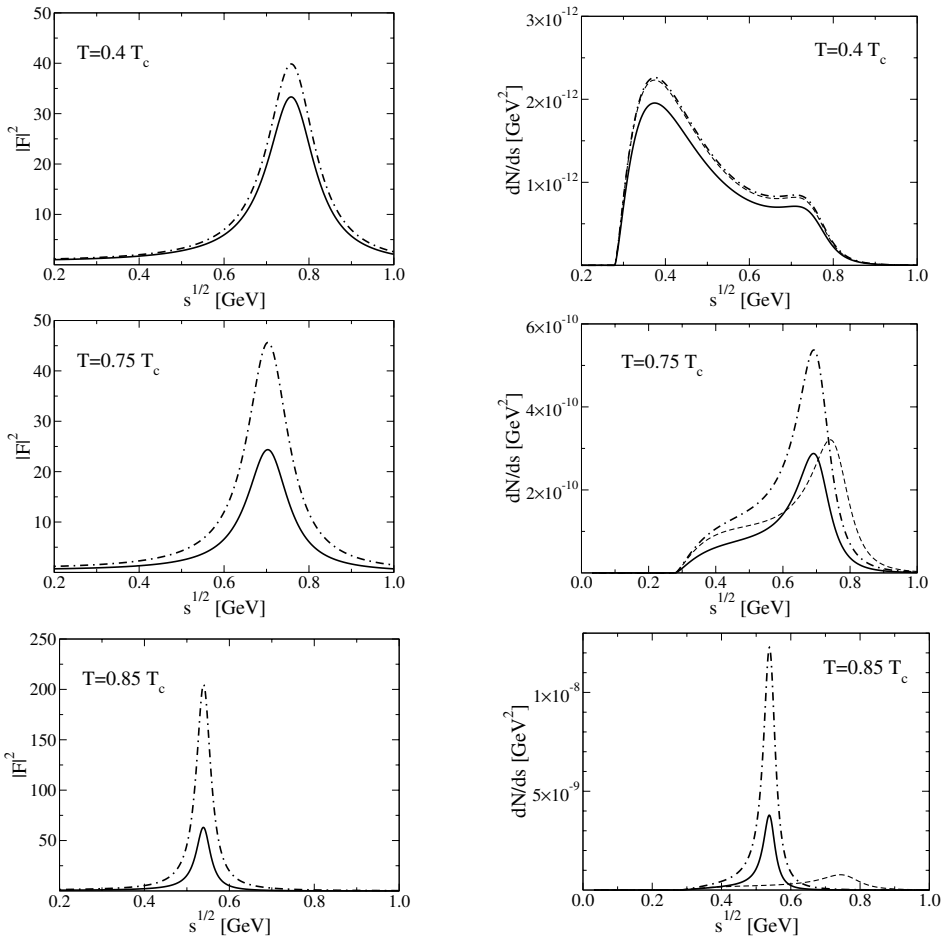

Fig. 7.7 Electromagnetic form factor of the pion (left) and dilepton production rate (right) as a function of the invariant mass $\sqrt{s}$ for various temperatures, from [Harada and Sasaki 2006] (copyright 2006 by the APS). The solid lines include the effects of the violation of the VD. The dashed-dotted lines correspond to the analysis assuming the VD. In the dashed curves in the right-hand figures, the parameters at zero temperature were used.

These results illustrate the qualitatively different predictions of HLS/VM from those of standard linear sigma models. Dramatic effects are expected once the temperature reaches the flash temperature. Up to that temperature, nothing much is

expected to happen. The violation of the VD is quite striking in both the pionic form factor and the dilepton rate and the dropping mass effects are particularly prominent in the dilepton rate. Noteworthy are the dramatic reduction in strength due to the VD violation and the sharp peak structure of the dilepton spectral function. These are unambiguously predicted effects, subject of course to the correctness of the interpretation of the intrinsic temperature dependence inferred from outside and of ignoring quark mass effects not taken into account. *They are bona-fide predictions, readily falsifiable both by lattice and laboratory experiments if one can zero in very near the vicinity of the critical temperature.*

7.4.3.3 *Confronting nature*

Confronting experiments such as dilepton production in heavy-ion collisions requires that in addition to the temperature effect discussed above, density effect be taken into account. As mentioned, the HLS/VM theory makes a clear-cut statement as to what one should expect very near the critical point, T_c and n_c. But departing from the VM fixed point, in contrast to the temperature case, no clear and systematic understanding of density effects exists. This means that it would be difficult at this stage to check whether or not VM is realized in nature since the experiments so far performed on various spectral functions cannot zero in to the vicinity of the VM fixed point where the prediction is unequivocal. In fact the available experiments, both CERN/RHIC and JLab, probe mostly the density regime near nuclear matter density and as mentioned at various places in the volume, processes that occur near nuclear matter density and at a temperature far away from T_c cannot yield pristine signal for the chiral property of the vacuum that is predicted by HLS/VM. The variety of complications, though interesting, that obstruct the search for such signals, have been discussed in [Brown and Rho 2005; Brown, Holt, Lee and Rho 2006]. These "background" effects will have to be cleanly sorted out before making a confrontation with the theory. So far this has not been done in the literature.

7.4.4 ρ^0/π^- *ratio in peripheral collisions*

The concept of hadronic freedom described above gives an extremely simple description of the STAR ratio on ρ^0/π^- measured in a peripheral collision of heavy ions at RHIC by the STAR collaboration [STAR Collaboration 2004].

In describing what happens as the system expands and the temperature cools from T_c down to T_{flash} at which the hadrons decay, we choose the 32 degrees of freedom for the ρ, π, σ [15] and a_1 in the $SU(4)$ multiplet (for up and down flavors) that come down from above T_c as described in [Brown, Lee and Rho 2005; Brown, Gelman and Rho 2006]. These are the light degrees of freedom found in

[15] Here following the convention in the field, σ is to stand for the scalar we labeled as ϕ in the rest of the volume. It should not be confused with the scalar multiplet that make up the longitudinal components of the ρ in HLS theory.

the quenched lattice calculation [Asakawa, Hatsuda and Nakahara 2003] and used in [Brown, Lee, Rho and Shuryak 2004]. It has been suggested that the entropy at T_c in lattice calculations correspond to that of massless bosons. Below T_c, the hadronic freedom is operative with the mesons nearly massless (not strictly massless due both to the non-zero quark mass and to $T \neq T_c$). One assumes that the pion which as pseudo-Goldstone has a small non-zero mass, stays more or less constant as temperature drops from T_c to T_{flash}. Now in HLS/VM, near T_c,[16] the width drops rapidly as the mass drops. As mentioned (*i.e.* Eq. (7.16)), including the p-wave penetration factor would make it drop as fast as [Shuryak and Brown 2003]

$$\frac{\Gamma_\rho^\star}{\Gamma_\rho} \sim \left(\frac{\langle \bar{q}q \rangle^\star}{\langle \bar{q}q \rangle} \right)^5 . \tag{7.107}$$

Assume for simplicity that the effective gauge coupling in medium denoted g^* begins to scale only above $T_{flash} \approx T_{freezeout} \approx 120$ MeV in peripheral collisions when the soft glue has begun to melt. This is analogous to the behavior in density where it is empirically established that the scaling of g^*/g sets in only at $n \gtrsim n_0$ [Brown and Rho 2004a].

Table 7.2 $\Gamma^\star$ as function of temperature. For the point at 120 MeV we have switched over to the Shuryak and Brown value for $\Gamma^\star/\Gamma$.

T	$m_\rho^\star/m_\rho$	$\Gamma^\star/\Gamma$
[175 MeV	0	0
164 MeV	0.18	0
153 MeV	0.36	0.01
142 MeV	0.54	0.05
131 MeV	0.72	0.22
120 MeV	0.90	0.67

Our next task is, then, to reverse the process by which the mesons lost their masses by the melting of the soft glue as T increased from ~ 120 MeV to the chiral restoration temperature T_c, in order to show how the mesons get their masses back; *i.e.* go on-mass-shell in free space.

In Table 7.2 is shown the calculated evolution of the mass and width of the ρ as the temperature drops from T_c. At $T \sim 120$ MeV which is the temperature at which the soft glue begins to melt and the ρ is 90% on-shell, the ρ meson decays into two pions. Down to that temperature, the width $\Gamma(\rho \to 2\pi)$ is too small to do much before then. The meson has to be nearly (free-space) on-shell before it can decay. Once on-shell, it decays very rapidly. The same argument holds for a_1 and other mesons in the $SU(4)$ multiplet.

[16] The most recent lattice measurement reports $T_c = 192$ MeV for 2 light-quark plus 1 heavy-quark systems. In [Brown, Lee and Rho 2005], T_c of 175 MeV was assumed.

It suffices to do a simple counting of the degrees of freedom relevant at the flash point. In total, 66 pions result at the end of the first generation from the 32 $SU(4)$ multiplet, *i.e.* ρ (18), a_1 (27), a_0 (4), π (3), σ (2) and $\epsilon \equiv f(1285)$ (12) where the number in the parenthesis is the number of pions emitted. Excluded from the counting are the ω and η since they leave the system before decaying. Leaving out the three π^-'s coming from the ρ^0 decays which are reconstructed in the measurement, we obtain

$$\frac{\rho^0}{\pi^-} \approx 3/(22-3) \approx 0.16. \tag{7.108}$$

Of course not all of the vector and axial vector mesons will have decayed. There could be a few left over. On the other hand, some pions will come from the π, σ group of initial degrees freedom. Now the above estimate of 0.16 for the $\frac{\rho^0}{\pi^-}$ ratio assumed all vector and axial-vector mesons decayed into pions at the flash temperature. This means that (7.108) should be taken as a lower limit. If one takes the numbers in Table 7.2 literally and assume a dynamical time of 1 fm/c, one finds that only 42 of the 66 total number of pions have been emitted at $T \approx 120$ MeV. If we take $42/3$ π^--mesons, we will have

$$\frac{\rho^0}{\pi^-} \approx 0.21 \tag{7.109}$$

which we can take as an upper limit. Thus, we arrive at the range of prediction [Brown, Lee and Rho 2005]

$$0.16 \lessapprox \frac{\rho^0}{\pi^-} \lessapprox 0.21. \tag{7.110}$$

This is in a surprising accord with the observed value [STAR Collaboration 2004]

$$(\frac{\rho^0}{\pi^-})_{STAR} = 0.169 \pm 0.003(\text{stat}) \pm 0.037(\text{syst}), \tag{7.111}$$

considering that the standard scenario would be off by several orders of magnitude, *i.e.* by a factor of $\gtrsim 400$ compared with the equilibrium value. This surprising result can be understood as follows. Because of the decreased width due to the hadronic freedom, the ρ meson goes through *only one generation* before it freezes out in the peripheral collisions in STAR. But there is no equilibrium at the end of the first generation. Had the ρ possessed its (free-space) on-shell mass and width with $\sim$ five generations as in the standard scenario, it is clear that the $\frac{\rho^0}{\pi^-}$ ratio would be much closer to the equilibrium value.

Chapter 8

Hadrons In The Sliding Vacua Of Nuclear Matter

Before entering into hadronic matter at high density that is the main subject of the following chapters, we need to check how the formalism developed in the preceding chapters fares with many-nucleon systems under normal conditions that have been studied both theoretically and experimentally since many decades and more or less understood quantitatively. To do this, we look at nuclei and nuclear matter in the framework that takes into account the change of hadron – both nucleon and meson – properties as the "vacuum" changes (or "slides") in hot/dense matter. It will turn out that this approach to nuclear physics is rather novel and hence exploratory.[1]

Naively, one would expect the change in the intrinsic mass of hadrons and coupling constants, in particular the mass of the nucleon, dropping as a consequence of the "melting" of the condensate (described in the preceding chapter and below) as density increases in nuclear medium to affect strongly the quantities well measured and well explained in the conventional description in the properties of nuclei. It is therefore important to check whether the change in the masses and coupling constants would not upset the agreement obtained without dropping masses and coupling constants. As a spin-off, we will encounter certain cases where predictions unforseen in the standard approach can be made. These can be taken as (albeit indirect) evidence for the predicted behavior.

8.1 Brown-Rho Scaling

What is often referred to in the literature as "Brown-Rho scaling" (BR scaling or BSR for short) has figured in several previous chapters, addressing the role of chiral symmetry in hadronic medium, finite as well as infinite. As stressed, this scaling property, strictly speaking, can be applied directly *only* in the vicinity of chiral

[1] The traditional approach is to start with a Lagrangian whose parameters are fixed at $T = n = 0$ and then compute as many terms as feasible in perturbation series in a strong coupling regime. This way of approaching nuclear dynamics seems to work when density is low or the number of nucleons involved in the interaction is small as we saw in Chapter 4, but there are reasons to expect that it would not work for heavy nuclei and nuclear matter at large temperature/density we are primarily interested in.

restoration. This point has been sharpened by Harada and Yamawaki [Harada and Yamawaki 2003] who showed that the scaling should be identified with the intrinsic dependence on background (temperature/density) of the quark condensates in QCD correlators. Unfortunately, the BR scaling behavior as originally put forward in [Brown and Rho 1991] has largely been misinterpreted in the literature in applying to many-nucleon systems away from the chiral transition point. This was mostly due to the fact that the original argument used to arrive at BR scaling in [Brown and Rho 1991] was couched in a highly simplified language of the Skyrme model applied to many-nucleon systems in the mean field approximation. A much more complete discussion was given in Chapter 6 where the Skyrme model, implemented with a scalar "dilaton" encoding (a part of) the trace anomaly of QCD but without vector mesons, was used to formulate a unified approach to both the vacuum change due to density and the excitations on top of the changed vacuum. However, as stressed there, the Skyrme model without the vector meson degrees of freedom is not adequate enough to address the intricate problem in the manifestation of chiral symmetry in nuclei and nuclear matter.

As proposed in the preceding chapters, the most realistic approach would be to take a skyrmion model incorporating as many vector mesons as possible, ultimately an infinite tower of them as in holographic dual QCD described in Chapter 5 and apply it to dense medium in a way similar to what was done in Chapter 6. Such a formulation is yet to come, so we will present the mean field formulation of [Brown and Rho 1991], now given with more precision than in the original formulation, and then specify in what way the relation should be understood.

8.1.1 *Intrinsic density dependence via dilaton*

Let us first elaborate on how the broken scale symmetry and chiral symmetry are intricately interwound. In Chapter 7, the general notion was presented in the context of hot medium, but here we are specifically concerned with density effects appropriate for nuclei and nuclear matter. Limiting ourselves to the chiral limit where the quark masses are ignored, we shall now state BR scaling in a more precise way. For this, we exploit the observations that: (1) chiral invariance is spontaneously broken even without explicit breaking, (2) scale invariance is broken both explicitly *and* spontaneously, but the spontaneous breaking can take place *only if* there is explicit breaking, (3) the spontaneous breaking of chiral symmetry induces the spontaneous breaking of scale invariance, but (4) when chiral symmetry is restored, explicit breaking of scale invariance *remains* as long as the gauge coupling is nonzero. What these observations imply is that we can write the effective Lagrangian as a sum of terms,

$$\mathcal{L} = \mathcal{L}_S(U, A_\mu, \chi) + \mathcal{L}_H + \cdots \tag{8.1}$$

where $\mathcal{L}_S$ is chirally and scale invariant involving the chiral field U, hidden local vector fields A_μ and dilaton field χ associated with the "soft glue" and $\mathcal{L}_H$ is scale non-invariant but chirally invariant. One can associate the soft glue to the former and the "hard glue" to the latter. The ellipses in (8.1) stand for terms that break chiral invariance, *e.g.*, quark mass terms and break *explicitly* the scale invariance. Now let us assume that the scale invariance is broken by the vacuum so that the χ field picks up a vacuum expectation value (VEV),

$$\langle\chi\rangle = \chi_0 \neq 0. \tag{8.2}$$

Writing

$$\chi = \chi_0 + \chi' \tag{8.3}$$

and substituting it into (8.1), one obtains a Lagrangian which has the scale symmetry broken *both* explicitly and spontaneously. The trace of energy-momentum tensor calculated from the resulting Lagrangian will then receive contributions from both the spontaneous breaking in $\mathcal{L}_S$ and the explicit breaking in $\mathcal{L}_H$. The Lagrangian used in [Brown and Rho 1991] belongs to this class of constructions using the Skyrme Lagrangian with the hard glue integrated out. At the mean field level, the skyrmion Lagrangian gives the BR scaling

$$m_B^*/m_B \approx m_M^*/m_M \approx (\langle\bar{q}q\rangle^*/\langle\bar{q}q\rangle)^r \tag{8.4}$$

where the subscript B stands for the ground-state light-quark baryon (as a skyrmion or a bound state of N_c constituent quarks), M for light-quark mesons, r is a non-negative constant and the asterisk for in-medium quantity dependent on density. We recall that although not explicitly mentioned, some of the arguments used there were inferred from a hidden local symmetry structure such as for instance the mass formula for the vector meson *etc.* [2] Note, however, they were made in the mean field approximation which means that the scaling essentially addressed the "intrinsic density/temperature dependence" of HLS theory, not the full HLS theory which should include non-negligible dense (thermal) loop corrections as well as many-body interactions that follow from the Lagrangian.

To meaningfully confront Nature, the full panoply of quantum loop terms would have to be calculated.

8.1.2 *Scaling of baryon masses*

The reasoning based on hidden local symmetry addressed directly meson properties in medium. There the simple scaling followed from the vector manifestation scenario of hidden local symmetry theory $\mathrm{HLS}_{K=1}$ for the lowest-lying vector mesons and

[2] The scaling for the pion mass written down in [Brown and Rho 1991] is most likely incorrect because the pion mass breaks both chiral and scale invariance and one should not apply the simple scaling argument to the pion mass. Therefore to the order considered there, the pion mass will be taken not to scale with density or temperature. We will come back to this matter below

other excitations above them. In order to address baryon masses within the same framework, one would have to bring in skyrmions to describe the baryon sector. This point has been stressed repeatedly in the preceding chapters. In the absence of reliable work on skyrmions with HLS in medium, it is difficult to say with certainty how baryon masses behave in dense (as well as hot) medium.

As a first guess, one might think that as in temperature discussed in the preceding chapter, there will be a "flash density" analogous to the flash temperature at which nucleons cease to be the correct degrees of freedom and must be replaced by something else, perhaps quasiquarks or constituent quarks. This means that it may not be correct to apply the scaling to the nucleon mass going beyond the "flash density." In the absence of model-independent guide, *e.g.*, lattice, precisely where this happens or what the mechanism is is not known at present. But if one assumes that at some density, say, above that of nuclear matter, nucleons transform into quasiquarks, then one might assign the same BR scaling (8.4) to quasiquarks as for vector mesons. In fact, this was done in the preceding chapter in establishing the vector manifestation at high density. In this way one can adopt a "universal" scaling for both mesons and baryons – as bound states of quasiquarks – as in the original BR scaling up to certain density. This is the picture, *i.e.* Eq. (8.4), we will adopt in what follows in this chapter. The readers, however, should be warned that there are caveats to this which could invalidate the baryon part of (8.4), especially near chiral restoration. One of them was mentioned in Chapter 6 where it was seen that a skyrmion transforms in dense matter into half-skyrmions with a pseudo-gap structure. There the skyrmion mass does not scale to zero (since the pion decay constant does not vanish at that point) although the chiral order parameter goes to zero. One other possibility is the parity-doublet structure discussed in the next subsection. There are also constraints such as "anomaly matching" when one is approaching the VM fixed point where massless excitations appear. One should keep this matter as an open issue until verified by experiments.

8.1.3 *Parity-doubled sigma model*

One of possible alternative scenarios to BR scaling is the parity-doubled nucleon model defined by a linear sigma model [DeTar and Kunihiro 1989; Nemoto, Jido, Oka and Hosaka 1998 ; Zschiesche, Tolos, Schaffner-Bielich and Pisarski 2006; Wilms, Giacosa and Rischke 2007] that contains, in addition to the usual sigma model mesons, a parity doublet of nucleons $\psi_{1,2}$ [3]

$$\begin{aligned}\mathcal{L} = &\bar{\psi}_1 i\gamma\cdot\partial\psi_1 + \bar{\psi}_2 i\gamma\cdot\partial\psi_2 + m_0(\bar{\psi}_2\gamma_5\psi_1 - m_0(\bar{\psi}_1\gamma_5\psi_2)\\ &+a\bar{\psi}_1(\sigma + i\gamma_5\vec{\tau}\cdot\vec{\pi})\psi_1 + a\bar{\psi}_2(\sigma + i\gamma_5\vec{\tau}\cdot\vec{\pi})\psi_2\\ &+\mathcal{L}_M + \cdots\end{aligned} \tag{8.5}$$

[3] Although obvious, we warn that the σ that figures here is not the σ of hidden local symmetry theory.

with

$$\mathcal{L}_M = \frac{1}{2}(\partial_\mu \sigma)^2 + \frac{1}{2}(\partial_\mu \vec{\pi})^2 - \frac{\lambda}{4}(\sigma^2 + \vec{\pi}^2 - v^2)^2 + \cdots . \tag{8.6}$$

Here ellipses stand for terms that involve coupling to massive vector mesons. The heavier degrees of freedom – vector mesons – are needed for short-distance physics for fully capturing nuclear dynamics of many-nucleon systems. For this discussion, however, we don't need their explicit form. It suffices to recognize that they can be incorporated consistently with chiral symmetry.

What makes this model different from standard sigma models and HLS models is that there is a chirally invariant mass term $\sim m_0$, that is to say, a term which remains invariant under the transformation

$$\psi_{1L(R)} \to g_L(g_R)\psi_{1L(R)}, \quad \psi_{2L(R)} \to g_R(g_L)\psi_{2L(R)}. \tag{8.7}$$

The presence of m_0 suggests that chiral restoration does not necessarily require that the nucleon mass be zero in the chiral limit. There can be a doublet of massive nucleons in the chirally restored phase. Now such a Lagrangian implemented with the lightest vector mesons ρ and ω including nonlinear terms may be used to describe nuclear matter as well as chiral restoration. Such a study has been made [Zschiesche, Tolos, Schaffner-Bielich and Pisarski 2006]. It seems to provide a reasonable description of nuclear matter. However, the critical density and nature of the chiral restoration transition – which is represented by the degeneracy of the doublet – turn out to be overly sensitive to the parameters of the Lagrangian. For instance, if the odd-parity partner of the nucleon is identified with $N'(1535)$, then the chiral restoration transition comes out to be of first order with the critical density at $n \approx 10n_0$. If on the other hand, one takes the N' mass to be 1.2 GeV and the physical pion mass $m_\pi \approx 140$ MeV, then the transition is a smooth cross-over at $n_0 \sim 3n_0$. With such diverse predictions, it is clearly not possible to assess the viability of the model. Even if viable, it would be difficult to pin down the nature of the transition in this model. What is significant for the issue at hand among the results of the model is that a large value of the chiral-invariant baryon mass is required to be compatible with nuclear incompressibility, *viz*,

$$m_0 \sim 0.8 \ \text{GeV}. \tag{8.8}$$

This large value implies first of all that the baryon mass must violate strongly the BR scaling. From nuclear physics point of view, such a large constant would seem to be inconsistent with what will be discussed below regarding various static properties of nuclei. It raises two immediate questions: One, fundamental, on how such a large m_0 is generated in QCD and two, phenomenological, on how well it fares with nature. The first implies that the mechanism for generating baryon masses can be basically different from the standard one associated with quark condensate. As for the second, the scenario has to confront a large battery of low-energy chiral dynamics and see whether they are consistent with nature. It is not clear that the

latter has cleared the test. Study made so far is inconclusive [Wilms, Giacosa and Rischke 2007].

In this volume, while we have no strong argument against the parity-doubler scenario, we will simply adopt the "conventional" scenario with $m_0 = 0$ and see how far one can go without getting into conflict with nature, although there is a problem which we would have to ultimately settle that has to do with the consistency with the 't Hooft anomaly matching condition. Ultimately we hope to be able to make a statement as to whether the parity-doublet picture can be dismissed or not.

8.1.4 *Constraints from anomaly matching?*

At the VM fixed point, chiral symmetry is assumed to be restored. In HLS theory, we have certain zero-mass excitations (in the chiral limit) that are presumably composites of the QCD degrees of freedom, quarks and gluons. For instance in $\mathrm{HLS}_{K=1}$, there are the pions, the massless σ's (longitudinal components of the massive ρ) and the massless ρ's. In $\mathrm{HLS}_{K=2}$, there are, in addition to what's in $\mathrm{HLS}_{K=1}$, the massless a_1's and the longitudinal components of the massive a_1's. The massless vector mesons are expected to decouple from the vector and axial vector correlators that control the physical observables we are looking at in this volume. However, one wonders whether the presence of various zero-mass excitations at the critical point does not get into conflict with some fundamental constraints imposed by QCD. One known constraint is the so-called 't Hooft anomaly matching condition ['t Hooft 1980] mentioned in Introduction. In the context of the present discussion, the condition, briefly, is the requirement that the global anomalies of a low-energy effective theory equal those of the fundamental ultraviolet theory, QCD in our case.

To apply the 't Hooft condition, consider the anomaly in $\pi^0 \to 2\gamma$. The anomaly is given in QCD by the triangle diagram saturated by the N_c quarks. 't Hooft condition then is that the massless excitations at the VM in HLS which are supposed to be the composites of the fundamental theory QCD give the same anomaly as the QCD itself.

Let us see what the 't Hooft condition implies in HLS/VM. For $\mathrm{HLS}_{K=1}$, there are the pions that match the triangle anomaly of QCD. This fact is encoded in the Wess-Zumino term. The massless ρ and the σ do not contribute. However, if there were massless quasiquarks, they could contribute in the same way as the current quarks of QCD (*i.e.* through the triangle diagram modulo the factor of N_c). This means that anomaly with the pions and quasiquarks does not match that of QCD. This suggests that other massless degrees of freedom are needed to cancel the anomaly contributed by the quasiquarks or else one would have to exclude the quasiquarks from the theory. It would be interesting to study what the infinite tower structure of AdS/QCD or holographic dual QCD (hQCD) would bring in at the chiral restoration phase transition.

8.1.5 *Modernizing BR scaling*

Taking into account the developments given in the preceding chapters, in particular, the hadronic freedom – and ignoring the caveats given above, we can write down a modernized and more specific BR scaling that supersedes the relation (8.4). Define $\mathcal{P} \equiv (T, n)$ and let M_h and m_h stand for the parametric mass and pole mass, respectively, of $h = \rho, \omega, q$ where q stands for quasiquark. Then the modernized BR scaling should read [Brown, Harada, Holt, Rho and Sasaki 2008]

$$\frac{M_h^*}{M_h} \approx \frac{f_\pi^*}{f_\pi}, \quad \mathcal{P} < \mathcal{P}_{flash}, \tag{8.9}$$

$$\frac{M_h^*}{M_h} \approx \frac{m_h^*}{m_h} \approx \frac{g^*}{g} \approx \frac{\langle \bar{q}q \rangle^*}{\langle \bar{q}q \rangle} \quad \mathcal{P} \geq \mathcal{P}_{flash}. \tag{8.10}$$

Due to the usual strong interactions, (8.9) does not contain the pole mass which has no simple scaling below the flash point whereas the VM behavior allows the pole mass to scale as the parametric mass beyond the flash point as in (8.10). Note also that the scaling in (8.9) is with the physical pion decay constant while that in (8.10) is with the gauge coupling. This relation is to be used for processes that probe chiral symmetry in hadronic matter.

8.2 Chiral Fermi Liquid

It is currently accepted that nuclear matter can be described as a Fermi liquid, and Landau Fermi liquid theory is applicable to it. Similarly, heavy nuclei could be described in terms of Landau Fermi liquid suitably adjusted to finite number of nucleons as was formulated by Migdal [Migdal 1967]. Thus ultimately one might be able to derive Fermi liquid from QCD proper, but we are quite far from achieving it. One may hope that lattice calculations could soon give some hints of how to do the job. But although lattice technique is impressively advanced, nuclei and nuclear matter are still very far from being tackled. Thus there seems to be no other way at present than effective field theories. In what follows, we will describe how to implement the notion of scaling masses and coupling constants in nuclear many-body problems.

8.2.1 *Double-decimation approach*

One might construct a "bare Lagrangian" at the chiral scale $\Lambda_\chi \sim 4\pi f_\pi$ inputting as much information as possible of QCD properties and then try to get to to nuclei and nuclear matter by standard field theory technique, such as *e.g.*, chiral perturbation theory. Because of multiple scales involved in nuclear systems, however, this has not been feasible in one step. We will have to do this in multiple steps. What we adopt here is probably the simplest that works, and that is what is called "double decimations" in the renormalization group equation (RGE for short) sense proposed

in [Brown and Rho 2004a]. This consists of two decimations. The first involves going from a chiral scale, which is more or less the matching scale Λ_M à la Harada and Yamawaki at which effective field theories are matched to the fundamental theory QCD, to the Fermi surface scale $\Lambda_{\rm FS}$ at which the Fermi surface is defined. How this could be achieved was discussed in a general context by Lynn some years ago [Lynn 1993] who made the conjecture that the Fermi surface could arise from $SU(2)_L \times SU(2)_R$ chiral effective field theory as a chiral soliton liquid. This conjecture has not yet been transformed into a workable scheme but it is an appealing one. It will be simply assumed in this volume that such a chiral liquid can be formed.

Once the Fermi surface is established, the "second decimation" is made by using three observations [Friman and Rho 1996]. First, Shankar [Shankar 1994] showed that given an effective Lagrangian built around the Fermi surface, decimating fluctuations toward the Fermi surface leads to the "Fermi liquid fixed point" with the quasiparticle mass $m^\star$ and quasiparticle interactions $\mathcal{F}$ being the fixed point parameters. Second, Matsui established [Matsui 1981] that Walecka mean field theory is *equivalent* to Landau Fermi liquid theory. Finally, it has been shown that Walecka mean-field theory can be obtained in the mean field of either an effective chiral Lagrangian in which (vector and scalar) massive degrees of freedom are present or an effective chiral Lagrangian with higher-dimension operators (such as four-Fermi operators) [Gelmini and Ritzi 1995; Park, Min and Rho 1996; Brown and Rho 1996p]. The strategy then is to endow the parameters of the effective Lagrangian with density dependence inherited by matching to QCD at the matching scale, namely, the *intrinsic background dependence* [Friman and Rho 1996]. We shall call this approach "chiral Fermi liquid approach" (or CFLA for short). It will be shown below that this procedure gives correct energy and momentum densities of nuclear matter that are consistent with thermodynamic properties. For this BR scaling has an indispensable role for the nucleon in medium in contrast to what is given by the parity-doubled nucleon picture.

8.2.2 *Scaling masses and Landau-Migdal parameters*

Our first task in this subsection is to establish a mean-field relation between Landau's Fermi liquid theory for nuclear matter and the *intrinsic density dependence* imposed upon the parameters by the Wilsonian matching to QCD correlators. It is important to keep in mind that the scaling relations established near the Fermi liquid fixed point are valid only in the neighborhood of the nuclear matter density and cannot be extrapolated to densities much beyond one or two times nuclear matter. They will be totally irrelevant near chiral restoration point at which the vector manifestation holds rigorously, directly signalling the specific features of chiral symmetry. This is the reason why obsevables probing matter in the vicinity of nuclear matter density including dilepton processes in heavy ion collisions do not provide a clean litmus for effects of "partial chiral symmetry restoration," contrary to what some people have thought.

The connection we are interested in is clearly not direct in the absence of a formal derivation of Landau Fermi liquid from an effective chiral field theory. One can, however, make use of what has been established [Matsui 1981] between Walecka mean field theory and Landau Fermi liquid theory. [4] To do this, we need a chiral Lagrangian (for $N_f = 2$) which *in the mean field subsumes the double decimations* mentioned above. There are two alternative but equivalent effective Lagrangians to use for this step:

(M1) One is an effective chiral Lagrangian that involves just the nucleon and pion fields, that is expected to result when all heavy degrees of freedom (vector and scalar mesons, baryon excitations *etc.*) are formally integrated out, *i.e.*

$$\mathcal{L}_\chi = \bar{N}[i\gamma_\mu(\partial^\mu + iv^\mu + g_A^\star\gamma_5 a^\mu) - M^\star]N - \sum_i C_i^\star(\bar{N}\Gamma_i N)^2 + \cdots \quad (8.11)$$

where the induced vector and axial vector "fields" are given by $v_\mu = -\frac{i}{2}(\xi^\dagger\partial_\mu\xi + \xi\partial_\mu\xi^\dagger)$ and $a_\mu = -\frac{i}{2}(\xi^\dagger\partial_\mu\xi - \xi\partial_\mu\xi^\dagger)$ with $\xi = e^{i\tau\cdot\pi/2f_\pi}$, $M^\star$ is the BR-scaling nucleon mass, the ellipses stand for terms with higher number of nucleon fields and the Γ_i's represent Dirac and flavor matrices as well as derivatives involving pions, consistent with chiral symmetry and other symmetries assumed, which can be approximated for our purpose by [5]

$$\sum_i C_i^\star(\bar{N}\Gamma_i N)^2 \approx -\frac{C_{\tilde{\phi}}^{\star\,2}}{2}(\bar{N}N)^2 + \frac{C_{\tilde{\omega}}^{\star\,2}}{2}(\bar{N}\gamma_\mu N)^2 + \frac{C_{\tilde{\rho}}^{\star\,2}}{2}(\bar{N}\gamma_\mu\tau N)^2 + \cdots . \quad (8.12)$$

The four-Fermi-interaction terms correspond to contributions coming from the exchange of mesons $\tilde{m}$ as well as from the localization of certain nonlocal terms that are typically given by pion loop corrections. As we saw in holographic dual QCD (Chapter 6), higher members of the tower of vector mesons (ρ, ω *etc*) can play an important role in the four-Fermi interactions. Although scalar degrees of freedom are not usually incorporated in HLS theory, we assume that they can be incorporated in a manner consistent with the HLS strategy. In practical calculations, the tower is replaced by the lowest excitations assuming that they dominate, but it would be helpful to remember that what is involved is the tower.

(M2) The other is a hidden local symmetric Lagrangian that contains a set of vector mesons coupled in a chiral-invariant way to (pseudo-)Goldstone bosons and nucleons. The simplest form is that of Walecka's linear Lagrangian with all other fields omitted but implemented with BR scaling represented by the

[4] Later we will describe a recent attempt to establish a microscopic connection.

[5] In medium, Lorentz invariance is broken and hence we should distinguish the time component and space component of the four vector γ_μ in (8.12) with different coefficients. In our case considered below, we will be dealing with the space part of $C_{\tilde{\omega}}^\star$ and $C_{\tilde{\rho}}^\star$ when we discuss the Landau parameter F_1. This distinction will be made by the subscript (t,s) for the (time,space) component on the coefficient C.

asterisk,[6]

$$\mathcal{L}_{walecka} = \bar{N}(i\gamma_\mu(\partial^\mu + ig_v^\star\omega^\mu) - M^\star + h^\star\phi)N$$
$$-\frac{1}{4}F_{\mu\nu}^2 + \frac{1}{2}(\partial_\mu\phi)^2 + \frac{m_\omega^{\star\,2}}{2}\omega^2 - \frac{m_\phi^{\star\,2}}{2}\phi^2 + \cdots \qquad (8.13)$$

In Eqs. (8.11) and (8.13), the ellipses stand for higher-dimension operators allowed by the symmetries involved. It would be more realistic to take into account the infinite tower of vector mesons, but in practice we will be considering only the lowest members in what follows.

As mentioned above, the equivalence for nuclear matter in mean field of (8.11) and (8.13) has been established. This can be understood as follows. One can think of (8.13) as arising as an effective chiral Lagrangian that incorporates a tower of vector mesons in hidden local symmetry theory in which fermions figure. The parameters of such a Lagrangian will have the *intrinsic* density dependence as described in Chapter 7 resulting from the matching to QCD in medium at the matching scale $\Lambda_M \sim \Lambda_\chi$. We interpret the Lagrangian (8.11) to result when the (tower of) vector mesons are integrated out as described in Chapter 5. Now the intrinsic density dependence of the parameters of the effective chiral Lagrangian indicated by the asterisk inherited from matching to QCD in medium will then be identified with BR scaling. This is the basic premise of our approach. It is in this sense that BR scaling should be understood. It is important to keep in mind – as stressed throughout this volume – that physical quantities such as pole mass of hadrons are in general intricate functions of these intrinsically density-dependent parameters.

To arrive at Landau Fermi-liquid for nuclear matter from a chiral Lagrangian, *e.g.*, (8.11), we need some definitions. Start with the interaction between two quasiparticles on the Fermi surface of the form (neglecting tensor interactions):

$$\mathcal{F}(\vec{p},\vec{p}') = F(\cos\theta) + F'(\cos\theta)(\vec{\tau}\cdot\vec{\tau}') + G(\cos\theta)(\vec{\sigma}\cdot\vec{\sigma}') + G'(\cos\theta)(\vec{\tau}\cdot\vec{\tau}')(\vec{\sigma}\cdot\vec{\sigma}'), \qquad (8.14)$$

where θ is the angle between $\vec{p}$ and $\vec{p}'$. The function $F(\cos\theta)$ can be expanded in Legendre polynomials,

$$F(\cos\theta) = \sum_l F_l P_l(\cos\theta), \qquad (8.15)$$

with analogous expansions for the spin- and isospin-dependent interactions. The coefficients F_l *etc.* are the Landau Fermi liquid parameters.[7]

[6] We are showing only the degrees of freedom appropriate for symmetric nuclear matter among the vector mesons, so the isovectors (and also the pions) are not explicit. The field tensor is therefore $F_{\mu\nu} = \partial_\mu\omega_\nu - \partial_\nu\omega_\mu$. The isovector degrees of freedom can, and indeed will, be taken into account whenever needed.

[7] We are addressing Fermi liquid in the context of strong interaction (nuclear) physics. Therefore when we say Landau (Fermi-liquid) parameters, we mean Landau-Migdal parameters since it is Migdal [Migdal 1967] who formulated nuclear matter in terms of Landau Fermi liquid theory.

In Landau theory, an important quantity is the single-quasiparticle energy with momentum $\vec{p}$. In the nonrelativistic approximation with Eq. (8.11), it takes the form[8]

$$\epsilon(p) = \frac{p^2}{2M^\star} + C_{\omega_t}^{*2}\langle N^\dagger N\rangle + \Sigma_\pi(p) \tag{8.16}$$

where $\Sigma_\pi(p)$ is the self-energy (Fock term) from the pion exchange graph, shown in Fig. (8.1).

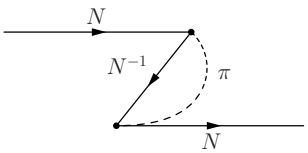

Fig. 8.1 The one-pion exchange (Fock term) contribution to the nucleon self energy. Here N^{-1} stands for "quasi-hole."

The self-energy contribution from the vector meson (second term on the right hand side of (8.16)) corresponds to the diagram shown in Fig. (8.2). The Landau effective mass m_L^* is related to the quasiparticle velocity at the Fermi surface

$$v_F = \frac{\mathrm{d}}{\mathrm{d}p}\epsilon(p)|_{p=k_F} = \frac{k_F}{m_L^*} = \frac{k_F}{M^\star} + \frac{\mathrm{d}}{\mathrm{d}p}\Sigma_\pi(p)|_{p=k_F} \tag{8.17}$$

where m_L^* is the Landau quasiparticle mass, the asterisk representing density dependence. Using Galilean invariance, Landau derived a relation between the effective mass of the quasiparticles and the velocity dependence of the effective interaction described by the Fermi-liquid parameter F_1:

$$\frac{m_L^*}{m_N} = 1 + \frac{F_1}{3} = (1 - \frac{\tilde{F}_1}{3})^{-1}, \tag{8.18}$$

where m_N is the free-space mass of the nucleon and $\tilde{F}_1 = (m_N/m_L^*)F_1$. The corresponding relation for relativistic systems follows from Lorentz invariance and has been derived by Baym and Chin [Baym and Chin 1976].

With the four-Fermi interaction (8.12), there are two distinct velocity-dependent terms in the quasiparticle interaction, namely the spatial part of the current-current interaction and the exchange (or Fock) term of the one-pion-exchange. In the nonrelativistic approximation, their contributions to $\tilde{F}_1$ are

$$\tilde{F}_1 = \tilde{F}_1^\omega + \tilde{F}_1^\pi \tag{8.19}$$

[8]From here on, $\tilde{\omega}$ ($\tilde{\rho}$) will be replaced by ω (ρ) unless otherwise noted.

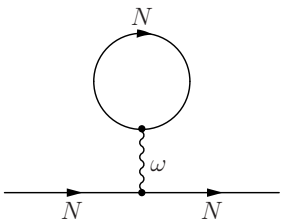

Fig. 8.2 The lowest ω-meson contribution to the nucleon self energy.

with

$$\tilde{F_1^\omega} = \frac{m_N}{m_L^*} F_1^\omega = -C_{\omega_s}^{*\,2} \frac{2k_F^3}{\pi^2 M^\star}, \tag{8.20}$$

$$\tilde{F_1^\pi} = -3\frac{m_N}{k_F}\frac{\mathrm{d}}{\mathrm{d}p}\Sigma_\pi(p)|_{p=k_F}. \tag{8.21}$$

The M^* in the denominator in (8.20) comes from the non-relativistic approximation of the spatial part of the current-current correlator with the nucleon in the background of the medium.

Using Eqs. (8.17) and (8.18), we find

$$(\frac{m_L^*}{m_N})^{-1} = 1 - \frac{1}{3}\tilde{F_1} = \frac{m_N}{M^\star} + \frac{m_N}{k_F}\frac{\mathrm{d}}{\mathrm{d}p}\Sigma_\pi(p)|_{p=k_F}, \tag{8.22}$$

which leads to the important result

$$\Phi^{-1} \equiv \frac{m_N}{M^\star} = 1 - \frac{1}{3}\tilde{F_1^\omega}. \tag{8.23}$$

This connects the *scaling* of the mass associated with the quark condensate to the *contribution* to the Landau parameter F_1 coming from the ω exchange in medium. There are two important points to underline here. First, the Landau parameters are the fixed point quantities in a (Wilsonian) renormalization group equation as explained by Shankar [Shankar 1994], and hence the relation (8.23) should hold in the vicinity of the saturation density of nuclear matter. Second, the ω-exchange contribution to the Landau parameter F_1 is due to the velocity-dependent part of the potential, $\sim \vec{p}_1 \cdot \vec{p}_2/m_N^2$ which is an $\mathcal{O}(p^2)$ term in the usual naive power counting. Nonetheless, it is this chirally non-leading term in the four-Fermi interaction that appears on the same footing with the chirally leading terms in the ω and the scalar (ϕ) tadpole graphs. This indicates that the conventional power counting valid in the absence of matter needs to be modified in the presence of a Fermi sea, suggesting that it is highly non-trivial to arrive at nuclear matter in effective field theory based chiral perturbation. This matter is discussed in [Brown and Rho 2004a].

The pion contribution to F_1 is completely fixed by the (pseudo-)Goldstone boson

nature of the pion and is given for a given Fermi momentum k_F by

$$\frac{1}{3}\tilde{F_1^\pi} = -\frac{3f_{\pi NN}^2 m_N}{8\pi^2 k_F}[\frac{m_\pi^2+2k_F^2}{2k_F^2}\ln\frac{m_\pi^2+4k_F^2}{m_\pi^2} - 2] \tag{8.24}$$

where $f_{\pi NN} = \frac{g_{\pi NN}m_\pi}{2m_N} \approx 1$ is the non-relativistic πN coupling constant. At normal nuclear matter density with $k_F \approx 2m_\pi$, it is

$$\frac{1}{3}\tilde{F_1^\pi} = -0.153. \tag{8.25}$$

This numerical value will be used below.

8.2.3 *Thermodynamic consistency*

At first sight, it seems worrisome to have the intrinsic density dependence, although "required" by the matching to QCD at a given scale, appear in a Lagrangian treated at a mean field level. For instance, one might worry that the energy density and the current density of the system so obtained might violate, respectively, thermodynamic consistency such as the energy-momentum conservation and charge conservation in the electromagnetic response functions *etc.* We will discuss the issue of charge conservation in the convection current in the next section. Here we address the consistency issue with the energy-momentum tensor. We shall be somewhat more detailed on this matter than elsewhere because we consider this matter highly intricate and poorly appreciated in the nuclear physics community.

Given the energy-density $\mathcal{E}$ computed in mean field with the Lagrangian (8.13),[9] one may wish to calculate the pressure from this quantity. One would find that a naive calculation does not give correctly $\frac{1}{3}\langle T_{ii}\rangle$ where $T_{\mu\nu}$ is the conserved energy-momentum tensor. This means that the density in the masses and coupling constants cannot be treated as a C-number independent of matter fields in deriving, by Noether theorem, the energy-momentum tensor. Now the question is: how do we treat the field dependence of the intrinsic density in the scaling masses and constants?

There may be several equivalent solutions to this problem. One possible solution to this problem goes as follows [Song, Min and Rho 1998]. We start by defining[10]

$$\check{\rho}u^\mu \equiv \bar{N}\gamma^\mu N \tag{8.26}$$

with unit fluid 4-velocity

$$u^\mu = \frac{1}{\sqrt{1-\boldsymbol{v}^2}}(1,\boldsymbol{v}) = \frac{1}{\sqrt{\rho^2-\boldsymbol{j}^2}}(\rho,\boldsymbol{j}) \tag{8.27}$$

[9] One can equivalently work with the Lagrangian (8.11), but (8.13) is more convenient for comparing with other works in the literature.

[10] In this subsection, we are using the notation ρ as the number density instead of n used elsewhere. There should be no confusion with the vector meson ρ which will be distinguished when it appears.

with the baryon current density

$$\boldsymbol{j} = \langle \bar{N}\boldsymbol{\gamma}N\rangle \tag{8.28}$$

and the baryon number density

$$\rho = \langle N^\dagger N\rangle = \sum_i n_i. \tag{8.29}$$

We will take n_i to be given by the Fermi distribution function, $n_i = \theta(k_F - |\boldsymbol{k}_i|)$ at $T = 0$. We should replace the ρ that appears in the masses and constants in (8.13) by $\check{\rho}$. The definition of $\check{\rho}$ makes our Lagrangian formally Lorentz-invariant. The resulting Lagrangian is highly non-linear, with the coefficients being functionals of the bilinear nucleon field $\check{\rho}$, which in the mean field, gives the Fermi-liquid fixed point theory. With this, the Euler-Lagrange equation of motion for the nucleon field is

$$\begin{aligned}\frac{\delta\mathcal{L}}{\delta\bar{N}} &= \frac{\partial\mathcal{L}}{\partial\bar{N}} + \frac{\partial\mathcal{L}}{\partial\check{\rho}}\frac{\partial\check{\rho}}{\partial\bar{N}} \\ &= [i\gamma^\mu(\partial_\mu + ig_v^\star\omega_\mu - iu_\mu\check{\Sigma}) - M^\star + h^*\phi]N \\ &= 0\end{aligned} \tag{8.30}$$

with

$$\begin{aligned}\check{\Sigma} &= \frac{\partial\mathcal{L}}{\partial\check{\rho}} \\ &= m_\omega^\star\omega^2\frac{\partial m_\omega^\star}{\partial\check{\rho}} - m_\phi^\star\phi^2\frac{\partial m_s^\star}{\partial\check{\rho}} - \bar{N}\omega^\mu\gamma_\mu N\frac{\partial g_v^\star}{\partial\check{\rho}} - \bar{N}N\frac{\partial M^\star}{\partial\check{\rho}}.\end{aligned} \tag{8.31}$$

This additional term that we identify with what is referred to in many-body theory as "rearrangement terms" plays a crucial role in what follows.[11] The equations of motion for the bosonic fields are

$$(\partial^\mu\partial_\mu + m_\phi^{\star 2})\phi = h^*\bar{N}N \tag{8.32}$$

$$\partial_\nu F_\omega^{\nu\mu} + m_\omega^{\star 2}\omega^\mu = g_v^\star\bar{N}\gamma^\mu N. \tag{8.33}$$

We start with the conserved canonical energy-momentum tensor constructed à la Noether from the Lagrangian (8.13):

$$\begin{aligned}\theta^{\mu\nu} &= i\bar{N}\gamma^\mu\partial^\nu N + \partial^\mu\phi\partial^\nu\phi - \partial^\mu\omega_\lambda\partial^\nu\omega^\lambda \\ &\quad -\frac{1}{2}[(\partial\phi)^2 - m_\phi^{\star 2}\phi^2 - (\partial\omega)^2 + m_\omega^{\star 2}\omega^2 - 2\check{\Sigma}\bar{N}\gamma\cdot uN]g^{\mu\nu}.\end{aligned} \tag{8.34}$$

[11] The notion of density-dependent parameters in many-body problems is of course an old one [Kohn and Sham 1965].

We shall compute thermodynamic quantities from (8.34) using the mean field approximation which amounts to taking

$$N = \frac{1}{\sqrt{V}} \sum_i a_i \sqrt{\frac{E_{\kappa_i} + m_N^\star}{2E_{\kappa_i}}} \begin{pmatrix} \chi \\ \frac{\boldsymbol{\sigma}\cdot\boldsymbol{\kappa}_i}{E_{\kappa_i}+m_N^\star}\chi \end{pmatrix} \exp\left(i\boldsymbol{\kappa}_i \cdot \boldsymbol{x} - i(g_v^\star \omega_0 - u_0\Sigma + E_i)t\right)$$

$$h^*\phi = C_h^2 \langle \bar{N} N \rangle = C_h^2 \sum_i n_i \frac{m_N^\star}{\sqrt{\boldsymbol{\kappa}_i^2 + m_N^{\star 2}}} \tag{8.35}$$

$$g_v^\star \omega = C_v^2(\rho, \boldsymbol{j}) = C_v^2 \sum_i n_i \left(1, \frac{\boldsymbol{\kappa}_i}{\sqrt{\boldsymbol{\kappa}_i^2 + m_N^{\star 2}}}\right)$$

where a_i is the annihilation operator of the nucleon i, with

$$n_i = \langle a_i^\dagger a_i \rangle, \tag{8.36}$$

and

$$\Sigma = \langle \check{\Sigma} \rangle, \tag{8.37}$$

$$\boldsymbol{\kappa}_i \equiv \boldsymbol{k}_i - C_v^2 \boldsymbol{j} + \boldsymbol{u}\Sigma, \tag{8.38}$$

and

$$E_{\kappa_i} = \sqrt{\boldsymbol{\kappa}_i^2 + m_N^{\star 2}} \tag{8.39}$$

with the effective nucleon mass m_N^* – which is the same as the Landau m_L^* defined above – given by

$$m_N^* = M^* - h^* \langle \phi \rangle. \tag{8.40}$$

Here χ is the spinor and $\boldsymbol{\sigma}$ is the Pauli matrix. We have defined

$$C_v(\check{\rho}) \equiv \frac{g_v^\star(\check{\rho})}{m_\omega^\star(\check{\rho})} \tag{8.41}$$

and

$$C_h(\check{\rho}) \equiv \frac{h}{m_s^\star(\check{\rho})} \equiv \frac{1}{\tilde{C}_h(\check{\rho})}. \tag{8.42}$$

In this approximation, the energy density is

$$\begin{aligned} \mathcal{E} &= \langle \theta^{00} \rangle \\ &= \langle i\bar{N}\gamma^0\partial^0 N + \frac{1}{2}m_s^{\star 2}\phi^2 - \frac{1}{2}m_\omega^{\star 2}\omega^2 + \check{\Sigma}\bar{N}/uN \rangle \\ &= \frac{1}{2}C_v^2(\rho^2 + \boldsymbol{j}^2) + \frac{1}{2}\tilde{C}_h^2(m_N^\star - M^\star)^2 + \sum_l n_l \sqrt{\boldsymbol{\kappa}_l^2 + m_N^{\star 2}} - \Sigma \boldsymbol{u}\cdot\boldsymbol{j}. \end{aligned} \tag{8.43}$$

Note that the Σ-dependent terms cancel out in the co-moving frame ($\boldsymbol{v} = 0$), so that the resulting energy-density is identical to what one would obtain from the

Lagrangian in the mean field with the density-dependent parameters taken as field-independent quantities.

Given the energy density (8.43), the pressure can be calculated by (at $T = 0$)

$$\begin{aligned} p &= -\frac{\partial E}{\partial V} = \rho^2 \frac{\partial \mathcal{E}/\rho}{\partial \rho} = \mu\rho - \mathcal{E} \\ &= \frac{1}{2} C_v^2(\rho)\rho^2 - \Sigma_0\rho - \frac{1}{2}\tilde{C}_h^2(\rho)(m_N^\star - M^\star(\rho))^2 \\ &\quad - \frac{\gamma}{2\pi^2}\left(E_F(\frac{m_N^{\star 2}}{8}k_F - \frac{1}{12}k_F^3) - \frac{m_N^{\star 4}}{8}\ln[(k_F + E_F)/m_N^\star] \right) \end{aligned} \tag{8.44}$$

where μ is the chemical potential – the first derivative of the energy density with respect to ρ in the comoving frame ($\boldsymbol{v} = 0$):

$$\mu \equiv \frac{\partial}{\partial \rho}\mathcal{E}|_{\boldsymbol{v}=0} = C_v^2\rho + E_F - \Sigma_0 \tag{8.45}$$

with $E_F = \sqrt{k_F^2 + m_N^{\star 2}}$ and $\Sigma_0 = \langle \check{\Sigma} \rangle_{\boldsymbol{v}=0}$. To check that this is consistent, we calculate the pressure from the energy-momentum tensor (8.34) in the mean field at $T = 0$:

$$\begin{aligned} p_t &\equiv \frac{1}{3}\langle \theta_{ii} \rangle_{\boldsymbol{v}=0} \\ &= \frac{1}{3}\langle i\bar{N}\gamma_i\partial_i N - \frac{1}{2}(m_\omega^{\star 2}\omega^2 - m_s^{\star 2}\phi^2 - 2\check{\Sigma}N^\dagger N)g_{ii}\rangle_{\boldsymbol{v}=0} \\ &= \frac{1}{2}C_v^2(\rho)\rho^2 - \frac{1}{2}\tilde{C}_h^2(\rho)(m_N^\star - M^\star(\rho))^2 - \Sigma_0\rho \\ &\quad - \frac{\gamma}{2\pi^2}\left(E_F(\frac{m_N^{\star 2}}{8}k_F - \frac{1}{12}k_F^3) - \frac{m_N^{\star 4}}{8}\ln[(k_F + E_F)/m_N^\star] \right). \end{aligned} \tag{8.46}$$

This agrees with (8.44). Thus our equation of state conserves energy and momentum.

We showed that a simple effective chiral Lagrangian with BR scaling parameters is thermodynamically consistent, a point which is important for studying nuclear matter under extreme conditions. It is clear, however, that this does not require that the masses appearing in the Lagrangian scale according to BR scaling only. What is shown in this subsection is that masses and coupling constants could depend on density without getting into inconsistency with general constraints of chiral Lagrangian field theory.

8.2.4 *Meaning of $C^*_{\omega_s}$*

It is tempting to assume that $C^*_{\omega_s}$ is saturated by the lowest-lying ω meson in medium and identify $C^*_{\omega_s} \propto g^*_{\omega NN}/m^*_\omega$. This would imply a constraint for $C^*_{\omega_s}$ by Eq. (8.23). But this is not entirely correct. The reason is that C_ω can receive contributions from higher-lying states of ω quantum numbers (as we have seen in holographic dual QCD discussed in Chapters 5 and 6) as well as loop corrections

that renormalize the coefficient of the four-Fermi interactions as one would expect if one were to derive the Landau Fermi-liquid parameters from a fundamental theory. We therefore must eschew making a direct connection between Φ and the scaling m_V^*/m_V for the vector mesons from (8.23). It should be understood as a mean value. We shall treat the latter in the section below.

8.2.5 *Many-body forces*

The thermodynamically consistent interpretation of BR scaling implies that certain many-body force effects are summed in the observables. To illustrate this point which plays an important role of BR scaling in nuclear matter, we look at the Lagrangian (8.13) in which the BR scaling parameters are functionals of the nucleon bilinear $\check{\rho}$,

$$\begin{aligned}\mathcal{L} = &\bar{N}(i\gamma_\mu(\partial^\mu + ig_v^\star(\check{\rho})\omega^\mu) - M^\star(\check{\rho}) + h^\star(\check{\rho})\phi)N \\ &-\frac{1}{4}F_{\mu\nu}^2 + \frac{1}{2}(\partial_\mu\phi)^2 + \frac{m_\omega^\star(\check{\rho})^2}{2}\omega^2 - \frac{m_\phi^\star(\check{\rho})^2}{2}\phi^2 + \cdots . \end{aligned} \tag{8.47}$$

Since up to the nuclear matter density only the masses seem to scale, let us look at a meson mass, say, m_ω^*. Now making a Taylor expansion, we have

$$m_\omega^*(\check{\rho})^2 = m_\omega^*(0)^2 + (\bar{N}\gamma_0 N)\frac{\partial}{\partial\check{\rho}}m_\omega^*(\check{\rho})^2|_{\check{\rho}=0} + \cdots . \tag{8.48}$$

The same expansion applies to other fields such as the scalar, the ρ *etc* that can be implemented in the Lagrangian. When inserted into a two-body potential, the second term gives rise to a three-body potential, the next term a four-body potential and so on. This means that when used as a BR scaling mass in a two-body potential, it simulates effects of n-body forces for $n > 2$. One would then think that when one does a full many-body calculation that includes a generic three-body potential, it would include the leading effect of BR scaling in addition to other contributions that have nothing to do with BR scaling. This is true to a certain extent.

However there is more in this that needs to be highlighted. First of all, in the standard chiral counting as discussed in Chapter 4, n-body forces for $n > 2$ are subleading to the 2-body forces, so the higher-body forces are expected to be suppressed. Here in contrast, all certain important n-body effects are subsumed in two-body potentials. Secondly it is consistent with the Fermi-liquid fixed point structure. These features presumably account for the phenomenological successes described below.

8.3 Observables in Finite Nuclei

In this section, we apply the formalism developed above to finite nuclei, check the consistency required and then determine the parametric masses and coupling

constants. These parameters will then be used in the next section to describe nuclear matter. For this section, the Lagrangian (8.11) is found to be more convenient.

8.3.1 *Nuclear magnetic moment*

The first case we consider is the nuclear magnetic moment, in particular the convection current of a nucleon sitting on top of a Fermi sea with a momentum $\vec{p}$, $|\vec{p}| = k_F$. It is given by

$$\vec{J} = \frac{\vec{p}}{m_N} g_l \tag{8.49}$$

where as before m_N is the nucleon mass in free space and g_l is the orbital gyromagnetic ratio. Note that it is the free-space nucleon mass that figures here. First we shall consider the isoscalar magnetic moment for which the gyromagnetic ratio is simply

$$(g_l)_{isoscalar} = 1/2. \tag{8.50}$$

This is the entire story – there cannot be any correction to this. It is the charge conservation that requires that the mass that appears in the expression be the free-space mass. One might naively expect that the mass could be the BR-scaling mass $M^\star$ but without further corrections (namely, "backflow" in the language of many-body theory), that would be inconsistent with the charge conservation. This is analogous to Kohn's theorem [Kohn 1961] in the electron gas system where the cyclotron frequency involves free electron mass and not an effective mass. The question we have to ask is: How does one reconcile with the charge conservation when one starts with the BR scaling mass M^*?

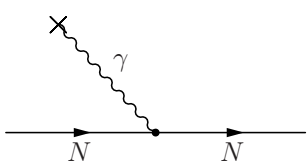

Fig. 8.3 The single particle EM current.

Starting with the Lagrangian (8.11)) suitably gauged with $U(1)_{EM}$, the single particle convection current from the Lagrangian corresponding to Fig. 8.3 is

$$\vec{J}_1 = \frac{\vec{p}}{2M^*} \tag{8.51}$$

where M^* is the BR-scaling nucleon mass. This gives the gyromagnetic ratio

$$(g_l)_{is1} = \frac{1}{2}\frac{m_N}{M^*}. \tag{8.52}$$

Thus a naive simple-minded calculation gives a wrong gyromagnetic ratio. This has been often used as an argument against the notion of BR scaling. Now in order to remedy the defect, we have to consider that we have other degrees of freedom. The pion-exchange (Fock) term Fig. 8.1, when the photon couples to the pion, can give a single-particle current, but this is purely isovector, so it does not contribute to the isoscalar current. The only non-vanishing contribution at the next order is found to be

$$(g_l)_\omega = -\frac{1}{6}C^{\star\ 2}_{\omega_s}\frac{2k_F^3}{\pi^2}\frac{1}{M^*} = \frac{1}{6}\tilde{F}_1^\omega = \frac{1}{2}(-\frac{m_N}{M^*}+1). \tag{8.53}$$

The easiest way to derive (8.53) is to compute the negative-energy sea contribution linear in nuclear density, Fig. 8.4. One can also derive it from four-Fermi interactions coupled to the electromagnetic current via nucleon convection current where all anti-nucleons and vector mesons are integrated out. The former corresponds to approximating the coefficient of the four-Fermi-EM vertex by the pair term. Note that the subscripts ω and ρ in Fig. 8.4 represent the whole tower of vector mesons with the respective quantum numbers. In practice (which is put in doubt in view of holographic dual picture), one takes only the lowest-lying vector mesons known accurately experimentally. The offending single-particle contribution (8.52) is canceled by a part of the "exchange current" (8.53) to give the sum

$$(g_l)_{isoscalar} = (g_l)_{is1} + (g_l)_\omega = \frac{1}{2} \tag{8.54}$$

as required by charge conservation. For this calculation, what is important is the relation (8.23) between the Landau parameter F_1 (or rather $\tilde{F}_1^\omega$) and the scaling quantity $\Phi \equiv M^*/m_N$ which relates a Landau fixed point parameter to the scaling.

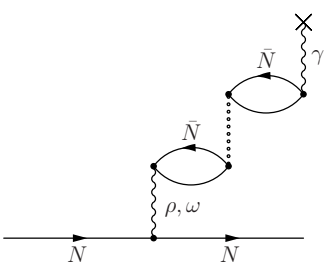

Fig. 8.4 The polarization contribution to the current. The backward-going lines correspond to negative energy states (anti-nucleons) while the lines without arrows represent nucleon states that are blocked by the filled Fermi sea. The exchanged vector mesons ρ and ω should be considered as representing the whole towers rather than the ground state vector mesons.

So far we have dealt with the isoscalar part. Now we turn to the isovector component. There will be contributions from the exchange of isovector mesons, namely, the π and the ρ. They are computed in exactly the same way as in the isoscalar part. The isovector single-quasiparticle gyromagnetic ratio is

$$(g_l)_{v1} = \frac{m_N}{2M^*}\tau_3 \tag{8.55}$$

and the contributions from the isovector mesons ρ and π are, respectively,

$$(g_l)_\rho = -\frac{1}{6}C^{*\ 2}_{\rho_s}\frac{2p_F^3}{\pi^2}\frac{1}{M^*}\tau_3 = \frac{1}{6}(\tilde{F}_1^\rho)'\tau_3 \tag{8.56}$$

and

$$(g_l)_\pi = \frac{1}{6}((\tilde{F}_1^\pi)' - \tilde{F}_1^\pi)\tau_3. \tag{8.57}$$

Thus with the help of Eq. (8.23),

$$(g_l)_{isovector} = \left(\frac{1}{2} + \frac{1}{6}(\tilde{F}_1' - \tilde{F}_1)\right)\tau_3 \tag{8.58}$$

where

$$\tilde{F}_1 = \tilde{F}_1^\omega + \tilde{F}_1^\pi, \tag{8.59}$$

$$\tilde{F}_1' = (\tilde{F}_1^\pi)' + (\tilde{F}_1^\rho)'. \tag{8.60}$$

The total gyromagnetic ratio for the nucleon is therefore

$$g_l = \frac{1+\tau_3}{2} + \delta g_l \tag{8.61}$$

with

$$\delta g_l = \frac{1}{6}(\tilde{F}_1' - \tilde{F}_1)\tau_3 \tag{8.62}$$

which is the celebrated "anomalous gyromagnetic ratio." This was first derived by Migdal [Migdal 1967] using Landau's Fermi liquid theory arguments. The derivation made here makes the connection between Fermi liquid theory and mean field chiral field theory incorporating BR scaling [Friman and Rho 1996], leading via Eq. (8.23), to

$$\delta g_l = \frac{4}{9}\left[\Phi^{-1} - 1 - \frac{1}{2}\tilde{F}_1^\pi\right]. \tag{8.63}$$

This relation suggests an intricate connection between the chiral structure of the vacuum in medium subsumed in Φ and the Fermi liquid interactions at the fixed point, which are many-body interactions in the conventional many-body theory. To ultimately understand this relation which links the complex QCD vacuum and many-body interactions, it may be necessary to understand the connection between

the Fermi-liquid fixed point and topology in emerging dynamics in many-body interactions as discussed by Horăva [Horăva 2005].

8.3.2 *Deducing $\Phi(n_0)$ from experiment*

One can compare the prediction (8.63) with the experimental value for g_l from the total photo-absorption on proton measured in heavy nuclei [Nolte, Baumann, Rose and Schumacher 1986; Schumacher *et al.* 1994],

$$\delta g_l^p = 0.23 \pm 0.03. \tag{8.64}$$

Substituting (8.25) for $\tilde{F_1^\pi}(n_0)$ into Eq. (8.63), this gives

$$\Phi(n_0) \simeq 0.78. \tag{8.65}$$

This is the value we shall use most of the time. If we make an interpolation between $n = 0$ and $n = n_0$ in the form

$$\Phi(n) = \frac{1}{1 + y\frac{n}{n_0}}, \tag{8.66}$$

then we find

$$y \simeq 0.28. \tag{8.67}$$

Now given (8.65) and (8.24), we can use Eq. (8.22) to predict the Landau mass which is the physical effective mass of the nucleon

$$\frac{m_L^\star}{m_N} \simeq 0.69. \tag{8.68}$$

There is a QCD sum-rule calculation that agrees with this [Furnstahl, Jin and Leinweber 1996]. We should stress – and this will be repeated below – that the scaling (8.66) with (8.67) is valid only in the vicinity of the nuclear matter density.

8.3.3 *Relation between the Landau mass m_L^* and the axial coupling constant g_A*

The Landau mass (8.22) can be related via (8.23) to the BR scaling Φ and the pionic contribution to the Landau parameter F_1 as

$$\frac{m_L^\star}{m_N} = \Phi\left(1 + \frac{1}{3}F_1^\pi\right) = \left(\Phi^{-1} - \frac{1}{3}\tilde{F}_1^\pi\right)^{-1}. \tag{8.69}$$

Let us now consider getting the scaling of the nucleon mass from the Skyrme model (see Chapter 6) that has two parameters f_π and e, the former related to the current algebra term and the second to the Skyrme quartic term. A simple scaling argument

in the Skyrme model as used in deriving the BR scaling leads to the relation [Rho 1985; Brown and Rho 1991]

$$\frac{m_L^\star}{m_N} \approx \Phi(\rho)\sqrt{\frac{g_A^\star}{g_A}}. \tag{8.70}$$

Equations (8.69) and (8.70) give

$$\frac{g_A^\star}{g_A} = \left(1+\frac{1}{3}F_1^\pi\right)^2 = \left(1-\frac{1}{3}\Phi\tilde{F}_1^\pi\right)^{-2}. \tag{8.71}$$

Let us see what (8.71) predicts at nuclear matter density. Using $\Phi(n_0) \simeq 0.78$ determined above and $\frac{1}{3}\tilde{F_1^\pi}(n_0) \simeq -0.153$ calculated in (8.25), we obtain for $g_A = 1.26$

$$g_A^\star \simeq 1.0. \tag{8.72}$$

This is in good agreement with what has been determined in analyses in finite nuclei. See, *e.g.*, [Buck and Perez 1984; Radha *et al.* 1997].

8.3.4 *Pion decay constant in medium*

From deeply bound pionic nuclei, the ratio f_π^*/f_π has been deduced [Kienle and Yamazaki 2004]. What has been found is

$$(f_\pi^\star(0.6n_0)/f_\pi)^2 = 0.78 \pm 0.05. \tag{8.73}$$

To see what this corresponds to in terms of the extrapolation of the type (8.66), we write

$$f_\pi^\star(n)/f_\pi = \frac{1}{1+x\frac{n}{n_0}}. \tag{8.74}$$

From (8.73), one gets

$$x \simeq 0.22 \tag{8.75}$$

which gives

$$f_\pi^*(n_0)/f_\pi \simeq 0.81 \tag{8.76}$$

which is consistent within the error bar with the prediction (8.65).

8.3.5 *Effect on tensor forces*

Historically the BR scaling was deduced from something that is intrinsically nuclear physics. It was in particular the structure of tensor forces in nuclei that suggested that hadronic masses might be scaling in dense medium. The notion that tensor

forces in nuclei must be strongly influenced was formally discussed in [Brown and Rho 1990] although it goes back to earlier times.

Working with an HLS Lagrangian in the large N_c limit, we consider the tensor forces generated by meson exchanges. We are to consider the graphs at tree order. At tree order, we have the pion exchange and ρ exchange with the nucleon treated in non-relativistic approximation ($1/m_N$ corrections coming in at higher order in the chiral counting), with the parameters of the Lagrangian endowed with the intrinsic density dependence. In the presence of the pions and the vector mesons as in HLS theory and treating at the tree level, the tensor force between two nucleons in free space (*i.e.* $n = 0$) has two components, the pionic and the ρ. In momentum space,

$$V_T = V_T^\pi + V_T^\rho \tag{8.77}$$

where

$$V_T^\pi(q) = -\frac{f_{\pi NN}^2}{m_\pi^2}(\tau_1 \cdot \tau_2)\left[\frac{(\sigma_1 \cdot \mathbf{q})(\sigma_2 \cdot \mathbf{q}) - \frac{1}{3}((\sigma_1 \cdot \sigma_2)q^2}{q^2 + m_\pi^2}\right], \tag{8.78}$$

$$V_T^\rho(q) = \frac{f_{\rho NN}^2}{m_\rho^2}(\tau_1 \cdot \tau_2)\left[\frac{(\sigma_1 \cdot \mathbf{q})(\sigma_2 \cdot \mathbf{q}) - \frac{1}{3}((\sigma_1 \cdot \sigma_2)q^2}{q^2 + m_\rho^2}\right]. \tag{8.79}$$

Here $f_{\pi NN}^2/4\pi = 0.08$, $f_{\rho NN}^2/m_\rho^2 \simeq 2f_{\pi NN}^2/m_\pi^2$ and

$$f_{\rho NN} = g_{\rho NN}\frac{(1 + \kappa_V^\rho)m_\rho}{2m_n} \tag{8.80}$$

with $\kappa_V^\rho = 6.6 \pm 0.6$.

Now how do we go to an effective tensor force valid in medium?

In the leading order approximation (*i.e.* mean field), it suffices to put asterisks on the parameters that figure for the ρ meson, given that the pion mass m_π and the pion-nucleon coupling $f_{\pi NN}$ remain unscaled. Up to nuclear matter density, the ρ scales with $\Phi(n)$. As mentioned in Chapter 7, we do not know theoretically how the ρNN coupling constant $g_{\rho NN}$ scales except very near chiral restoration. The only information we have is from phenomenology that suggests that up to $n \approx n_0$, $g_{\rho NN}^* \approx g_{\rho NN}$. Thus $f_{\rho NN}$ can be taken unscaled at least up to the nuclear matter density. This means that all that is needed is to scale the ρ mass in (8.79) as $m_\rho^* \approx \Phi(n)m_\rho$. The resulting tensor force is shown and compared to the free-space force in Fig. 8.5. This shows that there is a substantial reduction of the tensor force at $r \sim 1$ fm. Various physical consequences of this effect is discussed in [Brown and Rho 1990]. Although this important effect was pointed out a long time ago, little attention has been paid to this in the community of nuclear structure physics. However, a recent development highlights a spectacular effect of BR scaling in nuclear physics which we discuss briefly. It concerns with the ^{14}C dating beta decay [Holt, Brown, Kuo, Holt and Machleidt 2007]. What is noteworthy in this development is that it offers one more indication – perhaps the most striking of them all – that the BR scaling manifests itself in a highly subtle way compounded

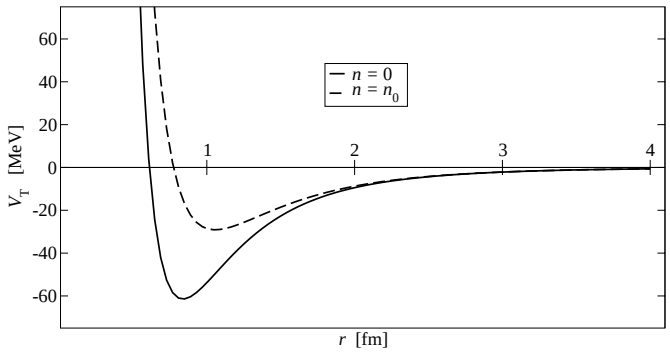

Fig. 8.5 The radial part of the nuclear tensor force in coordinate space (of Eqs. (8.78) and (8.79)) from π and ρ meson exchange at zero density (solid line) and nuclear matter density with $\Phi(n_0) = 0.80$ (broken line).

with what appears to be mundane many-body effects. This is in line with what we encountered in the nuclear anomalous gyromagnetic ratio discussed above.

The unusually long half-life, $\tau_{1/2} \simeq 5730$ yr, of the $^{14}\mathrm{C}(J^\pi = 0^+, T = 1)$ to $^{14}\mathrm{N}(J^\pi = 1^+, T = 0)$ β transition has long been a puzzle for the nuclear shell model for more than half a century. While the decay is mediated by an allowed Gamow-Teller matrix element, the decay rate is suppressed by nearly six orders of magnitude, indicating that the transition matrix element accidentally vanishes. There are two prominent factors that lead to this surprising aspect in the transition.

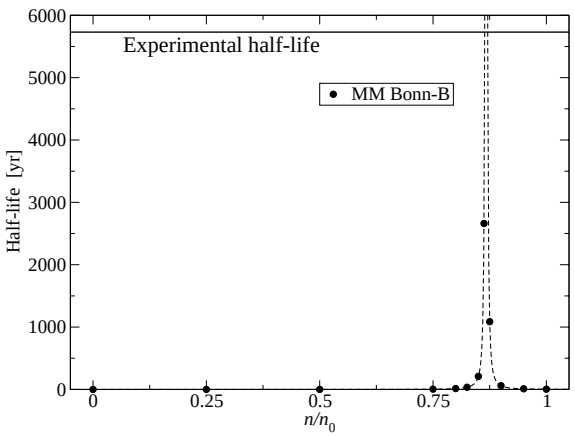

Fig. 8.6 The half-life of $^{14}\mathrm{C}$ calculated using the medium-modified Bonn-B potential.

The first is that the initial and final states are of two holes in the doubly closed shell at mass number 16, namely $^{16}\mathrm{O}$. Being just below the double shell closure, the

nuclear density is close to that of nuclear matter. The second is that the Gamow-Teller transition involved is extremely sensitive to the nuclear tensor force. These two play a crucial role in zeroing in onto the effect of Brown-Rho scaling.

To calculate the relevant matrix element of the Gamow-Teller operator, one decimates a realistic NN potential à la Wilsonian renormalization to a shell-model scale at which two-hole configurations in the $p_{1/2}$ and $p_{3/2}$ shells interact, thereby obtaining an effective potential of the V_{low-k} type [Bogner, Kuo, Schwenk, Entem and Machleidt 2003]. As mentioned in Chapter 4, the resulting effective potential should not depend upon the detailed short-distance structure of the basic NN potential as long as it has the correct long-distance feature given by chiral symmetry and fit to scattering data to the lab momentum ~ 2 fm^{-1}. In the calculation of [Holt, Brown, Kuo, Holt and Machleidt 2007], the V_{low-k} was obtained from the Bonn-B potential. Now put in LS-coupling, the wavefunctions for the ^{14}C and ^{14}N ground states are

$$\begin{aligned}\psi_i &= x\left|{}^1S_0\right\rangle + y\left|{}^3P_0\right\rangle \\ \psi_f &= a\left|{}^3S_1\right\rangle + b\left|{}^1P_1\right\rangle + c\left|{}^3D_1\right\rangle .\end{aligned} \tag{8.81}$$

In terms of these wavefunctions, the Gamow-Teller matrix element $M_{\rm GT}$ is given by

$$\sum_k \langle\psi_f||\sigma(k)\tau_+(k)||\psi_i\rangle = -\sqrt{6}\left(xa - yb/\sqrt{3}\right). \tag{8.82}$$

It is known that the amplitudes x and y have the same sign, so the Gamow-Teller matrix element can vanish only if a and b have the same sign, which requires that the $\left\langle{}^3S_1\right| V_{\rm eff}\left|{}^3D_1\right\rangle$ matrix element furnished by the tensor force be large enough. Indeed the two terms in the Gamow-Teller matrix element (8.82) are found to cancel each other when the matter density reaches $\sim 0.85n_0$. In Fig. 8.6 is shown the half-life of ^{14}C as a function of density. One can see that the half-life is near zero except in the range of 0.75-1.0 n_0 where it diverges as $1/\Delta^2$ as $\Delta \to 0$. [12] The splitting between the 1^+_1 and 0^+_1 levels in ^{14}N is found to be also quite sensitive and neatly provides a support for the life-time calculation as one can see in Fig. 8.7. It turns out, however, that beta transitions from excited states of ^{14}C are relatively insensitive to density and hence to Brown-Rho scaling.

8.3.6 *Warburton ratio*

Combining the Brown-Rho scaling with the notion of the chiral filter presented in Chapter 4 allows us to calculate certain processes in heavy nuclei which, up to date, cannot be accessed by the RigEFT. The striking example is the $\Delta J = 0$ first

[12] Corrections from forbidden terms, relativistic terms *etc.* in the weak current would of course soften the divergence but the qualitative feature will not be modified.

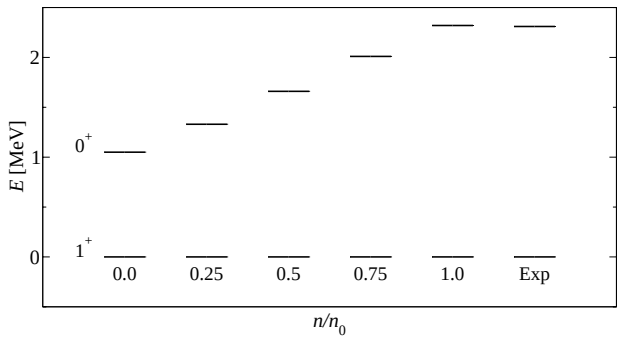

Fig. 8.7 The splitting between the 1_1^+ and 0_1^+ levels in ^{14}N for different values of the nuclear density. Also included is the experimental value.

forbidden β decay

$$A(J^{\pm}) \to A'(J^{\mp}) + e^-(e^+) + \bar{\nu}(\nu), \quad \Delta T = 1 \tag{8.83}$$

where A and A' are the initial and final nuclei involved in the transition. This transition is largely mediated by the time component of the axial current (*i.e.* axial charge) A_0^a. In nuclear systems, this operator is chiral-filter protected in the sense that the main correction to the single-particle axial charge operator is given by the "soft-pion" term (4.30), which is completely fixed by chiral symmetry. Furthermore at the mean field level, the intrinsic density dependence prescribed by hidden local symmetry says that the same operator is effective in heavy nuclei if the coefficient of the operator $1/F_\pi$ is replaced by the *parametric* pion decay constant $1/F_\pi^*$ scaling with density. This observation led to an extremely simple calculation of the correction to the axial-charge matrix element for the process (8.83) [Kubodera and Rho 1991; Friman, Rho and Song 1999]. This prediction has been tested by experiments.

The convenient quantity to look at is the Warburton ratio [Warburton 1991] defined as

$$\epsilon_{MEC} \equiv \frac{M^{exp}}{M_1^{sp}} \tag{8.84}$$

where M^{exp} is the measured axial charge matrix element and M_1^{sp} is the matrix element *calculated* in the impulse approximation. The numerator of (8.84) is experimental but the denominator is theoretical since it is a matrix element of the single-particle operator with free-space coefficients computed with the SNPA (standard nuclear physics approach) wave functions discussed in Chapter 4. As such, the ratio ϵ_{MEC} is at best semi-empirical with caveats attached to the extraction of the axial-charge matrix element from the observed decay rate and the calculation

of M_1^{sp}. Nonetheless one can make a semi-quantitative test of the prediction using this ratio.

In terms of the BRS factor $\Phi(n)$ valid near the nuclear saturation density (*i.e.* Fermi liquid fixed point), the prediction is [Friman, Rho and Song 1999]

$$\epsilon_{MEC}^{th} = \frac{1}{\Phi}(1+\delta) \tag{8.85}$$

where δ is given by the soft-pion exchange term governed by the vertex (4.30) (given in Chapter 4) corrected by a small amount from vector mesons. Numerically one finds for the densities $n = n_0/2$ and $n = n_0$

$$\epsilon_{MEC}^{th}|_{n=n_0/2} \approx 1.63, \quad \epsilon_{MEC}^{th}|_{n=n_0} \approx 2.06. \tag{8.86}$$

The experimental extraction of the ratio leads to the values : $\epsilon_{MEC}^{exp} = 1.60 \pm 0.05$ for $A = 50$ and 2.01 ± 0.10 for $A = 208$ (see [Brown and Rho 2002] for details including references to the experimental papers). With due considerations of the caveats mentioned above, this is a striking confirmation of the power of MEEFT as well as the notion of BR scaling.

8.3.7 *"Observing" the dropping vector meson masses*

We have thus far looked at indirect manifestation of BR scaling in the properties of nuclei. The overall picture that emerges is consistent with the notion of BR scaling and HLS/VM. There is no indication that the way the "mass" behaves in the vicinity of nuclear matter density contradicts the theory. One would, however, like to see a "smoking gun" signal for the vacuum-induced effect that says something definite about the origin of hadron mass.

There have been extensive discussions on whether or not there is evidence for medium-modifications of the ρ meson properties following the CERES and NA60 experiments on dilepton production in heavy ion collisions. For review, see [Rapp and Wambach 2000]. It has been stated, albeit without rigor, throughout the volume that dileptons are not good signals for chiral symmetry: Although the description is clean very near the chiral restoration point, the strength of the lepton coupling to the ρ and ω meson is strongly suppressed by the vector-dominance violation due to the VM effect. Why this is so is clear from what we have discussed so far but will be stated in a much more precise term later. It suffices to mention here that the experiments performed so far did not succeed to zero in on those dileptons coming from dense/hot medium where the vector manifestation is operative. Since the jury is not out on the controversy, we will not dwell in detail on this issue. [13] Given the confused situation, one can only say that the observations are not inconsistent with

[13] For a recent argument that the dilepton experiments, in particular, the NA60, have little to do with the properties of the ρ meson vis-à-vis with chiral symmetry, see [Brown, Harada, Holt, Rho and Sasaki 2008].

the scaling $m^*_\rho(n_0)/m_\rho \simeq 0.78$ as required by BR scaling and obtained in QCD sum rule calculations.[14]

A number of experimental evidences for BR scaling have been reported in the literature. One early case was the measurement of the in-medium mass of ρ^0 in the ^{3}He$(\gamma, \rho^0)ppn$ reactions [Lolos *et al* 1998]. Exploiting tagged photon energies below the ρ^0 production threshold on a free nucleon, Lolos *et al* measured the decay product in $\rho^0 \to \pi^+\pi^-$. The observed shift was $\delta m_{\rho^0} = 160 \pm 35$ MeV. Given that the nucleus probed is light, this is a huge mass shift. Also considering that the final state is strongly interacting, what is gotten may not be a "snap-shot" picture of the in-medium ρ^0. The situation is not clear at this moment.

A much cleaner evidence comes from the behavior of the ω meson in medium, not via dileptons, but in the Wess-Zumino-term induced anomalous process

$$\gamma + A \to \omega + X \to \pi^0\gamma + X' \tag{8.87}$$

where A, X and X' represent nuclei. The invariant mass $M_{\pi\gamma}$ measured by Trnka *et al* [Trnka *et al.* 2005] is shown in Fig. (8.8). What makes this process cleaner is that coming from the anomalous (*i.e.* Wess-Zumino) term, it is protected by topological constraints, so freer of mundane strong interaction effects. Furthermore, it does not suffer from such VM effect as the violation of vector dominance which suppresses the dilepton productions near the chiral transition point as discussed in Chapter 7. The measurement was made with the Nb target whose average density is roughly 0.6 times n_0. Extrapolating to normal nuclear matter density, the authors of [Trnka *et al.* 2005] deduced

$$m^*_\omega(n_0)/m_\omega \simeq 0.84. \tag{8.88}$$

In view of the fact that using a finite nucleus and extrapolating to nuclear matter density is a rough procedure – and since one expects important fluctuations around the bulk property that tracks the vacuum change, this scaling is not inconsistent with what we found for the ρ meson, $m^*_\rho(n_0)/m_\rho \simeq 0.78$ – which as mentioned above, could represent an average value for the infinite tower of vector mesons in the ρ channel. Generically the pole mass of the vector meson measured in experiments is expected to read as

$$m^*_V = {a^*}^{1/2} g^* F^*_\pi + (\Delta M)_V \tag{8.89}$$

which consists of the parametric mass (first term) involving the hidden gauge coupling g and the pion decay constant F_π and a medium-dependent quantum correction $(\Delta M)_V$. It is the parametric mass ${a^*}^{1/2} g^* F^*_\pi$ that should scale universally and

[14] QCD sum-rule calculations are still fraught with uncertainties as well as misinterpretations thereof and it will be premature for us to make definite statement about what are available in the literature. It should, however, be mentioned that there is at least one set of sum-rule calculations which agree with our results for $m^\star_\rho(n_0)/m_\rho$ and $m^\star_L(n_0)/m_N$. The calculation by Jin and Leinweber [Jin and Leinweber 1995] finds $m^\star_\rho/m_\rho|_{n=n_0} = 0.78 \pm 0.08$ and that by Furnstahl *et al* [Furnstahl, Jin and Leinweber 1996] $m^\star_N/m_N|_{n=n_0} = 0.67 \pm 0.05$.

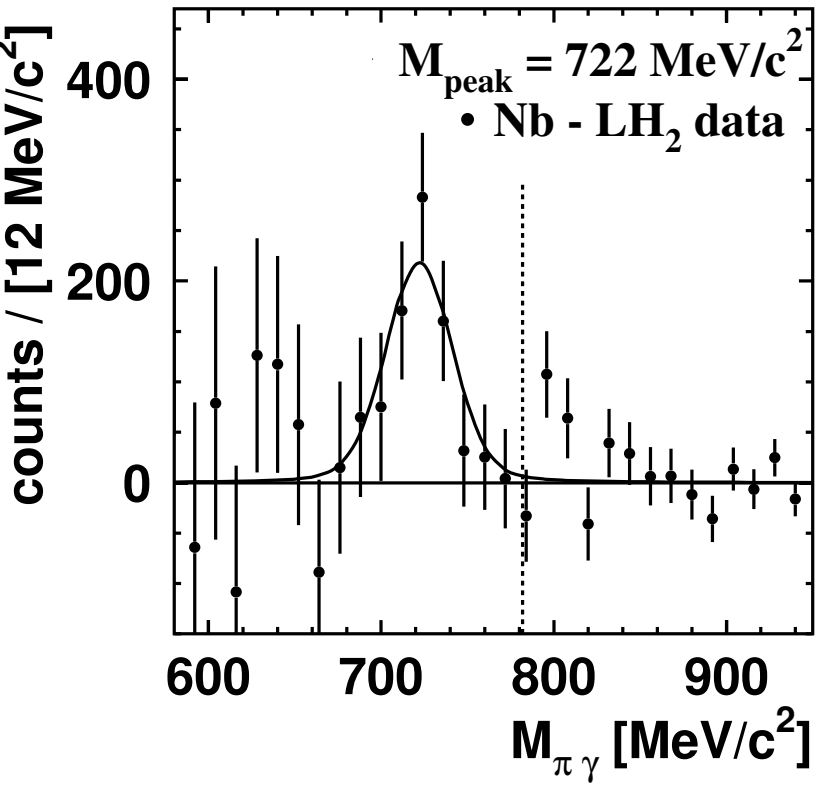

Fig. 8.8 The mass shift in the ω meson channel measured in the process $\gamma + A \to \omega + X \to \pi^0\gamma + X'$. From [Trnka *et al.* 2005] (copyright 2005 by the APS).

the medium-loop corrections $(\Delta M)_V$ that receive contributions from the coupling of the vector mesons to medium excitations will differ between the ρ and ω even if the assumed symmetry is $\mathrm{U(N}_f\mathrm{)}$ that puts the ρ and ω in the same multiplet in the medium-free space. One should also not forget the caveat mentioned before: that far away from the VM fixed point, there is nothing which says that the second term of (8.89) could not swamp the first term, thereby wiping out the signal from the intrinsic dependence on the quark condensate that is lodged in the gauge coupling g.

8.4 Dropping Masses and Nuclear Matter

In this section, we apply the "chiral Fermi liquid field theory" described above to the structure of nuclear matter and then compare with a microscopic derivation of Fermi liquid theory starting with an NN potential.

8.4.1 *Nuclear matter in chiral Fermi liquid approach*

As mentioned before, in calculating nuclear matter starting from an effective field theory Lagrangian, we can equivalently use, in mean field, either (8.11) or (8.13). To compare with the linear Walecka model,[15] it is more convenient to take the Lagrangian (8.13).

Once the scaling factor is picked, then the mass parameters that we have to fix are the free-space masses of the ω, the N, and the scalar ϕ (or the σ in the standard nuclear physics notation). The nucleon and vector meson masses are given in the Particle Data Booklet, but the mass of ϕ is an unknown (ϕ being an effective interpolating field) and we take it to be ~ 700 MeV. The constant h in (8.13) is to be fixed self-consistently by identifying

$$m_L^\star/m_N = M^\star - h\langle\phi\rangle^\star \tag{8.90}$$

with (8.69). The density-driven running of the coupling constant $g_v^\star$ is not known by the theory except near the phase transition which is irrelevant to our problem. However, the situation is not so bad. As before, we can rely on the empirical observation [Brown and Rho 2004a] that $g_v^\star$ (related to the HLS coupling g in medium) remains more or less constant up to the equilibrium density and then runs proportionally to the running of the vector meson mass above that density. A straightforward mean-field calculation yields for the above set of constants and properties the following nuclear matter quantities [Song, Brown, Min and Rho 1997; Song 2001]:

$$B = 16.1 \text{ MeV}, \quad k_F = 258 \text{ MeV}, \ K = 259 \text{ MeV} \tag{8.91}$$

where B is the binding energy, k_F the equilibrium Fermi momentum and K the compression. The corresponding Landau mass is given by

$$m_L^\star/m_N = 0.675. \tag{8.92}$$

The values (8.91) and (8.92) should be compared with the standard "empirical values"[Furnstahl and Serot 2000]

$$B = 16.0 \pm 0.1 \text{ MeV}, \quad k_F = 256 \pm 2 \text{ MeV}, \ K = 250 \pm 50 \text{ MeV},$$
$$m_L^\star/m_N = 0.61 \pm 0.03. \tag{8.93}$$

Given the extreme simplification of the calculation, a precise comparison may not be very meaningful, but the point to note is that the simple picture is surprisingly consistent with nature. It has not been rigorously shown but it is plausible that many-body effects as described in Section 8.2.5 together with the Fermi-liquid fixed point structure play a crucial role here in giving the correct description of nuclear matter.

[15] One can do much better by including nonlinear terms as discussed in [Song, Brown, Min and Rho 1997], but this procedure is quite arbitrary and does not provide insight into their origins.

8.4.2 *Microscopic approach to Landau Fermi liquid with Brown-Rho scaling*

In the chiral Fermi liquid field theory approach described above, we have used two established results to by-pass the first to go to the second decimation. Now let us see how one can go about doing the first decimation.

To be in line with what has been developed in this volume, let us consider a generalized hidden local symmetry (GHLS) theory discussed in Chapter 5 that contains a complete set of relevant degrees of freedom for nuclear matter, say, π, ρ, ω, a_1, ϕ *etc.*, matched to QCD at a matching scale Λ_M.[16] There are no explicit baryon degrees of freedom in this theory. We shall take it for granted that if needed, baryons can be generated naturally as skyrmions even though no one has arrived at nuclear dynamics starting from a GHLS. As in the preceding chapters, one simply introduces baryon fields explicitly as matter fields and couples them in a hidden local symmetric way. This is what is done in standard chiral perturbation theory with global chiral symmetry with pions and nucleons as the only explicit degrees of freedom. Now the crucial ingredient to be taken into account is that through the Wilsonian matching, the "bare" Lagrangian so obtained carries parameters such as masses and coupling constants endowed with an intrinsic background (temperature or density) dependence that tracks the properties of chiral symmetry.

Given the "bare" Lagrangian so determined, one then can proceed in three steps, as follows:

(M1) First one constructs NN potentials in chiral perturbation theory with the vector mesons treated à la Harada and Yamawaki [Harada and Yamawaki 2003] – here hidden local symmetry plays a crucial role. Again such a potential has not yet been derived, but we see no reason why it cannot be constructed: the chiral perturbation procedure is as well formulated in HLS theory as in the standard approach without the vector degrees of freedom.

(M2) Next, one performs a (Wilsonian) renormalization-group decimation to the "low-k" scale [17] Λ_{low-k} to obtain the V_{low-k} [Bogner, Kuo, Schwenk, Entem and Machleidt 2003]. The scale Λ_{low-k} defines the *first decimation* and depends upon what one does for the next decimation. To confront NN scattering data available for the purpose, the convenient choice turns out to be $\Lambda_{low-k} \approx 2$ fm^{-1}. The NN potential constructed in the step (M1) above should then be consistent with scattering data up to that momentum scale.

(M3) The potential V_{low-k} so derived is then fed into the Green's function integral equation for the Landau parameters F [Abrikosov, Gor'kov and Dzyaloshinski 1965]. This step corresponds to the *second decimation* to the Fermi surface.

A calculation of this type should then give a microscopic derivation of chiral Fermi liquid effective theory described in the preceding subsection. Such a calculation

[16] The GHLS Lagrangian did not contain the scalar ϕ. Here we are adding it by hand.

[17] We can identify this scale with Λ_{FS} introduced above.

has been performed by Holt *et al.* [Holt, Brown, Holt and Kuo 2006] but using a phenomenological NN potential and implementing Brown-Rho scaling in an indirect way. The approach is identical to what was done in the calculation of the carbon-14 dating transition described above. Since V_{low-K} is universal for all potentials that have the correct long-range behavior typically given by pions and are fit to NN scattering to ~ 2 fm^{-1} [Bogner, Kuo, Schwenk, Entem and Machleidt 2003], there will be little difference from the result based on GHLS for the first decimation except for the fact that the phenomenological potentials as used in [Schwenk, Friman and Brown 2002] lack the *intrinsic density dependence (IDD)*. [18] This means that the potential as it stands applied to the second decimation in dense medium [Schwenk, Friman and Brown 2002] cannot be reliable unless Brown-Rho scaling is suitably implemented. In phenomenological models where the scalar meson ϕ figures as in Bonn potential, Brown-Rho scaling can be effectively, but approximately, implemented by inserting scalar tadpoles on the propagators of all the degrees of freedom involved and this is what has been done in [Holt, Brown, Holt and Kuo 2006].[19] In this work, the Landau interaction parameters are expressed as a sum of two terms: a "driving term" and an "induced term." The induced term representing the exchange term constrained by the Pauli principle is computed using a technique developed by Babu and Brown (called Babu-Brown induced interaction) [Babu and Brown 1973]. The standard Landau theory is then applied to computing the energy density, Landau effective mass, compression modulus *etc.* that figure for the description of nuclear matter. Now had the above procedure been followed in GHLS, the theory would have Brown-Rho scaling automatically incorporated as an IDD. However, since Holt *et al.* take, for the step (M1), phenomenological potentials in which the intrinsic density dependence (IDD) required by matching to QCD is missing and the result would essentially be the same as in [Schwenk, Friman and Brown 2002], Brown-Rho scaling has to be added explicitly. What is significant is that they find that without IDD, nuclear matter cannot be described correctly. Indeed, with the Brown-Rho scaling implemented as described, the calculation of [Holt, Brown, Holt and Kuo 2006] provides a satisfactory microscopic description of Fermi liquid structure of nuclear matter, thereby providing a *derivation* of the chiral Fermi liquid field theory.

There are several highly non-trivial lessons one can learn from what was obtained above. One, one can think of this as a confirmation of the soundness of the double decimation procedure. Two, both the microscopic approach [Holt, Brown, Holt and Kuo 2006] and the effective field theory approach [Song, Brown, Min and Rho 1997] – which complement each other – indicate the importance of Brown-Rho scaling in the structure of nuclear matter. Three, there must be a relation – presumably complicated – between the Φ and the microscopic potential V_{low-k} valid at nuclear

[18] That such a V_{low-k} should be universal and insensitive to short-distance uncertainty is the basis of what is called MEEFT or "more effective effective field theory" described in Chapter 4.

[19] The tadpole insertion is equivalent to doing the mean-field approximation with the nucleon bilinear $\check{\rho}$ in the Lagrangian (8.47).

matter density. Finally, it is clear that the connection between Brown-Rho scaling and many-body interactions is highly intricate and needs to be carefully assessed depending on the environment where the system is probed. This observation allows us to sharpen the assertion made before: That only very close to the critical point is the scaling directly locked to the chiral order parameter $\langle \bar{q}q \rangle^{\star}$, and near the normal nuclear matter density, the connection, if any, is highly compounded with many-body interactions. This is evidenced by the subtle interplay between, to name a few, the Fermi liquid fixed point parameter F_1, the ω-mass scaling, the anomalous orbital gyromagnetic ratio in nuclei, the working of tensor forces *etc.*

This page intentionally left blank

Chapter 9

Strangeness In Dense Medium

Although we have argued by means of the vector manifestation that the hidden local symmetry approach could be most reliable very near the chiral restoration density as very near the critical temperature, we have not yet dealt with dense matter beyond the nuclear matter density. In this chapter, we treat many-baryon systems possibly relevant to the interior of compact stars, in particular the process that can be most profitably accessed starting from the VM fixed point, namely, the condensation of negatively charged kaon, K^-.

Going above the normal nuclear matter density, before reaching the conjectured super-dense matter which can be described in terms of well-controlled perturbative QCD, *i.e.* color-flavor-locked superconductivity, there can be a multitude of phase changes from normal nuclear matter to "exotic" states. Possible such non-normal-nuclear states are pion condensation, kaon condensation, hyperon matter *etc.* In this chapter, we will develop arguments that the first, and possibly the last, phase change that occurs as the density increases beyond that of nuclear matter is kaon (*i.e.* K^-) condensation.[1] In our description, this will be the crucial phase change that will determine the fate of massive stars, say, form stable neutron stars or collapse to black holes. Possible other phases that can figure afterwards at higher densities are unlikely to be relevant.[2] Even if observations established that quark matter is present in compact stars, kaon condensation could play a non-negligible role as a doorway to it. This will be discussed in the next chapter. The specific feature of kaon condensation *proper* that enters into the physics of compact stars will not be treated in this chapter.

In approaching the state of matter present in the interior of compact stars, we will start from three different vantage points and arrive at the concurring result that

[1] In this chapter, unless otherwise noted, "kaon" will stand for the negatively charged kaon.

[2] Pion condensation is a possible phase and has been extensively discussed since 1970's (see [Rho and Wilkinson 1979]) but no evidence for the condensation or even precursor has shown up in experiments. There are theoretical reasons why it cannot occur before kaon condensation, so we shall ignore it here. The hyperon matter cannot be ruled out but it involves complications that cannot be given a reliable treatment in the framework adopted in this volume. Furthermore there are reasons to believe that it is not very relevant to the process in question. We will only briefly comment on it as we go along.

kaons must condense in the vicinity of $3n_0$ before anything else happens. This then leads us to the conclusion that kaon condensation is the most likely phase transition to take place in hadronic matter in the density regime *that is relevant* to the fate of compact stars. This is a rather strong point but has the virtue of being falsifiable as we will specify. We will confront this conclusion with astrophysical observations in Chapter 11.

9.1 Kaon Condensation from Matter-Free Vacuum

The approach most frequently resorted to for treating high density matter up to chiral restoration is chiral perturbation theory, pioneered by Kaplan and Nelson [Kaplan and Nelson 1986]. Here the assumption is that by doing higher chiral perturbation calculations with a chiral Lagrangian constructed in a matter-free environment and assuring such properties as unitarity, one can access possible such phase changes as meson condensations. This is what we will do first. But before going into more detailed treatments, we first look at the problem in an extremely simplified way that captures the essence of the process.

9.1.1 *Kaon condensation as "restoration" of explicit chiral symmetry breaking*

Suppose that the s quark mass were comparable to the chiral (u, d) quark mass, so kaons were (nearly) degenerate with pions. In this case, there would be no reason why kaons should condense in preference to pions. Therefore one can think that kaons condense because the s quark is massive, and what matter density does is to "restore" the chiral symmetry explicitly broken by the s-quark mass. To see how this comes about, it is found to be simplest to take the V-spin projection of the Goldstone boson sphere onto the V-spin circle, composed of K^- and a scalar σ in the $SU(3)$ chiral Lagrangian [Brown, Kubodera and Rho 1987]. The Hamiltonian for explicit chiral symmetry breaking – which is of $\mathcal{O}(p^2)$ in the chiral power counting – is then given by

$$\begin{aligned} H_{\chi SB} &= \Sigma_{KN}\langle\bar{N}N\rangle\cos\theta + \frac{1}{2}m_K^2 {f_\pi}^2\sin^2\theta \\ &\simeq \Sigma_{KN}\langle\bar{N}N\rangle\left(1-\frac{\theta^2}{2}\right) + \frac{1}{2}m_K^2 {f_\pi}^2\theta^2 + \cdots \end{aligned} \tag{9.1}$$

where θ is the chiral angle defined in Fig. 9.1 and f_π is the physical pion decay constant. The last expression is obtained for small fluctuations θ. Here we have taken mean field in the baryon sector. Dropping the term independent of θ, we find

$$ {m_K^\star}^2 = m_K^2\left(1-\frac{\Sigma_{KN}\langle\bar{N}N\rangle}{f_\pi^2 m_K^2}\right)^{1/2} . \tag{9.2}$$

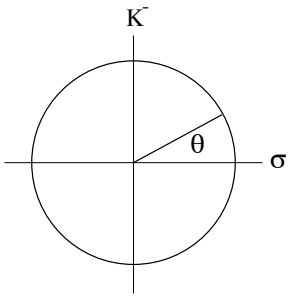

Fig. 9.1 Projection onto the σ-K^- plane. The angular variable θ represents fluctuation toward kaon mean field.

The KN sigma term is

$$\Sigma_{KN} = \frac{(m_u + m_s)\langle N|\bar{u}u + \bar{s}s|N\rangle}{(m_u + m_d)\langle N|\bar{u}u + \bar{d}d|N\rangle}\sigma_{\pi N} \tag{9.3}$$

where $m_{u,d,s}$ are the current quark masses and $\sigma_{\pi N}$ is the pion sigma term. Lattice calculations [Dong, Lagae and Liu 1996] give

$$\Sigma_{KN} \simeq 389(14) \text{ MeV}. \tag{9.4}$$

We can go one order higher in the "effective mass" of the kaon (9.2) by incorporating what is called "range term" which turns out to be important quantitatively [Lee 1996]. It amounts to changing Σ_{KN} to

$$\Sigma_{KN}^{\text{eff}} = \left(1 - 0.37\frac{\omega_{K^-}^2}{m_K^2}\right)\Sigma_{KN} \tag{9.5}$$

where ω_{K^-} is the (anti)kaon energy

$$\omega_{K^-} = V_{TW}^{K^-} + \sqrt{k^2 + {m_{K^-}^\star}^2}. \tag{9.6}$$

In addition to the scalar attraction (which can be thought of as giving the kaon an effective mass), there is the vector attraction given by the Weinberg-Tomozawa term – which is the leading term, *i.e.* $\mathcal{O}(p)$, in the chiral counting,

$$V_{\text{TW}}^{K^-} = -\frac{3}{8f_\pi^2}n \approx -60 \text{ MeV}\frac{n}{n_0} \tag{9.7}$$

where n_0 is the nuclear matter density.

In a neutron star the electron chemical potential μ_{e^-}, which in the progenitor of SN1987A was ~ 220 MeV [Thorsson, Prakash and Lattimer 1994], is the driving force towards kaon condensation [Brown, Thorsson, Kubodera and Rho 1992]. Once the *in-medium* kaon mass $m_{K^-}^\star$ is less than μ_e, then the degenerate electrons in the electron cloud in the neutron star can lower the energy by changing into a kaon condensate. The kaons are bosons, so they will immediately go into an s-state condensate, which lowers the pressure substantially from that of the degenerate

electrons in the cloud in the neutron star. After this drop in pressure, the neutron star will go into a black hole in a light-crossing time.

The above essentially outlines the calculation of kaon condensation as it stood for many years. It gave the critical density at $n_c \lesssim 3n_0$. In the literature, the matter is made a lot more complicated – and one tends to get lost in details – in the effort to make the model "more realistic." We will see that approached from different vantage points, things can be considerably simpler.

9.1.2 *Doing heavy baryon χPT*

Let us be more "complicated" and more systematic than what we were with the V-spin picture. For this we look at a chiral Lagrangian written next-to-leading order (NLO) in chiral expansion with the baryons, which we write in the form that we need:

$$\begin{aligned}\mathcal{L} = & \frac{f^2}{4}\mathrm{Tr}\,(\partial_\mu U\partial^\mu U^\dagger) + \kappa\mathrm{Tr}\,(\mathrm{Tr}\mathcal{M}U + h.c.) \\ & + \mathrm{Tr}B^\dagger i\partial_0 B + i\mathrm{Tr}B^\dagger[V_0, B] - D\mathrm{Tr}B^\dagger\vec{\sigma}\cdot\{\vec{A}, B\} - F\mathrm{Tr}B^\dagger\vec{\sigma}\cdot[\vec{A}, B] \\ & + b\mathrm{Tr}B^\dagger\,(\xi\mathcal{M}\xi)\,B + d\mathrm{Tr}B^\dagger B\,(\xi\mathcal{M}\xi + h.c.) + h\mathrm{Tr}B^\dagger B\,(\mathcal{M}U + h.c.) + \cdots .\end{aligned} \tag{9.8}$$

where

$$\begin{pmatrix} V^\mu \\ -iA^\mu \end{pmatrix} = \frac{1}{2}\left(\xi^\dagger\partial^\mu\xi \pm \xi\partial^\mu\xi^\dagger\right) \tag{9.9}$$

with $U = \xi^2 = \exp(2i\pi/f)$ where $\pi = \pi^a\lambda^a/2$ is the octet pseudoscalar (pseudo-Goldstone) field and $B = B^a\lambda^a/2$ is the octet baryon field. The constant f will be specified later. The mass matrix $\mathcal{M}$ in (9.8) is taken diagonal $\mathcal{M}^\dagger = (m_u, m_d, m_s)$ which is counted as $\mathcal{O}(p^2)$. As suggested before, one can view this Lagrangian – consisting only of the baryon and pion fields – as a truncated one in which the higher tower of vector mesons than the ground state have been integrated out and the baryons are put in by hand as local fields in place of the skyrmions – which are point-like in the infinite tower – in the HLS Lagrangian discussed in the preceding chapters. For the treatment we will make here, we will not need the full panoply of the fields given above. Finally the ellipses stand for three classes of higher order terms: (A) terms quadratic in derivatives acting on the meson fields, (B) terms linear in $\mathcal{M}$ and powers of derivatives and (C) terms higher order in $\mathcal{M}$ *etc.* We shall be focusing on s-wave kaon condensation. Since we will be considering here the mean field, the higher order terms (A) to (C) will not be needed for the moment. How to go beyond the mean field with (9.8) for the process in question is not yet fully worked out, although much work has been done in high orders for the scattering of kaons off nucleons and nuclei. One early such attempt will be presented later.

Of course for kaon scattering off nucleons or nuclei, the (A) and (B) terms can be important and need to be included as we will remark later.

Now given the Lagrangian (9.8), how to pick the parameters in the Lagrangian depends on what one does with the Lagrangian. If one were to do a systematic chiral expansion, then the parameters could be fit to experiments *at each order* in the chiral expansion. In considering kaon condensation, however, it is not at all clear that there is a simple and straightforward counting rule because of the multiple scales involved in dense medium as pointed out in the preceding chapter and in particular the potential importance of the background dependence of the parameters as one finds in HLS theory in medium described in Chapters 7 and 8. Here we will adopt the simplest possible strategy and fix the parameters to empirical values at tree order and use them for the mean field calculation. The result we obtain in this way should therefore be taken with caution if one wants to confront nature. Later we will improve this approach by implementing the "intrinsic background dependence (IBD)" taken into account in the form of BR scaling.

The parameters are fixed as follows.

(M1) From weak leptonic pion decay, we have $f_\pi \approx 93$ MeV. We shall take this value for f, setting $f \approx f_\pi$ although the physical kaon decay constant is bigger, $f_K \approx 113$ MeV.

(M2) From nuclear β decay and semi-leptonic hyperon decay, we get $F \approx 0.46$ and $D \approx 0.80$ so that the axial-vector constant for the nucleon $g_A = 1.26$. Other parameters can be expressed in terms of the current s-quark mass m_s.

(M3) From the Gell-Mann-Oakes-Renner (GMOR) relation (at the lowest order in the mass matrix) for the pseudoscalar meson asses, we can determine

$$m_s \kappa \approx (182 \text{ MeV})^4. \tag{9.10}$$

(M4) From tree-order baryon mass splitting, $m_\Sigma - m_N = 2dm_s$, $m_\Lambda - m_N = \frac{2}{3}(d-2b)m_s$ and $m_\Xi - m_N = 2(d-b)m_s$, we obtain

$$bm_s \approx -67 \text{ MeV}, \tag{9.11}$$

$$dm_s \approx 134 \text{ MeV}. \tag{9.12}$$

(M5) The coefficient h is related to the KN sigma term $\Sigma_{KN} \equiv \frac{1}{2}(\bar{m}+m_s)\langle p|\bar{q}q + \bar{s}s|p\rangle$ with $\bar{m} = (m_u + m_d)/2$ which in terms of the parameters of the Lagrangian is $\Sigma_{KN} = -(b/2 + d + 2h)m_s$. The sigma term has been reliably measured with a quoted accuracy of 3 to 5% error bar on lattice [Dong, Lagae and Liu 1996] $\Sigma_{KN}^{lattice} = 362$ MeV from which we get

$$hm_s \approx -231 \text{ MeV}. \tag{9.13}$$

Now we have a fully determined Lagrangian density that can be used at the mean field level.

9.1.3 *Kaon condensation driven by electrons*

Politzer and Wise discussed kaon condensation triggered by pion condensation [Politzer and Wise 1991]. The assumption in their treatment was that pions condense before kaons do. This was reviewed in CND-I and since we do not think that this is a scenario chosen by nature, we won't discuss it here. Instead we will consider the process where kaon condensation is driven by electrons with high chemical potential proposed in [Brown, Thorsson, Kubodera and Rho 1992] as we did in the preceding subsection.

The key idea is that in "neutron star" matter, energetic electrons – reaching hundreds of MeV in kinetic energy in dense "neutron star" matter – can decay into kaons if the kaon mass falls below the electron chemical potential:

$$e^- \to K^- + \nu. \tag{9.14}$$

This process can go into chemical equilibrium with the beta decay $n \to p + e^- + \nu_e$ with the neutrinos diffusing out. This means that the chemical potentials satisfy

$$\mu_{K^-} = \mu_{e^-} = \mu_n - \mu_p \ . \tag{9.15}$$

Let x denote the fraction of protons generated by (9.14) and the neutron beta decay, so

$$n_n = (1-x)n, \qquad n_p = xn \tag{9.16}$$

and define

$$n \equiv u n_0 \tag{9.17}$$

with n_0 being the nuclear matter density. With the addition of protons, we gain in energy through the "nuclear symmetry energy" by the amount

$$E_s/V = \epsilon_s[(1-2x)^2 - 1]n_0 u = -4x(1-x)\epsilon_s n_0 u \tag{9.18}$$

where we have assumed, for simplicity, that the symmetry energy depends on the density linearly with the constant ϵ_s determined from nuclei,

$$\epsilon_s \approx 32\text{MeV}. \tag{9.19}$$

More sophisticated – and somewhat complicated – formulas for symmetry energy that have been studied (*e.g.*, those of Prakash *et al.* [Prakash, Ainsworth and Lattimer 1988]) could be used, but for our purpose, this form should suffice. In any event the symmetry energy above nuclear matter density is not well known, so this constitutes one of the major uncertainties in our discussion. Further progress in understanding nuclear matter under extreme conditions would be of help.

The energy density in mean field is easy to compute from (9.8). Dropping pions which do not contribute in the mean field if pion condensation does not take place,

we get the simple result

$$\tilde{E}/V \equiv \tilde{\epsilon} = \tilde{\epsilon}(0) + (m_K^2 - \mu^2)|v_K|^2 + n\Delta\epsilon \tag{9.20}$$

where $\tilde{\epsilon}(0)$ represents the sum of the kinetic energy density of the symmetric nuclear matter and the isospin independent part of the nuclear interaction contribution, and

$$\Delta\epsilon = -\frac{1}{2f^2}\left[\mu(1-x) + 2\mu x - (4h+2d)m_s\right]|v_K|^2 - 4x(1-x)\epsilon_s + \cdots \tag{9.21}$$

The first term in the square bracket of (9.21) is the neutron contribution through vector exchange (namely, the V_0 term in (9.8)) and the second the corresponding proton contribution. The factor of 2 for the proton contribution can be easily understood by the fact that the K^-p interaction with vector meson exchanges is twice as attractive as the K^-n interaction. Defining

$$\hat{\mu} = \mu + \frac{n_0 u}{4f^2}(1+x) \tag{9.22}$$

we can rewrite (9.20)

$$\begin{aligned}\delta\epsilon &\equiv \tilde{\epsilon} - \tilde{\epsilon}(0) \\ &= \left[(m_K^*)^2 - \hat{\mu}^2 + \frac{n_0^2 u^2}{16f^4}(1+x)^2\right]|v_K|^2 - 4x(1-x)\epsilon_s n_0 u + x n_0 u \mu\end{aligned} \tag{9.23}$$

where

$$(m_K^*)^2 = m_K^2 + \frac{n_0 u}{2f^2}(4h+2d)m_s. \tag{9.24}$$

The charge neutrality condition $\partial\Delta\epsilon/\partial\mu = 0$ is simply gotten by balancing the negative charge of the kaon against the positive charge of the proton, *i.e.*

$$\hat{\mu} = x\frac{n_0 u}{2|v_K|^2} \tag{9.25}$$

while the beta equilibrium,

$$\partial\tilde{\epsilon}/\partial x = 0, \tag{9.26}$$

gives

$$\hat{\mu} \approx \frac{n_0 u}{2f^2}(1+x) = \frac{16f^2}{|v_k|^2}x(1-2x)\epsilon_s. \tag{9.27}$$

The Eqs. (9.25) and (9.27) determine μ and x in terms of v_K and u. Then setting the coefficient of $|v_K|^2$ equal to zero determines the critical density in the standard way. The numerical value depends on both the coefficient h which governs the KN sigma term Σ_{KN} and the symmetry energy ϵ_s. As mentioned, the lattice data [Dong, Lagae and Liu 1996] gave a rather accurate value for $hm_s \approx -231$ MeV in free space. However it is not clear that the value needed is actually the free-space value instead of an effective one *sliding* with the vacuum structure – that is, intrinsic background

dependence taken into account – and hence it is not clear that the value determined on lattice is what one should use. Given also the ignorance on the symmetry energy for $n \gtrsim n_0$, all one can say at the present stage of our theoretical understanding is that the critical density falls in the range[3]

$$2 \lesssim \frac{n_c^K}{n_0} \lesssim 4 \tag{9.28}$$

as found in the more complete treatment of [Thorsson, Prakash and Lattimer 1994] for the range -310 MeV $\lesssim hm_s \lesssim -134$ **MeV** (and with some dependence on the precise value and function of the symmetry energy). This more elaborate treatment confirms essentially the toy-model result given in the preceding subsection. In fact this range would remain the best one can get for the process even if one were to do "high-order" chiral perturbation calculations. Furthermore, as will be argued, going to higher order from the Lagrangian (9.8) does not have much sense.

9.1.4 *Constraints from kaon-nuclear scattering*

In approaching an "exotic" kaonic matter as kaon condensation and dense strange nuclei – "strange nugget" to be described below – from the matter-free vacuum where the Lagrangian (9.8) was defined, the question invariably posed is: Does the Lagrangian correctly describe kaon-nucleon and kaon-nuclear scattering? Obviously all approaches that purport to arrive at phase changes with a Lagrangian well defined in the vacuum and have some sort of contact with the fundamental theory QCD require a positive answer to this question.

9.1.4.1 $\Lambda(1405)$

Viewed from kaon-nuclear scattering, the most important ingredient left out from the above discussion based on (9.8) is the $\Lambda(1405)$ that figures importantly in the threshold K^-p scattering. Without $\Lambda(1405)$, one cannot describe the empirically well-determined threshold branching ratios for $K^-p \to X$, where X is the final state indicated below:

$$\begin{aligned}
\gamma &= \frac{|\mathcal{T}_{\pi^+\Sigma^-}|^2}{|\mathcal{T}_{\pi^-\Sigma^+}|^2} \\
R_c &= \frac{\sum_{i=\pi^\pm\Sigma^\mp} |\mathcal{T}_i|^2}{\sum_{j=\pi^0\Lambda,\pi^0\Sigma^0,\pi^\pm\Sigma^\mp} |\mathcal{T}_j|^2} \\
R_n &= \frac{|\mathcal{T}_{\pi^0\Lambda}|^2}{\sum_{i=\pi^0\Lambda,\pi^0\Sigma^0} |\mathcal{T}_i|^2} \ .
\end{aligned} \tag{9.29}$$

Approaching this problem quantitatively in a microscopic way requires a coupled channel treatment [Borasoy, Nissler and Weise 2005]. Since $\Lambda(1405)$ lies only about

[3] In this and next chapters, we denote the critical density for kaon condensation by n_c^K and the one for chiral restoration by $n_c^{\chi SR}$.

25 MeV below the K^-p threshold, kaon-nucleon scattering near threshold is very subtle and needs to be treated carefully. However for our purpose, such a sophistication is a luxury. In fact, a much more expedient and simpler way, while capturing the essential physics at high density, is to treat $\Lambda(1405)$ as much of an "elementary field" as the nucleon and the hyperons are [Lee, Min and Rho 1996]. This is because kaon condensation taking place far away from the threshold is mostly insensitive to the detailed structure of $\Lambda(1405)$.

One of the main justifications for considering $\Lambda(1405)$ as an interpolating "elementary" field is that in the skyrmion description, $\Lambda(1405)$ is an $SU(2)$ skyrmion bound to a kaon to give a baryon with the parity opposite to that of the hyperon Λ. This makes $\Lambda(1405)$ as *elementary* as $\Lambda(1116)$, a member of the octet baryons to which the nucleon belongs. Now the skyrmion is a baryon in QCD in the large N_c limit – a point-like soliton in the large 't Hooft limit as we saw in holographic dual QCD model [Hong, Rho, Yee and Yi 2007a; Hong, Rho, Yee and Yi 2007b], so the zero-width $\Lambda(1405)$ is just the large N_c baryon as the N, $\Lambda(1116)$ *etc.* are.[4]

Taken as an elementary field, then $\Lambda(1405)$ denoted hereafter as $\Lambda^\star$, couples to even-parity baryons and the kaon by a term – to leading order in the chiral Lagrangian – of the form

$$\delta\mathcal{L} = (\sqrt{2}g_{\Lambda^\star}\bar{\Lambda}^\star_v \mathrm{Tr}(v\cdot AB_v) + h.c.) \tag{9.30}$$

with $A_\mu = i\{\xi^\dagger, \partial_\mu\xi\}/2$. Now the $\Lambda^\star KN$ coupling constant, $g_{\Lambda^\star}$, can be fixed from the empirical decay width $\Gamma_{\Lambda^\star} = 50$ MeV through $\Lambda^\star \to \pi\Sigma$ with $m_{\Lambda^\star} = 1405$ MeV (it comes out to be $g^2_{\Lambda^\star} = 0.15$). With (9.30), the $O(p^2)$ chiral Lagrangian can explain quantitatively the ratios (9.29) as well as other threshold properties [Lee, Min and Rho 1996].

Now what does this $\Lambda(1405)$ do to kaon condensation?

The most important way the $\Lambda(1405)$ enters in the process is the correlation involving "particle-hole" excitations. This is typically many-body in nature. There are two classes of correlations to consider. One is the usual nuclear particle-hole excitations involving no strangeness and the other strange particle-non-strange hole excitations for which $\Lambda(1405)$ figures for the s-wave kaon condensation. Hyperons enter for p-wave processes. These correlations can be mediated by four-Fermi interactions.

[4]There have been discussions in the literature, based on coupled channel calculations, as to whether there are actually two near-by states of the quantum numbers of $\Lambda(1405)$ instead of one that we are adopting here. In the kaon-skyrmion bound-state picture, there can be only one such state. Given that the bound-state picture represents QCD in the large N_c limit, it must be what QCD predicts. This is confirmed in large-N_c analysis of a coupled channel calculation involving the channels $\bar{K}N$, $\pi\Sigma$, $\eta\Lambda$ and $K\Xi$ [Hyodo, Jido and Roca 2007]. Therefore our treatment with a single elementary $\Lambda(1405)$ field should be amply good enough for our argument. The two-pole structure, if real, might be important near the KN threshold, but will be totally irrelevant for the same reason that the $\Lambda(1405)$ is irrelevant, for kaon condensation.

Since we are dealing with s-wave kaon interaction, the most important configuration that K^- can couple to is the $\Lambda^\star$ particle-nucleon hole (denoted as $\Lambda^\star N^{-1}$ with N either a proton (p) or neutron (n)). We shall return to non-strange particle-hole correlations when we treat density effects on the basic constants of the Lagrangian (*i.e.* BR scaling). Here we focus on the former type. Now for the s-wave in-medium kaon self-energy, the relevant four-Fermi interactions that involve a $\Lambda^\star$ can be reduced to a simple form involving two unknown constants

$$\mathcal{L}_{4-fermi} = C^S_{\Lambda^\star}\bar{\Lambda}^\star_v\Lambda^\star_v \mathrm{Tr}\bar{B}_v B_v + C^T_{\Lambda^\star}\bar{\Lambda}^\star_v\sigma^k\Lambda^\star_v \mathrm{Tr}\bar{B}_v\sigma^k B_v \tag{9.31}$$

where $C^{S,T}_{\Lambda^\star}$ are the dimension -2 (M^{-2}) parameters to be fixed empirically and σ^k acts on the baryon spinor.

We shall denote the sum of these contributions to the kaon self-energy by $\Pi_{\Lambda^\star}$. A simple calculation gives

$$\begin{aligned}\Pi_{\Lambda^\star}(\omega) = &-\frac{g^2_{\Lambda^\star}}{f^2}\left(\frac{\omega}{\omega + m_B - m_{\Lambda^\star}}\right)^2\left\{C^S_{\Lambda^\star}n_p\left(n_n + \frac{1}{2}n_p\right) - \frac{3}{2}C^T_{\Lambda^\star}n_p^2\right\}\\ &-\frac{g^4_{\Lambda^\star}}{f^4}n_p\left(\frac{\omega}{\omega + m_B - m_{\Lambda^\star}}\right)^2\omega^2\left(\Sigma^p_K(\omega) + \Sigma^n_K(\omega)\right)\end{aligned} \tag{9.32}$$

where $g_{\Lambda^\star}$ is the renormalized $KN\Lambda^\star$ mentioned above, and $\Sigma^N_K(\omega)$ is given by

$$\Sigma^N_K(\omega) = \frac{1}{2\pi^2}\int_0^{k_{F_N}} d|\vec{k}|\frac{|\vec{k}|^2}{\omega^2 - M^2_K - |\vec{k}|^2}\ . \tag{9.33}$$

While the second term of (9.32) gives repulsion corresponding to a Pauli quenching, the first term can give either attraction or repulsion depending on the sign of $(C^S_{\Lambda^\star}[n_n + \frac{1}{2}n_p] - \frac{3}{2}C^T_{\Lambda^\star}n_p)$ with the constants $C^{S,T}_{\Lambda^\star}$ being the only parameters that are not determined by on-shell data.

These additional parameters $C^{S,T}_{\Lambda^\star}$ in the four-Fermi interactions in the strange particle-hole sector require experimental data involving nuclei and nuclear matter. In principle these constants could be fixed from kaonic atom data. In order to fix both of these constants, we would need data over a wide range of nuclei. One sees in (9.32) that for the symmetric matter, what enters is the combination $(C^S_{\Lambda^\star} - C^T_{\Lambda^\star})$. At present, this is the only combination that we can pin down reasonably reliably from kaonic atom data. That leaves one parameter unfixed. We shall pick $C^S_{\Lambda^\star}$. We parameterize the proton and neutron densities by the proton fraction x and the nucleon density $u = n/n_0$ as before:

$$n_p = xn\ ,\ \ n_n = (1-x)n\ ,\ \ n = un_0. \tag{9.34}$$

Table 9.1 Self-energies for kaonic atoms in nuclear matter ($x = 0.5$) in unit of M_K^2 for $g_{\Lambda^\star}^2 = 0.25$ and $(C_{\Lambda^\star}^S - C_{\Lambda^\star}^T)f^2 = 10$. $\Delta V \equiv M_K^\star - M_K$ is the attraction (in unit of MeV) at given density.

u	M_K^*	ΔV	$-n\mathcal{T}^{free}$	$-n\delta\mathcal{T}^{free}$	$\Pi_{\Lambda^\star}^1$	$\Pi_{\Lambda^\star}^2$
0.2	424.6	−70.37	−0.0673	0.0034	−0.1998	0.007607
0.4	390.0	−105.0	−0.0920	0.0084	−0.3024	0.006641
0.6	364.3	−130.7	−0.1173	0.0143	−0.3610	0.005635
0.8	342.6	−152.4	−0.1462	0.0207	−0.3996	0.004794
1.0	323.5	−171.5	−0.1789	0.0274	−0.4250	0.004088
1.2	306.2	−188.8	−0.2150	0.0343	−0.4404	0.003483
1.4	289.9	−205.1	−0.2540	0.0413	−0.4460	0.002945

Using the presently available kaonic atom data [Friedman, Gal and Batty 1994][5]

$$\Delta V = S_{K^-} + V_{K^-} \approx -(200 \pm 20) \ \text{MeV} \ \text{ at } \ u = 0.97 \tag{9.35}$$

we have for $x = 1/2$

$$(C_{\Lambda^\star}^S - C_{\Lambda^\star}^T)f^2 \approx 10. \tag{9.36}$$

This value is obtained by taking the difference between the observed value and the leading-order contribution (*i.e.* the Weinberg-Tomozawa term and the sigma term with the constants fixed in free space). We take (9.36) as the standard value although we will show other values for comparison. The results will be quite insensitive to this quantity. The real part of the kaonic atom potential for $x = 0.5$ obtained for $(C_{\Lambda^\star}^S - C_{\Lambda^\star}^T)f^2 \approx 10$ is listed in Table 9.1.

Now the parameter $C_{\Lambda^\star}^S$ can be determined if the mass shift of the $\Lambda^\star$ in medium is known. To in-medium one-loop order, two graphs of Fig. 9.2 contribute to the mass shift. A simple calculation gives

$$\delta m_{\Lambda^\star} = \sum_{i=a,b} \delta\Sigma_{\Lambda^\star}^{(i)}(\omega = m_{\Lambda^\star} - m_B) \tag{9.37}$$

where

$$\begin{aligned} \delta\Sigma_{\Lambda^\star}^{(a)}(\omega) &= -\frac{g_{\Lambda^\star}^2}{f^2}\omega^2 \left(\Sigma_K^p(\omega) + \Sigma_K^n(\omega)\right) \\ \delta\Sigma_{\Lambda^\star}^{(b)}(\omega) &= -C_{\Lambda^\star}^S(n_p + n_n). \end{aligned} \tag{9.38}$$

[5] A recent analysis [Barnea and Friedman 2007] supports this value. We should, however, note that there has been considerable controversy on the interpretation of the kaonic atom data and the jury is not out yet on this issue. (The situation up to the time of writing of this volume is summarized by Gal [Gal 2007; Friedman and Gal 2007].) The ultimate verdict will have to come from experiments, as the calculations that find a much shallower depth of the potential than quoted here – described below – cannot be ignored as they are based on systematic account of terms that are "faithful" to chiral perturbation theory approached bottom-up from the matter-free vacuum. Here and in what follows, we shall take the deeper potential since it is consistent with our point of view, but the alternative interpretation should be considered as also viable until proven otherwise empirically. We should stress that this controversy does not affect the main result of this analysis.

The superscript (a, b) stands for the figures (a) and (b) of Fig. 9.2. The contribution from Fig. 9.2a is completely given with the known constants. The dependence on the unknown constant $C^S_{\Lambda^\star}$ appears linearly in the Fig. 9.2b. For the given values adopted here, the mass shift is numerically

$$\delta m_{\Lambda^\star}(u, x, y) = [r(u, x) - 150.3 \times u \times y] \ \text{MeV} \tag{9.39}$$

where $y = C^S_{\Lambda^\star} f^2$ and $r(u, x) \equiv \delta\Sigma^{(a)}_{\Lambda^\star}$ with the numerical values given in Table 9.1.

One can see from Eq. (9.39) that the shift in the $\Lambda^\star$ mass in medium is primarily controlled by the constant $C^S_{\Lambda^\star}$. For symmetric matter ($x = 1/2$, $u = 1$), the shift is zero for $y = 0.41$ and linearly dependent on the y value for non-symmetric matter. At present we have no empirical information as to whether the medium lowers or raises the mass of the $\Lambda^\star$, so it is really a free parameter, but it is reasonable to expect that, if any, the shift cannot be very significant. We consider, therefore, that a reasonable value for y is $\mathcal{O}(1)$. Again it will turn out that the resulting critical density is extremely insensitive to $y = C^S_{\Lambda^\star} f^2$.

9.1.4.2 *Influence on kaon condensation*

Let us now look how the critical density is influenced by the effect of $\Lambda(1405)$. Including (9.32) as well as other in-medium two-loop terms and the nuclear symmetry energy in the form of (9.18), one can straightforwardly (numerically) calculate the critical density as described above. It is found that the critical density is remarkably insensitive *both* to $(C^S_{\Lambda^\star} - C^T_{\Lambda^\star})f^2$ and to $C^S_{\Lambda^\star} f^2$ as one can see in Table 9.2. The result then is that kaon condensation is expected to occur in the same range as before:

$$2 \lesssim n_c/n_0 \lesssim 4. \tag{9.40}$$

The remarkable result that the $\Lambda(1405)$ plays a totally insignificant role for the critical density can be seen in the dispersion formula for K^- in medium, that is, the

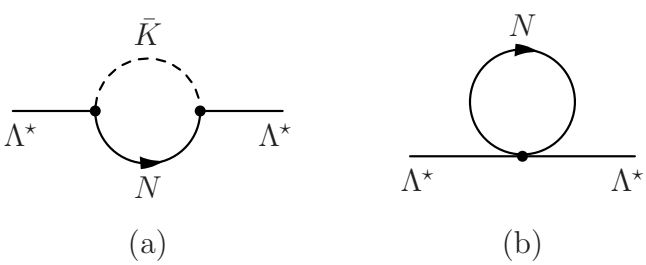

Fig. 9.2 In medium one-loop diagrams contributing to the mass shift of $\Lambda(1405)$.

Table 9.2 Critical density u_c in in-medium two-loop chiral perturbation theory for $g^2_{\Lambda^\star} = 0.25$ and $F(u) = u$ which corresponds to the choice of the symmetry energy (9.18).

$(C^S_{\Lambda^\star} - C^T_{\Lambda^\star})f^2$	$C^S_{\Lambda^\star} f^2 = 100$	$C^S_{\Lambda^\star} f^2 = 10$	$C^S_{\Lambda^\star} f^2 = 0$
1	2.25	3.25	4.51
10	2.24	3.13	3.69
100	2.18	2.66	2.77

inverse propagator of the kaon in dense medium as shown in the schematic figure Fig. 9.3. The $\Lambda(1405)$ is very important near the K^-p threshold below $\omega = M_K$ but becomes less influential as one approaches the pole mass in the medium "$M^\star_K$".

It is striking that changing the two constants associated with $\Lambda(1405)$ by two orders of magnitude changes the critical density by only a few %. In particular, with $(C^S_{\Lambda^\star} - C^T_{\Lambda^\star})f^2 \approx 10$ as suggested by the kaonic atom data, varying $C^S_{\Lambda^\star} f^2$ from zero to 100 changes the critical density by less than a factor of 2. For a given mass shift of the $\Lambda(1405)$ governed by the constant $C^S_{\Lambda^\star} f^2$, shifting the kaon-nuclear attraction by two orders of magnitude affects the critical density only by $\sim 20\%$. There must be a deep reason for this surprising result.

In order to see what it is, we have to understand that while the attraction induced by the presence of $\Lambda(1405)$ is essential for *triggering* kaon condensation, its influence on the critical behavior near the critical temperature is highly insensitive to the strength with which $\Lambda(1405)$ participates in generating the attraction. The effective four-Fermi interaction (9.31) is an irrelevant operator, so as one approaches the kaon condensation point, it gets suppressed. But it is an analog to what is amusingly called a "dangerously irrelevant term" in condensed matter physics where the role of such terms is pronounced.

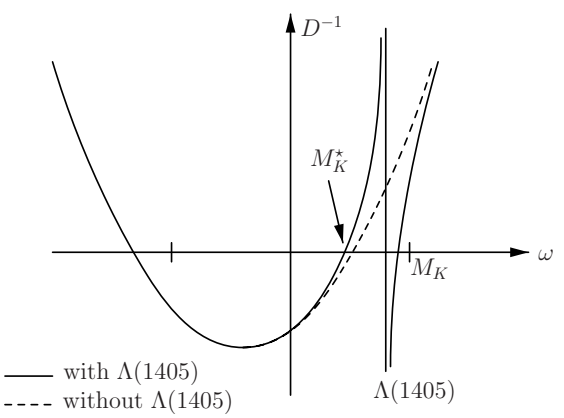

Fig. 9.3 Schematic diagram of dispersion relation D^{-1} with and without $\Lambda(1405)$ contribution.

9.1.4.3 *"Dangerously irrelevant terms"*

To understand the role of $\Lambda(1405)$ discussed above, it is quite instructive to resort to a renormalization group argument. We shall follow the argument given in [Lee, Rho and Sin 1995] for generic meson condensation in strong interaction physics. So it would apply to both pion condensation and kaon condensation. The technique used is the one developed by Shankar [Shankar 1994] for Landau Fermi liquid theory. There is a distinct difference, however, between boson condensation and Fermi liquid in that while a "mass" term is *relevant* in the renormalization group sense, so figures importantly in the condensation process, the effective mass in Fermi liquid is a fixed point quantity, so it does not flow in the latter. This is because the Fermi surface is fixed by fiat.

Let the meson field be denoted as Φ. We will focus on two terms, one "mass term" and the other "interaction term," with the action written schematically (apart from the kinetic energy term)

$$S = S_M + S_I \tag{9.41}$$

where

$$S_M = \int d\omega d^3q \tilde{M} \Phi^* \Phi, \tag{9.42}$$

$$S_I = \int (d\omega d^3q)^2 (d\epsilon d^3k)^2 h \Phi^* \Phi \Psi^\dagger \Psi \delta^4(\omega, \epsilon, q, k) \tag{9.43}$$

where Ψ is the baryon field containing nucleons, hyperons and $\Lambda(1405)$ *etc.* Of course both $\tilde{M}$ [6] and h subsume many terms with varying powers in the suitable expansion (*e.g.*, the chiral expansion in chiral perturbation theory). [7] For our discussion we need not specify them here.

The scaling law for the fields involved, under scaling transformation determined from the kinetic term (which is required to be invariant under the scaling), shows that the "mass" term is *relevant* but the interaction (h) term is *irrelevant*. Now the RGEs are found by making the scale change $\Lambda \to s\Lambda$ with $0 < s < 1$ where Λ is the cut-off scale [Lee, Rho and Sin 1995],

$$\frac{d\tilde{M}}{dt} = \tilde{M} - Dh, \tag{9.44}$$

$$\frac{dh}{dt} = -h/2 \tag{9.45}$$

where $t = -\ln s$ and $D = dn$ with $d > 0$ is a constant depending on Λ/k_F where

[6] Tilde represents that it contains other "mass-like" terms.

[7] For instance, h will contain, aside from the kaon mass, leading $O(p)$ term of $\sim \frac{\omega}{f_\pi^2} K^\dagger K N^\dagger N$, the next-to-leading order $O(p^2)$ terms, $\sim \frac{\Sigma}{f_\pi^2} K^\dagger K N^\dagger N$ *etc.*

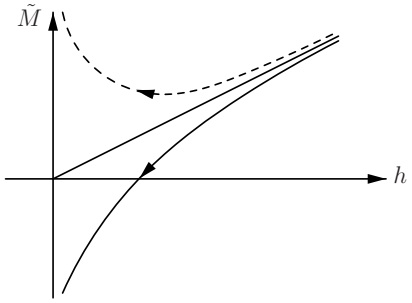

Fig. 9.4 Schematic diagram of RGE flow for the mass $\tilde{M}$. The dotted line with arrow up shows the flow for $D < \frac{3}{2}\frac{\tilde{M}_0}{h_0}$ and the solid line with arrow down for $D > \frac{3}{2}\frac{\tilde{M}_0}{h_0}$.

k_F is the Fermi momentum of the baryonic system. The solutions to the RGEs are

$$\tilde{M}(t) = (\tilde{M}_0 - \frac{2}{3}Dh_0)e^t + \frac{2}{3}Dh_0e^{-t/2}, \tag{9.46}$$

$$h(t) = h_0e^{-t/2}. \tag{9.47}$$

As one decimates down with $s \to 0$ ($t \to \infty$) integrating out higher lying modes, the boson-fermion interaction gets exponentially suppressed. We see that if $D < \frac{3}{2}\frac{\tilde{M}_0}{h_0}$, then the $\tilde{M}$ flows toward $+\infty$. On the other hand, for

$$D > \frac{3}{2}\frac{\tilde{M}_0}{h_0} \tag{9.48}$$

the $\tilde{M}$ is bound to turn negative, signalling instability against condensation. This can be seen in Fig. 9.4. Now $D = dn$ and $d > 0$, so that means that (9.48) can be satisfied by dialling the density. What matters is the "dangerously irrelevant term" figuring in h_0 that drives flow toward condensation while more irrelevant terms get suppressed.

What we learn from this toy model exercise is that while the relevant mass term triggers meson condensation, it is the *least* irrelevant interaction term that determines the flow of renormalization group and ultimately the fate of the ground state. In the chiral limit, there is no boson mass since it is a Goldstone particle and chiral symmetry protects the system from condensing. This is also the case when chiral symmetry is lightly broken since any small repulsive irrelevant interaction can reverse the direction leading to non-condensation. It is thus the substantial symmetry breaking in the strange-quark sector that is responsible for boson condensation.

9.1.5 *Role of kaon-nuclear potential in kaon condensation*

9.1.5.1 *Chiral perturbation approach*

We have so far treated kaon condensation using an effective field theory in the mean field approximation. However going bottom-up, one would like to check whether the same Lagrangian describes satisfactorily observable quantities like kaon-nuclear scattering, kaonic atoms *etc.*, some aspect of which was discussed above as a constraint. The mean field treatment applied to the possible phase change does not guarantee that the Lagrangian used is good for on-shell processes which typically require doing higher order chiral perturbation, taking into account various coupled channels (*e.g.*, $\pi\Sigma$, $\pi\Lambda$, $\eta\Sigma$, $\eta\Lambda$ *etc.*), and implementing unitarity. There have been several works along this line, starting with a given chiral Lagrangian and calculating higher-order terms in chiral perturbation theory, and then extrapolating to high densities to see whether kaon condensation takes place at low enough density to be relevant in compact stars.

A typical procedure in this class of approaches is to pick the leading chiral-order term in the chiral Lagrangian, build the relevant potentials for coupled channels and solve the coupled equations in suitable approximations. The driving term typically is the Weinberg-Tomozawa term – encapsulated in the term $i\mathrm{Tr}B^\dagger[V_0, B]$ in (9.8) – which provides a sizable attraction between $\bar{K}$ and nucleons,

$$V_{\bar{K}} \approx -\frac{3}{8F_\pi^2} n \sim -57\frac{n}{n_0}\ \mathrm{MeV} \tag{9.49}$$

where $F_\pi \approx f_\pi \approx 93$ MeV is taken. This term – plus higher chiral order terms of the Lagrangian – treated as a potential, iterated to all orders within an in-medium coupled channel approach constrained by the $\bar{K}N$-$\pi\Sigma$-$\pi\Lambda$ data near the $\bar{K}N$ threshold gives rise to a strongly attractive potential [Waas, Kaiser and Weise 1996; Waas, Rho and Weise 1997]

$$V_{\bar{K}} = -\frac{2\pi}{\mu_{KN}} b_0(n) n(r) \tag{9.50}$$

with the in-medium $\bar{K}N$ isoscalar scattering length $b_0(n) = \frac{1}{2}(a_{K^-p}(n) + a_{K^-n}(n))$ and $\mathrm{Re}V_{\bar{K}}(n_0) \sim -110$ MeV.

As is often the case, implementing certain symmetries manifest in a field theory into a potential model framework does not necessarily yield a unique result. In doing so, there is a risk of losing a certain aspect of QCD symmetries and dynamics at the expense of other constraints such as unitarity, self-consistency *etc.* For instance, the matching to QCD that results in the intrinsic density dependence in the parameters of the Lagrangian is totally lacking in this approach. Imposing self-consistency in the propagators in the Lippmann-Schwinger equation determining $b_0(n)$ without assuring chiral symmetry and other QCD constraints can lead to a shallower potential, $\mathrm{Re}V_{\bar{K}}(n_0) \sim -(40-60)$ MeV as found in [Ramos, Magas, Oset and Toki 2007]. Such a shallow potential, while perhaps fully consistent with the

data for kaon-nuclear processes near the $\bar{K}N$ threshold, cannot possibly lead to kaon condensation at a density $n \lesssim 4n_0$. It also poorly describes kaonic atoms as elaborated below [Gal 2007].

9.1.5.2 *Kaonic atom and deeply bound kaonic nuclei*

The approach described above corresponds to what was referred to as "one-step decimation" in Chapter 8. As noted there, even approaching nuclear matter at one go is not straightforward. A more expedient approach required a "double-decimation" strategy. This was thought mainly due to the existence of the Fermi sea and the Fermi-liquid fixed point.

Now kaon condensation – and the possible formation of deeply bound kaonic nuclear states – require going beyond that region. We are therefore led to question whether one can reach such extreme states by fluctuating *perturbatively* around the matter-free vacuum. This feature is already observed in kaonic atom data.

In Fig. 9.5 are shown the potentials for various models and the χ^2 as obtained in the analysis of kaonic atom data [Barnea and Friedman 2007]. One notes that linear density approximation for the optical potential – marked "$t\rho$" – which is similar to the "self-consistent" chiral model of [Ramos, Magas, Oset and Toki 2007], gives shallow potentials whereas nonlinear dependence can lead to deep potentials such as those marked "F" and "DD." Purely from the phenomenological point of view, the shallow potential obtains a much poorer fit to kaonic atom data than what the deeper potential does. From theoretical point of view, the linear density approximation can only probe the surface and not the interior of a nucleus, hence cannot be sensitive to dense regime. In terms of what has been developed in HLS theory in Chapter 7, this may be interpreted as a consequence of the absence of the intrinsic background dependence (IBD) of the parameters of the chiral Lagrangian required by the matching to QCD.

9.1.6 *Kaon condensation with Brown-Rho scaling*

Departing from the strict bottom-up approach anchored on free-space data, we turn to the HLS/VM approach with the matching at a scale Λ_M to QCD to inherit the "intrinsic background (density or temperature) dependence" in the parameters in the bare Lagrangian with which to do quantum theory. The deeply attractive K^--nuclear potential indicates what the behavior in density of those parameters can be. The strategy is the "double-decimation" that was used in Chapter 8 to fluctuate around the Landau Fermi liquid fixed point to calculate the anomalous gyromagnetic ratio and axial charge transitions. Here we are looking at the response to the strangeness probe brought by the kaons in the medium. As there, the response is given by mean-field quantities modified by the "intrinsic density dependence."

Consider the s-wave KN interaction relevant to K-nuclear interactions in symmetric nuclear matter where the isospin dependence drops out. Looked bottom-up,

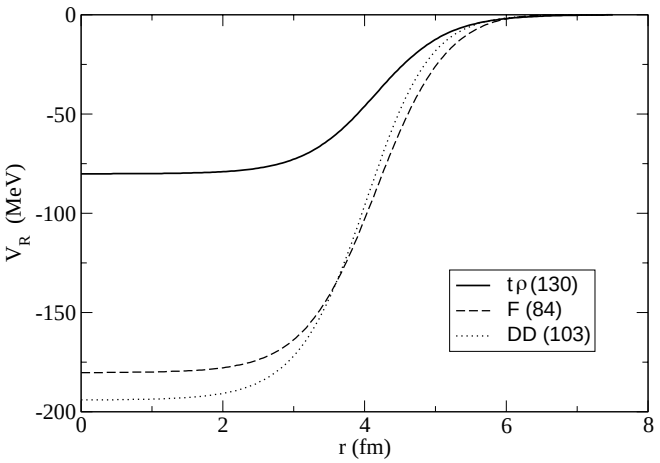

Fig. 9.5 Real part of the K^--Ni optical potential for various models and the values of χ^2 for 65 data points in parentheses taken selectively from [Barnea and Friedman 2006] (copyright 2006 by the APS) that should be referred to for more precise details.

the most relevant terms are the Weinberg-Tomozawa term and the sigma term

$$\mathcal{L}_{KN} = \frac{-6i}{8f^2}(\overline{B}\gamma_0 B)\overline{K}\partial_t K + \frac{\Sigma_{KN}}{f^2}(\overline{B}B)\overline{K}K \equiv \mathcal{L}_\omega + \mathcal{L}_\sigma \tag{9.51}$$

where $K^T = (K^+ K^0)$. The four-Fermi interactions involving Λ^* and p-wave kaon-nucleon interactions are assumed to be suppressed in the vicinity of kaon condensation as argued above. The constant f in (9.51) which in medium-free space is the pion decay constant f_π will be modified à la Brown-Rho scaling. We shall denote the medium quantity by $F_\pi^\star$. In chiral perturbation expansion, the first term corresponds to $\mathcal{O}(p)$ and the second term to $\mathcal{O}(p^2)$. There is one more $\mathcal{O}(p^2)$ term proportional ∂_t^2, *i.e.* the range term, which we will discuss later.

One can associate the first term of (9.51) with what one obtains by integrating out the ω meson as in the baryon sector. The resulting K^-N vector potential in medium can then be deduced in the same way as for the N-nuclear vector interaction V_N:

$$V_{K^\pm} = \pm\frac{3}{8F_\pi^{\star 2}}n \tag{9.52}$$

where $F_\pi^\star$ is the (parametric) effective constant that depends on the background, *i.e.* density. To do this, we assume that the constituent (or quasi) quark description with the ω meson coupling to the kaon as a *matter field* becomes applicable: the ω coupling to the kaon which has one nonstrange quark is 1/3 of the ω coupling

to the nucleon which has three nonstrange quarks. Then in mean field, the vector K-nuclear interaction is related to the vector N-nuclear interaction as

$$V_{K^\pm} \approx \pm\frac{1}{3}V_N. \tag{9.53}$$

Now what about the second term of (9.51)?

As in the baryon sector, one may couple the dilaton (scalar) χ field to the kaon field. (This χ may or may not be related to ϕ in Walecka model or σ in the linear sigma model.) But with the kaon considered as a pseudo-Goldstone field, the only way to couple them without using derivatives is through the symmetry breaking term. This should then be related to the sigma term. On the other hand, if the kaon is treated as a *matter field* as suggested by its coupling to the ω-meson field – a reasonable assumption in medium in view of the fact that *all* non-strange hadron masses other than that of Goldstone bosons drop – then we can use the coupling

$$\mathcal{L}_\sigma = \frac{1}{3}(2m_K)g_\chi^\star\overline{K}K\chi \tag{9.54}$$

where the factor 1/3 accounts again for one non-strange quark in the kaon as compared with three in the nucleon and the factor $(\sqrt{2m_K})^2$ is inserted for the kaon wavefunction normalization. When the χ field is integrated out as was done with the ω meson, we will get, analogously to the nucleon case,

$$\mathcal{L}_\sigma = \frac{1}{3}(2m_K)\frac{g_\chi^{\star\,2}}{m_\chi^{\star\,2}}\overline{B}B\overline{K}K. \tag{9.55}$$

Comparing with the second term of (9.51), we find

$$\frac{\Sigma_{KN}}{f^2} \approx \frac{1}{3}(2m_K)\frac{g_\chi^{\star\,2}}{m_\chi^{\star\,2}}. \tag{9.56}$$

Although this relation may be unfamiliar to the readers, it can be understood by recalling the dual role that the kaon plays in the structure of hyperons: On the one hand, the kaon is "light" enough to be considered as a (pseudo-)Goldstone boson so the skyrmion picture with $SU(3)$ collective coordinates applies; on the other hand, it can be considered as "heavy" enough so that it can be treated as a matter field (rather than a Goldstone field) as in the Callan-Klebanov model [Callan and Klebanov 1985]. It is surprising, but true, that the kaon mass can be tuned in such a way that one can go from the Callan-Klebanov picture with the "heavy" quark to the Goldstone limit [Kaplan and Klebanov 1990]. The reference [Min, Oh, Park and Rho 1994] describes how these two descriptions can be joined smoothly in the case of the kaon and heavier mesons. It is shown there that as the mass of a pseudoscalar boson Φ (such as the D meson) increases above the chiral scale $\sim$ 1 GeV, the heavy-meson field can be taken to transform like a massive matter field, eventually exhibiting heavy-quark symmetry. It is this dual character of the kaon that is likely reflected in (9.56) in the background where the masses of other hadrons scale down:

the Goldstone boson nature of the kaon gives the left-hand side of Eq. (9.56), while the massive matter field character of the kaon in medium supplies the right-hand side. The situation resembles the overlapping in the strange-quark hadron sector of the "top-down" approach starting from heavy-quark symmetry and the "bottom-up" approach starting from chiral symmetry as discussed in [Min, Oh, Park and Rho 1994]. In the present case, the overlapping region seems to be located between $\sim n_0$ and $\sim 2n_0$ in density, that is, the "flash density" defined in Chapter 8. As mentioned, this is also the regime where constituent quarks replace nucleons as relevant fermionic degrees of freedom.

Given the KN sigma term, we could determine independently what f is in medium. However, since the strange-quark mass is not well-known in medium, we cannot determine the (in-medium) sigma term accurately even if the $\bar{s}s$ content of the nucleon could be measured on lattice. Suppose we take it from lattice gauge calculations [Dong, Lagae and Liu 1996], $\Sigma_{KN} = 362$ MeV $\approx 2.6 m_\pi$. Then the left- and right-hand sides of (9.56) are equal if we set[8]

$$f \to F_\pi^\star. \tag{9.57}$$

This is consistent with the scaling for the ω-meson exchange leading to the relation (9.53). It follows from (9.51) with f replaced by $F_\pi^\star$ that the scalar kaon-nuclear potential is

$$S_{K^\pm} \approx \frac{1}{3} S_N. \tag{9.58}$$

• Predicting for kaon-nuclear potential

Given Walecka mean fields for nucleons, we can now calculate the corresponding mean-field potential for K^--nuclear interactions in symmetric nuclear matter. From the results obtained above, we have

$$S_{K^-} + V_{K^-} \approx \frac{1}{3}(S_N - V_N). \tag{9.59}$$

Phenomenology in Walecka mean-field theory gives $(S_N - V_N) \lesssim -600$ MeV for $n = n_0$ [Serot and Walecka 1986]. This leads to the prediction that at nuclear matter density

$$S_{K^-} + V_{K^-} \lesssim -200 \text{ MeV}. \tag{9.60}$$

This agrees with the result of the analysis in K-mesic atoms made by Friedman, Gal and Batty quoted in (9.35) [Friedman, Gal and Batty 1994].

[8] This constant is not to be identified with the physical pion decay constant in medium that would vanish at the chiral phase transition. As mentioned, this quantity most likely stops decreasing at a matter density of order of $\gtrsim n_0$ and stays more or less constant beyond.

• Predicting for kaon condensation

In applying the above mean-field argument to kaon condensation in compact-star matter to chiral $\mathcal{O}(p^2)$, we need to make two additions to the Lagrangian (9.51). The first is that the compact-star matter relevant to the problem consists of roughly 85% neutrons and 15% protons, so we need to take into account the ρ-meson exchange in addition to the ω exchange. The ρ exchange between K^- and neutrons (protons) gives repulsion (attraction), equal in magnitude to 1/3 of the attraction from the ω-exchange. The second correction has to do with an $\mathcal{O}(p^2)$ term in the Lagrangian proportional to ω_K^2 (where ω_K is the kaon frequency) associated with "1/m" corrections in chiral expansion. The effect of this term is to cut down the scalar exchange given by the second term of (9.51) by the factor $F \simeq (1 - 0.37\frac{\omega_K^2}{m_K^2})$ (this factor is explained in [Lee 1996]). This term was referred to above as "range term."

We are now in position to estimate roughly the critical density for kaon condensation using the resulting mean-field theory. Let us start with Walecka mean fields for nucleons in symmetric nuclear matter. We take for illustration the following values from the analyses in the literature:

$$V_N(n = n_0) \approx 275 \text{ MeV}, \quad S_N(n = n_0) \approx -350 \text{ MeV}. \tag{9.61}$$

These are, in fact, the values calculated from the Bonn two-body potential in a relativistic Brueckner-Hartree-Fock approach [Brockmann and Machleidt 1984] and, thus, have some grounding in a microscopic theory. As Brockmann and Machleidt point out, these are more or less central values for those used in Walecka mean-field calculations. Now at $n \approx n_0$, $F \simeq (1 - 0.37\frac{\omega_K^2}{m_K^2}) \approx 0.86$ and so

$$S_{K^-}(n = n_0) \approx -\frac{1}{3} \times 350 \times 0.86 \text{ MeV} \approx -100 \text{ MeV}. \tag{9.62}$$

This is valid for K^- independently of the isospin content of the matter. For symmetric nuclear matter, our scaling gives

$$V_{K^-}(n = n_0) \approx -\frac{1}{3} \times 275 \text{ MeV} \approx -92 \text{ MeV}. \tag{9.63}$$

Thus for K^- in nuclear matter, we get $(S_{K^-} + V_{K^-}) \approx -192$ MeV which is consistent with the K-mesic atom data. For a matter of 85% neutrons and 15% protons appropriate in compact stellar matter, we get instead

$$V_{K^-}(n = n_0) \approx -92 \times (0.85 \times \frac{2}{3} + 0.15 \times \frac{4}{3}) \text{ MeV} \approx -71 \text{ MeV}. \tag{9.64}$$

At $n \approx n_0$, therefore, the attraction in the stellar matter of the given composition would be

$$S_{K^-} + V_{K^-} \approx -171 \text{ MeV}. \tag{9.65}$$

As shown in dense skyrmion matter, when used in the mean field, the constant F_π^* should stop decreasing beyond $\sim n_0$. We can understand this as follows. Normally, a linear extrapolation with density, although commonly employed in Walecka mean field calculations, cannot be strictly correct, because correlations, Pauli blocking, *etc.* tend to cut down attraction progressively with increasing density. On the other hand, our effective coupling constant, starting from chiral Lagrangians, is $1/f^{\star 2}$ where $f^\star$ is the physical in-medium decay constant $f_\pi^\star$, which steadily increases with density. We believe that the two effects essentially cancel making the $F_\pi^\star$ stay constant at $n \gtrsim n_0$. This gives an alternative explanation to the observation made in Chapter 7 (see Eqs. (7.42) and (7.43)), Thus the mean fields can be taken to extrapolate linearly in density. We will see below that this is what happens when looked at from the VM fixed point.

Given our estimate (9.65), we see that

$$\omega_{K^-}(2n_0) \approx 495 - 342 \approx 153 \text{ MeV}. \tag{9.66}$$

From the equation of state for dense stellar matter available in the literature (*e.g.*, PAL [Prakash, Ainsworth and Lattimer 1988]), we have the chemical potential for electrons

$$\mu_e(2n_0) \approx 173 \text{ MeV} \tag{9.67}$$

for either $K_0 = 180$ MeV or 240 MeV where K_0 is the compression modulus for nuclear matter. Since kaon condensation occurs when $\omega_K^\star = \mu_K = \mu_e$, we expect $n_c \sim 2n_0$. This agrees well with the $O(p^3)$ chiral perturbation result $n_c \approx 2.3n_0$ in [Lee, Brown, Min and Rho 1995] when the BR scaling is incorporated. Note, however, that by using the above linear extrapolation in the mean fields, we have implicitly assumed a definite parametrization for BR scaling for $n \gtrsim n_0$.

9.2 From the Vector Manifestation Fixed Point to Kaon Condensation

9.2.1 *Simplification at the VM*

The density range predicted thus far $2 < n/n_0 \lesssim 4$ is near the critical density at which chiral symmetry is expected to be restored. In the HLS framework, the chiral symmetry restoration point is the same as the VM fixed point of hidden local symmetry. So in this picture, kaons must be condensing not far from the VM fixed point. At the VM fixed point, the theory simplifies tremendously as the hidden gauge coupling g goes to zero and the parameter a to 1. The *physical* pion decay constant f_π, through an interplay of quadratic divergence from pion loop, also goes to zero at that point. Now it is very plausible therefore that kaon condensation could be better described starting from the VM fixed point – assuming the VM does exist in nature – than from the vacuum where $g \gg 1$ and $a \simeq 2$. As we discussed in

Chapter 5, there are indeed a variety of processes which can be efficiently treated starting from the VM fixed point, fluctuating with small gauge coupling constant and with an a near 1. To cite a few examples given there:

- The chiral doubling of heavy-light hadrons predicted more than a decade ago using sigma model built on the (matter-free) vacuum [Nowak, Rho and Zahed 1993; Bardeen and Hill 1994] and confirmed by the BaBar and CLEO collaborations in D mesons can be very simply understood in terms of HLS/VM in the light-quark sector starting from the VM fixed point [Harada, Rho and Sasaki 2004]. Here a remains equal to 1 to the order considered.
- The π^+-π^0 mass splitting can be very well reproduced in HLS theory with $a = 1$ and $g \neq 0$ [Harada, Tanabashi and Yamawaki 2003]. [9]
- In the *presence of baryonic matter*, even when one is far away from the VM fixed point, a flows precociously to 1. For instance, $a \approx 1$ in the EM form factor for the nucleon as discussed in [Brown and Rho 2004a].
- As discussed in Chapter 7, in the presence of temperature, a flows to 1 and vector dominance in the EM form factor of the pion breaks down maximally at chiral restoration, with a potential consequence on dilepton processes in heavy ion collisions [Harada and Sasaki 2004].

The idea then is to start with a bare Lagrangian fixed by Wilsonian matching to QCD at the matching scale Λ_M and then make perturbative corrections in terms of the departure from the VM fixed point. The closer to the fixed point, the smaller the corrections are expected to be.

Now near the VM fixed point, the quark condensates are rotated out – which is of course strictly true in the chiral limit but we will assume it here, so the sigma term which is "more irrelevant" than the Weinberg-Tomozawa term will no longer be important. Furthermore, the similarly irrelevant four-point interactions that intervene to drive kaon condensation when initiated from the matter-free vacuum such as those involving $\Lambda(1405)$ and p-wave interactions involving hyperons discussed above, both of which are of the same chiral order [10] or suppressed relative to the sigma term, would have flowed to zero at the VM fixed point, a feature which was exploited above when Brown-Rho scaling was implemented bottom-up. We recall that this feature emerged from the in-medium two-loop order chiral perturbation calculation in [Lee, Brown, Min and Rho 1995; Lee 1996]. What's left are then "weak" interactions between the relevant degrees of freedom, pions, kaons, quasiquarks and vector mesons ρ, ω. The leading term is

[9] That $a = 1$ is also of the special importance in connection with the notion of "little Higgs" and "theory space locality" in the Standard Model. The emergence of hidden local symmetry and the notion of theory space locality are relevant for extending low-energy effective field theory to the regime where the effective theory breaks down and should be "ultraviolet" completed to a fundamental theory. See [Harada, Tanabashi and Yamawaki 2003].

[10] Recall that in HLS theory, chiral perturbation expansion is defined with the vector meson mass on the same scale as the pion mass and since near the VM, the vector mass is of $\mathcal{O}(g)$, the chiral perturbative scheme should work better than at the matter-free vacuum.

then the *effective* Weinberg-Tomozawa-type term from the exchange of the ω-meson and the ρ-meson between the kaon and the baryonic matter, *all subject to the VM scaling*.

Now once kaon condensation sets in with $\langle K^- \rangle \neq 0$, isospin, among others, is spontaneously broken with the consequence that the Fermi seas get distorted. From that density on, the system would be oblivious – if back reaction is ignored – to the VM of chiral symmetry. In fact if one were to approach the chiral restoration point from the kaon condensed state, the scenario could be totally different from approaching it from the usual Fermi liquid state of normal nuclear matter. This point will be taken up in the next chapter in a different context. This would seem to imply that the VM may not be a suitable starting point of studying the condensation phenomenon. This worry, however, is unfounded. The reason is that as far as the hadronic dynamics is concerned, the presence of the Fermi sea of electrons does not affect how kaons behave in matter, so kaons will simply flow towards the VM fixed point. The condensation takes place when the effective kaon mass drops to the level of the electron chemical potential at which the electron will decay into the kaon and neutrino as Eq. (9.14) bolstered by boson condensation. Up to the point of the decay, it is the VM that governs the dynamics. The back-reaction by the electrons on the hadronic flow should be negligible.

9.2.2 *Toward kaon condensation*

The calculation reduces simply to computing the effective Weinberg-Tomozawa term for which we assume that the quasiquark notion is applicable in the density regime $n \gtrsim n_0$, say, in the vicinity of the "flash density" n_{flash} defined before. Now we need to calculate RGE flow with the gauge coupling g and the parameter a as in the density region $n_{flash} \lesssim n \lesssim n_c^{\chi SR}$. The only other quantity (apart from g^* and a^*) that we have to consider is the parametric pion decay constant F_π^*, since kaons will couple to the quarks with the constant $1/F_\pi^*$. We need this constant at the matching scale Λ_M^*. For this we observe that F_π^* does not scale appreciably in the matter-free space as found by Harada and Yamawaki [Harada and Yamawaki 2003] and also in dense matter as discussed in [Harada, Kim and Rho 2002]. A physical argument in support of this property was given in Sec. 9.1.6. Thus it will be sufficient to know what it is at the nuclear matter density and assume that it does not change much from there to the critical point. This information comes from the analysis of deeply bound pionic atoms [Suzuki *et al.* 2004] which shows that the in-medium parametric F_π must be decreased

$$F_\pi \to f_\pi^\star(n_0) \approx 0.8 F_\pi \tag{9.68}$$

$\sim 20\%$ at $n = n_0$ and stays more or less unchanged in movement towards chiral restoration. In [Brown, Lee, Park and Rho 2006] it was shown that the Walecka vector mean field used so much in nuclear physics already had this increase in it, so that it is part of the usual phenomenology of nuclear physics.

Since the gauge coupling constant g is near zero in the hadronic freedom region, quantum loop corrections can be ignored. It suffices therefore to do the mean field calculation (*i.e.* tree contributions). For the neutron fraction x_n and proton fraction x_p in a compact star, the potential felt by the kaon will then be

$$V_{K^-} = -\frac{1}{a^* F_\pi^{*2}} \left(\frac{x_n}{2} + x_p\right) n. \tag{9.69}$$

We have included ρ as well as ω exchange so as to make a typical neutron star charge up at density corresponding to chiral restoration $n_c^{\chi SR}$. In this picture, this is the only important contribution to the effective mass of the kaon. Other terms are suppressed by the hadronic freedom effect. Now let us see how the effective kaon mass behaves near the chiral phase transition density $n_c^{\chi SR} \sim 4n_0$. For this we take $a^* = 1$ and $F_\pi^*/F_\pi \simeq 0.8$. Then we find

$$\frac{[g_V^{\star\,2}/m_V^{\star\,2}]_{\text{fixed point}}}{[g_V^2/m_V^2]_{\text{zero density}}} = \frac{[aF_\pi^2]_{\text{zero density}}}{[a^\star F_\pi^{\star\,2}]_{\text{fixed point}}} = \frac{2}{0.8^2} \simeq 3.1. \tag{9.70}$$

For $x_n \approx 0.9$ corresponding to the neutron-star matter, we have from (9.69)

$$V_{K^-}(n = 4n_0) \approx -516 \text{ MeV}. \tag{9.71}$$

This suggests that the kaon mass must vanish at the chiral transition density.

Let us move down to the flash point $\sim 3n_0$. At this density, taking into account the flow of a, we find

$$m_K^*(\frac{3}{4} n_c^{\chi SR}) \frac{4}{3} \simeq m_{K^-}/4 \simeq 165 MeV. \tag{9.72}$$

This is somewhat smaller but not too far from the electron chemical potential expected at that density, ~ 220 MeV [Thorsson, Prakash and Lattimer 1994]. Considering the roughness of the estimate, it seems reasonable to identify the flash point as the kaon condensation critical density n_c^K. We note that were it not for the presence of the electron Fermi sea, the flow of the star matter would end up at the VM fixed point at $n_c^{\chi SR}$. However, the decay of electrons into kaons stops the hidden local symmetry (HLS) flow.

9.3 Dense Kaonic Nuclei as Strange Nuggets: "*KaoN*"

So far we have been discussing dense (infinite) kaonic matter with a focus on kaon condensation. It is tempting to speculate that a kaon-condensed star with an average density $\sim 3n_0$ could be considered as a giant nucleus consisting of clusters of $nnpK^-$ (that we shall call $KaoN$ for short) much as α-clusters in heavy nuclei. The K^- in the cluster at that density is bound by a few hundreds of MeV. This is represented in terms of an effective in-medium kaon mass of ~ 300 MeV. The challenge for the experimentalists is to determine in terrestrial laboratories whether such a

chunk of matter exists in nature. In order to phrase this challenge in a more precise term, let us imagine that we scoop one chunk of $KaoN$ out of the kaon condensed compact-star matter. Such a droplet does not exist in the normal condition. It is more like the "ice-9" in Kurt Vonnegut's novel "Cat's Cradle" (Bantam Doubleday Dell Publishing Group, Inc. New York, 1963).[11] But can the condition be met such that a stable $KaoN$ be produced in the laboratory? That's the question recently addressed by Yamazaki and Akaishi [Akishi, Doté and Yamazaki 2005].

In this section we look at this problem in light of what we discussed above.

9.3.1 *With standard potentials*

Standard chiral perturbation approaches without taking into account the intrinsic density dependence of HLS theory are unlikely to admit dense $KaoN$s or kaon condensation at a relevant density. The question one might raise is what happens when the four-body $pnnK^-$ system is solved exactly instead of in chiral perturbation theory. Suppose that one has accurate two-body as well as n-body forces (for $n > 2$) that may be determined either theoretically, or more likely by fitting to free-space experimental data. The objective is to solve the many-body problem exactly. In the SNPA (standard nuclear physics approach) to few-body systems considered in Chapter 4, this was done via Monte Carlo technique using two-body and three-body forces. Such a calculation would describe the system taking fully into account *many-body correlations* mediated by the given interactions *determined in free-space*.

Up to date, the full four-body treatment of the $pnnK^-$ system has not yet been made, but a Faddeev calculation of the three-body ppK^- system is available [Shevchenko, Gal and Mareš 2007]. Although the system is not of the configuration for the kaon nugget of the would-be compact star we are interested in, this calculation offers the possibility to study how the exact treatment differs from the perturbative scheme. In addition there are experimental efforts to see a bound K^-pp system in a reaction $K^-pp \to \Lambda p$.

This problem involves the coupled channels $\bar{K}NN$-$\pi\Sigma N$. In order to render the Faddeev calculation feasible, a few approximations are made. First, possible three-body forces are ignored. Next, two-body potentials are expressed in separable forms and fit to experiments in all two-body processes involved, a procedure consistent with the spirit of the standard nuclear physics approach (SNPA) used in Chapter 4. The calculation is rather involved, requiring careful accounts of various channels involved. However the result is rather simple. Due largely to the attraction that is found in the two-body K^-p interaction, namely, the Weinberg-Tomozawa term, the system can be bound. There is no surprise here. The binding energy found comes out to be in the range $B \sim 55 - 70$ MeV, somewhat larger than what one finds in chiral perturbation calculations [Ramos, Magas, Oset and Toki 2007]. However

[11] The ice-9 is the fictional matter of water in the ice form at room temperature. This analogy was suggested to the author by Gerry Brown.

the width is large $\Gamma \sim 90 - 110$ MeV which is due mainly to the open channel $\pi\Sigma N$. What one can conclude from these results [Shevchenko, Gal and Mareš 2007; Gal 2007] is that even though the binding energy is not small, such a large width would render the quasi-bound state difficult to see experimentally. Although it is not obvious what n-body forces (with $n > 2$) will do, there is nothing to suggest that the four-body K^-NNN system would have a large enough binding energy and density to form a $KaoN$ stable against the decay to $\pi\Sigma NN$.

9.3.2 *With non-standard potentials*

Since the approach with the standard potentials extracted from on-shell data, whether it is chiral perturbation theory or exact many-body solution, cannot produce a dense $KaoN$, one possibility is to modify the potentials by incorporating certain properties that are not present in the matter-free space. Unlike the approaches described above such as fluctuating from the VM fixed point or doing mean field with Brown-Rho scaling in which no constraints from the matter-free space are imposed, here the potentials are first extracted from free-space information, but certain ingredients absent in the free-space attributed to many-body correlations are to be implemented *in addition* so as to produce a dense $KaoN$. So the question is: what must one do to the potential to obtain a $pnnK^-$ system in which a kaon is bound by a binding energy of $\gtrsim 200$ MeV and at a density of $\sim 3n_0$? This is the question posed by Akaishi *et al.* [Akishi, Doté and Yamazaki 2005] [12].

One could treat all together three related systems, $pppK^-$, $ppnK^-$ and $pnnK^-$. Here we will focus on the $KaoN$, hence the $pnnK^-$ system.

One starts with the $\bar{K}$-nuclear attraction (9.49) which increases linearly in density. This formula is strictly valid at low density, so cannot be naively extrapolated to high density. As we noted above, the iteration of this potential in coupled equations increases the attraction, so a more realistic treatment of density dependence might make the potential more attractive than the *bare* potential (9.49). Such a density dependence in the potential indicates that the greater the density of the nucleonic matter, the larger the attraction felt by the kaon in medium. This is an induced attraction by the presence of the kaon as the "core" system shrinks and becomes denser. It would be absent without a K^- embedded in the system. This attraction gets a further enhancement by the increased kaon coupling to the medium going as as $\sim 1/F_\pi^*(n)$. However this induced attraction will be counter-balanced by the repulsion generated by the shrinking of the core system of three nucleons, thus stabilizing the $KaoN$. Such an attraction is absent in the chiral and exact many-body treatments described above that do not support $KaoN$s. It will therefore be tenuous if not impossible for a RigEFT-type approach

[12] This work was motivated to give a theoretical description of the dense strange tribaryons $S^0(3115)$ and $S^1(3140)$ announced to have been observed in 2004. These states have not been reconfirmed by subsequent experiments. For our purpose, whether or not such states do exist is not the issue here.

(discussed in Chapter 4) applied to dense matter, *i.e.* [Hyodo and Weise 2007; Weise and Härtle 2008], to arrive at the structure needed for $KaoN$s.

9.3.3 *KaoN as an "Ice-9" nugget*

We describe here a chiral model that closely resembles Akaishi *et al*'s picture, namely, a topological soliton model consisting of a $\bar{K}$ bound to a $B = 3$ skyrmion. Consider the holographic dual QCD discussed in Chapters 5 and 6. In this model, the *pnn* core system will be a $B = 3$ instanton in 5 dimensions or skyrmion in an infinite tower of vector mesons in 4 dimensions. As with the $B = 1$ instanton [Hong, Rho, Yee and Yi 2007b], the soliton will be tiny and hence dense in the 't Hooft and large N_c limit. The system will be stabilized by the Coulomb term from the Chern-Simons term. Now when a K^- is embedded in the $B = 3$ instanton background, there will be two sources of attraction as in the Callan-Klebanov bound state model for hyperons [Callan and Klebanov 1985]. One is the attractive potential generated by the normal component of the chiral Lagrangian and the other by the anomalous component associated with the Wess-Zumino term that comes from the Chern-Simons term. In the Callan-Klebanov model, the Wess-Zumino term plays a crucial role for binding a K^- to the skyrmion to give the hyperon $\Lambda(1116)$ and its odd-parity partner $\Lambda(1405)$. It is also the Wess-Zumino term that may be responsible for non-binding of K^+ to the soliton to give the pentaquark. In this model, both the "induced attraction" generated by the kaon interacting with the tiny and dense instanton and the counter-balancing repulsion of the squeezed instanton suggested by Akaishi *et al* are naturally present.[13]

Up to date, there is no such calculation available to report on. There is no such calculation even in the Skyrme model for the $KaoN$ system. Fortunately, however, there is an initial work on the same K^-pp system discussed above in terms of the Faddeev calculation. It is essentially the Callan-Klebanov approach applied to the K^-pp system. The K^- gets bound to the soliton, particularly by the Wess-Zumino term which is coupled to the baryon current, so the higher density of the system, the greater the binding becomes.

The presently available calculation consists of taking the ansatz for the chiral field in the form [Nishikawa and Kondo 2007]

$$U = U(1)U_K U(2) \tag{9.73}$$

where $U(1)$ and $U(2)$ are the skyrmion fields located at $\mathbf{r}_1 = \mathbf{r} - \mathbf{R}/2$ and $\mathbf{r}_2 = \mathbf{r} + \mathbf{R}/2$ respectively, U_K is the kaon field $U_K = e^{i\hat{K}}$ with $\hat{K} = \frac{\sqrt{2}}{f_\pi}\begin{pmatrix} 0 & K \\ K^\dagger & 0 \end{pmatrix}$ and $K^T = (K^+ K^0)$. Solving the equation of motion and collective-quatizing in the

[13] The pentaquark story given in Chapter 6 is anchored on this repulsion in the Callan-Klebanov model which is another story. As discussed in Chapter 7, the role of the infinite tower is mocked up in Harada-Yamawaki's HLS/VM model with the parameter a going toward the fixed point $a = 1$.

manner identical to one soliton problem à la Callan and Klebanov, one can get the energy of the system as a function of $R = |\mathbf{R}|$ which is the separation distance of the two protons. Since the product ansatz cannot correctly describe short-distance properties, we cannot expect the calculation to give a quantitative picture. One can, however, see that as the two nucleons are close together so the density gets higher, the attraction is strongly enhanced. The authors [Nishikawa and Kondo 2007] find that for the separation distance between two nucleons $\sim 1 \gtrsim R \gtrsim 2.5$ fm, the attraction can give rise to the binding energy in the range $\sim 485 \gtrsim$ B.E. $\gtrsim 145$ MeV. In compact stars treated in the next chapter, the matter is compressed to high density by gravity, so that the $KaoN$ will be dense and benefit from the strong attraction at short distance. There will be counter-balancing repulsion in the NN interaction, but as will be explained in the next chapter, the vector manifestation will weaken the repulsion at high density.

Clearly a more realistic Lagrangian and ansatz will be needed to pin down the correct estimate. But what we learn from the result is that this is a serious matter to be settled if we wish to properly address the issues of dense kaon nuggets and condensation.

While awaiting a realistic calculation of this type for the $K^- pp$ as well as $KaoN$ systems, preferably in the holographic QCD framework, we can tentatively conclude that an "ice-9" structure is a definite possibility in the effective field theory framework.

This page intentionally left blank

Chapter 10

Dense Matter For Compact Stars

The topic we will treat in this Chapter is the most intriguing part of the story – and the least understood at the moment. It is concerned with dense matter at low temperature relevant to the physics of compact stars. Processes studied at relativistic heavy ion colliders do not properly probe the regime of the dense stellar matter, since they involve high temperature as well as high density. Some closely related issues were treated in Chapter 9, touching on certain laboratory observations such as dense kaonic matter which could be produced in the terrestrial laboratories. Here we will look at what can happen when density increases to the order of 10 times the nuclear matter density that is expected to be found in the interior of compact stars.

In describing dense matter, we face both experimental and theoretical obstacles. Experimentally, there are no laboratory data to guide theorists. As discussed in Chapter 9, deeply bound kaonic nuclear systems could possibly be formed and provide direct information on self-bound nuclear systems at high density. Up to date, however, there are no confirmed experimental results. Furthermore there are no reliable theoretical tools to make predictions that could guide experimentalists. The lattice QCD suffers from the "sign problem" which does not allow going to high enough density. In the absence of model-independent guidance, one is compelled to resort to models, the most frequently employed one of which being the Nambu-Jona-Lasinio model and its cousins (with or without instanton and/or confinement effects). These models give a rich and fascinating landscape of phases involving hadrons and/or quarks, but lacking help from experiments, it is difficult to assess how reliable the plethora of model predictions are. We will nonetheless discuss some of what one learns from such models since they are interesting on their own merits and could perhaps be sharpened in the future with more data from various sources, in particular from up-coming terrestrial experiments.

10.1 Dense Hadronic Phase With and Without Exotica

Before we go into dense matter proper in which the microscopic degrees of freedom of QCD could figure explicitly, let us discuss in which way hadrons as *macroscopic* degrees of freedom could "dictate" the state of matter at high density. As we have stressed throughout this volume, one should of course keep in mind that one cannot make a clean distinction between what is microscopic and what is macroscopic except in certain special cases.

It is generally accepted that when density is high enough, hadronic matter will make transition to a color superconducting quark matter via the famous Cooper pairing [Rajagopal and Wilczek 2001]. The transition is believed to be of first order, and this is what one finds in most of the phase diagrams seen in the literature. The assumption made there is that the "door-way" state to color superconductivity is a normal Fermi liquid. There is, however, no rigorous proof to support this scenario since the only nonperturbative QCD machinery available, namely, lattice, is moot in this regime. We discussed in Chapter 6 a possible "pseudo-gap" phase with half-skyrmions that could emerge as *the* relevant degrees of freedom at the phase boundary. The existence of such a phase must have something to do with chiral symmetry since the phase change involved there is characterized by an order parameter tied to the quark condensate. Such a matter would entail, as we will show below, a non-normal Fermi liquid structure. Now even before reaching that point, if the vector manifestation of HLS takes place at the critical density, then a simple consideration based on fluctuations around the VM fixed point suggests, as we saw in the preceding chapter, that in compact stars, there will be kaon condensation aided by the electron chemical potential. If kaons are condensed below the would-be critical density for chiral restoration, then the Fermi surface would also be distorted and that would likely change the structure of the color superconducting matter in the quark phase. This matter will be discussed below.

If one were to approach from the standard nuclear physics point of view discussed in Chapter 4 and disregard the possibility of other degrees of freedom than just the nucleons, then one would conclude that nothing "interesting" happens to the hadronic matter in the density regime relevant in the stars. In the absence of rigorous QCD predictions, it will be ultimately up to observables from up-coming laboratory experiments or from compact stars to assess this "un-exciting" conclusion. We will have more to say on this in the next section where we will discuss some astrophysical observations, but in order to motivate the discussion that will come in that section, let us see what we can say from the presently available information on the mass and radius of the neutron stars. There are of course many more observables from the stars (see, among many others, [Lattimer and Prakash 2007] for review). Here we will focus on these two quantities – the mass and radius, and leave other matters to the future.

10.1.1 *Compact stars as dense neutron matter*

For nuclear physicists, one of the principal goals in studying compact stars is to learn about the equation of state (EOS) which is supposed to provide information on the phase structure of matter at high density. For instance the maximum mass of stable compact stars is known to be sensitive to the stiffness of neutron matter. The recent observation by Nice *et al.* of the neutron star PSR J0751+1807 (more on this in the next section) with mass $2.1 \pm 0.2\ M_{\odot}$ raises the possibility that the compact star matter cannot support the so-called "exotic" phases such as condensed kaons or hyperons or even ordinary or Cooper-paired quark matter.

For the sake of discussion, we will depart in this part of discussions from the principal thesis of this volume that the presence of multiple fixed points at various densities obstructs going directly from a free-space Lagrangian to one applicable to densities higher than that of the normal nuclear matter. Putting this caveat aside, we consider the energy density $\epsilon(n)$ of dense matter – from which the EOS is derived – inferred strictly from the information available in *free space*. The starting point will be the same as the SNPA (standard nuclear physics approach) to few-nucleon systems described in Chapter 4. It will consist of the following three steps: (1) First determine an accurate two-nucleon potential fit to scattering data measured accurately, say, to lab momenta $\sim 2\ \mathrm{fm}^{-1}$; (2) next implement the two-body potential with many-nucleon forces, typically three-body, consistent with few-body systems; (3) finally solve as accurately as possible the many-body Schrödinger equation and obtain the energy density $\epsilon(n)$ of the system with densities greater than the nuclear matter density. The first and second steps are constrained by measured data on few-body nuclear systems and the last requires highly sophisticated computational methods, *e.g.*, Monte-Carlo simulations.

One of the currently best state-of-art calculations involves one of the most "realistic" two-body potentials, *i.e.* Av18 [Wiringa, Stoks and Schiavilla 1995] we encountered in Chapter 4, implemented by the three-body force known as "UIX," best-fit to nuclear properties of few-nucleon systems. In Fig.10.1 is illustrated the qualitatively distinctive feature of the neutron star mass vs. radius as obtained by Akmal *et al.* [Akmal, Pandharipande and Ravenhall 1998] using the above-mentioned potentials. The precise numerical values should not be taken too seriously but one can see clearly from the results that the three-body force UIX, with the relativistic correction suitably incorporated, produces a strong repulsion at high density so that the maximum neutron star mass predicted therein could be considerably higher than that without the three-body force. The resulting stiffness of the EOS would very likely prevent entirely, or at least banish to much higher densities than relevant, such possible phase changes as kaon condensation, diquark Cooper pairing *etc.*

How solid is this prediction and are there loop-holes to the argument leading to it?

In order to assess the reliability of this prediction, the first question to ask is

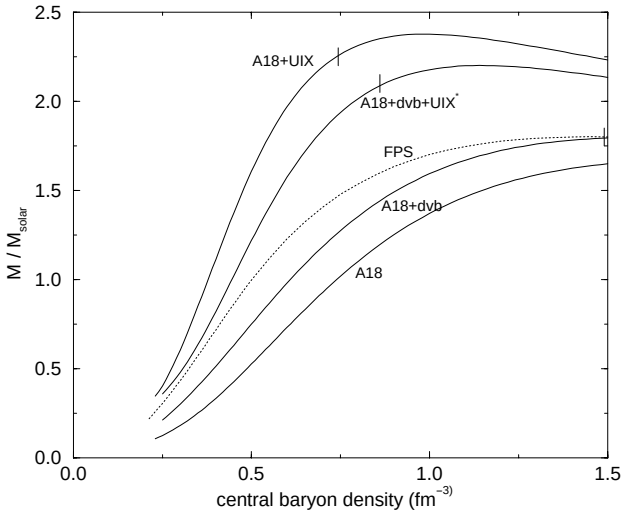

Fig. 10.1 Qualitative feature of neutron star mass versus radius for the nuclear models with and without repulsive three-body forces, as revealed in [Akmal, Pandharipande and Ravenhall 1998].

what is responsible in the potentials for such a repulsion. This question can be addressed in terms of what we learned from HLS with the vector manifestation.

10.1.2 *Working of the vector manifestation*

The first point to note is that the potentials used for Fig.10.1 are fit to zero-density and low-density regime, which means that the parameters that figure in the theory are free-space quantities. We shall now argue that the EOS of [Akmal, Pandharipande and Ravenhall 1998] based on the SNPA strategy lacks the "intrinsic background dependence" (IBD) in the parameters of the theory that is *indispensable for correctly encoding the complex vacuum structure of chiral symmetry in the strong interactions*. We suggest here that a proper account of the IBD can provide the mechanism to suppress the strong repulsion that is generated for densities $n > n_0$ by three-body forces in medium.

It was discussed in Chapter 8 that certain important part of the effect of many-body forces in dense medium can be embedded into the IBD with density providing the background. In hidden local symmetry theory, the IBD is encoded in the renormalization-group properties of QCD in the background of density. How this IBD maps onto many-body theory with many-body forces has not been fully worked out. However, one can give a plausible argument that when the IBD is properly taken into account, the repulsion due to three-body forces will be softened, if not totally eliminated, at densities $n > n_0$. It is possible to formulate the argument

in many-body Schrödinger formalism by introducing density-dependent parameters (*e.g.*, via Kohn-Sham density functional), but implementing relevant symmetries therein would be difficult and the result could be plagued with ambiguities. It can be best formulated in field theory language where the relevant symmetry, *i.e.* chiral symmetry, is manifest.

Consider the EFT Lagrangian (8.11) and (8.12) given in Chapter 8,

$$\mathcal{L}_\chi = \bar{N}[i\gamma_\mu(\partial^\mu + iv^\mu + g_A^\star\gamma_5 a^\mu) - M^\star]N - \sum_i C_i^\star(\bar{N}\Gamma_i N)^2 + \cdots \tag{10.1}$$

with

$$\sum_i C_i^\star(\bar{N}\Gamma_i N)^2 \approx +\frac{C_{\tilde{\omega}}^{\star\,2}}{2}(\bar{N}\gamma_\mu N)^2 + \frac{C_{\tilde{\rho}}^{\star\,2}}{2}(\bar{N}\gamma_\mu\tau N)^2 + \cdots . \tag{10.2}$$

Here the asterisk denotes the IBD in the parameters appearing in the EFT Lagrangian. In (10.2) are shown only those four-Fermi interactions that involve vector-meson exchanges. Other interactions are subsumed in the ellipses. As suggested in Chapter 8, we could take the $\tilde{\omega}$ to encapsulate entire contributions from the tower in the ω quantum number in the infinite tower HLS theory, and likewise for the $\tilde{\rho}$ and other terms that come from the localization of certain non-local terms that are typically given by loop corrections. Other four-Fermi interactions and higher-Fermi interactions are denoted by the ellipses. We will not need them for our purpose here.

Now we recall from Chapter 8 (see, *e.g.*, [Song, Brown, Min and Rho 1997; Song, Min and Rho 1998; Song 2001]) that chiral symmetry requires that the parameters of the theory with the "intrinsic density dependence" be given as *functionals* of the chirally-invariant density operator $\hat{n}(x) \equiv N^\dagger(x)N(x)$. Suppose now that the functional parameters in the matrix elements of the four-Fermi interactions (10.2) are expanded in power of the density operator $\hat{n}$. The resulting Lagrangian will contain six- and higher-Fermi fields and when mean field is taken, will give rise to density dependent parameters in the theory. This means that certain chirally symmetric n-body (with $n > 2$) interactions are subsumed in the IBD of the coefficients in (10.2) when truncated to the four-Fermi terms. Since the mean field using the Lagrangian (10.1) is equivalent to doing Landau Fermi liquid theory, certain important many-body effects are therefore encoded *chirally symmetrically* in the IBD of the parameters.

In this formulation, the repulsion resides in the ω channel in (10.2). In Harada-Yamawaki HLS theory, the parametric mass of the ρ and ω (or the lowest member of the tower) drops as density increases whereas the vector coupling g remains more or less unchanged up to $n \sim n_0$ and then decreases after the "flash density" $n_{flash} \gtrsim 2n_0$. This means the coefficient $C_{\tilde{\omega}}^{\star\,2}$ will increase as $g^2/m_\omega^{*\,2}$ with the falling mass up to, say, $n \sim n_0$ or slightly above. This repulsion up to that density provides the mechanism for the saturation of nuclear matter. From n_{flash}, the VM

(vector manifestation) starts becoming operative, with the gauge coupling and the mass falling at the same rate, so that the ratio g^{*2}/m_ω^{*2} will remain constant at higher density. The repulsion will cease accordingly.

The above discussion allows one to understand what takes place in Fig.10.1. Solving many-body Schrödinger equation with three-body forces, when interpreted in terms of HLS, accounts at least partly for the dropping m_ω^* without, however, any change in the vector coupling and hence accounting for the repulsion, but the mechanism for the vector manifestation (VM) behavior at higher density is missing in the theory, so the repulsion will continue as density increases. This is what causes the stiffness in the EOS. This is basically the same mechanism that, in the absence of HLS/VM, banished kaon condensation to a density $n \gtrsim 7n_0$ [Pandharipande, Pethick and Thorsson 1995]. The same problem arises in the description of dense skyrmion matter treated in Chapter 6, when the ω meson is introduced without properly taking into account the dropping vector coupling g_v implied by HLS/VM: the increasing ω repulsion requires that the ω mass increase rather than decrease as density increases beyond the flash density [Park, Rho and Vento 2004], which is at variance with BR scaling. This defect is removed when the decreasing of the gauge coupling g at increasing density is taken into account [Park, Rho and Vento 2008].

10.1.3 *Demise of the VM scenario by massive compact stars?*

The possibility presented above that the vector manifestation would prevent increasing repulsion as density increases beyond, say, the flash density could have a strong consequence on the possible formation of hybrid compact stars containing quark matter inside and nuclear matter at the mantle with mass $M \gtrsim 2M_\odot$. As will be briefly touched on in the section below, what is considered to be the most likely stable color superconducting phase at very high density is the LOFF crystalline phase of three-flavor quark matter [Alford, Schmitt, Rajagopal and Schäfer 2007] which also lends itself to a test in gravity-waves from LIGO. Let us assume for the sake of argument that such a crystalline state exists in the core of hybrid stars. Now in order to make transition from hadronic matter to the crystalline phase, it is found to be necessary that the normal hadronic state be very stiff, in fact *maximally* stiff within the stricture of the SNPA. Within the model framework available, namely, NJL model, bag models *etc.* for the dense phase, nuclear EOS's soft enough to accommodate possible phase changes such as kaon condensation cannot bring phase equilibrium between nuclear and quark matter. (For discussion on this matter, see [Ippolito, Ruggieri, Rishchke, Sedrakian and Weber 2007].)

That only very stiff nuclear EOS's can be matched to the crystalline structure implies that the compact stars of hybrid type of quark core and nuclear mantle can be massive, say, $M \gtrsim 2M_\odot$. In fact, several such massive stars seem to have been "observed." The most advertised of them all is the 2.1 solar mass pulsar of [Nice *et al.* 2005] to which we will return later, but there have been more recently announced

observations in NGC 6440 and NGC 6441 of millisecond pulsars of median mass $2.74 \pm 0.21 M_\odot$ [Friere *et al.* 2007]. If confirmed, the existence of such massive stars, which are readily accommodated with the crystalline color-superconducting matter but *not* with kaon condensation, would throw doubt on the viability of the VM scenario. Whether or not the determination of the 2.74 solar mass from the observation is valid is a highly controversial issue, and it will be sometime before the "jury" could be out. We should consider it as an open issue. This caution is more apt given that the 2.1 solar mass of [Nice *et al.* 2005] is now revised drastically down to $\sim 1.26 M_\odot$ as will be mentioned more precisely below. Nonetheless the possible caveat will have to be kept in mind in what follows as we inject the notion of the VM into the confrontation with astrophysical observations.

10.1.4 *Kaon condensation as a doorway to quark matter*

We now turn to dense matter, the density of which is $\gtrsim 2n_0$, in which exotic states could intervene. As in Chapter 9, we assume in parallel to the flash temperature in hot matter that beyond $n_{flash} \sim 2n_0$, the relevant fermion degrees of freedom are the quasiquarks or constituent quarks, not the baryons. Chiral symmetry is supposed to be realized in the Nambu-Goldstone mode whereas quarks and gluons are deconfined with the "soft" glues participating in chiral condensation. This is essentially the regime where the Manohar-Georgi chiral quark model [Manohar and Georgi 1984] should apply. This picture is one of two scenarios that emerge in holographic dual QCD à la Sakai-Sugimoto [Sakai and Sugimoto 2005; Sakai and Sugimoto 2006; Aharony, Sonnenschein and Yankielowicz 2007].

As argued in the preceding chapter, kaons will condense in compact-star matter (with electrons having large chemical potential) *before* the density reaches the critical density for the onset of ordinary quark matter or color superconductivity. We will show that once kaons are condensed, then the "normal" phase must be quite different from the Fermi-liquid state that is ascribed to nuclear matter. In addition to the half-skyrmion phase which is of "pseudo-gap" type presented in the next subsection, the kaon-condensed phase will constitute an anomalous doorway state to possible quark matter, so a possible transition to a superconducting state might be quite different from the standard scenario that involves a normal Fermi-liquid phase.

We can gain a qualitative idea of what might happen at densities above the flash density from the simple chiral quark model (χQM) of Manohar and Georgi [Manohar and Georgi 1984]. We expect basically similar results from more realistic models. The Lagrangian we will work with is of the form

$$\mathcal{L} = \mathcal{L}_0 + \mathcal{L}_M + \mathcal{L}_{m_\pi}, \tag{10.3}$$

where $\mathcal{L}_0$ is the chirally invariant Lagrangian that we write down explicitly as it is

needed for later discussions,

$$\mathcal{L}_0 = \bar{\psi}(iD^\mu + v^\mu)\gamma_\mu\psi + g_A\bar{\psi}\gamma_\mu\gamma_5 a^\mu\psi - M_0\bar{\psi}\psi + \frac{1}{4}f_\pi^2 \mathrm{tr}(\partial^\mu U^\dagger \partial_\mu U) - \frac{1}{2g_c^2}\mathrm{Tr}(G^{\mu\nu}G_{\mu\nu}) + \ldots . \tag{10.4}$$

Here D^μ is the covariant derivative with the gluon field, f_π is the (physical) pion decay constant, ψ is the quasiquark field, $v_\mu(a_\mu)$ is the induced vector (axial-vector) field defined in previous chapters, *e.g.*, Chapter 5, and $\mathcal{L}_M$ and $\mathcal{L}_{m_\pi}$ are respectively the chiral symmetry-breaking terms for the baryons and for the (pseudo-)Goldstone bosons, the explicit forms of which are not needed for the present discussion.

Although the Lagrangian (10.4) has been quite successfully used in matter-free space [Cheng and Li 1995], it should be more appropriate where the quasiquark concept is applicable, as in the density regime at and above the flash point. From the flash density to the chiral restoration density which can be identified with the VM fixed point [Harada, Kim and Rho 2002], the relevant fermion degrees of freedom are assumed to be the quasiquarks, and the hadronic freedom should become operative. We also assume that the "soft" glues participate in giving rise to the quasiquark masses as explained in Chapters 7 and 8, leaving behind "hard" glues which may be identified with the gluon fields that figure in (10.4). If one were to integrate out the "hard" gluon component, one would wind up with 4- and higher-Fermi interactions in the effective Lagrangian. These will play an important role in phase changes, including possible color superconductivity. Approaching kaon condensation in this way is a bottom-up one exploiting the hadronic freedom which shares the same property as in Chapter 9 where kaon condensation was approached top-down from the VM fixed point. In the same vein, we can make the same weak-coupling calculations, now going bottom-up.

Now what happens in this χQM picture when kaons are condensed? What we are interested in here is the behavior of the quark condensates in the presence of the condensed kaons. We consider in particular K^- since the electron-driven kaon condensation involves the negatively charged kaons. The quark condensates calculated from χQM given by the Lagrangian Eq. (10.4) take the form

$$\langle\bar{u}u\rangle_n = \langle\bar{u}u\rangle_{vac} + \frac{1}{2}\left[\frac{\partial\tilde{\epsilon}}{\partial m_u} + \frac{dM_u}{dm_u}\frac{\partial\tilde{\epsilon}}{\partial M_u} + \frac{dm_K^2}{dm_u}\frac{\partial\tilde{\epsilon}}{\partial m_K^2}\right] \tag{10.5}$$

$$\langle\bar{d}d\rangle_n = \langle\bar{d}d\rangle_{vac} + \frac{1}{2}\left[\frac{dM_d}{dm_d}\frac{\partial\tilde{\epsilon}}{\partial M_d} + \frac{dm_K^2}{dm_d}\frac{\partial\tilde{\epsilon}}{\partial m_K^2}\right] . \tag{10.6}$$

Here $M_{u,d}$ is the constituent quark mass and the possible dependence on the current quark mass of the physical quantities such as g_A, f_π *etc* is ignored. $\tilde{\epsilon}$ is the energy density of the system which we will compute in mean field including electron contributions and with the charge neutrality taken into account.[1] In that approximation,

[1] We remind the reader the well-known result in the field that the charge neutrality condition sets the kaon frequency ω_K equal to the chemical potential of the electron μ_e.

$\langle\bar{d}d\rangle$ does not depend on the kaon condensate $v \equiv |\langle K^-\rangle|$ since $\frac{dm_K^2}{dm_d} = 0$. Thus K^- condensation does not affect the d-quark condensate. It is the u-quark condensate which will be sensitive to kaon condensation. We look at the ratio

$$R \equiv \frac{\langle\bar{u}u\rangle_n}{\langle\bar{u}u\rangle_{vac}} = 1 - \frac{m_u}{m_\pi^2 f_\pi^2}[\frac{\partial\tilde{\epsilon}}{\partial m_u} + \frac{\sigma_u}{m_u}\frac{\partial\tilde{\epsilon}}{\partial M_u} + \frac{m_K^2}{m'}\frac{\partial\tilde{\epsilon}}{\partial m_K^2}] \,, \tag{10.7}$$

where $\sigma_u \equiv m_u dM_u/dm_u$ and $m' = m_u + m_s$. Given the electron chemical potential which is fed in from outside, one can readily compute the ratio R as a function of density n/n_0. The results are illustrated in Fig. 10.2 for reasonable values (see below) of the electron chemical potential.

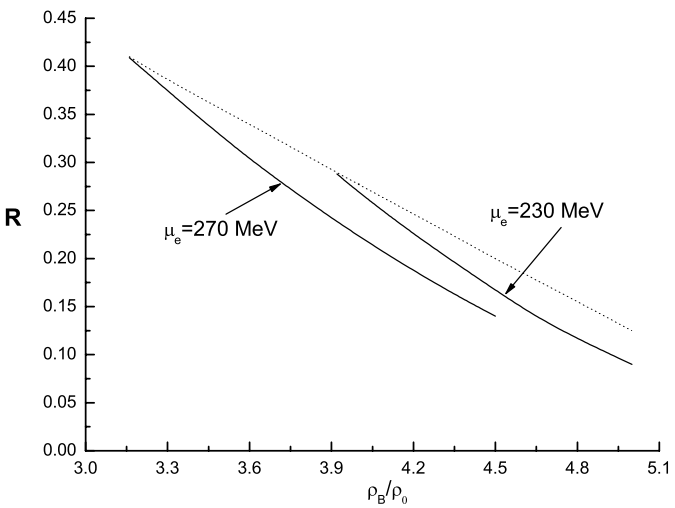

Fig. 10.2 $R \equiv \langle\bar{u}u\rangle_{\rho_B}/\langle\bar{u}u\rangle_{vac}$ calculated with (solid line) and without (dotted line) kaon condensation taken into account. The results are given for two different values of the electron chemical potential, μ_e= 230 and 270 MeV.

The point to note in the result is that the ratio R falls faster in density with kaon condensation than without. Since the d quark condensate, $\langle\bar{d}d\rangle$, is not affected by the presence of K^- condensation to the lowest order in density under consideration, we expect that in the kaon condensed phase $\langle\bar{u}u\rangle/\langle\bar{d}d\rangle \to 0$ as the density n increases. It is generally expected that chiral symmetry restoration characterized by $\langle\bar{u}u\rangle = \langle\bar{d}d\rangle = 0$ occurs in dense matter.[2] The above results indicate, however, that at densities between the critical density for kaon condensation n_c^K and that for

[2]Note however that even if $\langle\bar{u}u\rangle = \langle\bar{d}d\rangle = 0$, it could be that $f_\pi \neq 0$, a phenomenon that might be related to a pseudo-gap phenomenon as observed in dense skyrmion crystal matter described in Chapter 6.

chiral restoration $n_c^{\chi SR}$ ($n_c^K < n_B < n_c^{\chi SR}$), kaon condensation may lead to a phase characterized by $\langle\bar{u}u\rangle \simeq 0$, $\langle\bar{d}d\rangle \neq 0$, which represents partial "flavor-dependent restoration" of chiral symmetry.

An immediate consequence is that a K^- condensate gives rise to difference between the masses of the constituent u and d quarks. It is easy to show

$$M_u^\star = M_0 + m_u - \frac{m'}{2f_\pi^2}v^2$$
$$M_d^\star = M_0 + m_d \quad (= M_d) \tag{10.8}$$

with $m' = m_u + m_s$. Thus the presence of a K^- condensate induces additional $SU(2)$-isospin symmetry breaking on top of the small explicit isospin breaking due to $m_u - m_d \neq 0$. What this means is that the Fermi surfaces for the nucleons will be affected and is likely to influence the onset and structure of color superconductivity. In particular, the proton chemical potential will be increased, reducing the difference between the neutron and proton chemical potentials.

10.2 Skyrmion-Half-Skyrmion Transition

A potentially important phenomenon that can occur as a doorway to color superconductivity deviating strongly from Fermi-liquid structure – even if kaons had not condensed by then – is the half-skyrmion phase discussed in Chapter 6. In this phase, chiral symmetry is restored with vanishing quark condensate but the pion decay constant is not zero, which was characterized as a pseudogap phenomenon. In Chapter 6, this result was obtained using the Skyrme model which contains the pion field only. We discuss in this subsection what happens when hidden local symmetric vector mesons are incorporated. Although no results of quantitative analyses are available, one can have a qualitative idea of what can happen, using a hidden local symmetry Lagrangian of the type developed in the volume [Rho 2007b]. We will present an argument that the half-skyrmion phase corresponds to a phase in which Georgi's "vector mode/symmetry" [Georgi 1989a; Georgi 1989b] is realized as an emergent symmetry, emergent in the sense that the symmetry in question is not present in QCD proper.

QCD predicts that if the up, down and strange quark masses are equal so that the flavor $SU(3)$ is a good symmetry and small, then if density can be brought high enough, normal nuclear matter will make a transition to the color-flavor-locked (CFL) color superconducting state which will be discussed below. In the normal state, the quarks are confined and the $SU(3)_L \times SU(3)_R$ chiral symmetry is spontaneously broken down to the diagonal subgroup $SU(3)_{V=L+R}$. In the CFL state, the quarks are also confined and the global symmetry $SU(3)_c \times SU(3)_L \times SU(3)_R$ is spontaneously broken down to $SU(3)_{c+L+R}$ with the gluons getting higgsed and chiral symmetry also spontaneously broken. There thus seems to be "continuity"

in the excitation spectra from below to above the transition density [Schäfer and Wilzcek 1999].

We have argued in the preceding chapters that in low-energy effective theory of QCD below $n_c^{\chi SR}$, baryons can be described as skyrmions – albeit rigorously valid only at large number of colors N_c [Witten 1983]. Therefore the normal nuclear matter can be described as a skyrmion matter [Nowak, Rho and Zahed 1996]. Furthermore, as will be discussed below, the baryons in the CFL phase can also be viewed as skyrmions (referred to as "superqualitons" in [Hong, Rho and Zahed 1999]) and hence the CFL phase can be considered as *another* form of skyrmion matter (we shall refer to it as "superqualiton matter"). The phase transition from the normal nuclear matter to the CFL phase can thus be interpreted as a transition from the standard skyrmion matter to another form of skyrmion matter. Now the question raised here is: What is the nature of, or mechanism for, this transition between the two confined systems with spontaneously broken chiral symmetry, one above $n_c^{\chi SR}$ with a diquark condensate for its order parameter and one below $n_c^{\chi SR}$ with a quark-antiquark condensate? It seems plausible that a sort of quantum critical phenomenon is taking place here as in condensed matter systems [Sachdev 2000; Coleman and Schofield 2005].

10.2.1 *Half-skyrmions and emergence of "vector symmetry"*

Let us first recall the structure of skyrmion matter at high density constructed in Chapter 6.4.2 by putting the Skyrme Lagrangian on a crystal. It was found there that at some density $n_p > n_0$, the skyrmion matter in FCC makes a phase transition to a half-skyrmion matter in body-centered cubic (BCC) crystal. This phase was characterized by the chiral order parameter $\langle\bar{q}q\rangle \sim \langle\sigma\rangle = 0$, signalling the restoration of chiral symmetry with, however, the pion decay constant $f_\pi \neq 0$. At some higher density, say, $n_c^{\chi SR}$, f_π does also go to zero. We identified the phase between n_p and $n_c^{\chi SR}$ with a "pseudogap" phase in analogy to high T superconductivity. When the Skyrme Lagrangian was *minimally* gauged and supplemented with a dilaton scalar χ interpolating the gluon condensate representing the trace anomaly of QCD, it was found that the pseudogap structure remained intact, namely, the pion decay constant remained non-zero while the chiral condensate vanished and that the vector meson mass scaled as $\langle\chi\rangle^*$ which is non-zero in $n_p \leq n < n_c^{\chi SR}$. This meant that the vector meson mass was non-zero in the pseudogap phase. However, as noted above, the gauged Skyrme Lagrangian used in [Park, Rho and Vento 2004] does not capture fully the vector manifestation property of the HLS/VM theory. Although the scaling vector meson mass is reproduced by the VEV $\langle\chi\rangle^*$, so consistent with the property of BR scaling as we saw in Chapter 6, it does not exhibit the fixed point feature of HLS/VM.[3] In order to expose the characteristics of HLS/VM,

[3]This is due to the fact that the gauged Skyrme Lagrangian used there does not correctly reproduce the anomaly structure of hidden local symmetry theory present in $\mathrm{HLS}_{K=\infty}$ (or in $\mathrm{HLS}_{K=1}$ obtained by integrating out the higher-lying vector mesons). While the dilaton condensate plays

we go back to the notion that the vector mesons in the effective field theory are emergent degrees of freedom. The crucial observation, as stressed before, is that the chiral field $U = e^{2i\pi/F_\pi}$ can be written in terms of the left and right coset-space coordinates as

$$U = \xi_L^\dagger \xi_R \tag{10.9}$$

with the transformation under $SU(3)_L \times SU(3)_R$ as $\xi_{L,R} \to \xi_{L,R} g_{L,R}^\dagger$ with $g_{L,R} \in SU(3)_{L,R}$. The hidden local symmetry

$$\xi_{L,R} \to h(x)\xi_{L,R} \tag{10.10}$$

and the emergent gauge fields transforming

$$V_\mu \to h(x)(V_\mu - i\partial_\mu)h^\dagger \tag{10.11}$$

are encapsulated in the HLS Lagrangian given by Eq. (5.25)

$$\mathcal{L} = \frac{F_\pi^2}{4}\mathrm{Tr}\{|D_\mu \xi_L|^2 + |D_\mu \xi_R|^2 + \kappa |D_\mu U|^2\} \; - \frac{1}{2g^2}\,\mathrm{Tr}\,[V_{\mu\nu}V^{\mu\nu}] + \cdots \; . \tag{10.12}$$

Suppose one constructs dense skyrmion matter with (10.12) in the way that is done with the Skyrme Lagrangian. We expect that the skyrmion so constructed on crystal will fractionize at, say, $n = n_p$ into two half skyrmions, one given by $\xi_L^\dagger$ and the other by ξ_R. We can think of the former as "left-half-skyrmion" and the latter "right-anti-half-skyrmion," the product of which making up a single skyrmion. It is suggestive to think of this fractionization as an analog to the "deconfined quantum critical phenomenon" in the transition in condensed matter from the Néel magnetic phase to the valence-bond-solid (VBS) paramagnetic phase which is characterized by the deconfinement of a baby-skyrmion into two half baby-skyrmions [Senthil *et al.* 2004]. In this condensed matter example, half-skyrmions are confined (or bound) to skyrmions in the initial (Néel) and final (VBS) phases and the transition occurs via the fractionized (or deconfined) half-skyrmion phase. Similarly we can think of the phase transition from the normal baryonic matter to, say, the color-flavor locked superconducting state (described below) as a transition from a normal skyrmion matter to a "superqualiton" skyrmion matter via a half-skyrmion phase. Unlike in the condensed matter case where the monopole tunneling is understood to be at work for the confinement/deconfinement of the half skyrmions, however, the mechanism for such deconfinement at n_p in dense hadronic matter is not known. What is the most pertinent for our discussion is that the possible half-skyrmion phase could be a non-Fermi liquid state very much like in the condensed matter

the role of the intrinsic density dependence indispensable for vector manifestation, the repulsion that forces the ω mass to increase as density increases – which is at odds with the VM as discussed above – is an artifact of approximations made in the anomalous Lagrangian responsible for $\omega \to 3\pi$ decay. At the time of this writing, a work was in progress (with Y. Oh and D.-P. Min) to rectify this defect.

case and could crucially influence the mechanism for (a variety of) phase transitions to color superconducting states.

What is perhaps more interesting and significant is that the half-skyrmion (or pseudogap) state exhibits an emerging or "enhanced" symmetry. In $\mathrm{HLS}_{K=1}$ theory, the half-skyrmion state has the chiral $SU(3)_L \times SU(3)_R$ (for $N_f = 3$) restored. Thus for $n_p \leq n < n_c^{\chi SR}$,

$$(F_\sigma/F_\pi)^2 \equiv a = 1, \quad F_\pi \neq 0, \tag{10.13}$$

which corresponds to $\kappa = 0$ in Eq. (10.12). Note, however, that the gauge coupling $g \neq 0$, so the vector meson remains massive. Since the vector meson mass is non-zero, F_σ is the decay constant for the longitudinal component of the vector meson, not of a free scalar. g does go to zero, however, in the skyrmion matter at chiral restoration, *i.e.* $n = n_c^{\chi SR}$. This corresponds to Georgi's "vector limit." [4] As noted by Georgi, at this point the symmetry swells to $SU(3)^4$, with Σ_L and Σ_R transforming under independent $SU(3) \times SU(3)$ symmetries,

$$\xi_L \to h_L(x)\xi_L g_L^\dagger, \quad \xi_R \to h_R(x)\xi_R g_R^\dagger, \tag{10.14}$$

where $g_{L,R}$ and $h_{L,R}$ are the unitary matrices generating the corresponding global and local $SU(3)$ groups. The hidden local symmetry is the diagonal sum of $SU(3)_{h_L}$ and $SU(3)_{h_R}$. Away from the vector limit, the non-zero gauge couplings break the vector symmetry explicitly producing the nonzero vector meson mass and couplings for the transverse components of the vector mesons. In terms of this symmetry pattern, we see that the pseudogap phase is the regime where one has $a = 1$ ($\kappa = 0$) and weak gauge coupling $g \to 0$. We note that this is precisely the regime in which "hadronic freedom" is operative. This allows us to identify the onset density for the pseudogap phase n_p with the flash density n_{flash} – the density counterpart of the flash temperature T_{flash} – that figured importantly and extensively exploited in Chapters 7 and 9.

In what follows, for the reason of our total ignorance, we will simply ignore such intricacies as kaon condensation, deconfined half-skyrmion phase *etc.* as a doorway state to color-superconducting quark matter. We should of course keep this caveat in mind in discussing the possible role of quark matter in compact stars.

10.2.2 *Transition from the CFL phase to the normal nuclear phase*

So far we have been approaching the critical point from the normal matter side. Now what about approaching it from the CFL phase?

[4] In his formulation, Georgi considered that vector symmetry could encompass the situation where $g = 0$ and $\kappa = 0$ but $F_\pi \neq 0$. It is argued in [Harada and Yamawaki 2003] that with quantum corrections included, one cannot have $g = 0$ and $f_\pi \neq 0$ (where f_π is the physical pion decay constant) since this violates chiral Ward identity. The possible loop-hole to this no-go theorem is that there are collective excitations in dense medium and certain symmetries not present in QCD – such as this vector symmetry – could emerge from such excitations.

The first point to note for this matter is that the low-energy effective theory for the CFL phase is also a local flavor gauge theory. One can see this as follows. The CFL phase is characterized by the locking of color and flavor such that the color rotation is exactly compensated by the flavor rotation. The symmetry breaking pattern is

$$G = SU(3)_c \times SU(3)_L \times SU(3)_R \to H = SU(3)_{c+L+R} \tag{10.15}$$

where the additional $U(1)$ breaking is not indicated here since it does not concern us. Both chiral symmetry and the global color symmetry are spontaneously broken, so we have two sets of Goldstone bosons, one set scalars (denoted σ) and the other pseudoscalars (denoted π). The scalars are eaten up by Higgs mechanism to render the gluons massive while the pseudoscalars remain as physical Goldstone boson excitations. Let us write the coset coordinates in terms of the two Goldstone fields σ and π,

$$\xi^{\alpha}_{L(R)i} = \epsilon_{\alpha\beta\gamma}\epsilon^{ijk}\langle\psi^{\beta}_{L(R)j}\psi^{\gamma}_{L(R)k}\rangle \tag{10.16}$$

with $\xi_{L,R} = e^{\mp i\hat{\pi}/F_{\hat{\pi}}}e^{i\hat{\sigma}/F_{\hat{\sigma}}}$ where $F_{\hat{\pi},\hat{\sigma}}$ are the corresponding decay constants for the scalars involved. Here the fields are distinguished with a hat from those in the (low-density) Nambu-Goldstone phase. In (10.16), α is the color index and i the flavor index. The low-energy theory for the Goldstone bosons is the nonlinear sigma-model Lagrangian defined in the coset space G/H [Hong, Rho and Zahed 1999; Casalbuoni and Gatto 1999],

$$\mathcal{L} = \frac{F^2_{\hat{\pi}}}{4}\mathrm{Tr}(U^{\dagger}\partial^{\mu}U)^2 + \cdots \tag{10.17}$$

with

$$U = \xi^{\dagger}_L\xi_R \tag{10.18}$$

with $\xi_{L,R}$ transforming

$$\xi_{L(R)} \to h(x)\xi_{L(R)}g^{\dagger}_L(g^{\dagger}_R) \tag{10.19}$$

with $h \in P = c + L + R$ and $g_L(g_R) \in c + L(R)$. Now as in the normal phase formulated in [Bando *et al.* 1988; Harada and Yamawaki 2003], one exploits the gauge equivalence of the non-linear G/H theory to linear $G_{global} \times H_{local}$ theory that follows from the product form of (10.18). In this way of bringing in gauge degrees of freedom, the gauge fields are "hidden" in some sense as in the $n < n_c$ phase. However, there is a basic difference in the case of the $n > n_c$ phase because the local gauge fields are already present in the form of gluon fields. The color-flavor locking is accompanied by the color gauge fields higgsed and then transformed to flavor gauge fields by being dressed by the "pion cloud" in a way analogous to Wetterich's approach to spontaneously broken color in normal matter [Wetterich 2001]. Thus the vector fields are *not* really hidden in the sense described above;

they are actually explicit. At low energy, the two ways of looking at this phase above n_c should be equivalent, so we shall continue using the terminology "HLS" for this theory.

Given the HLS Lagrangin, the next step is to construct the skyrmion in the manner proposed in [Hong, Rho and Zahed 1999].[5] We expect that low-energy properties of the CFL phase will be given by the skyrmion matter (superqualiton matter in this case) and the transition from the skyrmion matter to the half-skyrmion matter arrived at from above n_c could be developed as from below. The transition is from one form of skyrmions (with the quark-antiquark condensate) to another form of skyrmions (with the di-quark condensate) and vice-versa.

We of course do not know what the mechanism for such a transition could be top-down as in the case of bottom-up. What we can suggest is that the quark-baryon continuity of [Schäfer and Wilzcek 1999] has an intermediate phase in which a deconfinement of a sort takes place. The deconfinement is manifested through the fractionization of a skyrmion into half-skyrmions, such a phase making a border between a normal skyrmion matter below n_c and on a CFL skyrmion matter above n_c. We suggest this as an illustration of a "smooth" cross-over in dense medium similar to what has been recently discussed for RHIC processes involving temperature-induced transition [Brown, Holt, Lee and Rho 2006; Brown, Gelman and Rho 2006]. In both cases, what figures are the collective modes in macroscopic variables, *not* in explicit QCD variables. Why not? After all, we are doing many-body problem as in condensed matter physics.

From the practical standpoint, we would like to know whether the presence of such a boundary phase between exterior neutron matter and interior CFL matter in compact stars can influence observable properties of compact stars!

10.3 QCD at High Density: Color Superconductivity (CSC)

At super-high density, QCD could make a reliable prediction of what the strongly interacting matter could be like. There is a compelling argument why at asymptotic density Cooper pairing of the quarks should take place and color superconductivity (CSC) should set in, making the CSC state the ground state. At an extremely high density, asymptotic freedom will operate, which means that one-gluon exchange will be dominant and the attraction in the color ani-triplet channel in diquarks will trigger the Cooper pairing. There is robust argument for the prediction that if quark masses are ignorable or if the chemical potential $\mu > m_s/\Delta$ where m_s is the strange quark mass (ignoring the up and down quark mass) and Δ is the gap, the

[5] Casalbuoni and Gatto pointed out in [Casalbuoni and Gatto 1999] that the chiral Lagrangian of [Hong, Rho and Zahed 1999] has the "enlarged" symmetry $G \times SU(3)$, not G. However this does not involve extraneous symmetry since what is being done in [Hong, Rho and Zahed 1999] is using the equivalent linear representation $G \times H_{local}$ with the gluon field appearing as the local gauge field, essentially what we are doing here.

color and flavor will be locked, breaking both the color and chiral symmetry, giving rise to the "color-flavor locked (CFL)" phase that we referred to above [Rajagopal and Wilczek 2001; Alford 2006a].

Whether or not compact star matter can actually access that asymptotic regime of density is highly problematic. For non-asymptotic density at which QCD non-perturbative effects cannot be ignored, various effective theories, principally NJL type, predict that there will be CSC of some sort. However, if the density does not overpower all other scales involved, namely the s-quark mass *etc.*, then the situation is quite complex, the details depending upon parameters and the description becoming highly model-dependent. There is a landscape of overflowing phases which are, to be sure, extremely interesting theoretically but are difficult to pin down, and it is not clear how relevant they are to Nature, even for compact stars, not to mention laboratory experiments. We will nonetheless touch on a few aspects of CSC to make our discussion complementary, although there is nothing concrete one can say as to how the variety of scenarios mesh with the structure of compact stars.

10.3.1 *Color-flavor locking (CFL)*

Perturbative QCD is applicable at asymptotic density much beyond the range of density relevant to nature, *i.e.* stable compact stars. Since the theory is well-defined at that density, let us see what we can learn by starting at an asymptotic density and going down in density making corrections in $1/\mu$ where μ is the chemical potential.

That the ground state at high density is color-superconducting is easy to understand [Alford 2006a]. In QCD, the interaction between quarks at high density becomes weak owing to the asymptotic freedom. At low temperature, the weakly interacting quarks will form Fermi surfaces. We know at low density that some channels of interactions are attractive since a dilute system is made up of nucleons that are bound states of the quarks. Now the Fermi surface is defined by the minimum of the free energy with the Fermi energy $E_F = \mu$, with μ the chemical potential. It costs no free energy to add a pair of particles or holes and if there are attractive interactions between them, then the free energy of the system will be lowered, so many pairs will be formed near the Fermi surface. Since the pairs are bosonic excitations, they will Bose-condense, making the ground state a superposition of different numbers of pairs breaking spontaneously the fermion number symmetry. The pair of quarks cannot combine to a singlet in color and the condensate which is the vacuum expectation value of a pair of quarks must therefore break color. Thus there will be color superconductivity.

If the density is very high such that μ is much greater than the current quark mass of the strange quark, so the quarks of different flavors have roughly the same Fermi momenta, then pairing will occur symmetrically in three flavors, up, down and strange. This is because first of all the QCD interaction is most attractive in the color channel that is antisymmetric, namely $\bar{\mathbf{3}}$, and next, pairing is most

favored in the channel that preserves rotational symmetry, that is, spin singlet (antisymmetric). Thus Pauli principle requires that the pair be flavor-singlet. This gives rise to the color flavor locking which can be summarized by the formula

$$\langle \psi_i^\alpha C\gamma_5 \psi_j^\beta \rangle \propto \epsilon^{\alpha\beta A}\epsilon_{ijA} \tag{10.20}$$

and the symmetry breaking in the pattern of

$$SU(3)_c \times SU(3)_L \times SU(3)_R \times U(1)_B \to SU(3)_{c+L+R} \times \mathbb{Z}_2 \tag{10.21}$$

where color indices α, β and flavor indices i, j run from 1 to 3 and C is the charge conjugation matrix. The symmetry $U(1)_A$ is assumed to stay broken by the axial anomaly. The baryon number symmetry ($U(1)_B$) is broken down to a $\mathbb{Z}_2$ symmetry under which all quark fields are multiplied by -1.

What follows from this CFL can be simply summarized [Alford 2006a]: (a) The color $SU(3)_c$ is completely broken spontaneously so since it is a local gauge symmetry, the octet of gluons become massive by Higgs mechanism. They map to the vector mesons present in the low-density space; (b) the nine quark modes arising from three colors times three flavors get gapped and fall into $\mathbf{8} \oplus \mathbf{1}$ with two gap parameters. The octet quasiquarks map to the baryons in the low-density space. The singlet quasiquark has a bigger gap, so is higher lying; (c) the flavor symmetry breaking in (10.21) gives rise to eight Goldstone bosons mapping to those in the low-density regime; (d) there remains an unbroken $U(1)$ symmetry corresponding to a "rotated electromagnetism" consisting of the original photon and one of the gluons (much like in the electroweak sector).

10.3.2 *Chiral Lagrangian for CFL*

The pattern of symmetry breaking described above is analogous to that of chiral symmetry at zero μ and zero T. In fact, if one is looking at the energy scale which is small compared with the pairing gap Δ, then all that enters are the pseudo-Goldstone bosons. The symmetry breaking (10.21) then indicates that one can describe low-energy excitations in terms of a chiral Lagrangian with the octet "pion" fields U, making a model-independent treatment feasible. This is an interesting theoretical issue regardless of whether it is realized in nature or not.

One can readily write down the effective Lagrangian in a derivative and mass expansion [Hong, Rho and Zahed 1999; Casalbuoni and Gatto 1999; Schäfer 2006b]

$$\begin{aligned}\mathcal{L} = {} & \frac{f_\pi^2}{4}\mathrm{Tr}[\nabla_0 U \nabla_0 U^\dagger - v_\pi^2 \partial_i U \partial^i U^\dagger] \\ & + [c_1(\mathrm{Tr}MU^\dagger)^2 + c_2\mathrm{Tr}(MU^\dagger)^2 + c_3\mathrm{Tr}(MU^\dagger)\mathrm{Tr}(M^\dagger U) + \mathrm{h.c.}) + \cdots\end{aligned} \tag{10.22}$$

where

$$\nabla_0 U = \partial_0 U + i\mu_L U - iU\mu_R \tag{10.23}$$

with

$$\mu_L = MM^\dagger/2k_F, \quad \mu_R = M^\dagger M/2k_f \tag{10.24}$$

where M is the quark mass matrix, and the ellipsis stands for higher derivative and higher mass terms. A standard trick is to elevate the chemical potential term $\mu_{L,R}$ to the time component of a gauge-field degree of freedom, *i.e.* $A_\mu = (\mu, \mathbf{0})$ and write the Lagrangian as a sum of a gauge invariant term and non-derivative terms involving the mass term. This Lagrangian is quadratic in the mass matrix M because of the Z_2 invariance left over. Terms linear in M can come from the instantons but they are found to be small, so are usually ignored.

As in the effective field theory in the vacuum, the parameters that appear in the Lagrangian (10.22) need to be extracted from either experiments or matching to the fundamental theory, QCD. The latter can be done at asymptotic density since theory is very well defined there. As for the density regime relevant to nature, as we describe below, it is not yet clear (1) whether CFL enters into the description and (2) even if it does, there is no experimental information that would allow the extraction of the parameters.

• **Matching to QCD**

Let us first discuss matching to QCD at an asymptotic density. At high density where the chemical potential μ is much greater than any relevant scale in the system, say, $\mu \gg \Lambda_{QCD}$, the only relevant low-energy degrees of freedom are (quark) particles and (quark) holes in the vicinity of the Fermi surface. We write the quark field characterized as

$$\psi_v = \psi_{v,+} + \psi_{v,-} \tag{10.25}$$

where $\psi_\pm = P_\pm \psi$ with $P_\pm = \frac{1}{2}(1 \pm \alpha \cdot \hat{v})$, the projection operator for the postive/negative energy state. For large μ, the negative energy state can be eliminated. The subscript v stands for the Fermi velocity which represents the patch on the Fermi surface. For large chemical potential, the QCD Lagrangian in the presence of the Fermi sea can then be expanded in $1/\mu$ and to leading order, after the field $\psi_{v,-}$ is eliminated by equation of motion, takes the form[6] [Hong 2000a; Hong 2000b]

$$\mathcal{L} = \psi^\dagger_{v,+}\left(iv\cdot D - \frac{D_\perp^2}{2\mu} - \frac{g\sigma_{\mu\nu}G_\perp^{\mu\nu}}{4\mu} + \cdots\right)\psi_{v,+} - \frac{1}{2}\mathrm{Tr}G_{\mu\nu}G^{\mu\nu} + \cdots . \tag{10.26}$$

This should be implemented with the mass term which can be computed in perturbation theory with the Lagrangian (10.26),

$$\delta\mathcal{L} = -\frac{1}{2k_F}\left(\psi^\dagger_{vL}MM^\dagger\psi_{vL} + \psi^\dagger_{vR}M^\dagger M\psi_{vR}\right). \tag{10.27}$$

[6] In the color-flavor locked case, we do not need to distinguish the color trace 'tr' and the flavor trace 'Tr', and the color gauge coupling g_c and the flaor gauge coupling g..

For ease of notation, we omit the subscript +, understanding that the negative energy quarks have been integrated out.

The Lagrangian (10.26) with (10.27) allows one to do a systematic perturbation calculation in power of $1/\mu$. This is fairly well formulated in the literature and we refer to recent lectures [Schäfer 2006b]. The parameters of (10.22) calculated therewith are [Son and Stephanov 2000; Schäfer 2006b]

$$f_\pi^2 = \frac{21 - 8\ln 2}{18}\left(\frac{k_F^2}{2\pi^2}\right), \quad v_\pi^2 = 1/3 \tag{10.28}$$

and

$$c_1 = -c_2 = \frac{3\Delta^2}{4\pi^2}, \quad c_3 = 0. \tag{10.29}$$

Given these parameters, one can calculate the pseudo-Goldstone mass formulas. From (10.22), one finds

$$m_{\pi^\pm}^2 = \frac{2c}{f_\pi^2} m_s(m_\mu + m_d), \quad m_{K^\pm}^2 = \frac{2c}{f_\pi^2} m_d(m_\mu + m_s) \tag{10.30}$$

(where c is an overall constant) which shows that the kaon is lighter than the pion, contrary to what happens in the low-density regime.

These results are all very nice and neat, but they are most likely useless in practice since the perturbative reasoning holds only at asymptotic density and cannot be used for confronting nature as they are at present. It should be understood, however, that with the parameters taken free, the Lagrangian (10.22) could remain valid at much lower – and relevant – density as we shall discuss below.

10.3.3 *"Un-hidden" local symmetry*

So far we discussed the lowest modes in the CFL phase, *i.e.* pions and kaons. Let us see how we can go up to the next energy scale which will be populated by vector mesons. To do this, we look at the symmetry breaking pattern. Ignoring the $U(1)_B$ symmetry associated with the baryon number (the $U(1)_A$ symmetry is broken by the anomaly), the unbroken global symmetry involved is $G = SU(3)_c \times SU(3)_L \times SU(3)_R$. Now according to (10.20), the color locks to L as well as to R as

$$SU(3)_c \times SU(3)_L \to SU(3)_{c+L}, \tag{10.31}$$

$$SU(3)_c \times SU(3)_R \to SU(3)_{c+R}. \tag{10.32}$$

Since the color is vectorial, this means that the L and R are broken down to the diagonal $V = L + R$ as well, so effectively the symmetry breaking is

$$G \to H \tag{10.33}$$

where

$$G = SU(3)_c \times SU(3)_L \times SU(3)_R, \tag{10.34}$$

$$H = SU(3)_P \tag{10.35}$$

with $P = c + V$. Since the chiral symmetry is broken, we have an octet of pseudoscalar Goldstone bosons denoted $\hat{\pi} = \lambda^a \hat{\pi}^a/2$ with λ being the Gell-Mann matrices. Since the global color symmetry is completely broken, there are an octet of scalar Goldstone bosons denoted $\hat{\sigma} = \lambda^a \hat{\sigma}^a/2$. We can express the coordinates $\xi \in G/H$ as before:

$$\xi^\alpha_{L(R)i} = \epsilon_{\alpha\beta\gamma}\epsilon^{ijk}\langle \psi^\beta_{L(R)j}\psi^\gamma_{L(R)k}\rangle \tag{10.36}$$

(where we have dropped spinor indices for economy in notation) in terms of the two sets of Goldstone fields. A convenient parametrization is

$$\xi_L(x) = e^{-i\hat{\pi}(x)/F_{\hat{\pi}}}e^{i\hat{\sigma}(x)/F_{\hat{\sigma}}}, \quad \xi_R(x) = e^{i\hat{\pi}(x)/F_{\hat{\pi}}}e^{i\hat{\sigma}(x)/F_{\hat{\sigma}}}. \tag{10.37}$$

Let $h \in SU(3)_c$ and $g_L(g_R) \in SU(3)_{L(R)}$ be the generators of the respective transformations. Then the ξ field transforms as

$$\xi_{L(R)} \to h\xi_{L(R)}g^\dagger_L(g^\dagger_R). \tag{10.38}$$

We still have the local gauge invariance associated with the gluons $G_\mu = \lambda^a G^a_\mu/2$ – which will eventually be spontaneously broken, so the degrees of freedom that we have are $\hat{\pi}$, $\hat{\sigma}$ and G_μ. To construct gauge-invariant theory with these fields, define the covariant derivative

$$D_\mu \xi_{L,R}(x) = (\partial_\mu - iG_\mu)\xi_{L,R}(x) \tag{10.39}$$

and write

$$\begin{aligned}\hat{\alpha}_{V\mu}(x) &\equiv (D_\mu\xi_L \cdot \xi^\dagger_L + D_\mu\xi_R \cdot \xi^\dagger_R)(-i/2),\\ \hat{\alpha}_{A\mu}(x) &\equiv (D_\mu\xi_L \cdot \xi^\dagger_L - D_\mu\xi_R \cdot \xi^\dagger_R)(-i/2).\end{aligned} \tag{10.40}$$

The leading-order Lagrangian with the lowest power of derivatives is

$$\mathcal{L}_{p^2} = F^2_{\hat{\pi}}\mathrm{Tr}(\hat{\alpha}_{A\mu})^2 + aF^2_{\hat{\pi}}\mathrm{Tr}(\hat{\alpha}_{V\mu})^2 \tag{10.41}$$

where a is a constant to be determined later. Adding the kinetic energy term for the gluons, we have

$$\mathcal{L}^{eff}_{CFL} = \mathcal{L}_{p^2} - \frac{1}{2g^2}\mathrm{Tr}(G_{\mu\nu})^2 + \cdots \tag{10.42}$$

with $G_{\mu\nu} = \partial_\mu G_\nu - \partial_\nu G_\mu - i[G_\mu, G_\nu]$. The ellipses stand for higher derivatives, quark mass terms and Wess-Zumino terms *etc.*

The fact that the color-flavor locking is operative is described by that $F_{\hat{\pi}} \neq 0$ and $a \neq 0$. Since the local gauge symmetry is spontaneously broken, the gluons

get higgsed and become massive. This can be seen in the unitary gauge which corresponds to setting $\hat{\sigma} = 0$ in (10.37). The mass formula is then

$$m_G^2 = aF_{\hat{\pi}}^2 g^2. \tag{10.43}$$

Note that this formula is a familiar one from low-energy chiral dynamics, *i.e.* "KSRF relation". We encountered this in $\mathrm{HLS}_{K=1}$ theory discussed in low-density (hadronic) regime.

The theory we have written down is to describe low-energy excitations solely based on symmetry. In medium, one has to take into account the fact that Lorentz invariance is broken, so the time and space components of various quantities have to be distinguished. This can be done readily. When distinguished, for instance, the mass formula (10.43) corresponds to the time component of the vector meson mass, *i.e.* Debye mass. The Debye mass, unknown at low density, can, however, be calculated at asymptotic density starting from (10.26). The result is given by $a = 1$ and $F_{\hat{\pi}}^2 = f_{\hat{\pi}}^2 = \frac{21-8\ln 2}{18}\left(\frac{k_F^2}{2\pi^2}\right)$. The space component of the vector mass, *i.e.* Meissner mass, can also be computed from (10.26) at asymptotic density: It is also given by (10.43) but with the space component of $F_{\hat{\pi}}^2$ which is $1/3$ of the time component. The ratio $F_{\hat{\pi}}^s/F_{\hat{\pi}}^t = 1/\sqrt{3}$ is the pion velocity.

The above relations are not expected to hold at lower density, that is, the parameters of the Lagrangian cannot be calculated in low orders of perturbation theory. This requires that the parameters be determined from experiments or on lattice.

A couple of comments are in order at this juncture.

First it should be mentioned that in the case at hand, as mentioned before, the vector degrees of freedom arise top-down "in reduction" from the QCD sector [Hong, Rho and Zahed 1999]. This is unlike in the hadronic sector where the top-down procedure starting from QCD *proper* is not available, though one can construct it from string theory via holography as in the Sakai-Sugimoto model, but then we cannot be sure that we are doing QCD.

Next, the way effective theories are "UV-completed" is different in the two sectors (hadronic and CFL sectors). In the hadronic sector, the low-energy effective theory is matched to OPE of QCD correlators whereas in the CFL phase, the matching is done in terms of weak-coupling QCD. While in the former, the "bare" Lagrangian is known from QCD information at realistic matching point, the one in the latter is unknown at the matching point unless one is considering a regime where asymptotic density is operative.

10.3.4 *Superqualitons as baryons*

We have mesonic excitations up to massive vector mesons. Now what about baryons in the spectrum? There are two ways of bringing in the baryons. One way is to simply introduce baryonic fields as effective fields as one does in the hadronic phase, leading to baryonic chiral Lagrangian. The other is to obtain them as solitons in

the Lagrangian (10.42). We shall fist describe the latter, going to the former later.

The argument that the Lagrangian (10.42) supports soliton as first suggested in [Hong, Rho and Zahed 1999; Hong, Hong and Park 2001] is the same as the one used for the skyrmion in the HLS theory described in Chapter 6. There are of course higher derivative terms and mass terms, but with (10.42) alone, the soliton can be stabilized by the kinetic energy term given that the vector meson mass is proportional to the chemical potential which is supposed to be much greater than the QCD scale and hence the kinetic energy gives rise to an effective quartic Skyrme term. Unlike in the hadronic sector, the Skyrme term does play an essential role for the superqualiton stabilization.

It has been established [Hong, Rho and Zahed 1999; Nowak, Rho, Wirzba and Zahed 2001] that there is also the familiar Wess-Zumino term that guarantees that the superqualiton is a fermion with spin 1/2. A rough calculation shows that the mass of the qualiton with the quantum number of the nucleon has a mass of order the gap Δ and that higher excitations are massive, so can be ignored. It remains to work out the detailed structure of baryon spectroscopy comparable to baryon chiral perturbation theory.

Instead of generating baryons via topology, one can introduce baryons as local fields and do chiral perturbation calculations as in the hadronic sector with baryon chiral perturbation theory. This way of doing things is particularly simple for studying baryon spectroscopy, including gapless fermionic modes. The connection between the soliton picture and chiral perturbation picture has not been established yet. As in the hadronic sector, the two pictures should be complementary, offering different aspects of the same object.

If one restricts to terms of $\mathcal{O}(M^2/(k_F\Delta))$, the baryon Lagrangian takes the form (see *e.g.* [Schäfer 2006b]),

$$\mathcal{L} = \mathrm{Tr}\left(B^\dagger i v^\mu D_\mu B\right) + \mathrm{Tr}\left(B^\dagger \gamma_5 \kappa_A B\right) + \frac{\Delta}{2}\{\mathrm{Tr}(B\gamma_5 B) - \mathrm{Tr}(B)\gamma_5 \mathrm{Tr}(B) + \mathrm{h.c.}\} \tag{10.44}$$

where

$$D_0 B = \partial_0 B + i[\kappa_V, B] \tag{10.45}$$

and

$$\kappa_{V,A} = \frac{1}{2}\left\{\xi \frac{M^\dagger M}{2k_F}\xi^\dagger \pm \xi^\dagger \frac{M M^\dagger}{2k_F}\xi\right\}. \tag{10.46}$$

In (10.44), the notation $BB = B^\alpha B^\beta C^{\alpha\beta}$ with C the charge conjugation matrix is used. To leading order in the strong coupling constant and in $1/k_F$, we have $D = F = 1/2$.

Ignoring terms of order m_u^2, m_d^2, the excitation energy of "proton" ($\hat{p}$) and "neutron" ($\hat{n}$) particles as well as $\hat{\Xi}^{-,0}$ holes is lowered by the strangeness effective

chemical potential $\mu_s = m_s^2/(2k_F)$ as $\omega = \Delta - \mu_s$ while the energy of $\hat{\Xi}^{-,0}$ particles and "proton" and "neutron" holes is raised by the same amount, $\omega = \Delta + \mu_s$. Corresponding baryon spectra have been studied in detail. Since we are not directly concerned with the baryon spectrum, we refer for details to the reference [Schäfer 2006b]. We just mention that when μ_s becomes as large as the gap Δ, the $(\hat{p}, \hat{n})$ and $(\hat{\Xi}^-, \hat{\Xi}_0)^{-1}$ excitations become gapless. A variety of other interesting phenomena can also occur. All these are theoretical speculations at present and lack either experimental or theoretical verifications.

10.3.5 *Kaon condensation in the CFL sector*

When μ_s reaches 2Δ, $\hat{K}^0$ mesons can condense. We briefly discuss this phenomenon and compare its structure to what happens with K^- condensation in the Nambu-Goldstone phase.

As noted, the larger strange-quark mass makes the kaons lighter than the pions with smaller current-quark mass. Because the expansion parameter is $m_s^2/(k_f\Delta)$, the greater the kaon mass the lower the critical density at which kaons can condense. This fact resembles the situation with kaon condensation in the Nambu-Goldstone mode obtained from the matter-free vacuum where the larger KN sigma term corresponding to larger symmetry breaking brings in more attraction when viewed bottom-up although the mechanism is quite different as one can see if one considers the hadronic kaon condensation from the vector manifestation fixed point.

To see the structure of kaon condensation in the case at hand, we look at the effective potential from (10.22)

$$V_{eff} = \frac{f_\pi^2}{4}\mathrm{Tr}[2\mu_L U \mu_R U^\dagger - \mu_L^2 - \mu_R^2] - c_1[(\mathrm{Tr}MU^\dagger)^2 - \mathrm{Tr}(MU^\dagger)^2] + \cdots . \quad (10.47)$$

The parameters of the Lagrangian are chosen in such a way that they are valid in the limit of large chemical potential as shown in (10.29). This potential favors neutral kaons, so one looks for the minimum of the potential with the ansatz

$$U = e^{i\alpha\lambda_4} \quad (10.48)$$

which gives the potential

$$V(\alpha) == f_{\hat{\pi}}^2 \left(\frac{1}{2} \left(\frac{m_s^2 - m^2}{2k_f} \right)^2 (\sin\alpha)^2 + {m_K^0}^2 (\cos\alpha - 1) \right) \quad (10.49)$$

with ${m_{\hat{K}}^0}^2 = (4c_1/f_{\hat{\pi}}^2)m(m + m_s)$. In the high density limit, $c_1 \approx \frac{3\Delta^2}{4\pi^2}$. Minimizing this potential with respect to α, one finds that $\hat{K}^0$ will condense, *i.e.* $\alpha \neq 0$, when $\mu_s > m_{\hat{K}}^0$,

$$\alpha = \cos^{-1}({m_{\hat{K}}^0}^2/\mu_S^2). \quad (10.50)$$

We can estimate from this the "critical" s-quark mass by setting the argument of $\cos^{-1}$ on the RHS equal to 1 the "critical" strange quark mass, given a value for the gap Δ. For $\Delta \sim 50$ MeV, one finds

$$m_s^c \sim 70 \text{ MeV}. \tag{10.51}$$

This rough estimate suggests that kaons could be condensed in compact stars if the latter were in a CSC phase.

It is interesting that kaons condense in both the Nambu-Goldstone phase and the CFL phase because the s-quark mass is in some sense "heavy." However the condensation phenomenon described here is different from the K^- condensation in the Nambu-Goldstone phase in that the latter is driven by the electron chemical potential while the former is not.

10.4 CSC at Non-Asymptotic Density

The CFL phase inevitable at superhigh density much greater than the quark masses and their differences will be stable for the strange quark mass that satisfies

$$M_s^2/\mu < 2\Delta_{CFL} \tag{10.52}$$

where Δ_{CFL} is the CFL pairing strength and M_s is the "effective" strange-quark mass $\approx m_s$. To have a rough idea of what we are talking about here, if one assumes the s-quark mass to be zero, then at $\mu \sim 500$ MeV, Δ_{CFL} comes out to be ~ 100 MeV. This is more or less an upper limit. In reality dealing with nature, in particular with compact stars, the chemical potential is not asymptotically high, possibly only a few times that of nuclear matter, and the paring strength cannot be so high. Furthermore the system of a compact star must be in electromagnetic and color neutrality, and is in equilibrium under the weak interaction. These conditions can cause the different colors and flavors to have different chemical potentials, and bring a "stress" on the CFL process. When the stress is too big, then the CFL state becomes unstable and gets replaced by other forms of pairing. This then generates a plethora of different phases depending upon the various intervening factors. The delineation of these phases becomes quite complicated. Perturbative QCD cannot handle these phases and at present, only model calculations can be performed [Buballa 2005]. Therefore lacking guidance from experiments, the situation is murky in theory. It is premature to think of what might happen in dense matter to be produced in the laboratories and presumed to be present in compact stars. Therefore we shall be brief on this matter, focusing mainly on what is understood better.

10.4.1 *Induced CFL*

An interesting possibility that a CFL phase might bypass the "stress" at a density low enough to be relevant to compact-star matter arises when the strength of the $U(1)_A$ anomaly is high. This could constitute a basis for the "hadron-quark" continuity advocated in this volume and possibly allow a model-independent treatment of CSC at non-asymptotic density. This may happen in a conspiracy between the quark-antiquark condensate $\langle\bar{q}q\rangle$ in the Nambu-Goldstone mode and the diquark condensate $\langle qq\rangle$ [Hatsuda, Tachibana, Yamamoto and Baym 2006]. The question addressed, namely, how a state characterized by $\sigma \sim \langle\bar{q}q\rangle$ changes over to the one characterized by $\mathcal{D} \sim \langle qq\rangle$ as density increases, has been addressed extensively in NJL model dealing with the normal component of the chiral Lagrangian [Buballa 2005]. But this is highly model-dependent and cannot be trusted. This matter can be studied model-independently, however, in terms of Ginzburg-Landau approach taking account of the axial anomaly of QCD [Hatsuda, Tachibana, Yamamoto and Baym 2006; Yamamoto, Hatsuda, Tachibana and Baym 2007].

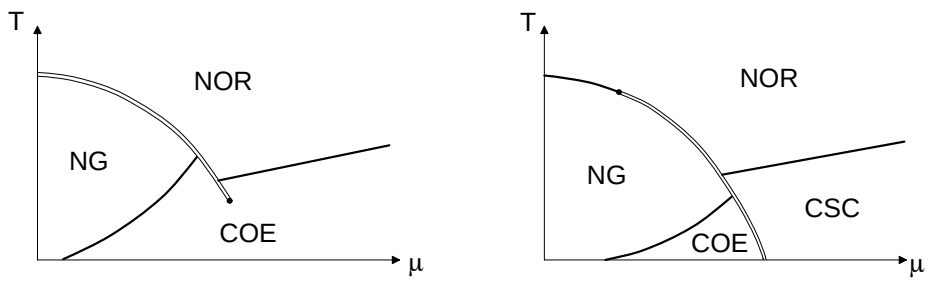

Fig. 10.3 Schematic phase structure in the T-μ plane for the case 1 (massless three-flavor; left) and for the case 2 (massless two-flavor; right) from [Yamamoto, Hatsuda, Tachibana and Baym 2007] (copyright 2007 IOP Publishing Ltd). The double (single) line indicates first-order (second-order) transition.

The symmetry involved for the two phases is $G = SU(3)_L \times SU(3)_R \times U(1)_B \times U(1)_A \times SU(3)_c$. Due to the axial anomaly, $U(1)_A$ is broken down to Z_6 which is responsible for the mass of η'. Define the condensates

$$\Sigma_{ij} = -\langle\bar{q}^i_R q^j_L\rangle, \tag{10.53}$$

$$\epsilon_{abc}\epsilon_{ijk} d^\dagger_{Lai} = \langle q^j_{Lb} C q^k_{Lc}\rangle \tag{10.54}$$

where i, j, k are the flavor indices and a, b, c the color indices, and $C = i\gamma^2\gamma^0$ is the charge conjugation operator. The Ginzburg-Landau approach is to write the free energy $\Omega(\Sigma, d)$ invariant under G except for the broken $U(1)_A$ in powers of the condensates. There are two cases to consider: (1) the 3-flavor chiral limit and (2) the chiral limit for 2 flavors (u and d) and the infinite s-quark mass. There is a third case where the s-quark mass is not too heavy to be ignored in the second case.

This case is a bit too complicated and we will skip it here. In the first case, we take the ansätze $\Sigma = \mathrm{diag}(\sigma, \sigma, \sigma)$ and $d_L = -d_R = \mathrm{diag}(d, d, d)$ and in the second, $\Sigma = \mathrm{diag}(\sigma, \sigma, 0)$ and $d_L = -d_R = \mathrm{diag}(0, 0, d)$. The free energy takes the following forms

$$\Omega_{case1} = \frac{a}{2}\sigma^2 - \frac{c}{3}\sigma^3 + \frac{b}{4}\sigma^4 + \frac{\alpha}{2}d^2 + \frac{\beta}{4}d^4 - \gamma d^2\sigma + \lambda d^2\sigma^2, \tag{10.55}$$

$$\Omega_{case2} = \frac{a}{2}\sigma^2 + \frac{b}{4}\sigma^4 + \frac{f}{6}\sigma^6 + \frac{\alpha}{2}d^2 + \frac{\beta}{4}d^4 + \lambda d^2\sigma^2 \tag{10.56}$$

where the subscript indicates the cases involved. The axial anomaly enters into the c and γ terms in the 3-flavor case (10.55) which are absent in the 2-flavor case (10.56).

The details of the phase structure depend on the parameters, most of which are known precisely neither from theory nor from experiments. The axial anomaly plays a role of an external field for the σ condensate in the presence of the diquark condensate d. The coefficients c and γ are related microscopically via the axial anomaly in QCD. In principle there can be four possible phases: normal (denoted NOR) phase for which $\sigma = d = 0$, color superconducting phase (denoted CSC) with $\sigma = 0$ and $d \neq 0$, Nambu-Goldstone phase (NG) with $\sigma \neq 0$ and $d = 0$ and coexisting phase (COE) with $\sigma \neq 0$ and $d \neq 0$. The phase structure is schematically shown in Fig. 10.3. What we focus on for our discussion is the low-temperature and high-μ regime in the neighborhood of the COE and CSC phases. In the absence of the anomaly term in the case (2), the two phases are separated by first-order phase transition while in the case (1), the COE phase permeates going continuously between the two phases, with the NG pion mixed with the CFL pion satisfying a generalized Gell-Mann-Oakes-Renner formula [Hatsuda, Tachibana, Yamamoto and Baym 2006]. How the continuity region opens and closes as a function of the s-quark mass is indicated in Fig. 10.4. The role of the s-quark mass is quite clear. The "gate of continuity" widens the closer the s-quark mass is to that of the chiral quark and is closed completely when the s-quark decouples as its mass increases. As we encountered in Chapter 9, in reality, the s-quark mass has a subtle ambidextrous role. It is neither too heavy nor too light. Hyperons can be better described in the skyrmion picture if the s-quark is considered as "heavy." On the other hand, the s-quark can be considered as "light" and allows chiral perturbation theory in terms of expansion in the s-quark mass to work. In the description of the kaon (K^-) condensation described top-down fluctuating from the VM fixed point [Brown, Lee, Park and Rho 2006], it was shown that kaons condense because the kaon is neither too heavy nor too light: In the two limits, there will be no condensation taking place. It is not clear as to what the role of the s-quark mass might be in the present circumstance.

What is the true nature of the phase structure in compact stars could be determined when the parameters of the Ginzburg-Landau free energy are determined from QCD.

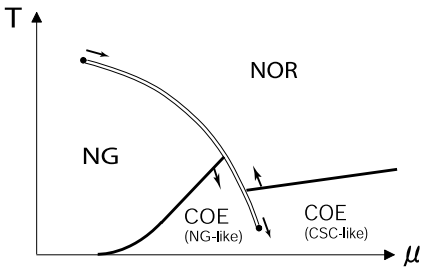

Fig. 10.4 Schematic phase structure with two light quarks (up and down) and a medium heavy quark (strange) from [Yamamoto, Hatsuda, Tachibana and Baym 2007]. The arrows show how the critical points and the phase boundaries move as the strange-quark mass increases toward the two-flavor limit.

10.4.2 *Landscape of non-CFL phases*

As noted, the strange-quark mass plays an important role on the fate of the CFL phase and the quark-hadron continuity. Model calculations (typically of NJL type) show qualitatively that if the gap is large, say, $\Delta \sim 100$ MeV – the value expected at $\mu \sim (1/2)$ GeV with $M_s = 0$ – then the CFL can be continuously connected to nuclear matter. However, if $M_s^2/(4\mu)$ (where M_s is the effective mass of the strange quark or more properly "quasiquark" mass) is of the order of the gap Δ in two-flavor CSC (2SC) or in the CFL phase, say, tens of MeV, the CFL phase can no longer be stable and cedes to gapless CFL (denoted gCFL) or to non-CFL forms of CSC, gapped or gapless. The gapless phases are also found to be unstable. The instability is manifested in that the Meissner mass M_M^2 becomes imaginary, namely, $M_M^2 < 0$. The instability of gapless modes can be due to spontaneous symmetry breaking of translational invariance. Such an instability implies that there could be other phases which are lower-lying. The nature of such phases cannot be fully unraveled without guidance from QCD proper.

What appears to be the most probable phase at non-asymptotic density that escapes from instability of various types such as magnetic instability is the position-dependent pairing known as the "LOFF" phase which can arise when different flavors pair with non-zero momentum so as to accommodate the tendency for the Fermi momenta to separate [Alford, Schmitt, Rajagopal and Schäfer 2007]. For instance, a single-plane-wave LOFF ansatz yields a state that has lower free energy than gCFL in the region where the gCFL makes transition to unpaired state with no Meissner instability. What could be the most favorable crystal structures is not yet clearly settled and is a hot topical issue at the time of this writing [Alford 2006b; Alford, Schmitt, Rajagopal and Schäfer 2007] and we will let the time settle the issue. In the next section, we will briefly discuss how the gravitational wave from LIGO may provide information on the existence of the crystalline structure in a rotating neutron star.

This page intentionally left blank

Chapter 11

Compact Stars

11.1 Objective

There will be, in the coming years, a number of experimental efforts to create cool dense matter in such laboratories as GSI and JPARC which could eventually provide crucial guidance for checking the theoretical ideas presented in the preceding chapter. But at present there are no solid experimental results to rely on. Given that the theoretical tools exploited for the plethora of phenomena proposed thus far are highly mode-dependent, we cannot use them with confidence to understand the variety of astrophysical phenomena. Besides, even if such an attempt were meaningful, a comprehensive and in-depth treatment of them all would require another volume. We shall therefore simply eschew making the attempt to do so in this chapter. Instead, we will limit ourselves to what we can do with some confidence that can be readily confirmed or refuted unambiguously..

Of all the possible processes in dense medium we have looked at, there is one process which we can treat with some confidence within the framework developed in this volume, namely, the effective field theory approach anchored on hidden local gauge symmetry, and that is the phase transition involving kaon condensation. As we have argued, the first serious phase change that can occur in dense hadronic matter as density increases beyond nuclear matter density is kaon condensation at a density $\sim 3n_0$. This has been arrived at from various vantage points, most reliable of which being from the vector manifestation fixed point of HLS theory. We have argued that the various objections that have been raised against the dominant role of kaon condensation, such as, *e.g.*, many-body repulsion, hyperons, $\Lambda(1405)$ *etc.* are ineffective in the vicinity of the vector manifestation fixed point around which kaons condense and that once kaons condense, stars more massive than a certain maximum mass cannot be stable against gravitational collapse, which would render the rich – and interesting – variety of quark phases mentioned in Chapter 10 *inaccessible* to astrophysical observations, hence most likely irrelevant. What we shall do in this chapter is simply to examine what the consequences of kaon condensation are on compact-star observables. There is one great advantage in taking this drastically

simplified approach and that is that it is readily falsifiable. We will specify how this test can be achieved.

In what follows, we will closely follow the development recently summarized in [Brown, Lee and Rho 2008].

11.2 Star Observables

The commonly exploited neutron star property which can provide clues on the hadronic equation of states in dense medium is the masses of the neutron stars.[1] It is now fairly well accepted that the maximum mass is set by the dense matter equation of state at density $\gtrsim 2n_0$ (where $n_0 \sim 0.16\text{fm}^{-3}$). The radius of neutron star can also provide valuable information. However, it is determined by the variation of the symmetry energy of the matter as a function of density in the range of 1-2 n_0, so the size of the neutron star is strongly dependent on the outer low-density crust, and hence the radius is rather insensitive to the properties of the dense inner core. In addition, the determination of the neutron star radius from the observation is extremely difficult and strongly model-dependent.

It is now well understood that most of the information from neutron stars comes from the surface region where the density is relatively low compared to the normal nuclear matter density. Whatever information there can be on extreme dense matter inside neutron stars therefore faces difficulty in penetrating through the outer-layer density crust. The possible exception is the information carried by the neutrinos because they can easily escape the outer low density crust. Recent research indicates that the neutrino signals can provide critical information on inner dense medium.

In what follows, we will first review the specific theoretical tool – out of the variety given in the volume – that will be used to obtain the neutron star equation of states. Later we will discuss the current status of the observations which are related to the properties of neutron stars, with a focus on the mass and radius.[2]

11.3 Chiral Dynamics in the Core of Compact Stars

The basic assumption we make in the discussion that follows is that as baryon density increases beyond the nuclear matter density, the first crucial phase transition that determines the fate of stars is kaon condensation at $\sim 3n_0$. We study what the phase change does to the compact stars, neutron stars vs. black holes.

[1] "Neutron star" is a misnomer for the compact stars we will consider in this chapter. "Nuclear star" would be more appropriate. But following the practice in astrophysics, we will use the nomenclature "neutron star" for stable compact stars.

[2] The writing of this chapter was aided invaluably by Chang-Hwan Lee.

11.3.1 *TOV equation*

To obtain the mass and radius of a neutron star, one has to solve the general relativistic hydrodynamic equation. Most commonly used equation is the Tolman-Oppenheimer-Volkov (TOV) equation in which mean field approximation is made. With given pressure and energy density in the mean field approximation, the structure of a spherically symmetric neutron star can be determined by solving the TOV equations [Shapiro and Teukolsky 1983]

$$\begin{aligned}\frac{dM(r)}{dr} &= 4\pi r^2 \frac{\epsilon(r)}{c^2}\,,\\ \frac{dP(r)}{dr} &= -\frac{GM(r)\epsilon(r)}{c^2 r^2}\left[1+\frac{P(r)}{\epsilon(r)}\right]\left[1+\frac{4\pi r^3 P(r)}{c^2 M(r)}\right]\left[1-\frac{R_s(r)}{r}\right]^{-1}\end{aligned} \tag{11.1}$$

where $M(r)$ is the enclosed gravitational mass, $\epsilon(r)$ is the energy density inclusive of the rest mass density, $P(r)$ is the pressure, and $R_s(r) = 2GM(r)/c^2$ is the Schwarzschild radius with a given mass $M(r)$. The hydrostatic equilibrium is assumed in the above equations.

Various equations of state, $P(n)$ and $\epsilon(n)$ with baryon number density $n(r)$, have been suggested. Once the central density $n(r = 0)$ is given, by solving Eq. (11.1) numerically, one can obtain the mass and size of neutron stars. By varying $n(r = 0)$, the maximum mass of neutron stars can be obtained. It is generally accepted that what truly matters is how soft or stiff the EOS is, independently of what mechanism is at work. A stiff equation of state gives higher maximum mass, and a soft equation of state, such as kaon condensation that we are considering, gives lower maximum mass. Empirical constraints on the equation of state are available only in low-density ($n \lesssim n_0$) region, so the extrapolation beyond is required. The claim made in this volume is that an effective field theory makes a prediction that is reliable for kaon condensation at the lowest density as density increases, rendering other phase transitions so far predicted for higher densities unlikely to be relevant for the physics of compact stars. Our first effort, therefore, is to see what we can learn from it in light of the proposal that *baryon number density plays the pivotal role in determining the fate of massive stars*. Ultimately, the observations should tell us whether the scenario we develop is correct or not.

11.3.2 *Neutron stars with kaon condensation "light"*

Here we will set up a schematic model specifically suitable for compact star matter that encodes the characteristic features of kaon condensation treated more generally in Chapter 9. Though highly simplified, it brings out the essential idea of how things work out in exhibiting the important consequences of the medium modification of kaon properties on the structure and evolution of compact objects in astrophysics, especially the maximum mass of neutron stars. There have been many studies on this subject. For our purpose, the most suitable approach is to use the schematic

description of Li *et al.* [Li, Lee and Brown 1997] on cold, neutrino-free neutron stars that are in chemical equilibrium under β decay processes. Two scenarios are considered: one without and the other with kaon condensation. In the first case, we need to find the ground state for a system of nucleons, electrons and muons in chemical equilibrium, while in the second scenario, we construct the ground state of a system of nucleons, electrons, muons and kaons in chemical equilibrium. The ground state energy density and pressure are then used in the TOV equation to calculate neutron star properties. The results obtained in this schematic model are supported by the more sophisticated and realistic calculation of [Thorsson, Prakash and Lattimer 1994] for the range of parameters prescribed by the theory described in Chapter 9.

In the absence of kaons, the chemical equilibrium conditions require that the chemical potentials satisfy

$$\mu = \mu_n - \mu_p = \mu_e = \mu_\mu, \tag{11.2}$$

and in the presence of kaons,

$$\mu = \mu_n - \mu_p = \mu_e = \mu_\mu = \mu_K. \tag{11.3}$$

In both cases μ is the overall charge chemical potential. The local charge neutrality can be imposed by minimizing the thermodynamical potential [3]

$$\Omega = \varepsilon_N + \varepsilon_K + \varepsilon_L - \mu(\rho_p - \rho_K - \rho_e - \rho_\mu). \tag{11.4}$$

A large variety of different energy densities of nucleons (ε_N) exist in the literature. The result of Li *et al.* [Li, Lee and Brown 1997] on which the argument developed below relies exploits ε_N of Furnstahl *et al.* [Furnstahl, Tang and Serot 1995], so we will show the results based on it. It is consistent with our scheme since the energy density of [Furnstahl, Tang and Serot 1995] is essentially the same as the BR-scaling formulation of [Song, Brown, Min and Rho 1997] described in Chapter 8.

The energy density of leptons is

$$\varepsilon_L = \varepsilon_e + \eta(\mu - m_\mu)\varepsilon_\mu \ , \tag{11.5}$$

where η is the Heaviside function ($\eta(x) = 1$ if $x > 0$ and $\eta(x) = 0$ if $x < 0$). The electron and muon energy densities are, respectively,

$$\varepsilon_e = \frac{\mu^4}{4\pi^2}, \tag{11.6}$$

and

$$\varepsilon_\mu = \frac{m_\mu^4}{8\pi^2}\left[t(1+2t^2)\sqrt{1+t^2} - \ln(t+\sqrt{1+t^2})\right], \tag{11.7}$$

[3] Here and in what follows, we denote the number density by ρ instead of n. There will be no confusion with the vector meson ρ since the meson does not figure here explicitly.

where $t = K_{F_\mu}/m_\mu$ with $K_{F_\mu}^2 = \mu^2 - m_\mu^2$. The energy density of kaons in the chiral perturbation theory is

$$\varepsilon_K = -f_\pi^2 \frac{\mu^2}{2} \sin^2\theta + 2m_K^2 f_\pi^2 \sin^2\frac{\theta}{2} + \mu x\rho$$
$$-\mu(1+x)\rho \sin^2\frac{\theta}{2} - 2f_\pi^2 a_{\bar{K}} \rho \sin^2\frac{\theta}{2}, \tag{11.8}$$

where f_π is the (physical) pion decay constant, $x = \rho_p/\rho$ is the proton fraction, and the "chiral angle" θ is defined in terms of the kaon amplitude $v_K = \langle K \rangle$,

$$\theta = \frac{\sqrt{2} v_K}{f_\pi}. \tag{11.9}$$

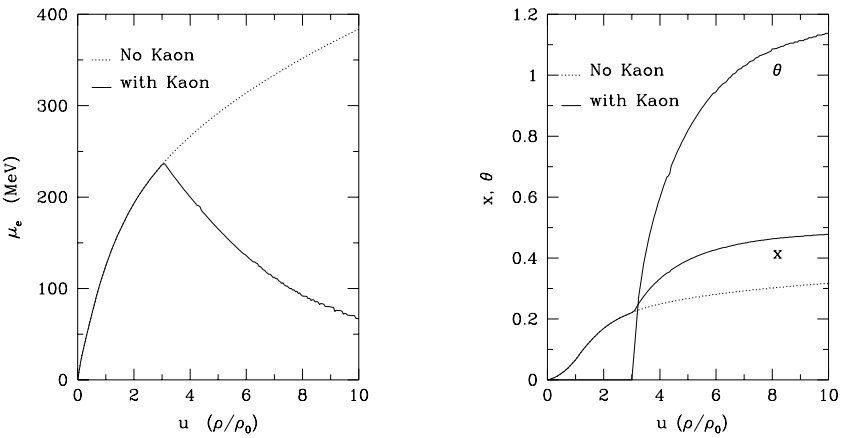

Fig. 11.1 Electron chemical potential (left panel) and proton fraction and chiral angle (right panel) as a function of nucleon density.

The energy density ε of the ground state of the system is obtained by extremizing Ω with respect to x, μ, and θ. The pressure of the system is then obtained from the energy density

$$P = \rho \left(\frac{\partial(\varepsilon/\rho)}{\partial\rho} \right). \tag{11.10}$$

The energy density ε and pressure P are then used in the TOV equation to obtain the properties of neutron stars.

The above constitutes the basic ingredient that also went into a more detailed calculation of [Thorsson, Prakash and Lattimer 1994]..

The results of the Li *et al*'s calculation are as follows: In Fig. 11.1 is shown the electron chemical potential as a function of nucleon density. Without kaon condensation, the electron chemical potential continues to increase with nucleon

density. When kaons are included, the electron chemical potential first increases up to about three times normal nuclear matter density until kaon condensation sets in. Then it decreases as the electrons convert to K^-'s. Thus based on the kaon in-medium properties as constrained by heavy-ion data and the nuclear equation of state that encodes the vector manifestation property of HLS, Li *et al.* [Li, Lee and Brown 1997] find that the critical density for kaon condensation to be about $3\rho_0$, consistent with the critical density arrived at in Chapter 9. Also shown in Fig. 11.1 are the proton fraction x and the chiral angle θ as a function of nucleon density. The solid and dotted curves are obtained with and without kaons, respectively. Once kaon condensation sets in, the proton fraction increases rapidly to become comparable to the neutron fraction. This reduces the asymmetry parameter, and hence the symmetry energy, of the system. The chiral angle, or the condensate amplitude, rises rapidly near the threshold, and then slowly saturates to about 60^0. [4]

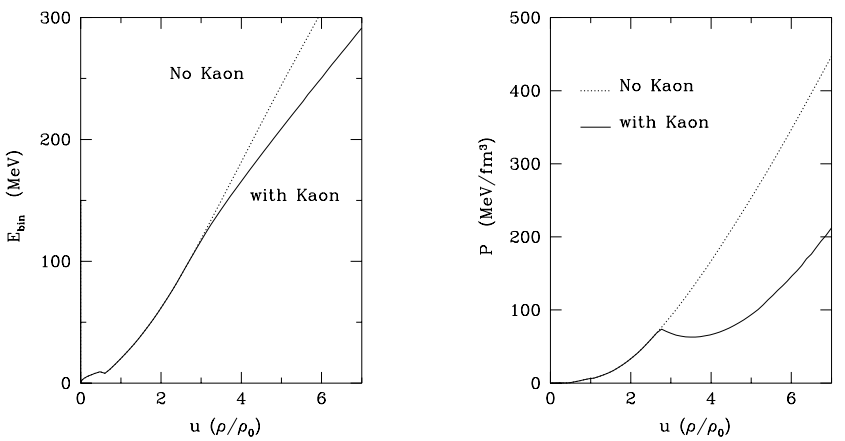

Fig. 11.2 Energy density (left panel, $m_N\rho$ is subtracted) and pressure (right panel) as a function of nucleon density.

In Fig 11.2 we show the energy density and the pressure of the system as a function of nucleon density, for both with and without kaon condensates. For densities lower than 0.08 fm^{-3} (*i.e.* $\sim \frac{1}{2}\rho_0$), the empirical equation of state was used as in [Thorsson, Prakash and Lattimer 1994]. Both the energy density and pressure are seen to be lowered once kaon condensation sets in. The effect is particularly strong in the pressure. It can be seen that the softening of the equation of state by kaon condensation is appreciable.

[4]This estimate is based on mean-field approximation, so may be unreliable at this angle. For a more realistic description, one would have to do higher (chiral) order calculations along the line developed in the preceding chapters and this has not been done yet in a satisfactory way.

The results for neutron star mass as a function of central density ρ_{cent} are shown in Fig. 11.3. Without kaons, the maximum neutron star mass in this model reaches about $2M_\odot$. When kaon condensates are present, the maximum mass of neutron stars is about $1.5M_\odot$. The dependence of neutron star mass on radius is shown in Fig. 11.3. With kaon condensation, the radius of maximum mass neutron star increases. These are the characteristic features of kaon condensation at a density $\sim 3\rho_0$ that constitute the basis of the Brown-Bethe scenario on the maximum stable neutron star mass to be discussed below. We will present the evidence that they control the fate of compact stars between becoming neutron stars and collapsing into black holes.

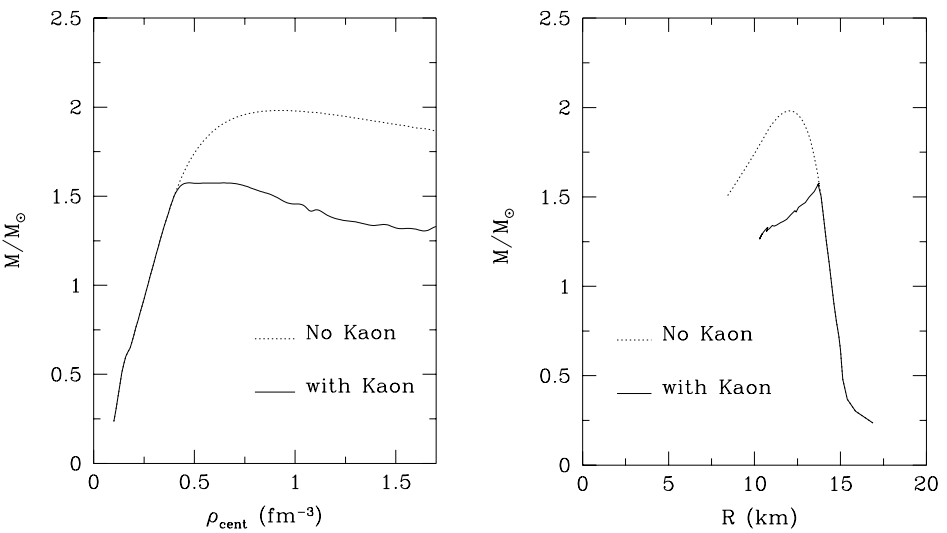

Fig. 11.3 Neutron star mass as a function of central density (left panel) and the radius (right panel).

In the remainder of this chapter, we confront the phase structure of dense matter sketched above in a highly simplified – but qualitatively correct – form with nature, in particular with the fate of compact stars. As announced, we will restrict ourselves to the scenario based on kaon condensation and its consequence on.whether a collapsed star will go into a neutron star or a black hole. For a much more comprehensive discussion covering a wide-range of scenarios including highly model-dependent alternatives that have been discussed in the literature, the readers are invited to refer to the extensive reviews, *e.g.*, [Lattimer and Prakash 2004; Lattimer and Prakash 2007].

11.4 Maximum Neutron Star Mass

11.4.1 M_{NS}^{max} à la Brown-Bethe

The quantity that is most pertinent to us is the maximum stable mass of neutron star proposed by Brown and Bethe [Brown and Bethe 1994] which will be denoted M_{NS}^{max}. The Brown-Bethe proposal is that compact stars more massive than M_{NS}^{max} can only be in the form of black holes. Whether or not this scenario is viable as it stands in confrontation with nature is reviewed in [Brown, Lee and Rho 2007]. Here we describe the reasoning that led to this result.

In the study of neutron stars, a key tool used in astrophysics is the Eddington accretion as the maximum possible rate. An explanation in a non-technical term goes as follows.

Matter falling on a neutron star is bound to the neutron star gravitationally by $\sim 20\%$ of its rest mass because of the great mass of the neutron star. This binding energy is used to produce radiation, say in the form of photons, which are emitted from the surface of the neutron star. These photons scatter off the incoming matter, which can be taken to be hydrogen, and deposit their momentum in it, by Thomson scattering. The outward pressure from the scattering of photons by the hydrogen is sufficient to counteract the inward gravitational force. This, then, gives a maximum rate of accretion in the neighborhood of rates $\sim \dot{M}_{\rm Edd}$ known as the Eddington limit [5]

$$\dot{M}_{\rm Edd} = R_6\ 1.5 \times 10^{-8} M_{\rm NS} {\rm yr}^{-1} \tag{11.13}$$

where R_6 is the radius of the neutron star in units of 10^6 cm – a typical neutron star radius – and $M_{\rm NS}$ is the mass of the neutron star in units of the mass of our sun $M_\odot$. Now the processes that we are interested in, such as common envelope evolution of

[5] For those unfamiliar with astrophysical terminologies, some definitions might be useful. The Eddington luminosity defined by

$$L_{\rm Edd} = \frac{4\pi c G M}{\kappa} \approx 1.3 \times 10^{38} \frac{M}{M_\odot}\ {\rm erg\ s}^{-1} \tag{11.11}$$

has been considered to be the limit of the luminosity in stellar evolution. Here, M is the mass of the accreting star, and $\kappa = \sigma_T N_A$, where σ_T is the Thomson cross section and N_A is Avogadro's number. The total luminosity can be connected to the mass accretion rate by

$$L = \epsilon L_{\rm Edd} = \epsilon\eta \dot{M}_{\rm Edd} c^2, \tag{11.12}$$

where $\epsilon\eta$ is the efficiency for converting gravitational energy to radiation energy. The Eddington mass-accretion rate is then given by (11.13). The so-called "hypercritical accretion" sets in when $\dot{M} > 10^4 \dot{M}_{\rm Eddington}$.

The hypercritical accretion could set in in a neutron star in the dense environment of a stellar envelope. Such a situation could occur in the scenario for the formation of binary pulsars, in which the spiral-in of the neutron star through the companion supergiant expels the envelope, which is hydrodynamically coupled to the drag from the neutron star, leaving a helium star as companion. Except in very extended stars, radiation pressure is unable to limit the accretion to the Eddington rate [Brown 1995].

stars take a time $\sim$ years. Given the 10^{-8} factor in Eq. (11.13), accretion at the order of the Eddington rate is unimportant and can be neglected.

Consider specifically the common envelope evolution of the first born neutron star with the helium core of the $20M_\odot$ star. The common envelope evolution takes only a few years, so in terms of Eddington limit for mass accretion of $1.5 \times 10^{-8} M_\odot$ yr^{-1}, the accretion is quite negligible, accounting for the fact it has generally been neglected in the literature to date. However, the rate of accretion continuously increases, so there is no reason to assume the Eddington rate to hold forever. Ultimately, the density of matter falling onto the neutron star becomes sufficiently high so that the photons originating from the neutron star random walk in the framework of the infalling matter and move out at a lower velocity than the infalling matter, so that the photons are swept back onto the neutron star by the adiabatic inflow. Now with the increase in the rate of accretion, scaled with Eddington rate

$$\dot{m} = \frac{\dot{M}}{\dot{M}_{\rm Edd}}, \tag{11.14}$$

in the region of rates $\dot{m} \sim 1$, the cutting off of increase in accretion above that value sets in. The increase of accretion from $\dot{m} \sim 1$ to 10^4 is thought to be complicated and not well understood, but from $\dot{m} \sim 10^4$ onward, the accretion again becomes simple with uniform flow.

In the scenario of Bethe and Brown [Bethe and Brown 1998], neutrinos were trapped in the collapse of large stars, so the photons were obviously trapped to give hypercritical accretion. Given two giant progenitors going through the evolution, the lowest mass in the problem will be the neutron star mass $M_{\rm NS}$. Bethe and Brown [Bethe and Brown 1998] found that the accretion was $\sim 10^8$ to 10^9 times Eddington accretion and assuming that the classical accretion argument – due to Bondi – applies, they found that the first-born neutron star would accrete $\sim 1M_\odot$ in the common envelope evolution during the red giant phase of the remaining giant and then send the primary into a black hole of mass $\sim 2.4M_\odot$. Based on the softening of the EOS given by kaon condensation at $\sim 3n_0$, they arrived at the conclusion that stars that are more massive than $M_{NS}^{max} \sim 1.5M_\odot$ are in black holes.

11.4.2 *Cosmological constraint on M_{NS}^{max}?*

Clearly in the Brown-Bethe scenario, the lower the M_{NS}^{max}, the more black holes will be formed in the collapse of stars. There are several immediate questions one can raise here. The first question is: why is the M_{NS}^{max} tuned to around 1.5 $M_\odot$? Why not lower and why not higher?

In the context of the main thesis developed here, the above question addresses the location of kaon condensation density. If the critical density were lower, then the M_{NS}^{max} would be lower than $\sim 1.5M_\odot$. The M_{NS}^{max} cannot be lower than the mass of the Hulse-Taylor binary pulsar of $1.44M_\odot$ which undoubtedly exists. Furthermore,

there would be lack of ^{12}C in the Galaxy as explained in [Brown and Bethe 1994], so even if the Hulse-Taylor pulsar were absent in nature, M_{NS}^{max} could not go below.

Now what about the maximum value for M_{NS}^{max}? The higher the M_{NS}^{max}, the lower the number of black holes in the Galaxy. The argument of Brown and Bethe is that if kaons condense around $3n_0$, then any compact star with mass $\gtrsim 1.5M_\odot$ would go into a black hole. This scenario clearly predicts that there would be a lot more black holes formed in the collapse of stars than if a star of mass $\sim 2.1M_\odot$ as suggested by Nice *et al.*'s J0751+1807 were confirmed to exist. It is interesting to note that the Brown-Bethe scenario is consistent with the cosmological argument, called "cosmological natural selection (CNS)," by L Smolin that requires that the black hole production in the universe should be maximized [Smolin 1997]. Needless to say, the connection between kaon condensation and the black hole population in the universe is an intriguing possibility. It should be stressed that both the Brown-Bethe scenario and Smolin's CNS would be *unambiguously falsified* if, for instance, quark stars with the LOFF phase – the most likely color superconducting state described in Chapter 10 – were found to exist.

11.5 Formation of Double Neutron Star Binaries

We do see double neutron star binaries, so the first-born neutron star cannot always go into a black hole. If the two giant progenitors are so close in mass that they burn helium at the same time, then they would go into a helium common envelope evolution, the one star sending He across the Roche Lobe into the other and the other one sending its expanding helium to the first star [Brown 1995]. Helium burning takes up 10% of the star lifetime, most of the time being spent in the main sequence hydrogen burning. Going from lifetimes to masses, Brown and Bethe predict that two neutron stars in a binary must be within 4% of each other in mass so as to be stable.[6]

The compilation of masses of double neutron star binaries in Table 11.1 [Lattimer and Prakash 2007] illustrates the tenability of the argument given above. In J1518+49 the uncertainties are too large to say anything, except that the largest error $+0.45M_\odot$ is in the direction of equalizing the masses. In the next three binaries the masses are very close. In fact, B2127+11 is in the globular cluster and often considered to have resulted from the exchange of neutron stars formed in different binaries. However, they do satisfy the Brown-Bethe nearly equal mass scenario.

[6]There is, however, one proviso. That is that the lower mass neutron stars in the double pulsars J0737−3039 and J1756−2251 go through not only the hydrogen burning red giant but also a helium burning red giant. The temperature for helium burning in low mass stars must be greater than in higher mass stars in order to ensure a sufficiently high central temperature because of the energy loss through the surface. During the helium burning red giant, ~ 0.1 to $0.2M_\odot$ can be deposited on the first born neutron star by the helium star companion, and the first born neutron star should be that much more massive than the other, in addition to the possible $\sim 4\%$ difference in mass because they must burn helium at the same time.

Table 11.1 Compilation of NS-NS binaries

Object	Mass ($M_\odot$)	Companion Mass ($M_\odot$)
J1518+49	$1.56^{+0.13}_{-0.44}$	$1.05^{+0.45}_{-0.11}$
B1534+12	$1.3332^{+0.0010}_{-0.0010}$	$1.3452^{+0.0010}_{-0.0010}$
B1913+16	$1.4408^{+0.0003}_{-0.0003}$	$1.3873^{+0.0003}_{-0.0003}$
B2127+11C	$1.349^{+0.040}_{-0.040}$	$1.363^{+0.040}_{-0.040}$
J0737−3039A	$1.337^{+0.005}_{-0.005}$	$1.250^{+0.005}_{-0.005}$ (J0737−3039B)
J1756−2251	$1.40^{+0.02}_{-0.03}$	$1.18^{+0.03}_{-0.02}$

Using a flat distribution for the Initial Mass Function, Lee *et al.* [Lee, Park and Brown 2007] calculated in hypercritical accretion what the masses of primary and secondary neutron stars would be in the scenario shown in Fig. 11.4 in which case the primary (first-born) neutron star is assumed not to go into a black hole, but the neutron star of mass it ends up with after accretion is assumed to be stable. One sees that the primary star, the pulsar, has high $\sim 84\%$ probability of ending up with mass between 1.8 and $2.3M_\odot$. This is not seen at all in Table 11.1, so it is natural to assume that these must all have gone into black holes.

Note that only the primary pulsar masses (the first born pulsar in the double pulsar) would be affected by the accretion; the companion masses lie on the lower thin band in Fig. 11.4. In the figure, the primary pulsar masses of 5 double neutron star binaries are indicated in filled circles. J1518+49 have a large uncertainty in the masses, so they are left out. The *à priori* probability for the primary pulsar masses to lie on the lower thin band within $0.2M_\odot$ uncertainty due to the possible accretion during the He giant phase, given no other possibility than to remain neutron stars, comes out to be

$$P = (0.16)^5 \simeq 1 \times 10^{-4}. \tag{11.15}$$

There is negligible probability assuming random neutron star masses that the two neutron stars in each of 5 binaries are all within 4% of each other in mass.

11.6 Neutron Stars Heavier than M_{NS}^{max}?

There are "observed" neutron stars whose masses exceed the Brown-Bethe M_{NS}^{max}. Can these be accounted for if kaon condensation always sets in for density greater than $n_c^K \sim 3n_0$?

In addition to the neutron star-neutron star binaries discussed above, there are X-ray binaries whose mean mass is $\sim 1.53M_\odot$ but in which some are more massive than M_{NS}^{max}. Among them, the notable one is Vela X-1 with mass $(1.86 \pm 0.16)M_\odot$. There are also neutron star-white dwarf binaries with a mean mass of $1.58M_\odot$,

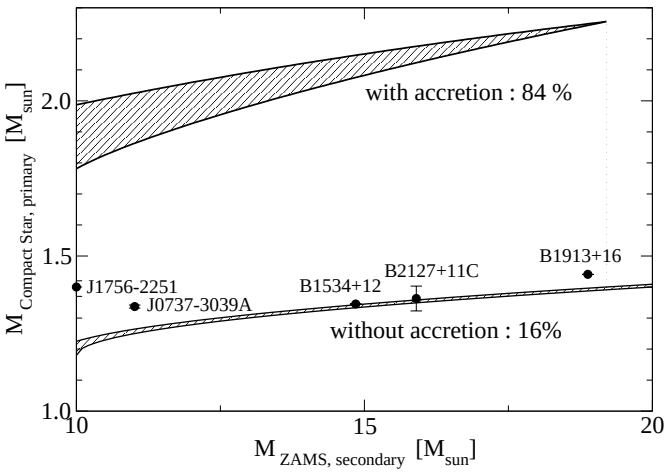

Fig. 11.4 Masses of primary compact stars with and without accretion during H red giant stage of secondary star. The filled circles show the primary (more massive) pulsar masses in double neutron star binaries. The corresponding secondary ZAMS (zero age main sequence) masses were obtained from the secondary (less massive) pulsar masses using Eq. (8) of Lee *et al* [Lee, Park and Brown 2007]. Note that the 84% corresponds to $M_{\text{Compact Star,primary}} > 1.8M_{\odot}$. There is uncertainty in the final primary compact star masses due to the extra mass accretion, $\sim 0.1M_{\odot} - 0.2M_{\odot}$, during He giant stage. This may increase the primary compact star masses for both 'with-' and 'without-accretion'. Note that with the maximum neutron star mass of $1.8M_{\odot}$, all primary compact stars with accretion would go into low-mass black holes.

among which some are considerably more massive than M_{NS}^{max}. Most striking among them is the J0751+1807 with the published mass 2.10 ± 0.20 [Nice *et al.* 2005] which, however, has been reduced to $1.26^{+0.14}_{-0.12}$ by new measurement.

The question then is: If kaon condensation is inevitable for density $\gtrsim 3n_0$, how did these massive stars escape from collapse to black hole? Are there loop-holes to the kaon condensation scenario and/or the Brown-Bethe argument? We briefly discuss this issue.

11.6.1 *Vela X-1*

The X-ray binaries have large error bars, so the situation is not clear. The most serious candidate is the Vela X-1 [7] as mentioned. If it is confirmed that Vela X-1 does have a mass as large as $\sim 1.86M_{\odot}$, then we will have to entertain the possibility that there can be several scenarios for the formation of stable neutron stars. So how solid is the evidence for the large mass of Vela X-1?

Here are some of the assessment by the observers on the system:

[7] The Vela X-1 is made up of an $18M_{\odot}$ B-star and a neutron star. The center of mass is well within the giant.

- A caveat noted by [Van Paradijs *et al.* 1977a]: "Another systematic effect, due to the distortion of the primary may be quite important in the case of X-ray binaries with a small mass ratio as the Vela X-1 system. In such a system the radial velocities of certain individual surface elements of the primary are much greater than the orbital velocity of the center of mass of this star, in the case of synchronous rotation. When the primary is tidally distorted and has a variation of effective temperature and gravity across its surface, it is by no means clear that the observed radial velocity, which is given by some spectrophotometric average over the surface, can be identified with the motion of the center of mass of the object."
- In a follow-up to the discussion of [Van Paradijs *et al.* 1977a], the authors stated: "In a previous paper we presented a numerical study of the effect of the deformation of the primary on its apparent radial velocity. The apparent velocity amplitude can in some cases increase by up to 30%, thereby increasing the apparent mass of the compact object by approximately the same amount." [Van Paradijs *et al.* 1977b]
- We note that the light curve is known to vary substantially from night to night. Indeed, in Barziv *et al* [Barziv *et al.* 2001] from which the large neutron star mass is taken, the authors say "The best estimate of the mass of Vela X-1 is $1.86M_{\odot}$. Unfortunately, no firm constraints on the equation of state are possible, since systematic deviations in the radial-velocity curve do not allow us to exclude a mass around $1.4M_{\odot}$ as found for other neutron stars."

There are also possibilities that the massive stars are not neutron stars but black holes.

11.6.2 *Neutron star-white dwarf binaries*

Next we consider the neutron star-white dwarf binaries.

In Table 11.2 taken from [Lattimer and Prakash 2004], are listed the neutron-star, white-dwarf binaries in which the central value of the neutron star mass is $\geq 1.5M_{\odot}$. It should be noted that given the errors involved, there is no neutron star mass other than in J0751+1807 which is definitely above M_{NS}^{max}.

On the other hand, sufficient of the central values of the neutron stars in binaries with white dwarf lie above $1.5M_{\odot}$ that it should be considered significant although it has been argued by Lee *et al.* [Lee, Park and Brown 2007] that the maximum neutron star mass must be less than $1.8M_{\odot}$, otherwise the spectrum of double neutron star binaries would be completely different from that shown in Table 11.1.

Up to date, the largest measured mass published in the literature is in J0751+1807, a neutron star in a binary with white dwarf, with mass $2.10^{+0.20}_{-0.20}M_{\odot}$ [Nice *et al.* 2005]. However at 95% confidence level, the mass is $2.1^{+0.4}_{-0.5}M_{\odot}$ so it could be as low as $1.6M_{\odot}$ at this level. Clearly it could be $1.8M_{\odot}$ with not unrea-

Table 11.2 Neutron star masses in neutron-star, white dwarf binaries in which the central value of the neutron star mass is $\geq 1.5 M_\odot$

Name	Pulsar Mass ($M_\odot$)
J1713+0747	$1.54^{+0.007}_{-0.10}$
B1855+09	$1.57^{+0.12}_{-0.11}$
J0751+1807	$2.10^{+0.20}_{-0.20}$
J1804−2718	< 1.70
J1012+5307	$1.68^{+0.22}_{-0.22}$
J0621+1002	$1.70^{+0.12}_{-0.29}$
J0437−4715	$1.58^{+0.18}_{-0.18}$
J2019+2425	< 1.51

sonable probability. Furthermore the recently re-measured value $1.26^{+0.14}_{-0.12} M_\odot$ (see below) goes in the direction of confirming this interpretation.

Neutron stars in binaries in some globular clusters have been reported with masses substantially above M_{NS}^{max}. For example, the relativistic periastron advance for the two eccentric systems in the globular cluster Terzan 5, I and J, indicates that at least one of these pulsars has a mass of $1.68 M_\odot$ at 95% confidence. As mentioned, there have been observations in NGC 6440 and NGC 6441 of millisecond pulsars of median mass $2.74 \pm 0.21 M_\odot$ [Friere *et al.* 2007]. All these are, however, highly controversial and need to be reconfirmed to be taken as a serious case against our scenario. In any event, the situation in globular clusters could be very different from Galactic. With very low metalicity, their stars resemble more Population II stars than Galactic ones. This should, however, not make a difference in the calculation of kaon condensation and its consequences since we find that *the condensation depends only on the baryon number density.*

11.6.3 *Two-branch scenario*

We seem to have two drastically different observations, one the collapse of the SN1987A into a black hole with mass $\gtrsim M_{NS}^{max}$ [Brown and Bethe 1994] that is consistent with the Brown-Bethe scenario and the existence of stars more massive than M_{NS}^{max}. Can one reconcile the two observations if they are real?

Haensel *et al.* [Haensel, Bejger and Zdunik 2007] have proposed an interesting way to reconcile the Brown and Bethe $M_{\rm NS}^{max}$ with the Nice *et al.* [Nice *et al.* 2005] $2.1 M_\odot$ neutron star or other massive stars that deviate from $M_{\rm NS}^{max}$, *i.e.* two branches of neutron stars — reconciling a $2 M_\odot$ pulsar and SN1987A. Two scenarios of neutron star formation were considered. Here we interpret the two scenarios in terms of two possibilities in our language. In the first scenario the formation of the strangeness core is rapid; this is the case of the double neutron star binaries in which the hypercritical accretion from the evolving companion onto the first-born neutron

star, the pulsar, is at a rate of $\sim 10^8 \dot{M}_{\rm Edd}$, so that the total accretion time is ~ 1 year. In the second scenario the neutron star is already present when the main sequence progenitor of the white dwarf begins to evolve. The neutron star accretes matter (and is spun up) by accretion from the companion red giant in stable mass transfer. The rate of mass transfer is $\lesssim \dot{M}_{\rm Edd}$, so it is $\sim 10^8$ times slower than in the first case. Models of quark deconfinement (producing quark matter) are found in which the condition $M_{\rm NS}^{max} \gtrsim 2M_\odot$ is satisfied.

The Haensel *et al.* reconciliation is ingenious and deserves to be paid attention. However in view of the recent development on Nice *et al.*'s $2.1M_\odot$ neutron star mentioned below, reconciliation of that type does not seem called for. We would nonetheless suggest that the reasoning for the two tracks of Haensel *et al* is not valid for the case at hand. Of the two possible phases, quark matter and kaon condensation, the former phase would be favored at high temperature, as is found in collapses like 1987A, and the latter in a cool scenario like the $\sim 10^8$ yr accretion from an evolving main sequence star onto the neutron star to make a neutron-star, white-dwarf binary. In 1987A the collapsing star heats up, to a temperature $\sim$ 25 MeV in the center, because of Joule heating. The latter is accomplished by the $\sim$ 100 MeV highly degenerate neutrinos leaving their degeneracy energy in the center of the forming neutron star as they leave with energies determined by the surface temperature. On the other hand, the temperature from accretion onto neutron stars in the white-dwarf, neutron-star binary evolution is much less than 1 MeV, so the thermal neutrino emission is almost negligible. Thus, the collapse into strangeness condensation would be favored by the more massive of the two stars in a double-track scenario and the transition into a black hole by strangeness condensation in the collapse of a large star would favor quark matter. In other words, the two tracks of Haensel *et al* would be filled in the different way, if indeed they were.

11.6.4 *New measurement of the neutron star mass in J0751+1807*

A new value for the mass of J0751+1807[8] measured anew is now $1.26^{+0.14}_{-0.12}M_\odot$ to replace the old value $(2.1 \pm 0.2)M_\odot$. This removes the necessity for two branches of neutron stars, with which we had troubles noted just above. In fact, the 2.1 $M_\odot$ cannot be right on a general ground: Were it correct, the spectrum of neutron-star masses would be completely different from what it is.

11.7 Outlook

According to the scenario most natural in the spirit developed in the preceding chapters and here – but yet to be confirmed, the collapsing stars face two fates

[8] As announced by D. Nice in the McGill meeting on "40 Years of Pulsars," August 12-17, 2007, http://www.ns2007.org.

depending upon whether binaries are stabilized with a mass difference of $\lesssim 4\%$ or not. In the former case, we will have neutron stars with their masses $\lesssim M_{NS}^{max}$. In the latter case, stars more massive than M_{NS}^{max} will collapse into black holes. The suggestion was that *the matter density plays the pivotal role on the fate of compact stars*, with possible caveats due to metalicity which we have not taken into account in considering the effect of kaon condensation.

The outstanding question for the future is: What is the implication of this scenario on the structure of matter at high density in the interior of stable compact stars?

Even if we accept that kaon condensation sets in to make the mass of stable stars $\lesssim M_{NS}^{max}$ and sends heavier stars into black holes, it is still possible that density in double pulsars is high enough for the system to make further phase transitions. Whether and how this can occur has not been studied with reliable tools to enable us to know what can actually happen. This is an open problem. As mentioned, once kaon is condensed, the matter is highly non-Fermi liquid, so possible phase changes, if any, will take place from a "normal" phase which is poorly understood as in high T_c superconductivity. For instance, the possible half-skyrmion coupled to "emerging" nonabelian gauge fields, possibly the infinite vector fields of hQCD, could further complicate, or on the contrary, simplify the door-way state to possible color superconductivity. Thus theoretically the situation is totally unknown.

At present, observational data are inconclusive. For instance, some neutron stars are observed to be spinning at a rate that would exclude extremely stiff density dependent EOS such as the one described in Chapter 10.1.1. Also rapidly cooling neutron stars in several young supernova remnants indicate high rates of neutrino emission in their interiors consistent with the presence of softening phases. However the majority of stars that are thermally emitting are consistent with relatively slow standard cooling rates (see [Lattimer and Prakash 2007] for an extensive review).

Of all the multitude of scenarios painting a vast landscape of possible phases that are possible beyond $\sim 2n_0$, the simplest and readily falsifiable scenario proposed up to date is the one based on the thesis developed in this volume, namely, the Brown-Bethe scenario anchored on kaon condensation. The possible exploration of the landscape will depend upon the falsification or confirmation of the precise prediction which may be succinctly stated as [Brown, Lee and Rho 2007]: "Find a double pulsar with mass difference substantially greater than $\sim 4\%$, then the proposed Brown-Bethe scenario would be ruled out."

Suppose that no such double pulsars are found. While this would not mean that such pulsars don't exist in nature, it would be suggestive [Brown, Lee and Rho 2007] that for stars with mass $\gtrsim M_{NS}^{max}$, *"all ends with baryon number density* $\sim 3n_0$*, and there is only 'nothingness,' the space-time volume of the black hole, beyond."* This is a strong statement. One can think of two possibilities. One is that such phenomena predicted model-independently by QCD as color-flavor locked color superconductivity, even if existent at super-high density, will be hidden in the "black-hole

nothingness" inaccessible to the (astrophysical) observers. The other possibility is that there is a loop-hole, hitherto undiscovered, to the black-hole scenario, allowing the matter in compact stars that meet the Brown-Bethe constraint to go over to a color superconducting state of some variety.

If, on the other hand, one such double-pulsar system – at odds with the Brown-Bethe constraint – were found, the door would be wide open to all the variety of exotic scenarios conceived thus far, generating exciting developments both in theory and in observations [Schaffner-Bielich 2007]. This of course would not invalidate the notion of hidden local symmetry *per se* but would put in grave doubt some of the basic assumptions made to reach the state of dense matter we have.

Whatever the outcome the Brown-Bethe prediction may turn out to be, an observation of a structure indicative of a phase signalling quark matter in any form, be that in the terrestrial laboratories or space observatories, will be the most exciting development in this field. Indeed it has been suggested that such a signal could be "seen" in the gravitational waves from LIGO, in particular in the form of neutron star "ellipticity" that measures the breaking strain of solid in the interior of a spinning neutron star [Owen 2005; Haskell, Andersson and Samuelsson 2007]. The presence mentioned in Chapter 10.4.2 of the LOFF crystalline structure in a color superconducting phase supporting superfluid rigid states with shear moduli 20 to 1000 times that of a conventional neutron star – with which the argument of this volume is at odds – could be a source of such gravitational wave [Mannarelli, Rajagopal and Sharma 2007]. There is a preliminary indication from the presently available gravitational wave data from the LIGO [Haskell, Andersson and Samuelsson 2007] that compact objects do not contain such crystalline core. However whether or not such a signal can be unequivocally identified with a specific solid structure is however by no means clear. It must involve a complicated interplay of the crust and interior of the star and sorting out all other effects than what is looked for cannot be clear-cut. Furthermore there can be a variety of different forms of solid structure at high density. For instance, a compact star that is in the form of dense skyrmion crystal described in Chapter 6 could also be a source for ellipticity.

This page intentionally left blank

Bibliography

Abrikosov, A.A., Gor'kov, L.P. and Dzyaloshinski, L.YE. (1965) *Quantum field theoretical methods in statistical physics* (Pergamon Press, London, 1965).

Adkins, G.S. and Nappi, C.R. (1984) Stabilization of chiral solitons via vector mesons, *Phys. Lett.* **B137**, pp. 251-256.

Adkins, G.S., Nappi, C.R. and Witten, E. (1983) Static properties of nucleons in the Skyrme model, *Nucl. Phys.* **B228**, pp. 552-566.

Aharony, O., Sonnenschein, J. and Yankielowicz, S (2007) Holographic model of deconfinement and chiral symmetry restoration, *Ann. Phys.* **322**, pp. 1420-1443.

Akaishi, Y., Doté, A. and Yamazaki, T. (2005) Strange tribaryons as $\bar{K}$-mediated dense nuclear matter, *Phys. Lett.* **B613**, pp. 140-147.

Akmal, A., Pandharipande, V.R. and Ravenhall, D.G. (1998) The equation of state of nucleon matter and neutron star structure, *Phys. Rev.* **C58**, pp. 1804-1828.

Alford, M. (2006a) Color superconductivity and the strange quark, *AIP Conf. Proc.* **806**, pp. 293-302.

Alford, M. (2006b) Color superconductivity in ultra-dense quark matter, hep-lat/0610046.

Alford, M.G., Schmitt, A., Rajagopal, K. and Schäfer, T. (2007) Color superconductivity in dense quark matter, arXiv:0709.4635 [hep-ph].

Alkofer, R., Hong, H.T. and Zahed, I. (1991) NJL soliton in matter, *J. Phys. G: Nucl. Part.* **17**, pp. L59-66.

Ando, S., Song, Y.-H., Park, T.-S., Fearing, H.W. and Kubodera, K. (2003) Solar-neutrino reactions on deuteron in effective field theory, *Phys. Lett.* **B555**, pp. 49-56.

Aoki, Y., Endrödi, G., Fodor, Z., Katz, S.D. and Szabó, K.K. (2006) The order of the quantum chromodynamics transition predicted by the standard model of particle physics, *Nature*, pp. 675-677.

Appelquist, T., Fleming, G.T. and Neil, E.T. (2007) Lattice study of the conformal window in QCD-like theories, arXiv:0712.0609 [hep-th].

Arkani-Hamed, N., Georgi, H. and Schwartz, M.D. (2003) Effective field theory for massive gravitons and gravity in theory space, *Ann. Phys.* **305**, pp. 96-118.

Asakawa, M., Hatsuda, T. and Nakahara, Y. (2003) Hadronic spectral functions above the QCD phase transition, *Nucl. Phys.* **A715**, pp. 863-866.

Atiyah, M.F. and Manton, N.S. (1989) Skyrmions from instantons, *Phys. Lett.* **B222**, pp. 438-442.

Babu, S. and Brown, G.E. (1973) Induced interactions, *Ann. Phys.* **78**, pp. 1-38.

Bahcall, J.N., Pinsonneault, M.H. and Basu, S. (2001) Solar models: Current epoch and time dependences, neutrinos, and helioseismological properties, *Astrophys. J.* **555**, pp. 990-1012.

Bando, M., Kugo, T. and Yamawaki, K. (1988) Nonlinear realization and hidden local symmetries, *Phys. Rept.* **164**, pp. 217-314.

Bardeen, W.A. and Hill, C.T. (1994) Chiral dynamics and heavy quark symmetry in a solvable toy field theoretic model, *Phys. Rev.* **D49**, pp. 409-425.

Barnea, N. and Friedman, E. (2007) Radial sensitivity of kaonic atoms and strongly bound $\bar{K}$ states, *Phys. Rev.* **C75**, pp. 022202-4.

Barziv, O., Kaper, L., van Kerkwijk, M.H., Telting, J.H. and Van Paradijs, J. (2001) The mass of neutron star in Vela X-1, *Astron. Astrophys.* **377**, pp. 925-944.

Baskaran, G. and Anderson, P.W. (1988) Gauge theory of high temperature superconductors and strongly correlated Fermi systems, *Phys. Rev.* **B37**, pp. 580-583.

Bass, S.D. (2005) The spin structure of the proton, *Rev. Mod. Phys.* **77**, pp. 1257-1302.

Battye, R.A., Krusch, S. and Sutcliffe, P.M. (2006) Spinning skyrmions and the Skyrme parameters, *Phys. Lett.* **B626**, pp. 120-126.

Battye, R.A. and Sutcliffe, P.M. (2006) Skyrmions with massive pions, *Phys. Rev.* **C73**, pp. 055205-4.

Baumann, P. *et al.* (1998) Meson exchange enhancement in first forbidden beta transitions: The Case of ^{50}K and ^{38}Ca, *Phys. Rev.* **C58**, pp. 1970-1979.

Baym, G. and Chin, S.A. (1976) Landau theory of relativistic Fermi liquids, *Nucl. Phys.* **A262**, pp. 562-538.

Bedaque, P.F. and Schäfer, T. (2002) High density quark matter under stress, *Nucl. Phys.* **A697**, pp. 802-822.

Bedaque, P.F. and U. van Kolck (2002) Effective field theory for few nucleon systems (2002), *Ann. Rev. Nucl. Part. Sci.* **52**, pp. 339-396.

Benayoun, M., David, P., DelBuono, L., Leitner, O. and O'Connell, H.B. (2007) The dipion mass spectrum in e^+e^- annihilation and τ decay: A dynamical (ρ, ω, ϕ) mixing approach, arXiv:0711.4482 [hep-ph].

Bethe, H.A. and Brown, G.E. (1998) Evolution of binary compact objects which merge, *Astrophys. J.* **506**, pp. 780-789.

Bijker, R. and Iachello, F. (2004) Re-analysis of the nucleon space- and time-like electromagnetic form-factors in a two-component model, *Phys. Rev.* **C69**, pp. 068201-4.

Bijnens, J., Colangelo, G. and Gasser, J. (1994) K_{l4} decays beyond one loop, *Nucl. Phys.* **B427**, pp. 427-454.

Birse, M.C. (1994) Does the effective Lagrangian for low-energy QCD scale?, *J. Phys.* **G20**, pp. 1287-1292.

Bogner, S.K., Kuo, T.T.S., Schwenk, A., Entem, D.R. and Machleidt, R. (2003) Towards a model-independent low momentum nucleon-nucleon interaction, *Phys. Lett.* **B576**, pp. 265-272.

Borasoy, B., Nissler, R. and Weise, W. (2005) Chiral dynamics of kaon-nucleon interactions revisited, *Eur. Phys. J.* **A25**, pp. 79-96.

Brihaye, Y., Hill, C.T. and Zachos, C.K. (2004) Bounding gauged skyrmion masses, *Phys. Rev.* **D70**, pp. 111502-4.

Brockmann, R. and Machleidt, R. (1984) Nuclear saturation in a relativistic Brueckner-Hartree-Fock approach, *Phys. Lett.* **B149**, pp. 283-287.

Brodsky, S.J. and de Teramond, G.F. (2006) Hadronic spectra and light-front wavefunctions in holographic QCD, *Phys. Rev. Lett.* **96**, pp. 201601-4.

Brower, R.C., Polchinski, J., Strassler, M.J. and Tan, J.-I. (2007) The pomeron and gauge/string duality, *JHEP* **12**, pp. 005-62.

Brown, G.E. (1995) Neutron star accretion and binary pulsar formation, *Astrophys. J.* **440**, pp. 270-279.

Brown, G.E. and Bethe, H.A. (1994) A scenario for a large number of low-mass black holes in the galaxy, *Astrophys. J.* **423**, pp. 659-664.

Brown, G.E., Gelman, B.A. and Rho, M. (2006) Matter formed at Brookhaven Heavy Ion Collider, *Phys. Rev. Lett.* **96**, pp. 132301-4.

Brown, G.E., Harada, M., Holt, J.W., Rho, M. and Sasaki, C. (2008) A hidden gauge theory for dileptons in relativistic heavy ion collision, to appear.

Brown, G.E., Holt, J.W., Lee, C.-H. and Rho, M. (2006) Late hadronization and matter formed at RHIC: Vector manifestation, BR scaling and hadronic freedom, *Phys. Rept.* **439**, pp. 161-191.

Brown, G.E., Kubodera, K. and Rho, M. (1987) Strangeness condensation and "clearing" of the vacuum., *Phys. Lett.* **B192**, pp. 273-278.

Brown, G.E., Lee, C.-H., Park, H.J. and Rho, M. (2006) Study of strangeness condensation by expanding about the fixed point of the Harada-Yamawaki vector manifestation, *Phys. Rev. Lett.* **96**, pp. 062303-4.

Brown, G.E., Lee, C.-H. and Rho, M. (2005) Chemical equilibration in relativistic heavy ion collisions, *Nucl. Phys.* **A747**, pp. 530-563.

Brown, G.E., Lee, C.-H. and Rho, M. (2006) Vector manifestation of hidden local symmetry, hadronic freedom, and the STAR ρ^0/π^- ratio, *Phys. Rev.* **C74**, pp. 024906-6.

Brown, G.E., Lee, C.-H. and Rho, M. (2007) Recent developments on kaon condensation and its astrophysical implications, arXiv:0708.3137 [hep-ph].

Brown, G.E., Lee, C.-H. and Rho, M. (2008) Kaon condensation, black holes and cosmological natural selection, in preparation.

Brown, G.E., Lee, C.-H., Rho, M. and Shuryak, E. (2004) The $\bar{q}q$ bound states and instanton molecules at $T \gtrsim T_C$, *Nucl. Phys.* **A740**, pp. 171-194.

Brown, G.E., Lee, C.-H., Rho, M. and Thorsson, V. (1993) From kaon nuclear interactions to kaon condensation, *Nucl. Phys.* **A567**, pp. 937-956.

Brown, G.E. and Rho, M. (1979) The little bag, *Phys. Lett.* **B82**, pp. 177-180.

Brown, G.E. and Rho, M. (1988) The chiral bag, *Comments Part. Nucl. Phys.* **18**, pp. 1-42.

Brown, G.E. and Rho, M. (1990) In-medium stiffening of the nucleon nucleon spin-isospin interaction, *Phys. Lett.* **B237**, pp. 3-7.

Brown, G.E. and Rho, M. (1991) Scaling effective Lagrangians in a dense medium, *Phys. Rev. Lett.* **66**, pp. 2720-2723.

Brown, G.E. and Rho, M. (1996) Chiral restoration in hot and/or dense matter, *Phys. Rep.* **269**, pp. 333-380.

Brown, G.E. and Rho, M. (1996) From chiral mean field to Walecka mean field and kaon condensation, *Nucl. Phys.* **A596**, pp. 503-514.

Brown, G.E. and Rho, M. (2002) On the manifestation of chiral symmetry in nuclei and dense nuclear matter, *Phys. Rept.* **363**, pp. 85-171.

Brown, G.E. and Rho, M. (2004a) Double decimation and sliding vacua in the nuclear many-body problem, *Phys. Rep.* **396**, 1-39.

Brown, G.E. and Rho, M. (2004b) Matching the QCD and hadron sectors and medium-dependent masses; hadronization in relativistic heavy-ion collisions, *Phys. Rep.* **398**, 301-325.

Brown, G.E. and Rho, M. (2005) NA60 and BR scaling in terms of the vector manifestation: Formal consideration, arXiv: nucl-th/0509002; NA60 and BR scaling in terms of the vector manifestation: A Model approach, arXiv: nucl-th/0509001

Brown, G.E., Rho, M. and Weise, W. (1986) Phenomenological delineation of the quark - gluon structure from nucleon electromagnetic form-factors, *Nucl. Phys.* **A454**, pp. 669-690.

Brown, G.E., Thorsson, V., Kubodera, K. and Rho, M. (1992) A novel mechanism for kaon condensation in neutron star matter, *Phys. Lett.* **B291**, pp. 355-362.

Buballa, M. (2005) NJL model analysis of quark matter at large density, *Phys. Rept.* **407**, pp. 205-376.

Buck, B. and Perez, S.M. (1984) New look at magnetic moments and beta decays of mirror nuclei, *Phys. Rev. Lett.* **50**, pp. 1975-1978.

Callan, C.G. and Klebanov, I.R. (1985) Bound state approach to strangeness in the Skyrme model, *Nucl. Phys.* **B262**, pp. 365-382.

Carlson, J. and Schiavilla, R. (1998) Structure and dynamics of few nucleon systems, *Rev. Mod. Phys.* **70**, pp. 743-842.

Casalbuoni. R. and Gatto, D. (1999) Effective theory for color flavor locking in high density QCD, *Phys. Lett.* **B464**, pp. 111-116.

Castillejo, L., Jones, P.S.J., Jackson, A.D. and Verbaarschot, J.J.M. (1989) Dense skyrmion systems, *Nucl. Phys.* **A501**, pp. 801-812.

Chemtob, M. and Rho, M. (1971) Meson exchange currents in nuclear weak and electromagnetic interactins, *Nucl. Phys.* **A163**, p. 1-55.

Chen, J.-W., Rupak, G. and Savage, M.J. (1999a) Nucleon-nucleon effective field theory without pions, *Nucl. Phys.* **A653**, pp. 386-412.

Chen, J.-W., Rupak, G. and Savage, M. (1999b) Suppressed amplitudes in $np \to d\gamma$, *Phys. Lett.* **B464**, pp. 1-11.

Cheng, M. *et al.* (2006) The transition temperature in QCD, *Phys. Rev.* **D74**, pp. 054507-15.

Cheng, T.P. and Li, L.-F. (1995) Flavor and spin contents of the nucleon in the quark model with chiral symmetry, *Phys. Rev. Lett.* **74**, pp. 2872-2875.

Chodos, A. and Thorn, C.B. (1975) Chiral invariance in the bag model, *Phys. Rev.* **D12**, pp. 2733-2743.

Coleman, P. and Schofield, A.J. (2005) Quantum criticality, *Nature* **433**, pp. 226-229.

Cremer, J.G., Miller, G.A., Wu, J.M.S. and Yoon, J.-H. (2005) Quantum opacity, the RHIC HBT purzzle, and the chiral phase transition, *Phys. Rev. Lett.* **94**, pp. 102301-4.

Damgaard, P.H., Nielsen, H.B. and Sollacher, R. (1992a) Smooth bosonization: The Cheshire cat revisited, *Nucl. Phys.* **B385**, pp. 227-250.

Damgaard, P.H., Nielsen, H.B. and Sollacher, R. (1992b) Smooth bosonization: The Massive case., *Phys. Lett.* **B296**, pp. 132-138.

Damgaard, P.H., Nielsen, H.B. and Sollacher, R. (1994) Gauge-symmetric approach to effective Lagrangians: The η' meson from QCD, *Nucl. Phys.* **B414**, pp. 541-578.

Da Rold, L. and Pomarol, A. (2005) Chiral symmetry breaking from five-dimensional spaces, *Nucl. Phys.* **B721**, pp. 79-97.

DeTar, C. and Kunihiro, T. (1989) Linear sigma model with parity doubling, *Phys. Rev.* **D39**, pp. 2805-2808.

Diakonov, D. and Petrov, V. (2000) Nucleons as chiral solitons, *At the frontier of particle physics: Handbook of QCD* ed by M. Shifman (World Scientific, Singapore, 2001) vol. 1, pp. 359-415.

Dong, J.J., Lagae, J.-F. and Liu, K.F. (1996) $\pi N\sigma$ term, $\bar{s}s$ in nucleon and scalar form factor: A lattice study, *Phys. Rev.* **D 54**, pp. 5496-5500.

Dorey, N. and Mattis, M.P, (1995) From effective Lagrangians, to chiral bags, to Skyrmions with the large-N_c renormalization group, *Phys. Rev.* **D52**, pp. 2891-2914.

Ellis, J.R. and Lanik, J. (1985) Is scalar gluon observable?, *Phys. Lett.* **B150**, pp. 289-294.

Earlich, J., Katz, E., Son, D.T. and Stephanov, M.A. (2005) QCD and a holographic model of hadrons, *Phys. Rev. Lett.* **95**, pp. 261602-4.

Epelbaum, E. and Meissner, U.-G. (2006) On the renormalization of the one-pion exchange potential and the consistency of Weinberg's power counting, nucl-th/0609037.

Eto, M., Nitta, M., Ohashi, K. and Tong, D. (2005) Skyrmions from instantons inside domain walls, *Phys. Rev. Lett.* **95**, pp. 252003-4.

Filippone, B.W. and Ji, X.-D. (2001) The spin structure of the nucleon, *Adv. Nucl. Phys.* **26**, pp.1-88.

Freire, P.C.C. *et al* (2007) Eight new millisecond pulsars in NGC 6440 and NGC 6441, arXiv:0711.0925.

Freund, P.G.O. and Nambu, Y. (1968) Scalar field coupled to the trace of the energy-momentum tensor, *Phys. Rev.* **174**, pp. 1741-1743.

Friedman, E. and Gal, A. (2007) Strange atoms, strange nuclei and kaon condensation, arXiv:0710.5890 [nucl-th].

Friedman, E., Gal, A and Batty, C.J. (1994) Density dependent K-nuclear optical potentials from kaonic atoms, *Nucl. Phys.* **A579**, pp. 518-538.

Friman, B. and Rho, M. (1996) From chiral Lagrangians to Landau Fermi liquid theory of nuclear matter, *Nucl. Phys.* **A606**, pp. 303-319.

Friman, B. , Rho, M. and Song, C. (1999) Scaling of chiral Lagrangians and Landau Fermi liquid theory for dense hadronic matter, *Phys. Rev.* **C59**, pp. 3357-3370.

Frishman, Y., Hanany, A. and Karliner, M. (1996) On the stability of quark soliton, *Sakharov Conference*, pp.20-32; hep-ph/9507206

Fuchs, T., Gegelia, J. and Scherer, S. (2004) Electromagnetic form-factors of the nucleon in relativistic baryon chiral perturbation theory, *J. Phys.* **G30**, pp. 1407-1426.

Fujikawa, K. (2006) Geometric phases and hidden local gauge symmetry, *Phys. Rev.* **D72**, pp. 025009-14.

Fukuda, S. *et al.* (Super-Kamiokande Coll.) (2001) Constraints on neutrino oscillations using 1258 days of Super-Kamiokande solar neutrino data, *Phys. Rev. Lett.* **86**, pp. 5656-5660.

Furnstahl, R.J., Jin, X.-M. and Leinweber, D.B. (1990) New QCD sum rules for nucleons in nuclear matter, *Phys. Lett.* **B387**, pp. 253-258.

Furnstahl, R.J. and Serot, B. (2000) Parameter counting in relativistic mean field models, *Nucl. Phys.* **A671**, pp. 447-460.

Furnstahl, R.J., Tang, H.-B. and Serot, B.D. (1995) Vacuum contribution in a chiral effective Lagrangian for nuclei, *Phys. Rev.* **C 52**, pp. 1368-1379.

Gal, A. (2007) Overview of $\bar{K}$-nuclear theory and phenomenology: Search for narrow quasibound states, *Prog. Theor. Phys. Supple.* **168**, pp. 556-564.

Gårdestig, A. and Phillips, D.R. (2006) How low-energy weak reactions can constrain three-nucleon forces and the neutron-neutron scattering length, *Phys. Rev. Lett.* **96**, pp. 232301-4.

Gelmini, G. and Ritzi, B. (1995). Chiral effective Lagrangian description of bulk nuclear matter, *Phys. Lett.* **B357**, pp. 431-434.

Georgi, H. (1984) *Weak interactions and modern particle theory* (The Benjamin/Cummings, Menlo Park, Calif. 1984).

Georgi, H. (1989) New realization of chiral symmetry, *Phys. Rev. Lett.* **63**, pp. 1917-1919.

Georgi, H. (1990) Vector realization of chiral symmetry, *Nucl. Phys.* **B331**, pp. 311-330.

Goldhaber, A.S. and Manton, N.S. (1987) Maximal symmetry of the Skyrme crystal, *Phys. Lett.* **B198**, pp. 231-234.

Goldstone, J. and Jaffe, R.L. (1983) The baryon number in chiral bag models, *Phys. Rev. Lett.* **51**, pp. 1518-1521.

Gottlieb, S., Liu, W., Toussaint, D., Renken, R.L. and Sugar, R.L. (1987) The quark number susceptibility of high temperature QCD, *Phys. Rev. Lett.* **59**, pp. 2247-2250.

Haensel, P., Bejger, M. and Zdunik, J.L. (2007) Two branches of neutron stars – reconciling a $2M_{\odot}$ pulsar and SN1987A, asXiv:0705.4594 [astro-ph].

Hammer, H.W. (2005) Few-body physics in effective field theory, *J. Phys.* **G31**, pp. S1253-S1261.

Harada, M., Kim, Y. and Rho, M. (2003) Vector manifestation and fate of vector mesons in dense matter, *Phys. Rev.* **D66**, pp. 016003-15.

Harada, M., Kim, Y., Rho, M. and Sasaki, C. (2003) The vector and axial vector susceptibilities and effective degrees of freedom in the vector manifestation, *Nucl. Phys.* **A727**, pp. 437-463.

Harada, M., Kim, Y., Rho, M. and Sasaki, C. (2004) The pion velocity at chiral restoration and the vector manifestation, *Nucl. Phys.* **A730**, pp. 379-391.

Harada, M., Matsuzaki, S. and Yamawaki, K. (2006) Implications of holographic QCD in ChPT with hidden local symmetry, *Phys. Rev.* **D74**, pp. 076004-9.

Harada, M., Rho, M. and Sasaki, C. (2004) Chiral doubling of heavy light hadrons and the vector manifestation of hidden local symmetry, *Phys. Rev.* **D70**, pp. 074002-14.

Harada, M. and Sasaki, C. (2002) Vector manifestation in hot matter, *Phys. Lett.* **B537**, pp. 280-286

Harada, M. and Sasaki, C. (2004) Vector manifestation and violation of vector dominance in hot matter, *Nucl. Phys.* **A736**, pp. 300-338.

Harada, M. and Sasaki, C. (2005) Dropping ρ and a_1 meson masses at chiral phase transition in the generalized hidden local symmetry," *Phys. Rev.* **D73**, pp. 036001-17.

Harada, M. and Sasaki, C. (2006) Thermal dilepton production from dropping ρ based on the vector manifestation, *Phys. Rev.* **D74**, 114006-14.

Harada, M., Tanabashi, M. and Yamawaki, K. (2003) π^+-π^0 mass difference in the hidden local symmetry: A dynamical origin of little Higgs, *Phys. Lett.* **B568**, pp.103-108.

Harada, M. and Yamawaki, K. (2001) Wilsonian matching of effective field theory with underlying QCD, *Phys. Rev.* **D64**, pp. 014023-37.

Harada, M. and Yamawaki, K. (2003) Hidden local symmetry at loop: A new perspective of composite gauge bosons and chiral phase transition, *Phys. Rept.* **381**, pp. 1-234.

Haskell, B., Andersson, N., Jones, D.I. and Samuelsson, L. (2007) Are neutron stars with crystalline color-superconducting cores relevant for the LIGO experiment?, *Phys. Rev. Lett.* **99**, pp. 231101-4.

Hatsuda, T., Tachibana, M., Yamamoto, N. and Baym, G. (2006) New critical point induced by the axial anomaly in dense QCD, *Phys. Rev. Lett.* **97**, pp. 122001-4.

Heiselberg, H. and Pandharipande, V. (2000) Recent progress in neutron star theory, *Ann. Rev. Nucl. Part. Sci.* **50**, pp. 481-524.

Hidaka, Y., Morimatsu, O. and Ohtani, M. (2006) Renormalization group equations in a model of generalized hidden local symmetry and restoration of chiral symmetry, *Phys. Rev.* **D73**, pp. 036004-28.

Hill, C.T. (2002) Topological solitons from deconstructed extra dimensions, *Phys. Rev. Lett.* **88**, pp. 04160-4.

Hill, C.T. and Zachos, C.K. (2005) Dimensional deconstruction and Wess-Zumino-Witten terms, *Phys. Rev.* **D71**, pp. 046002-5.

Hirn, J. and Sanz, V. (2005) Interpolating between low and high energy QCD via a 5D Yang-Mills model, *JHEP* **12**, pp. 030-071.

Hirn, J., Rius, N. and Sanz, V. (2006) Geometric approach to condensates in holographic QCD, *Phys. Rev.* **D73**, pp. 085005-9.

Holt, J.W., Brown, G.E., Holt, J.D. and Kuo, T.T.S. (2006) Nuclear matter with Brown-Rho-scaled Fermi liquid interactions, *Nucl. Phys.* **A785**, pp. 322-338.

Holt, J.W., Brown, G.E., Kuo, T.T.S., Holt, J.D. and Machleidt, R. (2007) Shell-model description of the ^{14}C dating β-decay with Brown-Rho-scaled NN interactions, arXiv.0710.0310 [nucl-th].

Holzwarth, G. (1996) Electro-magnetic nucleon form factors and their spectral functions in soliton models, *Z. Phys.* **A356**, pp. 339-350.

Hong, D.K. (2000a) An Effective field theory of QCD at high density, *Phys. Lett.* **B473**, pp. 118-125.

Hong, D.K. (2000b) Aspects of high density effective theory in QCD, *Nucl. Phys.* **B582**, pp. 451-476.

Hong, D.K., Hong, S.T. and Park, Y.J. (2001) Bosonization of QCD at high density, *Phys. Lett.* **B499**, pp. 125-134.

Hong, D.K., Rho, M., Yee, H.-U. and Yi, P. (2007a) Chiral dynamics of baryons from string theory, *Phys. Rev.* **D76**, pp. 061901-5.

Hong, D.K., Rho, M., Yee, H.-U. and Yi, P. (2007b) Dynamics of baryons from string theory and vector dominance, *JHEP* **09**, pp. 063-117.

Hong, D.K., Rho, M., Yee, H.-U. and Yi, P. (2007c) Nucleon form factors and hidden symmetry in holographic QCD, *Phys. Rev.* **D77**, pp. 014030-8.

Hong, D.K., Rho, M. and Zahed, I. (1999) Qualitons at high density, *Phys. Lett.* **B468**, pp. 261-269.

Horăva, P. (2005) Stability of Fermi surfaces and K-theory, *Phys. Rev. Lett.* **95**, pp. 016404-4.

Horowitz, G. and Polchinski, J. (2006) Gauge/gravity duality, *Towards Quantum Gravity* (Cambridge University Press), gr-qc/0602037.

Hosaka, A. and Toki, H. (1996) Chiral bag model for the nucleon, *Phys. Rept.* **277**, pp. 65-188.

Houghton, C. and Magee, S. (2007) The effect of pion mass on Skyrme configurations, *Europhys. Lett.* **77**, pp. 11001-3.

Hyodo, T., Jido, D. and Roca, L. (2007) The N_c behavior of the two $\Lambda(1405)$ poles in chiral dynamics, arXiv:0712.3347 [hep-ph].

Hyodo, T. and Weise, W. (2007) Effective $\overline{K}N$ interactions based on chiral SU(3) dynamics, arXiv:0712.1613 [nucl-th].

Igarashi, Y., Johmura, M., Kobayashi, A. Otsu, H., Sato, T. and Sawada, S. (1985) Stabilization of skyrmions via ρ mesons, *Nucl. Phys.* **B259**, pp. 721-729.

Ippolito, N.D., Ruggieri, M., Rischke, D.H., Sedrakian, A. and Weber, F. (2007) Equilibrium sequences of non-rotating and rapidly rotating crystalline color-superconducting hybrid stars, arXiv:0710.3874.

Isgur, N and Wise, M.B. (1989) Weak decays of heavy mesons in the static quark approximation, *Phys. Lett.* **B232**, pp. 113-117.

Iwasaki, Y., Kanaya, K., Kaya, S., Sakai, S. and Yoshie, T. (2004) Phase structure of lattice QCD for general number of flavors, *Phys. Rev.* **D69**, pp. 014507-21.

Jackson, A.D. and Rho, M. (1983) Baryons as chiral solitons, *Phys. Rev. Lett.* **51**, pp 751-754.

Jaikumar, P. and Ouyed, R. (2006) Skyrmion stars: Astrophysical motivations and implications, *Astrophys. J.* **639**, pp. 354-362.

Jenkins, E. and Manohar, A.V. (1991) Baryon chiral perturbation theory using a heavy fermion Lagrangian, *Phys. Lett.* **B255**, pp. 558-562.

Jin, X.-M. and Leinweber, D.B. (1995) Valid QCD sum rules for vector mesons in nuclear matter, *Phys. Rev.* **C52**, pp. 3344-3352.

Johnson, K. (1975) The M.I.T. Bag Model, *Acta Phys. Polon.* **B6**, pp. 865-919.

Kaplan, D.B. (1991) Qualitons, *Nucl. Phys.* **B351**, pp. 137-160.

Kaplan, D.B. (2005) Five lectures on effective field theory, nucl-th/0510023.
Kaplan, D.B. and Klebanov, I.R. (1990) The role of a massive strange quark in the large N Skyrme model, *Nucl. Phys.* **B335**, pp. 45-66.
Kaplam, D.B. and Nelson, A.E. (1986) Strange goings on in dense nucleonic matter, *Phys. Lett.* **B175**, pp. 57-63.
Karch, A., Katz, E., Son, D.T. and Stephanov, M.A. (2006) Linear confinement and AdS/QCD, *Phys. Rev.* **D74**, pp. 015005-18.
Kienle, P. and Yamazaki, T. (2004) Pions in nuclei, a probe of chiral symmetry restoration, *Prog. Part. Nucl. Phys.* **52**, pp. 85-132.
Kim, Y., Kubodera, K., Min, D.-P., Myhrer, F. and Rho, M. (2007) Kaon condensation and quark-antiquark condensate in dense matter, *Nucl. Phys.* **A792**, pp. 249-263.
Kitazawa, M., Rischke, D.H. and Shovkovy, I.A. (2006) Stable gapless superconductibity at strong coupling, *Phys. Lett.* **B637**, pp. 367-373.
Kohn, W. (1961) Cyclotron resonance and de Haas-van Alphen oscillations of an interacting electron gas, *Phys. Rev.* **123**, pp. 1242-1244.
Kohn, W and Sham, L.J. (1965) Self-consistent equations including exchange and correlation effects, *Phys. Rev.* **140**, pp. A1133-A1138.
Kong, X. and Ravndal, F. (2001) Proton-proton fusion in effective field theory, *Phys. Rev.* **C64**, pp. 044002-14.
Kovtun, P., Son, D.T. and Starinets, A.O. (2005) Viscosity in strongly interacting quantum field theories from black hole physics, *Phys. Rev. Lett.* **94**, pp. 111601-4.
Kubodera, K., Delorme, J. and Rho, M. (1978) Axial currents in nuclei, *Phys. Rev. Lett.* **40**, pp. 755-758.
Kubodera, K. and Rho, M. (1991) Axial charge transitions in heavy nuclei and in-medium effective chiral Lagrangians, *Phys. Rev. Lett.* **67**, pp. 3479-3483.
Kugler, M and Shtrikman, S. (1989) Skyrmion crystals and their symmetries, *Phys. Rev.* **D40**. pp. 3421-3429.
Lattimer, J. and Prakash, M. (2004) The physics of neutron stars, *Science* **304**, pp. 536-542.
Lattimer, J. and Prakash, M. (2007) Neutron star observations: Prognosis for equation of state constraints, *Phys. Rept.* **442**, pp. 109-165.
Lee, C.-H. (1996) Kaon condensation in dense stellar matter, *Phys. Rept.* **275**, pp. 255-341.
Lee, C.-H., Brown, G.E., Min, D.-P. and Rho, M. (1995) An effective chiral Lagrangian approach to kaon-nuclear interactions: Kaonic atom and kaon condensation, *Nucl. Phys.* **A585**, pp. 401-449.
Lee, C.-H., Min, D.-P. and Rho, M. (1996) The Role of $\Lambda(1405)$ in kaon-proton interactions, *Nucl. Phys.* **A602**, pp. 334-346.
Lee, C.-H., Park, H.J. and Brown, G.E. (2007) Merger of compact objects, astro-ph/0607442.
Lee, H.-J., Min, D.-P., Park, B.-Y., Rho, M. and Vento, V (1999) The proton spin in the chiral bag model: Casimir contribution and Cheshire Cat Principle, *Nucl. Phys.* **A657**, pp. 75-94.
Lee, H.-J., Park, B.-Y., Min, D.-P., Rho, M. and Vento, V. (2003) A unified approach to high density: pion fluctuations in skyrmion matter, *Nucl. Phys.* **A723**, p. 427-446.
Lee, H.-J., Park, B.-Y., Rho, M., and Vento, V. (2003) Sliding vacua in dense skyrmion matter, *Nucl. Phys.* **A726**, pp. 69-92.
Lee, H.-J., Park, B.-Y., Rho, M., and Vento, V. (2004) The pion velocity in dense skyrmion matter, *Nucl. Phys.* **A741**, pp. 161-178.
Lee, H.K., Rho, M. and Sin, S.-J. (1995) Renormalization-group flow analysis of meson condensations in dense matter, *Phys. Lett.* **B348**, pp. 290-296.

Lee, S.-H. (1989) Gluon condensates above T_c, *Phys. Rev.* **D40**, pp. 2484-2486.

Lepage, G.P. and Brotsky, S.J. (1980) Exclusive processes in perturbative quantum chromodynamics, *Phys. Rev.* **D22**, pp. 2157-2198.

Li, G.Q., Lee, C-H. and Brown, G.E. (1997) Kaon production in heavy-ion collisions and maximum mass of neutron stars, *Phys. Rev. Lett.* **79**, pp. 5214-5217.

Lolos, G.J. *et al* (1998) Evidence for ρ^0 mass modification in the $^3\mathrm{He}(\gamma,\rho^0)ppn$ reactions, *Phys. Rev. Lett.* **80**, pp. 241-244.

Lynn, B.W. (1993) Chiral $SU(2)_L \times SU(2)_R$ liquids: A Theory of heavy nuclei and neutron stars, *Nucl. Phys.* **B402**, pp. 281-322.

Machleidt, R. (2001) The high-precision, charge-dependent Bonn nucleon-nucleon potential, *Phys. Rev.* **C63**, pp. 024001-32.

Machleidt, R. and Entem, D.R. (2005) Recent advances in the theory of nuclear forces, *Phys. Conf. Ser.* **20**, pp. 77,

Mannarelli, M., Rajagopal, K. and Sharma, R. (2007) The strength of crystalline color superconductors, arXiv:0710.03331 [hep-ph].

Manohar, A. and Georgi, H. (1984) Chiral quarks and the nonrelativistic quark model, *Nucl. Phys.* **B234**, pp. 189-212

Marcucci, L.E., Riska, D.O. and Schiavilla, R. (1998) Electromagnetic structure of the trinucleons, *Phys. Rev.* **C58**, pp. 3069-3084.

Marcucci, L.E., Schiavilla, R., Viviani, M., Kievsky, A., Rosati, S. and Beacom, J.F. (2001) Weak proton capture on ^{3}He, *Phys. Rev.* **C63**, pp. 015801-28.

Matevosyan, H.H., Miller, G.A. and Thomas, A.W. (2005) Comparison of nucleon form factors from lattice QCD against the light front cloudy bag model and extrapolation to the physical mass regime, *Phys. Rev.* **C71**, pp. 055204-14.

Matsui, T. (1981) Fermi liquid properties of nuclear matter in a relativistic mean-field theory, *Nucl. Phys.* **A370**, pp. 365-388.

Migdal, A.B. (1967) *Theory of finite nuclear system and application to atomic nuclei* (Interscience Publishers/John Wiley, 1967).

Miller, D.E. (2000) Gluon condensates at finite temperature, e-Print: hep-ph/0008031.

Miller, D.E. (2007) Lattice QCD calculations for the physical equation of state, *Phys. Rept.* **443**, pp. 55-96.

Min, D.-P., Oh, Y.-S., Park, B.-Y. and Rho, M. (1994) Heavy quark symmetry and skyrmions, *Int. J. Mod. Phys.* **E4**, pp. 47-122.

Morley, P.D. and Kislinger, M.B. (1979) Relativistic many-body theory, quantum chromodynamics and neutron stars/supernova, *Phys. Rept.* **51**, pp. 63-110.

Nadkarni, S., Nielsen, H.B. and Zahed, I. (1984) Bosonization relations for bag boundary conditions, *Nucl. Phys.* **B253**, pp. 308-322.

Narison, S. (1988) Beautiful mesons from QCD spectral sum rules, *Phys. Lett.* **B210**, pp. 238-248.

Narison, S. (2003) Open charm and beauty chiral multiplets in QCD, *Phys. Lett.* **B605**, pp. 319-325.

Nemoto, Y., Jido, D., Oka, M. and Hosaka, A. (1998) Decays of $1/2^-$ baryons in chiral effective theory, *Phys. Rev.* **D57**, pp. 4124-4135.

Nice, D.J. *et al.* (2005) A 2.1 solar mass pulsar measured by relativistic orbital decay, *Astrophys. J.* **634**, pp. 1242-1249.

Nielsen, H.B. and Wizba, A. (1987) The Cheshire Cat principle applied to hybrid bag models, *Proceedings: Les Houches Workshop on the Elementary Structure of Matter, Springer-Verlag*, Mar 24 - Apr 2, 1987.

Niemi, A.J. (2006) Could the spin-charge separation be the source of confinement?, *AIP Conf. Proc.* **806**, pp. 114-123; hep-ph/0510288.

Nishikawa, T. and Kondo, Y. (2007) A study of the ppK^- system in the Skyrme model, hep-ph/0703100.

Nogga, A., Timmermans, R.G.E. and van Kolck, U. (2005) Renormalization of one-pion exchange and power counting, *Phys. Rev.* **C72**, pp. 054006-15.

Nolte, R., Baumann, A., Rose, K.W. and Schumacher, M. (1986) Effect of exchange currents in E1 sum rule and orbital g-factor in ^{209}Bi, *Phys. Lett.* **B173**, pp. 388-391.

Nowak, M.A., Rho, M., Wirzba, A. and Zahed, I. (2001) $\pi^0 \to \gamma\gamma$ in dense QCD, *Phys. Lett.* **B497**, pp. 85-90.

Nowak, M.A., Rho, M. and Zahed, I. (1993) Chiral effective action with heavy quark symmetry, *Phys. Rev.* **D48**, pp. 4370-4374.

Nowak, M.A., Rho, M. and Zahed, I. (1996) *Chiral Nuclear Dynamics* (World Scientific, Singapore, 1996)

Nowak, M.A., Rho, M. and Zahed, I. (2004) Chiral doubling of heavy-light hadrons: BaBar 2317-MeV/c^2 and CLEO 2463-MeV/c^2 discoveries, *Acta Phys. Polon.* **B35**, pp. 2377-2392

Orear, J. (1978) Evidence for a proton core, *Phys. Rev.* **18**, pp. 2484-2490.

Oset, E. and Toki, H. (2006) A critical analysis on deeply bound kaonic states in nuclei and the KEK experiment, nucl-th/0609070.

Owen, B.J. (2005) Maximum elastic deformtions of compact stars with exotic equation of state, *Phys. Rev. Lett.* **95**, pp. 211101-4.

Pandharipande, V.R., Pethick, C.J. and Thorsson, V. (1995) Kaon energies in dense matter, *Phys. Rev. Lett.* **75**, pp. 4567-4570.

Park, B.-Y., Min, D.-P., Rho, M. and Vento, V. (2002) Atiyah-Manton approach to skyrmion matter, *Nucl. Phys.* **A707**, pp. 381-398.

Park, B.-Y., Min, D.-P. and Rho, M. (2004) Kaon-soliton bound state approach to the pentaquark states, *Phys. Rev.* **D70**, pp. 114026-31.

Park, B.-Y., Rho, M. and Vento, V. (2004) Vector mesons and dense skyrmion matter, *Nucl. Phys.* **A736**, pp. 129-145.

Park, B.-Y., Rho, M. and Vento, V. (2008) The role of the dilaton in dense skyrmion matter, arXiv:0801.1374 [nucl-th].

Park, H.-J., Lee, C.-H. and Brown, G.E. (2006) The problem of mass: Mesonic bound states above T_c, *Nucl. Phys.* **A774**, pp. 889-892.

Park, T.-S. *et al.* (2003) Parameter free effective field theory calculation for the solar proton fusion and hep processes, *Phys. Rev.* **C67**, pp. 055206-21.

Park, T.-S., Kubodera. K., Min, D.-P. and Rho, M. (2001) Effective field theory for nuclei: Confronting fundamental questions in astrophysics, *Nucl. Phys.* **A684**, 101-112.

Park, T.-S., Min, D.-P., Kubodera, K. and Rho, M. (2002) Effective field theory approach to $\vec{n} + \vec{p} \to d + \gamma$ at threshold, *Phys. Lett.* **B472**, pp. 232-242.

Park, T.-S., Min, D.-P. and Rho, M. (1993) Chiral dynamics and heavy fermion formalism in nuclei. 1. Exchange axial currents, *Phys. Rept* **.233**, pp. 341-395.

Park, T.-S., Min, D.-P. and Rho, M. (1995) Radiative neutron-proton capture in effective chiral Lagrangians, *Phys. Rev. Lett.* **74**, pp. 4153-4156.

Park, T.-S., Min, D.-P. and Rho, M. (1996) Chiral Lagrangian approach to exchange vecor currents in nuclei, *Nucl. Phys.* **A596**, p. 515-552.

Pavon Valderrama, M. and Ruiz Arriola, E. (2005) Renormalization of the deuteron with one pion exchange, *Phys. Rev.* **C72**, pp. 054002-20.

Pavon Valderrama, M. and Ruiz Arriola, E. (2006) Renormalization of NN interaction with chiral two pion exchange potential: Non-central phases, *Phys. Rev.* **C74**, pp. 064004-19; Erratum-ibid.**C75**, pp. 059905.

Petronzio, R., Vergata, S. Simula, S. and Ricco, G. (2003) Possible evidence of extended objects inside the proton, *Phys. Rev.* **D67**, pp. 094004, Erratum-ibid. **D68**, pp. 099901-11.

Phillips, D.R. (2007) Chiral effective theory predictions for deutron form factor ratios at low Q^2, *J. Phys.* **G34**, pp. 365-388.

Pieper, S.C. and Wiringa, R.B. (2001) Quantum Monte Carlo calculations of light nuclei, *Ann. Rev. Nucl. Part. Sci.* **51**, pp. 53-90.

Pieper, S.C., Wiringa, R.B. and Carlson, J. (2004) Quantum Monte Carlo calculations of excited states in A=6-8 nuclei, *Phys. Rev.* **C70**, pp. 054325-10.

Piette, B.M.A.G. and Probert, G.I. (2007) Towards Skyrmion stars: Large baryon configurations in the Einsten-Skyrme model, *Phys. Rev.* **D75**, pp. 125023-9.

Politzer, H.D. and Wise, M.B. (1991) Kaon condensation in nuclear matter, *Phys. Lett.* **B273**, pp. 156-162.

Prakash, M., Ainsworth, T.L. and Lattimer, J.M. (1988) Equation of state and the maximum mass of neutron stars, *Phys. Rev. Lett.* **61**, pp. 2518-1522.

Radha, P.B. *et al.* (1997) Gamow-Teller strength distributions in f-p shell nuclei, *Phys. Rev.* **C56**, pp. 3079-3086.

Rajagopal, K. and Wilczek, F. (2001) The Condensed matter physics of QCD, *At the frontier of particle physics: Handbook of QCD* ed by M. Shifman (World Scientific, Singapore, 2001) Vol. 3, pp. 2061-2151.

Ramos, A., Magas, V.K., Oset, E. and Toki, H. (2007) Theoretical view on bound antikaon-nuclear states, nucl-th/0702019

Rapp, R. and Wambach, J. (2000) Chiral symmetry restoration and dileptons in relativistic heavy ion collisions, *Adv. Nucl. Phys.* **25**, 1-164.

Rho, M. (1974) Quenching of axial-vector coupling constant in beta-decay and pion nucleus potential, *Nucl. Phys.* **A231**, pp. 493-503.

Rho, M. (1982) Pions and the chiral bag, *Prog. Part. Nucl. Phys.* **8**, pp. 103-146.

Rho, M. (1985) Axial currents in nuclei and the skyrmion size, *Phys. Rev. Lett.* **54**, pp. 767-770.

Rho, M. (1991) Exchange currents from chiral Lagrangians, *Phys. Rev. Lett.* **66**, pp. 1275-1278.

Rho, M. (1994) The Cheshire Cat hadrons, *Phys. Rept.* **240**, pp. 1-148; corrected and updated with errata "The Cheshire Cat hadrons revisted," in hep-ph/0206003.

Rho, M. (2002) 10th Taiwan Lectures on "Effective field theories for nuclei, nuclear matter and dense matter," nucl-th/0202078.

Rho, M. (2004) Pentaquarks, skyrmions and the vector manifestation of chiral symmetry, *Nagoya 2004, Dynamical symmetry breaking*, pp. 197-206; hep-ph/0502049.

Rho, M. (2006) Predictiveness of effective field theory in nuclear physics, nucl-th/0610003.

Rho, M. (2007a) Hidden local symmetry and the vector manifestation of chiral symmetry in hot and/or dense matter, *Prog. Theor. Phys. Suppl.* **168**, pp. 519-526.

Rho, M. (2007b) Hidden local symmetry and dense half-skyrmion matter, arXiv:0711.3895 [nucl-th].

Rho, M., Goldhaber, A.S. and Brown, G.E. (1983) Topological soliton bag model for baryons, *Phys. Rev. Lett.* **51**, pp. 747-750.

Rho, M. and Wilskinson, D.H. (1979) *Mesons In Nuclei*, Vol. I, II & III (North-Holland, Amsterdam 1979).

Riska, D.O. and Brown, G.E. (1972) Meson exchange effects in $n + p \to d + \gamma$, *Phys. Lett.* **38B**, pp. 193-195.

Sachdev, S. (2000) *Quantum phase transitions* (Cambridge University Press 2000).

Sakai, T. and Sugimoto, S. (2005) Low energy hadron physics in holographic QCD, *Prog. Theor. Phys.* **113**, pp. 843-882.

Sakai, T. and Sugimoto, S. (2006) More on a holographic dual of QCD, *Prog. Theor. Phys.* **114**, pp. 1083-1118.

Sasaki, C. (2004) Non-renormalization theorem originating in a new fixed point of the vector manifestation, *Nucl. Phys.* **A739**, pp. 151-165.

Sasaki, C. (2005) Chiral phase transition in QCD and vector manifestation, Nagoya University thesis, hep-ph/0504073.

Sasaki, S. and Yamazaki, T. (2007) Nucleon form factors from quenched lattice QCD with domain wall fermions, arXiv:0709.3150 [hep-lat].

Schäfer, T. (2006a) The CFL phase and m_s: An effective field theory approach, nucl-th/0602067.

Schäfer, T. (2006b) Effective field theories of dense and very dense matter, nucl-th/0609075.

Schäfer, T. and Wilczek, F. (1999) Continuity of quark and hadron matter, *Phys. Rev. Lett.* **82**, pp. 3956-3959.

Schaffner-Bielich, J. (2007) Signals of the QCD phase transition in the heavens, arXiv:0709.1043 [astro-ph].

Schumacher, M. *et al.* (1994) The enhancement of giant-dipole strength and its consequences for the effective mass of the nucleon and the electromagnetic polarizabilities and quadrupole sum-rule of the nucleon, *Nucl. Phys.* **A576**, pp. 603-625.

Schwenk, A., Brown, G.E. and Friman, B. (2003) Low momentum nucleon-nucleon interaction and Fermi liquid theory, *Nucl. Phys.* **A703**, pp. 745-769.

Scoccola, N.N., Min, D.P., Nadeau, H. and Rho, M. (1989) The strangeness problem: An $SU(3)$ skyrmion with vector mesons, *Nucl. Phys.* **A505**, pp. 497-524.

Serot, B.D. and Walecka, J.D. (1986). The relativistic nuclear many-body problem, *Adv. Nucl. Phys.* **16**, pp. 1-327.

Senthil, T. *et al.* (2004) Deconfiend quantum critical points, *Science* **303**, pp. 1490-1494.

Shankar, R. (1994) Renormalization group approach to interacting fermions, *Rev. Mod. Phys.* **66**, pp. 129-192.

Shapiro, S.L. and Teukolsky, S.A. (1983) *Black holes, white dwarfs and neutron stars* (Wiley, New York 1983).

Shevchenko, N.V., Gal, A. and Mareš, J. (2007) Faddeev calculation of K^-pp quasibound state, *Phys. Rev. Lett.* **98**, pp. 082301-4.

Shifman, M.A., Vainshtein, A.I. and Zakharov, V.I. (1979a) QCD and resonance physics: Sum rules, *Nucl. Phys.* **B147**, pp. 385-447.

Shifman, M.A., Vainshtein, A.I. and Zakharov, V.I. (1979b) QCD and resonance physics: Applications, *Nucl. Phys.* **B147**, pp. 448-518.

Shuryak, E.V. and Brown, G.E. (2003) Matter induced modification of resonances at RHIC freezeout, *Nucl. Phys.* **A717**, pp.322-335.

Skyrme, T.H.R. (1962) A unified field theory of mesons and baryons, *Nucl. Phys.* **31**, pp. 556-569.

Smolin, L. (1997) *The Life of the Cosmos* (Oxford University Press, New York and Oxford, 1997).

Son, D.T. and Stephanov, M.A. (2000) Inverse meson mass ordering in color flavor locking phase of high density QCD, *Phys. Rev.* **D61**, pp. 074012-9.

Son, D.T. and Stephanov, M.A. (2002) Pion propagation near the QCD chiral phase transition, *Phys. Rev. Lett.* **88**, pp. 202302-5; Real-time pion propagation in finite-temperature QCD, *Phys. Rev.* **D66**, pp. 076011-23.

Son, D.T. and Stephanov, M.A. (2004) QCD and dimensional deconstruction, *Phys. Rev.* **D69**, pp. 065020-33.

Song, C. (2001) Dense nuclear matter: Landau Fermi liquid theory and chiral Lagrangian with scaling, *Phys. Rept.* **347**, pp. 289-371.

Song, C., Brown, G.E., Min. D.-P. and Rho, M. (1997) Fluctuations in "Brown-Rho scaled" chiral Lagrangians, *Phys. Rev.* **C56**, pp. 2244-2260.

Song, C., Min, D.-P. and Rho, M. (1998) Thermodynamic properties in Brown-Rho scaled chiral Lagrangians, *Phys. Lett.* **B424**, pp. 226-234.

Song, Y.-H., Lazauskas, R., Park, T.-S. and Min, D.-P. (2007) Effective field theory approach to the M1 properties of A=2 and 3 nuclei, *Phys. Lett.* **B656**, pp. 174-181.

STAR Collaboration (2004) ρ production and possible modification in $Au + Au$ and $p + p$ collisions at $s(NN)^{1/2} = 200$ GeV, *Phys. Rev. Lett.* **92**, pp. 092301-4.

Stoks, V. G. J., Klomp, R. A. M., Terheggen, C. P. F. and de Swart, J. J. (1994) Construction of high quality NN potential models, *Phys. Rev.* **C49**, pp. 2950-2962.

Suzuki, K. *et al.* (2004) Precision spectroscopy of pionic 1S states of Sn nuclei and evidence for partial restoration of chiral symmetry in the nuclear medium, *Phys. Rev. Lett.* **92**, pp. 072302.

Tanabashi, M. (1993) Chiral perturbation to one loop including ρ meson, *Phys. Lett.* **B316**, pp.534-541.

Tanabashi, M. (1996) Formulations of spin 1 resonances in the chiral lagrangian, *Phys. Lett.* **B384**, pp. 218-226.

't Hooft, G. in *Recent developments in gauge theories* (Plenum Press 1980), pp. 135.

Thomas, A.W. (1982) Chiral symmetry and the bag model: A new starting point for nuclear physics, *Adv. Nucl. Phys.* **13**, pp. 1-137.

Thomas, A.W., Theberge, S. and Miller, G.A. (1981) The cloudy bag model of the nucleon, *Phys. Rev.* **D24**, pp. 216-229.

Thorsson, V., Prakash, M. and Lattimer, J.M. (1994) Composition, structure and evolution of neutron stars with kaon condensation, *Nucl. Phys.* **A 572**, pp.693-731.

Trnka, D. *et al.* (2005) First observation of in-medium modifications of the ω meson, *Phys. Rev. Lett.* **94**, pp. 192303-4.

Vafa, C. and Witten, E. (1984) Restrictions on symmetry breaking in vector-like gauge theories, *Nucl. Phys.* **B234**, pp. 173-188.

Van Paradijs, J., Takens, R. and Zuiderwijk, E. (1977a) Systematic distortions of the radial velocity curve of HD 77581/Vela X-1/ due to tidal deformation, *Astron. Astrophys.* **57**, pp. 221-227.

Van Paradijs, J., Zuiderwijk, E.J., Takens, R.J., and Hammerschlag-Hensberge, G (1977b) Spectroscopic orbit and the masses of the components of the binary X-ray source 3U 0900-40/HD 77581, *Astron. Astrophys. Suppl.* **30**, pp. 195-211.

Waas, T., Kaiser, N. and Weise, W. (1996) Effective kaon masses in dense nuclear and neutron matter, *Phys. Lett.* **B379**, pp. 34-38.

Waas, T., Rho, M. and Weise, W. (1997) Effective kaon mass in dense baryonic matter: Role of correlations, *Nucl. Phys.* **A617**, pp. 449-463.

Warburton, E.K. (1991) Mesonic enhancement of the weak axial vector current evaluated from beta decay in the lead region, *Phys. Rev. Lett.* **66**, pp. 1823-1826

Weigel, H. (1996) Baryons as three flavor solitons, *Int. J. Mod. Phys.* **A11**, pp. 2419-2544.

Weinberg, S. (1967) Precise relations between the spectra of vector and axial vector mesons, *Phys. Rev. Lett.* **18**, pp. 507-509 .

Weinberg, S. (1979) Phenomenological Lagrangians, *Physica* **A96**, pp. 327-340.

Weinberg, S. (1990) Nuclear forces from chiral Lagrangians, *Phys. Lett.* **B251**, pp. 288-292.

Weinberg, S. (1991) Effective chiral Lagrangians for nucleon-pion interactions and nuclear forces, *Nucl. Phys.* **B363**, pp. 3-18.

Weinberg, S. (1997a) What is quantum field theory, and what did we think it is?, hep-th/9702027.

Weinberg, S. (1997b) Effective field theories in the large-N limit, *Phys. Rev.* **56**, pp. 2303-2316.

Weise, W. and Härtle, R. (2008) Chiral SU(3) dynamics and antikaon-nuclear quasibound states, arXiv:0801.1467 [nucl-th].

Wetterich, C. (2001) Spontaneously broken color, *Phys. Rev.* **D64**, pp. 036003-38.

Wilczek, F. (2006) Did the Bing Bang boil?, *Nature* **443**, pp. 637-638.

Wilms, S., Giacosa, F. and Rischeke, D.H. (2007) Pion-nucleon scattering within a gauged sigma model with parity-doubled nucleons, nucl-th/0702076.

Wiringa, R.B. (2006) Pair counting, pion-exchange forces and the structure of light nuclei, *Phys. Rev.* **C73**, pp. 034317-27.

Wiringa, R.B., Stoks, V.G.J. and Schiavilla, R. (1995) An accurate nucleon-nucleon potential with charge independence breaking, *Phys. Rev.* **C51**, pp. 38-51.

Witten, E. (1983) Global aspects of current algebra, *Nucl. Phys.* **B223**, pp. 422-432.

Witten, E. (1998) Baryons and branes in anti de Sitter space, *JHEP* **07**, pp. 006-37.

Yamamoto, N., Hatsuda, T., Tachibana, M. and Baym, G. (2007) Hadron-quark continuity induced by the axial anomaly in dense QCD, *J. Phys.* **G34**, pp. S635-638.

Zschiesche, D., Tolos, L., Schaffner-Bielich, J. and Pisarski, R.D. (2006) Cold, dense matter in a SU(2) parity doublet model, nucl-th/0608044.

Zahed, I. and Brown, G.E. (1986) The Skyrme model, *Phys. Rept.* **142**, pp. 1-102.

Zarembo, K. (2001) Possible pseudogap phase in QCD, *JETP Lett.* **75**, p. 59-62.

Zumino, B. (1970) Effective Lagrangians and broken symmetries, in *1970 Brandeis lectures on "Elementary particles and quantum field theory"*, Vol. 2, Cambridge, Mass. 1970, pp. 437-500.

Index